

Historic, Archive Document

Do not assume content reflects current scientific knowledge, policies, or practices.

**UV-B Monitoring Workshop: A Review of the Science
and Status of Measuring and Monitoring Programs**

**10-12 March 1992
Washington, D.C.**

Sponsored by the

***Alternative Fluorocarbons
Environmental Acceptability Study***

and the

***Cooperative State Research Service
U.S. Department of Agriculture***

Conducted and Reported on by

***Science and Policy Associates, Inc.
The West Tower, Suite 400
1333 H Street, NW
Washington, D.C.***

**United States
Department of
Agriculture**



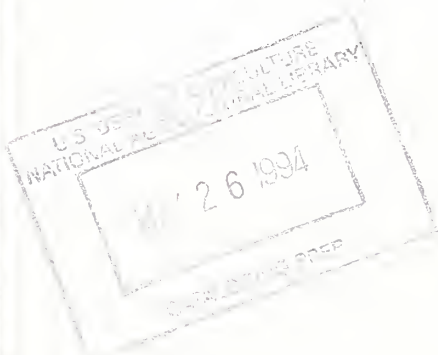
National Agricultural Library

USDA, National Agricultural Library
NAL Bldg
10301 Baltimore Blvd
Beltsville, MD 20705-2351

a GC253
49
1992

UV-B MONITORING WORKSHOP: A REVIEW OF THE SCIENCE
AND STATUS OF MEASURING AND MONITORING PROGRAMS

10-12 March 1992
Washington, D.C.



Sponsored by the

*Alternative Fluorocarbons
Environmental Acceptability Study*

and the

*Cooperative State Research Service
U.S. Department of Agriculture*

Conducted and Reported on by

*Science and Policy Associates, Inc.
The West Tower, Suite 400
1333 H Street, NW
Washington, D.C.*

The opinions described in this report are those of the speakers and do not necessarily represent those of the sponsoring organizations. While every effort has been made to summarize the presentations accurately, we cannot guarantee the complete absence of errors.

CONTENTS

Introduction	1
Status of Knowledge on UV-B and Potential Effects – The WMO/UNEP Stratospheric Ozone and UNEP Environmental Effects Assessments, 1991	1
UV-B Radiation Changes	2
Changes in Biologically Active UV Radiation Reaching the Earth's Surface	2
Effects on Human Health	3
Effects on Terrestrial Plants	4
Effects on Aquatic Ecosystems	4
Spectral Responses of Biological Systems	5
Biological Action Spectra	5
UV-B Measurement and Monitoring Programs	6
NSF UV-B Monitoring in Polar Regions	6
European Communities STEP UV-B Program: Instrument Comparison	6
USDA/CSRS Instrument Development and Preliminary Network	7
High Altitude UV-B Measurements and Trends in Switzerland	7
UV-B Controlling Factors and Variability	8
Comparison of Measurements from the Robertson-Berger Meter and Dobson Networks	8
U.S. Robertson-Berger Meter Network and Instrument Characterization	9
Ancillary Measurements	10
Department of Energy Atmospheric Radiation Measurement Program	10
International Network for Detection of Stratospheric Change	10
Role of Satellites in UV-B Monitoring	11
Potential for Satellite Measurements of Surface UV Climatology	11
Non-U.S. National UV Research and Monitoring Programs	12
New Zealand	12
Sweden	13
United Kingdom	14
Statistical Considerations in Network Design and Trend Analysis	14
Network Design and Trend Analysis	14

Commentary of Invited Experts	15
Instrumentation	15
Environmental Effects Assessment and Future Needs	15

Appendix A: Agenda

Appendix B: List of Participants

Appendix C: Presentation Materials

UV-B Radiation Changes	C-1
<i>Richard McKenzie, New Zealand Department of Scientific and Industrial Research</i>	
Changes in Biologically Active UV Radiation Reaching the Earth's Surface	C-23
<i>Sasha Madronich, National Center for Atmospheric Research</i>	
Effects on Human Health	C-58
<i>Margaret Kripke, University of Texas</i>	
Effects on Terrestrial Plants	C-64
<i>Joe Sullivan, University of Maryland</i>	
Effects on Aquatic Ecosystems	C-83
<i>Robert Worrest, U.S. Environmental Protection Agency</i>	
Action Spectroscopy and Stratospheric Ozone Depletion	C-89
<i>Thomas Coohill, Western Kentucky University</i>	
NSF UV-B Monitoring in Polar Regions	C-113
<i>C. Rocky Booth, Biospherical Instruments, Inc.</i>	
European Communities STEP UV-B Monitoring Program: Instrument Intercomparison	C-121
<i>Brian Gardiner, British Antarctic Survey</i>	
<i>Ann Webb, University of Reading</i>	
USDA/CSRS Instrument Development and Preliminary Network	C-129
<i>Lee Harrison, State University of New York, Albany</i>	
High Altitude UV-B Measurements and Trends	C-142
<i>Mario Blumthaler, University of Innsbruck</i>	
UV-B Controlling Factors and Variability	C-147
<i>John Frederick, University of Chicago</i>	

Comparison of Measurements from R-B and Dobson Meters	C-162
<i>John Frederick, University of Chicago</i>	
U.S. R-B Meter Network and Instrument Characterization	C-177
<i>John DeLuigi, National Oceanic and Atmospheric Administration</i>	
The Department of Energy Atmospheric Radiation Measurement Program	C-226
<i>Gerald Stokes, Pacific Northwest Laboratory</i>	
International Network for the Detection of Stratospheric Change	C-230
<i>Michael Kurylo, National Aeronautics and Space Administration</i>	
Potential for Satellite Measurements of Surface Ultraviolet Climatology	C-250
<i>Dan Lubin, California Space Institute, University of California, San Diego</i>	
UV-B Monitoring and Research in New Zealand	C-276
<i>Richard McKenzie, New Zealand Department of Scientific and Industrial Research</i>	
UV-B Monitoring Activities in Sweden	C-279
<i>Ulf Wester, Swedish Radiation Protection Institute</i>	
Broad-Band Solar Radiation Measurements in the United Kingdom	C-297
<i>Colin Driscoll, U.K. National Radiological Protection Board</i>	
Statistical Considerations in Network Design and Data Analyses	C-305
<i>William Hill, University of Wisconsin, Madison</i>	
<i>Lane Bishop, Allied-Signal Corporation</i>	
Commentary on UV-B Effects Research	C-323
<i>Jan van der Leun, University of Utrecht</i>	

INTRODUCTION

The Alternative Fluorocarbons Environmental Acceptability Study (AFEAS) sponsored a workshop on 10-12 March 1992 to address the current status of knowledge of ultraviolet-B (UV-B) radiation and its effects, and the status of measurement and monitoring programs. Presentations were made by an international group of 24 experts, providing background for discussions of the specifications for irradiance measurements – wavelength range, resolution (adequacy of integrated or multiple fixed-wavelength measurements), accuracy, sites, etc. The goal of the latter half of the workshop, which was jointly sponsored by AFEAS and the Cooperative State Research Service, U.S. Department of Agriculture (CSRS/USDA), was to develop specifications for instruments whose cost and operation would allow for their placement at a large number of sites throughout the United States. Necessary ancillary measurements, calibration requirements, number of monitoring sites, siting criteria, etc. were discussed. The recommendations that evolved from these discussions are published in a separate report by CSRS/USDA.

The CSRS/USDA previously held a workshop on UV-B monitoring in Denver, Colorado in January 1991. The goal of the Denver workshop was to define specifications for state-of-the-art spectral irradiance measurements and instrumentation. The March 1992 meeting provided supplemental information necessary to develop a nationwide monitoring program in the United States that would complement efforts being made by other countries. Invited experts presented the current understanding of the potential effects of UV-B radiation, status of UV-B measurement and monitoring programs, spectral responses of biological systems, role of satellites in monitoring, need for ancillary measurements, and statistical considerations in network design and trend analysis (see agenda, Appendix A). The list of workshop participants is provided in Appendix B. This report summarizes the presentations given by the invited speakers; presentation materials are provided in Appendix C.

The workshop was organized Dr. J. Richard Soulen (AFEAS) and Dr. James Gibson (Colorado State University), and was conducted and reported on by Science and Policy Associates, Inc. We are indebted to the speakers for checking the accuracy of the summaries of their presentations, which are provided below.

STATUS OF KNOWLEDGE ON UV-B AND POTENTIAL EFFECTS – THE WMO/UNEP STRATOSPHERIC OZONE AND UNEP ENVIRONMENTAL EFFECTS ASSESSMENTS, 1991

This session of the workshop provided a review of relevant aspects of two major reports: the 1991 WMO/UNEP Scientific Assessment of Ozone Depletion and the 1991 update of the Environmental Effects of Ozone Depletion report.

UV-B Radiation Changes

Richard McKenzie
New Zealand Department of Scientific and Industrial Research

Increases in UV-B effects are most likely to appear first in the Southern Hemisphere where stratospheric ozone losses have been more severe, tropospheric ozone has not increased, and aerosol concentrations are lower. The following conclusions were presented:

- Stratospheric ozone levels have been decreasing in both hemispheres.
- Trends in UV-B are not well established.
- The effects of ozone changes are evident in spectral data.
- Models and measurements agree for ozone and solar zenith angle effects.
- UV radiation levels at the Earth's surface are currently greater in the Southern Hemisphere than in the Northern Hemisphere.
- Due to the complexity of heterogeneous chemistry, existing models underestimate changes in the observed ozone levels. Therefore, they cannot be used to accurately predict future changes in UV radiation reaching the Earth's surface.
- A high quality spectral monitoring program is needed. Requirements for such a program involve determination of resolution/range, frequency and coverage, calibration (field of view, irradiance, and wavelength scales), site selection, and supporting measurements.

Changes in Biologically Active UV Radiation Reaching the Earth's Surface

Sasha Madronich
National Center for Atmospheric Research

Measurements of UV trends have historically been performed with Robertson-Berger (R-B) meters, spectral radiometers, and Dobson instruments. Measurements of UV data are available from the R-B meter network of 25 U.S. stations and 11 non-U.S. stations. The number of operating stations has varied over time; there are currently only 17 active sites. The R-B meter measurements show a decrease of 0.5% to 1.1% per year of integrated, annual UV radiation from 1974 to 1985. Because the meters are located in mostly urban and near-urban sites, it has been suggested that this decrease could be due to an increase in local pollution around the R-B meters. Spectral irradiance measurements have been taken at too few sites and for too short a time period to determine statistically significant UV distribution and trend information. Spectral radiometers do, however, confirm the theory for large ozone changes. Dobson ozone instruments provide direct observational evidence for global-scale change in the relative intensity of different wavelengths inside the UV-B range. This information comprises the data from which ozone columns and their long-term trends are derived.

Data indicate that the global-scale ozone distribution has been changing over the past ten years. Recent total ozone measurements (TOMS Version 6) imply an increase of annual DNA-

damage weighted UV-B over large geographical areas of the Earth. In the Northern Hemisphere trends range from 5% per decade at 30°N to about 11% per decade in the polar region, while in the Southern Hemisphere the trends are 5% per decade at 30°S, 10% per decade at 55°S, and 40% per decade at 85°S. In the equatorial region (30°S to 30°N), trends are not statistically significant.

Various factors affect the amount of UV radiation reaching the Earth's surface. Analyses of recent studies indicate that a 2% per decade decrease in UV-B can be expected with current tropospheric ozone trends. In some locations, the amount of UV-B radiation reaching the ground may have been reduced by 3-10% and 6-18% due to increases in tropospheric ozone and sulfuric aerosols, respectively. Efforts to improve air quality may accentuate the potential increases in UV-B associated with the depletion of stratospheric ozone.

Effects on Human Health

*Margaret Kripke
University of Texas*

An increase in UV-B radiation can have various direct and indirect effects on human health. UV-B exposure can affect the incidence of skin cancer and ocular damage, and could potentially affect the incidence and severity of certain infectious diseases. The potential immunological impacts of UV radiation are not limited to fair-skinned populations; effects on the immune system are observed in deeply pigmented individuals as well.

It is estimated that a sustained 10% reduction in stratospheric ozone would result in approximately a 26% increase in non-melanoma skin cancer (NMSC) worldwide or 300,000 new cases per year. For NMSC, UV radiation effects are cumulative; incidence is proportional to lifetime UV-B exposure. Therefore, with increased UV-B irradiation, skin cancer is expected to occur at a younger age. The data are much less certain for melanoma skin cancer. The role of UV-B radiation in melanoma skin cancer is complex and the mechanisms are unknown. The incidence of melanoma skin cancer, however, has been related to acute UV-B exposure and could also occur at a younger age with a reduction in stratospheric ozone. A 10% ozone reduction is estimated to result in a 20% increase or 4,500 new cases.

Cataracts are responsible for 17 million cases of blindness each year (50% of the world's cases). A 1% stratospheric ozone loss is predicted to result in a 0.6% increase in cataract incidence or 100,000 new cases per year. The known ocular effects due to increased UV-B radiation include photokeratitis (snowblindness), early presbyopia, lens capsule deformation, and ocular melanoma.

Animal models showing the effects of UV-B radiation on the immune system suggest that UV-B exposure decreases immune functions, which contribute to UV-induced skin cancer and melanoma. Skin immunity, some systemic immune responses, phagocytosis, and immunity to infectious diseases (Herpes simplex virus, Leishmania, Mycobacteria, Candida) are impaired by UV irradiation. The effect that sunscreens may have in protecting the immune system is open to question. In humans, studies have shown that increased exposure to UV-B causes damage to immune cells in the skin, alters proportions of white blood cells, decreases the initiation of immune responses in skin (contact allergy), and causes long-lasting, specific immune suppression. Studies have also shown that pigmentation in humans is not protective against immune system effects.

Effects on Terrestrial Plants

*Joe Sullivan
University of Maryland*

In the past two decades, many studies have been conducted that evaluated the potential consequences of increased UV-B radiation on plants. Most studies have used artificial lamp sources to simulate enhanced UV-B radiation fluences. These studies have repeatedly shown the tremendous variability that exists among plants in their sensitivity to UV-B radiation. Various responses have been reported including changes in leaf secondary chemistry (flavonoid accumulation), alterations in leaf anatomy and morphology, reductions in net carbon assimilation capacity (photosynthesis), and changes in biomass allocation and growth. However, specific information is lacking on many key species. The large variation in plant response makes it extremely difficult to extrapolate effects of UV-B radiation to species or ecosystems for which there is little or no information.

Much progress has been made in the past several years in the assessment of the implication of increasing UV-B radiation on plant growth and productivity. More realistic irradiation technology (modulated UV-B enhancement and UV-B reduction techniques) has been developed and our understanding of the molecular basis of the accumulation of flavonoids in response to UV-B radiation has increased. Data are now being obtained on the possible consequences of increasing UV-B radiation on species other than agricultural species. The interaction of multiple environmental changes is also being studied.

Additional research is needed for a thorough understanding of how UV-B radiation damages plants, how repair and mitigation processes are controlled, and of the genetic basis and heritability of UV-B sensitivity. To adequately assess the consequences of ozone depletion on ecosystem dynamics or productivity, more studies will need to be conducted. Areas of particular concern are the potential interactive effects of UV-B radiation, such as competition, plant/pest interactions and potential effects on nutrient cycling or decomposition rates.

Effects on Aquatic Ecosystems

*Robert Worrest
U.S. Environmental Protection Agency*

Increased UV-B radiation due to stratospheric ozone depletion may have potential effects on aquatic ecosystems. UV-B radiation impacts marine organisms by affecting their adaptive strategies (motility, orientation), impairing important physiological functions (photosynthesis, enzymatic reactions), and influencing the developmental stages (young of finfish, shrimp larvae, crab larvae). In addition to damaging DNA, UV-B radiation affects enzymes and other proteins, eliciting photodynamic responses. These responses can have the following possible consequences for aquatic ecosystems:

- reduced biomass production, resulting in a reduced food supply to humans;
- altered species composition and biodiversity;
- decreased nitrogen assimilation by prokaryotic microorganisms, possibly leading to a nitrogen deficiency for higher plant ecosystems; and
- reduced sink capacity for atmospheric carbon dioxide.

A recent study led by Dr. Raymond Smith (University of California, Santa Barbara) involved collecting phytoplankton samples along transects both outside of and under the ozone hole in the Southern Ocean (Smith et al., *Science*, 255: 952-959, 1992). Results indicated that as the ozone layer thinned, sea surface- and depth-dependent ratios of UV-B irradiance to total irradiance increased and that UV-B inhibition of photosynthesis increased. A 6-12% reduction in primary production associated with ozone depletion was estimated for the duration of the study. The ability of phytoplankton to adapt to increases in UV-B is unlikely because generation of protective pigments in phytoplankton is stimulated by an increase in UV-A radiation, not UV-B, and decreased stratospheric ozone will only affect UV-B radiation.

Uncertainties regarding the effects of increased levels of UV-B radiation on aquatic systems still remain, including problems of extrapolating laboratory findings to the open sea, and the nearly complete absence of data on long-term effects and ecosystem responses. Research is needed on adaptive strategies and the effects of cumulative UV-B radiation doses.

SPECTRAL RESPONSES OF BIOLOGICAL SYSTEMS

Biological Action Spectra

Thomas Coohill
Western Kentucky University

Action spectroscopy is of central importance to photobiological studies. Accurate information is needed to assess the potential effects on living organisms caused by an increase in UV radiation reaching the Earth's surface due to the depletion of stratospheric ozone. Of immediate use would be a series of action spectra for general biological effect that would typify responses to increased UV-B radiation. This would require that data be collected at a variety of wavelengths that include, at least, the full UV-B range. Further extension of the system to longer wavelengths would be preferable for estimating other cellular responses, including repair. Such a spectrum would provide biologists with a common starting point, similar to the erythral action spectrum widely quoted as a typical response to UV for human skin. Because of the absorption properties of ozone and the solar UV spectrum, increases in the UV flux at the Earth's surface would be concentrated in the UV-B range. How these small increases in energy would affect living cells and ecosystems is still an issue, but detrimental effects have been suggested and, in some cases, reported (e.g., plants).

More action spectra need to be generated, especially for plants. Studies using plant cells in culture might be able to identify the chromophores involved in plant responses to UV. Field studies using intact plants and polychromatic sources added to the ambient background will be essential for realistic estimates of effect. It is apparent that no single action spectrum or solar effectiveness spectrum can currently be considered to be general enough to predict the varied responses of all biological systems to wavelengths throughout the solar UV range 290 to 380 nanometers (nm). However, reasonable estimates can be made for plant damage due to UV-B and a portion of UV-A. The usefulness of these spectra are limited. They will be replaced in the future by more accurate and common spectra as they are generated. The availability and use of numerous cell mutants has made a large contribution to the understanding of the responses of bacteria, fungi, and mammalian cells to UV. If common assays and irradiation procedures are followed, then a generalized plant damage action spectrum may be forthcoming and will add to

the body of animal cell data already generated. If the data are clearly listed in tabular form, comparisons will be possible. Of course, as is also the case for the widely used action spectrum for human skin erythema, no common spectrum will suffice to substitute for any specific spectrum for any given response. The photobiological community will be asked to provide realistic action spectra developed under natural conditions.

UV-B MEASUREMENT AND MONITORING PROGRAMS

NSF UV-B Monitoring in Polar Regions

*C. Rocky Booth
Biospherical Instruments, Inc.*

The UV Radiation Monitoring Network was established by the U.S. National Science Foundation (NSF) in 1988 in response to predictions of increased UV radiation in the polar regions resulting from stratospheric ozone depletion. Biospherical Instruments, Inc., under contract to Antarctic Support Associates, directed by NSF, is responsible for the network and for distributing data to the scientific community.

The network consists of five automated all-weather spectroradiometers placed in strategic locations in the Antarctic and the Arctic. Instruments were stationed at Palmer, McMurdo, the South Pole, and Ushuaia, Argentina in 1988-89 and at Pt. Barrow, Alaska in 1990. The instruments make high spectral resolution measurements of irradiance over the spectral range of 280-600 nm with a typical resolution of 0.7 nm. From the high spectral resolution data, a variety of biological dosage calculations of UV exposure can be calculated. In this presentation, daily dose data from all five sites were computed using Setlow's DNA dose weighting. The 1990 season highs at McMurdo, Palmer, and Ushuaia were driven by persistent ozone depletion extending into early December when day lengths were approaching a maximum. In October 1991, Palmer and Ushuaia experienced the season's highest averaged doses during a transient in ozone depletion caused by movement of the ozone hole. At McMurdo and the South Pole, although ozone depletion strongly influenced UV, day length contributed significantly to causing the maximum daily dose to occur near the summer solstice, as was also the case at Barrow. The data, which represent episodes of ozone depletion for different sites covering the 1990 and 1991 ozone seasons, are available on CD ROM (ISO9660 format) from Biospherical Instruments, Inc.

European Communities STEP UV-B Program: Instrument Comparison

*Brian Gardiner, British Antarctic Survey
Ann Webb, University of Reading*

In order to investigate the compatibility of available instruments in Europe, a field comparison was conducted in Greece in July 1991 under the auspices of the European Commission. Six spectroradiometer designs were represented, with the following attributes in common: diffraction gratings, a mechanical scanning mechanism, and a photomultiplier. The diversity of the instruments offered an excellent perspective of the relative advantages of the various features, but also made interpretation difficult.

Lamp calibrations and sky calibrations were performed. The results of the lamp calibrations indicated good agreement between the instruments in their relative spectral response, but considerable discrepancies in the absolute calibrations. If these discrepancies were solely due

to errors in the calibrations performed at the home institutes before the instruments were brought to the intercomparison meeting, they would all agree on the ratio of the outputs of two different lamps. However, this was not the case – the spectrometers were divided as to the value of this ratio, falling roughly into two groups. The lamp calibrations will need to be improved before reliable solar irradiance spectra can be obtained on an absolute scale, because every sky spectrum ultimately depends on a lamp for its calibration. For the sky calibrations, the instruments tended to agree on the absolute irradiances slightly better than for the lamp experiment. Where they disagreed there was usually an identifiable reason. For example, differences in slit functions gave rise to very repeatable fluctuations in the ratio of the output from two instruments. Some variations in the ratio between pairs of spectrometers were dependent on solar zenith angle, and are probably due to imperfect cosine response in the diffusers. The wavelength calibration of most instruments was satisfactorily stable.

Developments in this program will be aimed at improving the absolute calibration of the spectrometers, determining the effect of critical parameters such as slit function, dark current and stray light, and the investigation of cosine and azimuth response in individual instruments. The first step will be the construction of a mobile lamp unit that will enable more frequent intercalibration than has been possible in the past.

USDA/CSRS Instrument Development and Preliminary Network

*Lee Harrison
State University of New York, Albany*

The Solar Ultraviolet Monitoring Network for the Biosphere, funded by the U.S. Department of Agriculture Cooperative State Research Service, was created to develop, test, and deploy two prototype high accuracy ultraviolet spectrometers suitable for extended autonomous field operation. These instruments will be put into operation for one year, thereby starting the Biosphere Monitoring Program. One of the instruments will be located at the Southern Great Plains Clouds and Radiation Testbed facility of the DOE Atmospheric Radiation Measurement (ARM) program near Ponca City, Oklahoma. The second site has not yet been determined.

The new spectroradiometer under development will consist of Lambertian foreoptics, a dual ¼ meter Ebert grating monochromator, a Peltier cooled photomultiplier detector operated in the photon counting regime, and an on-board control and data telemetry computer. The instrument will also implement the automated shadowband technique to permit separate measurements of the total horizontal irradiance and the direct beam irradiance. Because the engineering efforts involved with producing the instrument have just begun, there have been no results of integrated system performance. There have been some results, however, from the testing of the Lambertian inlet optic or cosine diffuser; these results are described in detail in Appendix C.

High Altitude UV-B Measurements and Trends

*Mario Blumthaler
University of Innsbruck*

Measurements from an alpine high mountain station (3,500+ meters) in Switzerland were made to determine the sensitivity of the R-B meter to changes in ozone. Data indicate that a 1% reduction in ozone results in a $1.1 \pm 0.2\%$ increase of the meters reading relevant for daily totals

of the annual mean. An analysis of cloudless days since 1981 indicates that there has been a slight increase of solar UV-B irradiance of $7 \pm 3\%$ per decade.

UV-B Controlling Factors and Variability

*John Frederick
University of Chicago*

Many factors control surface UV-B irradiances. These factors include absorption in the atmosphere, absorption at the Earth's surface, and scattering to space. Other factors such as latitudinal, temporal, and seasonal variations also affect surface UV-B irradiances. Factors that must be incorporated into models include solar zenith angle (or elevation of sun above horizon), stratospheric composition (molecular scattering, absorption by ozone, scattering by aerosols), and tropospheric composition (molecular scattering, absorption by gaseous pollutants, scattering by haze and particulates, and scattering by clouds). An objective of ground-based UV spectral irradiance measurements is to determine how clouds, haze, and gaseous pollutants alter the transmission of the troposphere. To achieve this, the magnitude and variability in the ratio of actual UV spectral irradiance to the UV spectral irradiance for a clear, unpolluted atmosphere must be determined. This ratio will depend on meteorological conditions, season, and location. With this focus, surface UV irradiances are not redundant with column ozone measurements made from satellites or the Dobson network.

Research has been conducted using an R-B meter to measure the influence of gaseous air pollutants on trends in erythral irradiance. Data were presented that described the annual cycle in erythral irradiance at North American latitudes, annually integrated erythral irradiances based on Dobson stations, 11 years of UV irradiance measurements using the R-B meter, and the attenuation of erythral irradiance by ozone, nitrogen oxide, and sulfur dioxide in the boundary layer.

Comparison of Measurements from R-B and Dobson Meters

*John Frederick
University of Chicago*

Two data sets were compared to examine the trends in UV radiation and ozone: 1) UV radiation measurements from R-B meters located at Bismarck, North Dakota and Tallahassee, Florida (1974-1985), and 2) simulated R-B signals based on a radiative transfer code using Dobson column ozone measurements from Bismarck and Tallahassee as inputs, with the computed spectral irradiance weighted by the R-B meter response function. Both data sets are expressed as monthly mean, daytime integrated radiation levels (in relative units). Analyses of these data have led to the following conclusions:

- Year-to-year variations in R-B meter readings are not explained solely by variations in ozone. Cloudiness must make a major contribution to the year-to-year variability.
- Trends in the R-B data sets for clear skies are consistent with trends computed using Dobson ozone data for months when the absolute radiation levels are greatest.

- Negative trends (in percent of the monthly mean signal per decade) exist in the R-B data sets for the months of low signal levels. These trends differ in sign from predictions based on Dobson ozone data.
- Based on this analysis alone, it is not possible to determine the origin of the discrepancy between trends computed for months of low signal levels.

Robertson-Berger Meter Network and Instrument Characterization

John DeLuisi

National Oceanic and Atmospheric Administration

R-B meters were placed at different latitudes and longitudes in the United States in the 1970s for monitoring seasonal and regional variations in UV radiation. There are currently 17 R-B meter sites in the network. Seven of these meters have been studied for their spectral response characteristics and a publication of the results is in press (*Journal of Photochemistry and Photobiology*). Since this initial study, all R-B meters in the network have been characterized with regard to their spectral response attributes.

The solar response functions (SRFs) measured were quite similar in shape in the wavelength region of importance (300-330 nm). However, the wavelength positions among them varied by a few nanometers. These variations are partially due to experimental error and variations in the optical components such as filter and substrate thickness. The displacements have only a small impact on the agreement among the meters when they are calibrated to agree with a standard, as is done for the network instruments. However, if each instrument were separately calibrated for absolute irradiance, then considerable differences would result among them because the differences in their SRFs would become important. The agreement among them is improved if all instruments are calibrated to agree with the same daily total value. Because these measurements have not been previously made, it is not possible to determine if a drift has occurred. Comparison of the mean of seven SRFs with the R-B meter SRFs published in the 1970s show virtually no difference. Improper calibration of the response level of a network of R-B type meters can result in a drift, or false trend, in the network data. Examining the SRFs after one or more years of additional field operation should help resolve this issue. The recording units were not evaluated, but they show signs of aging. An upgraded unit would greatly improve data quality.

The following summarize the conclusions of the study:

- The shape of the R-B meter SRFs in the present network appears not to have changed significantly with time.
- The design principle of the R-B meter might be sufficient for a stable, long-term UV sensor.
- The temperature dependence of the R-B meter optical head should receive attention, although it is believed not to be responsible for instrument drift.
- Drifts in the network of instruments can be avoided by proper calibration if the SRFs remain stable.

- More work is needed to quantify the cosine response of R-B meters.

ANCILLARY MEASUREMENTS

DOE Atmospheric Radiation Measurement Program

*Gerald Stokes
Pacific Northwest Laboratory*

The Department of Energy's Atmospheric Radiation Measurement (ARM) Program focuses on radiative transfer, cloud life cycle, and cloud properties, with an emphasis on process studies. The main component of ARM is the Cloud and Radiation Testbed, a flexible experimental facility designed to ease the comparison of model predictions and observational data. ARM experimental approaches include instantaneous radiative fluxes, a single column model, data fusion and assimilation, and hierarchical diagnosis. Information on instantaneous radiative fluxes provide concurrent characterization of the state of the atmosphere and the consequent fluxes and their associated moments taken over both space and time under clear sky, general overcast, and broken cloud conditions. Measurements are made of radiation, other surface fluxes, basic meteorological parameters, cloud distribution, and aerosols. The radiation measurements include broad-band radiometry, spectral measurements, flux divergence, and USDA UV-B measurements made by Dr. Lee Harrison. The surface fluxes of concern are latent heat, sensible heat, and precipitation. ARM will make measurements in five general areas: southern U.S. Great Plains (North Central Oklahoma, South Central Kansas), the Tropical Western Pacific Ocean, the North Slope of Alaska (penetrating to the marginal ice zone), Eastern North Pacific or Atlantic Ocean, and the Gulf Stream (off the coast of Eastern North America). The first site will be operational in spring of 1992, with one site per year coming on line for the next four years.

International Network for Detection of Stratospheric Change

*Michael Kurylo
National Aeronautics and Space Administration*

The Network for Detection of Stratospheric Change (NDSC) consists of a set of international remote sounding research stations for observing and understanding the physical and chemical state of the stratosphere. The network is complemented by secondary stations, satellite measurements, and existing monitoring networks. Ozone and key ozone related parameters are measured. The NDSC is a major component of the international upper atmosphere research effort and has been endorsed by national and international scientific agencies, including the International Ozone Commission. NDSC is co-sponsored by NASA, NOAA, and the Chemical Manufacturer's Association (CMA), and includes commitments from several foreign government agencies as well.

The primary goals of the program include the following:

- To provide early and continuous detection of stratospheric changes and to discern the cause of the changes.
- To gain a better understanding of the temporal and spatial variability of the atmosphere's composition and structure.

- To obtain data that can be used to test and improve multi-dimensional stratospheric chemical and dynamical models.
- To provide an independent calibration of satellite sensors of the atmosphere.

Remote sensing instruments for the NDSC program were selected on the basis that they were capable of continuous, long-term field operation, potentially in remote locations. Depending on the specific site characteristics, such as geography and meteorology, each of the primary NDSC stations will be equipped with several instruments such as lidars, microwave sensors, and spectrometers.

The network's data will make a major contribution toward understanding stratospheric change. The NDSC data protocol is aimed at achieving both high data quality and ready data access. The main features of the protocol include establishing scientific collaboration for the optimum testing and verification of measurements, archiving preliminary analyses of measurements within one year after measurement, and making data available to the public through a centralized scientific archiving and distribution facility that will be accessible by electronic transfer.

ROLE OF SATELLITES IN UV-B MONITORING

Potential for Satellite Measurements of Surface UV Climatology

*Dan Lubin
California Space Institute*

Frederick and Lubin (*Journal of Geophysical Research*, 93(D4), 3825-3832, 1988) demonstrated that satellite measurements of atmospheric ozone and cloud reflectance may be used in conjunction with radiative transfer theory to compute the budget of biologically active UV radiation in the Earth-atmosphere system. This study showed that satellite data, such as those provided by instruments aboard Nimbus-7, can provide an excellent diagnostic tool by showing the relative importance of ozone absorption and cloud scattering as a function of latitude. Trend analysis or prognostic applications set more stringent requirements on the quality of the satellite data. The satellite instrument measuring cloud reflectance should have some on-board or otherwise acceptable radiometric calibration and the data must be taken for a sufficient period of time for trend analysis.

To date, the longest and most comprehensive time history of satellite cloud reflectance measurements is found in the International Satellite Clouds and Climatology Project (ISCCP) data set. However, the primary satellite instrument providing the ISCCP cloud reflectance measurements, the Advanced Very High Resolution Radiometer (AVHRR), has no on-board radiometric calibration. There have been respectable efforts to perform ground-truthing calibrations of AVHRR using images of the world's deserts, but it is uncertain if such ground-truthing can make radiometric error bars small enough for surface UV-B trend analysis. The best measurements of cloud reflectance to date have been provided by the Earth Radiation Budget Experiment (ERBE), which included on-board radiometric calibration. ERBE lasted from 1985-1990, and the future generation of ERBE-type instruments will probably provide the most useful data for estimating surface UV-B trends. Major changes in global cloud cover or cloud optical

thickness could alter the surface UV irradiance by an amount comparable to that predicted by long-term trends in ozone.

NON-U.S. NATIONAL UV RESEARCH AND MONITORING PROGRAMS

New Zealand

*Richard McKenzie
Department of Scientific and Industrial Research*

Prior to 1989, the only spectroradiometric UV data available in New Zealand was from two short measurement campaigns in 1980 and 1988. In 1988, the Department of Scientific and Industrial Research (DSIR) initiated a program to characterize the spectrum of solar UV radiation reaching the ground in New Zealand. An instrument was developed at DSIR to enable routine measurements of cosine weighted UV irradiances incident on a horizontal surface at the ground. The goals of the UV measurement program are to determine the climatology associated with UV radiation, to identify regional differences in irradiances, to understand the reasons for the variability of UV radiation, and to detect any long-term trends.

The measurement system is based on a small, commercially available double monochromator (focal length 100 mm, f-number f3, dispersion 10 nm/mm), which was modified and temperature controlled to improve its stability. The instrument includes several novel features. A custom-made diffuser is used to improve the cosine response; the mounting of this diffuser incorporates a light baffle to improve stray light rejection. A shadow band can be positioned so that the direct component of solar radiation can be masked from the instrument. This enables the diffuse and direct components of UV spectra to be studied independently. The spectral range covered is 290-450 nm and the instrument bandpass is approximately 1 nm. The spectrum is sampled continuously at 0.2 nm intervals, and this oversampling enables the logged spectra to be accurately aligned using a computer algorithm that compares the logged spectrum with a reference spectrum. A photomultiplier tube detector is used, and the wide dynamic range necessary is achieved by allowing the high voltage that controls its gain to vary during the scan. Both the multiplier signal and the high voltage that controls the gain are logged. A supplementary diode detector samples broadband UV continuously during scans and the statistics of this data are logged so that the intensity changes due to cloud cover during the scanning interval (200 seconds) can be identified. With the present system, useful measurements at 1 nm resolution are limited to irradiances greater than 10^{-3} $\mu\text{W}/\text{cm}^2/\text{nm}$, which corresponds to a lower limit in wavelength in the region 290 to 295 nm (depending on the sun angle and ozone amount). This is a useful lower limit for many applications of relevance to the biosphere. The instrument specifications, calibration, quality control procedures, performance, and results from the first year of operation are discussed in McKenzie et al., "Solar Ultraviolet Spectro Radiometry in New Zealand: Instrumentation and Sample Results from 1990," *Applied Optics* (accepted 1992).

Efforts are continuing to extend geographic coverage and improve the quality of UV measurements in New Zealand through the deployment of new instruments and through participation in intercomparison studies with other instruments. In addition, studies investigating the possible use of real time satellite data (e.g., cloud cover, ozone fields) to infer UV irradiance levels are in progress.

Sweden

Ulf Wester
Swedish Radiation Protection Institute

The Swedish Radiation Protection Institute has initiated and funded projects in Sweden to measure and map biologically active UV radiation. Swedish UV data have been obtained from studies with spectroradiometers, mathematical models, an R-B meter (since 1983), other UV monitors (since 1989), and a network for solar UV monitoring (since 1990). The following instruments are employed:

- A Dobson ozone spectrophotometer was used by the Department of Meteorology of the University of Uppsala (59.9°N) from 1951 to 1966. The instrument has been modernized and is used by the Swedish Meteorological and Hydrological Institute (SMHI) at Vindeln (64.1°N). This study is funded by the Swedish Environmental Protection Agency.
- Laboratory UV-spectroradiometers have been used since 1980 for solar UV measurements, mostly in Stockholm (59.4°N). The spectral data from these instruments have been stored.
- A Brewer ozone spectroradiometer has been operated at the SMHI in Norrköping (58.6°N) since 1983. In addition to measurements of stratospheric ozone, the instrument is specially designed for spectral irradiance measurements in the UV-B region, and was used for such measurements during 1983-85. Since 1985, it has primarily been used to monitor ozone.
- A Berger UV-B Sunburn Meter has been operated by SMHI in Norrköping since 1983.
- Two specially built filter radiometer-instruments for measuring both natural global UV-B at 306 nm and UV-A at 360 nm have been monitoring solar UV since 1983 continuously in Norrköping and with some interruption in Luleå (65.5°N). Data from these instruments have not yet been evaluated. A third instrument of the same type has been monitoring solar UV in Stockholm since 1989.
- One erythema MED-meter was tested at SMHI in Norrköping in 1989.

A new project has been started with the goal of providing seasonal and geographical mapping of UV exposure data and statistics in Sweden. Six MED-monitors and four UV-A monitors have been placed at five meteorological stations: Lund (55.7°N), Norrköping (58.6°N), Borlänge (60.5°N), Umeå (63.8°N), and Kiruna (67.8°N). The installations were initiated in 1990 and completed in the summer of 1991. Data will be gathered by SMHI using an automatic data collection network for a five-year period, after which there will be a final evaluation of the results and statistics.

United Kingdom

Colin Driscoll
National Radiological Protection Board

In 1988, the National Radiological Protection Board (NRPB) set up three monitoring stations to make continuous measurements of terrestrial solar radiation at different latitudes in the United Kingdom. These were located at the NRPB centers at Chilton (52°N), Leeds (54°N), and Glasgow (56°N). Measurements of visible, UV-A, and erythemally weighted UV radiation have been made concurrently using a system based on three commercially available broad-band detectors. The measurements were designed to provide information regarding the range of variation of solar UV radiation at different latitudes with the time of year; the effects of various factors that affect the terrestrial measurement of solar UV radiation, such as cloud cover; and establishment of baseline levels for natural UV radiation with which measurements from artificial sources of UV radiation could be compared. It is proposed to extend the measurement network to cover the range of latitudes (50°N to 60°N) appropriate to all of the United Kingdom. In addition, there is interest in developing a measurement network at various locations throughout Europe, especially at latitudes less than 40°N. This is important due to the increasing number of populations that work, live, or take holidays in this region.

STATISTICAL CONSIDERATIONS

Network Design and Data Analysis

William Hill, University of Wisconsin
Lane Bishop, Allied-Signal Corporation

The basic statistical considerations in network and trend analysis are trend detection, coverage or representativeness, sampling, and quality assurance. To detect a trend, several statistical factors must be considered. These include noise level, autocorrelation, length of record, sampling rate, spatial correlation, model selection, and the quality assurance of data. Coverage or representativeness issues are related to distance and location, design factors (e.g., cloudiness), and ancillary measurements. Depending on the information to be inferred from the data and trends, some important societal factors such as population, pollution, and urbanization, must also be taken into account. The availability of ancillary measurements (e.g., column ozone, aerosol and particulates, surface albedo) is also an issue. For sampling, if a model is based on a fixed solar zenith angle, dawn to dusk data will be needed. Day-to-day autocorrelation will influence the number of days per month the sampling should be done. Network quality assurance considerations include calibration checks, quality control charts to assess special cause changes (e.g., drifts), robustness of measurements to viewing conditions, intercomparison with similar or ancillary instrumental data, and comparison of results with model calculations.

The following conclusions and recommendations were presented:

- Determine trend detection target using statistical knowledge of model and variation. Trend detection for a monitoring site is a function of the model, noise level, autocorrelation, and time record.
- Select sites that represent viewing and societal factors. Use statistical design to minimize the number of sites.

- Use a sampling plan that is based away from model and data considerations (e.g., auto and spatial correlation).
- Design a quality assurance plan early in the network design and deployment that ensures that the network will be above reproach.

COMMENTARY FROM INVITED EXPERTS

Instrumentation

Arthur Schmeltekopf

National Oceanic and Atmospheric Administration, retired

Dr. Schmeltekopf offered commentary on the development of a national UV-B monitoring network. He presented three options for instrumentation, requiring varying levels of effort. The simplest option was based on the R-B meter and one band pass, complemented with satellite data to indicate cloud cover. This option would have inadequacies, but could be sufficient for some aspects of UV monitoring. Alternatively, a monitoring program could use complex instruments capable of measuring many other aspects related to UV-B irradiance such as ozone, aerosols, etc. This option would be expensive, perhaps prohibitively so, and would require more effort to maintain the instruments, to gather the data, and to analyze the data. As a compromise, a program could be designed to measure a few wavelengths and to use models and measurements available from other programs, from which calculations of ozone level and irradiance changes with time could be made.

Before deciding on any option, the designers of a program must decide what they want their program to be able to do and the information necessary to achieve these goals. Sufficient scoping should be done so that the investigators are aware of existing programs and can use these to complement or enhance their system.

Environmental Effects Assessment and Future Needs

Jan van der Leun

University of Utrecht

Dr. van der Leun provided commentary on the effects aspect of UV-B research. The uncertainties associated with the effects of atmospheric changes (i.e., ozone depletion) are great. The primary factor behind our interest in atmospheric changes is to determine how these changes might impact our lives, either directly or indirectly. Despite this interest in effects, most research has been conducted on atmospheric processes. Funding for research on the consequences of increased UV-B radiation is disproportionately low – typically less than 1% of what is made available for atmospheric research related to ozone depletion. We now know that the atmosphere will be affected for the next 100 years or longer due to natural and anthropogenic influences, therefore knowledge is needed to determine what potential effects can be expected. A major change in emphasis is needed toward the effects side of research. Effects research is necessary to provide policy makers with relevant information, so that they can evaluate response strategies for future challenges. A better understanding of the potential effects is needed in order to address the most significant issues in a timely manner.

Appendix A: Agenda

UV-B MONITORING WORKSHOP

10-12 March 1992

Sheraton City Centre
1143 New Hampshire Avenue NW
Washington, DC

AGENDA

TUESDAY, MARCH 10

Moderator: Igor Sobolev, AFEAS

- 8:00 Registration
- 8:30 Welcoming Remarks – *Dick Soulen, AFEAS*
- 8:40 Workshop Objectives – *Jim Gibson, Colorado State University*
- 8:50 Introductory Comments – *Patrick Jordan, USDA/CSRS*

SESSION 1 – CURRENT STATUS OF KNOWLEDGE ON UV-B AND POTENTIAL EFFECTS

- 9:05 WMO/UNEP Scientific Assessment: 1991, Chapter 11: UV Radiation Changes – *Richard McKenzie, DSIR, New Zealand*
- 9:25 UNEP Environmental Effects Assessment: 1991, Chapter 1: Changes in Biologically Active Ultraviolet Radiation Reaching the Earth's Surface – *Sasha Madronich, NCAR*
- 9:45 Discussion
- 9:50 UNEP Environmental Effects Assessment: 1991, Chapter 2: Human Health – *Margaret Kripke, University of Texas*
- 10:10 UNEP Environmental Effects Assessment: 1991, Chapter 3: Terrestrial Plants – *Joe Sullivan, University of Maryland*
- 10:30 UNEP Environmental Effects Assessment: 1991, Chapter 4: Aquatic Ecosystems – *Bob Worrest, U.S. EPA*
- 10:50 Discussion
- 10:55 BREAK

SESSION 2 – SPECTRAL RESPONSES OF BIOLOGICAL SYSTEMS

- 11:10 Biological Action Spectra – *Thomas Coohill, Western Kentucky University*
- 11:30 Discussion

SESSION 3 – UV-B MEASUREMENT AND MONITORING PROGRAMS: STATUS AND PLANS

- 11:35 NSF UV-B Monitoring in Polar Regions – *Rocky Booth, Biospherical Instruments*

- 11:55 European Communities STEP UV-B Program: Instrument Intercomparison – *Brian Gardiner, British Antarctic Survey, and Ann Webb, University of Reading, UK*
- 12:15 USDA/CSRS Instrument Development and Preliminary Network – *Lee Harrison, SUNY-Albany*
- 12:35 Discussion
- 12:45 LUNCH (*on your own*)
- 2:00 UV-B Measurements and Trends – *Mario Blumthaler, University of Innsbruck, Austria*
- 2:20 UV-B Controlling Factors and Trends – *John Frederick, University of Chicago*
- 2:40 Discussion
- 2:45 RB Meter Network and Instrument Characterization – *John DeLuisi, NOAA*
- 3:05 Comparison of Trends from RB and Dobson Meters – *John Frederick, University of Chicago*
- 3:25 Discussion
- 3:35 BREAK

SESSION 4 – ANCILLARY MEASUREMENTS: STATUS AND PLANS OF OTHER MONITORING PROGRAMS

- 3:45 DOE Atmospheric Radiation Measurement (ARM) Program – *Gerry Stokes, Pacific Northwest Laboratory*
- 4:05 Network for the Detection of Stratospheric Change (NDSC) Program – *Michael Kurylo, NASA Headquarters*
- 4:25 Discussion

SESSION 5 – ROLE OF SATELLITES IN UV-B MONITORING

- 4:30 Potential for Satellite Measurements – *Dan Lubin, California Space Institute – UCSD*
- 4:50 Discussion
- 5:00 Adjourn for the day

WEDNESDAY, MARCH 11

Moderator: Igor Sobolev, AFEAS

- 8:30 Opening Remarks

SESSION 6 – NON-U.S. NATIONAL UV RESEARCH AND MONITORING PROGRAMS

- 8:40 New Zealand – *Richard McKenzie, DSIR, New Zealand*
- 9:00 Sweden – *Ulf Wester, Swedish Radiation Protection Institute*
- 9:15 U.K. – *Colin Driscoll, U.K. National Radiological Protection Board*

9:30 Discussion

SESSION 7 – STATISTICAL CONSIDERATIONS IN NETWORK DESIGN AND TREND ANALYSIS

9:35 Network Design and Data Analysis – *William Hill, University of Wisconsin*
9:55 Discussion

10:00 BREAK

SESSION 8 – COMMENTARY FROM INVITED EXPERTS

10:15 Instrumentation – *Arthur Schmeltekopf, NOAA - Retired*
10:35 Discussion

10:45 Network Design and Data Analysis – *Lane Bishop, Allied-Signal*
11:05 Discussion

11:15 UNEP Environmental Effects Assessment and Future Needs –
Jan van der Leun, University of Utrecht, The Netherlands
11:35 Discussion

11:45 LUNCH (*on your own*)

SESSION 9 – MEASUREMENT REQUIREMENTS AND INSTRUMENT SPECIFICATIONS FOR
USDA/CSRS UV-B MONITORING NETWORK

Moderator: Jim Gibson, CSU

1:15 Introductory Remarks – *Jim Gibson, Colorado State University*
1:30 Future USDA/CSRS UV-B Monitoring and Research Plans – *Dan Tompkins,*
USDA/CSRS
1:45 Discussions
5:00 Adjourn for the Day

THURSDAY, MARCH 12

Moderator: Jim Gibson, CSU

8:00 Continue Discussions and Formulate Recommendations

12:00 Workshop Adjourned

*The workshop is sponsored by the Alternative Fluorocarbons Environmental
Acceptability Study (AFEAS) and the U.S. Department of Agriculture
Cooperative State Research Service (USDA/CSRS).*

*The workshop is conducted by Science and Policy Associates, Inc. (Washington, DC)
Workshop Staff: Katie Smythe, Whitney Carroll, Susie Keeley*

Appendix B: List of Participants

UV-B MONITORING WORKSHOP

10-12 March 1992
Washington, DC

PARTICIPANTS

Dr. S.P.S. Anand
Applied Research Corporation
8201 Corporate Drive, Suite 1120
Landover, MD 20785
Tel: 301/459-8442
Fax: 301/731-0765

Mr. Stephen Bannasch
TERC
2067 Massachusetts Ave.
Cambridge, MA 02140
Tel: 617/547-0430
Fax: 617/349-3535

Dr. William F. Barnard
AREAL (MD-75)
U.S. EPA
Research Triangle Park, NC 27711
Tel: 919/541-2205
Fax: 919/541-4609

Dr. John M. Barnes
NAPAP
722 Jackson Place NW
Washington, DC 20503
Tel: 202/296-1002
Fax: 202/296-1009

Mr. David J. Beaubien
Yankee Environ. Systems, Inc.
101 Industrial Road, Box 746
Turners Falls, MA 01376
Tel: 413/863-0200
Fax: 413/863-0255

Ms. Julie Bedford
Science & Policy Associates, Inc.
The West Tower, Suite 400
1333 H St., NW
Washington, DC 20005
Tel: 202/789-1201
Fax: 202/789-1206

Mr. Daniel Berger
Solar Light Company, Inc.
721 Oak Lane
Philadelphia, PA 19126
Tel: 215/927-4206
Fax: 215/927-6347

Dr. R. Hilton Biggs
University of Florida
1119 Fifield Hall
Gainesville, FL 32611
Tel: 904/392-6888
Fax: 904/392-5653

Dr. Mario Blumthaler
Institut für Medizinische Physik
Universität Innsbruck
Müllerstrasse 44
A-6020 Innsbruck, Austria
Tel: (43) 512/507-2426
Fax: (43) 512/507-2429

Mr. C. Rocky Booth
Biospherical Instruments Inc.
4901 Morena Blvd, Suite 1003
San Diego, CA 92117
Tel: 619/270-1315
Fax: 619/270-1513

Ms. Whitney Carroll (AFEAS)
Science & Policy Associates, Inc.
The West Tower, Suite 400
1333 H St., NW
Washington, DC 20005
Tel: 202/898-0906
Fax: 202/789-1206

Dr. Stan Coloff
Bureau of Land Management (Code 220)
18th & C Streets NW
Washington, DC 20240
Tel: 202/653-9210
Fax: 202/653-9118

Dr. Thomas P. Coohill
Dept. Physics and Astronomy
Western Kentucky University
Bowling Green, KY 42101
Tel: 502/745-4357
Fax: 502/745-6471

Dr. Lee W. Cooper
Oak Ridge National Laboratory
Environmental Sciences Division
P.O. Box 2008/MS 6038
Oak Ridge, TN 37831-6038
Tel: 615/574-7812
Fax: 615/576-8646

Dr. David Correll
Environmental Research Center
Smithsonian Institution
P.O. Box 28
Edgewater, MD 21037
Tel: 301/261-4190
Fax: 301/261-7954

Mr. Robert F. Crabbs, Jr.
Research Support Instruments, Inc.
10610 Beaver Dam Road
Cockeysville, MD 21030
Tel: 410/785-6250
Fax: 410/785-1228

Dr. Arne Dahlback
c/o Norwegian Institute for Air Research
P.O. Box 64
N-2001 Lillestrom
Norway
Tel: 47 6 814170
Fax: 47 6 819247

Dr. Helen M. Dalaski
Smithsonian Environmental
Research Center
P.O. Box 28
Edgewater, MD 21037
Tel: 301/261-4690
Fax: 301/261-7954

Dr. Anne H. Datko
USDA-NRICGP
Aerospace Building, Room 323
901 D Street SW
Washington, DC 20250-2200
Tel: 202/401-4871
Fax: 202/401-6488

Dr. Bruce S. David
Optronic Laboratories, Inc.
4470 35th Street
Orlando, FL 32811
Tel: 407/422-3171
Fax: 407/648-5412

Dr. John DeLuisi
NOAA, ERL/CMDL
325 Broadway
Boulder, CO 80303-3328
Tel: 303/497-6824
Fax: 303/497-6290

Dr. Colin Driscoll
National Radiology Protection Board
Didcot, Chilton
Oxfordshire OX1 0RQ
United Kingdom
Tel: 44/235 831600
Fax: 44/235 833891

Dr. Shyam Dube
University of Maryland
Center for Agricultural Biotechnology
2111 Agricultural/Life Science
Surge Building
College Park, MD 20742-2351
Tel: 301/405-1583
Fax: 301/314-9075

Ms. Philippa Duff
Science & Policy Associates, Inc.
The West Tower, Suite 400
1333 H St., NW
Washington, DC 20005
Tel: 202/789-1201
Fax: 202/789-1206

Dr. D.D. Duncan
Johns Hopkins University
Applied Physics Laboratory
Johns Hopkins Road
Laurel, MD 20723-6099
Tel: 301/953-5000 ext. 8548
Fax: 301/953-1093

Dr. Jerry W. Elwood
U.S. Department of Energy
Office of Energy Research
Environmental Sciences Division, ER-74
Washington, DC 20585
Tel: 301/903-4583
Fax: 301/903-5051

Dr. Edwin Fiscus
USDA/NCSU
Air Quality Research Program
1509 Varsity Drive
Raleigh, NC 27695
Tel: 919/515-3311
Fax: 919/515-3593

Dr. James Franklin (AFEAS)
Solvay S.A.
Rue de Ransbeek 310
1120 Brussels Belgium
Tel: 32-2-264-2202
Fax: 32-2-264-3061

Dr. John Frederick
Department of Geophysical Sciences
University of Chicago
5734 S. Ellis Ave
Chicago, IL 60637
Tel: 312/702-3237
Fax: 312/702-9505

Mr. David Frederickson
LI-COR, Inc.
4421 Superior Street
P.O. Box 4425
Lincoln, NE 68504
Tel: 402/467-3576
Fax: 402/467-2819

Dr. Brian G. Gardiner
British Antarctic Survey
High Cross, Madingley Rd.
Cambridge CB3 0ET, U.K.
Tel: 44-223-61188
Fax: 44-223-62616

Dr. James H. Gibson
Natural Resource Ecology Laboratory
Colorado State University
Fort Collins, CO 80523
Tel: 303/491-1978
Fax: 303/491-1965

Dr. Dennis C. Gitz, III
Miami University
Department of Botany
Miami University
Oxford, Ohio 45056
Tel: 513/529-4273 or 4200
Fax: 513/529-4243

Dr. Bill Graver
SAIC
803 West Broad Street
Falls Church, VA 22046
Tel: 703/241-7900
Fax: 703/538-3750

Mr. Frederick H. Hallet
White Consolidated Industries, Inc.
1317 F St., NW, Suite 510
Washington, DC 20004
Tel: 202/638-7878
Fax: 202/638-7887

Mr. Robert Hampson
NIST
Bldg. 222, Room A260
Gaithersburg, MD 20899
Tel: 301/975-2571
Fax: 301/926-4513

Mr. Gerry A. Hapka
Du Pont Company
1007 Market Street, D7020
Wilmington, DE 19898
Tel: 302/774-9466
Fax: 302/774-1189

Dr. Lee Harrison
Atmospheric Sciences Research Center
SUNY-Albany
Albany, NY 12205
Tel: 518/442-3811
Fax: 518/442-3867

Dr. Douglass Hayes
Smithsonian Environ. Research Center
Serc Solar Radiation Laboratory
6325 Executive Boulevard
Rockville, MD 20852
Tel: 301/443-9255 or 9253
Fax: 301/443-4132

Mr. Donald Heath
STX
2883 Springdale Lane
Boulder, CO 80303
Tel: 303/449-0557
Fax: 303/449-3973

Dr. William Hill
Center for Quality & Productivity
University of Wisconsin
610 Walnut Street, 1575 WARF Bldg.
Madison, WI 53706-1693
Tel: 608/263-2520
Fax: 608/263-1425

Mr. David B. Hobbie
Climate Institute
324 4th St., NE
Washington, DC 20002
Tel: 202/547-0104
Fax: 202/547-0111

Mr. Hans Jaspers (AFEAS)
Akzo Chemicals BV, Chem. Div.
Stationsstraat 48, P.O. Box 247
3800 AE Amersfoort
The Netherlands
Tel: 31/33-676315
Fax: 31/33-676157

Dr. J. Patrick Jordan
Director, CSRS
U.S. Department of Agriculture
14th Street & Independence Av, SW
Washington, DC 20250
Tel:
Fax:

Mr. F. Paul Kapinos
U.S. Geological Survey, National Center
12201 Sunrise Valley Drive
Reston, VA 22092
Tel: 703/648-6876
Fax: 703/648-5295

Dr. John R. Kelly
Battelle Ocean Sciences
397 Washington Street
Duxbury, MA 02332
Tel: 617/934-0571
Fax: 617/934-2124

Dr. James Kinsey
Applied Research Corporation
8201 Corporate Drive, Suite 920
Landover, MD 20785
Tel: 301/459-8833
Fax: 301/731-0765

Dr. Margaret L. Kripke
Dept. of Immunology
The University of Texas
M.D. Anderson Cancer Center
1515 Holcombe Blvd. - Box 178
Houston, Texas 77030
Tel: 713/792-8578
Fax: 713/794-1322

Dr. Donald Krizek
Climate Stress Laboratory/ARS
U.S. Department of Agriculture
Room 206 B-001 BARC-W
Beltsville, MD 20705
Tel: 301/504-5324 or 5607
Fax: 301/504-6626 or 7521

Dr. Michael Kurylo
NASA Headquarters - Code EEU
600 Independence Avenue SW
Washington, DC 20546
Tel: 202/453-1483
Fax: 202/755-5032

Mr. Edward H. Lee
USDA/ARS
Bldg. 001, Room 206
Beltsville, MD 20705
Tel: 301/504-6528
Fax: 301/504-7521

Mr. Peter Leigh
NOAA
Universal Bldg., Room 518
1825 Connecticut Ave., NW
Washington, DC 20235
Tel: 202/606-4366
Fax: 202/606-4355

Dr. Joel Levy
U.S. EPA, Global Change Division
ANR-445
401 M St., SW
Washington, DC 20460
Tel: 202/260-5533
Fax: 202/260-4710

Mr. Jean-Marie Libre (AFEAS)
Elf Atochem S.A.
4, Cours Michelet
La Défense 10, Cédex 42
92091 Paris France
Tel: 33 (1) 69007887
Fax: 33 (1) 69007021

Dr. Ted Loder
Institute for the Study of Earth,
Oceans, and Space
University of New Hampshire
Durham, New Hampshire 03824
Tel: 603/862-3151
Fax: 603/862-1915

Dr. Janice Longstreth
Battelle Pacific Northwest Laboratory
370 L'Enfant Promenade SW
Washington, DC 20024-2115
Tel: 202/646-7784
Fax: 202/646-7838

Dr. Daniel Lubin
California Space Institute (MC A-021)
University of California, San Diego
La Jolla, CA 92093
Tel: 619/534-6369
Fax: 619/534-7452

Dr. Lester Machta
Air Resources Lab, NOAA
1335 East-West Highway
Silver Spring, MD 20910
Tel: 301/713-0684
Fax: 301/713-0119

Dr. Sasha Madronich
NCAR
P.O. Box 3000
Boulder, CO 80307-3000
Tel: 303/497-1430
Fax: 303/497-1400

Dr. Hillel Magid (AFEAS)
Allied-Signal Inc.
Buffalo Research Laboratory
20 Peabody Street
Buffalo, NY 14210
Tel: 716/827-6258
Fax: 716/827-6207

Mr. Archie McCulloch (AFEAS)
ICI Chemicals & Polymers Ltd.
P.O. Box 8, The Heath
Runcorn, Cheshire WA7 4QD
United Kingdom
Tel: 44-928-51-3835
Fax: 44-928-58-1204

Dr. Tom McElroy
Atmospheric Environment Service
Environment Canada
4905 Dufferin Street
Toronto, Ontario M3H 5T4
Canada
Tel: 416/739-4630
Fax: 416/739-4281

Dr. Mack McFarland (AFEAS)
E.I. du Pont de Nemours & Co., Inc.
Fluorochemicals Division
1007 Market Street (B-13221)
Wilmington, DE 19898 USA
Tel: 302/774-5076
Fax: 302/774-8416

Dr. Jack McKay
Research Support Instruments
10610 Beaver Dam Road
Hunt Valley, MD 21030
Tel: 410/785-6250
Fax: 410/785-1228

Dr. Richard McKenzie
DSIR Physical Sciences
Lauder, Central Otago 9182
New Zealand
Tel: 64-3-4473411
Fax: 64-3-4473348

Ms. Marian Morys
Solar Light Co.
721 Oak Lane
Philadelphia, PA 19126
Tel: 215/927-4206
Fax: 215/927-6347

Dr. S. Robert Orfeo (AFEAS)
Allied-Signal Inc.
Buffalo Research Lab
20 Peabody Street
Buffalo, NY 14210
Tel: 716/827-6243
Fax: 716/827-6207

Dr. Polly Penhale
Polar Programs Division
National Science Foundation
1800 G Street NW
Washington, DC 20550
Tel: 202/357-7894
Fax: 202/357-7894

Dr. Kenneth E. Pickering
USRA/NASA/GSFC
Code 916
Greenbelt, MD 20771
Tel: 301/286-2097
Fax: 301/286-3460

Dr. R. Jack Pickering
U.S. Geological Survey
National Center, MS 416
12201 Sunrise Valley Drive
Reston, VA 22092
Tel: 703/648-6875
Fax: 703/648-5295

Dr. Hugh Pitcher
Battelle Pacific Northwest Lab
901 D St., SW
Suite 900
Washington, DC 20029-2115
Tel: 202/646-7815
Fax: 202/646-5233

Dr. Boyd W. Post
USDA/CSRS
329 L Aerospace Bldg.
901 D Street SW
Washington, DC 20250-2200
Tel: 202/401-5016
Fax: 202/401-1706

Dr. Ata Qureshi
Climate Institute
324 4th St., NE
Washington, DC 20002
Tel: 202/547-0104
Fax: 202/547-0111

Dr. James D. Regan
Dept. of Biological Sciences
Florida Institute of Technology
New Bourne, Florida 32901
Tel: 407/768-8000 ext. 8811
Fax: 407/952-1818

Mr. Tim Richardson
Vital Technologies
65 James Street
Bolton, Ontario
Canada L7E 3G5
Tel: 416/951-0096
Fax: 416/951-0097

Mr. Shunichi Samejima (AFEAS)
Asahi Glass America, Inc.
1185 Ave. of the Americas, 30th Floor
New York, NY 10036
Tel: 212/764-3155
Fax: 212/764-3384

Dr. Arthur Schmeltekopf
410 E Fork Road
Marshall, NC 28753
Tel: 704/689-5265

Dr. J. Thomas Schriempf
Research Support Instruments, Inc.
10610 Beaver Dam Road
Hunt Valley, MD 21030
Tel: 410/785-6250
Fax: 410/785-1228

Mr. Joseph Scotto
NCI
Executive Plaza North
6130 Executive Blvd., Room 431
Rockville, MD 20892
Tel: 301/496-4153
Fax: 301/402-0081

Dr. Gunther Seckmeyer
GSF
Inglostadter, Landstrasse 7
D-8042 Neuherberg Germany
Tel: 49 89 3187 2989
Fax: 49 89 3187 3383

Dr. Hans Joachim Semmler (AFEAS)
Hoechst Aktiengesellschaft
F+E / GB-A, D 729
P.O. Box 800320, Bruningstrasse 50
D-6230 Frankfurt 80 Germany
Tel: 49-69-3055973
Fax: 49-69-331507

Mr. James D. Shomper
Du Pont Company
1007 Market Street, D7081
Wilmington, DE 19898
Tel: 302/774-6403
Fax: 302/773-6880

Mr. Lee R. Shugart
Oak Ridge National Laboratory
Environmental Sciences Division
P.O. Box 2008, MS 6036
Oak Ridge, TN 37831-6036
Tel: 615/576-5269
Fax: 615/576-8543

Dr. Wilbert R. Skinner
University of Michigan
2455 Hayward Street
Ann Arbor, MI 48109-2143
Tel: 313/747-3960
Fax: 313/763-5567

Dr. William H. Smith
Yale University
School of Forestry & Env. Sci.
370 Prospect St.
New Haven, CT 06511
Tel: 203/432-5149
Fax:

Ms. Katie Smythe (AFEAS)
Science & Policy Associates, Inc.
The West Tower – Suite 400
1333 H Street NW
Washington, DC 20005
Tel: 202/898-0906
Fax: 202/789-1206

Dr. Igor Sobolev (AFEAS)
Chemical & Polymer Technology, Inc.
5 Rita Way
Orinda, CA 94563
Tel: 510/376-6402
Fax: 510/376-6402

Dr. Susan Solomon
NOAA Aeronomy Laboratory
325 Broadway
Boulder, CO 80303
Tel:
Fax:

Mr. Steven F. Somerstein
Lockheed Company
ORG: 9720, B-254G
1111 Lockheed Way
Sunnyvale, CA 94089-3504
Tel: 408/742-7274
Fax: 415/354-5002 or 408/756-8048

Dr. J. Richard Soulen (AFEAS)
Technical & Management Services Inc.
P.O. Box 388
Bloomfield Hills, MI 48303
Tel: 313/642-6568
Fax: 313/258-6769

Dr. Valrey Soyfer
Laboratory of Molecular Genetics
George Mason University
4400 University Drive
Fairfax, VA 22030-4444
Tel: 703/993-2180
Fax: 703/993-2175

Mr. Warren Spaeth
ARM-DOE
Battelle Pacific Northwest Laboratory
370 L'Enfant Promenade, SW, Suite 900
Washington, DC 20024
Tel: 202/646-5246
Fax: 202/646-7843

Dr. Knut Stamnes
Geophysical Institute
Department of Physics
University of Alaska
Fairbanks, AK 99775-0800
Tel: 907/474-7368
Fax: 907/474-7290

Dr. Gerald Stokes
Pacific Northwest Laboratories
P.O. Box 999 (Mail Stop K1-74)
Richland, WA 99352
Tel: 509/375-3816
Fax: 509/375-2698

Dr. Norton Strommen
World Agriculture Outlook Board
USDA
Room 5133, South Bldg.
Washington, DC 20250
Tel: 202/720-9805
Fax:

Dr. Joe Sullivan
Department of Botany
University of Maryland
College Park, MD 20742
Tel: 301/405-1626
Fax: 301/314-9082

Dr. Tove Svendby
University of Oslo
Department of Physics
P.O. Box 1048, Blindern
N-0316 Oslo, Norway
Tel: 47/2-855658
Fax: 47/2-855671

Dr. Ambler Thompson
NIST
Div. of Radiometric Physics
Building 220, Room B 306
Gaithersburg, MD 20899
Tel: 301/975-2333
Fax: 301/840-8551

Dr. Dan Tompkins
USDA/CSRS Aerospace Bldg.
901 D Street SW
Washington, DC 20250-2200
Tel: 202/401-4603
Fax: 202/401-4888

Mr. Dennis Trout
EPA/Global Change Research Program
Room WT 611H/RD-682
401 M St., SW
Washington, DC 20460
Tel: 202/260-5991
Fax: 202/260-6370

Dr. Jan C. van der Leun
Institute of Dermatology
State University Hospital - Utrecht
Heidelberglaan 100, PO Box 85500
NL-3584 CX Utrecht The Netherlands
Tel: 31/30-507386
Fax: 31/30-541822

Mr. Maurice Verhille (AFEAS)
Elf Atochem S.A.
4, Cours Michelet
La Défense 10, Cédex 42
92091 Paris France
Tel: 33/1-4900-8476
Fax: 33/1-4900-7252

Dr. F.A. Vogelsberg, Jr. (AFEAS)
E.I. du Pont de Nemours & Co., Inc.
1007 Market Street (B-13237)
Wilmington, DE 19898
Tel: 302/774-3267
Fax: 302/774-8416

Dr. Judy Walrath
Du Pont Company
1007 Market Street, N11510-6
Wilmington, DE 19898
Tel: 302/773-4552
Fax: 302/773-6030

Dr. Ann R. Webb
Department of Meteorology
University of Reading
2 Earley Gate, Whiteknights Rd.
P.O. Box 239
Reading RG6 2AU U.K.
Tel: 44/734-318954
Fax: 44/734-352604

Dr. Eckard Wellmann
Biologisches Institut 11 der Universität
Schanzlestrasse 1
D-7800 Freiburg, Germany
Tel: 49-761-203-2664
Fax: 49-761-203-2712

Dr. Ulf Wester
Swedish National Institute
for Radiation Protection
P.O. Box 60204
S-104 01 Stockholm, Sweden
Tel: 46-8-729-7100 or 7171
Fax: 46-8-311714

Dr. Robert C. Worrest (formerly with the U.S. EPA)
CIESIN
1825 K Street, NW
Suite 805
Washington, D.C. 20006
Tel: 202/775-6600
Fax: 202/775-6622

Dr. William Yu
ITI, Inc.
12310 Herrington Manor Drive
Silver Spring, MD 20904
Tel: 301/890-3022
Fax: 301/890-5595

Appendix C: Presentation Materials

UV Radiation Changes

Dr. Richard McKenzie
Department of Scientific and Industrial Research

Scientific Assessment of Ozone Depletion: 1991

Preprint: December 17, 1991

Co-Chairmen:

Robert T. Watson, NASA
Daniel L. Albritton, NOAA

Sponsored by:

World Meteorological Organization
United Nations Environment Programme
National Aeronautics and Space Administration
National Oceanic and Atmospheric Administration
U. K. Department of Environment

Chapter 11. Ultra-Violet Radiation Changes

Lead authors:

R. L. MCKENZIE, M. Ilyas, J. E. Frederick, V. Filyushkin

Additional Contributors:

A. Wahner, P. Muthusubramanian, C. E. Roy, K. Stamnes,
M. Blumthaler, S. Madronich

SCIENTIFIC SUMMARY

A major consequence of ozone depletion is an increase in solar UV radiation received at the Earth's surface. This chapter discusses advances that have been made since the previous assessment [WMO, 1990] to our understanding of UV radiation. The impacts of these changes in UV on the biosphere are not included, because they are discussed in the Effects Assessment [UNEP, 1991]. The major conclusions and recommendations are:

1. Significant improvements in the UV data base have occurred since the last assessment. Spectral measurements are becoming available, but to determine trends long-term accurate measurements of UV are required at unpolluted sites.

2. Biologically damaging UV has been observed to more than double during episodes of ozone depletion in Antarctica. Smaller episodic enhancements have been measured in Australia. The observed enhancements are consistent with the results of radiative transfer calculations for clear sky conditions.

3. An Erythema Radiative Amplification factor (RAF) of 1.25 ± 0.20 has been deduced from measurements of ozone and UV at a clean air site. This is in agreement with the RAF derived from model calculations (RAF = 1.1 at 30°N).

4. There is an apparent discrepancy between observed UV trends from the Robertson-Berger (RB) network and those calculated from TOMS ozone data. Cloud variability, increases in tropospheric ozone and aerosol extinctions may have masked the UV increase due to ozone depletion. In addition, the data record available for comparison is short, and the instrument calibration (which is critical) is still in question. However, at a high altitude European observatory, the observed positive trends in UV appear to be larger than expected. Further studies of the effects of cloud and aerosol on UV are required.

5. Clear-sky radiative transfer calculations using ozone fields measured by the TOMS instrument show that during the 1980s erythemally active UV has increased significantly at latitudes poleward of 30°, with larger increases in the Southern Hemisphere, particularly at high latitudes.

6. Significant increases in UV effects are most likely to appear first in the Southern Hemisphere where in the summer, historical ozone levels are lower and the Earth-Sun separation is a minimum. Further, in the Southern Hemisphere, stratospheric ozone losses are more severe, tropospheric ozone has not increased, and aerosol concentrations are lower.

7. Existing chemical models underestimate the changes in the observed ozone fields. Therefore they cannot be used to accurately predict future changes in UV fields.

11.1. UV MEASUREMENTS AND ANALYSES

11.1.1 Interpretation of UVB Time Series Data

The most comprehensive time series of UVB data are those from the Robertson-Berger (RB) network. However, a study by *Scotto et al.* [1988] showed no increase in UVB at observation sites in USA, despite the decrease in stratospheric ozone. Investigations to understand the reasons for this surprising result have continued. Increases in tropospheric ozone that more than compensated for stratospheric ozone losses were proposed by *Brühl and Crutzen* [1989]. However, recent analyses of TOMS data and tropospheric ozone trends suggest an increase in UVB should still have been observed [UNEP, 1991]. Increasing local pollution at the measurement sites has also been suggested. Since the industrial revolution, reductions in Northern Hemisphere UVB have already occurred due to aerosol extinction. The decreases in UVB caused by increases in aerosols since the industrial revolution probably exceed the increases due to ozone depletion (Fig 11.1, from *Liu et al.* [1991]). On a local scale, changes in pollution at the network sites may therefore be significant in the analysis period (1974-1985).

The RB meters have a relatively low sensitivity to ozone depletion. Typically a 1% reduction in ozone produces a reduction of less than 1% in the RB weighted irradiance [UNEP 1991], and it is possible that the trends in UVB irradiance measured by the RB network have been masked by natural variability in cloud cover. A study by *Beliaevsky et al.* [1991] argues that because of natural cloud variability, decades of data would be required before UVB trends would be detectable without supporting measurements.

Frederick and Weatherhead [1991] have examined RB data from two sites in the US (Bismarck and Tallahassee) at which Dobson ozone data were available (Fig. 11.2). They concluded that monthly trends in the RB data are consistent with expectations based on Dobson column ozone measurements for the months of high UVB irradiance, April through September. However, large differences exist between modeled and clear-sky results in the period November through February. The reason for this discrepancy is unknown at present. We understand that the calibration of this network is currently being evaluated, and a publication is likely to appear. With the information currently available, there are still questions about the calibration of this network.

RB data obtained from the high altitude European observatory at Jungfraujoch has been used in conjunction with measurements of global radiation (G) between 300 and 2000 nm, to eliminate cloud and aerosol effects, and reveal trends in UVB [Blumthaler and Ambach, 1990]. Updated measurements that include data from 1990 (M. Blumthaler, private communication, 1991) are shown in Fig 11.3. The plot shows the departures from the long term mean in the ratio UVB/G. The data show irregular variations, but unlike the US data, there is a superimposed trend, which corresponds to UVB increases of $10 \pm 5\%$ per decade, which is larger than that expected (Madronich, 1991) from the changes in ozone measured over the same period (Chapter 2). However, the effects of the 1982 El Chichon volcanic eruption on this data may be significant either through its possible influence on ozone which was anomalously low at these latitudes in 1983 [WMO, 1990], or through changes in the wavelength-dependent aerosol optical depth [Kent et al., 1991].

There has been an increasing awareness that spectral measurements are required to study the effects of changes in ozone on UV radiation. The RB response does not accurately represent any of the diverse biological action spectra of interest [UNEP, 1991], whereas spectral data can be accurately convolved with various action spectra. In addition, the spectral information enables greater confidence in instrument calibration, and identification of the reasons for any changes in UV. For example, spectral measurements have enabled ozone column amounts to be deduced.

and facilitated determination of cloud and aerosol effects [Stamnes *et al.*, 1990]. The time series of UV spectral measurements is too short at present to determine trends, but useful insights have nevertheless been gained already from analyses of this type of data.

11.1.2 Effects of Antarctic Ozone Depletion

In 1988 the National Science Foundation established four sites for monitoring solar ultraviolet and visible radiation in the high latitude Southern Hemisphere. Three of these sites are on the Antarctic continent, at the South Pole, McMurdo, and Palmer Station, and one is located at Ushuaia, Argentina. Results from McMurdo [Stamnes *et al.*, 1990], and from Palmer Station on the Antarctic peninsula [Lubin *et al.*, 1989; Lubin and Frederick, 1991] have appeared in the literature. To date the focus has been on changes in surface ultraviolet irradiance associated with the springtime depletion in ozone.

The ultraviolet radiation field over Antarctica varies with the solar elevation, clouds and haze, and the atmospheric ozone amount. Over Palmer Station (latitude 64.8°S) clouds, in a monthly averaged sense, reduce the surface ultraviolet irradiance to approximately 50-60% of the values that would prevail under perpetually clear skies. The springtime depletion in ozone constitutes a relatively recent perturbation to the highly variable radiation background. The two issues to consider here are (a) the magnitude of the reduction in ozone and (b) the timing of the reduction relative to the normal seasonal cycle in solar radiation.

Figure 11.4 presents two spectra of surface ultraviolet irradiance measured at local noon from Palmer Station on day numbers 293 (Oct 19) and 349 (Dec 14) of 1988 [Lubin *et al.*, 1989]. The former date was the day of minimum ozone, while the latter is near summer solstice. Based solely on solar elevation, one would expect the largest irradiances in December. Figure 11.4 shows this to be the case at wavelengths longer than 315 nm. However, at shorter wavelength, the measured irradiances for October equal and then exceed those in December. This is the manner in which a reduction in ozone appears in ultraviolet radiation at the earth's surface. Although the enhanced irradiances exist at wavelengths where the absolute energy flux is small, living cells are quite sensitive to damage in the spectral region from 300 to 315 nm.

The springtime ozone depletion of 1988 had vanished from the Antarctic peninsula by mid-November. However, during 1990 reduced ozone amounts persisted over Palmer Station well into December. The combination of low ozone and high solar elevation led to unusually large irradiances as shown in Figure 11.5 [Frederick and Alberts, 1991]. The points denote ratios of the noontime irradiance measured at 306.5 nm, near the peak of the biologically-weighted spectrum, to that at 350.0 nm, where absorption by ozone is insignificant. Use of this irradiance ratio removes the influence of clouds, to a good approximation, so the points indicate variations associated with ozone only. The solid line represents computed ratios based on the ozone climatology of Nagatani *et al.* [1988] in which any springtime ozone reduction is small. The dashed line indicates double the climatological prediction. Approximately 20% of the days during the spring of 1990 had irradiance ratios in excess of the climatological prediction by a factor of two or more, and the enhancement persisted into early December when the daylight period is long. Measurements from McMurdo during 1990 yielded similar results, with ozone depletions persisting in December to give enhancements in biologically weighted radiation by a factor of three [Stamnes *et al.*, 1991]. The variations in observed UVB irradiances in Antarctica have been shown to be consistent with the results of radiative transfer calculations [Stamnes *et al.*, 1990].

The minimum ozone levels over Antarctica occur in October. At this time, solar elevations are relatively low, so that the maximum UV fluxes occur later in the year. However, the transmission of sea-ice has a strong seasonal maximum in spring so that organisms that live under the ice sheet may be at risk [Troedahl and Buckley, 1989]. In terms of the potential

ecological effects, the duration of the ozone depletion is likely to be an important quantity. When ozone amounts remain low into December, the instantaneous and 24 hour integrated ultraviolet irradiances discussed above can be far in excess of the maximum values experienced in Antarctica prior to the 1980s.

11.1.3 Global Effects

UVB perturbations have also been seen at mid latitudes in the Southern Hemisphere, from episodic intrusions of ozone poor air from the Antarctic ozone hole. For example, *Roy et al.* [1990] showed an association between high UVB levels in Melbourne Australia and ozone-depleted air arriving from Antarctica in late 1987. Figure 11.6 shows the strong anticorrelation between UVB (integrated over the wavelength range 285-315 nm) and ozone. The impacts of the ozone changes on the observed UV are consistent with model predictions, although calculated irradiances are 10% smaller.

The Southern Hemisphere is where increases in UV stresses are most likely to appear first. Historically, UV levels there have been high because of the lower ozone amounts in summer compared with the Northern Hemisphere, and because the Earth-Sun separation is smallest in January. Further, in the Southern Hemisphere stratospheric ozone losses are more severe, tropospheric ozone has not increased, and aerosol concentrations are lower [*McKenzie*, 1991].

In absolute terms, even small percentage decreases in ozone are important in the tropics, since UVB levels there are already large. A 10% decrease in ozone in the tropics would lead to a UVB increase which is larger than the total UVB at mid-latitudes [*Ilyas*, 1989]. In view of this sensitivity, more tropical measurements of UV are clearly required, even though the most recent analyses of TOMS satellite ozone indicate that there have been no changes of statistical significance at equatorial latitudes.

11.1.4 Radiative Amplification Factor Deduced from Measurements

A suitable long term data base does not yet exist to enable global UV trends due to ozone depletion to be determined. It has, however, been demonstrated that under similar observing conditions (i.e same ozone, sun angle, clear skies), any changes between 1980 and 1988 in the measured spectral distribution of UV at Lauder, New Zealand (45°S, 170°E), were small [*Bittar and McKenzie*, 1990]. Since December 1989, spectral measurements from Lauder have been made routinely at fixed solar zenith angles (SZAs) and near local noon, whenever weather conditions permit. Typical spectra obtained at midday in winter and summer are shown in Fig. 11.7a. The figure also shows the erythmal weighting function [*McKinlay and Diffey*, 1987] used in the analyses that follow in the remainder of this chapter. The integrated midday erythmal irradiance in winter (Fig 11.7b) is only 10% of that in summer, due mainly to differences in the SZA.

Seasonal variations in ozone are large at mid-latitude sites, enabling these measurements to be used to investigate the relationship between UV and ozone (and other factors such as cloud cover and sun angle). Observations obtained at fixed SZAs over a year were used, and variations due to seasonal changes in the Sun-Earth separation were removed using a simple trigonometric correction. Data from 1990 was used in the analysis. In this period, variations in aerosol extinction were relatively small.

Figure 11.8 shows the relationship between ozone column and erythemally weighted UVB

for SZA = 60°. The influence of clouds and SZA on UVB dominate over ozone effects. Clouds frequently reduce the irradiances by 50% or more (no observations are attempted if rain is imminent). The clear-sky subset of this data was used to deduce the increase in erythral UV (EUV) that would result from a 1% decrease in ozone. This Radiative Amplification Factor ($RAF = -(d(EUV)/EUV) / (d(O_3)/O_3)$) was then used to reconstruct the curves in the figure. Similarly, RAFs were derived for other SZAs. Figure 11.9 shows these RAFs as a function of SZA. The spread of results between morning and afternoon UV measurements, and between TOMS and Dobson ozone data indicates the uncertainty in the measurements. Thus the RAF derived from these measurements is 1.25 ± 0.20 [McKenzie *et al.*, 1991].

The computed daily integrated RAF for this action spectrum at 30°N is 1.1, and is insensitive to cloud and tropospheric aerosol variations [UNEP, 1991]. However, the calculated effect of an ozone redistribution from the stratosphere to the troposphere will lead a decrease in UV for small solar zenith angles [Brühl and Crutzen, 1989], but may lead to an increase for large solar zenith angles [Tsay and Stamnes, 1991a]. Stratospheric aerosols (from volcanos) have a similar effect [Tsay and Stamnes, 1991b], so that impacts of ozone vertical redistributions and stratospheric aerosols on UV will depend on latitude and season

11.2 CHANGES IN ULTRAVIOLET RADIATION BASED ON MEASURED AND COMPUTED OZONE AMOUNTS

11.2.1 Objectives and Limitations

This section presents computed changes in UV irradiances based on ozone values taken from measurements and two-dimensional models. Consistent with the focus of this assessment on the stratosphere, the present work addresses only those changes in UV irradiance related to changes in column ozone. The results should not be interpreted as the changes which have actually occurred, but rather as the changes which would have occurred if column ozone were the only variable. In particular, the calculations do not account for a change in the partitioning of ozone between the stratosphere and troposphere and assume clear, pollution-free skies. All results were obtained with the radiative transfer model described by Frederick and Lubin [1988].

This analysis reports the "erythral irradiance" integrated over the entire daylight period. This is defined by the convolution over wavelength of the action spectrum for erythema [McKinlay and Diffey, 1987] with the computed spectral irradiance incident on the ground, integrated from sunrise to sunset. The absolute erythral irradiance, in joules per square meter of horizontal area, depends on the action spectrum being normalized to unity at wavelengths less than 298 nm. The extension of the spectrum to 400 nm implies that the weighted irradiance has a weaker sensitivity to changes in ozone than was the case with older action spectra, which terminated at shorter wavelengths. It is important to recognize that the values reported here depend on the action spectrum adopted. While the action spectrum for erythema is a standard reference, it is not appropriate to all biological responses. For example, using the action spectrum appropriate for damage to DNA, the sensitivity to ozone is increased, while for photosynthesis inhibition, the RAF is near 1 [UNEP, 1991]. A biologically weighted irradiance provides an index of the radiation dose received by an organism, but quantitative predictions must be based on an established relationship between dose and response. A large percentage change in irradiance may or may not correspond to a large percentage change in biological response. Similarly, small percentage changes in irradiance are not necessarily insignificant. Such considerations receive further attention in the companion "Effects Assessment" document.

Figure 11.10 presents contours of daytime integrated erythral irradiance as functions of

latitude and month. The column ozone values used here are from the TOMS Version 6 data set for the year 1980. The patterns are as expected from the elevation of the sun and the duration of daylight. Large absolute values exist in the tropics and in the summer hemisphere, while a sharp latitudinal gradient exists in winter. These results represent the baseline case against which to measure percentage changes in irradiance over periods of years.

11.2.2 Changes in Erythral Radiation Based on TOMS Ozone Measurements

Figure 11.11 gives the percent change in daytime integrated erythral irradiance from 1980 to 1990 as functions of latitude and month based on zonally and monthly averaged measurements from TOMS. The results show increases of 8-12% in the mid-to-high latitude winter and spring of the Northern Hemisphere. The changes from 1980 to 1990 are typically 4-8% in the Northern mid-latitude summer and 4-12% in the Southern summer. Note that the largest percentage changes appear in winter when the absolute irradiances are small. The cross-hatched area in Figure 11.11 is a region of large gradients in irradiance associated with the prolonged Antarctic ozone depletion of 1990. The UV enhancements in this region are in excess of 25%.

The annually integrated irradiance is a useful index which incorporates both the large annual cycle in radiation and the seasonal changes in ozone. Figure 11.12 presents the percent change in annually integrated erythral irradiance between 1980 and 1990 as a function of latitude. The changes are near zero within 30° latitude of the equator but become positive at latitudes poleward of 30° in each hemisphere. The increases reach 10% at high northern latitudes. The extended high latitude, southern hemisphere ozone depletion of 1990 led to large ultraviolet irradiances in late spring and early summer. These influence the annually integrated irradiances, giving enhancements of 10-24% compared with 1980 at latitudes poleward of 60°S .

11.2.3 Predicted Changes in Erythral Radiation Based on Computed Ozone Values

Current chemical models seriously underestimate the ozone losses observed by TOMS between 1980 and 1990 (see Chapter 2). Therefore they cannot be used to accurately predict future changes in UV fields. Nevertheless, the models are qualitatively in agreement that ozone losses due to atmospheric chlorine will reach a peak around the year 2000, when the peak chlorine loading is expected to maximize given full or near-full compliance with the Montreal Protocol (see Chapter 8, scenario "A"). Erythral UV levels are expected to be enhanced by a factor of two over 1990 levels by 2000, with a gradual reduction thereafter. By 2020, UV levels are expected to have reverted to 1990 levels. It must be stressed however that these are crude estimates, because the model simulations are incomplete.

References

- Beliaevsky, A. V., V. M. Zakharov, G. M. Kruchenitsky, The effect of cloudiness on the detection of UV-B irradiance trends caused by total ozone depletion, *Optics of the Atmosphere* (Russian), submitted 1991.
- Bittar, A., and R. L. McKenzie, Spectral UV intensity measurements at 45°S: 1980 and 1988, *J. Geophys. Res.*, 95, 5597-5603, 1990.
- Blumthaler, M., and W. Ambach, Indication of increasing solar ultraviolet-B radiation flux in alpine regions, *Science*, 248, 206-208, 1990.
- Brühl, C., and P. J. Crutzen, On the disproportionate role of tropospheric ozone as a filter against solar UV-B radiation, *Geophys. Res. Lett.*, 16, 7, 703-706, 1989.
- Frederick, J. E., and A. D. Alberts, Prolonged enhancement in surface ultraviolet radiation during the Antarctic spring of 1990, *Geophys. Res. Lett.*, in press 1991.
- Frederick, J. E., and D. Lubin, The budget of biologically active ultraviolet radiation in the earth-atmosphere system, *J. Geophys. Res.*, 93, 3825-3832, 1988.
- Frederick, J. E., and E. C. Weatherhead, Temporal changes in surface ultraviolet radiation: a study of the Robertson-Berger meter and Dobson data records, *Photochem. Photobiol.*, submitted 1991.
- Ilyas, M. The danger of ozone depletion in the tropics, *Search*, 20, (5), 148-149, 1989.
- Kent, G. S., M. P. McCormick and S. K. Schaffner, Global climatology of the free tropospheric aerosol from 1.0 μ M satellite occultation measurements, *J. Geophys. Res.*, 96, 5249-5267, 1991.
- Liu, S. C., S. A. McKeen, and S. Madronich, Effect of anthropogenic aerosols on biologically active ultraviolet radiation, *Geophys. Res. Lett.*, in press 1991.
- Lubin, D., J. E. Frederick, C. R. Booth, T. Lucas, and D. Neuschuler, Measurements of enhanced springtime ultraviolet radiation from Palmer Station, Antarctica, *Geophys. Res. Lett.*, 16, 783-785, 1989.
- Lubin, D., and J. E. Frederick, The ultraviolet radiation environment of the Antarctic peninsula: The roles of ozone and cloud cover, *J. Appl. Meteor.*, 30, 478-493, 1991.
- Madronich, S., Implications of recent total atmospheric ozone measurements for biologically active radiation reaching the Earth's surface, *Geophys. Res. Lett.*, in press 1991.
- McKenzie, R. L., Application of a simple model to calculate latitudinal and hemispheric differences in ultraviolet radiation, *Weather and Climate*, 11, 3-14, 1991.
- McKenzie, R. L., W. A. Matthews and P. V. Johnston, The relationship between erythemal UV and ozone, derived from spectral irradiance measurements, *Geophys. Res. Lett.*, in press 1991.
- McKinlay, A. F., and B. L. Diffey, A reference action spectrum for ultraviolet induced erythema in human skin, in *Human Exposure to Ultraviolet Radiation: Risks and Regulations* (Eds. W. R. Passchler and B. F. M. Bosnjakovic), Elsevier, Amsterdam, 83-87, 1987.
- Nagatani, R. M., A. J. Miller, K. W. Johnson, and M. E. Gelman, An Eight-Year Climatology of Meteorological and SBUV Ozone Data, *NOAA Technical Report NWS 40*, Camp Springs, MD, 125 pp, 1988.
- Roy, C. R., H. P. Gies, and G. Elliot, Ozone depletion, *Nature*, 347, 235-236, 1990.
- Scotto J. and G. Cotton, Biologically effective ultraviolet radiation: surface measurements in the US, *Science*, 239, 762-764, 1988.
- Stamnes, K., Z. Jin, J. Slusser, C. Booth and T. Lucas, Three-fold enhancements of biologically effective ultraviolet levels at McMurdo Station Antarctica during the 1990 ozone "hole", *Science*, submitted 1991.
- Stamnes, K., J. Slusser, M. Bowen, C. Booth, and T. Lucas, Biologically effective ultraviolet radiation, total ozone abundance, and cloud optical depth at McMurdo Station, Antarctica: September 15, 1988 through April 15, 1989, *Geophys. Res. Lett.*, 17, 2181-2184, 1990.
- Trodahl, H. J., and R. G. Buckley, Ultraviolet levels under sea ice during the Antarctic spring, *Science*, 245, 194-195, 1989.

- Tsay S. -C., and K. Stamnes, Ultraviolet radiation in the Arctic: The impact of potential ozone depletion and cloud effects, *J. Geophys. Res.*, in press 1991a.
- Tsay, S. -C. and K. Stamnes, The stratosphere as a modulator of ultraviolet radiation into the biosphere, *Surveys in Geophysics*, in press 1991b.
- UNEP *Environmental Effects Panel Report*, Chapter 1, Changes in biologically active ultraviolet radiation reaching the Earth's surface, S. Madronich, L. O. Bjorn, M. Ilyas, and M. M. Caldwell, 1991.
- WMO, *Scientific Assessment of stratospheric ozone: 1989*, World meteorological organization Global Ozone Research and Monitoring Project-Report No. 20, Eds D. L. Albritton and R. T. Watson, 1990.
- Yue, G. K., M. P. McCormick, and E. W. Chiou, Stratospheric aerosol optical depth observed by the Stratospheric Aerosol and Gas Experiment II: decay of the el Chichon and Ruiz volcanic perturbation, *J. Geophys. Res.*, 96, 5209-5219, 1991.

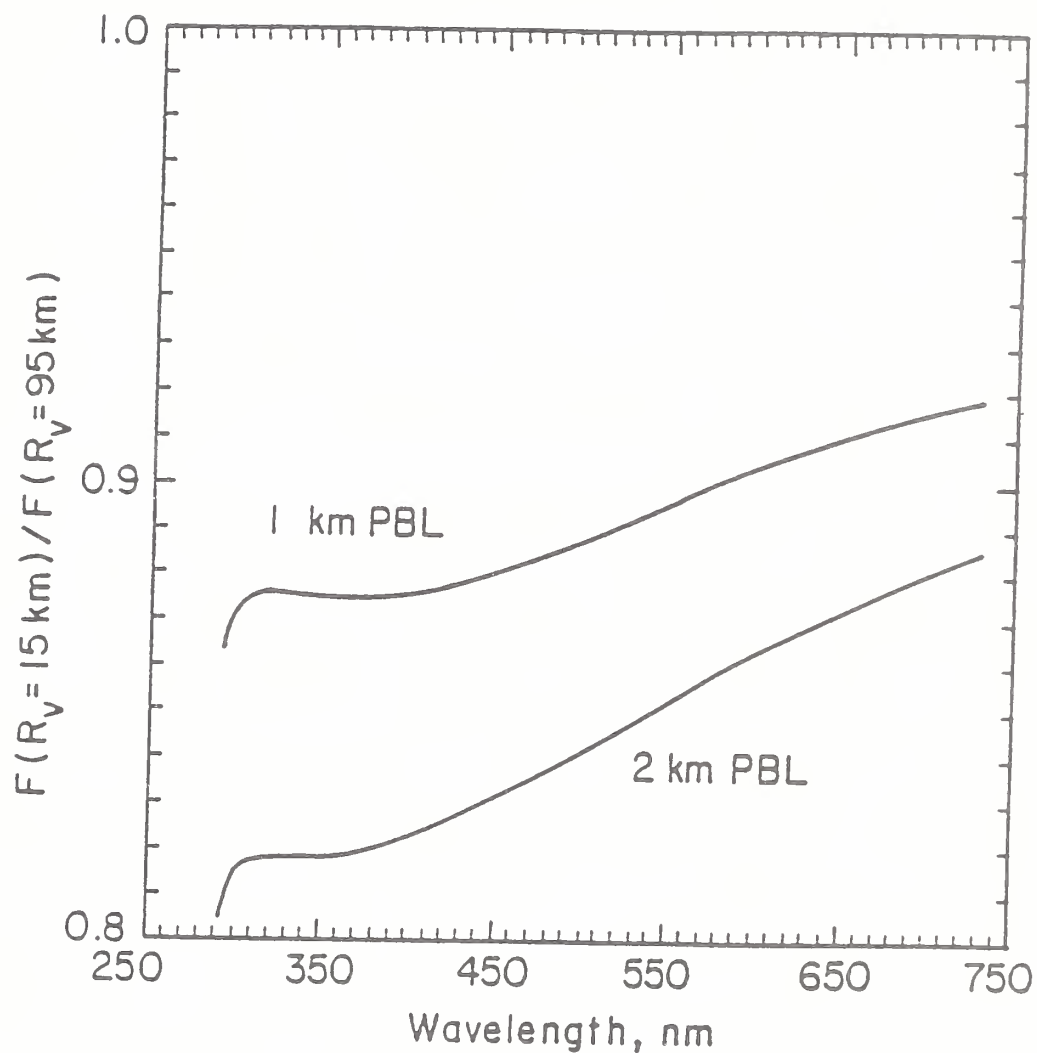


Fig. 11.1. Ratio of daily surface solar radiation for 15 km visual range (typical Northern Hemisphere) to that for 95 km visual range (clean air) as a function of wavelength, for assumed aerosol boundary layer heights of 1 and 2 km (from *Liu et al.*, [1991]).

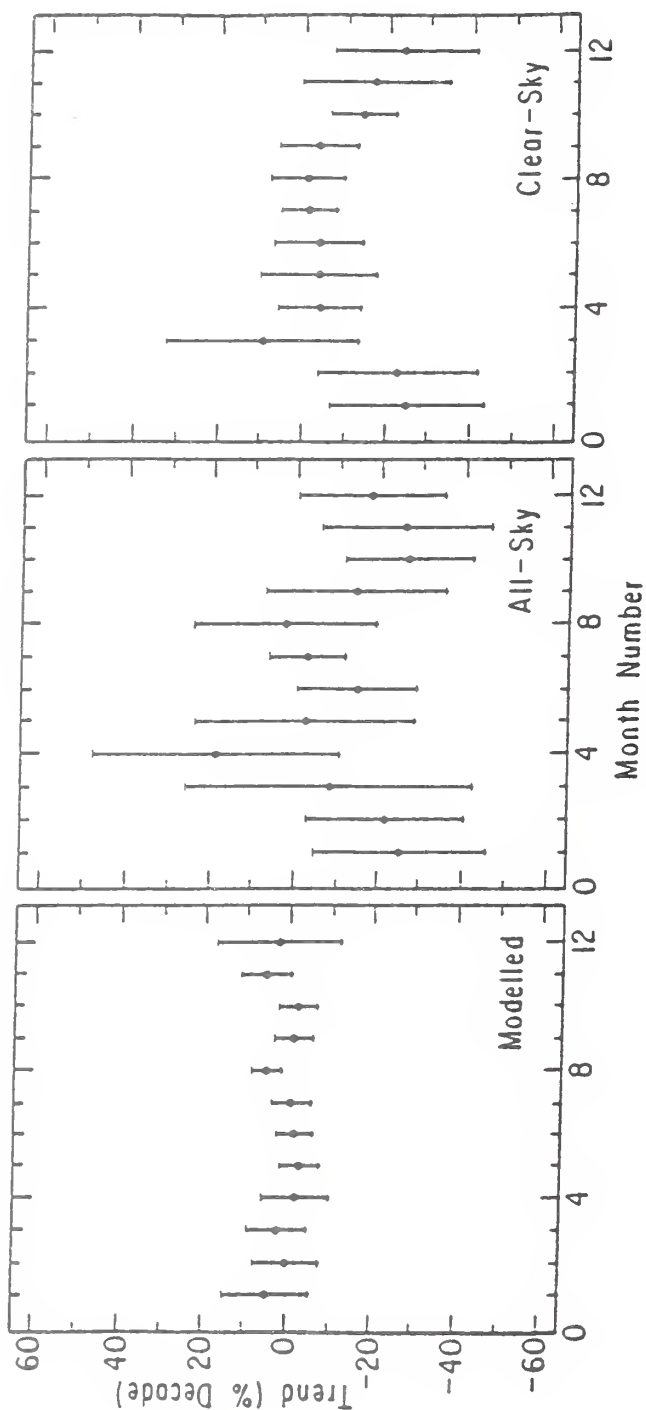


Fig. 11.2. Trends by month of the year in the Robertson-Berger (RB) meter data set for Bismarck USA, derived for the period 1974-1985. Error bars denote 95% confidence limits. Left panel: Results derived from radiative transfer calculations using Dobson ozone data as inputs. Center panel: Trends in the entire RB data set, including the influence of clouds. Right panel: Trends in a clear-sky subset of the RB data base (from *Frederick and Weatherhead* [1991]).

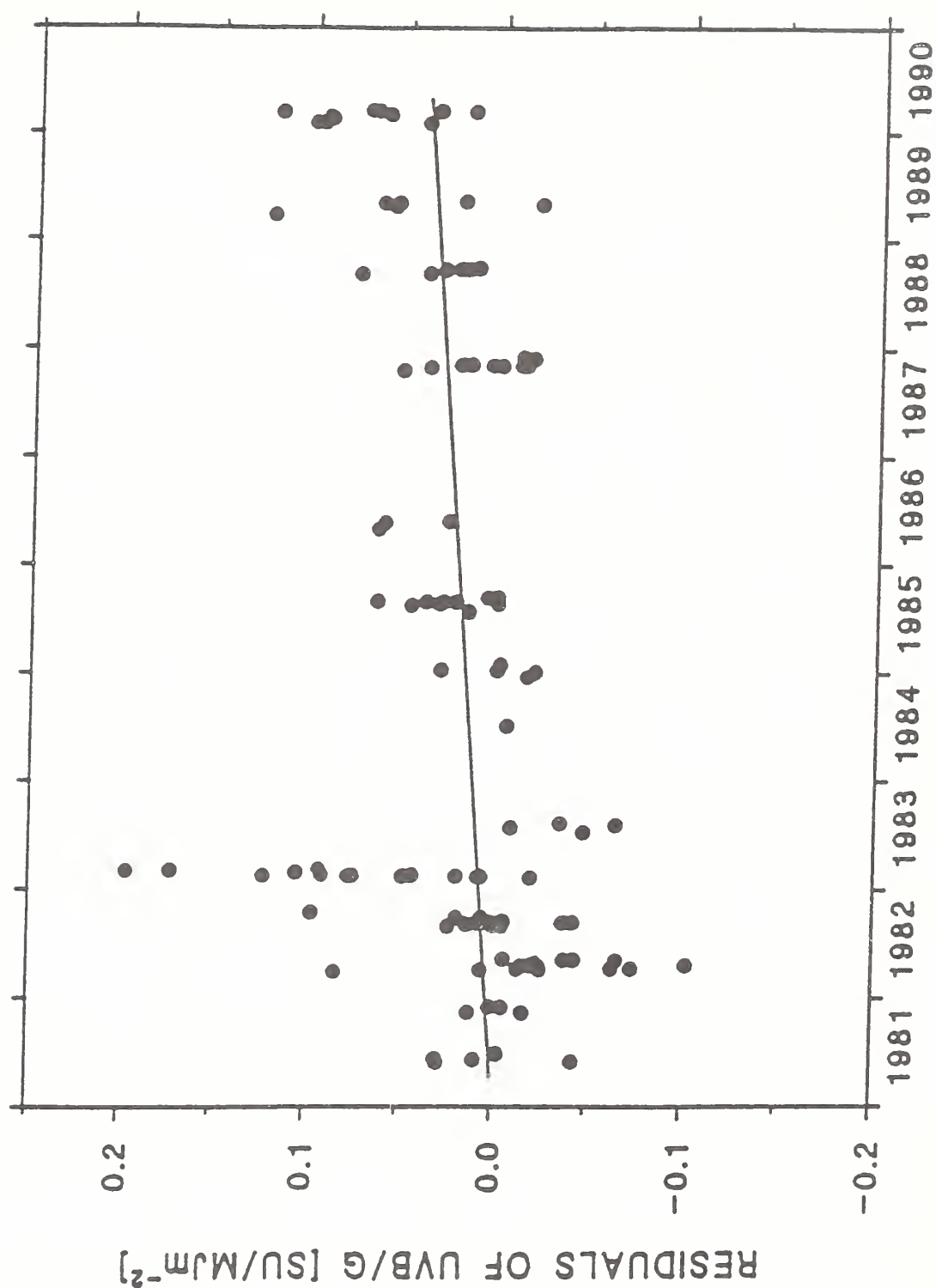


Fig. 11.3. Long-term tendency of the residuals from the long term means of the ratios UVB/G, measured at Jungfraujoch observatory between 1981 and 1990. The regression line is also shown (from *Blumhauer and Ambach* [1991]).

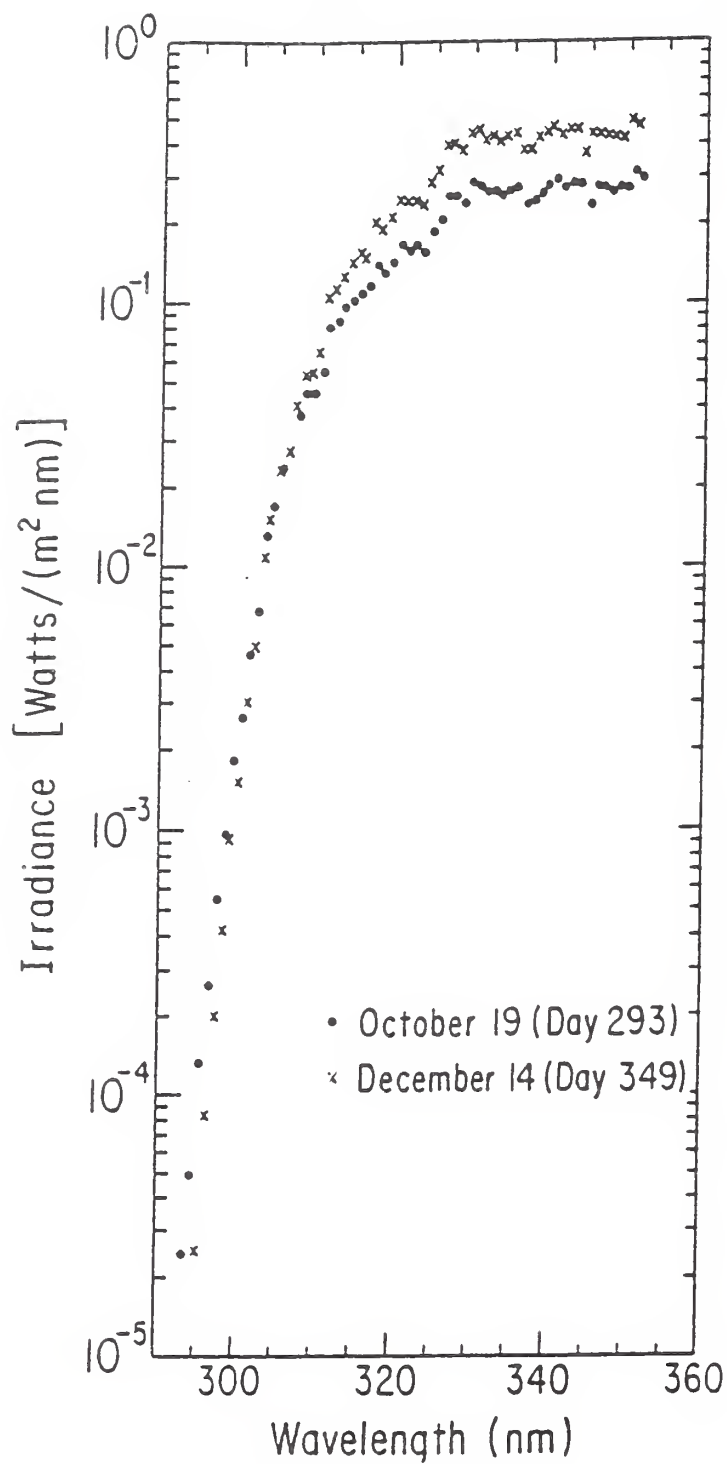


Fig. 11.4. Spectra of ultraviolet solar irradiance measured at local noon from Palmer Station, Antarctica in 1988. Day number 293 (Oct. 19) is the time of minimum ozone, while day number 349 (Dec. 14) is representative of conditions near summer solstice.

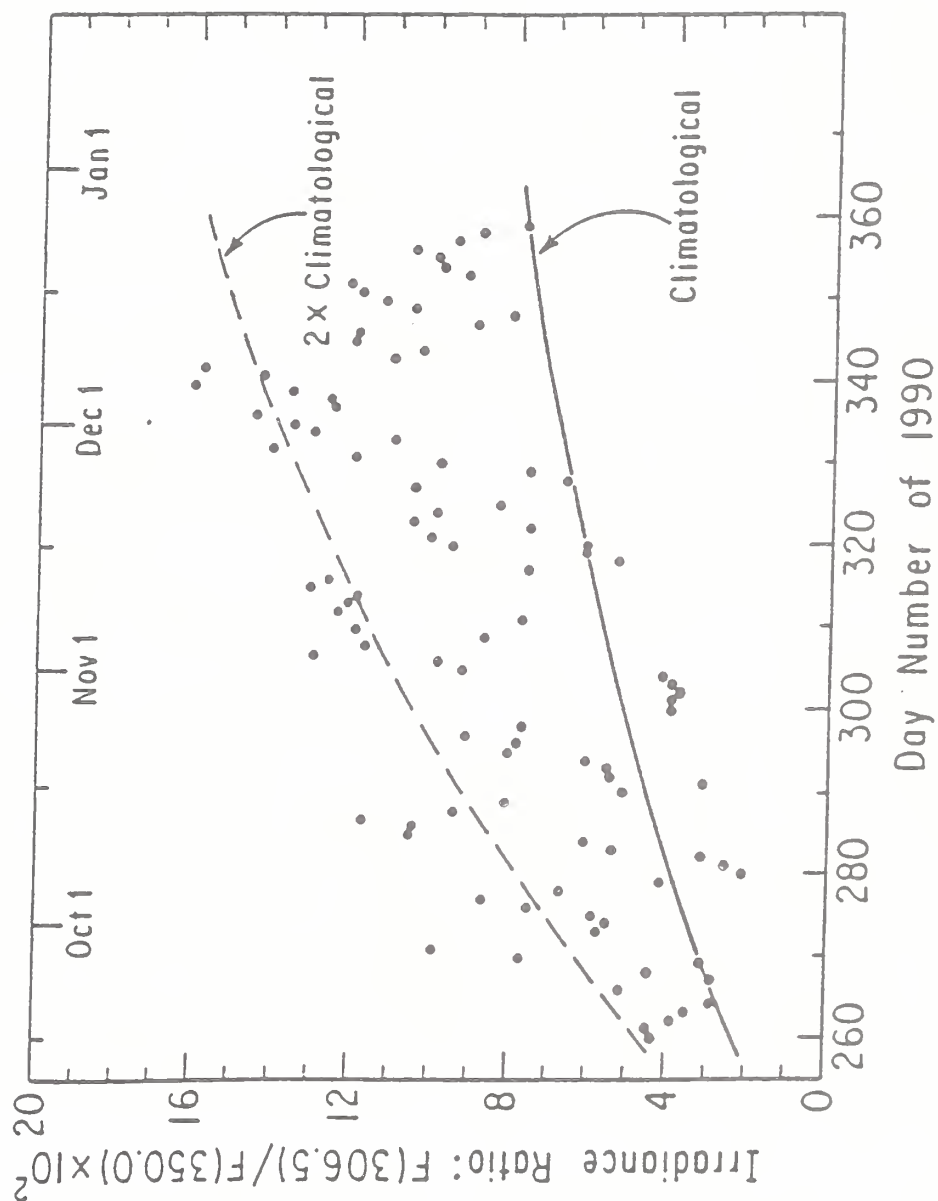


Fig. 11.5. Ratios of noontime solar irradiance at 306.5 nm to that at 350.0 nm (points) for the Austral spring of 1990 at Palmer Station. The solid curve labelled "climatological" is a calculation based on ozone amounts which are typical of those in the absence of a depletion. The dashed curve is twice the climatological irradiance ratio.

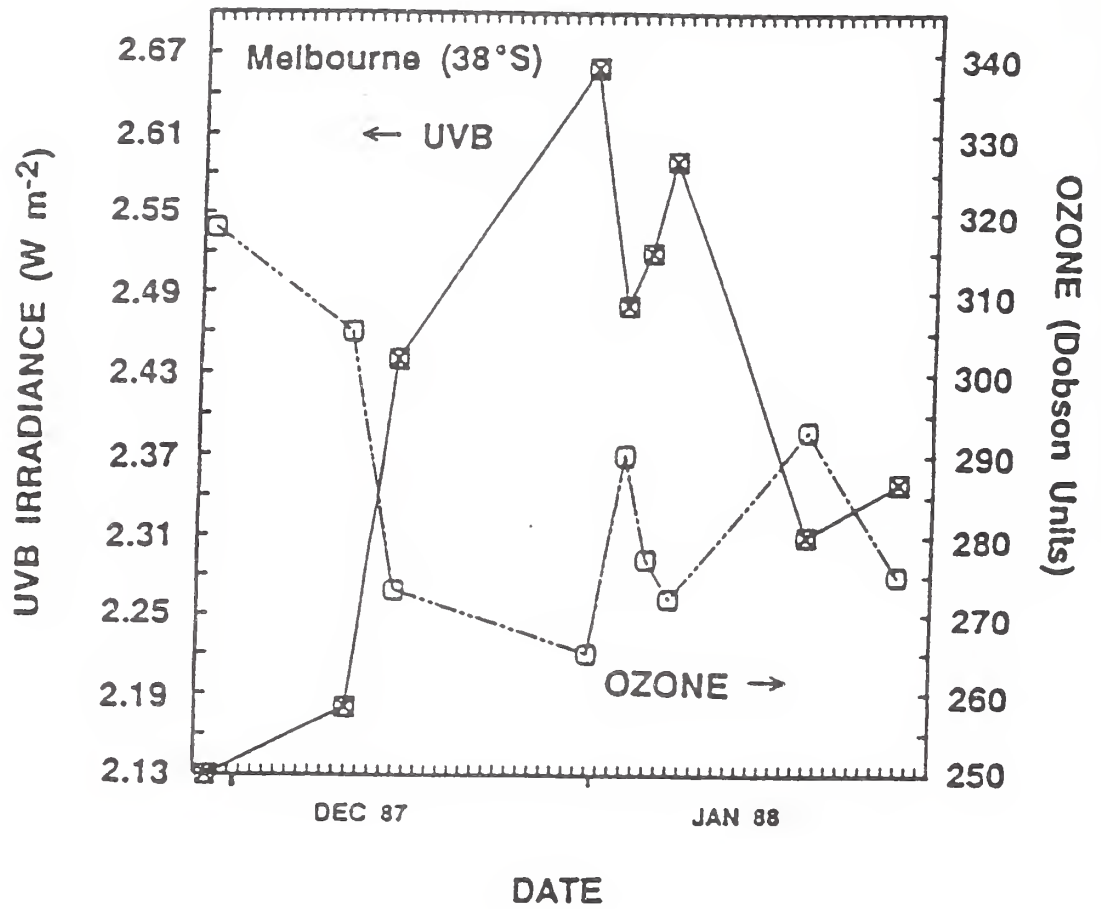


Fig. 11.6 Comparison of solar UVB radiation (285-315 nm) and ozone at Melbourne, Australia (38°S), during the intrusion of ozone poor air in December 1987 and January 1988 (from Roy *et al.*, [1990]).

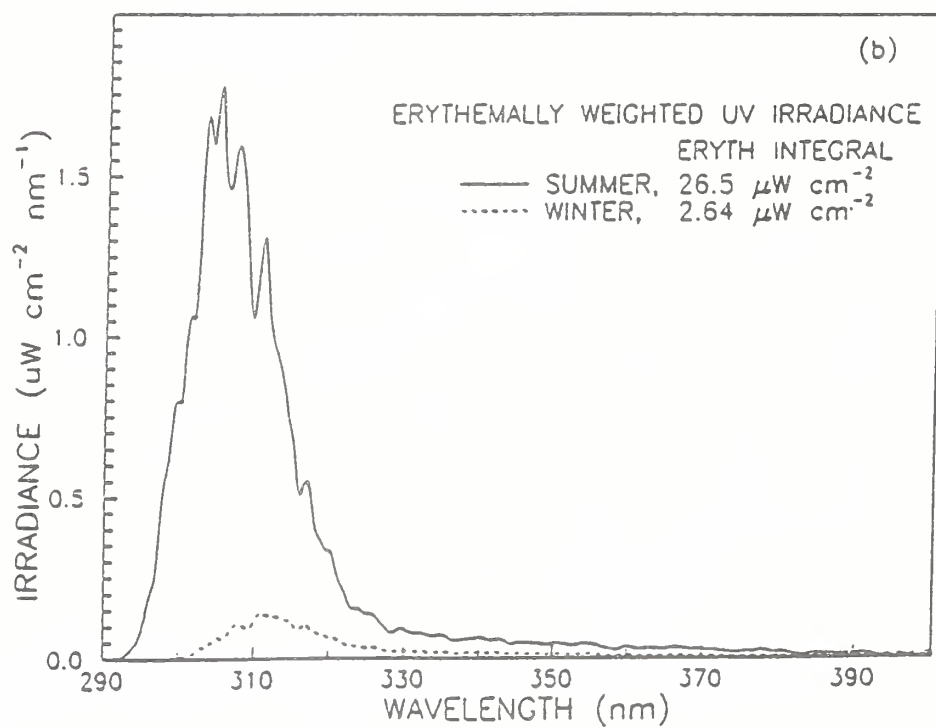
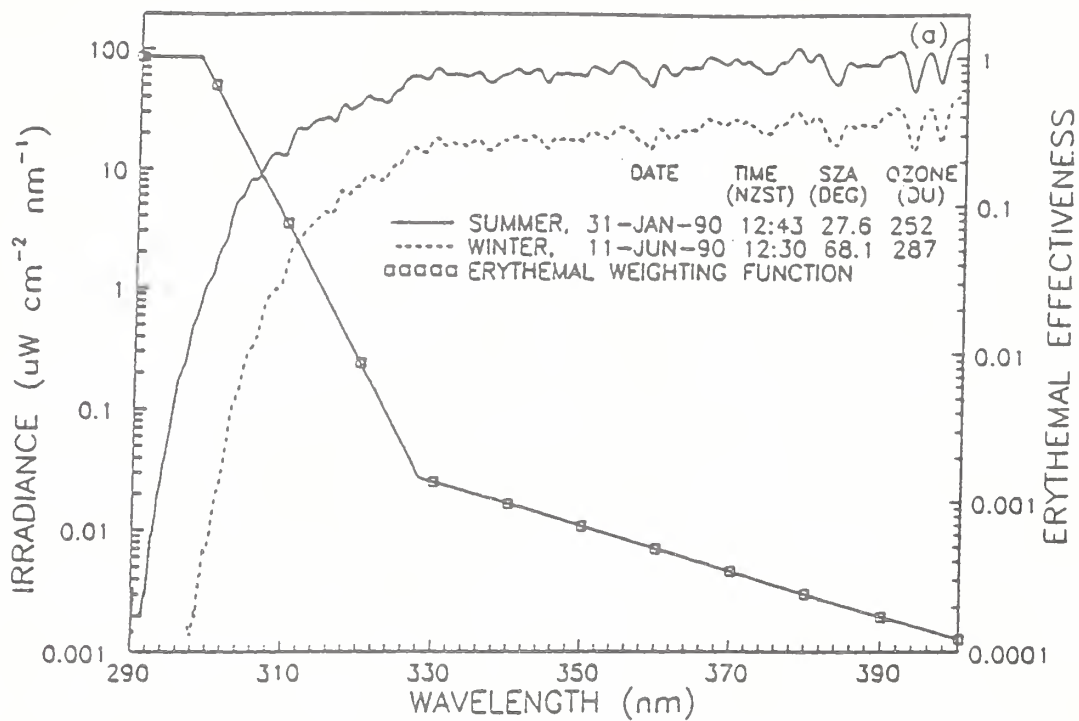


Fig. 11.7. (a) Typical noon spectra of UV irradiance at midlatitudes for summer and winter, showing the erythemal action spectrum used in the calculations that follow, (b) corresponding erythemally weighted irradiances.

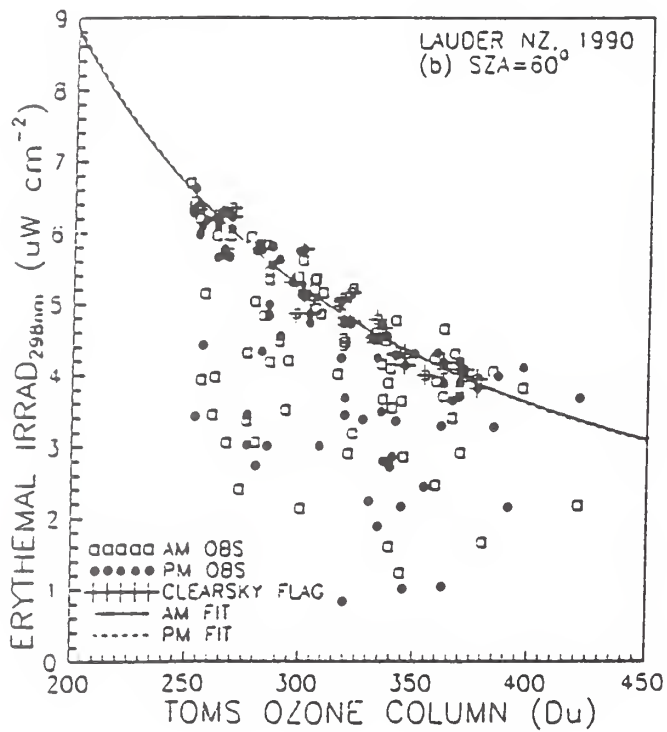
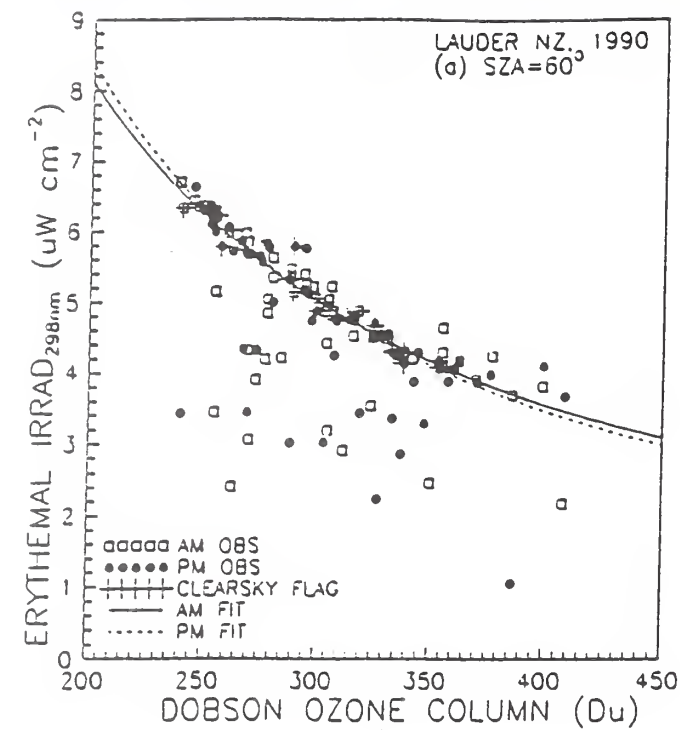


Fig. 11.8. Relationship between erythral UV (EUV) measured at SZA = 60°, and ozone (and cloud) measured at the same site (a) Ozone measured by Dobson, (b) ozone measured by TOMS. Observations that were positively identified as being cloud-free are flagged. The best-fit values of $RAF = -(d(EUV)/EUV) / (d(O_3)/O_3)$ to these points were found for both morning and afternoon observations, and used to construct the fitted curves shown.

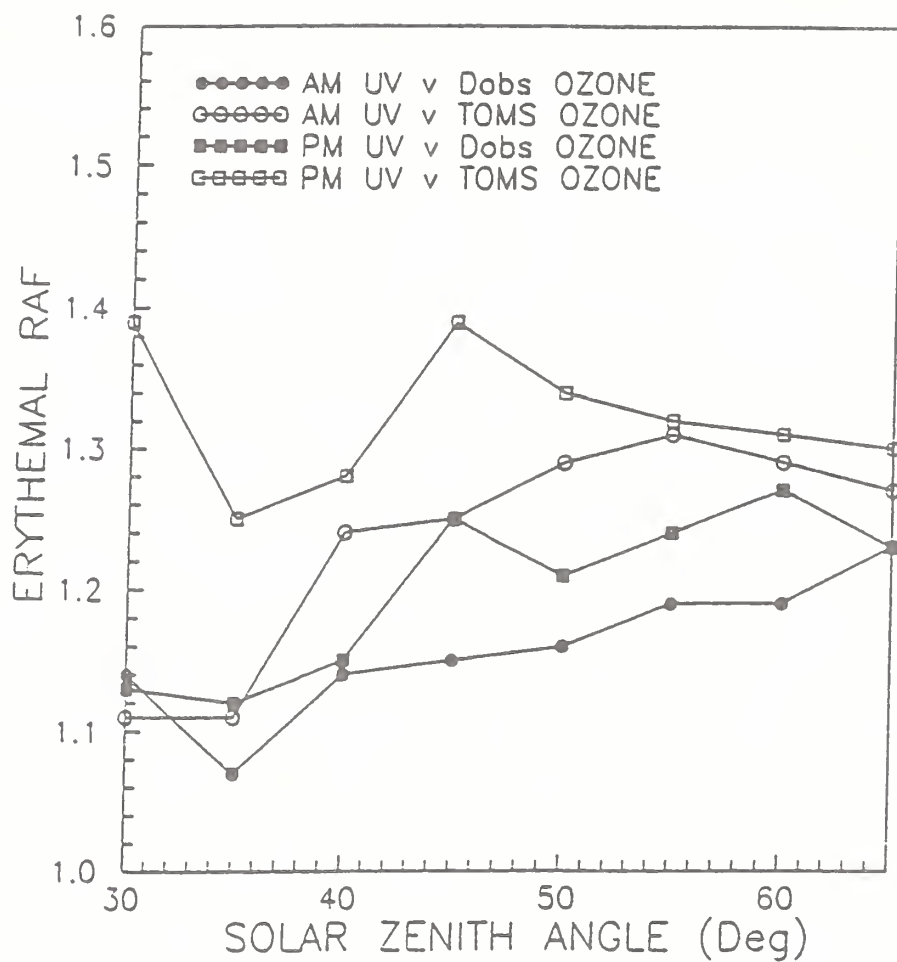


Fig. 11.9. RAFs as functions of solar zenith angle, deduced from measurements of erythemally weighted UV irradiance and total ozone. Results have been separated into morning and afternoon observations, and the RAFs are deduced for both Dobson and TOMS ozone measurements.

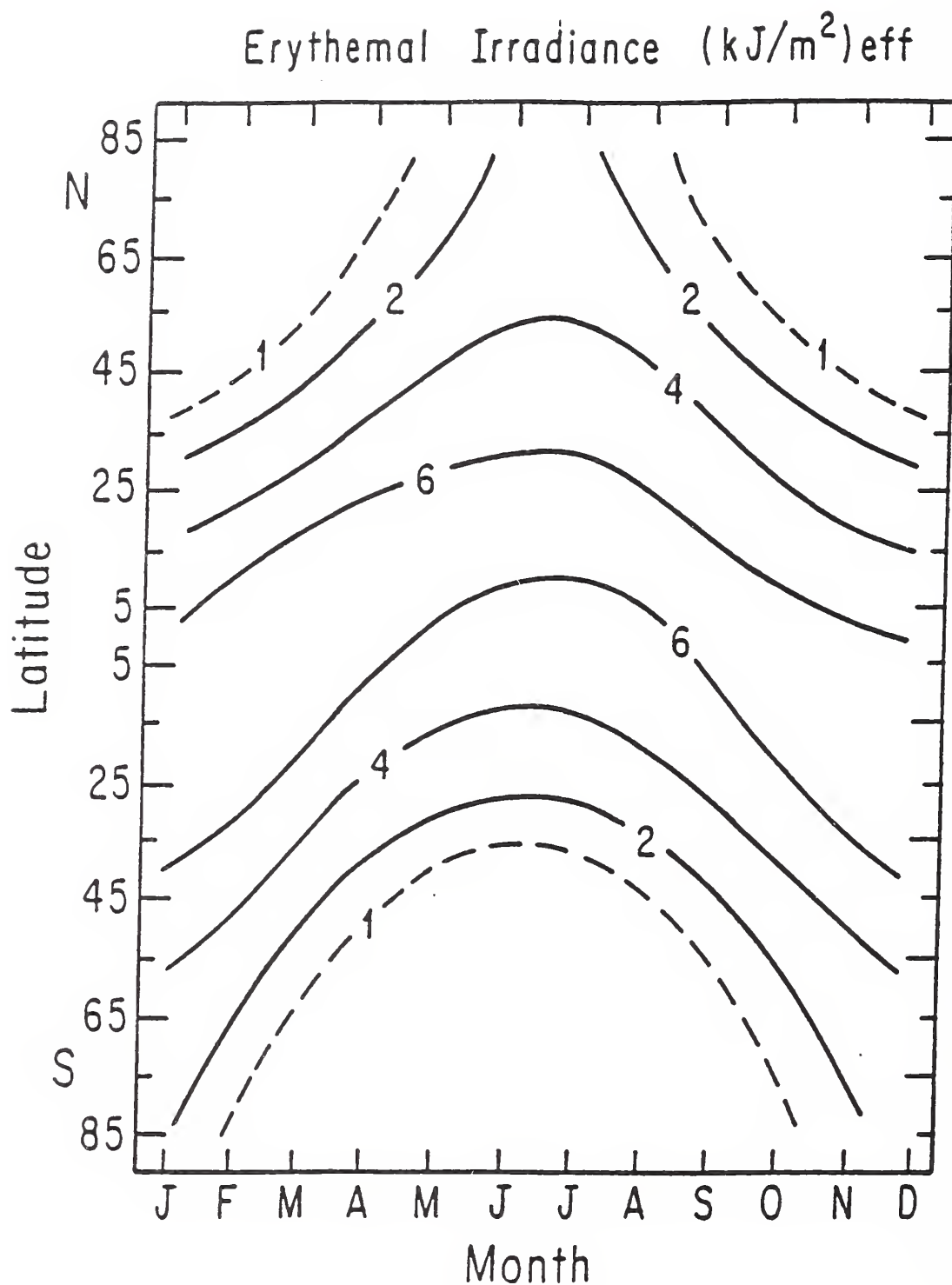


Fig. 11.10. Latitudinal and monthly distribution of daytime integrated erythematous irradiance in kilojoules per square meter of horizontal area based on TOMS zonally averaged column ozone measurements from 1980.

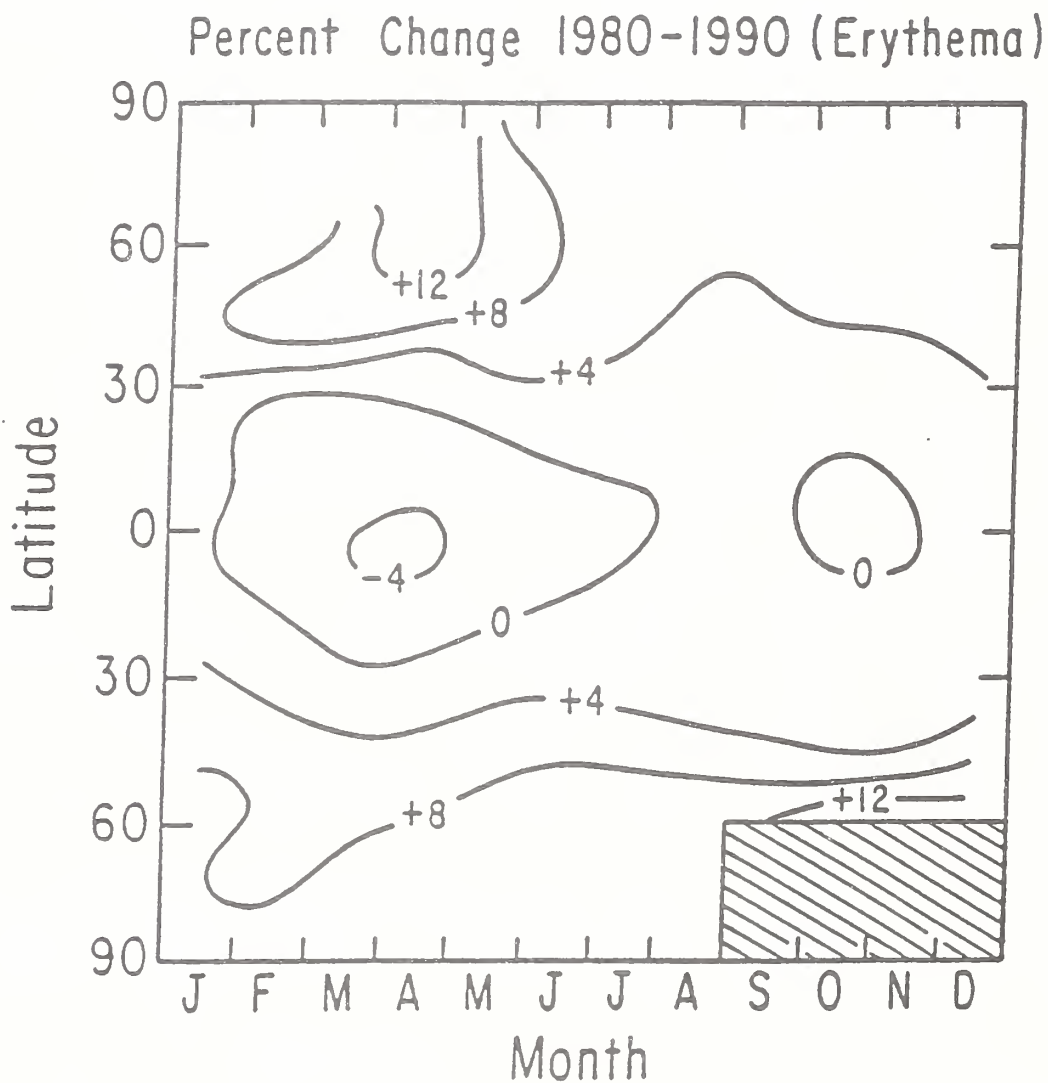


Fig. 11.11. Percentage changes in daytime integrated erythemal irradiance as functions of latitude and month based on column ozone changes measured by the TOMS instrument from 1980 to 1990.

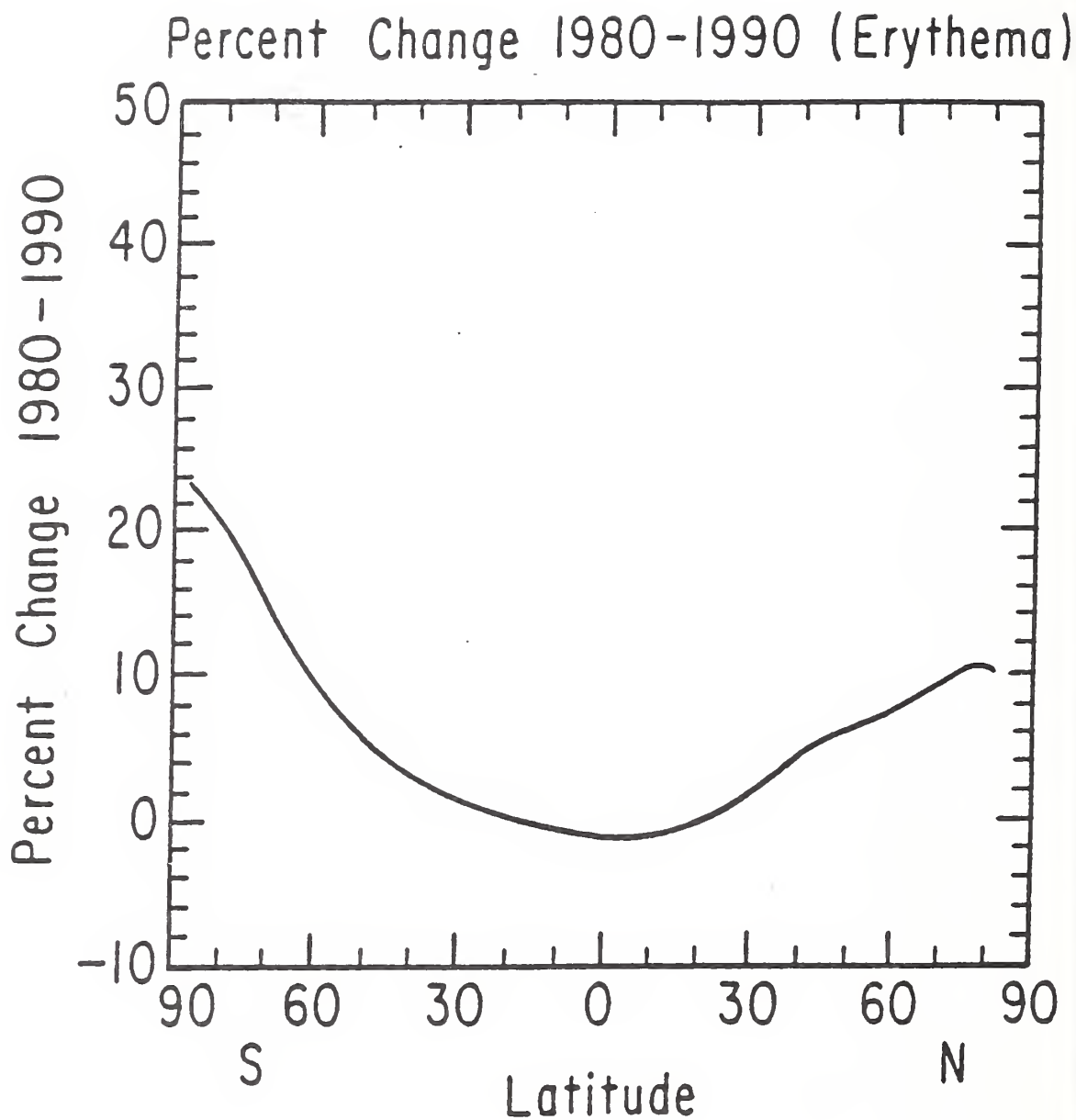


Fig. 11.12. Percentage change in annually integrated erythemal irradiance between 1980 and 1990 as a function of latitude.

**Changes in Biologically Active UV Radiation
Reaching the Earth's Surface**

**Dr. Sasha Madronich
National Center for Atmospheric Research**



Review of:

UNEP 1991:

S. Madronich, L. O. Björn, M. Ilyas, and M. M. Caldwell, Chapter 1: changes in biologically active ultraviolet radiation reaching the earth's surface, in *Environmental Effects of Ozone Depletion: 1991 Update*, (J. Van der Leun and M. Tevini, eds.), United Nations Environment Programme, November 1991.

Liu et al. 1991:

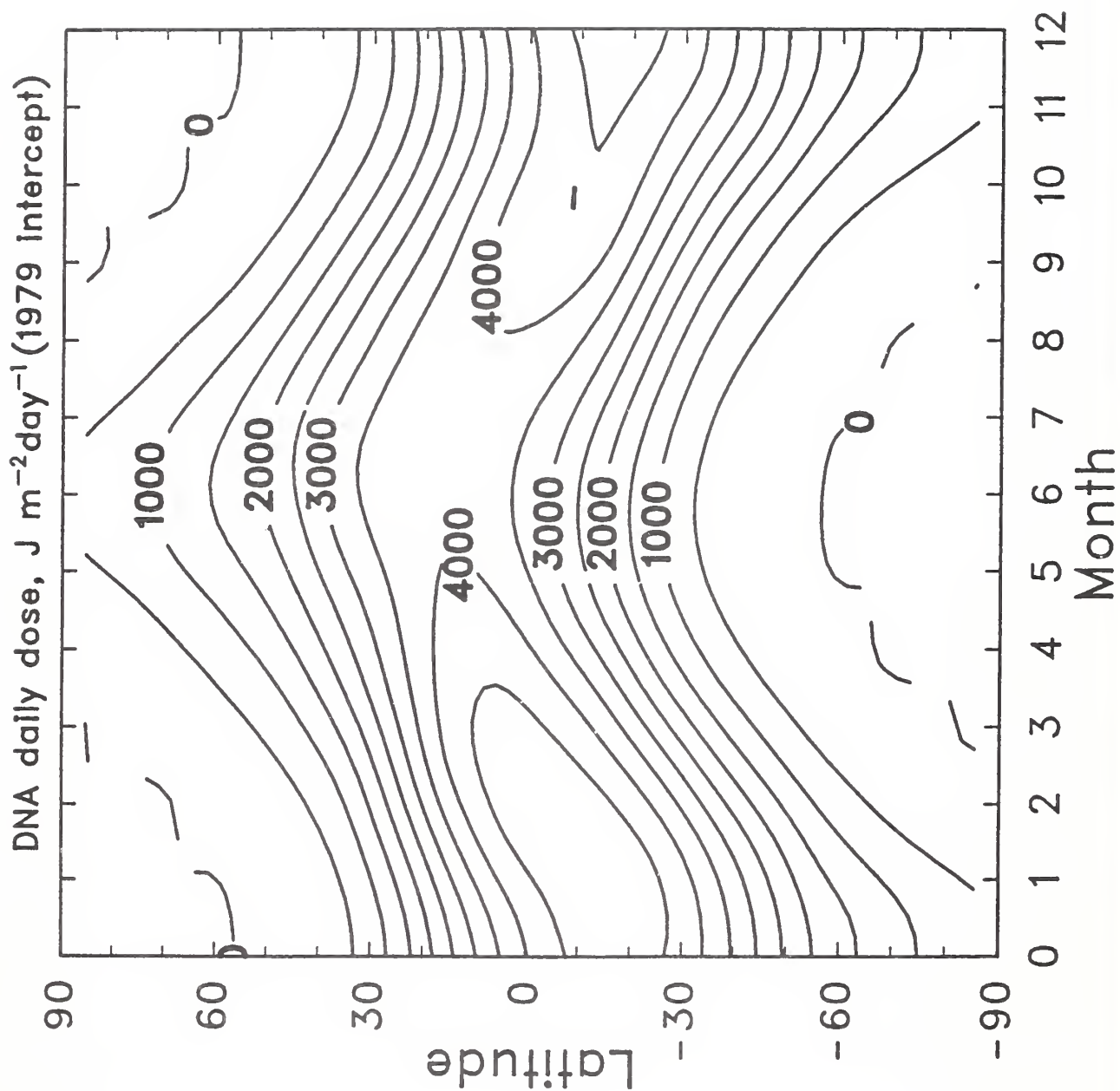
S. C. Liu, S. A. McKeen, and S. Madronich, Effect of anthropogenic aerosols on biologically active ultraviolet radiation, *Geophys. Res. Lett.*, 18, 2265-2268, December 1991.

Madronich 1992:

S. Madronich, Implications of recent total atmospheric ozone measurements for biologically active ultraviolet radiation reaching the Earth's surface, *Geophys. Res. Lett.*, 19, 37-40, January 1992.

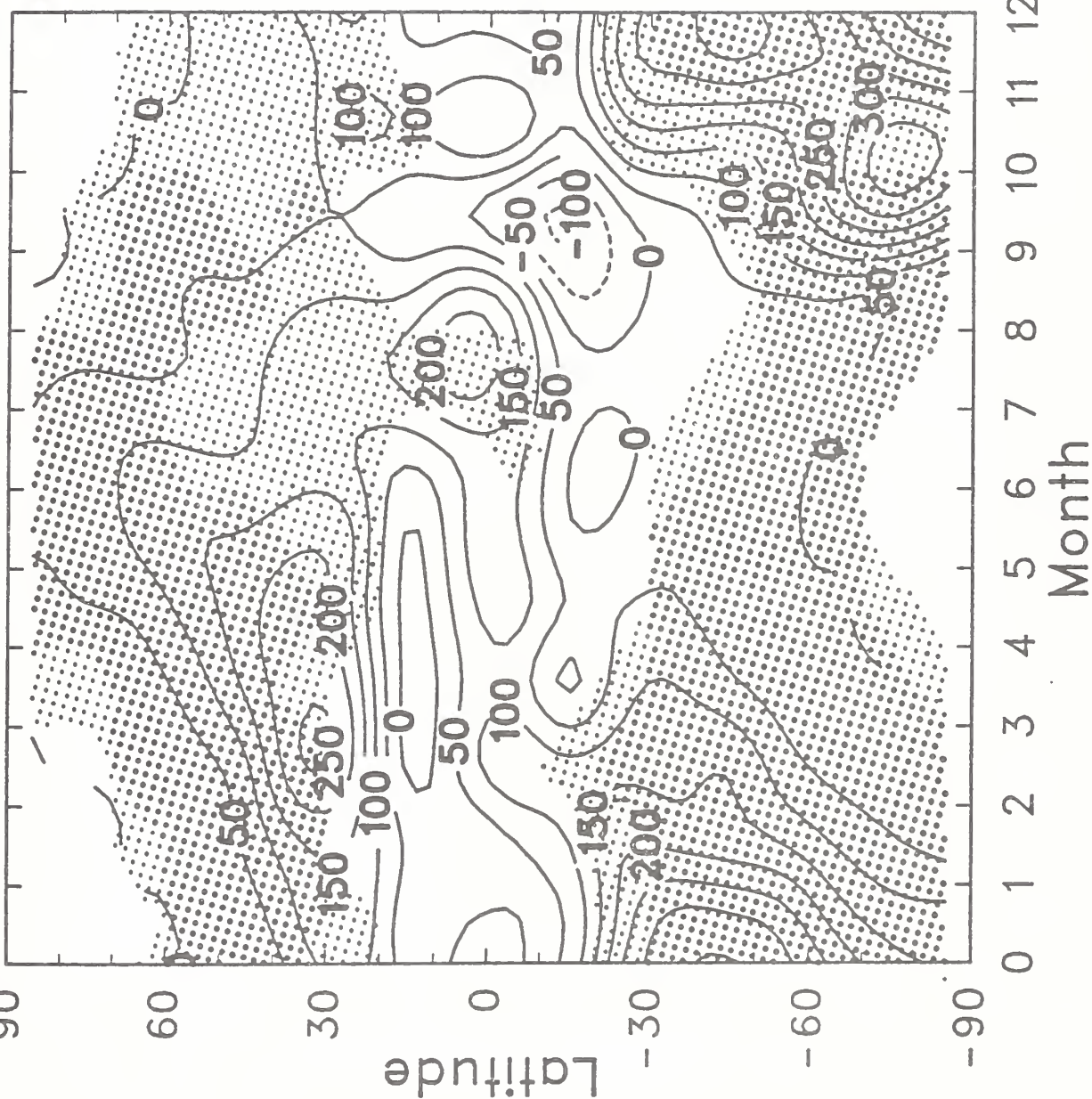
Madronich and Granier, 1992:

S. Madronich and C. Granier, Impact of recent total ozone changes on tropospheric ozone photodissociation, hydroxyl radicals, and methane trends, *Geophys. Res. Lett.*, March 1992.



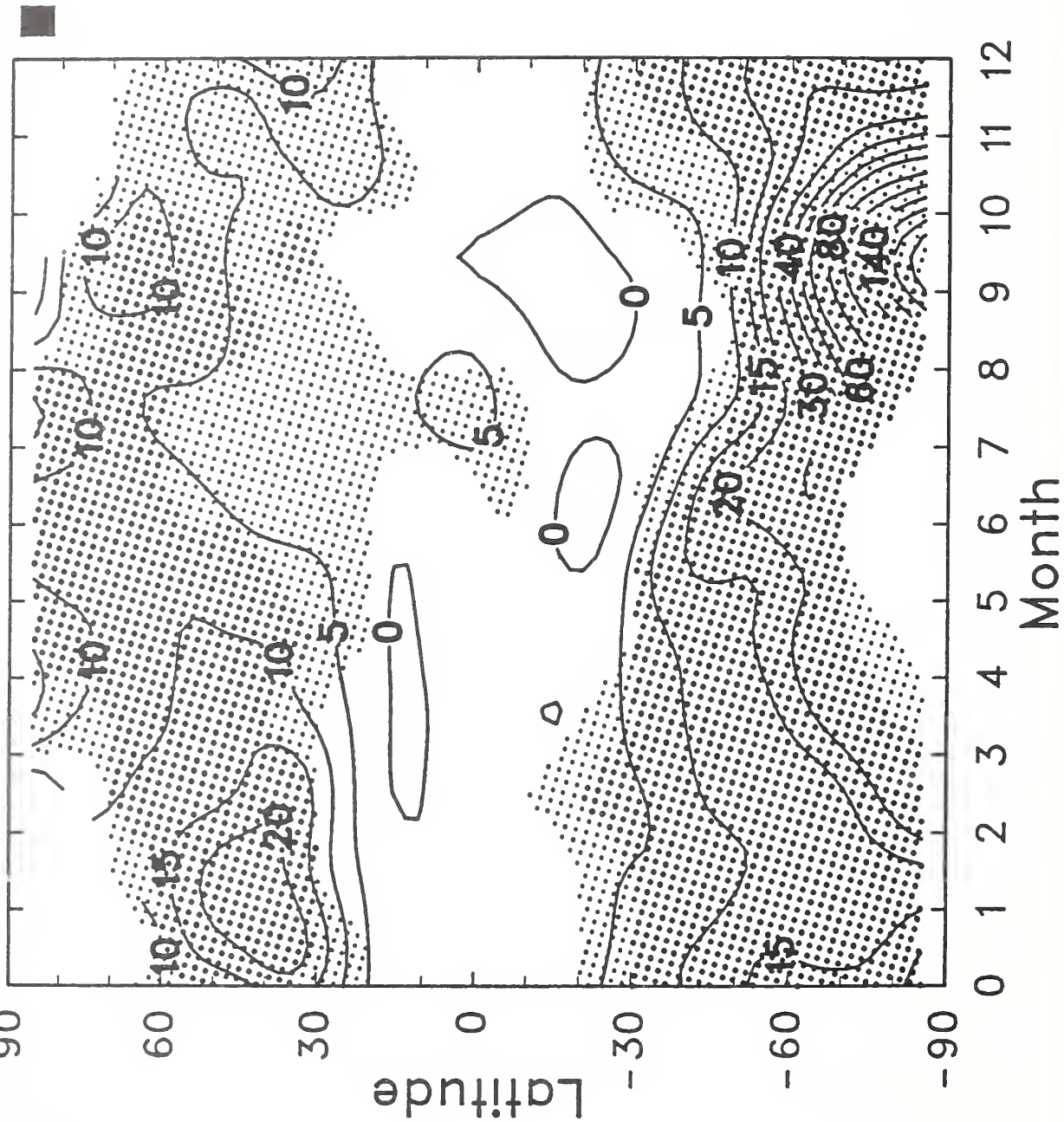
UNEP 91

DNA daily dose change, $\text{J m}^{-2}\text{day}^{-1}$ per decade (1979-1989)

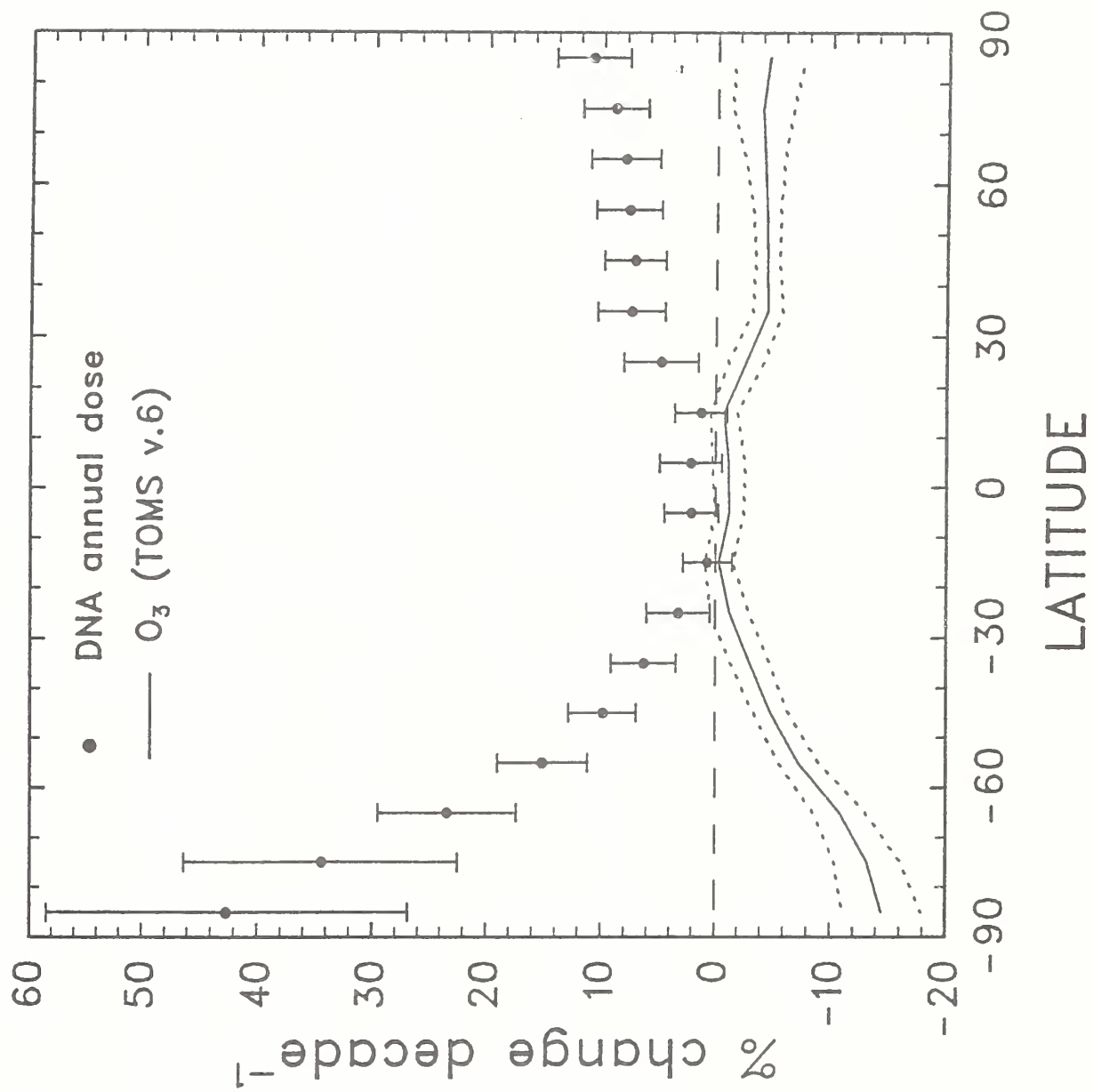


492

DNA daily dose change, $\text{J m}^{-2}\text{day}^{-1}$ per decade (1979-1989)



M92
UNIP91



UNEP 91

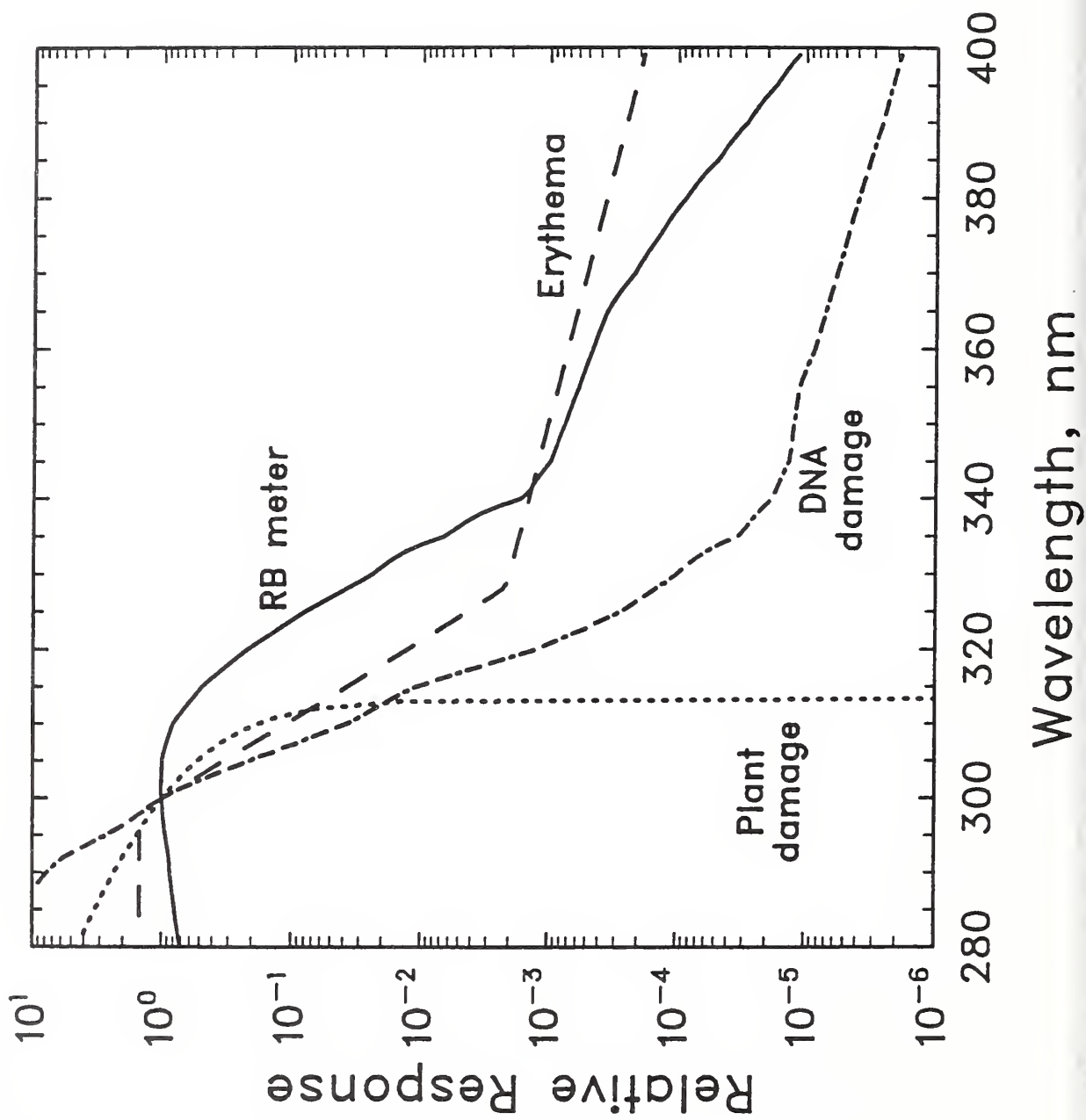


Table 1: Trends in annual integral, percent per decade, over 1979-1989.

Latitude	Total ozone	RB meter	Erythema induction	Plant damage	DNA damage
85 N	-4.5±3.0	5.1±1.5	4.7±1.4	14.8±4.3	10.1±3.2
75 N	-4.0±2.7	3.9±1.3	4.1±1.4	10.8±3.4	9.0±2.9
65 N	-4.2±1.7	3.4±1.3	4.0±1.5	8.9±3.3	8.1±3.0
55 N	-4.4±1.2	3.3±1.2	4.0±1.5	8.1±3.0	7.7±2.9
45 N	-4.5±1.0	3.1±1.0	4.0±1.4	7.2±2.6	7.2±2.7
35 N	-4.5±1.3	3.0±1.1	4.3±1.6	7.0±2.7	7.5±3.0
25 N	-2.7±1.6	1.8±1.1	2.8±1.9	4.2±2.8	4.8±3.3
15 N	-0.7±1.2	0.5±0.8	0.8±1.4	1.1±1.9	1.3±2.3
5 N	-1.2±1.4	0.8±1.0	1.3±1.6	1.8±2.3	2.2±2.7
5 S	-1.2±1.3	0.8±0.8	1.3±1.4	1.8±2.0	2.1±2.4
15 S	-0.3±1.2	0.2±0.8	0.4±1.3	0.6±1.8	0.7±2.2
25 S	-1.2±1.7	1.0±1.1	1.8±1.7	2.7±2.5	3.3±2.8
35 S	-3.1±1.7	2.3±1.1	3.5±1.6	5.6±2.6	6.3±2.9
45 S	-4.9±1.5	3.7±1.1	5.3±1.6	9.3±2.8	9.9±3.0
55 S	-7.3±1.7	6.0±1.5	7.7±1.9	15.4±4.0	15.1±3.9
65 S	-10.8±2.2	9.5±2.3	11.4±2.8	25.4±6.6	23.4±6.1
75 S	-13.2±2.8	12.8±3.9	15.0±4.8	39.0±13.4	34.4±11.9
85 S	-14.5±3.4	15.6±5.1	16.8±5.7	53.9±20.2	42.7±15.8

Uncertainties are one standard deviation.

M 92

Table 1.1 Radiation Amplification Factors (RAFs) at 30°N.

Effect	RAF		Reference
	January	July	
DNA Related			
Mutagenicity and Fibroblast killing	[1.7] 2.2	[2.7] 2.0	Zölzer and Kiefer, 1984; Peak et al., 1984
Fibroblast killing	0.3	0.6	Keyse et al., 1983.
Cyclobutane pyrimidine dimer formation	[2.0] 2.4	[2.1] 2.3	Chan et al., 1986.
(6-4) photoproduct formation	[2.3] 2.7	[2.3] 2.5	Chan et al., 1986.
Generalized DNA damage	1.9	1.9	Setlow, 1974
HIV-1 activation	[0.1] 4.4	[0.1] 3.3	Stein et al., 1989.
Plant Effects			
Generalized plant spectrum	2.0	1.6	Caldwell et al., 1986.
Inhibition of growth of cress seedlings	[3.6] 3.8	3.0	Steinmetz and Wellmann, 1986.
Isoflavonoid formation in bean	[0.1] 2.7	[0.1] 2.3	Wellmann, 1985.
Inhibition of phytochrome induced anthocyanin synthesis in mustard	1.5	1.4	Wellmann, 1985.
Anthocyanin formation in maize	0.2	0.2	Beggs and Wellmann, 1985.
Anthocyanin formation in sorghum	1.0	0.9	Yatsushashi et al., 1982.
Photosynthetic electron transport	0.2	0.1	Jones and Kok, 1966.
Photosynthetic electron transport	0.2	0.2	Bornman et al., 1984.
Overall photosynthesis in leaf of <i>Rumex patientia</i>	0.2	0.3	Rundel, 1983.
Membrane Damage			
Glycine leakage from <i>E. coli</i>	0.2	0.2	Sharma and Jagger, 1979.
Alanine leakage from <i>E. coli</i>	0.4	0.4	Sharma and Jagger, 1979.
Membrane bound K ⁺ -stimulated ATPase inactiv.	[0.3] 2.1	[0.3] 1.6	Imbrie and Murphy, 1982.
Skin			
Elastosis	1.1	1.2	Kligman and Sayre, 1991.
Photocarcinogenesis, skin edema	1.6	1.5	Cole et al., 1986.
Photocarcinogenesis (based on STSL)	1.5	1.4	Kelfkens et al., 1990.
Photocarcinogenesis (based on PTR)	1.6	1.5	Kelfkens et al., 1990.
Melanogenesis	1.7	1.6	Parrish et al., 1982.
Erythema	1.7	1.7	Parrish et al., 1982.
Erythema reference	1.1	1.1	McKinlay and Diffey, 1987.
Skin cancer in SKH-1 hairless mice (Utrecht)	1.4	1.3	de Gruijl, 1991.
Eyes			
Damage to cornea	1.2	1.1	Pitts et al., 1977.
Damage to lens (cataract)	0.8	0.7	Pitts et al., 1977.
Movement			
Inhibition of motility in <i>Euglena gracilis</i>	1.9	1.5	Häder and Worrest, 1991.
Materials damage			
Yellowness induction in poly vinyl chloride	0.2	0.2	Andrady et al., 1989.
Yellowness induction in polycarbonate	0.4	0.4	Andrady et al., 1991.
Other			
Immune suppression	[0.4] 1.0	[0.4] 0.8	DeFabo and Noonan, 1983.
Tropospheric rate coefficient for O ₃ + hv → O ₂ + O(¹ D)	1.8	1.6	Madronich (in press), 1991.
Robertson-Berger meter	0.8	0.7	Urbach et al., 1974.

Values in brackets show effect of extrapolating original data to 400 nm with an exponential tail, for cases where the effect is larger than 0.2 RAF units.

Tropospheric Ozone

100 years ago

10 ppb

Today (industrialized regions)

20 to 40 ppb

Trends

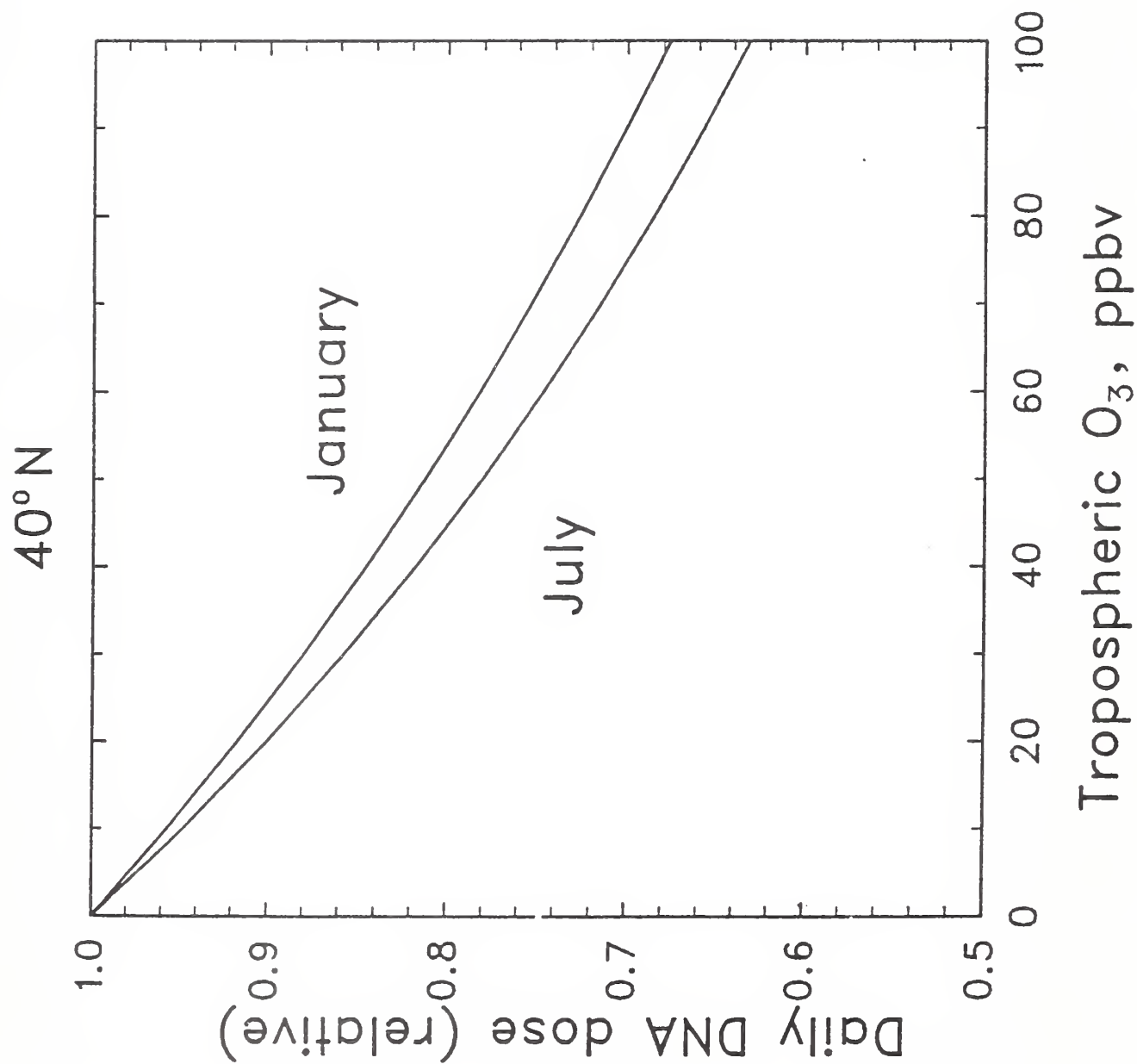
NH

+ 1% / year

SH

0 or slightly negative

UNEP 91



Univ. of

Tropospheric ozone: Effect on UV

Long term (industrialized regions) -5 to -15 %

Trends (NH) -1 to -2 % / decade

Trends (SH) 0

UNEP 91

Tropospheric Sulfate Aerosols

Ground level Visible Range at 2 % contrast

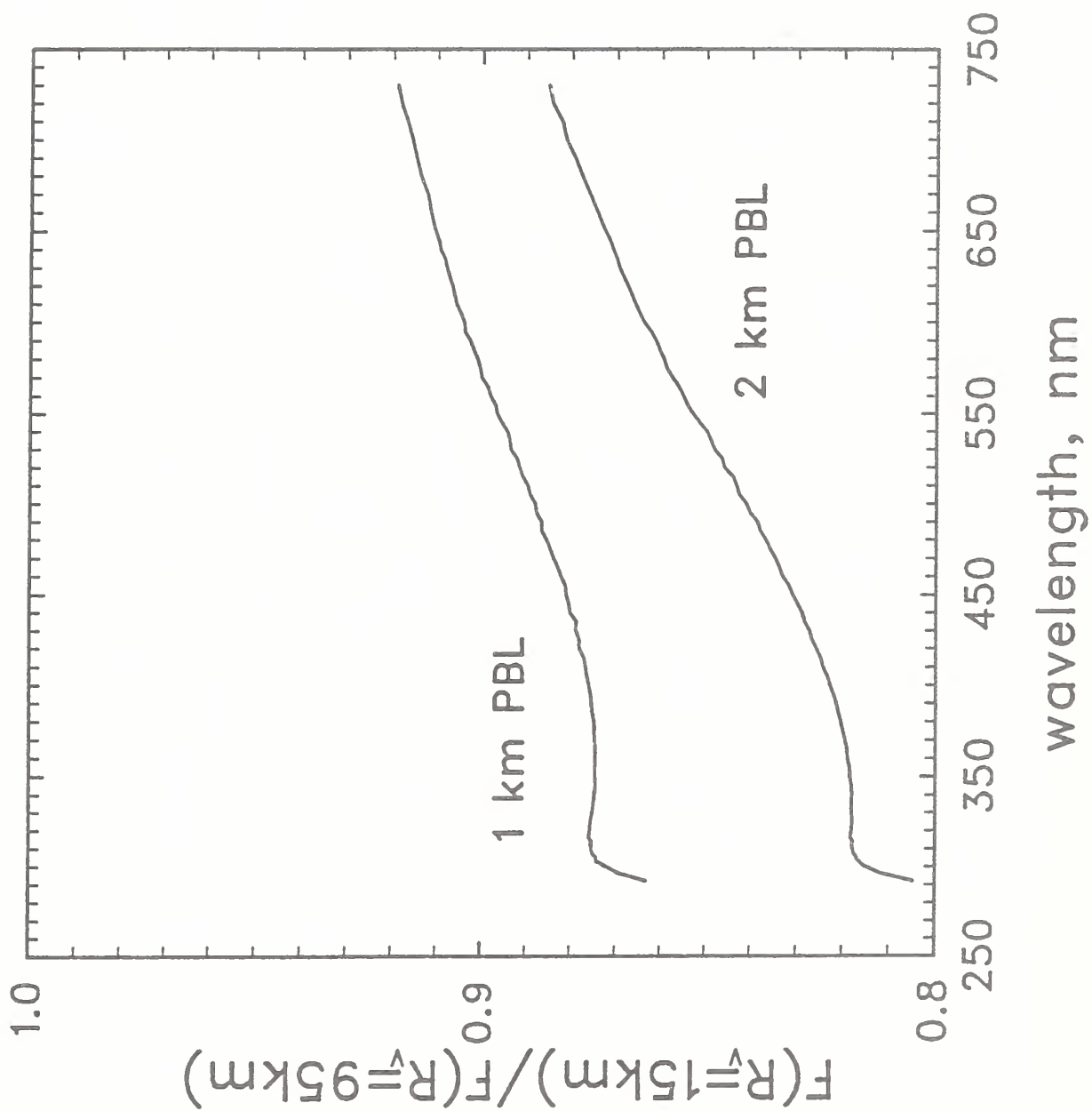
Pre-industrial visible range 95 km

Today (industrialized regions) 15 to 25 km

Trends (industrialized regions) variable

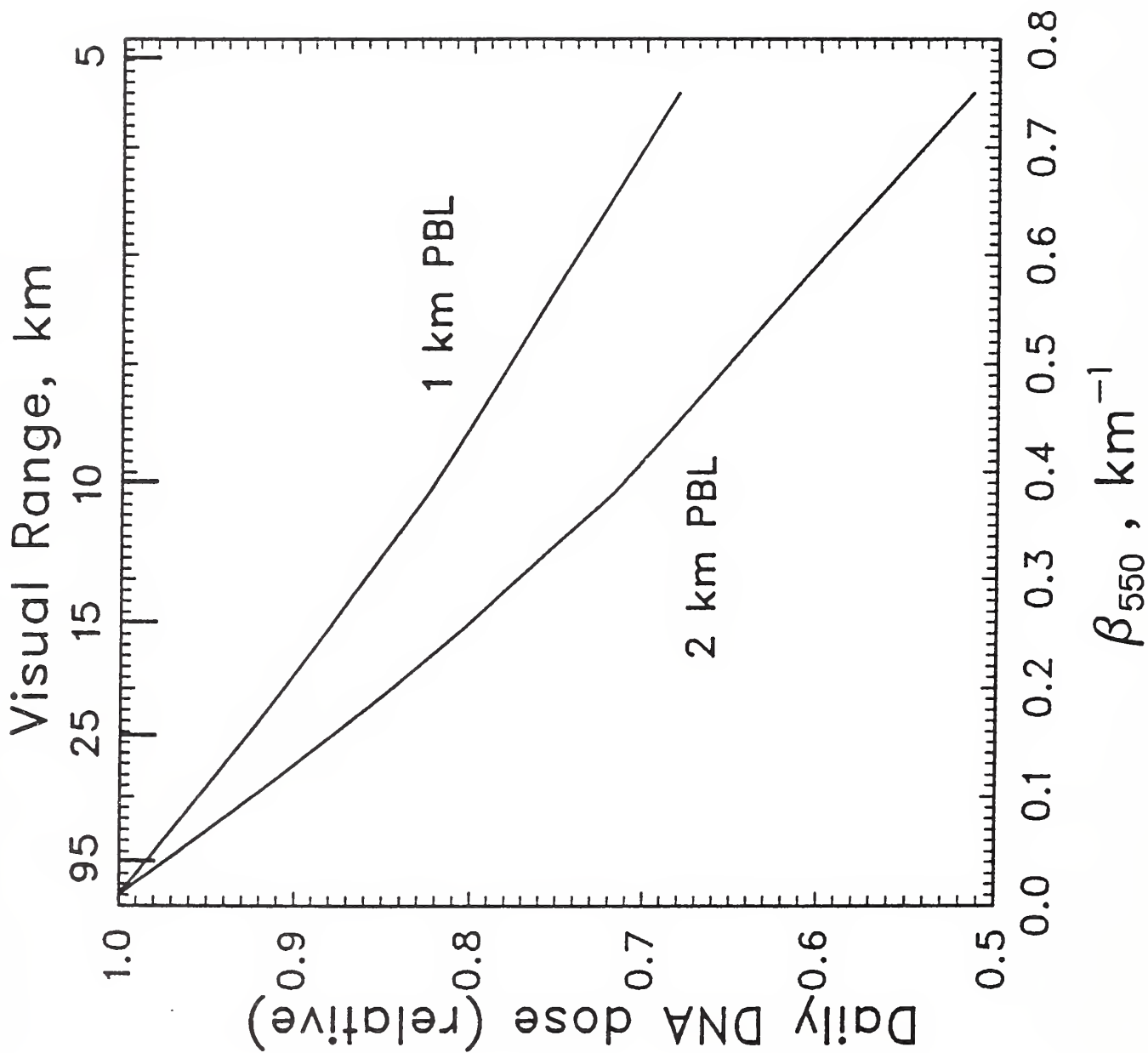
LAU 91

UNEP 91



LMM 91

WMO 91



$L_m q_1$
 $U_{WEP} q_1$

Tropospheric aerosols: Effect on UV

Long term (industrialized regions) -5 to -18 %

Trends variable

Long 91

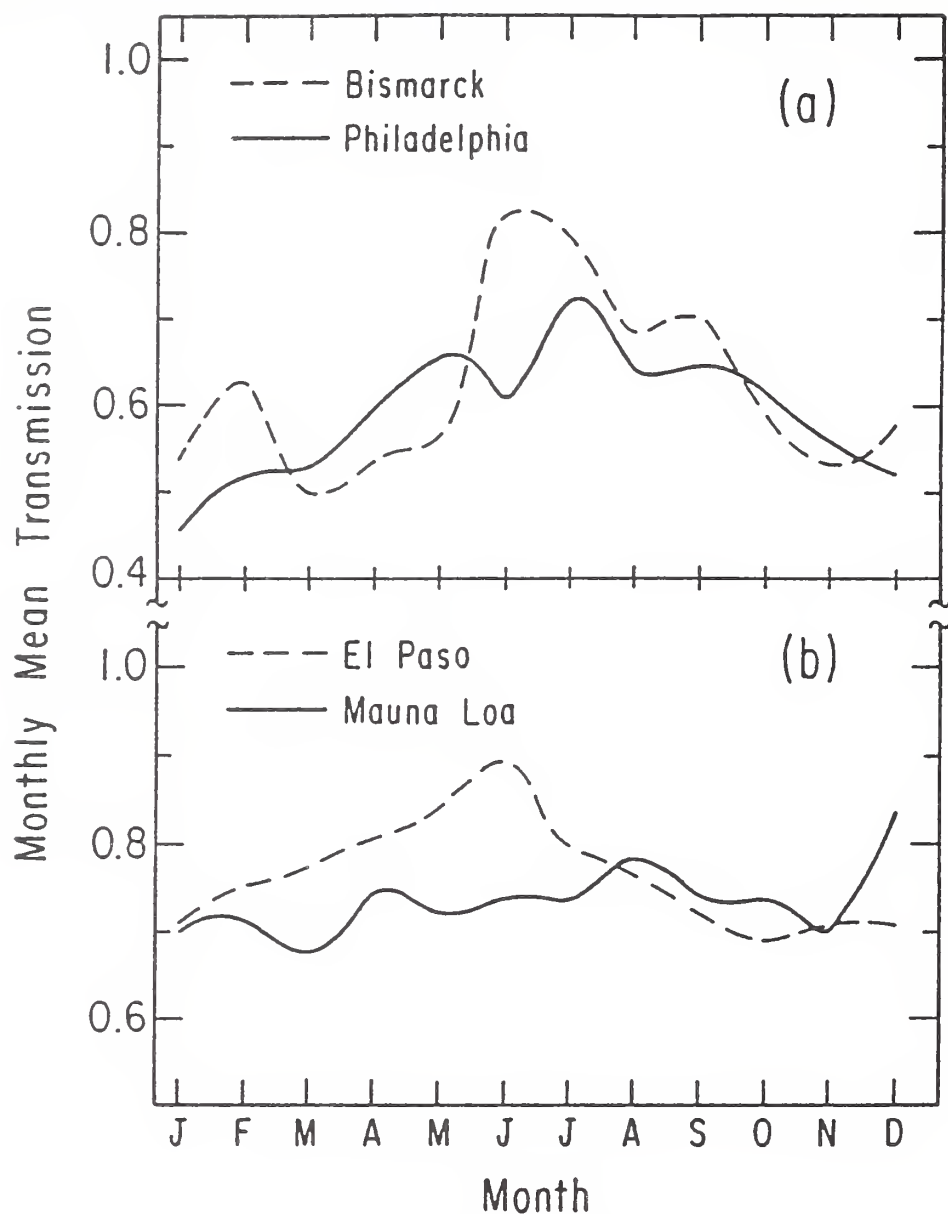


FIG. 3. Monthly mean transmissions relative to clear skies provided by cloud cover. (a) Bismarck and Philadelphia. (b) El Paso and Mauna Loa.

Reprinted from JOURNAL OF CLIMATE, Vol. 3, No. 3, March 1990
American Meteorological Society

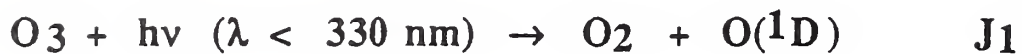
Tropospheric Influence on Solar Ultraviolet Radiation: The Role of Clouds

JOHN E. FREDERICK AND HILARY E. SNELL*

SOLAR INTERACTIONS

- Significant global scale decreases in total ozone have occurred over the past ten years.
- All other factors being constant, there is no scientific doubt that decreases in total ozone will increase UV-B radiation at ground level.
- Tropospheric ozone and aerosols may have masked the consequences of stratospheric ozone depletion for UV-B in some industrialized regions.
- It is likely that in areas remote from anthropogenic emissions, the UV-B changes due to stratospheric ozone depletion would be only partially compensated by tropospheric ozone and aerosol increases.
- There are no reliable estimates of the direction or magnitude of effects of any cloud cover trends on UV-B.
- Efforts to improve local and regional air quality may bring to light the increases in UV-B associated with the depletion of stratospheric ozone.

Effects on tropospheric chemistry



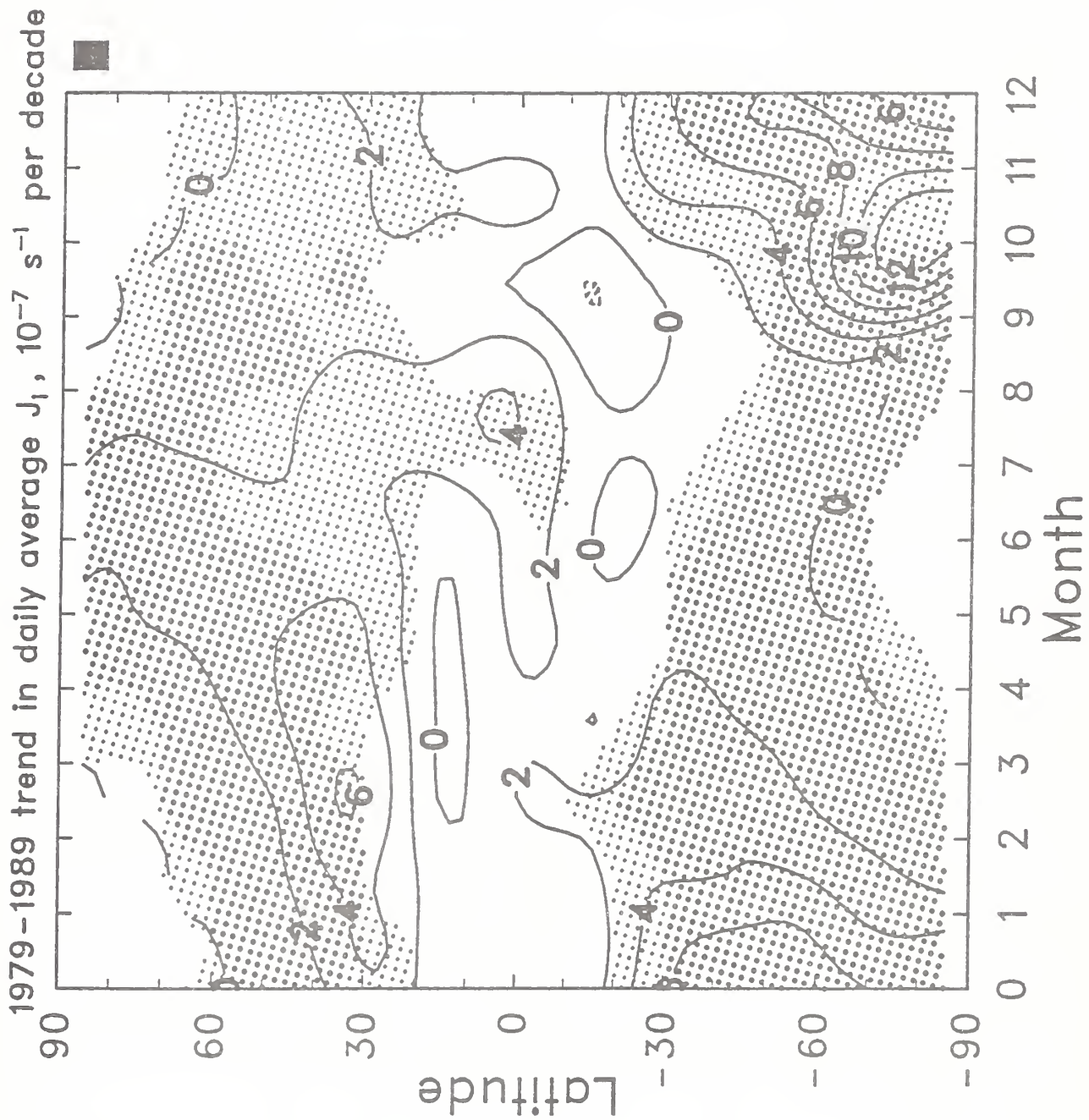
$\text{X} = \text{CO}, \text{CH}_4, \text{NHMC}, \text{NO}_2, \text{SO}_2, \text{DMS}, \text{ etc.}$

J_1 has increased (1979-1989):

NH + 3.8 ± 2.7 % /decade

SH + 4.1 ± 2.7 % / decade

MG 92



MG92

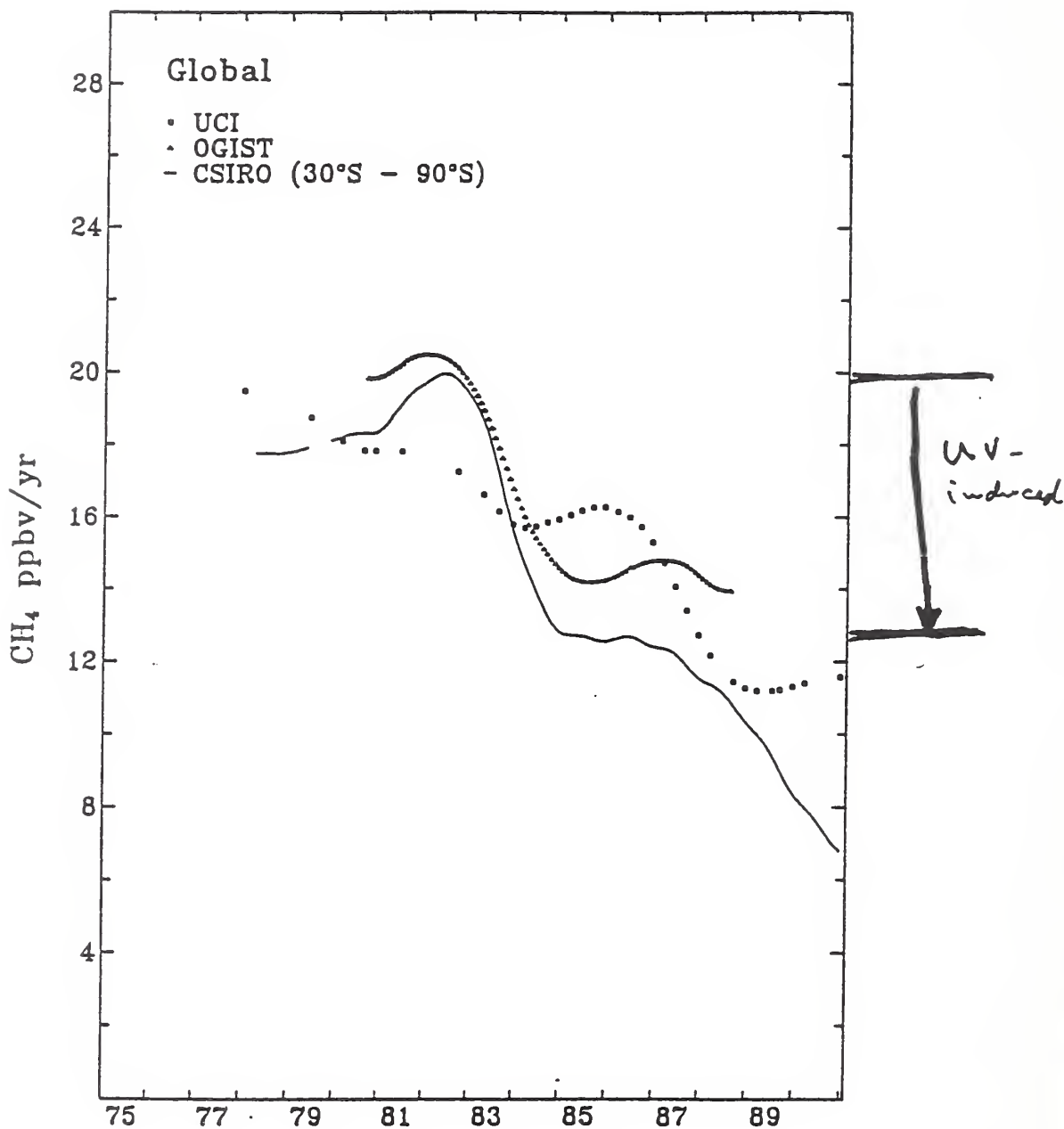


Figure 1.9. The global and Southern Hemispheric CH₄ trends from 1978-1990. The trends are obtained from spline fits to the long term CH₄ data records (Blake and Rowland, 1988, 1991; Rowland, 1990; Khalil and Rasmussen, 1990a; Fraser et al., 1986a, 1990; Fraser, 1991).

WMO91 → NG92

CHAPTER 1

CHANGES IN BIOLOGICALLY ACTIVE ULTRAVIOLET RADIATION REACHING THE EARTH'S SURFACE

*S. Madronich (USA), L.O. Björn (Sweden), M. Ilyas (Malaysia),
and M.M. Caldwell (USA)*

1991 REPORT SUMMARY

Significant global scale decreases in total ozone have occurred over the years 1979-1989. All other factors being constant, there is no scientific doubt that such decreases in total ozone will increase ultraviolet-B (UV-B) radiation (280-315 nm) at ground level. Calculations based on the measured ozone trends indicate increases in UV-B over large areas of earth. In the northern hemisphere, the annual DNA-damage weighted dose (one estimate of biologically active UV radiation) is estimated to have increased by 5% per decade at 30°N and about 10% per decade in the polar region. In the southern hemisphere, the trends are +5% per decade at 30°S, +15% per decade at 55°S, and +40% per decade at 85°S. In the equatorial region (30°S to 30°N) no statistically significant trends are found. In addition,

large UV-B increases have been directly measured during spring and early summer in the Antarctic.

UV-B penetration to the surface of the earth is also affected by tropospheric ozone, aerosols, and clouds. Increases in tropospheric ozone and aerosols since the pre-industrial era may have decreased UV-B levels in industrialized regions by amounts comparable to the increases estimated from stratospheric ozone change over the period 1979 to 1989. It is likely that, in areas remote from anthropogenic sources of aerosols and other precursors of tropospheric ozone, the calculated UV-B changes due to stratospheric ozone decreases would be only partially compensated by the possible effect of clouds. There are no reliable estimates of the direction or magnitude of the effect of any cloud cover trends on UV-B.

1989 REPORT SUMMARY

With the depletion of the ozone layer, the atmosphere becomes more transparent to solar ultraviolet radiation. Only a certain type of ultraviolet radiation is affected, that in a wavelength range of 280 to 315 nm, which is called UV-B radiation. Both the intensity and quality (wavelength composition) of the UV-B are affected by changes in ozone; the intensity increases and the wavelength composition is shifted to proportionately more radiation at shorter wavelengths. These changes must be evaluated with respect to biological responses and other phenomena affected by increased UV-B because these effects are usually very dependent on the quality of the UV-B. This is done by computing changes in "effective UV-B."

Concern about ozone reduction revolves around ozone in the stratosphere where most of the total atmospheric ozone resides (ca. 90+%). Ozone in the troposphere may be increasing, at least in local urban areas. For filtering sunlight, it is the total ozone column that is important. Thus, the net change of ozone in the upper and lower atmosphere is of consequence. In addition to ozone, effective UV-B is affected by the position of the sun in the sky (solar elevation angle) and cloud cover. Even without changes in the ozone layer, there are strong seasonal and latitudinal differences in effective UV-B. Under cloudless skies, the UV-B is much more intense in the summer months than during other seasons, and, at any time of the year, it is much stronger at lower than higher latitudes.

Apart from the Antarctic ozone hole, there have already been general reductions in stratospheric ozone. Using ozone layer thickness data from satellite observations, computations show that effective UV-B on clear days should have increased by as much as 10% at temperate latitudes during the cooler months of the year. The absolute increments of effective UV-B at tropical and temperate latitudes during the warmer months are calculated to be at least as great as the increased UV-B associated with the Antarctic ozone hole.

INTRODUCTION

Reductions in stratospheric ozone due to anthropogenic influences may allow the penetration of more UV-B radiation (280-315 nm wavelength) to the lower atmosphere and the surface of earth. UV-B radiation affects many chemical and biological processes. Its potential increases are of considerable concern, as UV-B has adverse effects on living tissue. Since the publication of the 1989 United Nations Environmental Programme report on the effects of stratospheric ozone depletion [UNEP, 1989], new information has become available on the changes in the composition of the atmosphere and the interpretation of the new data. There have also been some significant revisions of previously reported measurements.

The modification of UV-B by known changes in stratospheric ozone is, in principle, well understood, because the ozone absorption spectrum has been measured with sufficient accuracy [DeMore *et al.*, 1990]. Geometric parameters, such as variations in the earth-sun distance and the angle of incidence of solar radiation at the top of the atmosphere (a function of time of day, year, and latitude) are easily calculated. The theory behind the absorption and scattering of radiation is well established, and atmospheric transmission is easily computed for idealized conditions (horizontally homogeneous gas phase atmosphere of known composition). The dependence of surface UV-B on these simple parameters was reviewed in the earlier UNEP Report [UNEP, 1989; see also Dahlback *et al.*, 1989; Frederick *et al.*, 1989; Moan *et al.*, 1989]. Figure 1.1 shows the resulting latitudinal and seasonal distribution of surface UV-B radiation weighted by the DNA action spectrum.

Other environmental factors known to affect the UV-B levels include surface reflections, clouds, aerosols, and various tropospheric pollutants. These factors tend to be highly variable in both space and time, and may account for some of the conflicting trends in the few available long-term observational records of

Predictions of increased UV-B associated with computed ozone reductions over the century period from 1960 to 2060 are shown for two scenarios of CFC release rates. The first is for CFC release as permitted by the Montreal Protocol agreements. The second scenario involves a more stringent control whereby CFC release is reduced to 5% of the levels of the first scenario by the year 2000 and held constant thereafter. The second scenario results in increased effective UV-B levels that are less than half the values computed for the first scenario.

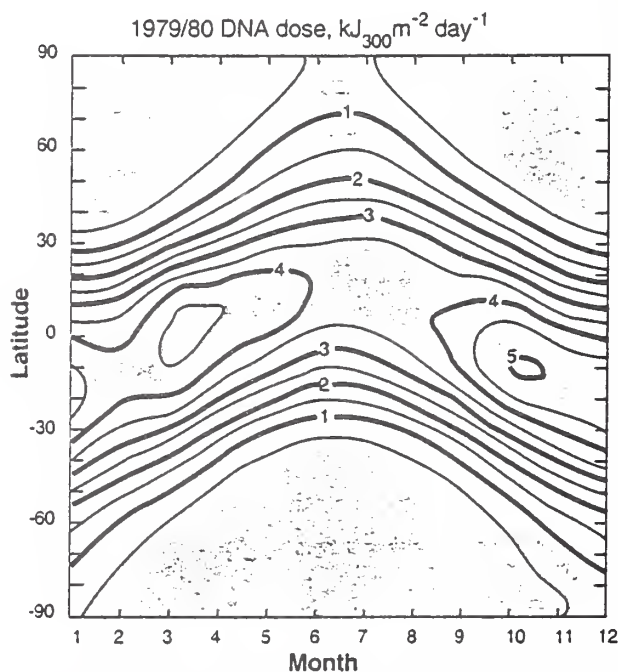


Figure 1.1 Daily effective UV-B dose, illustrated for DNA damage [Setlow, 1974], computed for cloudless skies using TOMS ozone column data for the years 1979 and 1980.

UV-B radiation. The potential effects of these environmental factors were acknowledged in the earlier report [UNEP, 1989], but no quantitative estimates were made at that time.

This update to the 1989 UNEP Report addresses the changes in UV radiation resulting from new total ozone measurements, as well as from possible long-term changes in tropospheric ozone, aerosols, and clouds. Of particular interest are the possible trends in tropospheric pollutants, to the extent that these may partially offset or supplement the UV-B increases due to stratospheric ozone reduction. Most of the UV-B estimates are made on the basis of the spectral dependence of DNA damage proposed by Setlow [1974]. Therefore, we have also included, for comparison, a compilation of the sensitivity to ozone changes for several other biological and chemical photo-processes.

RECENT MEASUREMENTS OF UV RADIATION TRENDS

At the present time, there are insufficient direct measurements of UV-B at the earth's surface available for constructing a global climatology, or to estimate long-term trends on extended geographic scales. Problems in obtaining reliable climatology measurements and trends include (1) the ambiguities in constructing a detector which fairly represents the sensitivity of different biological and chemical targets (with different wavelength dependencies, and sensitivity to different orientations), (2) the difficulties of maintaining accurate field instrument calibrations over a period of many years, (3) the practical limitations in the deployment of a global monitoring network, especially with the potential for bias from locally polluted areas, and (4) the absence of a baseline, long-term, historical UV record.

The most comprehensive UV data are from the Robertson-Berger (R-B) meter network of 25 United States stations and 11 non-U.S. stations, with varying lengths of operation [Cotton, 1990]. In the United States, the R-B meter measurements of integrated, annual UV radiation decreased from 1974 to 1985, between 0.5% and 1.1% per year [Scotto et al., 1988]. Aside from possible problems in the long-term calibration of the R-B meters, this result was seen as somewhat surprising in view of stratospheric ozone depletion. Grant [1988] suggested that local pollution may have accounted for the decrease, since the R-B meters operated mostly in urban and near-urban sites. In the Soviet Union, Garadzha and Nezval [1987] found a 12% decrease in the R-B meter measurements of UV radiation in Moscow between 1968 and 1983, with a concurrent 15% increase in turbidity, and a 13% increase in cloudiness. R-B meter data obtained at a station in the Swiss Alps (3.6 km above sea level) showed increases of $0.7 \pm 0.2\%$ per year between 1981 and 1989 [Blumthaler and Ambach, 1990].

Detailed spectral irradiance measurements are being made at a few locations [Stamnes et al., 1988; Henriksen et al., 1989a, 1989b; Bittar and McKenzie, 1990; Henriksen et al., 1990; Stamnes et al., 1990; Lubin et al., 1991], but the geographical coverage and time span of these measurements are too small to extract statistically significant UV distribution and trend information. However, the spectral measurements provide useful platforms for the validation of radiative transfer models that are used to calculate UV radiation under a variety of conditions. For example, measurements at the McMurdo and Palmer stations in Antarctica clearly demonstrated the enhancement of UV radiation under the springtime ozone holes of 1988,

1989, and 1990 [Stamnes et al., 1990; Lubin et al., 1991]. Furthermore, increased UV levels were detected in Melbourne in December 1987, concurrent with the reduced ozone levels thought to be associated with the break-up of the polar vortex in the late spring [Roy et al., 1990].

There is also direct observational evidence for global-scale change in the relative intensity of different wavelengths inside the UV-B range. This information is available from the Dobson ozone measuring instruments, and is essentially the raw data from which ozone columns and their long-term trends are derived [Bojkov et al., 1990].

OZONE-RELATED CHANGES

Since October 1978, measurements of the vertical ozone column over the globe have been made from the Total Ozone Mapping Spectrometer (TOMS) aboard the Nimbus 7 satellite. The TOMS monitors solar radiation reflected from the atmosphere at four UV wavelengths, and the amount of ozone present is calculated from the ratio of the radiation measured at different wavelengths. Due to difficulties in correcting for the progressive deterioration of optical components, the TOMS ozone trends derived previously [WMO, 1988; WMO, 1989; UNEP, 1989] have been recently re-examined. Herman et al. [1991] have developed a new correction procedure based on an internally self-consistent calibration with different wavelength pairs. The revised TOMS ozone column data (version 6) are now in agreement with standard measurements (overpass comparisons with the ground-based Dobson standard instrument No. 83).

The revised TOMS data have been analyzed statistically by Stolarski et al. [1991] for the 11.6 year period between November 1978 and May 1990. The integrated ozone column between latitudes 65°S to 65°N was found to have decreased by 3%, at a rate of change of $-0.26 \pm 0.14\%$ per year, after eliminating the effects of the 11 year solar cycle (1.5% variation in ozone over the cycle) and the quasi-biennial oscillation (1% variation in ozone over the cycle). Statistically significant (two standard deviations, or 2σ) negative ozone trends were found southward of 30°S at all times of the year, between 30°N - 60°N in the winter and spring, and between 50°N - 60°N in the summer. The strongest declines were observed in the Antarctic spring (-2.0% to -3.0% per year), and at latitudes 40°N - 50°N in the late winter (-0.8% per year). The decreases in the southern mid- and high- latitudes seem to be explained by the heterogeneous chemistry in the polar vortex, and the subsequent break up of the vortex and mixing of ozone-poor air to lower latitudes.

Dobson measurements in the northern hemisphere [Bojkov *et al.*, 1990] show weaker trends than the TOMS data. Because of the different geographical coverage and time records (1970-1986 for Dobson data and 1978-Present for TOMS data), a direct comparison between these two data sets is not possible, especially in view of the increasing anthropogenic gas trends and the associated non-linearities of the atmospheric chemistry. The relative importance of recent trends has been demonstrated by Frederick *et al.* [1991], who showed that in the latitude band of 40°N-52°N, UV-B trends that were estimated from Dobson measurements are significantly greater over the years 1970-1988, than during the 1957-1988 data record.

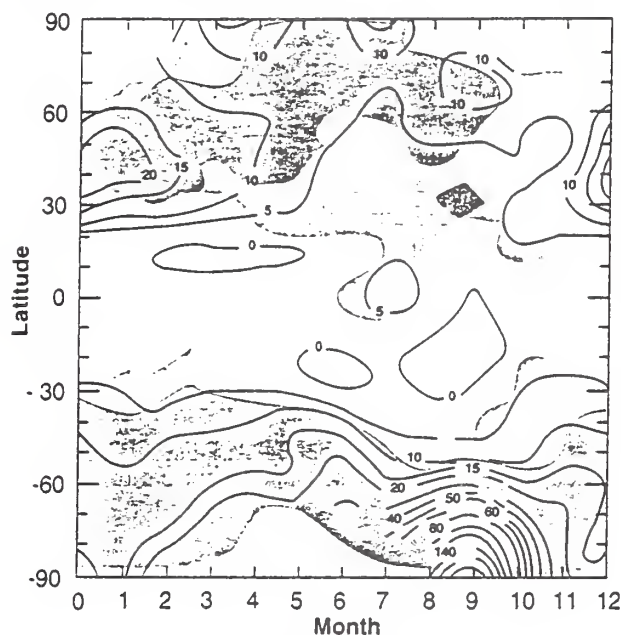


Figure 1.2 Trend in daily effective UV-B dose for DNA damage [Setlow, 1974] for cloudless skies, computed using TOMS data over the 11 year period 1979-1989, and expressed as percent per decade. White areas indicate regions of no light (polar winter) and regions where the trends are within 1 σ of zero (no trend); orange areas are within 2 σ ; green areas differ from zero by more than 2 σ [Madronich, 1991].

The revised TOMS data have recently been analyzed to estimate the trends in biologically active UV radiation [Madronich, 1991]. Daily UV doses were averaged for each month between January 1979 and December 1989, for 10° latitude increments. A linear fitting of the average daily doses for each month produced a seasonally and latitudinally dependent trend. Figure 1.2 shows the trends in surface UV radiation weighted with the generalized DNA damage spectrum of Setlow [1974]. These values, calculated for cloudless, aerosol-free conditions, show statistically significant (2 σ) increases of 5% to 20% per decade for daily doses of UV radiation in the 30°N-60°N band during late winter and early spring, 5% to 10% increases in summer poleward of 60°N, and 5% or greater

increases poleward of 30°S from spring to late fall. The strong enhancement of UV-B radiation under “ozone hole” conditions in the Antarctic spring is apparent. No statistically significant trends are seen in the tropics. However, it should be noted that in the tropics, the UV-B radiation levels are normally higher than elsewhere, so that even small fractional changes may result in substantial increases in total UV-B doses.

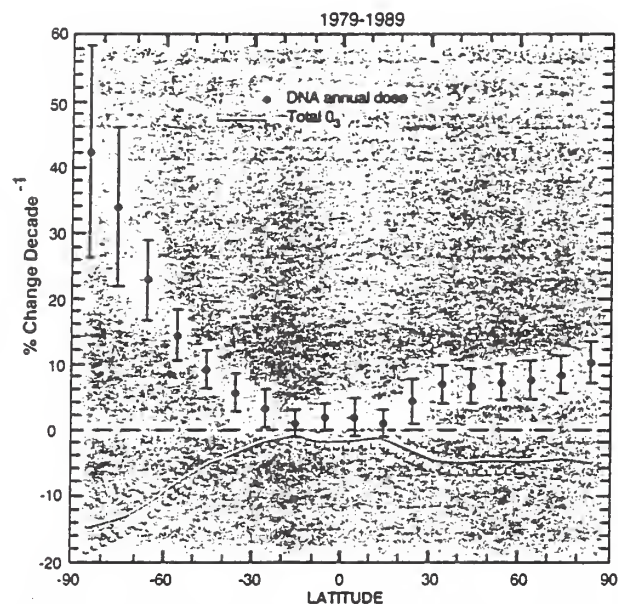


Figure 1.3 Trend in the annually integrated effective UV-B dose for DNA damage [Setlow, 1974] for cloudless skies, computed using TOMS data over the 11 year period 1979-1989, and expressed as percent per year. Also shown are the ozone column trends (solid lines) and 1 σ uncertainties (dotted lines). Zero trend is shown by dashed line [Madronich, 1991].

Cumulative yearly UV-B doses are a function of not only the annually averaged ozone column, but also of its seasonal variation of both ozone and radiation. Since the most severe ozone depletions seem to occur in the late winter and spring [Stolarski *et al.*, 1991], when unperturbed radiation levels are expected to be relatively low, it is of some interest to examine how the seasonality affects trends in cumulative annual UV-B doses. Figure 1.3 shows that statistically significant (2 σ) trends are present in both hemispheres poleward of 30°, and increase towards the pole. In the northern hemisphere, values range between 5% per decade to 11% per decade, while in the southern hemisphere values increase rapidly with latitude, from 10% per decade at 45°S to about 40% per decade at 85°S. Again, no trend is observed in the tropics.

Tropospheric ozone accounts for about one tenth of the total ozone column [WMO, 1989], but is highly variable in both time and space, making it difficult to accurately establish its current global distributions and

trends. Tropospheric ozone sources include intrusions of stratospheric air into the troposphere, and tropospheric photochemical production from nitrogen oxides, carbon monoxide, and hydrocarbons, all of which have significant natural and anthropogenic sources. High amounts of ozone have been observed in several urban areas, and on a regional scale in industrialized countries where chemical precursor concentrations are highest [Finlayson-Pitts and Pitts, 1986; Logan, 1989]. A particularly large positive trend in tropospheric ozone was reported recently by Staehelin and Schmid [1991]. Their analysis of 20 years (1969-1988) of ozone balloon soundings over Payerne, Switzerland showed significant increases in tropospheric ozone concentrations of approximately 1.4% per year at 900 mbar, 1.6% per year at 800 mbar, and 1.0% per year in the upper troposphere. The largest increments occurred in the last seven years of the data record.

In areas remote from industrial activity, tropospheric ozone concentrations are substantially lower. Typically high concentrations and increasing trends are found in the northern hemisphere, with slightly negative trends in the southern hemisphere. For example, measurements through the 1970s and 1980s by Oltmans et al. [1989] indicate increases in surface ozone of $(0.79 \pm 0.44)\%$ per year at Barrow, Alaska and $(0.78 \pm 0.42)\%$ per year at Mauna Loa, Hawaii, but decreases at Samoa of $(0.26 \pm 0.65)\%$ per year and at the South Pole of $(0.46 \pm 0.37)\%$ per year. It is still unclear whether the trends in remote measurements reflect increased photochemical production in the troposphere or fluctuations in transport from the stratosphere or other latitudes.

The trends in tropospheric ozone add to the uncertainty of the TOMS total ozone column data, since the TOMS does not fully detect tropospheric ozone [Klenk et al., 1982]. It is unclear how much of the tropospheric trend is convolved in the total ozone trends derived from TOMS data. Stolarski et al. [1991] used an assumed 50% efficiency for tropospheric ozone detection to estimate that the tropospheric trend detected by Staehelin and Schmid [1991] is small compared to the trend in total ozone (about 1/10 of the total ozone column trend in winter at 45°N, and about 1/20 in summer).

Tropospheric ozone can contribute to the UV-B optical depth of the atmosphere by absorbing radiation transmitted through the stratosphere. The computation of the effect of tropospheric ozone is complicated by the fact that 50% to 100% of the UV-B radiation reaching the lower troposphere is diffuse, due to scattering by air molecules (Rayleigh scattering). Brühl and Crutzen [1989] have pointed out that this scattering changes the average photon pathlength through tropospheric ozone.

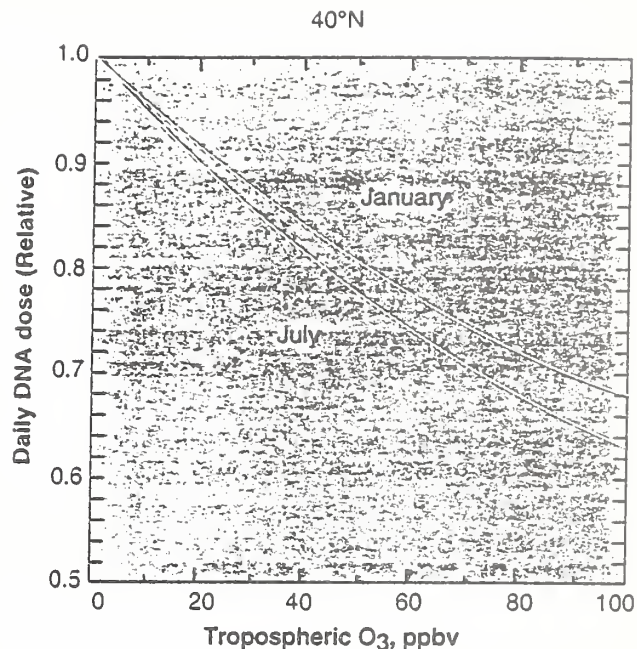


Figure 1.4 Effect of tropospheric ozone on daily UV-B dose for DNA damage [Setlow, 1974] by tropospheric ozone, calculated assuming a constant ozone mixing ratio from sea level to 10 km.

The pathlengths for diffuse light are generally longer than those for the direct solar beam if the solar zenith angles are less than 60°. Thus, for geographical regions and seasons having prevailing zenith angles less than 60°, tropospheric ozone absorbs UV radiation more effectively than stratospheric ozone, on a molecule by molecule basis. This effect is reversed at the large prevailing zenith angles typical of polar regions and mid-latitude winters. Figure 1.4 illustrates the sensitivity of DNA daily dose rates to tropospheric ozone, assuming a constant ozone mixing ratio in the troposphere between 0 and 10 km, for 40°N. The difference between the summer and winter curves is due largely to the seasonal change in prevailing zenith angles. Penkett [1989] has suggested that, based on the observed tropospheric ozone increases, on the negative R-B meter trends of Scotto et al. [1988], and on the modeling by Brühl and Crutzen [1989], UV levels may actually be decreasing in the northern hemisphere.

Figure 1.4 may also be used for obtaining an approximate estimate of the effects of tropospheric ozone changes on DNA-weighted UV-B radiation. For example, Staehelin and Schmid [1991] reported that ozone concentrations at 800 mbar have increased from around 34 ppb in 1969 to approximately 46 ppb in 1989. From Figure 1.4, the corresponding change in UV-B radiation is about -4% over this 20 year period, or -2% per decade. This value is significantly smaller than the +5% to +11% per decade increase derived from the TOMS data (see Figure 1.3), which already contains some of the tropospheric ozone trend, albeit with

reduced sensitivity. Thus we estimate that the combined trend in UV in the northern hemisphere is in the range of +3% to +11% per decade.

Longer term tropospheric ozone increases may have been significant in some industrialized regions. Volz and Kley [1988] have examined the historical record to estimate that between 1876-1910, annual average ozone concentrations at Montsouris, France were near 10 ppb, while current summer values in rural regions of industrialized countries may be 6-22 ppb higher [Logan, 1985]. From Figure 1.4 it can be estimated that this amounts to a UV-B reduction of 3%-10% at such industrialized locations. However, it is unknown whether such large reductions also apply to remote regions of the troposphere.

AEROSOL-RELATED CHANGES

The tropospheric aerosol content of the atmosphere has been identified as a major factor in determining the amount of radiation reaching urban and suburban areas [UNEP, 1989], and has been invoked qualitatively to explain negative trends in UV radiation at some urban locations [Garadzha and Nezval, 1987; Grant, 1988]. A recent study by Liu et al. [1991] suggests that aerosols may have caused substantial reductions of UV radiation on a much larger geographical scale in industrialized countries. Estimates of the mean annual average visual

range, measured horizontally at 550 nm, show a decrease from about 95 ± 45 km in pre-industrial times (background), to 15-25 km in the mid-1970s, for rural regions of the eastern United States and western Europe. Most of this aerosol consists of sulfate particles produced by atmospheric photo-oxidation of anthropogenic SO_2 emissions. SO_2 emissions in the United States have generally increased from the beginning of this century through the 1950s and 1960s. In more recent times, they have remained relatively steady or have declined in some regions, while continuing to increase in others [NRC, 1986].

The relation between aerosol extinction, visual range, and DNA daily dose is illustrated in Figure 1.5, for mid-summer, 40°N conditions [Liu et al., 1991]. DNA dose reductions of about 6% to 18% from background radiation may have occurred due to aerosol scattering and absorption. The changes are comparable to, or larger than, the UV enhancements estimated from the TOMS ozone column measurements and the tropospheric ozone changes. This may partially explain the observed declines in UV measured with the R-B meters [Scotto et al., 1988; Garadzha and Nezval, 1987].

As with tropospheric ozone, the temporal and geographical distribution of tropospheric aerosols is highly variable, and the global climatology and trend analyses are uncertain [Kent et al., 1991]. Future trends in atmospheric aerosol loading need to be monitored carefully. Because of concern about the environmental impacts of acidic precipitation, there may be significant reductions of sulfur emissions in some regions, particularly those from coal combustion. Some of this "pollution shield" [Grant, 1988] will be removed, and the effects of stratospheric ozone depletion may become more evident in large-scale regions of industrialized countries.

Stratospheric aerosols may also change the amount of UV radiation reaching the surface of the earth. Michelangeli et al. [1991] recently studied the radiative effects of stratospheric aerosols following the 1982 eruption of El Chichón. Using an optical depth of 0.25 (measured by DeLuise et al. [1983] over Mauna Loa in the plume of this eruption), surface UV changes of +45% at 290 nm, +3% at 295 nm, -5% at 300 nm, -11% at 310 nm, -7% at 315 nm, and -6% at 320 nm were calculated. The increases at short wavelengths appear to result from photon pathlength changes in highly absorbing layers of stratospheric ozone. However, the absolute radiation reaching the surface at those wavelengths is exceedingly small. We have applied these changes to the calculation of the DNA-damage weighted dose rate under similar conditions, and find a net decrease of about -8%. This attests to the dominance

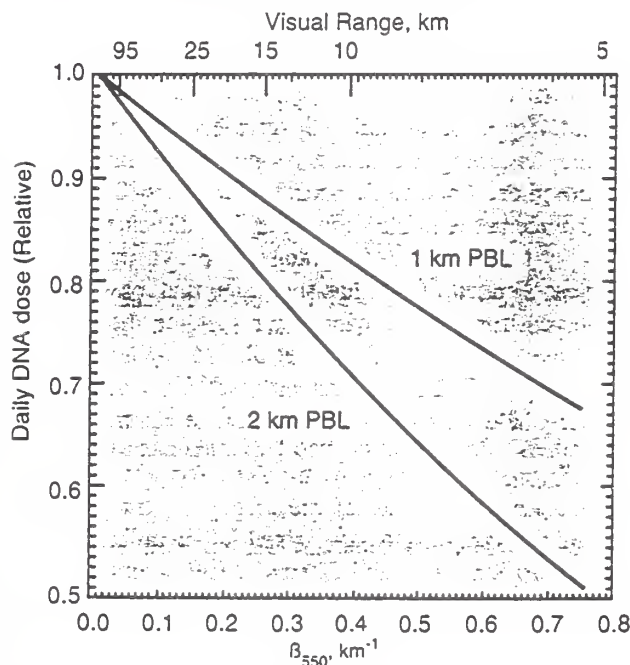


Figure 1.5 Ratio of daily DNA dose with aerosols to DNA dose in aerosol-free atmosphere (Rayleigh visual range of 386 km), for different aerosol loadings. The lower scale gives the ground-level total extinction coefficient at 550 nm, which is related to the visual range (V.R.) by the expression $\beta_{550} = 3.912/\text{V.R.}$ Results for two different planetary boundary layer heights (PBL) are shown [Liu et al., 1991].

of the ~310 nm peak response of the spectral dose rate. Volcanic aerosols tend to be distributed through the stratosphere and then decay with a time constant of between 0.5 and 1.5 years, so that the associated optical depths become much smaller [Yue *et al.*, 1991]. However, heterogeneous chemistry on the sulfate particles may impact the stratospheric ozone, particularly in the presence of chlorine. This remains a current subject of study [Hoffman and Solomon, 1989; Brasseur *et al.*, 1990], especially in view of the 1991 eruption of Mt. Pinatubo.

CLOUD-RELATED CHANGES

The effect clouds have on surface UV radiation is clearly significant. However, because cloud cover and type are highly variable, extensive averaging is required to assess their effect on UV climatology and trends. A comprehensive assessment is largely lacking at the present time, although some progress has been made in describing both temporally and spatially averaged contributions of clouds to surface UV.

The average attenuation by a complete cloud cover may range, depending on the type of cloud and the solar zenith angle, between 56% [Buttner, 1938] and 90% [Josefsson, 1986]. Parameterizations of transmission in relation to cloud type have been proposed [Haurwitz, 1948; Jones *et al.*, 1981]. Ilyas [1987] examined the dependence of measured UV-A radiation on visually estimated fractional cloud coverage at Penang, Malaysia and found an approximately linear reduction of UV with increasing cloud amount, down to 46% of the clear sky values during complete cloud cover. Frederick and Snell [1990] analyzed 1974 R-B meter readings from four United States stations, and found annual mean reductions of 27% at Mauna Loa, Hawaii, 22% at El Paso, Texas, 38% at Philadelphia, Pennsylvania, and 33% at Bismarck, North Dakota. In another study, Frederick and Lubin [1988] estimated the reduction of UV-B due to clouds based on measurements from the solar backscattered ultraviolet (SBUV) instrument aboard the Nimbus 7 satellite for July 1979. Their results suggest that the average UV reduction (relative to cloudless skies) was around 30% at 60°S and 60°N, approximately 10% at 20°S and 20°N, and near 20% at the Equator. All of these empirically-derived reductions may be dependent on the particular locations and seasons, and should be applied with some caution.

There are even greater uncertainties about how cloud distributions and optical properties will change in response to global change. Different global climate models show significantly different cloud-climate couplings [Cess *et al.*, 1989]. Cloud optical properties may be altered through changes in condensation nuclei

production by sulfates derived from natural sources, such as dimethyl sulfide from the ocean, and anthropogenic sources, such as SO₂ from coal combustion [Charlson *et al.*, 1987]. A first attempt to study the effect of cloud climate change on UV radiation was reported by Madronich [1990]. Taking results from two climate models, and using a 2°K sea surface temperature increase as a surrogate for climate change [Cess *et al.*, 1989], UV-B radiation for July was calculated to increase by 5%-10% in the regions between 45°S and 45°N, and decrease poleward of these latitudes. More recently, Bachelet *et al.* [1991] examined the predictions of three different climate models for a doubled CO₂ scenario, and used the Ilyas [1987] parameterization to estimate the effect of clouds on UV-B in rice-growing regions of South East Asia. Again, both the sign and the magnitude of the cloud changes (and therefore the UV-B changes) were model-dependent. Because of the high uncertainties in predicting future cloud changes, these results should not be regarded as predictive, but rather as indicative of the fact that substantial changes in cloud cover may affect UV radiation to an extent comparable to moderate changes in stratospheric ozone, tropospheric ozone, and aerosol loadings. Clearly more work is needed to establish the UV consequences of the current cloud climatology and trends.

RADIATION AMPLIFICATION FACTORS

The results presented so far have been expressed in terms of the generalized DNA damage spectrum of Setlow [1974]. Various biological and chemical processes have different responses to the ultraviolet spectrum (action spectra), and therefore to ozone depletion. To avoid showing analogs of *Figures 1.1* through *1.5* for each of the many processes of interests, we present in *Table 1.1* a comparison of the Radiation Amplification Factors (RAFs) for some of these processes. The RAFs are defined as the change (fractional differential) in the effective daily dose relative to the change (fractional, negative differential) in the total ozone column. For example, a 1% ozone reduction will cause an increase in fibroblast killing (second entry of *Table 1.1*) of 0.3% in January and 0.6% in July.

It should be noted that RAFs provide an indication of how the composite radiation at different wavelengths changes as filtering by ozone is altered. Thus, they are useful for assessing relative changes in potentially effective UV-B radiation. They do not, however, incorporate the absolute sensitivity of biological processes, which also depend on other factors including repair mechanisms and other environmental stresses.

Table 1.1 Radiation Amplification Factors (RAFs) at 30°N.

Effect	RAF		Reference
	January	July	
DNA Related			
Mutagenicity and Fibroblast killing	[1.7] 2.2	[2.7] 2.0	Zölzer and Kiefer, 1984; Peak et al., 1984.
Fibroblast killing	0.3	0.6	Keyse et al., 1983.
Cyclobutane pyrimidine dimer formation	[2.0] 2.4	[2.1] 2.3	Chan et al., 1986.
(6-4) photoproduct formation	[2.3] 2.7	[2.3] 2.5	Chan et al., 1986.
Generalized DNA damage	1.9	1.9	Setlow, 1974
HIV-1 activation	[0.1] 4.4	[0.1] 3.3	Stein et al., 1989.
Plant Effects			
Generalized plant spectrum	2.0	1.6	Caldwell et al., 1986.
Inhibition of growth of cress seedlings	[3.6] 3.8	3.0	Steinmetz and Wellmann, 1986.
Isoflavonoid formation in bean	[0.1] 2.7	[0.1] 2.3	Wellmann, 1985.
Inhibition of phytochrome induced anthocyanin synthesis in mustard	1.5	1.4	Wellmann, 1985.
Anthocyanin formation in maize	0.2	0.2	Beggs and Wellmann, 1985.
Anthocyanin formation in sorghum	1.0	0.9	Yatsuhashi et al., 1982.
Photosynthetic electron transport	0.2	0.1	Jones and Kok, 1966.
Photosynthetic electron transport	0.2	0.2	Bornman et al., 1984.
Overall photosynthesis in leaf of <i>Rumex patientia</i>	0.2	0.3	Rundel, 1983.
Membrane Damage			
Glycine leakage from <i>E. coli</i>	0.2	0.2	Sharma and Jagger, 1979.
Alanine leakage from <i>E. coli</i>	0.4	0.4	Sharma and Jagger, 1979.
Membrane bound K ⁺ -stimulated ATPase inactiv.	[0.3] 2.1	[0.3] 1.6	Imbrie and Murphy, 1982.
Skin			
Elastosis	1.1	1.2	Kligman and Sayre, 1991.
Photocarcinogenesis. skin edema	1.6	1.5	Cole et al., 1986.
Photocarcinogenesis (based on STSL)	1.5	1.4	Kelfkens et al., 1990.
Photocarcinogenesis (based on PTR)	1.6	1.5	Kelfkens et al., 1990.
Melanogenesis	1.7	1.6	Parrish et al., 1982.
Erythema	1.7	1.7	Parrish et al., 1982.
Erythema reference	1.1	1.1	McKinlay and Diffey, 1987.
Skin cancer in SKH-1 hairless mice (Utrecht)	1.4	1.3	de Gruijl, 1991.
Eyes			
Damage to cornea	1.2	1.1	Pitts et al., 1977.
Damage to lens (cataract)	0.8	0.7	Pitts et al., 1977.
Movement			
Inhibition of motility in <i>Euglena gracilis</i>	1.9	1.5	Häder and Worrest, 1991.
Materials damage			
Yellowness induction in poly vinyl chloride	0.2	0.2	Andrady et al., 1989.
Yellowness induction in polycarbonate	0.4	0.4	Andrady et al., 1991.
Other			
Immune suppression	[0.4] 1.0	[0.4] 0.8	DeFabo and Noonan, 1983.
Tropospheric rate coefficient for O ₃ + hv → O ₂ + O(¹ D)	1.8	1.6	Madronich (in press), 1991.
Robertson-Berger meter	0.8	0.7	Urbach et al., 1974.

Values in brackets show effect of extrapolating original data to 400 nm with an exponential tail, for cases where the effect is larger than 0.2 RAF units.

For the RAF computations, the spectral irradiance at the surface was calculated for 30°N conditions, using the 11.6 year average of the 1978-1990 TOMS ozone data, cloud-free and aerosol-free skies, 5% surface albedo, sea level, and a delta-Eddington radiative transfer scheme at 1 nm intervals over 280-400 nm. The daily dose was computed by the convolution of the spectral irradiance with the different process-specific action spectra, followed by an integration at 15 minute increments over the day. To obtain the RAFs, the calculation was repeated with 1% increments to ozone concentrations, applied equally at all altitudes. Additional details of the calculation are given in WMO [1989] where it was also shown that the RAFs are insensitive to many environmental conditions such as clouds, surface albedo, and aerosols, as long as these are maintained constant during the change in the total ozone column. Slightly different RAF values would be obtained if the total ozone column were increased by additions of stratospheric ozone or, alternatively, only the tropospheric ozone [Brihl and Crutzen, 1989]. Also, because of the non-linear nature of atmospheric transmission, the RAFs may be different for much larger changes in the ozone column.

Table 1.1 shows a large range of RAF values, from about 0.1 to about 4. While the RAFs for some processes appear reasonably established, there are significant uncertainties for others. An outstanding problem is the determination of action spectra in the long wavelength region (UV-A), since even relatively small "tails" can reduce the RAFs significantly. In compiling Table 1.1, exponential tail extrapolations were carried out in most cases, and those processes for which such extrapolation produced significant RAF decreases are shown in brackets. Also, in some cases, conflicting spectral information exists. For example, experiments on the duckweed *Wolffella hyalina* [Wan and Björn, 1991] lend support to the conclusion that the generalized plant action spectrum of Caldwell et al. [1986] is a reasonable approximation for the spectral dependence of the ultraviolet inhibition of biomass production by seed plants. On the other hand, limited data by Mitchell [1990], Holm-Hansen [1990], and Smith and Baker [1982] suggest that the action spectrum for UV inhibition of growth or photosynthetic carbon assimilation by phytoplankton is less steep, approaching the one determined by several groups for photosynthetic electron transport. Clearly, further work is needed to obtain accurate and representative action spectra.

It is important to note that RAF for R-B meters is substantially smaller than the RAFs for most of the biological and chemical processes of interest. This complicates the interpretation of some of the trends observed with R-B meters (see above). For example, if the increasing trend of +0.7% per year observed by

Blumthaler and Ambach [1990] is due to depletion of overhead ozone, the corresponding trends in biological effects may be amplified by the ratio of RAF values, e.g., +1.1% per year for erythema [McKinlay and Diffey, 1987], +1.9% per year for DNA damage [Setlow, 1974], and +1.6% per year for melanogenesis [Parrish et al., 1982]. If, however, the trends in R-B meter observations result from changes in tropospheric aerosols and cloud cover, which are only weakly dependent on wavelength, no significant RAF amplification is expected. This may be the case for the negative trends reported by Scotto et al. [1988] and Garadzha and Nezval [1987].

CONCLUSION

There is now compelling evidence that significant changes in the global-scale ozone distributions have been occurring over the past ten years. The most recent total ozone measurements (TOMS version 6) imply increases of annual DNA-damage weighted UV-B over large geographical areas of the earth. In the northern hemisphere the trends range from +5% per decade at 30°N to about +11% per decade in the polar region, while in the southern hemisphere the trends are +5% per decade at 30°S, +10% per decade at 55°S, and +40% per decade at 85°S. In the equatorial region (30°S to 30°N), trends are not statistically significant.

All other factors being constant, there is no scientific doubt that the calculated UV increases would be observed at the surface. However, other factors also affect the transmission through the atmosphere. In polluted urban and regional areas of industrialized countries, tropospheric ozone and sulfate aerosols have been generally increasing, although their variability is large and trends are difficult to estimate. Analysis of recent studies indicates that at most about 2% per decade decrease in UV-B can be expected from tropospheric ozone trends. However, large cumulative increases in tropospheric ozone and sulfate aerosols may have occurred over the last 100 years, and may have reduced the UV-B between 3% and 10% for ozone, and between 6% and 18% for sulfate aerosols in some locations. Tropospheric ozone and sulfate aerosols are believed to result primarily from human activities, and tend to be largest near industrialized and densely populated areas. Efforts to improve the air quality in these areas are likely to reduce their concentrations, and may bring to light the increases in UV-B associated with the depletion of stratospheric ozone. Furthermore, there is some concern about the fact that most of the UV monitoring is being carried out in industrialized regions of the northern hemisphere, where current UV reductions may be largest. In less industrialized regions, the atmosphere may be more transparent, but monitoring of the UV radiation is inadequate.

Tropospheric pollutants are likely to be much less important on the average global scale, and particularly in regions far from direct emissions sources. In these regions, it is expected that the depletion of stratospheric ozone will have its full impact on the UV-B radiation reaching the ground or the ocean surface. Due to the unfortunate absence of a suitable global UV-B monitoring network, no direct observational evidence is available, except in Antarctica, Australia, and New Zealand where the large springtime ozone hole and its break-up have stimulated great scientific interest. Here, measured and calculated UV-B increases are in reasonable agreement.

Future changes in cloud cover might affect the average intensity of UV-B radiation reaching the surface, by amounts comparable to that from moderate ozone and aerosol changes. At present, there are no reliable estimates of the sign or magnitude of current cloud cover trends, nor does it appear possible to make reliable predictions of the sign or magnitude of cloud cover changes which may result from anthropogenically driven climate change.

REFERENCES

- Andrady, A.L., A. Torikai, and K. Fueki, *J. Applied Polymer Sci.*, 37, 935, 1989.
- Andrady, A.L., K. Fueki, and A. Torikai, *J. Applied Polymer Sci.*, 42, 2105, 1991.
- Bachelet, D., P.W. Barnes, D. Brown, and M. Brown, Latitudinal and seasonal variation in calculated ultraviolet-B irradiance for rice-growing regions of Asia, *Photochem. Photobiol.*, 54, 411-422, 1991.
- Beggs, C.J. and E. Wellmann, Analysis of light controlled anthocyanin formation in coleoptiles of *Zea mays* L.: The role of UV-B, blue, red and far-red light, *Photochem. Photobiol.*, 41, 481-486, 1985.
- Bittar, A. and R.L. McKenzie, Spectral ultraviolet intensity measurements at 45°S: 1980 and 1988, *J. Geophys. Res.*, 95, 5597-5603, 1990.
- Blumthaler, M. and W. Ambach, Indication of increasing solar ultraviolet-B radiation flux in Alpine regions, *Science*, 248, 206-208, 1990.
- Bojkov, R., L. Bishop, W.J. Hill, G.C. Reinsel, and G.C. Tiao, A statistical trend analysis of revised Dobson total ozone data over the northern hemisphere, *J. Geophys. Res.*, 95, 9785-9807, 1990.
- Bornman, J.F., L.O. Björn, and H.-E. Akerlund, Action spectrum for inhibition by ultraviolet radiation of photosystem II activity in spinach thylakoids, *Photobiochem. Photobiophys.*, 8, 305-313, 1984.
- Brasseur, G.P., C. Granier, and S. Walters, Future changes in stratospheric ozone and the role of heterogeneous chemistry, *Nature*, 348, 626-628, 1990.
- Brühl, C. and P.J. Crutzen, On the disproportionate role of tropospheric ozone as a filter against solar UV-B radiation, *Geophys. Res. Lett.*, 16, 703-706, 1989.
- Buttner, K., Physik. Bio. Klim, Leipsiz, 1938 (quoted in Johnson et al., *Photochem. Photobiol.*, 23, 179-188, 1976.).
- Caldwell, M.M., L.B. Camp, C.W. Warner, and S.D. Flint, Action spectra and their key role in assessing biological consequences of solar UV-B radiation change, pp. 87-111 in *Stratospheric Ozone Reduction, Solar Ultraviolet Radiation and Plant Life*, R.C. Worrest and M.M. Caldwell (eds.), Springer-Verlag, Berlin, 1986.
- Cess, R.D., G.L. Potter, J.P. Blanchet, G.J. Boer, S.J. Ghan, J.T. Kiehl, H. Le Treut, Z.-X. Li, X.-Z. Liang, J.F.B. Mitchel, J.-J. Morcrette, D.A. Randall, M.R. Riches, E. Roeckner, U. Shlese, A. Slingo, K.E. Taylor, W.M. Washington, R.T. Wetherald, and I. Yagai, Interpretation of cloud-climate feedback as produced by 14 atmospheric general circulation models, *Science*, 245, 513-516, 1989.
- Chan, G.L., M.J. Peak, J.G. Peak, and W.A. Haseltine, Action spectrum for the formation of endonuclease-sensitive sites and (6-4) photoproducts induced in a DNA fragment by ultraviolet radiation, *Int. J. Radiat. Biol.*, 50, 641-648, 1986.
- Charlson, R.J., J. Langner, M.O. Andreae, and S.G. Warren, Oceanic phytoplankton, atmospheric sulphur, cloud albedo and climate, *Nature*, 326, 655-661, 1987.
- Cole, C.A., D. Forbes, and R.E. Davies, An action spectrum for UV photocarcinogenesis, *Photochem. Photobiol.*, 43, 275-284, 1986.
- Cotton, G.F., Robertson-Berger UV-B meter, in *Summary Report 1989*, Climate Monitoring and Diagnostics Laboratory Report No. 18, National Oceanic and Atmospheric Administration, Boulder, Colorado, December 1990.
- Dahlback, A., T. Henriksen, S.H.H. Larsen, and K. Stamnes, Biological UV-doses and the effect of an ozone layer depletion, *Photochem. Photobiol.*, 49, 621-625, 1989.

- De Fabo, E.C. and F.P. Noonan, Mechanism of immune suppression by ultraviolet radiation *in vivo*. I. Evidence for the existence of a unique photoreceptor in skin and its role in photoimmunology, *J. Exp. Med.*, 158, 84-98, 1983.
- de Gruijl, F.R., unpublished data, 1991.
- DeLuisi, J.J., E.G. Dutton, K.L. Coulson, T.E. DeFoor, and B.G. Mendonca, On some features of the El Chichón volcanic stratospheric dust cloud and a cloud of unknown origin observed at Mauna Loa, *J. Geophys. Res.*, 88, 6769-6772, 1983.
- DeMore, W.P., S.P. Sander, D.M. Golden, M.J. Molina, R.F. Hampson, M.J. Kurylo, C.J. Howard, and A.R. Ravishankara, Chemical kinetics and photochemical data for use in stratospheric modeling, *JPL Publication 90-1*, Jet Propulsion Laboratory, Pasadena, 1990.
- Finlayson-Pitts, B.J. and J.N. Pitts, *Atmospheric Chemistry: Fundamentals and Experimental Techniques*, John Wiley & Sons, New York, 1986.
- Frederick, J.E. and D. Lubin, The budget of biologically active ultraviolet radiation in the earth-atmosphere system, *J. Geophys. Res.*, 93, 3825-3832, 1988.
- Frederick, J.E., H.E. Snell, and E.K. Haywood, Solar ultraviolet radiation at the earth's surface, *Photochem. Photobiol.*, 51, 443-450, 1989.
- Frederick, J.E. and H.E. Snell, Tropospheric influence on solar ultraviolet radiation: The role of clouds, *J. Climate*, 3, 373-381, 1990.
- Frederick, J.E., E.C. Weatherhead, and E.K. Haywood, Long-term variations in ultraviolet sunlight reaching the biosphere: Calculations for the past three decades, *Photochem. Photobiol.*, in press, 1991.
- Garadzha, M.P. and Y.I. Nezval, Ultraviolet radiation in large cities and possible ecological consequences of its changing flux due to anthropogenic impact, in *Proc. Symp. on Climate and Human Health*, World Climate Programme Applications, Leningrad, WCAP Report No. 2, 64-68, 1987.
- Grant, W.B., Global stratospheric ozone and UV-B radiation, *Science*, 1111, 1988.
- Häder, D.-P. and R.C. Worrest, Effects of enhanced solar ultraviolet radiation on aquatic ecosystems, *Photochem. Photobiol.*, 53, 717-725, 1991.
- Haurwitz, B., Insolation in relation to cloud type, *J. of Meteorology*, 5, 110-113, 1948.
- Henriksen, K., K. Stamnes, G. Volden, and E.S. Falk, Ultraviolet radiation at high latitudes and the risk of skin cancer, *Photoderm.*, 6, 110-117, 1989a.
- Henriksen, K., K. Stamnes, and P. Ostensen, Measurements of solar UV, visible and near IR irradiance at 78°N, *Atmos. Environ.*, 23, 1989b.
- Henriksen, T., A. Dahlback, S.H.H. Larsen, and J. Moan, Ultraviolet-radiation and skin cancer. Effect of an ozone layer depletion, *Photochem. Photobiol.*, 51, 579-582, 1990.
- Herman, J.R., R. Hudson, R. McPeters, R. Stolarski, Z. Ahmad, X.-Y. Gu, S. Taylor, and C. Wellemeyer, A new self-calibration method applied to TOMS and SBUV backscattered ultraviolet data to determine long-term global ozone change, *J. Geophys. Res.*, 96, 7531-7545, 1991.
- Hoffman, D.J. and S. Solomon, Ozone destruction through heterogeneous chemistry following the eruption of El Chichón, *J. Geophys. Res.*, 94, 5029-5041, 1989.
- Holm-Hansen, O., UV radiation in Antarctic waters: Effect on rates of primary production, in response of marine phytoplankton to natural variations in UV-B flux, *Proc. of Workshop*, Scripps Institution of Oceanography, April 5, 1990, B. G. Mitchell, O. Holm-Hansen, and I. Sobolev, (eds.), Fluorocarbon Panel Report FC138-088, 1990.
- Ilyas, M., Effect of cloudiness on solar ultraviolet radiation reaching the surface, *Atmos. Environ.*, 21, 1483-1484, 1987.
- Imbrie, C.W. and T.M. Murphy, UV-action spectrum (254-405 nm) for inhibition of a K⁺-stimulated adenosine triphosphatase from a plasma membrane of *Rosa damascena*, *Photochem. Photobiol.*, 36, 537-542, 1982.
- Jones, F. L., R.W. Miksad, A.R. Laird, and P. Middleton, A simple method for estimating the influence of cloud cover on the NO₂ photolysis rate constant, *J. Air Pollut. Contr. Assoc.*, 31, 42-45, 1981.
- Jones, L.W. and B. Kok, Photoinhibition of chloroplast reactions. I. Kinetics and action spectrum, *Plant Physiol.*, 41, 1037-1043, 1966.
- Josefsson, W., Solar ultraviolet radiation in Sweden, *SMHI Reports - Meteorology and Climatology* 53, SMHI, Norrköping, 1986.
- Kelfkens, G., F.R. de Gruijl, and J. van der Leun, Ozone depletion and increase in annual carcinogenic ultraviolet dose, *Photochem. Photobiol.*, 52, 819-823, 1990.

- Kent, G.S., M.P. McCormick, and S.K. Schaffner, Global optical climatology of the free tropospheric aerosol from 1.0-mm satellite occultation measurements, *J. Geophys. Res.*, 96, 5249-5267, 1991.
- Keyse, S.M., S.H. Moses, and D.J. Davies, Action spectra for inactivation of normal and xeroderma pigmentosum human skin fibroblasts by ultraviolet radiation, *Photochem. Photobiol.*, 37, 307-312, 1983.
- Klenk, K.F., P.K. Bhartia, A.J. Fleig, V.G. Kaveeshwar, R.D. McPeters, and P.M. Smith, Total ozone determination from the backscattered ultraviolet (BUV) experiment, *J. Appl. Meteor.*, 21, 1672-1684, 1982.
- Kligman, L.H. and R.M. Sayre, An action spectrum for ultraviolet induced elastosis in hairless mice: Quantification of elastosis by image analysis, *Photochem. Photobiol.*, 53, 237-242, 1991.
- Liu, S.C., S.A. McKeen, and S. Madronich, Effects of anthropogenic aerosols on biologically active ultraviolet radiation, submitted to *Science*, May 1991.
- Logan, J.A., Tropospheric ozone: Seasonal behavior, trends, and anthropogenic influence, *J. Geophys. Res.*, 90, 10463-10482, 1985.
- Logan, J.A., Ozone in rural areas of the United States, *J. Geophys. Res.*, 94, 8511-8532, 1989.
- Lubin, D., B.G. Mitchell, J.E. Frederick, A.D. Alberts, C.R. Booth, T. Lucas, and D. Neuschuler, A contribution toward understanding the biospherical significance of Antarctic ozone depletion, *J. Geophys. Res.*, in press, 1991.
- Madronich, S., Changes in biologically damaging ultraviolet (UV) radiation: Effect of overhead ozone and cloud amount, pp. 30-31 in *Effects of Solar Ultraviolet Radiation on Biogeochemical Dynamics on Aquatic Environments, Report of a Workshop held in Woods Hole*, October 23-26, 1989, N.V. Blough and R.G. Zepp (eds.), Woods Hole Oceanographic Institution, Woods Hole, MA, 1990.
- Madronich, S., Implications of recent total atmospheric ozone measurements for biologically active ultraviolet radiation reaching the earth's surface, *Geophys. Res. Lett.*, in press; 1991.
- McKinlay, A.F. and B.L. Diffey, A reference action spectrum for ultraviolet induced erythema in human skin, in *Human Exposure to Ultraviolet Radiation: Risks and Regulations*, W. R. Passchler and B.F.M. Bosnjakovic (eds.), Elsevier, Amsterdam, 1987.
- Michelangeli, D.V., M. Allen, Y.L. Yung, R.-L. Shia, D. Crisp, and J. Eluszkiewicz, Enhancement of atmospheric radiation by an aerosol layer, *J. Geophys. Res.*, in press, 1991.
- Mitchell, B.G., Action spectra of ultraviolet photoinhibition of Antarctic phytoplankton and a model of spectral diffuse attenuation coefficients, in response of marine phytoplankton to natural variations in UV-B flux, *Proc. of Workshop*, Scripps Institution of Oceanography, April 5, 1990, B.G. Mitchell, O. Holm-Hansen, and I. Sobolev (eds.), Fluorocarbon Panel Report FC138-088, 1990.
- Moan, J., A. Dahlback, S. Larsen, T. Henriksen, and K. Stamnes, Ozone depletion and its consequences for the fluence of carcinogenic sunlight, *Cancer Research*, 49, 4247-4250, 1989.
- NRC Acid Deposition Long-Term Trends, National Research Council, National Academy Press, Washington, D.C., 1986.
- Oltmans, S.J., W.D. Komhyr, P.R. Franchois, and W.A. Matthews, Tropospheric ozone: Variations from surface and ECC ozonesonde observations, in *Ozone in the Atmosphere, Proceedings of the Quadrennial Ozone Symposium 1988 and Tropospheric Ozone Workshop*, Göttingen, Federal Republic of Germany, August 1988, R. Bojkov and P. Fabian (eds.), Deepak Publishing, Hampton, Virginia, 1989.
- Parrish, J.A., K.R. Jaenicke, and R.R. Anderson, Erythema and melanogenesis action spectra of normal human skin, *Photochem. Photobiol.*, 36, 187-191, 1982.
- Peak, M.J., J.G. Peak, M.P. Moehring, and R.B. Webb, Ultraviolet action spectra for DNA dimer induction, lethality, and mutagenesis in *Escherichia coli* with emphasis on the UV-B region, *Photochem. Photobiol.*, 40, 613-620, 1984.
- Penkett, S.A., Ultraviolet levels down not up (News and Views), *Nature*, 341, 283-284, 1989.
- Pitts, D.G., A.P. Cullen, and P.D. Hacker, Ocular effects of ultraviolet radiation from 295 to 365 nm, *Invest. Ophthalmol. Visual Sci.*, 16, 932-939, 1977.
- Roy, C.R., H.P. Geis, and G. Elliott, Ozone depletion, *Nature*, 347, 235-236, 1990.
- Rundel, R.D., Action spectra and the estimation of biologically effective UV radiation, *Physiol. Plantarum*, 58, 360-366, 1983.

- Scotto, J., G. Cotton, F. Urbach, D. Berger, and T. Fears, Biologically effective ultraviolet radiation: Surface measurements in the United States, 1974 to 1985, *Science*, 239, 762-764, 1988.
- Setlow, R.B., The wavelengths in sunlight effective in producing skin cancer: A theoretical analysis, in *Proceedings of the National Academy of Science*, 71, 3363-3366, 1974.
- Sharma, R.C. and J. Jagger, Ultraviolet (254-405 nm) action spectrum and kinetic studies of aniline uptake in *Escherichia coli* B/R, *Photochem. Photobiol.*, 30, 661-666, 1979.
- Smith, R.C. and K. Baker, Assessment of the influence of enhanced UV-B on marine primary productivity, pp.509-537, in *The Role of Solar Ultraviolet in Marine Ecosystems*, J. Calkins (ed.), Plenum Press, New York, 1982.
- Staehelin, J. and W. Schmid, Trend analysis of tropospheric ozone concentrations utilizing the 20-year data set of ozone balloon soundings over Payerne (Switzerland), *Atmos. Env.*, 25A, 1739-1749, 1991.
- Stamnes, K., K. Henriksen, and P. Ostensen, Simultaneous measurements of UV radiation received by the biosphere and total ozone amount, *Geophys. Res. Lett.*, 784-787, 1988.
- Stamnes, K., J. Slusser, M. Bowen, C. Booth, and T. Lucas, Biologically effective ultraviolet radiation, total ozone abundance, and cloud optical depth at McMurdo Station, Antarctica September 15, 1988 through April 15, 1989, *Geophys. Res. Lett.*, 17, 2181-2184, 1990.
- Stein, B., H.J. Rahmsdorf, A. Steffen, M. Litfin, and P. Herrlich, UV-induced DNA damage is an intermediate step in UV-induced expression of human immunodeficiency virus type 1, collagenase, c-fos, and metallothionein, *Mol. Cellular Biol.*, 9, 5169-5181, 1989.
- Steinmetz, V. and E. Wellman, The role of solar UV-B in growth regulation of cress (*Lepidium sativum* L.) seedlings, *Photochem. Photobiol.*, 43, 189-193, 1986.
- Stolarski, R.S., P. Bloomfield, R.D. McPeters, and J. R. Herman, Total ozone trends deduced from Nimbus 7 TOMS data, *Geophys. Res. Lett.*, 18, 1015-1018, 1991.
- UNEP, *Environmental Effects Panel Report*, J. C. van der Leun, M. Tevini, and R. C. Worrest (eds.), United Nations Environment Programme, Nairobi, Kenya, 1989.
- Urbach, F., D. Berger, and R.E. Davies, Field measurements of biologically effective UV radiation and its relation to skin cancer in man, in *Proceedings of the Third Conference on Climatic Impact Assessment Program*, A. J. Broderick and T. M. Hard (eds.), U.S. Dept. of Transportation, February 1974.
- Volz, A. and D. Kley, Evaluation of the Montsouris series of ozone measurements made in the nineteenth century, *Nature*, 332, 240-242, 1988.
- Wan and L.O. Björn, unpublished data, 1991.
- Wellmann, E., UV-B Signal/Response - Beziehungen unter natürlichen und artifiziellen Lichtbedingungen, *Ber. Deutsch. Bot. Ges.*, 98, 99-104, 1985.
- WMO, Report of the International Ozone Trends Panel, World Meteorological Organization, Global Ozone Research and Monitoring Project, Report No. 18, 1988.
- WMO, *Scientific Assessment of Stratospheric Ozone: 1989, Volume I*, World Meteorological Organization, Global Ozone Research and Monitoring Project, Report No. 20, 1989.
- Yatsushashi, H., T. Hashimoto, and S. Shimizu, Ultraviolet action spectrum for anthocyanin formation in broom sorghum first internodes, *Plant. Physiol.*, 70, 735-741, 1982.
- Yue, G.K., M.P. McCormick, and E.W. Chiou, Stratospheric aerosol optical depth observed by the stratospheric aerosol and gas experiment II: Decay of the El Chichón and Ruiz volcanic perturbations, *J. Geophys. Res.*, 94, 5209-5219, 1991.
- Zölzer, F. and J. Kiefer, Wavelength dependence of inactivation and mutation induction to 6-thioguanine-resistance in V79 Chinese hamster fibroblasts, *Photochem. Photobiol.*, 40, 49-53, 1984.

Effects on Human Health

**Dr. Margaret Kripke
University of Texas**

HEALTH EFFECTS OF UV-B RADIATION

SKIN CANCER

OCULAR EFFECTS

IMMUNE SYSTEM

SKIN CANCER

BASAL AND SQUAMOUS CELL CARCINOMA

- 1. Effects of UV-B are cumulative**
- 2. Incidence is proportional to life-time UV-B exposure**
- 3. 10% ozone loss = 26% increase in incidence (300,000 new cases)**
- 4. Will occur at a younger age**

SKIN CANCER

MELANOMA

- 1. Role of UV-B is complex**
- 2. Incidence is related to acute UV-B exposures**
- 3. 10% ozone loss = ??
20% increase in incidence (4,500 new cases); 3 to 20% increase in mortality**
- 4. May occur at younger age**

OCULAR EFFECTS

CATARACT

1. Responsible for 17M cases of blindness (half of world's cases)
2. 1% ozone loss = 0.6% increase in incidence (?) (100,000 cases)

PHOTOKERATITIS (snowblindness)

EARLY PRESBYOPIA (?)

LENS CAPSULE DEFORMATION (?)

OCULAR MELANOMA (?)

IMMUNE SYSTEM

ANIMAL MODELS

1. UV-B decreases immune functions

**UV-induced skin cancer, melanoma,
skin immunity, some systemic
immune responses, phagocytosis**

2. UV-B influences infectious diseases

**Herpes simplex virus, Leishmania
Mycobacteria, Candida**

3. Effects of sunscreens controversial

IMMUNE SYSTEM

HUMANS

- 1. Damage to immune cells in skin**
- 2. Altered proportions of WBC**
- 3. Decrease initiation of immune responses in skin (contact allergy)**
- 4. Long-lasting, specific immune suppression; genetically controlled**
- 5. Pigmentation is not protective**

Effects on Terrestrial Plants

**Dr. Joe Sullivan
University of Maryland**

Effects of UV-B Radiation on Crops and Terrestrial Ecosystems

Joe H. Sullivan, Dept. of Botany, University of Maryland,
College Park, MD 20742

INTRODUCTION

Continued depletions of the earth's stratospheric ozone layer is of concern because this ozone column is the primary attenuator of solar ultraviolet-B radiation (UV-B region, between 280 and 320 nm). A decrease in this ozone column would lead to increases in UV-B radiation between 290 and reaching the earth's surface. Though representing only a small fraction of the total solar electromagnetic spectrum, UV-B has a disproportionately large photobiological effect. One reason is that UV is readily absorbed by important macromolecules such as proteins and nucleic acids (Giese 1964). Therefore, it is not surprising that both plant and animal life are greatly affected by increases in UV-B radiation penetrating to the earth's surface.

Previous studies have shown that tremendous variability exists among plant species in sensitivity to UV-B radiation. Some species show sensitivity to current ambient levels of UV-B radiation (Bogenrieder and Klein 1978), while others are apparently unaffected by large UV enhancements (Sinclair *al.* 1990, Sullivan *et al.* 1992). This issue is complicated further by reports of equally large response differences among cultivars of a single species (Biggs *et al.* 1981, Teramura and Murali 1986).

A compilation of data from approximately two decades of study indicates that about one-third to one-half of all species studied are deleteriously affected by UV-B radiation levels above ambient. However, many species exhibit no such effects and this suggests that some plants are well-adapted to UV-B radiation. Of ten major terrestrial ecosystems, representatives of only four have been studied for UV-B radiation sensitivity (Table 1). The vast majority of the species tested have been annual agricultural species, which account for only approximately 9% of global net primary productivity (Table 1). During the past decade, only 12 field studies have examined the effects of UV radiation on the yield of some 22 crop and one tree species. Over half of these studies were conducted over only a single growing season and only two were conducted over more than two years (Teramura *et al.* 1990a, Sullivan and Teramura 1992). Thus, only scant information exists on the annual variation which occurs in field studies.

This paucity of data coupled with the wide range in sensitivity already described, makes any assessment of potential consequences of ozone depletion at the ecosystem

level quite speculative. This report summarizes the methodology generally utilized in UV-B radiation studies and results from some recent studies. This review is by no means exhaustive and will merely cite a few examples of some of the direct and indirect effects observed in plants when exposed to UV-B radiation. Several general reviews over the last three years which provide greater detail include Caldwell et al. 1989, Tevini and Teramura 1989, and Teramura 1990.

UV-B IRRADIATION METHODOLOGY

Most studies on the effects of UV-B radiation on plant growth or physiology have used artificial UV-B irradiation sources (sunlamps) to provide supplemental UV-B radiation to plants. Since the spectral output of sunlamps does not precisely match sunlight and due to the wavelength dependency of photobiological processes, some weighting function is generally utilized to determine the biological effectiveness of the UV-B irradiance supplied (Caldwell 1971, Coohill 1989). The UV-B supplementation may be provided by either a square-wave supply function (i.e. a constant or stepped supplemental irradiance for a specified period of time) or a modulated supply system which provides a designated supplemental irradiances proportional to that of natural sunlight (Fig. 1A). The advantage of the square-wave system lies in its simplicity and relatively low cost compared to the modulated system, which is much more realistic, especially under cloudy sky conditions (Fig. 1B), and ecologically relevant, but costs between four and five times as much as the square-wave systems.

Some other studies have utilized techniques to reduce natural solar UV-B irradiance and thus simulate ambient levels of UV-B radiation present at higher latitude or lower elevation locations for comparative purposes. In these studies, a reduction in UV-B radiation may be achieved either by means of UV-B filters (e.g. tents or shelters made of UV-B opaque materials such as polyester) or by positioning cuvettes containing ozone over the plants (Tevini et al. 1988). This latter method, though rather complex in design and expensive to construct and maintain, provides an excellent simulation of changes in solar UV-B radiation due to ozone depletion, since ozone rather than plastic filters are utilized to absorb natural solar radiation and artificial lamps are not required. Further advantages of this system are that it is adaptable for simulating a variety of UV-B radiation environments and the chambers can be further modified for control of other environmental factors such as temperature or CO₂ concentration. However, a disadvantage of this growth chamber technique is that only small potted plants can be evaluated and field conditions can not be precisely simulated.

UV-B PENETRATION INTO THE LEAF

In order for UV-B radiation to be effective in altering plant biochemistry, physiology or productivity, it must penetrate the leaf to sensitive targets and be absorbed by chromophores present. Beggs et al. (1986) summarized three general classes of protective responses to UV-B as 1) those that avoid damage by preventing UV-B from reaching sensitive targets (e.g. changes in leaf reflectance or epidermal absorbance), 2) those that minimize damage by growth delay, and 3) those that mitigate damage by repair mechanisms such as photoreactivation or post-transcriptional repair.

One response to UV-B radiation commonly reported is that of an increase in leaf thickness or specific leaf weight (SLW). For example Murali et al. (1988) reported that SLW increased in the soybean cultivar Williams but not in the Essex cultivar and further that this response was correlated with sensitivity differences between those two cultivars. Likewise, Bornman and Vogelmann (1991) reported increases in leaf thickness of 45% in Brassica campestris.

However, the mechanism of UV-B protection that has received the most attention by plant physiologists and ecologists has been that of the accumulation of UV-absorbing compounds in leaf tissue in response to UV-B radiation. Flavonoids are one group of compounds which may accumulate in the leaf epidermis in response to UV-B radiation. The role of flavonoids in UV-B radiation protection was hypothesized over two decades ago (Jagger 1967) and has since been considered frequently (e.g. Robberecht and Caldwell 1978, 1983, Sullivan and Teramura 1989, Tevini et al. 1991). The accumulation of flavonoids in the epidermis has been shown to reduce epidermal transmittance of UV-B radiation (Robberecht and Caldwell 1978).

Flavonoid accumulation is dependent upon a number of factors including both visible and UV fluence (Mohr and Drumm-Herrel 1983, Wellman 1983) and almost any other environmental stress such as drought, temperature, nutrient stress or pathogen/insect infestation (McClure 1986). The mechanistic basis of light or UV-induced accumulation appears to lie at the gene level as some key enzymes in the flavonoid biosynthetic pathway are induced by UV radiation. For example, it has been shown that UV-B radiation leads to increases in the levels of mRNA and enzymes, especially chalcone synthase and phenylalanine ammonia lyase (CHS and PAL), involved in flavonoid biosynthesis (Chappell and Hahlbrock 1984). This increase resulted in flavonoid accumulation (Beerhues et al. 1988).

However, several studies have indicated that the damaging effects of UV-B radiation may not be mitigated simply by an apparent increase in foliar flavonoid concentrations (Sisson

1981, Mirecki and Teramura 1984, Sullivan and Teramura 1989). Also, Barnes et al. (1987) reported that the photosynthetic apparatus of some plants from high elevation tropical areas was inherently more resistant to UV-B radiation than that of some other plants and that this was apparently not due to increases in flavonoid concentrations. Therefore a relationship between flavonoid accumulation and UV-protection often appears to exist, but a number of inconsistencies suggest that a simple correlation of flavonoid content and UV-B radiation tolerance may not always exist.

Clearly, anatomical and biochemical differences among species affect the penetration of UV-B radiation into the leaf. A recent survey of some 22 plant species (T.A. Day, personal communication) has shown a wide range of differences in the ability of UV-B radiation to penetrate through the epidermis. However, additional protective mechanisms, such as photoreactivation, where pyrimidine dimers may be repaired by a light-regulated DNA photolyase (Langer and Wellmann 1990), and other poorly understood mechanisms are also associated with UV-B radiation sensitivity. In conclusion, we are aware of several methods by which plants protect themselves from UV-B radiation but we lack many mechanistic details in our efforts to fully understand UV-B radiation sensitivity.

UV-B RADIATION EFFECTS ON PHOTOSYNTHESIS

The penetration of UV-B radiation through the epidermis may result in reductions in net carbon assimilation (photosynthesis). However, damage to photosynthetic mechanisms has not been observed in all species upon exposure to UV-B radiation (Beyschlag et al. 1988). Clearly some plants are well-protected from UV-B radiation damage as described above. However, in sensitive species, UV-B radiation may indirectly reduce photosynthesis by photodegradation of photosynthetic pigments, altering stomatal conductance or regulation, or by altering the visible light regime within the leaf due to anatomical (e.g. leaf thickness) or morphological (e.g. canopy architectural) changes. However, other studies have shown that UV-B radiation may reduce photosynthesis by direct effects on the photosynthetic machinery (e.g. Warner and Caldwell 1983, Tevini et al. 1991).

Direct damage to photosystem II, as indicated by changes in chlorophyll fluorescence, has been reported in isolated chloroplasts and cell suspensions (e.g. Smillie 1982, Iwanzik et al. 1983) and in intact tissue (Tevini et al. 1991, Bornman and Vogelmann 1991). Also diagnostic assessments of the responses of CO_2 assimilation to light and internal CO_2 concentration under enhanced UV-B radiation have demonstrated reductions in apparent quantum efficiency and RuBP (substrate) regeneration capacity (Sullivan and Teramura 1989 and 1990).

Measurements of reductions in assimilation capacity are not necessarily correlated with reduced growth. Some studies on the effects of UV-B radiation have shown changes in growth without observed reductions in photosynthetic rate and other studies have observed reductions in some aspect of photosynthesis without concurrent growth reductions. One reason for this apparent inconsistency of results lies in the wide range UV-B radiation sensitivity present among plant species and cultivars and may also be attributed to contrasting growth conditions and irradiation protocols between experiments. Another reason for this lack of consistent results may be that UV-B radiation damage and repair processes in plants are independent in terms of actual fluence response (e.g. each process is regulated by a unique fluence response) and that UV-B radiation effects vary on a temporal basis. This may be particularly true for long-lived species such as trees (Sullivan and Teramura 1989). Furthermore, in a recent study on loblolly pine, for example, reductions in net assimilations and damage to photosystem II was only detected during a very narrow "window" period during needle development (Fig. 2). It is possible that developmental changes in leaf chemistry or anatomy and increases in self-shading of foliage during shoot development may prevent further damage to the photosynthetic machinery and allow repair processes to mitigate previous damage. Therefore the timing (with respect to leaf phenology) of "point" measurements of photosynthesis or other indicators of UV-B radiation damage, may be critical in detecting damage due to UV-B radiation. Finally, the duration of the "window" period, if present, may be a particularly important determinant of the magnitude of UV-B radiation effectiveness or growth reduction.

GROWTH AND PRODUCTIVITY

A critical parameter assessed in most previous studies on the effects of UV-B radiation on plants is growth or productivity. This may be measured by biomass accumulation or seed yield. Since growth and seed production may differ considerably in controlled environment (e.g. growth chamber or greenhouse) studies compared to field studies this discussion will examine field studies only. Growth and yield may reflect a total integration of all stresses including microclimate, pests and competition. These parameters vary considerably from year to year and thereby contribute to annual variation in crop yield.

Two studies conducted over multiple field seasons have examined the effects of UV-B radiation on soybean yield. The first study was conducted over a two year period during 1981 and 1982 and UV-B radiation had little impact on biomass or yield of several soybean cultivars (Sinclair et al. 1990). These results contrast with a six-year study on two soybean cultivars conducted at the University of Maryland (Teramura et

al. 1990a). In that study two soybean cultivars were chosen for study in a field experiment conducted from 1981 to 1986 at Beltsville, Maryland. The results of that study demonstrated intraspecific differences in UV-B sensitivity in soybean yield and quality. However, the expression of these sensitivity differences to UV-B radiation was altered by other prevailing microclimatic factors. For the sensitive soybean cultivar, Essex, a simulated 25% ozone depletion reduced overall yield by 19-25% during 4 of the 6 years. No reductions in yield were detected in the 1983 and 1984 seasons, which were characterized as hot and dry with prolonged periods of drought.

Parallel field studies have shown that the effects of UV-B radiation are modified by concurrent environmental conditions. For example, under water stress (Sullivan and Teramura 1990) or mineral deficiency (Murali and Teramura 1985), soybeans are less susceptible to UV-B radiation, but under low levels of visible radiation, sensitivity to UV-B radiation increases (Warner and Caldwell 1983, Mirecki and Teramura 1984). Thus field studies conducted over several growing seasons are crucial to the realistic assessment of the potential impact of increasing UV-B radiation on plant productivity.

The contrasts in results obtained between the two studies above may have been due to differences in cultivar sensitivity, microclimate or irradiation protocols. However, it is apparent that the potential for UV-induced reductions in yield exists under some conditions and in some plant varieties. It is further apparent that studies of one or even two seasons may not be adequate to realistically assess the long-term consequences of ozone depletion on plant productivity.

In contrast to crops, few studies under any growth conditions, have been undertaken on woody perennials (trees), which account for over two-thirds of global net primary productivity and occupy as much as one-third of the land area of the United States (Whittaker, 1975). The examination of UV-B radiation effects on perennial species provides a unique opportunity to observe more subtle responses to protracted UV exposure which are impossible to investigate in annual species. For instance, it is presently unknown whether UV repair mechanisms can mitigate UV damage during the dormant period when ambient levels of solar UV are at their seasonal minima. Likewise, we have no information on whether the extensive physiological changes which accompany tissue hardening prior to entering the dormant period modify its sensitivity to subsequent UV exposure. The range of responses observed both inter- and intra-specifically suggests that extrapolations between annual and perennial species may not be feasible. Therefore, some direct field validation experiments

on key forest species are essential before realistic estimates of this nature can be made.

Only three studies have been completed on trees under field conditions and one of these examined the effects of exclusion of solar UV-B radiation (Bogenrieder and Klein 1982). Exclusion of naturally occurring UV-B radiation increased the growth of four broadleaf species but supplemental UV-B irradiation had no effects on growth in either Engelmann spruce or lodgepole pine (Kaufmann 1978). However, both of these studies were conducted over a single growing season.

Only one multiple year field study has been conducted to date on the effects of UV-B radiation on trees (Sullivan and Teramura 1992). In that study loblolly pine seedlings from four seed sources were grown in the field for three successive years. The results of that study showed that the effects of UV-B radiation accumulated over the three year period. After three years, biomass of plants from three of the four seed sources was significantly reduced by UV-B radiation simulating a 25% ozone depletion (Fig. 3) and similar reductions were observed in plants from two of the four seed sources at a simulated 16% depletion.

INDIRECT EFFECTS OF UV-B RADIATION

While reductions in productivity have been reported for several species, it is possible that, due to natural plant adaptations to UV-B radiation, total productivity may not be significantly altered by increasing UV-B radiation at the ecosystem level. However, significant changes may occur in community dynamics and in various ecosystem processes by indirect effects of increasing UV-B radiation. While data are extremely limited at this point, some of the potential consequences of ozone depletion at the ecosystem level are briefly discussed below.

Plant Competition

Changes in plant canopy morphology or architecture may alter competitive interactions without concurrent reductions in total productivity. Few data are available on this topic, but one multiple-year field and greenhouse study has shown that competition between wheat and a common competitor, wild oat, was changed, in favor of wheat, in response to UV-B radiation (Barnes et al. 1988). In that study and other related publications (e.g. Barnes et al. 1990, Beyschlag et al. 1988, Ryel et al. 1990), it was shown that alterations in growth form (e.g. internode length and branching), even in absence of reductions in biomass or photosynthetic carbon gain, were sufficient to quantitatively explain changes in competitive balance. Therefore, the absence of gross effects

of UV-B radiation on biomass does not necessarily preclude any ecological consequences of ozone depletion. Changes in plant architecture or biomass allocation, as described above, could result in changes in successional patterns and species composition in natural plant communities.

Plant-Pathogen/Plant Insect Interaction

Another important area where significant ecological effects could occur due to increasing UV-B radiation is in plant-pest interactions. Two recent studies have demonstrated that some plants may be more susceptible to damage from pathogens if preconditioned with UV-B exposure. Orth et al. (1990) showed that pretreatment with UV-B radiation predisposed cucumber (Cucumis sativus) cotyledons to greater disease severity than non-irradiated plants. More recently, Panagopoulos et al. (1991) have also shown that sugar beet (Beta vulgaris) exposed to 6.9 kJ m^{-2} UV-B radiation and infected with Cercospora beticola showed additive reduction in chlorophyll and fresh weight.

Almost no data exist on the implications of increasing UV-B radiation on plant-insect interactions. However, changes in foliar chemistry (e.g. flavonoid accumulation) in response to UV-B radiation suggest that significant effects could occur. In one preliminary study of field irradiated soybean (V. Krischik and C. Jones, personal communication), the feeding preference of Mexican Bean Beetle appeared to be for soybean (cv Clark) exposed to supplemental UV-B radiation compared to controls which received only natural UV-B radiation. This preference may have been related to concomitant increases in the flavonoid, kaempferol, since no feeding preference was detected in an isolate of Clark which produces only very small quantities of kaempferol. Similar results were obtained with cottonwood seedlings where the feeding preference of another specialist beetle (Chrysomalius scripta) was increased in response to UV-B radiation. However, in contrast, the generalist feeding Gypsy moth larvae (Lymantria dispar) fed significantly less on cottonwood exposed to supplemental UV-B radiation. It is presently unclear what the effects of increasing UV-B radiation would be on plant-pest interactions. However, our knowledge of the importance of plant secondary chemistry in plant-pest interactions and of the effects of UV-B radiation on plant secondary chemistry suggest that the potential for significant changes in these interactions could result from increasing UV-B radiation. More information is clearly needed in this area.

Interactive Effects of UV-B microclimate

Changes in global climate which alter the temperature and patterns of precipitation have been predicted due to increases in greenhouse gases in the atmosphere. Such changes in climate would occur in concert with increasing levels of UV-B

radiation reaching the earth. As previously discussed, UV-B radiation sensitivity is modified by the prevailing microclimate. Therefore, the ultimate impact of increased solar UV-B radiation on productivity may be dependent upon other environmental changes and species-specific interactions of these effects.

Interaction with Atmospheric CO₂

Atmospheric CO₂ concentrations have been increasing essentially since industrialization began and the concentration of CO₂ may double pre-industrial levels by the middle of the next Century (Gribbin 1981). Therefore, any potential interaction between CO₂ and UV-B radiation effects on plant productivity may be important in a realistic determination of the consequences of an increase in either parameter.

When studied independently, increases in UV-B radiation and CO₂ may be generally expected to elicit opposing responses. For example, plant growth is reduced by UV-B radiation but may increase under elevated levels of CO₂. In those instances where mechanisms are known, responses to UV-B and increased CO₂ result from different mechanisms. Therefore it is not clear whether increased CO₂ will mitigate damage from UV-B radiation.

Only a few studies have been published to date on the combined effects of increasing CO₂ and UV-B radiation. One study (Teramura et al. 1990b), was conducted on three crop species. In that study UV-B radiation reduced (wheat) or eliminated (rice) the CO₂ enhancement effect on growth or seed yield. These results suggest that in some cereal grains, overestimates of increased productivity due to future CO₂ enrichment could result if the solar irradiance environment is not considered. Further studies by Rozema et al. (1990), on three species and Ziska and Teramura (1992) on rice also indicated that the effects of UV-B radiation and CO₂ were independent, e.g. growth enhancements as a result of CO₂-enrichment tend to be reduced by the detrimental effects of UV-B radiation. We have also conducted greenhouse studies on the interactions of UV-B and elevated CO₂ in loblolly pine. The results from that study also indicate a lack of interactive effects in loblolly pine (J.H. Sullivan and A.H. Teramura, unpublished data).

The results above suggest that increased UV-B radiation could modify the response of plants to CO₂ enrichment. However, due to the difficulty in extrapolating greenhouse results to actual field conditions, field validations are needed before realistic estimates of potential effects can be made.

Interaction with Air Pollutants and Heavy Metal Contamination

Air pollutants (e.g. O_3 , SO_2 , etc.) and acid precipitation are increasing in many areas and currently result in tremendous damage to crops and other plant species. In addition, increases in air pollution and acid precipitation may be contributing to an accumulation of heavy metals in some areas. Almost no information exists on the multiple effects of air pollution or heavy metals and UV-B radiation. Concurrent increases in tropospheric ozone along with stratospheric ozone depletion provides a particularly complex issue. Since ozone absorbs UV-B radiation without regard to its location in the atmosphere, an increase in UV-B radiation might be compensated for (on a fluence basis) on a local and short-term basis by ozone or other tropospheric pollutants (Krupa and Kickert 1989, Penkett 1990). However, plant response on a physiological or productivity basis would most likely not show compensatory effects since the plant would experience alternating stresses (e.g. ozone one day and UV-B the next). No data are currently available with which to evaluate this on a realistic basis but such studies are needed.

One recent study has suggested that an increase in heavy metals may exacerbate UV-B radiation damage. Dube and Bornman (1991), found the addition of 5 millimolar cadmium chloride in addition to increased UV-B radiation reduced photosynthesis, chlorophyll concentration, height and dry matter accumulation in a synergistic fashion. These effects may be important in terms of changes in plant productivity; however, the mechanisms involved are not yet understood. Additional data are needed on multiple stress effects in general before we can adequately assess the consequences of ozone depletion on plant or ecosystem productivity.

SUMMARY AND CONCLUSIONS

A large number of studies have been conducted over the last two decades which evaluated the potential consequences of an increase in UV-B radiation. Most studies have utilized artificial lamp sources to simulate enhanced UV-B radiation fluences. Perhaps the most striking, though not surprising, outcome of these studies is that tremendous variability exists among plants in their sensitivity to UV-B radiation. Various responses have been reported including changes in leaf secondary chemistry (flavonoid accumulation), alterations in leaf anatomy and morphology, reductions in net carbon assimilation capacity (photosynthesis) and changes in biomass allocation and growth. However, we lack specific information on many key species and in fact we have no information at all on any representative from 6 of the 10 basic terrestrial ecosystems. The huge variation in plant response makes it extremely difficult to extrapolate effects of UV-B radiation to species on which we have no information or to the ecosystem

level, even for those ecosystems where we have some information.

However, much progress had been made in the last several years in our assessment of the implications of increasing UV-B radiation on plant growth and productivity. One area in which progress has been made is the development of more realistic irradiation technology (modulated UV-B enhancement and UV-B reduction techniques). Additionally we have also increased our understanding of the molecular basis for the accumulation of flavonoids in response to UV-B radiation and are increasing our quantitative and qualitative knowledge of light penetration into plant leaves. Finally we are now beginning to obtain some data on the possible consequences of increasing UV-B radiation on species other than agricultural species and on the interaction of multiple environmental changes.

Unfortunately, we still have a poor mechanistic understanding of how UV-B radiation damages plants, how repair and mitigation processes are controlled and of the genetic basis and heritability of UV-B sensitivity. Additional information is needed before we can adequately assess the consequences of ozone depletion on ecosystem dynamics or productivity. Areas of particular concern are the potential interactive effects of UV-B radiation with other environmental parameters and the assessment of potential indirect effects of UV-B radiation, such as competition, plant/pest interactions and potential effects on nutrient cycling or decomposition rates.

REFERENCES

- Barnes, P.W., S.D. Flint and M.M. Caldwell. 1987. Photosynthesis damage and protective pigments in plants from a latitudinal arctic/alpine gradient exposed to supplemental UV-B radiation in the field. *Arctic and Alpine Research* 19: 21-27.
- Barnes, P.W., P.W. Jordan, W.G. Gold, S.D. Flint and M.M. Caldwell. 1988. Competition, morphology and canopy structure in wheat (*Triticum aestivum* L.) and wild oat (*Avena fatua* L.) exposed to enhanced ultraviolet-B radiation. *Functional Ecology* 2: 319-330.
- Barnes, P.W., S.D. Flint and M.M. Caldwell. 1990. Morphological responses of crops and weeds of different growth forms to ultraviolet-B radiation. *Amer. J. Bot.* 77: 1354-1360.
- Beerhues L, H. Robenek and R. Wiermann. 1988. Chalcone synthesis from spinach (*Spinacia aleracea* L.) II. Immunofluorescence and immunogold localization *Planta* 173: 544-553.
- Beggs, C.J., U. Schneider-Ziebert and E. Wellmann. 1986. UV-B radiation and adaptive mechanisms in plants. pp 235-250

- In Stratospheric Ozone Reduction, Solar Ultraviolet Radiation and Plant Life. R.C. Worrest. and M.M. Caldwell (eds) Springer-Verlag Berlin Heidelberg.
- Beyschlag, W., P.W. Barnes, S.W. Flint and M.M. Caldwell. 1988. Enhanced UV-B radiation has no effect on photosynthetic characteristics of wheat (Triticum aestivum L.) and wild oat (Avena fatua L.) under greenhouse and field conditions. *Photosynthetica* 22: 516-525.
- Biggs, R.H., S.V. Kossuth & A.H. Teramura. 1981. Response of 19 cultivars of soybean to ultraviolet-B irradiance. *Physiol. Plant.* 53: 19-26.
- Bogenrieder, A. and R. Klein. 1978. Die abhangigkeit der UV-empfindlichkeit von der lichtqualitat bel der aufzucht (Lactuca sativa L.). *Angew. Botanik* 52: 283-293.
- Bogenrieder, A. and R. Klein. 1982. Does solar UV influence the competitive relationship of higher plants? pp 641-649. In The role of solar ultraviolet radiation in marine ecosystems. J. Calkins, ed. Plenum Press. New York.
- Bornman, J.F. and T.C. Vogelmann. 1991. The effect of UV-B radiation on leaf optical properties measured with fiber optics. *J. Exp. Bot.* 42: 547-554.
- Caldwell, M.M. 1971. Solar UV irradiation and the growth and development of higher plants. In *Photophysiology*, Vol. 6. Edited by A.C. Giese. Academic Press, New York.
- Caldwell, M.M., R. Robberecht and S.D. Flint. 1983. Internal filters: prospects for UV-acclimation in higher plants. *Physiol. Plant.* 58: 445-450.
- Caldwell, M.M., A.H. Teramura and M. Tevini. 1989. The changing solar ultraviolet climate and the ecological consequences for higher plants. *TREE*. 4: 363-367.
- Chappell, J. and K. Hahlbrock. 1984. Transcription of plant defense genes in response to UV light or fungal elicitor. *Nature (London)* 311:76-78.
- Coohill, T.P. 1989. Ultraviolet action spectra (280 nm to 380 nm) and solar effectiveness spectra for higher plants. *Photochem. Photobiol.* 50: 451-457.
- Dube, L.S. and J.F. Bornman. 1991. The response of young spruce seedlings to simultaneous exposure of ultraviolet-B radiation and cadmium. *Plant Physiol. Biochem.*
- Giese, A.C. 1964. Studies on ultraviolet radiation action upon animal cells. In *Photophysiology Vol. 2*, (Edited by A.C. Giese), pp. 203-245. Academic Press, NY-London.
- Gribbin, J. 1981. The politics of carbon dioxide. *New Sci.* 90: 82-84.
- Iwanzik W, M. Tevini, G. Dohnt, M. Voss, W. Weiss, P. Graber and G. Renger. 1983. Action of UV-B radiation on photosynthetic primary reactions in spinach chloroplasts. *Physiol. Plant.* 58: 401-407.
- Jagger, J. 1967. Introduction to research in ultraviolet photobiology. Prentice Hall, Englewood Cliffs, New Jersey.

- Kaufmann, M.R. 1978. The effect of ultraviolet (UV-B) radiation on Engelmann spruce and lodgepole pine seedlings. UV-B Biological and Climatic Effects Research (BACER). Final Report EPA-IAG-D-0168. EPA, Washington, DC.
- Krupa, S.W. and R.N. Kickert. 1989. The greenhouse effect: Impacts of ultraviolet-B (UV-B) radiation, carbon dioxide (CO₂), and ozone (O₃) on vegetation. *Env Pol* 61:263-393
- Langer, B. and E. Wellmann. 1990. Phytochrome induction of photoreactivation in Phaseolus vulgaris L. seedlings. *Photochem. Photobiol.* 52: 861-864.
- McClure, J.W. 1986. Physiology of flavonoids in plants. pp. 77-85. *In* Plant Flavonoids in Biology and Medicine: Biochemical, Pharmacological, and Structure-activity Relationships. V. Cody, E. Middleton and J.B. Harborne, eds. Alan Riss, Inc.
- Mirecki, R.M. and A.H. Teramura. 1984. Effects of ultraviolet-B irradiance on soybean. The dependence of plant sensitivity on the photosynthetic photon flux directly during and after leaf expansion. *Plant Physiol.* 74: 475-480.
- Mohr, H. and H. Drumm-Herrel. 1983. Coaction between phytochrome and blue/UV light in anthocyanin synthesis in seedlings. *Physiol. Plant.* 58: 408-414.
- Murali, N.S. and A.H. Teramura. 1986. Effectiveness of UV-B radiation on the growth and physiology of field-grown soybean modified by water stress. *Photochem. Photobiol.* 44: 215-220.
- Murali, N.S. and A.H. Teramura. 1985. Effects of ultraviolet-B irradiance on soybean. VI. Influence of phosphorus nutrition on growth and flavonoid content. *Physiol. Plant.* 63: 413-416.
- Murali N.S., A.H. Teramura and S.K. Randall. 1988. Response differences between two soybean cultivars with contrasting UV-B radiation sensitivities. *Photochem. Photobiol.* 47: 1-5.
- Orth, A.B., A.H. Teramura and H.D. Sisler. 1990. Effects of UV-B radiation on fungal disease development in Cucumis sativus. *Amer. J. Bot.* 77: 1188-1192.
- Panagopoulos, I., J.F. Bornman and L.O. Bjorn. 1992. Response of sugar beet plants to ultraviolet-B (280-320 nm) radiation and Cercospora leaf spot disease. *Physiol. Plant.* In press.
- Penkett, S.A. 1990. Ultraviolet levels down not up. *Nature* 341:283-284.
- Robberecht, R. and M.M. Caldwell. 1978. Leaf epidermal transmittance and of ultraviolet radiation and its implications for plant sensitivity to ultraviolet-radiation induced injury. *Oecologia (Berl.)* 32: 277-287.
- Robberecht, R. and M.M. Caldwell. 1983. Protective mechanisms and acclimation to solar ultraviolet-B radiation in Oenothera stricta. *Plant Cell Environ.* 6:.
- Rozema, J., G.M. Lenssen and J.W.M. van de Staaij. 1990. The combined effects of increased atmospheric CO₂ and UV-B

- radiation on some agricultural and salt marsh species. pp 68-71, In The greenhouse effect and primary productivity in European agroecosystems. (J. Goudriaan, H. van Keulen and H.H. van Laar, eds). Pudoc, Wageningen.
- Ryel, R.J., P.W. Barnes, W. Beyschlag, M.M. Caldwell and S.D. Flint. 1990. Plant competition for light analyzed with a multispecies canopy model. I. Model development and influenced of enhanced UV-B conditions on photosynthesis in mixed wheat and wild oat canopies. *Oecologia* 82: 304-310.
- Sinclair, T.R., O. N'Diaye and R.H. Biggs. 1990. Growth and yield of field-grown soybean in response to enhanced exposure to UV-B radiation. *J. Environ. Qual.* 19: 478-481.
- Sisson, W.B. 1981. Photosynthesis, growth and ultraviolet irradiance absorbance of Cucurbita pepo L. leaves exposed to ultraviolet-B radiation (280-315 nm). *Plant Physiol.* 67: 120-124.
- Smillie, R.M. 1982. Chlorophyll fluorescence in vivo as a probe for rapid measurement of tolerance to ultraviolet radiation. *Plant Sci. Letters.* 28:283-289.
- Sullivan, J.H. and A.H. Teramura. 1989. The effects of ultraviolet-B radiation on loblolly pine: 1. Growth, photosynthesis and pigment production in greenhouse-grown seedlings. *Physiol. Plant.* 77: 202-207.
- Sullivan, J.H. and A.H. Teramura. 1990. Field study of the interaction between supplemental UV-B radiation and drought in soybean. *Plant. Physiol.* 92: 141-146.
- Sullivan, J.H. and A.H. Teramura. 1992. The effects of ultraviolet-B radiation on loblolly pines 2. Growth of field-grown seedlings. *Trees.* In press.
- Sullivan, J.H., A.H. Teramura and L.H. Ziska. 1992. Variation in UV-B sensitivity in plants from a 3000 m elevational gradient in Hawaii. *Amer. J. Bot.* In press.
- Teramura, A.H. 1990. Implication of stratospheric ozone depletion upon plant production. *HortScience* 25: 1557-1560
- Teramura, A.H. and N.S. Murali. 1986. Intraspecific differences in growth and yield of soybean exposed to ultraviolet-B radiation under greenhouse and field conditions. *Environmental and Experimental Botany* 26: 89-95.
- Teramura, A.H., J.H. Sullivan and J. Lydon. 1990a. The effectiveness of UV-B radiation in altering soybean yield: A six year field study. *Physiol. Plant.* 80: 5-11.
- Teramura, A.H., J.H. Sullivan and L.H. Ziska. 1990b. The interaction of elevated UV-B radiation and CO₂ on productivity and photosynthesis in rice, wheat and soybean. *Plant Physiol.* 94: 470-475.
- Tevini, M. and A.H. Teramura. 1989. UV-B effects on terrestrial plants. *Photochem. Photobiol.* 50: 479-487.
- Tevini, M., J. Braun and F. Fieser. 1991. The protective function of the epidermal layer of rye seedlings against

- ultraviolet-B radiation. Photochem. Photobiol. 53: 329-333.
- Tevini, M., G. Fieser and P. Grusemann. 1988. Assessment of UV-B stress by chlorophyll fluorescence analysis. pp. 229-238. In Applications of chlorophyll fluorescence. H.K. Lichtenthaler, ed.). Kluwer, Dordrecht.
- Warner, C.W. and M.M. Caldwell. 1983. Influence of photon flux density in the 400-700 nm waveband of inhibition of photosynthesis by UV-B (280-320 nm) irradiation in soybean leaves: separation of indirect and immediate effects. Photochem. Photobiol. 38: 341-346.
- Wellman, E. 1983. UV radiation: Definitions, characteristics and general effects. In Encyclopedia of Plant Physiology, New Series. Vol. 16B. (W. Shropshire & H. Mohr, ed), pp. 745-756. Springer Verlag, Berlin.
- Whittaker, R.H. 1975. Communities and Ecosystems. MacMillan Co., New York.
- Ziska, L.E., A.H. Teramura and J.H. Sullivan. 1992. Physiological sensitivity to plants along an elevational gradient to UV-B radiation. Amer. J. Bot. In press.

Table 1. A survey of UV-B radiation studies by major terrestrial plant ecosystem (after Whittaker 1975).

Ecosystem in	Global NPP ($10^9 \text{ ton}^{-\text{Yr}}$)	Total Area (10^6 km^2)	Included UV Study
Tropical forest	49.9	24.5	no
Temperate Forest	14.9	12.0	yes
Savanna	13.5	15.0	no
Boreal Forest	9.6	12.0	no
Agricultural	9.1	14.0	yes
Woodland or Shrubland	6.0	8.5	no
Temperate Grassland	5.4	9.0	yes
Swamp or Marsh	4.0	2.0	no
Desert and Semidesert	1.7	42.0	no
Tundra and Alpine	1.1	8.0	yes

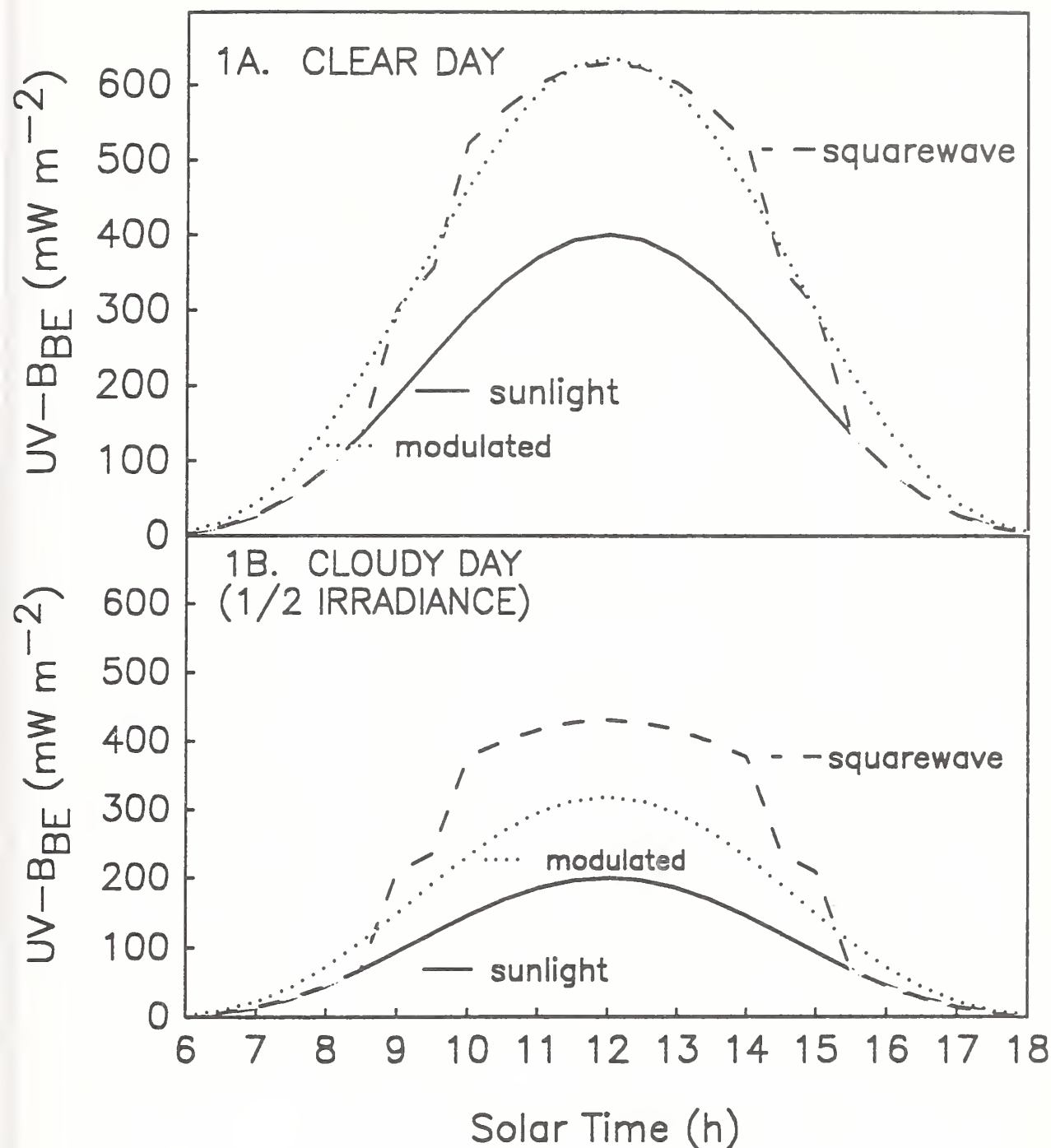


Figure 1. Representation of weighted UV-B irradiances ($UV-B_{BE}$), according to Caldwell's General Plant Weighting Function (Caldwell 1971) as predicted with an empirical model (Green et al. 1980) for natural sunlight ("sunlight"), and with supplemental UV-B simulating a 25% ozone depletion supplied with either a squarewave ("squarewave") or a modulated ("modulated") UV-B irradiation system. Theoretical conditions are for a clear day (1A) or a cloudy with total irradiance reduced by 1/2 (1B).

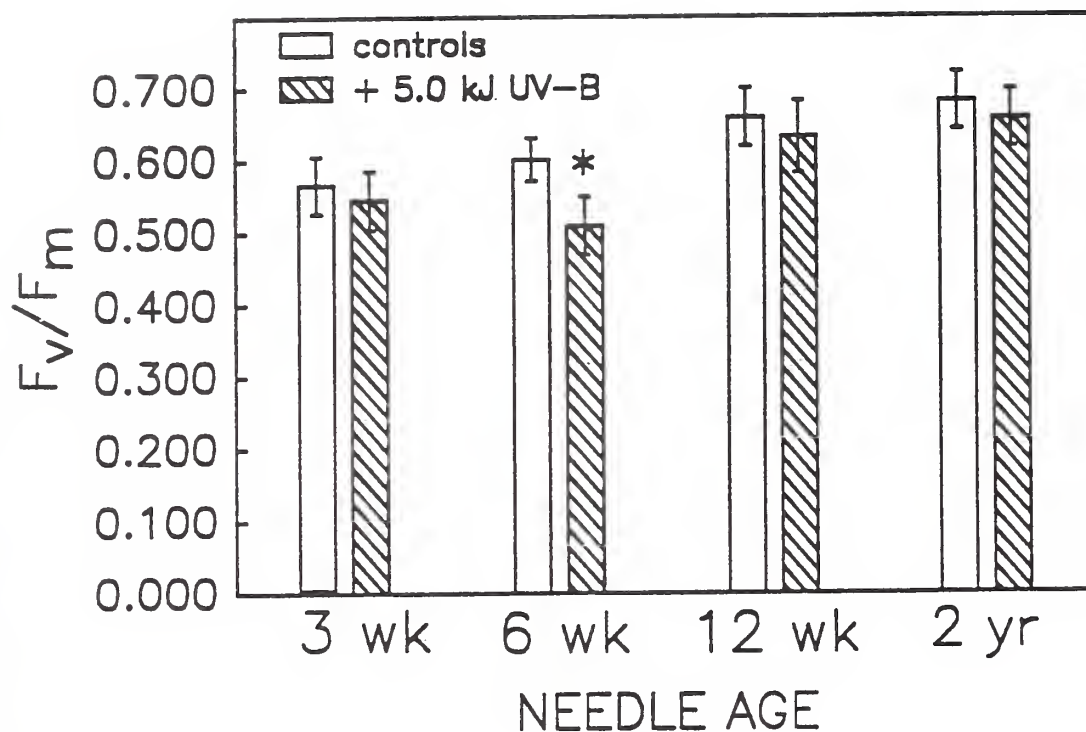


Figure 2. Photosynthetic efficiency, as measured by the ratio of variable to maximum fluorescence (F_v/F_m) with a portable chlorophyll fluorometer. Measurements were made after dark acclimation on plants grown under ambient or ambient + 5.1 kJ m⁻² UV-B radiation. The asterisk (*) represents a significant ($\alpha = 0.05$) difference between controls and supplemental UV-B irradiation (N = 12).

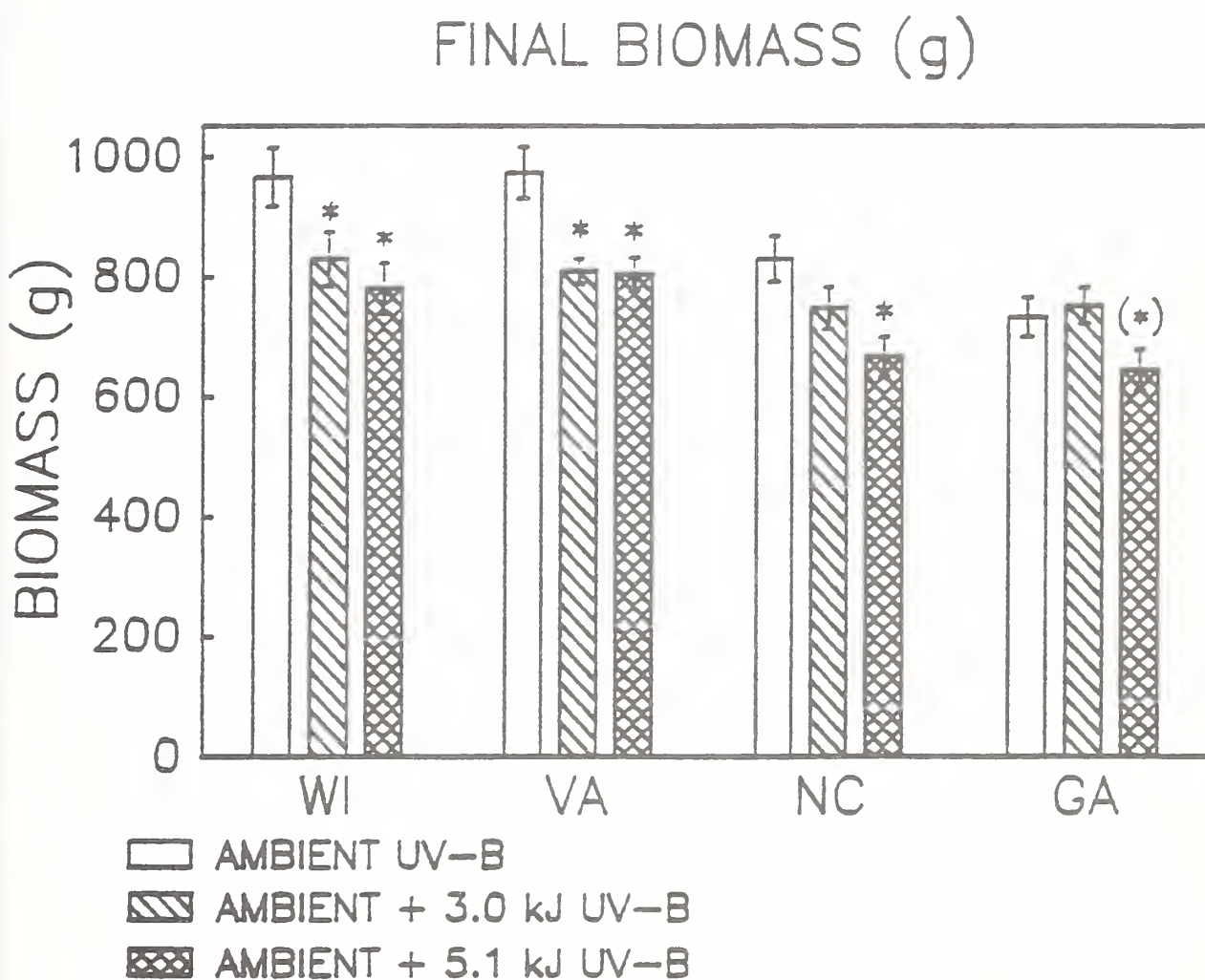


Figure 3. Biomass of loblolly pine from 4 seed sources after 3 years of growth in the field under ambient UV-B irradiances and those simulating a 16% or 25% ozone depletion over College Park, MD. Seed sources were open pollinated stands at; WI, eastern Maryland; VA, northern Virginia; NC, Piedmont North Carolina; GA, southern Georgia.

Effects on Aquatic Ecosystems

**Dr. Robert Worrest
U.S. Environmental Protection Agency**

STRATOSPHERIC OZONE DEPLETION: EFFECTS ON AQUATIC ORGANISMS

Robert C. Worrest
Office of Research and Development
U.S. Environmental Protection Agency,
Washington, DC 20460

Current Affiliation:
Consortium for International Earth Science Information Network (CIESIN)
1825 K Street NW, Suite 805
Washington, DC 20006

Introduction

Inadvertent alterations of the earth's atmosphere by human activities are now of regional and even global proportion. Increasing concern has been focused in the last two decades on the consequences of a reduction of ozone in the upper atmosphere. The problem is of truly global scale. Although individual nations and the international community have found stratospheric ozone reduction to be unacceptable, it will still take decades-to-centuries to reverse the depletion. Thus, anticipation of the consequences of stratospheric ozone reduction and efforts to mitigate such depletion are extremely important.

Based on a scientific assessment sponsored by WMO, UNEP, NASA, NOAA, and the UK Department of Environment (1991), there is undisputed evidence that the atmospheric concentrations of source gases important in controlling stratospheric ozone levels continue to increase on a global scale because of human activities. A reduction in ozone concentration will result in increased transmission of solar ultraviolet radiation through the stratosphere. Many adverse, serious effects of such an increase in exposure to this radiation have been identified, and the effects will continue well into the next century even with a vigorous mitigation program. To establish responsible regulations and mitigation options, we need to know more precisely what the effects of ozone depletion are likely to be. The potential effects may be to the point of seriously threatening many of the Earth's natural resources.

Although ozone constitutes a very small proportion of the stratosphere, it plays a major role in protecting life on this planet. The result of changes in the density of the total ozone column could, therefore, be far-reaching. The natural distribution of ozone in the Earth's atmosphere, concentrated most heavily in a diffuse layer in the stratosphere, is crucial in helping to protect humans, other biological systems, and man-made materials from the harmful effects of certain wavelengths of sunlight. Stratospheric

ozone exerts its beneficial effects by absorbing ultraviolet radiation in the 200- to 320-nm range, with reduced amounts of radiation in the 290- to 320-nm waveband (ultraviolet-B or UV-B radiation) penetrating to the Earth's surface. Depletion of the stratospheric ozone layer can, therefore, be expected to lead to damaging effects on human health and the environment (1) directly by increased penetration of UV-B radiation to the Earth's surface and (2) indirectly by the influences of changes in the vertical distribution of stratospheric ozone and water vapor that contribute to global warming effects and altered climatic conditions. If a decrease in total atmospheric ozone were to occur, exposure to solar radiation in the 290- to 320-nm waveband would increase at the surface of the earth.

Effects on Aquatic Organisms

For components of marine ecosystems, various experiments have demonstrated that UV-B radiation causes damage to fish larvae and juveniles, shrimp larvae, crab larvae, copepods, and plants essential to the marine food web. These damaging effects include decreased fecundity, growth, survival, and other reduced functions in these organisms (Worrest, 1982; U.S. EPA, 1987; Häder et al., 1989; Häder & Worrest, 1991; Häder et al., 1991). Although not nearly as important as light, temperature or nutrient levels, evidence indicates that ambient solar UV-B radiation is currently an important limiting ecological factor, and that even small increases of UV-B exposure could result in significant ecosystem changes (Damkaer, 1982).

Effects induced by solar UV-B radiation have been measured to a depth of more than 20 meters in clear waters and more than five meters in unclear water. The euphotic zone (i.e., those depths with levels of light sufficient for positive net photosynthesis) is frequently taken as the water column that reaches down to the depth at which photosynthetically active radiation is reduced 99%. In marine ecosystems, UV-B radiation penetrates approximately the upper 10% of the marine euphotic zone before it is reduced to 1% of its surface irradiance. Penetration of UV-B radiation into natural waters is a key variable in assessing the potential impact of this radiation on any aquatic ecosystem (U.S. EPA, 1987).

Smith et al. (1992) reported that phytoplankton communities confined to the near-surface waters of the marginal ice zone in the Antarctic region are potential targets of increased UV-B exposure resulting from springtime losses of ozone in that region. The authors speculated that the increased exposure would alter the dynamics of the marine ecosystem in the region, estimating that a minimum of six to twelve percent reduction in primary production, associated with ozone depletion, occurred during the duration of the measurements.

In marine plant communities a change in species composition rather than a decrease in net production would be the probable result of enhanced UV-B exposure (Worrest, 1983). A change in community composition at the

base of food webs may produce instabilities within ecosystems that likely would affect higher trophic levels (Kelly, 1986). The generation time of marine phytoplankton is in the range of hours to days; whereas the potential increase in ambient levels of solar UV-B irradiance will occur in the range of decades. The question remains as to whether the gene pool within species is variable enough to adapt during this relatively gradual (relative to the generation time of the target organisms) change in exposure to UV-B radiation. There is evidence that a decrease in column ozone abundance could diminish the near-surface season of invertebrate zooplankton populations. For some zooplankton, the time spent at or near the surface is critical for food gathering and breeding. Whether the population could endure a significant shortening of the surface season is unknown (Damkaer et al., 1980).

The direct effect of UV-B radiation on food-fish larvae closely parallels the effect on invertebrate zooplankton. Information is required on seasonal abundances and vertical distributions of fish larvae, vertical mixing, and penetration of UV-B radiation into appropriate water columns before effects of exposure to solar UV-B radiation can be predicted. However, in one study involving anchovy larvae, it was calculated that a 20% increase in UV-B radiation (which would accompany a 9% depletion of total column ozone) would result in the death of about 8% of the annual larval population (Hunter et al., 1982). This one study was performed in the laboratory, and even the control animals had significant mortality at the end of the normal larval period. This highlights the need for caution when trying to extrapolate conclusions to natural conditions when those conclusions are based on results from laboratory studies.

For many countries marine species supply more than fifty percent of the dietary protein. In many developing countries, this percentage is even larger. Research is needed to improve our understanding of how stratospheric ozone depletion could influence the world food supply. However, in the meantime, the nature of the potential global implications of any future effective steps to start to minimize stratospheric ozone depletion cannot wait for the outcome of such research.

Conclusions

Stratospheric ozone depletion has the potential to exert very substantial effects on the environment. However, our ability to predict with confidence and precision the likelihood of particular effects occurring and to quantify their anticipated ultimate scope varies greatly due to differences in the current level of our state of knowledge about particular types of effects. Table 1 illustrates differences in our state of knowledge regarding various types of anticipated effects and their potential global impact, as viewed by an expert subcommittee of EPA's Science Advisory Board and discussed by Kripke (1988). A major present dilemma is the fact that our current state of

knowledge is low with regard to certain effects that have the greatest potential for widespread global impacts. For example, the current state of knowledge concerning potential effects of increased UV-B radiation on immune system function is relatively low, but the global impact on human health could be quite high.

TABLE 1. POTENTIAL EFFECTS OF INCREASED UV-B RADIATION RESULTING FROM DECREASED STRATOSPHERIC OZONE¹

Effects	State of Knowledge	Potential Global Impact
Skin Cancer	Moderate to high	Moderate
Immune System	Low	High
Cataracts	Moderate	Low
Plant Life	Low	High
Aquatic Life	Low	High
Climate Impacts*	Moderate	Moderate
Tropospheric Ozone	Moderate	Low**
Polymers	Moderate	Low

*Contribution of both stratospheric ozone depletion itself and gases causing such depletion to climate changes, including sea level rise.

**Impact could be high in selected urban or rural areas typified by local or regional scale surface-level ozone air pollution problems.

¹Modified from SAB-EC-87-025 "Review of EPA's An Assessment of the Risks of Stratospheric Modification by the Stratospheric Ozone Subcommittee, Science Advisory Board, U.S. Environmental Protection Agency, March, 1987.

Additional research is needed to gain a more complete understanding of the effects of increased solar UV-B radiation on human health and the environment. Research priorities continue to relate to UV-B penetration into the water column and through ice. This basic physical information should then be used both in laboratory and field research to determine effects on phytoplankton and zooplankton. In addition, adaptive strategies of the plant and plankton communities need to be studied over extended periods of time as well as the effects of interactive stresses (temperature, salinity, etc.) and cumulative doses received over the lifetime of the organisms. And finally, plankton effects should be modeled into broader ecosystem dynamic patterns, which will feed into models of global carbon and nitrogen cycling.

References

- Damkaer, D.M. (1982) Possible influence of solar UV radiation in the evolution of marine zooplankton, In: Calkins, J. (ed.) *The Role of Solar Ultraviolet Radiation in Marine Ecosystems*, Plenum, New York.
- Damkaer, D.B. Dey, D.M., Heron, G.A., & Prentice, E.F. (1980) Effects of UV-B radiation on near-surface zooplankton of Puget Sound, *Oecologia* 44:149-158.
- Häder, D.-P., & Worrest, R.C. (1991) Effects of enhanced solar ultraviolet radiation on aquatic ecosystems, *Photochemistry and Photobiology* 53:717-725.
- Häder, D.-P., Worrest, R.C., & Kumar, H.D. (1989) Aquatic ecosystems, In: van der Leun, J.C., Tevini, M., & Worrest, R.C. (eds.) *Environmental Effects Panel Report*, United Nations Environment Programme, Nairobi, Kenya.
- Häder, D.-P., Worrest, R.C., & Kumar, H.D. (1991) Aquatic ecosystems, In: van der Leun, J.C., & Tevini, M. (eds.) *Environmental Effects of Ozone Depletion: 1991 Update*, United Nations Environment Programme, Nairobi, Kenya.
- Hunter, J.R., Kaupp, S.E., & Taylor, J.H. (1982) Assessment of the effects of UV radiation on marine fish larvae, In: Calkins, J. (ed.) *The Role of Solar Ultraviolet Radiation in Marine Ecosystems*, Plenum, New York.
- Kelly, J.R. (1986) How might enhanced levels of solar UV-B radiation affect marine ecosystems?, In: Titus, J.G. (ed.) *Effects of Changes in Stratospheric Ozone and Global Climate*, U.S. Environmental Protection Agency and United Nations Environment Programme, Washington, D.C.
- Kripke, M.L. (1988) Health effects of stratospheric ozone depletion: an overview. In: Schneider, T., Lee, S.D., Grant, L.D., Wolters, G. (eds.) *Atmospheric ozone research and its policy implications: third US-Dutch international symposium*; May; Nijmegen, The Netherlands. Amsterdam, The Netherlands: Elsevier.
- Smith, R.C., Prézelin, B.B., Baker, K.S., Bidigare, R.R., Boucher, N.P., Coley, T., Karentz, D., MacIntyre, S., Matlick, H.A., Menzies, D., Ondrusek, M., Wan, Z., & Waters, K.J. (1992) ozone depletion: ultraviolet radiation and phytoplankton biology in Antarctic waters, *Science* 255:952-959.
- U.S. EPA (1987) An assessment of the effects of ultraviolet-B radiation on aquatic organisms, In: Hoffman, J. (ed.) *Assessing the Risks of Trace Gases that Can Modify the Stratosphere*, pp. (12)1-33, USEPA 400/1-87/001C.
- WMO, UNEP, NASA, NOAA, UK Department of Environment (1991) Scientific Assessment of Ozone Depletion: 1991.

Worrest, R.C. (1982) Review of literature concerning the impact of UV-B radiation upon marine organisms, In: Calkins, J. (ed.) *The Role of Solar Ultraviolet Radiation in Marine Ecosystems*, pp. 429-458, Plenum, New York.

Worrest, R.C. (1983) Impact of solar ultraviolet-B (290-320 nm) upon marine microalgae, *Physiol. Plant.* 58:428-434.

Biological Action Spectra

**Dr. Thomas Coohill
Western Kentucky University**

Action Spectroscopy And Stratospheric Ozone Depletion

Thomas P. Coohill
Department of Physics & Astronomy
Western Kentucky University
Bowling Green, KY 42101, USA

Summary:

Action spectroscopy has a long history and is of central importance to photobiological studies. Action spectra were among the first assays to point to chlorophyll as the molecule most responsible for plant growth and to DNA as the genetic material. It is useful to construct action spectra early in the investigation of new areas of photobiological research in an attempt to determine the wavelength limits of the radiation region causing the studied response. But due to the severe absorption of ultraviolet radiation by biological samples, ultraviolet action spectra were first limited to small cells (bacteria and fungi). Advances in techniques (eg. single cell culture) and analysis allowed accurate action spectra to be reported even for mammalian cells. But precise analytical action spectra are often difficult to obtain when large, pigmented, or groups of, cells are investigated. Here some action spectra are limited in interpretation and merely supply a wavelength versus effect curve. When polychromatic sources are employed the interpretation of action spectra is even more complex and formidable. But such polychromatic action spectra can be more directly related to ambient responses. Since precise action spectra usually require the completion of a relatively large number of careful experiments using somewhat sophisticated equipment over a range of at least six wavelengths, they are often not perused. But they remain central to the elucidation of the effect being studied. The worldwide community has agreed that stratospheric ozone is depleting, with the possibility of a consequent rise in the amount of UVB (290-320 nm) reaching the earth's surface. It is therefore essential that new action spectra be completed for UVB effects on a large variety of responses of human, animal, and aquatic plants systems. Combining these action spectra with the known amounts of UVB reaching the biosphere can give rise to solar ultraviolet effectiveness spectra that, in turn, can give rise to estimates of effect. Preliminary estimates suggest that ozone layer depletion may seriously impact such important biological end-points as skin cancer, cataracts, the immune system, crop yields, and oceanic phytoplankton. So action spectra continue to play a central role in important photobiological research.

Action Spectroscopy:

Among the methods of obtaining and analyzing photobiological data, the technique known as action spectroscopy plays a central role in the initial characterization of bioresponses. Action spectroscopy is most simply defined as the measurement of a biological effect as a function of wavelength (λ). Crude action spectra (AS), the term "action

spectrum" was not coined until the nineteen forties (Kleczkowski, 1972), were first used in the nineteenth century to help identify chlorophyll as the chromophore most responsible for the growth of plants (Daubeny, 1836; Engelmann, 1882; Draper, 1884). In this century more sophisticated methods refined the analysis of AS such that it is now possible, in some instances, to make a reasonable determination of the molecule likely to contain the chromophore(s) responsible for the response being studied. It is this latter usage that has allowed such important identifications as the determination of DNA as the genetic material (Gates, 1930; Hollander and Emmons, 1941). This was possible because of the experimental availability of small unicellular organisms (such as bacteria and fungi) for photobiological studies. Such systems meet a variety of rather stringent criteria (see below) for reliable analysis of what I will term an analytical action spectrum. However, it is still possible to glean some information about the photoresponses of organisms that do not meet these criteria, although it may be impossible to identify either the molecule(s) or the mechanism(s) involved in the process being studied. It may not be possible to circumvent these limitations if a complex process, such as plant "growth", is to be analyzed. Action spectra for this latter process may be nothing more than a determination of effect as a function of wavelength and remain uninterpretable as to the mechanism causing the effect. But even here, such action spectra can be useful in estimating response to ambient or changing light exposures. A discussion of various types of AS follows.

Analytical Action Spectra (AAS)

If it is desirable and possible to do so, a carefully constructed AS can identify the absorbing chromophore. This can occur if the AS corresponds closely to the absorption spectrum of a molecule that can be shown to be affected by exposure to radiation in the λ region tested, and that, within reason, can be thought of as being involved in the metabolic process being studied. The affected chromophore, which has an energy level configuration that matches the energy of the incident photons, is not necessarily situated in the molecule that causes the ultimate effect. An energy transfer from the absorbing chromophore to the eventual target molecule can occur and can sometimes be measured (Jagger, 1967; Coohill, 1984; Coohill et al., 1987).

The following six fundamental conditions are necessary for the construction of an analytical action spectrum (for a more complete description see Jagger, 1967). First, at no λ should more than half of the incident radiation be absorbed by the sample before every participating chromophore is exposed. Ideally, each chromophore should be exposed to the same number of photons in order to have the same probability of responding, but this is never the case with biological samples. The higher the transmission of the sample, the more accurate the AAS can be. Thus, Gates (1930) was able to obtain a relatively rigorous AAS, because he used the bacteria E. coli and S. aureus which have cellular diameters of less than 2μ . He measured the absorption of a monolayer of these cells at 260 nm to be about 25% (Gates, 1930), saying in addition that a thin layer of such cells was "all but colorless in visible light, and so transparent that objects may be seen through it clearly and without distortion". Jagger (1967) estimated the amount of absorption to the center of an E. coli

cell, at this same λ , to be equal to or less than 15% (depending in the growth stage of the cell). Various measurements and calculations for mammalian cells show that more than half of the radiation at 260 nm will be absorbed before it reaches the center of a spherical cell (radius 10μ), while less than a third will be absorbed before it reaches the center of the nucleus of a flattened umbonate cell (Hatfield et al., 1970; Coohill, et al., 1979). Table 1 contains additional estimates for the absorption properties of various cells and viruses. Even with substantial absorption, reasonable AAS for such important mammalian cell functions as survival, mutation, and viral induction have been reported (Todd et al., 1968; Rothman and Setlow, 1979; Jacobson et al., 1980; Kantor et al., 1980; Doniger et al., 1981; Sutherland et al., 1981; Coohill et al., 1982). Significant absorption of UV radiation by multicellular organisms, such as plants, usually precludes an AAS, but useful AS have been constructed, some utilizing higher plants (Boegenrieder, 1982; Bornman, 1984; Caldwell et al., 1986; Jones and Kok, 1966; Negash, 1987; Tevini and Steinmüller, 1988).

The second criterion for a AAR is that scattering and absorption of radiation in front of the target chromophore should be either negligible, and thus satisfy the criterion of high transmission, or amenable to a "correction factor" for such shielding. For example, if the absorption and scattering properties of the membranes and cytoplasm, and their thicknesses, between the incident beam and a centrally located target chromophore, such as nuclear DNA, are known, then it may be possible to subtract these effects and predict the intensity and wavelength distribution of the radiation reaching the target molecules (Coohill and Deering, 1969; Coohill et al., 1979). Even better, if a target, such as adjacent pyrimidine molecules in DNA, is known to cause an effect, and if the consequent photoproduct (the pyrimidine dimer) can be measured, then an AS for dimer formation can be compared to an AS for cell killing, and, if similar, account for any observed shift in the peak of this spectrum compared to the absorption spectrum of isolated DNA (Coohill, 1984). If a detailed knowledge of the target chromophore or of the absorption and scattering events before the radiation impinges on the chromophore are not known, then any correction factor is suspect. For those cells that can change their size (Coohill and Deering, 1969) or shape (Coohill et al., 1979) it is sometimes possible to alter the exposure to the cell surface in such a manner as to expose the center of the cell to the same fluence (Coohill and Deering, 1969; Coohill et al., 1979). Again, these experimental modifications should be avoided if careful measurements of cellular dimensions are not available.

A third criterion demands that the absorption spectrum in vitro, for a given chromophore, be identical to its absorption spectrum in vivo, in order to compare it to a AAS. In addition, the quantum yield, which is the probability of a photochemical change in a chromophore that has absorbed a photon, should be the same for all the λ tested in the AAR. Otherwise the effect can vary with λ even without a change in the absorption of radiation by the chromophore. Although this should be tested, it rarely is, but it is often a safe assumption for biomolecules (Jagger, 1967).

The fifth criterion for an accurate AAS, involves the shape of the fluence effect curves ("survival" curves if cell killing is being measured). It should be possible to multiply each separate λ survival curve by a suitable fluence modification factor such that the curves are reasonably super imposable upon one another. This is an easily tested and crucial factor in determining whether one is looking at the same mechanism of action throughout the λ region being employed. This can often be complicated by the extent of the non responsive (shoulder) portion of the fluence effect curves, which, in turn may well be affected by extraneous factors, such as the amount of photochemical repair being accomplished during the assay period (Jagger, 1967; Caldwell et al., 1986).

The sixth, and often the easiest, criterion to test is whether the effect is the same regardless of the rate at which the exposure is given. In other words, if a given amount of radiation is delivered to a sample in a short time at one λ , but due to experimental constraints, over a longer time period at a different λ , does the efficiency of the process change? It is therefore imperative that each λ used be tested in fluence rate over as much of the range of fluence rates used at other λ as is possible. It is usually impossible to shorten each fluence rate to that of the briefest exposure, since sources do not usually emit at the same rate for each λ , so one normally extends the most effective λ to longer times. Often this reciprocity has to be tested over a fluence rate range of at least a factor of three.

Even if all of the above constraints are met, and they never are, there are experimental variables that can limit the reliability of any AS. These include, but are not limited to; the spectral purity of the radiation source; the accuracy of the dosimetry measurements; the placement of the dosimeter (ideally-at the sample); the presence of exogenous and/or endogenous "non-participating" chromophores; the ambient (even micro-environmental) conditions; the time in the life cycle (cellular) or growth cycle (developmental) of the exposed organism; the physical state of the target molecule (eg., DNA extended or coiled in chromatic); and numerous extraneous conditions. In addition, cells often harbor sophisticated and efficient methods for repairing photobiological damage (Jagger, 1967). Again, the extent of this repair during irradiation and before assay can significantly effect the measured response. All of these variables can given rise to errors in the interpretation of an AAS. Hence, "a particular action spectrum is a very specialized thing and may apply only under the conditions actually used to obtain it" (Jagger, 1967).

Even given the above constraints, AAS have been produced that have pointed to the answer for crucial biological questions. Perhaps the most famous AAS is that of Gates (1930) which showed, for the first time, that nucleic acid (presumably DNA), was the target molecule for the death of bacterial cells (both E. coli and S. aureus). This was the first clear evidence that the genetic material was DNA, not, as was then widely believed, protein (Fig. 1). Almost a decade later, even more tenable results for identification of the genetic material, were the AAS that involved cellular mutation by UV (Fig. 1). Knapp, Reuss, Risse, and Schreiber (1939) using the spores of Sphaerocarpus Donnellii, Stadler and Uber (1941) using the pollen of maize, and Hollander and Emmons (1941) using the fungus Trichophyton metagrophytes, all showed that UV in the region of about 265 nm was the

most effective λ for cellular mutation. Unlike cell killing, which could be caused by a variety of cellular dysfunctions, cell mutation was clearly thought to be a product of the genetic material. Hollander and Emmoms (1941) went on to compare these results with those for cell killing in these organisms and concluded that "the 265 nm maximum coincides with the high absorption coefficient of nucleic acids near this wavelength". The discrepancy at 218 nm in the correlation between the AS for fungal mutation (Fig. 1) and the absorption spectrum of DNA can easily be accounted for by the substantial absorption (75%) of UV by fungi at this λ before the radiation reaches the center of the cell, when compared to bacteria (45%) (Coohill, 1986). A correction for this fungal absorption value would raise that point in the figure to a level that essentially coincided with the absorption value of DNA at that λ . All of these studies and those of Gates (1930) preceded the biochemical work of Avery et al. (1944) which is usually regarded as the first "clear" evidence that DNA was the genetic material, ie. "Avery's bombshell".

Although AAS utilizing small cells flourished, it was difficult to extend these studies to larger (eg mammalian) cells because of the substantial absorption of UV by large cells and tissues (Fig. 2). Early attempts by Mayer and Schreiber (1934) failed to produce AS with the fine structure of those of Gates (1930), because they employed hanging-drop mammalian tissue samples that were essentially opaque to radiation near the peak of DNA absorption (260 nm). But, with the advent of single cell mammalian culture techniques, and with the unique flattened geometry that mammalian cells assume when in monolayer culture (Coohill et al., 1979) these studies began to appear in the late 1960's. The first AAS for mammalian cell killing (Todd et al, 1968) reported data similar to that of Gates (1930) with bacteria, but with a peak effect shifted slightly toward longer λ (peak 270 nm). This gave rise to the belief that both nucleic acids (peak absorption 260 nm) and proteins (peak absorption 280 nm) might contribute to reproductive death in these cells. However, once measurements of the AS for pyrimidine dimer production were available (Rothman and Setlow, 1979; Doniger et al., 1981; Enninga et al., 1986; Rosenstein and Mitchell, 1987), it could be shown that DNA alone was responsible for mammalian cell lethality by UVC (Coohill, 1984).

Polychromatic Action Spectra (PAS)

Many authors, perhaps realizing the futility of attempting to construct monochromatic AAS using multi-cellular organisms, have reported AS that employ polychromatic sources. These polychromatic AS (PAS) add to the complexity already inherent in the literature involving λ studies and bio-effects. These studies vary from irradiating the affected system with single UV wavelengths only (and then growing them under normal illumination ie., a "standard" AS), adding single wavelengths to a "white" light background, or generating a set of data using polychromatic sources that employ cutoff filters at successively shorter wavelengths. The former monochromatic system is accurate, the preferred way for determining the target chromophore, and the classical method for generating an analytical action spectrum, i.e. an accurate plot of biological effect as a function of single-wavelength irradiations. However, this system is highly artificial and

greatly removed from the natural setting. The polychromatic system is complex, tends to obscure individual chromophores, but is closest to natural field conditions. A major advantage of using polychromatic radiation in the development of PAS is that interactions of biological responses to different wavelengths (usually unknown) can be empirically incorporated into the composite spectrum. For example the involvement of photorepair systems or other cellular responses to longer wavelength radiation that might mitigate the damaging effect of shorter-wavelength radiation can be assessed without knowing about the nature or spectra for these repair and/or mitigating responses (Jagger, 1967; Caldwell, 1971; Beggs et al., 1985). It should be remembered that the monochromatic action spectra widely used for erythema (Parrish et al., 1978) and for DNA (Setlow, 1974) have proven useful in making general statements about biological responses to UV. The same would be true for more complex systems, such as plants. However, a PAS is useful because of its closer relation to the natural setting.

Stratospheric Ozone Depletion and Action Spectroscopy

So the field of action spectroscopy is quite complex. However, once again, it is an important first analysis in determining bioresponses to the natural environment. By 1988, the scientific community had reached agreement that a portion of the earth's protective stratospheric ozone layer was being depleted, largely by man-made chemicals (Frederick, 1990; Caldwell et al., 1989; Stolarski, 1988). This consensus was arrived at by the careful analysis of a substantial amount of data on the vertical ozone column, recorded by balloon, rocket, airplane, and other measurements. Earth based wavelength measurements in the UVB, largely conducted with "Dobson" meters confirmed the former experiments (Lubin et al., 1989; Frederick et al., 1989; World Meteorological Organization, 1989). But the amount of stratospheric ozone loss above temperate areas, especially in the northern hemisphere, was not enough (less than 10%) to cause alarm to the general public, even though (see below) this may have serious consequences for life on earth. It was the advent of the antarctic "ozone hole" that convinced the public, governmental agencies, and even skeptical scientists that the ozone layer was indeed being reduced, by as much as 50% in this case, and that this loss could be attributed, in large part, to human activities (Stolarski, 1988). The ozone hole (Farman et al., 1985) which appears only in the austral spring, was further observed to break up in the summer months and spin off depleted areas that caused severe temporary ozone losses above some major populated areas in the southern hemisphere (eg. reported 35% depletion above the city of Melbourne).

Although the list of chemical pollutants responsible for the loss of stratospheric ozone is long, one major group is the chlorofluorocarbons (CFC) invented in the 1930's (Rowland, 1989). These CFC are widely used in a variety of manufactured goods because of their stability, inertness, and long life. Thus many coolants, electronic solvents, foams, etc. contain CFC which are slowly released into the atmosphere where they can exist for up to one hundred years. About thirty years after release these CFC percolate into the

stratosphere where, via a reaction involving short wavelength ultraviolet radiation they produce free chlorine which destroys ozone. Each CFC molecule acts in a catalytic fashion to destroy about 100,000 ozone molecules.

Considering the geopolitical situation, a rapid response to this world wide threat produced the first Montreal Protocol in 1985, which addressed the problem directly by proposing limits on CFC production. Subsequently, these restraints have been made more stringent as additional data accumulates (Montreal Protocol, 1987). It is hoped that this treaty will turn off the source of CFC (and other offending gases) by the early twenty-first century. The use of transition chemicals, eg. HCFC, will be introduced to allow us to evolve to a series of chlorine free substitutes for CFC that are both safe and energy efficient. However, even if all CFC usage were to stop by the turn of the millennia, the release of the CFC already in the world, and their long lifetimes, means that the ozone layer will continue to be adversely affected until at least the mid-twenty first century.

The immediate question that this problem posed is, "what will this mean for the world?" The most important direct consequence of this loss of ozone is an increase in the amount of a certain portion of the UV spectrum reaching the earth's surface. This increase will be largely confined to the wavelength region 295-315 nm since shorter wavelengths are absorbed by other atmospheric components, while longer ones penetrate the current atmospheric column. This narrow region is a large fraction of the UVB (290-320 nm). Thus the effects of O₃ depletion can be assessed by estimating or measuring the additional consequences of increased UVB-exposure. These consequences are largely biological. Hence, a broad understanding of the UVB photobiology of living organisms is essential, if we are to estimate the worldwide effect of O₃ depletion. What follows is a general attempt at such estimations and a description of the use of AS for addressing the extent of this problem. Future estimates will follow as the amount of data collected on these systems increases. A goal is to provide the scientific, governmental, and public communities with reasonable, scientifically based values that can be used for determining appropriate responses to this worldwide problem.

Ultraviolet B Photobiology

The vast majority of biological organisms evolved after the initial formation of the stratospheric O₃ layer. This layer provided for living forms an umbrella of protection from the deleterious effects of UV by absorbing heavily those UV wavelengths below 320 nm. It is probably not a coincidence that the single most important molecule in living cells, ie. the genetic material DNA, has an absorption spectrum that peaks at 260 nm (well below 320 nm) and drops by three orders of magnitude at 320 nm (Fig. 3). In addition the molecules plastoquinone and plastoquinol, both important in photosynthesis, also absorb strongly at λ below 310 nm (Fig. 3). The percentage of UVB in the solar output reaching the top of the earth's atmosphere is less than 1.5% (20 Wm^{-2}); the amount reaching the earth's surface is less than 0.3% (2 Wm^{-2}) due to the filtering effect of atmospheric chemicals. Even so, there is enough ambient UVB reaching the biosphere to produce some damage to cellular

DNA. UV effects on DNA are widely reported and include such photochemical changes as pyrimidine dimers, 6-4 photoproducts, DNA-protein cross links, and lesions that can lead to single and double strand breaks (Peak and Peak, 1986; Mitchell and Nairn, 1989; Ananthaswamy and Pierceall, 1990). If left unrepaired, these lesions may lead to impairment, mutation, or even cell death (Churchill et al., 1991). For these reasons, some organisms avoid exposure to high levels of ambient UV, or are advised to do so in the case of humans, to prevent serious damage. The biochemical and physiological consequences of UV exposure to some biological system are well characterized and reasonably well understood (Jagger, 1967; Jagger, 1985) when compared with other insults, eg. ionizing radiation (Elkind and Whitmore, 1967).

Any analysis of biological responses to UV is complicated by a large number of variables (Caldwell et. al., 1986). For example, some plants have evolved in brilliant sunlight and would be expected to have developed defensive mechanisms to cope with high levels of UV. In addition, animals, especially humans, can avoid sunlight if they choose; terrestrial plants cannot. Shielding of component cells and tissues in higher organisms, or shielding of single cells by other cells in a system, is difficult to estimate. Plant cells are often highly pigmented and hence especially able to protect centrally located target molecules such as DNA (Coohill and Deering, 1969) from the harmful effects of UV. Pigmentation in animal cells varies. The wide variety of biological responses measured in plants also limits the degree to which comparisons between laboratories may be made (Caldwell, 1971; DeFabo et al., 1976; Halldal, 1967; Imbrie et al., 1982). Plants are exposed to many stresses in addition to UV radiation (Teramura, 1986, 1987; Tevini et. al., 1983). These include, but are not limited to, available nutrients, water stress, atmospheric composition, etc. Any attempt to provide a general picture of a typical plant's responses to these varied parameters is at best difficult and at worst impossible. Most animal experiments are confined to laboratory studies, often single cells or groups of cells in culture, a highly artificial situation (Coohill, 1984). A limited first approximation of the type of general data available from experiments with higher plants may be useful, and should follow from the plant work of Caldwell (1971) and Tevini (1988) and include the important results from their work and that of others (Bogenreider, 1982; Bornman et. al., 1984; Caldwell et. al., 1986; Jones and Kok, 1966; Steinmüller, 1986; Tevini and Steinmüller, 1988). Results reported for lower plants have already been compiled (Häder, 1988; Nultsch et. al., 1987). Data from animal, mostly mammalian cells in culture, are available from a variety of sources, partially summarized by Coohill (1984) and Coohill, et. al. (1987). So, the known depletion of stratospheric ozone, and the consequent increase in the amount of UVB (290 - 320 nm) radiation reaching the biosphere (Frederick and Lubin, 1988; Lubin et al., 1989), is of major concern to the worldwide community. Government agencies, the popular press, and others, are keenly aware of this environmental problem, and, as is correct, have turned to the photobiological community with the question "how will this affect life on earth".

Effectiveness Spectra (ES)

One obvious method of providing at least limited estimates for these effects is to obtain AS for a given effect, and combine this with the known (or estimated) ambient solar radiation expected due to various ozone depletion scenarios. Such an effectiveness spectrum (ES, Turro and Lamola, 1977) can be used to give first approximation preliminary estimates for the effects of this increased UVB on the biosphere.

For example, one could combine the AS for cell erythema with the known, and with an estimated depleted ozone layer, solar spectrum reaching the earth's surface to produce two ES and measure the increase in effect due to the latter (Fig. 4). Other well established AS could be used to produce similar ES that would allow reasonable estimates to be stated for the biological consequences of a decreased ozone layer. Preliminary attempts for some biological parameters, such as skin cancer, have already been made (Dahlback et al., 1989; Dahlback and Moan, 1990; Henricksen et al., 1990; Kelfkens et al., 1990; Urbach, 1989). For example, Henricksen et al. (1990) predicted a 2% increase in overall skin cancer for each 1% depletion of stratospheric ozone. Other estimates for these direct effects on human health are needed, eg. cortical cataracts (Taylor, 1989), and some are being proposed, eg. immune suppression (De Fabo et al., 1990).

But perhaps the most significant detrimental biological effects, even for human populations, will be those due to increased exposure to UVB of both terrestrial and aquatic organisms, especially plants. Data for UV effects on terrestrial higher plants is being collected, mainly for important crops, and, in some instances forest species (Sullivan and Teramura, 1988). Initial crop data show that several cultivars of some major crop species are sensitive to UVB. These include soybeans, beans, wheat, peas, rice, potato, squash, and cassava (Tevini et al., 1989; Tevini, 1988; Teramura, 1983; Teramura and Murali, 1986; Teramura, personal communication). Some studies show other cultivars of rice and wheat to be insensitive to UV (Tevini et al., 1989). Other crops appear to be UV resistant, eg. corn, peanuts, and cabbage (Tevini et al., 1989). Estimates of the extent of this sensitivity are difficult to make even for such vague assays as "yield". But the results cited above seem to show that decreases in yield quantity and quality may well occur under enhanced UVB exposure. Attempts to construct an ES from a generalized plant damage AS (Caldwell, 1971) or from a variety of end-points weighted for photosynthesis (Coohill, 1989) allow a preliminary estimate of a 1% decrease for each 1% decrease in the ozone layer (Fig. 5). However, it must be remembered that no one AS represents the general responses for higher plants. If crop yields diminish, certain human populations already near the limit of starvation may be dramatically effected.

All of the above ES show that the λ region 295 - 315 nm (ie., contained within the UVB) is the only region of the UV spectrum that will show an increase in biological effect due to ozone depletion.

Some scientists think that the first noticeable effect of a depleted ozone layer might be a reduction in the phytoplankton community in the world's oceans (Bidigare, 1989; El Sayed, 1988; El Sayed et al., 1989; Häder, 1986; Häder et al., 1987). Laboratory results show that some phytoplankton already appear to be at, or near, their UV stress limit. Small increases in UV-B may dramatically lower their reproductive rate. In oceanic populations the situation is more complex since photoplankton may move to lower positions in the water column to avoid additional UV. Such movement would also lower their photosynthetic efficiency. In addition, different species may predominate in the new solar UV surroundings. Field studies, though difficult, are being attempted (Mitchell et al., 1989). Estimates for the effects of additional UV on total phytoplankton mass vary widely (Smith, 1989) from dramatic (ie., a 4% decrease for each 1% decrease in ozone [El Sayed, 1988, 1989]), to negligible (no decrease, [Mitchell et al., 1989]), and even in some cases to an increase (Morel and Price, 1989). At present, a crude estimate would be that the total phytoplankton population could decrease as much as 1% for each 1% loss of ozone (Hader, personal communication). Since plankton account for more than half of the earth's biomass and, hence, fix more than half of the atmospheric CO₂, any reduction in their population will have drastic effects on the aquatic food chain and could contribute significantly to the greenhouse effect.

Conclusions

Thus, accurate information is needed to assess the potential effects on living organisms caused by an increase in the ultraviolet radiation reaching the earth's surface due to the depletion of stratospheric ozone. Of immediate use would be a series of action spectra for general biological effect(s) that would typify responses to increased UVB (290 - 320 nm). At minimum, this would require that data be collected at a variety of wavelengths that include, at least, the full UVB Range. Further extension of the system to longer wavelengths would be preferable, in part to estimate other cellular responses, including repair (Caldwell, 1984; Beggs et. al., 1985; Peak and Peak, 1986). Such a spectrum would provide biologists with a common starting point, similar to the erythral action spectrum widely quoted as a typical response to UV for human skin (Parrish et. al., 1978). Because of the absorption properties of ozone and the solar UV spectrum, increases in the UV flux at the earth's surface would be concentrated in the UVB (Frederick and Lubin, 1988; Worrest, 1986). How these small increases in incident energy would affect living cells and ecosystems (Caldwell, 1968) is still at issue, but detrimental effects have been postulated (Caldwell et. al., 1983; Tevini, 1988) and, in some cases, for example plants, reported (Teramura, 1983; 1986; Teramura and Murali, 1986; Teramura and Sullivan 1987; Tevini et. al., 1981, 1983).

So, once again, accurate AS are needed to answer key photobiological questions which are central to our understanding of the ecological consequences of human behavior. More AS have to be generated, especially for plants. Studies utilizing plant cells in culture might be able to identify the chromophores involved in plant responses to UV. Field studies utilizing intact plants and polychromatic sources added to the ambient background will be

essential for realistic estimates of effect. From the above it is apparent that no single action spectrum or solar effectiveness spectrum can currently be considered to be general enough to predict the varied responses of all biological systems to wavelengths throughout the solar UV range 290 to 380 nm. However, reasonable estimates can be made for plant damage by UVB (Caldwell et al., 1986) and a portion of UVA (Coohill, 1989). The usefulness of these spectra are limited and they will be replaced in the future by more accurate and common spectra as they are generated. The availability and use of numerous cell mutants has made a large contribution to the understanding of the responses of bacteria, fungi, and mammalian cells to UV. More plant mutant data, such as those reported by Galland (1983), are also needed. If common assays and irradiation procedures are followed, then a generalized plant damage action spectrum may be forthcoming and will add to the body of animal cell data already generated. If data are clearly listed in tabular form, comparisons will be facilitated. Of course, as is also the case for the widely used action spectrum for human skin erythema, no common spectrum, will suffice to substitute for any specific spectrum for any given response. But the photobiological community will be asked to provide "a realistic action spectrum, developed under more natural conditions" (Teramura, 1986), to allow government agencies (and others) to assume correct positions. Therefore, common attempts, though limited, may have widespread implications.

References

- Ananthaswamy, H. N. and W. E. Pierceall (1990) Molecular mechanisms of ultraviolet radiation carcinogenesis. Photochem. Photobiol. **52**, 1119-1136.
- Avery, O. T., C. M. MacLeod and M. McCarty (1944) Studies on the chemical nature of the substance inducing transformation of pneumococcal types. J. Exp. Med. **79**, 137-158.
- Beggs, C. J. A. Stolzer-Jehle and E. Wellmann (1985) Isoflavonoid formation as an indicator of UV-stress in bean (*Phaseolus vulgaris* L.) leaves. The significance of photorepair in assessing potential damage by increased solar UV-B radiation. Plant Physiol. **79**, 630-634.
- Björn, L. O. J. F. Bornman and E. Olsson (1986) Effects of ultraviolet radiation on fluorescence induction kinetics in isolated thylakoids and intact leaves. In: Stratospheric ozone reduction, solar ultraviolet radiation and plant life. Vol. G8, (Edited by R. C. Worrest and M. M. Caldwell), 185-197. NATO ASI Series, Springer-Verlag, Berlin.
- Bidigare, R. R. (1989) Potential effects of UV-B radiation on marine organisms of the southern ocean: distributions of photoplankton and krill during austral spring. Photochem. Photobiol. **50**, 469-477.
- Bogenrieder, A. (1982) Action spectra for the depression of photosynthesis by UV irradiation in *Lactuca stativa* l. and *Rumex alpinus* L. In *Biologic Effects of UV-B Radiation* (H. Baur, M. M. Caldwell, M. Tevini and R. C. Worrest, eds.), Proceedings of a workshop held in Munich-Neuherberg, 132-139.
- Bornman, J. F., L. O. Björn and H. E. Åkerlund (1984) Action spectrum for inhibition by ultraviolet radiation of photosystem II activity in spinach thylakoids. Photobiochem. Photobiophys. **8**, 305-313.
- Caldwell, M. (1968) Solar ultraviolet radiation as an ecological factor for alpine plants. Ecol. Monogr. **38**, 243-268.
- Caldwell, M. M. (1971) Solar UV irradiation and the growth and development of higher plants. In: *Photophysiology*. **6**, (Edited by A. C. Giese), 131-177.
- Caldwell, J. M., W. G. Gold, G. Harris and C. W. Ashurst (1983) A modulated lamp system for solar UV-B (280 - 320 nm) supplementation studies in the field. Photochem. Photobiol. **37**, 479-485.

- Caldwell, M. M. (1984) Effects of UV radiation on plants in the transition region to blue light. In *Blue Light Effect in Biological Systems*. (Edited by H. Senger) 20-28.
- Caldwell, M. M., L.B. Camp, C. W. Warner and S. D. Flint (1986) Action spectra and their key role in assessing biological consequences of solar UV-B radiation. In R. C. Worrest and M. M. Caldwell (eds.) *Stratospheric Ozone Reduction, Solar Ultraviolet Radiation and Plant Life*. 87-111.
- Caldwell, M. M., S. Madronich, L. O. Björn and M. Ilyas (1989) Ozone reduction and increased solar ultraviolet radiation. In "Environmental effects panel report", United Nations Environmental Program. ISBN 92 807 1245 4.
- Churchill, M. E., J. G. Peak and M. J. Peak (1991) Correlation between cell survival and DNA single-strand break repair proficiency in the Chinese hamster ovary cell lines AA8 and EM9 irradiated with 365 nm ultraviolet A radiation. Photochem. Photobiol. **53**, 229-236.
- Coohill, T. P. and R. A. Deering (1969) Ultraviolet light inactivation and photoreactivation of Blastocladiella emersonii. Radiat. Res. **39**, 374-385.
- Coohill, T. P., D. J. Knauer, and D. G. Fry, (1979) The effects of changes in cell geometry on the sensitivity to ultraviolet radiation of mammalian cellular capacity. Photochem. Photobiol. **30**, 565-572.
- Coohill, T. P., S. P. Moore, D. J. Knauer, D. G. Fry, T. J. Eichenbreener, and L. E. Bockstahler (1982) Action spectrum for the in vitro induction of simian virus 40 by ultraviolet radiation. Mutat. Res. **95**, 95-103.
- Coohill, T. P. (1984) Action spectra for mammalian cells in vitro. In *Topics in Photomedicine* (Edited by K. C. Smith), 1-37.
- Coohill, T. P. (1986) Virus-cell interactions as probes for vacuum-ultraviolet radiation damage and repair. Photochem. Photobiol. **44**, 359-363.
- Coohill, T. P., M. J. Peak and J.G. Peak (1987) The effects of the ultraviolet wavelengths of radiation present in sunlight on human cells in vitro. Photochem. Photobiol. **46**, 1043-1050.
- Coohill T. P. (1989) Ultraviolet action spectra (280 to 380 nm) and solar effectiveness spectra for higher plants. Photochem. Photobiol. **50**, 451-457.
- Coohill, T. P. and J. C. Sutherland (1989) Free-electron lasers in ultraviolet photobiology. J. Opt. Soc. Amer. B. **6**, 1079-1082.

- Dahlback, A., T. Henriksen, S. H. H. Larsen and K. Stamnes (1989) Biological UV-doses and the effect of an ozone layer depletion. Photochem. Photobiol. **49**, 621-625.
- Dahlback, A. and J. Moan (1990) Annual exposures to carcinogenic radiation from the sun at different latitudes and amplification factors related to ozone depletion. The use of different geometrical representations of the skin surface receiving the ultraviolet radiation. Photochem. Photobiol. **52**, 1025-1028.
- Daubeny, C. (1836) On the action of light upon plants and plants upon the atmosphere. Phil. Trans. Roy. Soc. London, 149-179.
- DeFabo, E. C., R. W. Harding and W. Shropshire, Jr. (1976) Action spectrum between 260 and 800 nanometers for the photoinduction of carotenoid biosynthesis in Neurospora crassa. Plant Physiol. **57**, 440-445.
- DeFabo, E. C., F. P. Noonan and J. E. Frederick (1990) Biologically effective doses of sunlight for immune suppression at various latitudes and their relationship to changes in stratospheric ozone. Photochem. Photobiol. **52**, 811-817.
- Doniger, J., E. D. Jacobson, K. Krell, and J. A. DiPaolo (1981) Ultraviolet light action spectra for neoplastic transformation and lethality of syrian hamster embryo cells correlate with spectrum for pyrimidine dimer formation in cellular DNA, Proc. Natl. Acad. Scie. U.S.A. **78**(4), 2378-2382.
- Draper, J. W. (1884) Note on decomposition of carbonic acid by the leaves of plants under the influence of yellow light. Phil. Mag., **25**, 159-173.
- El-Sayed, S. Z. (1988) Fragile life under the ozone hole. Nat. Hist. **97**, 72-83.
- El-Sayed, S. Z., F. C. Stephens, R. R. Bidigare and M. E. Ondrusek (1989) Potential effects of solar ultraviolet radiation on antarctic phytoplankton. In "Effects of solar ultraviolet radiation on biogeochemical dynamics in aquatic environments. WHOI-90-09, 141-142.
- Elkind, M. M. and G. F. Whitmore (1967) "Radiobiology of Cultured Mammalian Cells," Gordon and Breach, New York.
- Engelmann, T. W. (1882) Ueber Sauerstoffausscheidung von Pflanzensellen im Microspectrum. Bot. Zeit. **40**, 419-426.
- Enninga, I. C., R. T. L. Groenedijk, A. R. Filon, A. A. van Zeeland and J. W. I. M. Simmons (1986) The wavelength dependence of u.v.-induced pyrimidine dimer formation, cell killing and mutation induction in human diploid skin fibroblasts. Carcinogenesis **7**, 1829-1836.

- Farman, J. C., B. G. Gardiner and J. D. Shanklin (1985) Large losses of total ozone in Anatarctica reveal seasonal ClO_x/NO_x interaction. Nature, 315, 207-210.
- Frederick, J. E. and D. Lubin (1988) Possible long-term changes in biologically active ultraviolet radiation reaching the ground. Photochem. Photobiol. 47, 571-578.
- Frederick, J. E., H. E. Snell and E. K. Haywood (1989) Solar ultraviolet radiation at the earth's surface. Photochem. Photobiol. 50, 443-450.
- Frederick, J. (1990) Trends in atmospheric ozone and ultraviolet radiation: ? mechanisms and observations for the northern hemisphere. Photochem. Photobiol. 51, 757-763.
- Galland, P. (1983) Action spectra of photogeotropic equilibrium in phycomyces wild type and three behavioral mutants. Photochem. Photobiol. 37, 221-228.
- Gates, F. L. (1930) A study of the bactericidal action of ultraviolet light. III. The absorption of ultraviolet light by bacteria. J. Gen. Physiol. 14, 31-42.
- Häder D.P. (1986) Signal perception and amplification in photomovement of prokaryotes. Biochim. Biophys. Acta. 864, 107-122.
- Häder. D.P., R. C. Worrest. and H. D. Kumar (1987) Aquatic ecosystems. In "Environmental effect panel report", United National Environmental Program. ISBN, 92 807 1245-4.
- Häder, D. P. (1988) Ecological consequences of photomovement in microorganisms. J. Photochem. Photobiol B: Biol. 1, 385-414.
- Halldal, P. (1967) Ultraviolet action spectra in algology. Photochem. Photobiol. 6, 445-460.
- Hatfield, J. M. R., L. Schulze and D. Ernet (1970) Measurement of the ultraviolet absorption in specific parts of both living and fixed mammalian cells, using a specially designed microspectrophotometer. Exptl. Cell Res. 59, 484-486.
- Henriksen, T., A. Dahlback, S. H. H. Larsen and J. Moan (1990) Ultraviolet radiation and skin cancer. Effect of an ozone layer depletion. Photochem. Photobiol. 51, 579-582.
- Hollaender, A. and C. W. Emmons (1941) Wavelength dependence of mutation production in the ultraviolet, with special emphasis on fungi. Cold Spring Harbor Symp. Quant. Biol. 9, 179-186.
- Holmberg, M., Zs. Almasy, M. Langerberg and B. Niejahr (1985) The repair of strand breaks in human lymphocytes exposed to near UV-radiation (UVA) and far UV-radiation (UBC). Photochem. Photobiol. 41, 437-444.

- Imbrie, W. and T. M. Murphy (1982) UV action spectrum (254-405 nm) for inhibition of a K⁺-stimulated adenosine triphosphatase from the plasma membrane of Rosa Damascena. Photochem. Photobiol. 36, 537-542.
- Jacobson, E. D., K. Krell and M. J. Dempsey, (1980) The Wavelength dependence of ultraviolet light-induced cell killing and mutagenesis in L5178Y mouse lymphoma cells, Photochem. Photobiol. 33, 257-260.
- Jagger, J. (1967) Introduction to Research in Ultraviolet Photobiology.
- Jagger, J. (1985) Solar-UV actions on living cells. Praeger, NY.
- Jones, L. W. and B. Kok (1966) Photoinhibition of chloroplast reactions. I. kinetics and action spectra. Plant Physiol. 41, 1037-1043.
- Kantor, G. J., J. C. Sutherland and R. B. Setlow, (1980) Action spectra for killing non-dividing normal human and xeroderma pigmentosum cells, Photochem. Photobiol. 31, 459-464.
- Kantor, G. J. (1985) Effects of sunlight on mammalian cells. Photochem. Photobiol. 41, 741-746.
- Kelfkens, G., F. R. DeGruyl and Jan Van der Leun (1990) Ozone depletion and increase in annual carcinogenic ultraviolet dose. Photochem. Photobiol. 52, 819-823.
- Kleczkowski, A., (1972) Action spectra in their interpretation, In "Research Progress in Organic Biological and Medicinal Chemistry" (U. Gallo and L. Santamaria, ed.), Vol. 3 Part II, 48-70.
- Knapp, E., A. Reuss, O. Risse and H. Schreiber (1939) Quantitative analyses der mutationsauslösenden wirkung monochromatischen UV-lichtes Naturwiss. 27, 304.
- Lubin, D., J. E. Frederick, C. R. Both, T. Lucas and D. Nieschuler (1989) Measurements of enhanced springtime ultraviolet radiation from Palmer Station Antarctica. Geophys. Res. Lett. 16, 783-785.
- Mayer, E. and H. Schreiber (1934) Die wellenlangabhängigkeit der ultraviolettwirkung auf gewebeulturen (Reinkulturen), Protoplasma, 21, 34-61.
- Mitchell, B. G., M. Vernet and O. Holm-Hansen (1989) Ultraviolet radiation in antarctic waters: Particulate absorption and effects on photosynthesis. In "Effects of solar ultraviolet radiation on biogeochemical dynamics in aquatic environments", WHOI-90-09, 135-136.

- Mitchell, D. L. and R. S. Nairn (1989) The biology of the (6-4) photoproduct. Photochem. Photobiol. **49**, 805-819.
- Montreal Protocol (1987) Substances that deplete the ozone layer: Final Act UNEP Na. 87-6106.
- Morel, F. M. M. and N. M. Price (1989) Indirect effects of UV radiation on phytoplankton. In "Effects of solar ultraviolet radiation on biogeochemical dynamics in aquatic environments", WHOI-90-09, 110-112.
- Negash, L. (1987) Wavelength-dependence of stomatal closure by ultraviolet radiation in attached leaves of Eragrostis tef: action spectra under backgrounds. Plant Physiol. Biochem. **25**, 753-760.
- Nultsch, W., J. Pfau and M. Materna-Weide (1987) Fluence and wavelength dependence of photoinhibition in the brown alga Dictyota dichotoma. Mar. Ecol. Prog. Ser. **41**, 93-97.
- Nultsch, W. and D. P. Häder (1988) Photomovement in motile microorganisms - II. Photochem. Photobiol. **47**, 837-869.
- Parrish, J. A., R. R. Anderson, F. Urbach, and D. Pitts (1978) UV-A: Biological Effects of Ultraviolet Radiation with Emphasis on Human Responses to Longwave Ultraviolet. Plenum Press, NY
- Peak, J. J. and J. G. Peak (1983) Use of action spectra for identifying molecular targets and mechanisms of action of solar ultraviolet light. Physiol. Plant. **58**, 367-372.
- Peak, M. J. and J. G. Peak (1986) Molecular Photobiology of UVA. In The Biological Effects of UVA Radiation. (Edited by F. Urbach and R. W. Gange), 42056.
- Rosenstein, B. S. and D. L. Mitchell (1987) Action spectra for the induction of pyrimidine photoproducts and cyclobutane pyrimidine dimers in normal human skin fibroblasts. Photochem. Photobiol. **45**, 775-780.
- Rothman, R. H. and R. B. Setlow (1979) An action spectrum for cell killing and pyrimidine dimer formation in Chinese hamster V-79 cells. Photochem. Photobiol. **29**, 57-62.
- Rowland, F. S. (1989) Chlorofluorocarbons and the depletion of stratospheric ozone. Ameri Sci. **77**, 36-45.
- Rundel, R. D. (1983) Action spectra and estimation of biologically effective UV radiation. Physiol. Plant. **58**, 360-366.

- Setlow, R. B. (1974) The wavelengths in sunlight effective in producing skin cancer: A theoretical analysis. Proc. Nat. Accad. Sci. USA **71**, 3363-3366.
- Smith, R. C. (1989) Ozone, middle ultraviolet radiation and the aquatic environment. Photochem. Photobiol. **50**, 459-468.
- Stadler, L. J. and F. M. Uber (1941) Genetic effects of ultraviolet radiation in maize. IV. comparison of monochromatic radiation. Genetics **27**, 84-118.
- Steinmüller, D. (1986) On the effect of ultraviolet radiation (UV-B) on leaf surface structure and on the mode of action of cuticular lipid biosynthesis in some crop plants. Karler. Beitr. Entw. Ökophysiologie **6**, 1-174.
- Storlarski, R. S. (1988) The antarctic ozone hole. Sci. Amer. **258**, 30-36.
- Sullivan, J. H. and A. H. Teramura (1988) Effects of ultraviolet B irradiation on seedling growth in the Pinaceae. Amer. J. Botany, **75**, 225-230.
- Sutherland, B. M., N. C. Delhas and J. C. Sutherland, (1981) Action spectra for ultraviolet light-induced transformation of human cells to anchorage-independent growth, Cancer Res. **41**, 2211-2214.
- Taylor, H. R. (1989) The biological effects of UV-B on the eye. Photochem. Photobiol. **50**, 489-492.
- Teramura, A. H. (1983) Effects of ultraviolet-B radiation on the growth and yield of crop plants. Physiol. Plant. **58**, 415-427.
- Teramura, A. H. (1986) Interaction between UV-B radiation and other stresses in plants. In R. C. Worrest and M. M. Caldwell (eds.), Stratospheric Ozone Reduction, Solar Ultraviolet Radiation and Plant Life, 87-111.
- Teramura, A. H. and N. S. Murali (1986) Intraspecific differences in growth and yield of soybeans exposed to ultraviolet-B radiation under greenhouse and field conditions. Env. Exp. Bot. **26**, 89-95.
- Teramura, A.H. (1987) Current risks and uncertainties of stratospheric ozone depletion upon plants. In-assessing the risks of trace gases that can modify the stratosphere. Vol. 8: Technical support documentation ozone depletion and plants. U.S.E.P.A., EPA 400/1-87\001H, 1-77.
- Teramura, A. H. and J. H. Sullivan (1987) Soybean growth responses to enhanced levels of ultraviolet-B radiation under greenhouse conditions. Amer. J. Bot. **74**, 975-979.

- Tevini, M., W. Iwanzik and U. Thoma (1981) Some effects of enhanced UV-B radiation on the growth and composition of plants. Planta. **153**, 388-394.
- Tevini, M., W. Iwanzik and A. H. Teramura (1983) Effects of UV-B radiation on plants during mild water stress II. Effects on growth, protein and flavonoid content. Z. Pflanzenphysiol. **110**, 459-467.
- Tevini, M. (1988) The effects of UV radiation on plants. J. Photochem. Photobiol. **2**, 401-403.
- Tevini, M. and D. Steinmüller (1988) Personal communication
- Tevini, J., A. H. Teramura, G. Kulandaivelu, M. M. Caldwell, and L. O. Björn (1989) Terrestrial plants. In "Environmental effects panel report", United Nations Environmental Program. ISBN, **92**, 807 1245 4.
- Todd, P., T. P. Coohill and J. A. Mahoney, (1968) Responses of cultured chinese hamster cells to ultraviolet light of different wavelengths, Radiat. Res. **35**, 390-400.
- Turro, N. J. and A. A. Lamola, (1977) Photochemistry. In "The Science of Photobiology" (K. C. Smith, ed.), 87-112, Plenum Press, New York.
- Tyrrell, R. M. and M. Pidoux (1986) Endogenous glutathione protects human skin fibroblasts against the cytotoxic action of UVB, UVA and near-visible radiations. Photochem. Photobiol. **44**, 561-564.
- Tyrrell, R. M. and M. Pidoux (1987) Action spectra for human skin cells: estimates of the relative cytotoxicity of the middle ultraviolet, near ultraviolet and violet regions of sunlight on epidermal keratinocytes. Cancer Res. **47**, 1825-1829.
- Urbach, F. (1989) Potential effects of altered solar ultraviolet radiation on human skin cancer. Photochem. Photobiol. **50**, 507-513.
- World Meteorological Organization (1989) Scientific assessment of stratospheric ozone: 1989, Global Ozone Research and Monitoring Project, Geneva. In press.
- Worrest, R. C. (1986) The effect of solar UV-B radiation on aquatic systems: an overview. In: Titus, J. G. (ed.) Effects of changes in stratospheric ozone and global climate. Vol. 1. Overview, U.S. Environmental Protection Agency and United Nations Environmental Program. 175-191.

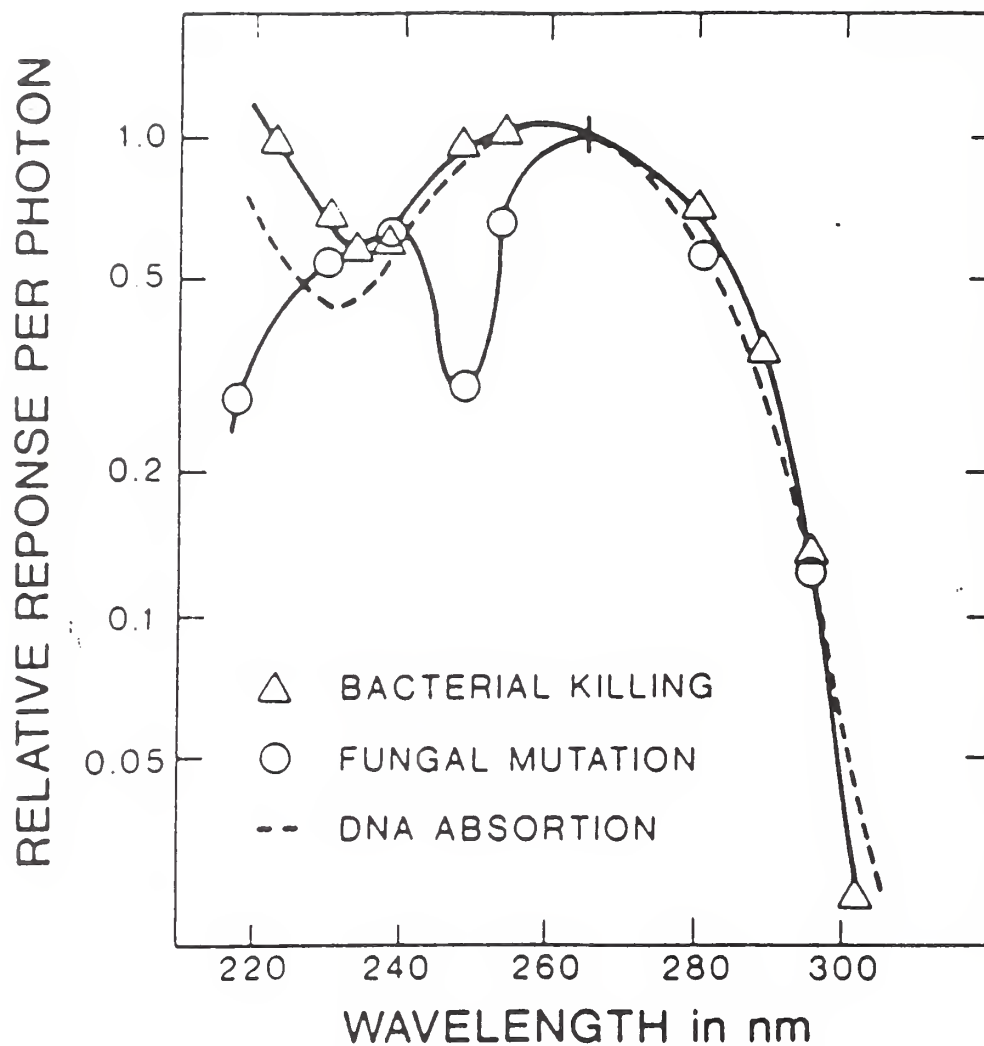


Figure 1. Analytical action spectrum for bacterial cell (Δ) killing (*S. aureus*) by UV radiation (Gates, 1930). This was, in retrospect, the first clear evidence that DNA was the genetic material. The dashed line is the absorption spectrum for DNA. AAS for mutation in the fungus (\circ) *T. metagrophytes* (Hollaender and Emmons, 1941). This corroborated the interpretation of Gates.

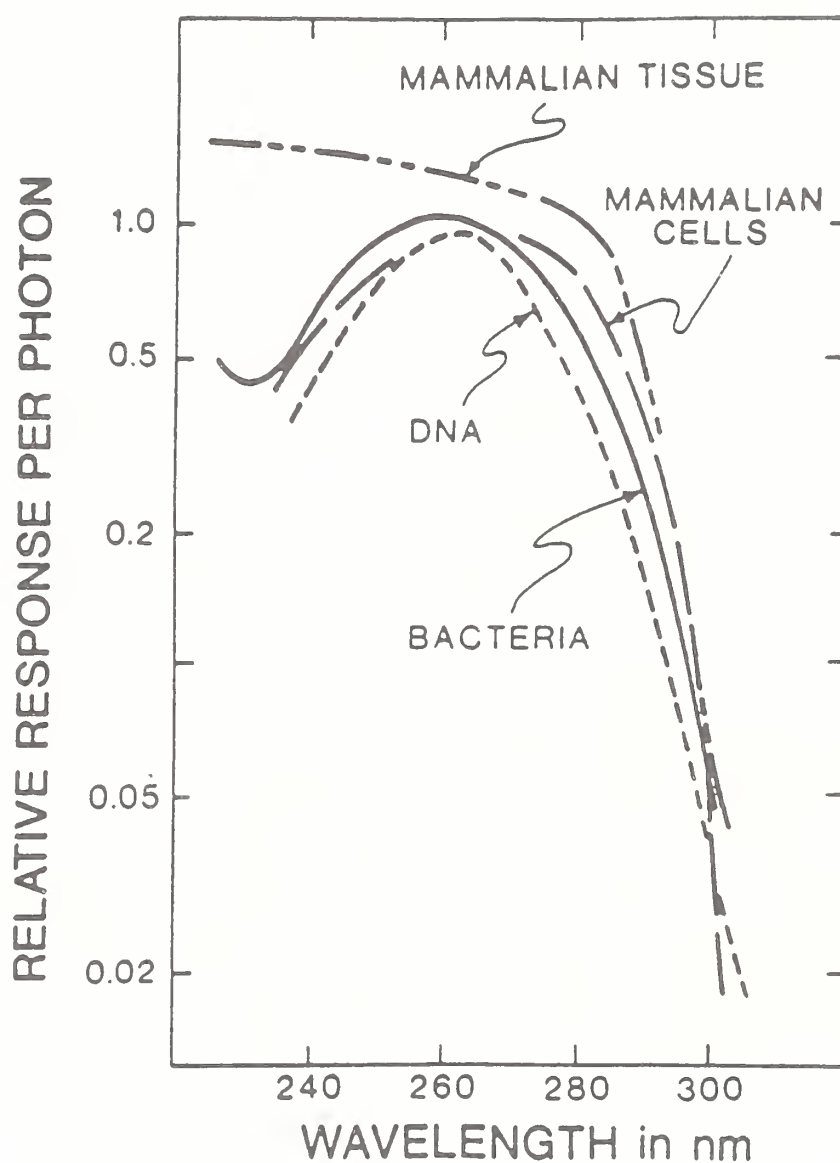


Figure 2. Action spectra for killing of bacteria (Gates, 1930), mammalian cells (Coohill, 1984), and mammalian tissue (Mayer and Schreiber, 1934). Also represented is the absorption spectrum for DNA (-----). Note that the fine structure inherent in the AS for bacteria and mammalian single cells is absent in the case of mammalian tissue. This is because the latter is essentially opaque to UV (see text).

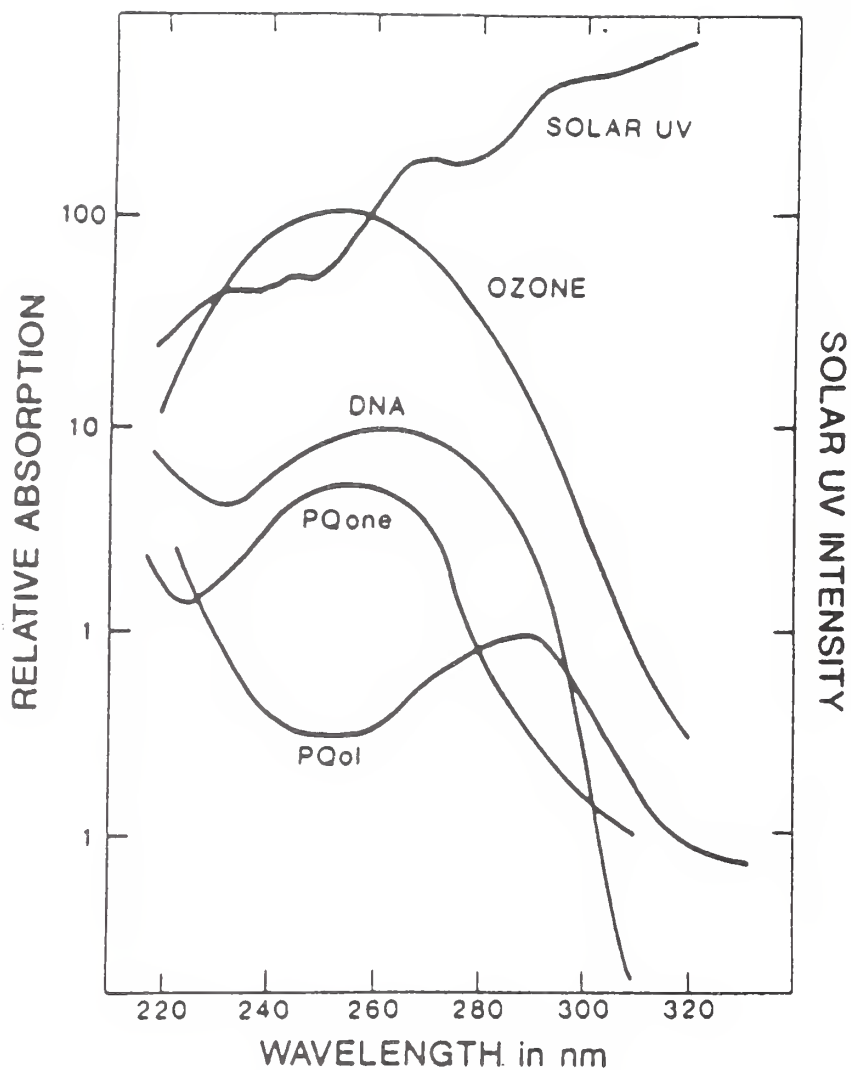


Figure 3 The umbrella-like protection from solar UV afforded to several important biomolecules by the absorption properties of ozone. Solar UV at the top of the atmosphere. Absorption spectra for ozone, DNA, plastoquinone, and plastoquinol.

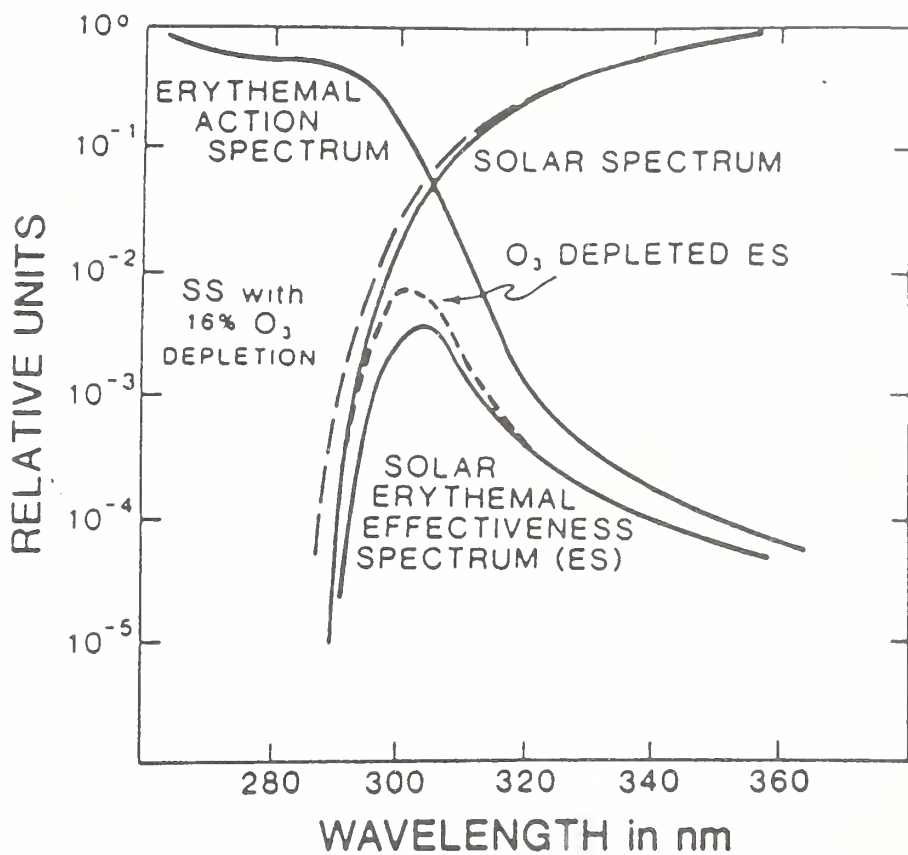


Figure 4 Erythemal action spectrum (Parrish *et al.*, 1978) and solar effectiveness spectrum (Jagger, 1985) for human skin. Added to the figure is the solar spectrum for a 16% O₃ depletion and the corresponding effectiveness spectrum for this additional UV radiation exposure.

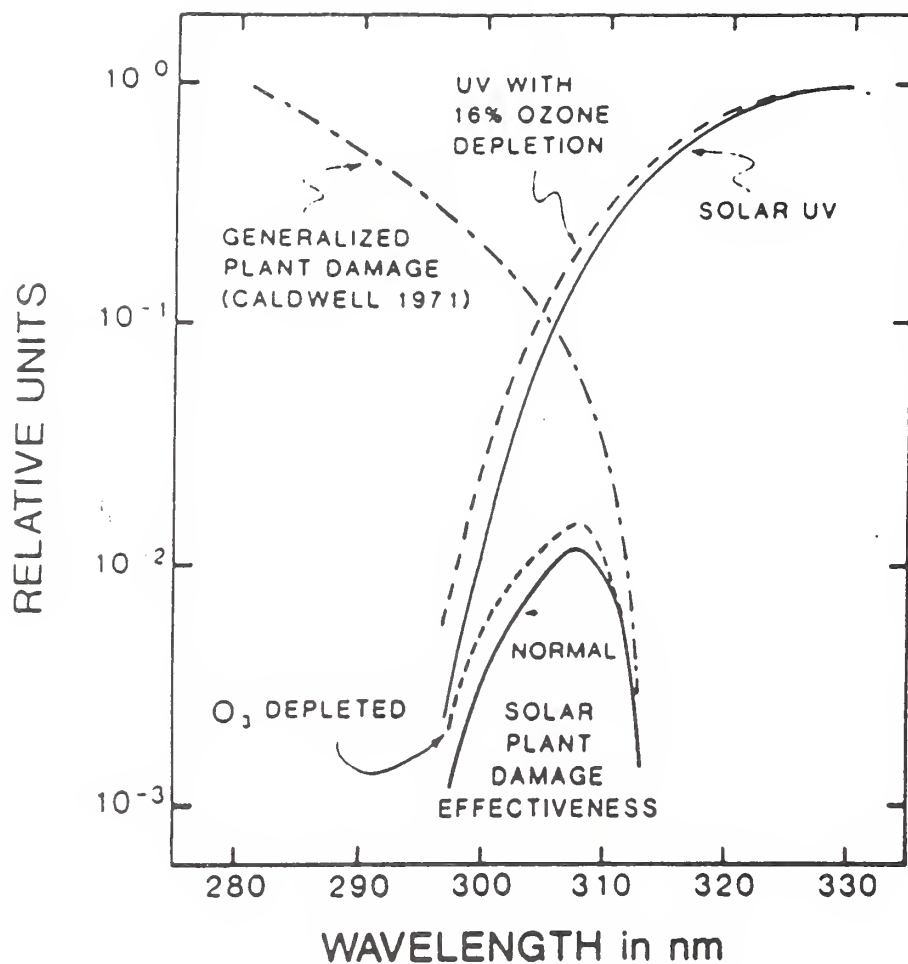


Figure 5 This figure (Coohill, 1989) shows the increase in solar plant damage due to a 16% decrease in ozone. The area under the O₃ depleted effectiveness spectrum (-----) is 17% greater than that for a normal solar effectiveness spectrum. Data such as this, approximately translate into a 1% increase in plant damage for each 1% decrease in O₃.

NSF UV-B Monitoring in Polar Regions

**C. Rocky Booth
Biospherical Instruments, Inc.**



Biospherical Instruments Inc.

C. R. BOOTH, T. LUCAS, S. DIAZ,

J. MORROW, J. TUSSON,

D. NEUSCHULER, AND

T. MESTECHKINA



NSF

UV Radiation Monitoring Network

United States National Science Foundation

Introduction

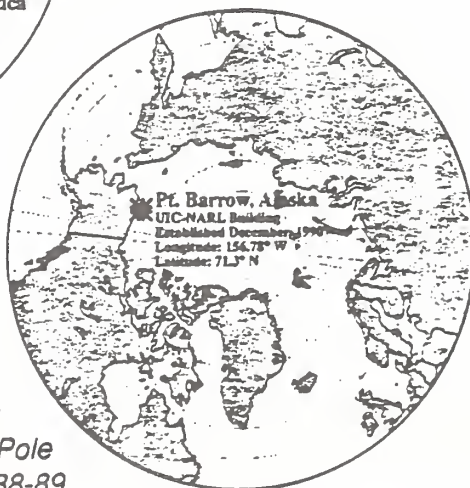
The Ultraviolet (UV) Radiation Monitoring Network was established by the United States National Science Foundation (NSF) in 1988 in response to predictions of increased UV radiation in the polar regions resulting from stratospheric ozone depletion. The network currently consists of five automated

spectroradiometers placed in strategic locations in Antarctica and the Arctic. The network makes high spectral resolution measurements of UV irradiance providing a variety of biological dosage calculations of UV exposure.

Biospherical Instruments Inc. (San Diego, CA), under contract to Antarctica Support Associates, directed by the National Science Foundation, is responsible for the network and distributing data to the scientific community.

This February 1992 update outlines the organization of the network, its instrumentation, and its operation. Data are presented contrasting episodes of ozone depletion for different sites covering the 1990 and 1991 ozone seasons.

Data Sets from the network (1989 to 1991v 1.0) are available on CD ROM (ISO9660 format). These are readable by a variety of platforms including PCs, Macs, and various workstations. For data availability consult C.R. Booth or Dr. Polly Penhale (NSF-DPP).



Instruments were stationed at Palmer, McMurdo, the South Pole and Ushuaia, Argentina in 1988-89 and at Pt. Barrow, Alaska in 1990.



Spectroradiometer System Description

Hardware and Operation

The SUV-100A spectroradiometer system features a 0.1 m double monochromator coupled to a photomultiplier tube (PMT) detector. Tungsten-halogen and mercury vapor lamps, operated under computer control, are used for automatic internal calibration of the optical system. In order to maximize stability, the monochromator and PMT are located in individual temperature controlled subassemblies.

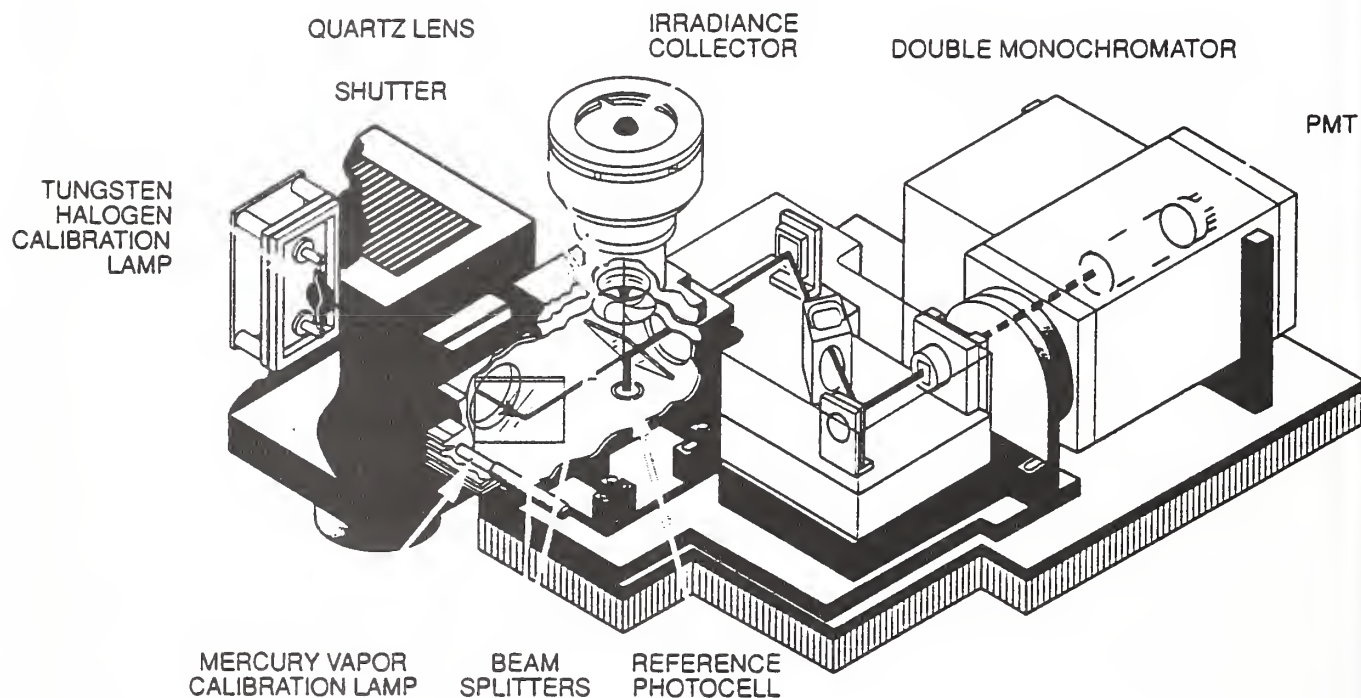
The system is designed to be operated unattended; human attention is required only for data transfer, periodic absolute calibrations, and maintenance of the system. Additional sensors that are attached to the SUV-

100A are scanned simultaneously with the PMT and also between high resolution PMT scans. These provide reference data which can be used to track instrument operation and can also be used to normalize data for time varying changes in atmospheric conditions.

Software

Software developed by Biospherical Instruments Inc. is used to manage calibration factors, perform data processing, display processed data, and create databases. Calculated values include solar zenith and azimuthal angles, spectral integrals, weighted doses, and standard meteorological spectral integrals. A series of databases tracking both irradiances, integrations, and system performance parameters is also available to researchers interested in more highly summarized data.

LIGHT PATH WITHIN THE SMDA (Exterior enclosure not shown)



DOUBLE SCANNING MONOCHROMATOR
 f/3.5 0.1 meter configured with 167 micron input/output slits and a 250 micron intermediate slit. Holographic grating with 200 grooves/mm blazed at 250 nm and driven by a stepping motor. Spectral bandwidth is a nominal 0.75 nm. Temperature of the monochromator is carefully controlled and monitored and is typically stable to $\pm 0.5^\circ \text{C}$.

SCANNING MONOCHROMATOR DETECTOR ASSEMBLY (SMDA)

SPECTRAL PYROMETER
 Auxiliary Sensor

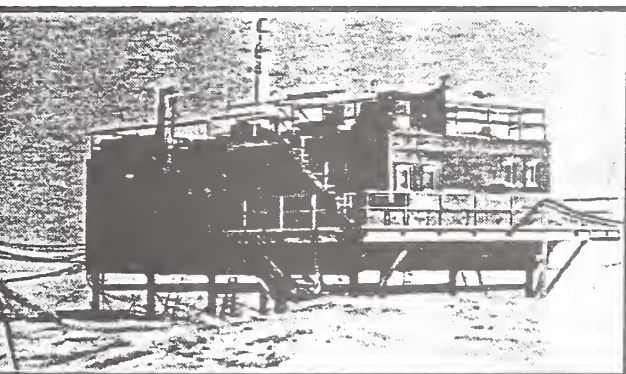
UV RADIOMETER
 Auxiliary Sensor

IRRADIANCE COLLECTOR
 TEFLON DIFFUSER

INTERMEDIATE
 CALIBRATION LAMP

ROOFBOX
 Environmentally sealed

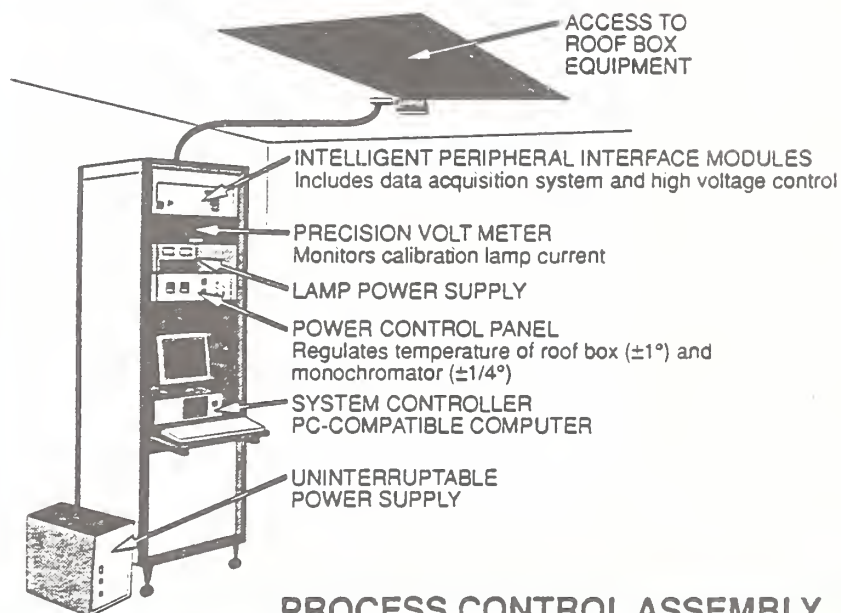
PHOTOMULTIPLIER TUBE (PMT)
 28 mm diameter 11 stage device with a bialkali cathode and a quartz window. It is housed in a cooled enclosure that is maintained at approximately 0°C to reduce dark current and noise.



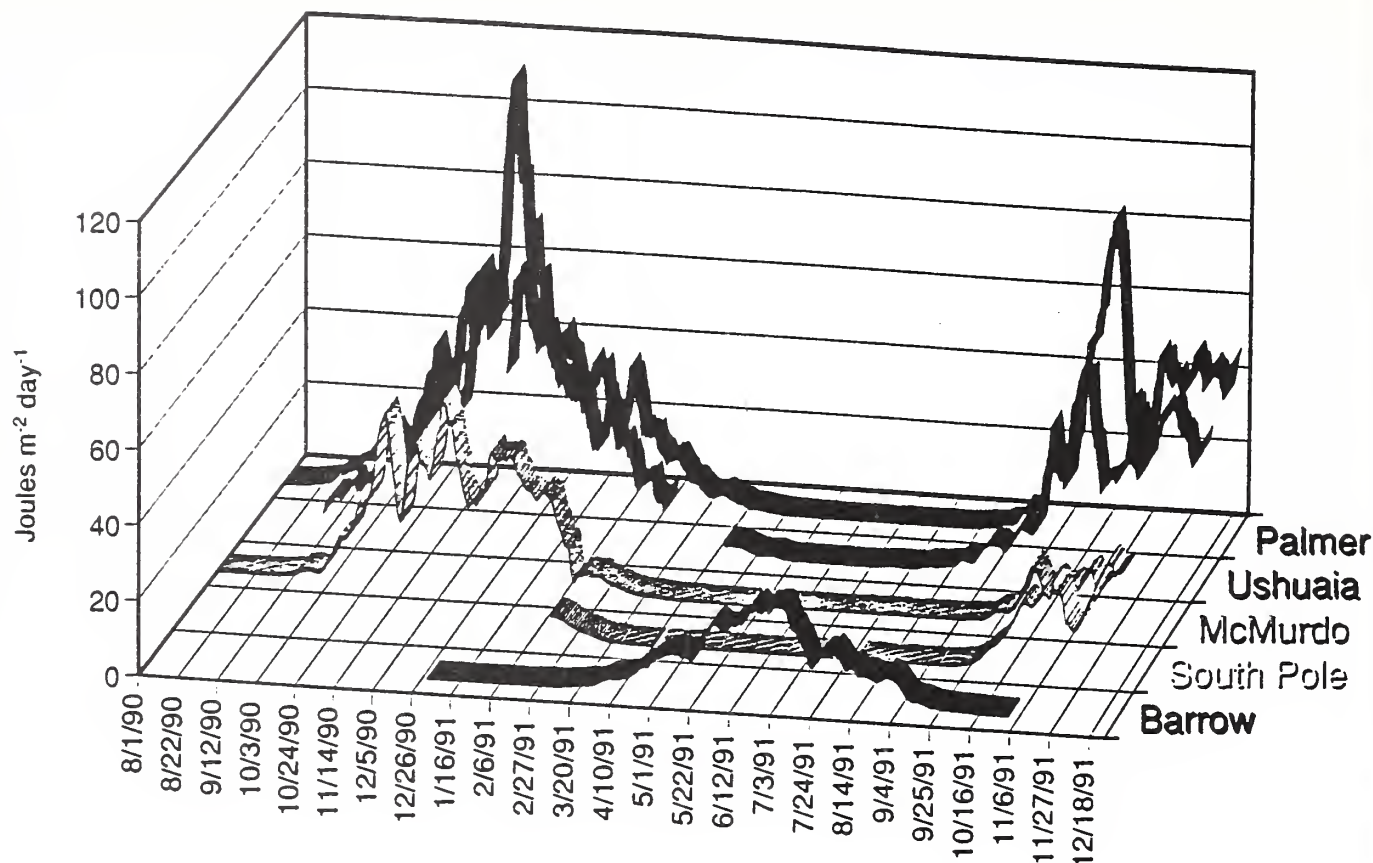
Clean Air Building, South Pole



Pt. Barrow, Alaska



PROCESS CONTROL ASSEMBLY



Daily Dose (Setlow): Seven-day Moving Average

Data from all five sites are presented in this seven-day moving average time series of daily dose computed using Setlow's DNA dose weighting. The units of dose are $\text{Joules m}^{-2} \text{ day}^{-1}$. The table below shows the maximum weekly averaged daily dose along with the date of the dose and the approximate ozone

values as measured by TOMS in Dobson Units (DU).

The 1990 season highs at McMurdo, Palmer, and Ushuaia were driven by persistent ozone depletion extending into early December when day lengths approached maximum. In October of 1991, Palmer and Ushuaia experienced the

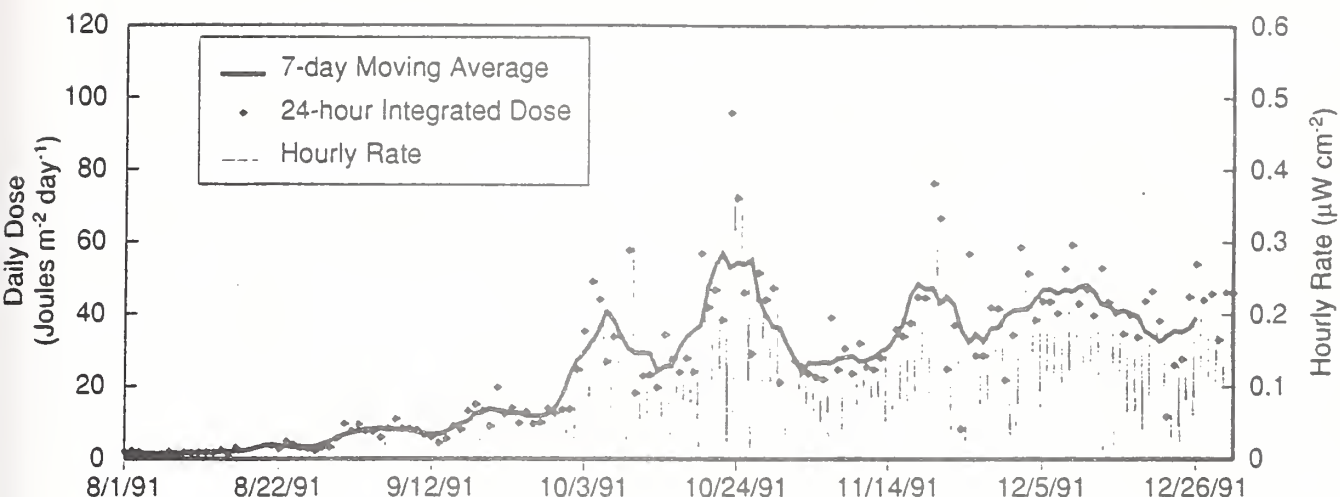
season's highest averaged doses during a transient in ozone depletion caused by movement of the ozone hole. At McMurdo and the South Pole, although ozone depletion strongly influenced UV, longer days contributed significantly to causing the maximum to occur near the summer solstice, as was also the case at Barrow.

1990 Season

Site:	McMurdo	Palmer	Ushuaia
Avg. Max. Dose:	49.45	113.07	75.00
Date:	12/2/90	12/4/90	12/27/90
TOMS Ozone:	≈270 DU	≈239 DU	≈290 DU

1991 Season

Site:	McMurdo	Palmer	Ushuaia	South Pole	Barrow
Avg. Max. Dose:	25.13	85.51	56.89	43.13	25.31
Date:	12/18/91	10/24/91	10/22/91	12/26/91	7/2/91
TOMS Ozone:		173 DU	245 DU		347 DU



Ushuaia: Setlow's DNA Dose Function Applied to Spectral Irradiance

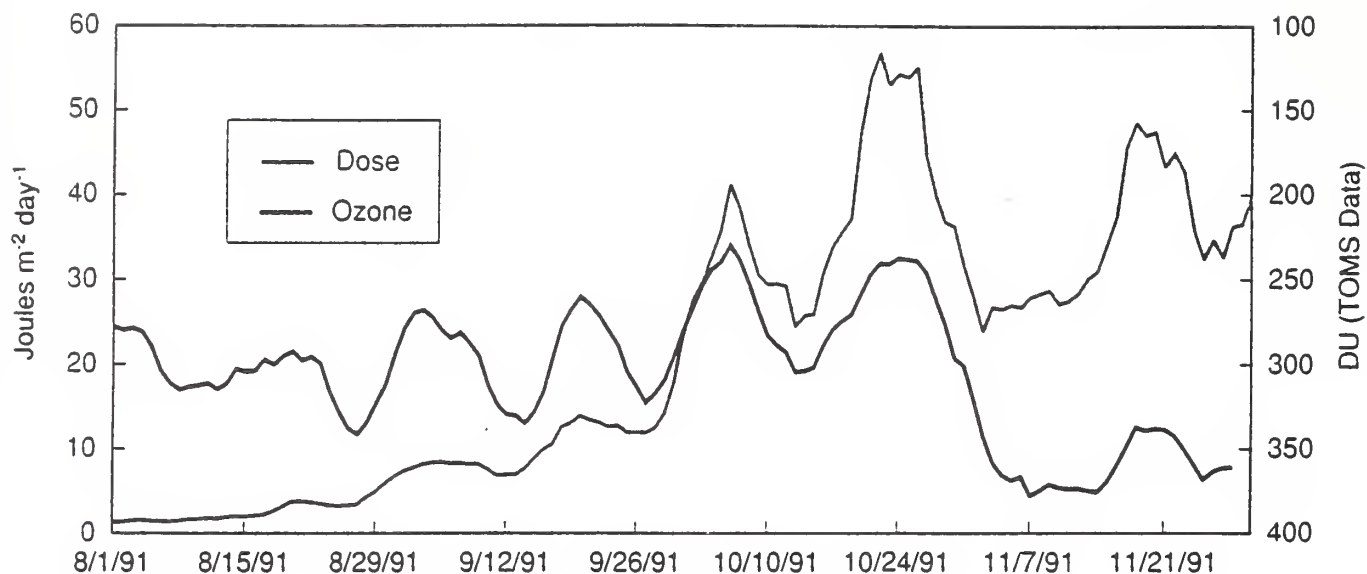
This plot shows dose weighted (Setlow 1974) irradiance expressed as the instantaneous dose rate measured hourly (light line), the daily dose (black diamonds), and averaged over seven days (heavy line). While the instantaneous rates are

higher in the spring, the influence of longer days toward summer tends to reduce the springtime (ozone depleted) daily doses relative to summer. This shows the importance of day length in considering the impact of ozone depletion. Note

that Ushuaia is a highly variable optical environment due to the closeness of mountains and the Beagle Passage (snows are not unusual even in spring and the weather changes frequently).



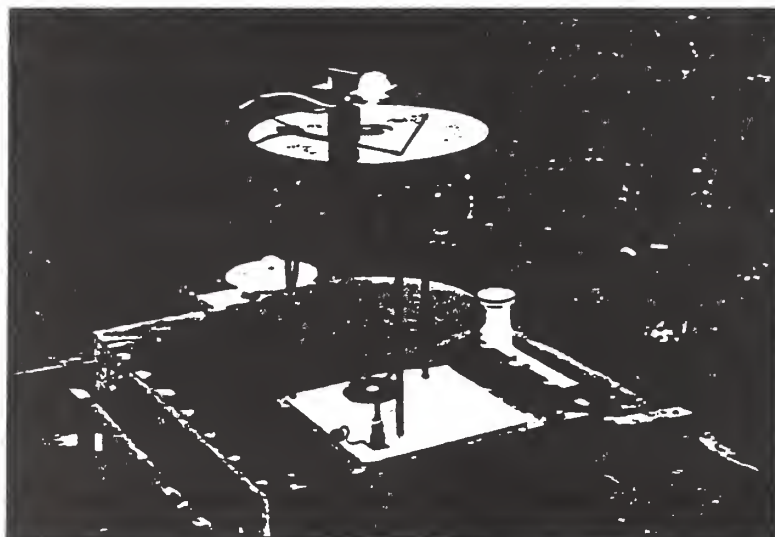
Ushuaia, Argentina



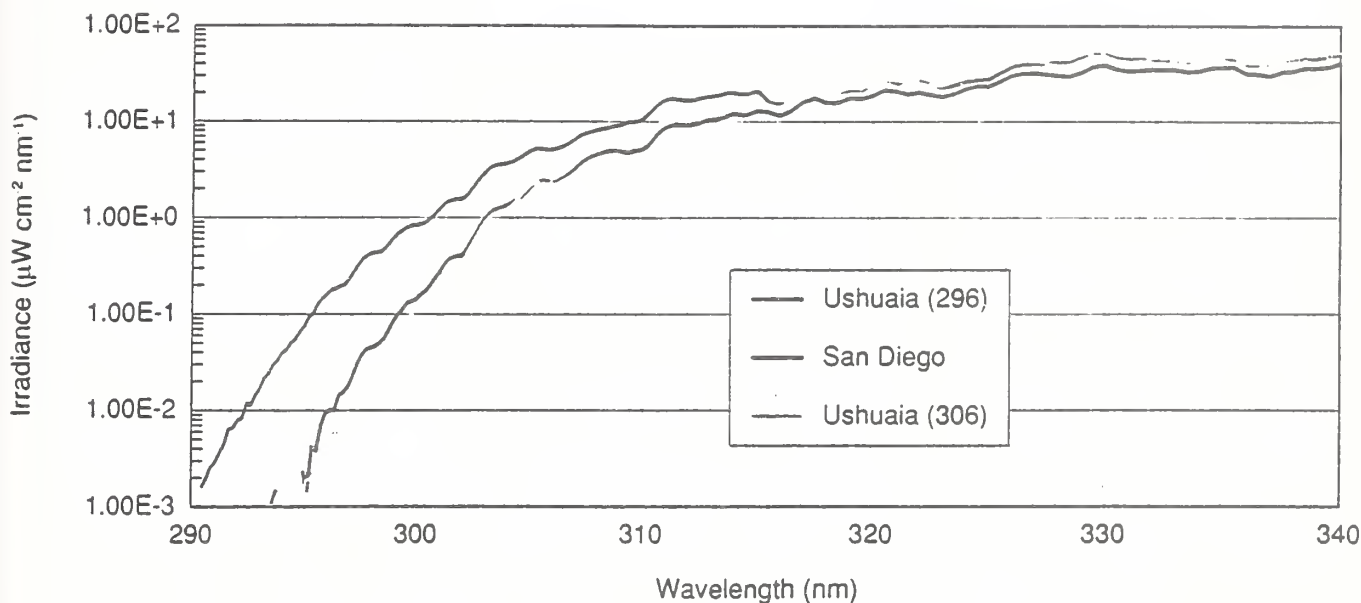
Ushuaia: Weekly Moving Averages Dose-weighted Irradiance and Ozone

In this 1991 data from Ushuaia, the Setlow (1974) dose weighting function is convolved with hourly spectral irradiance measurements. These data are integrated over 24 hours to compute a daily dose. The plot

shows seven-day moving averages. TOMS data (McPeters and Krueger, 1991) seven-day moving average in Dobson Units is also displayed (inverted scale).



Calibration unit shown without cover (Ushuaia, Argentina)



Contrasting Scans

In the plot above, spectral irradiance at Ushuaia recorded during a transient episode of ozone depletion occurring on 10/23/91 (ozone = 202 DU) is contrasted with a scan made just 10 days later when the ozone was much higher (396 DU). These scans are also compared with a scan recorded (coincidentally) on 10/23/90 at San Diego, CA.

The table on the right contrasts various measures of integrated irradiance between Ushuaia (ozone influenced) with San Diego. Solar zenith angles in all three cases were about 44°.

PARAMETER	VALUE	USHUAIA RELATIVE TO SAN DIEGO
UV-B	290/315 nm	102%
UV-B	290/320 nm	75%
UV-A	320/400 nm	19%
Visible	400/600 nm	4%
Spectral Integrals		
	289/294 nm	8320%
	294/298 nm	1574%
	298/303 nm	422%
	307/312 nm	100%
	317/322 nm	46%
	342/347 nm	23%
Erythema Doses	McKinney & Diffey 87 (CIE)	138%
Biological Doses	Setlow '74	299%
	Caldwell	199%

Publications that Utilize Data from the NSF UV Radiation Monitoring Network

Lubin, D., Fredenck, J. E. "Ultraviolet Radiation Environment of the Antarctic Peninsula: The Roles of Ozone and Cloud Cover". *J. of Applied Meteorology*, 30(4), 478-493, 1991.

Lubin, D., Fredenck, J. E. "Ultraviolet monitoring program at Palmer Station, spring, 1988. *Antarctic journal of the United States*, 1989, 24(5), p.172-174.

Lubin, D., Mitchell, B.G., J. E. Frederick, A. D. Alberts, C. R. Booth, T. Lucas, D. Neuschuler. "A contrioution toward understanding the biospherical significance of Antarctic ozone depletion". *Journal of Geophysical Research*, in press.

Lubin, D. and J. E. Frederick (1990). Column ozone measurements at Palmer

Station, Antarctica: vanations during the austral springs of 1988 and 1989. *Journal of Geophysical Research*, 95, 13883-13889.

Lubin, D. and J. E. Frederick (1991). Column ozone measurements of ozone and cloud properties from NSF UV-Monitor measurements at Palmer Station, Antarctica. *The Antarctic Journal of the United States*, in press.

Lubin, D. and J. E. Frederick (1991). The ultraviolet radiation environment of the Antarctic Peninsula: the roles of ozone and cloud cover. *Journal of Applied Meteorology*, 30, 478-493.

Smith, R. C., Z. Wan, and K. S. Baker. (1990). "Ozone depletion in Antarctica: Satellite and ground measurements, and

modeling under clear-sky conditions". *Journal of Geophysical Research*, in press.

Smith, R., K. Baker, D. Menzies, K. Waters. (1991). "Bio-optical measurements from the IceColors 90 cruise 5 Oct -21 Nov 1990". SIO Ref 91-13.

Smith, R., B. Prezlin R. Bidigare, D. Karentz, S. MacIntyre. (1991) "IceColors'90: Ultraviolet Radiation and phytoplankton biology in Antarctic Waters". *The Antarctic Journal of the United States*, in press.

Stamnes, K., J. Slusser, M. Bowen, C. Booth, and T. Lucas (1990). "Biologically Effective Ultraviolet Radiation, Total Ozone Abundance, and Cloud Optical Depth at McMurdo Station, Antarctica, September 15, 1988 through April 15, 1989". 1990. *Geophysical Res. Letters* (17), pp 2181-2184.

Stamnes, K., J. Slusser, and M. Boden (1991). "Total ozone abundance and effective cloud optical depth inferred from spectral irradiance measurements". *Applied Optics* 30 (4418-4426).

References

R. B. Setlow, The wavelengths in sunlight effective in producing skin cancer: a theoretical analysis, *Proc. Nat. Acad. Sci., USA*, Vol. 71, no. 9, pp. 3363-3366, 1974.

TOMS: Total Ozone Mapping Spectrometer. McPeters, R. D. and A. J. Krueger of NASA GSFC, members of the TOMS Nimbus Experiment and Ozone Processing Teams, and the National Space Science Data Center/World Data Center-A for Rockets and Satellites provided TOMS data. See for example, Krueger, A. J., P. E. Ardanuy, F.

S. Sechrist, L. M. Penn, D. E. Larko, S. D. Doiron, and R. N. Galimore. "The 1987 Airborne Antarctic Ozone Experiment - The Nimbus-7 TOMS Data Atlas". NASA Reference Publication 1201, March 1988.

DIN/CIE Dose"DIN/CIE Standard Dose:" McKinney and Diffey, 1987. "A reference action spectrum for ultra-violet induced erythema in human skin". Report from members of technical committee 2, Division 6, Photochemistry and Photobiology, CIE. Function equals 1 below 299nm.

"Caldwell" is the parameterization of Green, et al. for Caldwell's data on the relative photon effectiveness of UV-B irradiation to induce biological response when protein or nucleic acid chromophores are involved. Caldwell's work is in M. M. Caldwell, "Solar UV irradiation and the growth and development of higher plants" in *Photophysiology*, Ed. by A. C. Giese, Vol. 6, pp.131-177. Academic Press, New York. The parameterization is in A. E. S. Green, T. Sawada, and E. P. Shettle, "The middle ultraviolet reaching the ground", *Photochemistry and Photobiology*, 19, pp. 251-259 (1974).

Acknowledgments

The need for the rapid establishment of the UV monitoring program was recognized by Dr. Peter Wilkniss, Director, Division of Polar Programs, National Science Foundation. This project has been guided by Dr. Polly Penhale of NSF and Dr. Sue Weiler (NSF/DPP Consultant).

This research and monitoring activity was funded by contract AOT00010 to Biospherical Instruments from Antarctic Support Associates (ASA). ASA personnel involved include R. L. Murphy, R. Thomas, D. C. Shepherd, W. Coughran, M. Young, R. Faulhaber, E. Siefka, and R. Skane.

Dr. B. Mendonca of NOAA/CMDL assisted in providing operators and support for the installations at the South Pole and Barrow.

Dr. A. Kruger of NASA/GSFC provided TOMS Total Ozone data for comparison purposes.

S. Diaz of CONICET and I. Smolskaia of CADIC, are responsible for the Ushuaia, Argentina installation. Dr. J. Rabassa made this installation possible.

Barrow operators include Dr. D. Norton, D. Roghair, and NOAA/CMDL personnel D. Endres and C. Churylo. The Ukpeagvik Inupiat Corporation of Barrow provided assistance in the installation.

Special thanks goes to Dr. Steve Kottmeier and Mr. John Gress of ASA who work with us on a daily basis to make it possible to accomplish this project in Antarctica.

*Communications with
Biospherical Instruments Inc.:*

Telemail: R.BOOOTH/OMNET

Telephone: (619) 270-1315

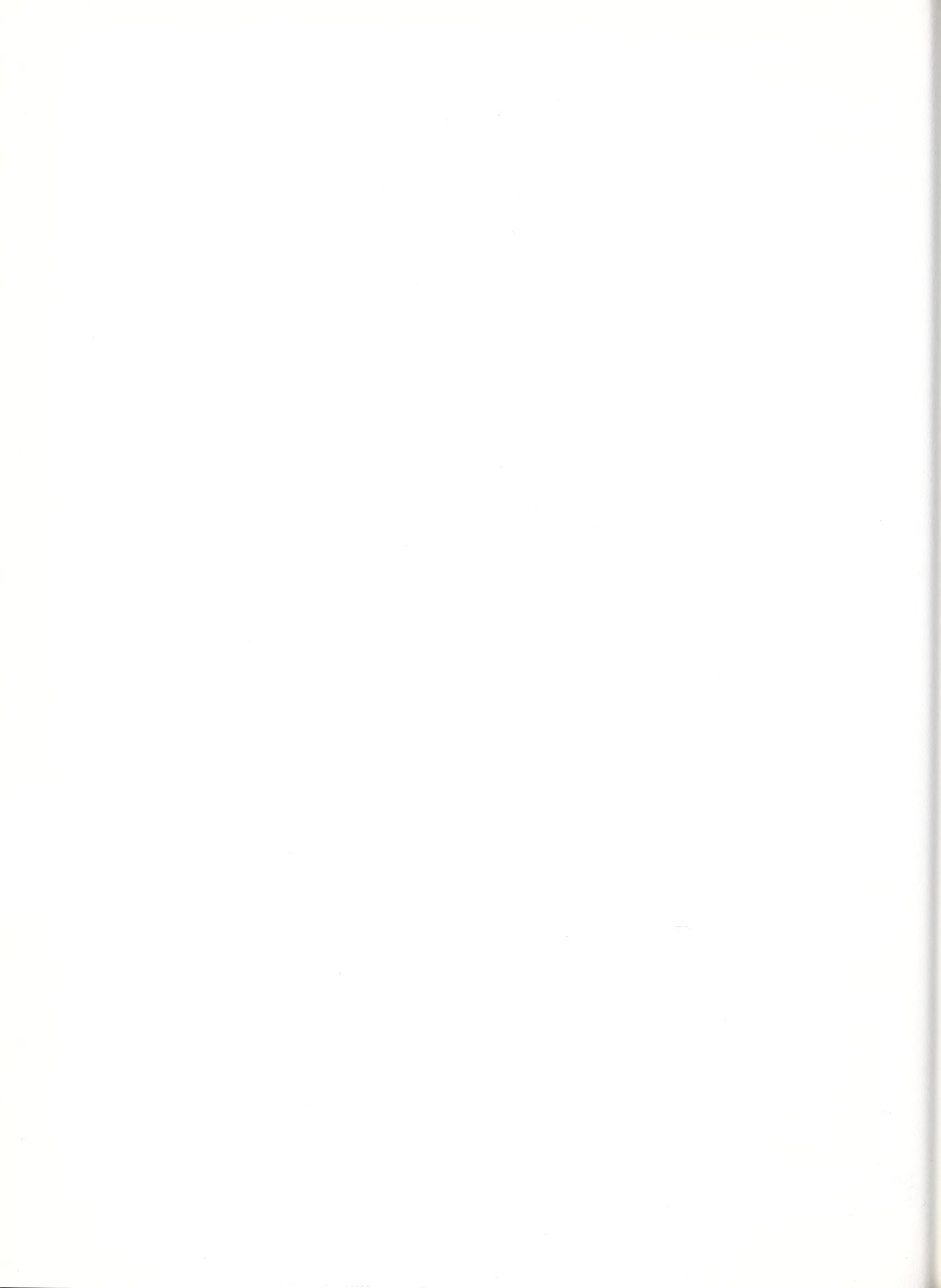
FAX: (619) 270-1513

Internet:
BOOTH@SSURF.UCSD.EDU

**European Communities STEP UV-B Program:
Instrument Intercomparison**

**Dr. Brian Gardiner
British Antarctic Survey**

**Dr. Ann Webb
University of Reading, U.K.**



European Communities STEP UV-B Program: Instrument Intercomparison

*Brian G. Gardiner
British Antarctic Survey
Madingley Road
Cambridge CB3 0ET, UK*

and

*Ann R. Webb
Dept. of Meteorology
University of Reading
2 Earley Gate
Reading RG6 2AU, UK*

If spectral measurements are to be recorded at different locations over a period of some years, it is essential to demonstrate that the results from the individual stations are compatible and that the procedures are stable. The establishment of a consistent and reliable calibration system is a necessary prerequisite, but it is also important to examine the response of the instruments in the field, with particular regard to the difficult cases such as short wavelengths and high solar zenith angles.

In order to investigate the compatibility of available instruments in Europe, a field comparison was carried out in Greece in July 1991 under the auspices of the European Commission. The University of Thessaloniki arranged the use of a site in the village of Panorama, overlooking the city. Observations were carried out from the flat roof of a school. This paper describes the instruments which took part, the results obtained, and the implications for future work. A complete report of the campaign is given in Gardiner and Kirsch (1991).

Six different types of spectroradiometer were represented, covering a wide range of characteristics. Four were double monochromators. One instrument had an integrating sphere, three had teflon diffuser plates, and two had quartz. Two of the instruments extended into the visible region. One had a restricted field of view. Some were fully automated, some weatherproof, and one could turn its receiving surface towards any part of the sky. Bandwidths and sampling intervals varied from one instrument to another. The designs ranged from developmental assemblies built by the operators to commercial products with custom-built modifications. The diversity of these instruments offered an excellent perspective on the relative advantages of the various features, but it undoubtedly made the interpretation more difficult. It was sometimes impossible to attribute a particular result to an individual spectrometer. Despite the variations in design, the instruments had some features in common: they all used diffraction gratings, a mechanical scanning mechanism, and a photomultiplier.

The instruments will be referred to by the abbreviations AI, AW, B, GB, GR and N, as follows. Their characteristics are shown in Table 1.

AI	Austria - Innsbruck	Institut für Medizinische Physik (M. Blumthaler)
AW	Austria - Wien	Universität für Bodenkultur, Vienna (P. Weihs)
B	Belgium	Institut d'Aéronomie Spatiale de Belgique (D. Gillotay)
GB	Great Britain	University of Reading (A. R. Webb)
GR	Greece	University of Thessaloniki (A. F. Bais)
N	Norway	University of Tromsø (T. Svenoe)

Table 1. Instrument Specifications

	AI	AW	B	GB	GR	N
Spectrometer type	Bentham DM150	JY DH10	JY DH10	Optronics 742	Brewer MK II	JY HR320
Focal length/mm	150	100	100	100	160	320
Gratings plane/concave holographic lines/mm	two plane yes 2400	two conc yes 1200	two conc yes 1200	two conc yes 1200	one plane yes 1800	one plane yes 1200
Bandwidth (FWHM)/nm	1.0	1.4	0.4	1.5	0.6	0.04
Step/nm usual finest	0.5 0.04	1.0 0.2	0.17 0.17	1.0 0.1	0.5 0.1	0.1 0.01
Usual range/nm from to	290 500	280 400	250 370	280 400	290 325	290 600
Direction of scan	up	up	down	up	up	up
Scan duration/s	180	120	192	235	185	390
Diffuser	teflon	integ. sphere	double quartz	teflon	teflon	quartz
Detector type	PM EMI 9558BQ	PM Hamam. 552U	PM Hamam. R292	PM S-20	PM	PM Hamam. R446
Weatherproof	no	no	no	no	yes	yes
Automatic	yes	no	yes	no	yes	yes
Temperature stabilised optics	yes	no	no	yes	no	no
Dark current removed	yes	yes	yes	yes	yes	no
Stray light removed	no	yes	yes	no	yes	no
Radiation standard	PTB	PTB	NIST	NIST	NIST	NIST
Main lamp/W	1000	1000	1000	1000		1000
Secondary lamp/W	100	37		200	200	

NIST National Institute of Standards and Technology

PTB Physikalisch-Technische Bundesanstalt

Lamp calibrations

Two types of intercalibration were performed: spectral scans of a standard lamp and spectral scans of the sky. The lamp facility was set up in a room without windows. A 1000-watt tungsten-halogen lamp was mounted on a portable optical bench, and the instrument under test was positioned on the optical axis of the bench with the aid of a small laser. As the calibrated beam was horizontal, the instrument had to be turned on its side to view the lamp at normal incidence. This is a questionable practice, as there is no way of knowing whether the spectrometer response changes when it is tilted. The AI instrument was free of this objection, as its optical head could be turned independently of the spectrometer, to which it was connected by a flexible optical fibre.

Each instrument was presented to the lamp in turn, the irradiance being controlled by monitoring the lamp current and fixing the distance from the lamp to the receiving surface. Two lamps were used: no. 102 in the first series of tests, and no. 104 in the second. The results of the lamp tests showed good agreement between the instruments in their relative spectral response, but considerable discrepancies in the absolute calibrations. Figure 1 shows the ratio of the output from the AI and GR instruments when exposed to lamp 102: there is no systematic variation with wavelength, despite the extensive differences between the designs of these two spectrometers. AI is a Bentham double monochromator fitted with a quartz fibre and operating up to 500 nm, whereas GR is a Brewer single monochromator restricted to the ultraviolet by a cut-off filter.

However, the instruments disagreed in their determination of the absolute irradiance of the lamp at the set distance. Figure 2 shows the severity of this problem. If these discrepancies were due solely to errors in the calibrations performed at the home institutes before the instruments were brought to the intercomparison, they would all agree on the ratio of the outputs of the two lamps. Figure 3 shows that the spectrometers were divided as to the value of this ratio, falling roughly into two groups. (The B instrument type is here represented by the NIST lamp certificate, as the lamp system was supplied by the Belgian team, whose instruments maintained their original calibration on this system.)

It is again noticeable that most of the spectrometers had little difficulty in reproducing the relative spectral output of the lamps, even when they disagreed about the absolute irradiance. The lamp calibrations will have to be improved before reliable global solar irradiance spectra can be obtained on an absolute scale: every sky spectrum depends ultimately on a lamp for its calibration. Either the instruments altered in sensitivity during the campaign or as they entered the calibration room (owing to the temperature or orientation of the instrument, for example), or the optical bench system suffers from significant errors in the field (due perhaps to current fluctuations, scattered light, or the exact positioning of the instruments). Future experiments will be planned to examine these possibilities.

Nevertheless, the lamp calibrations had several practical advantages over the sky scans, even for the establishment of relative spectral response. Results were obtainable down to 250 nm, well below the requirements of ground-based atmospheric work, and the smooth spectral output of the lamp eliminated any dependence on the slit function of the spectrometer. On the other hand, small shifts in the instrumental wavelength calibration would have passed unnoticed, and could account for some of the discrepancies: it might be advisable to allow suitable laser or gas discharge lines to enter the beam for part of a scan.

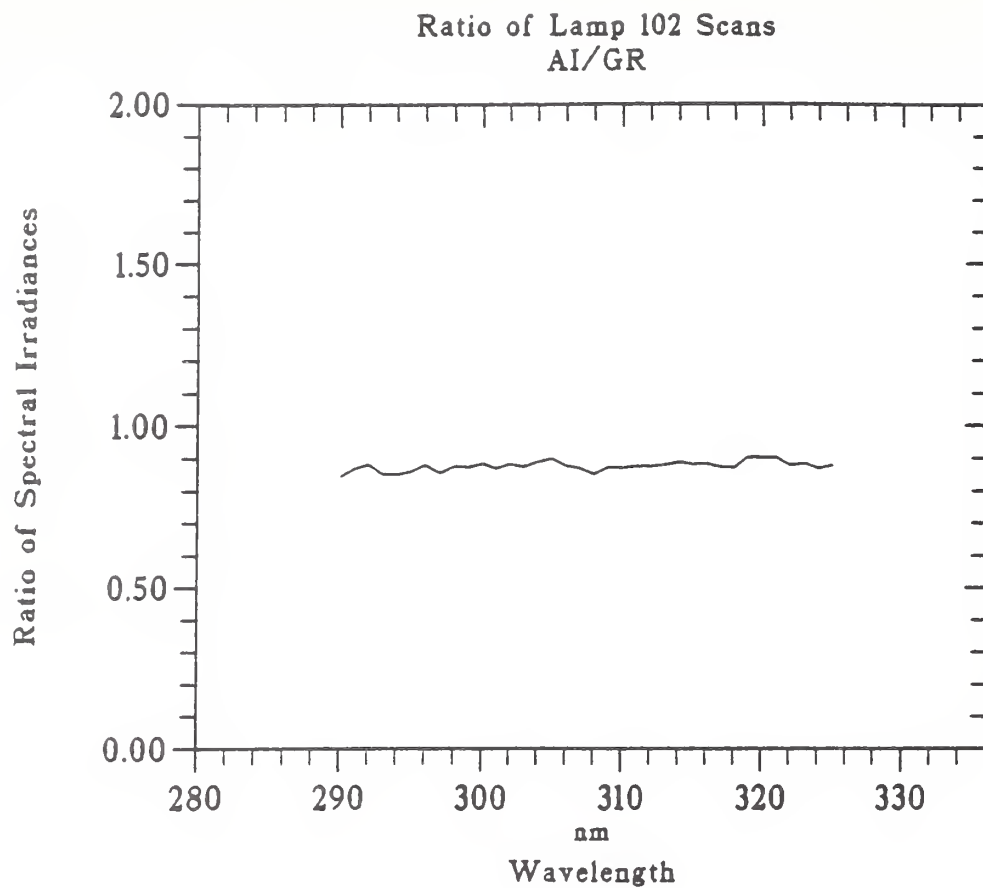


Figure 1

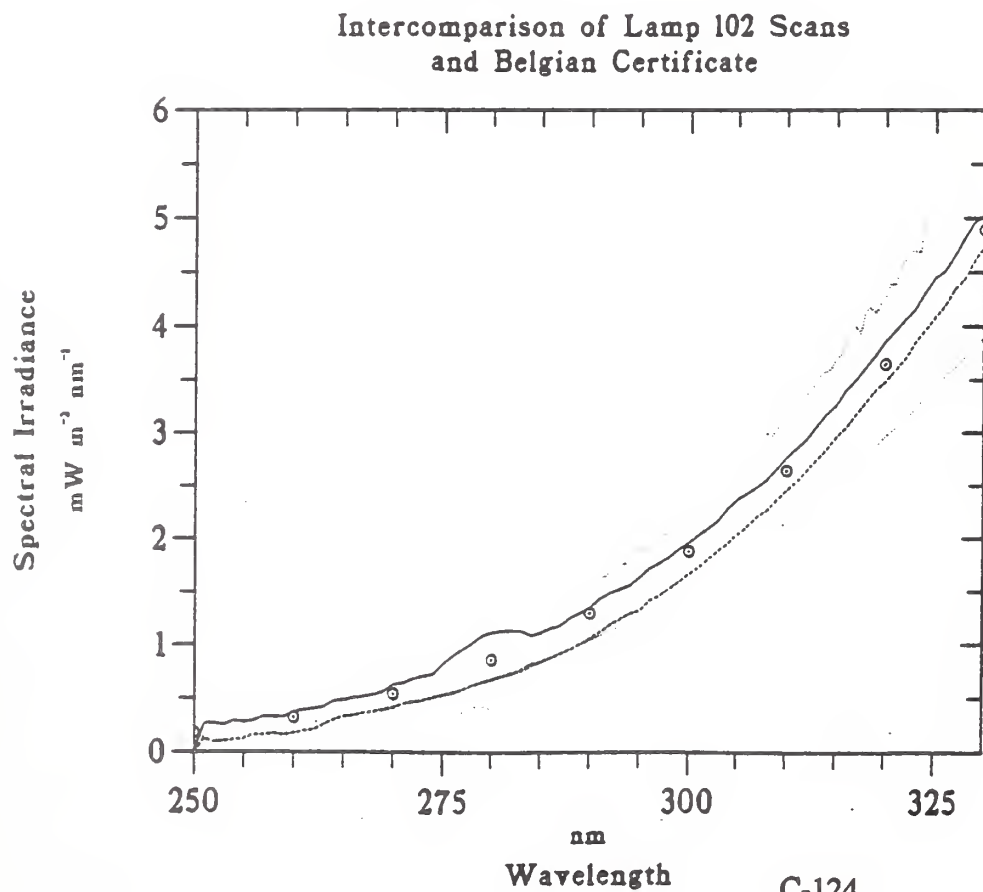


Figure 2

Ratios of Lamp Scans 102/104 Intercomparison with NIST 102/104

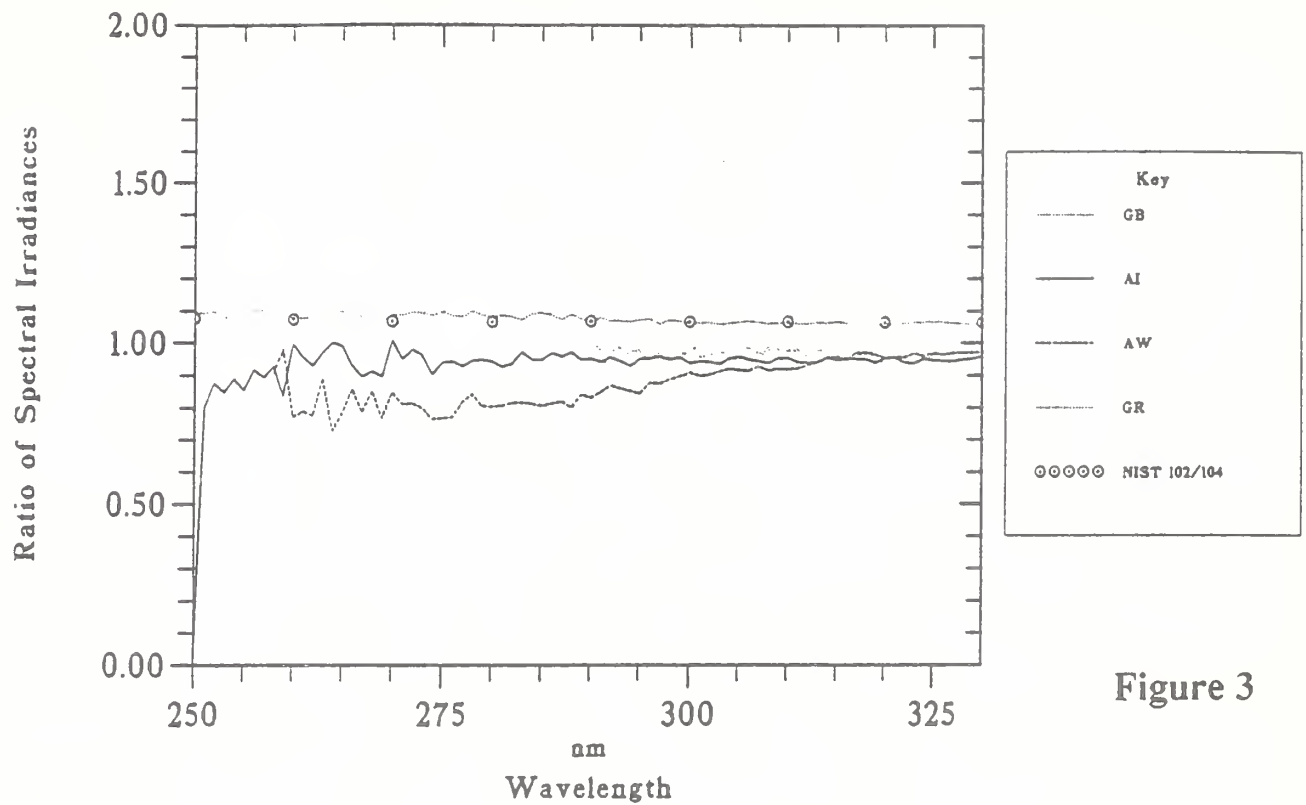


Figure 3

Ratios of Lamps 102, 104 and Sky Scans AI/GR 8 July 1991

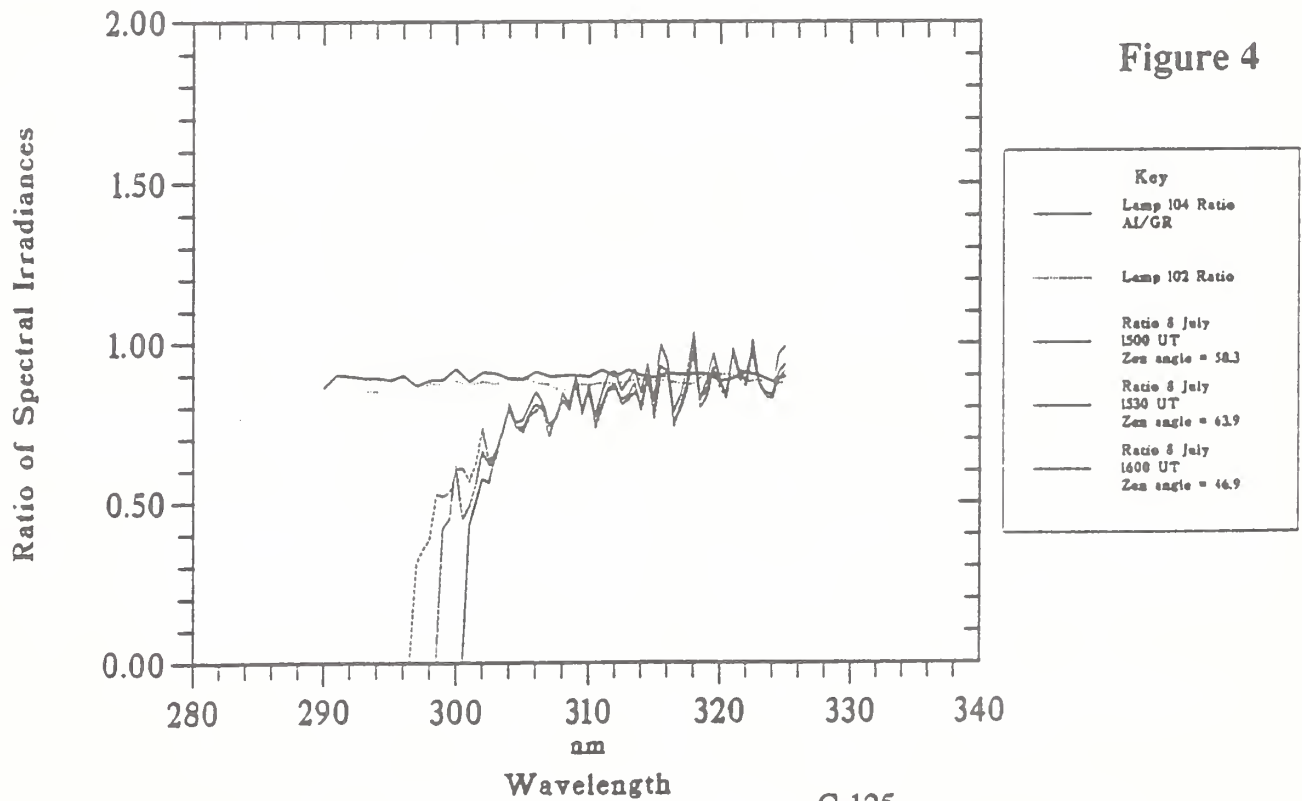


Figure 4

Observed Global Ultraviolet Irradiance
Greece 40°N
July 1991

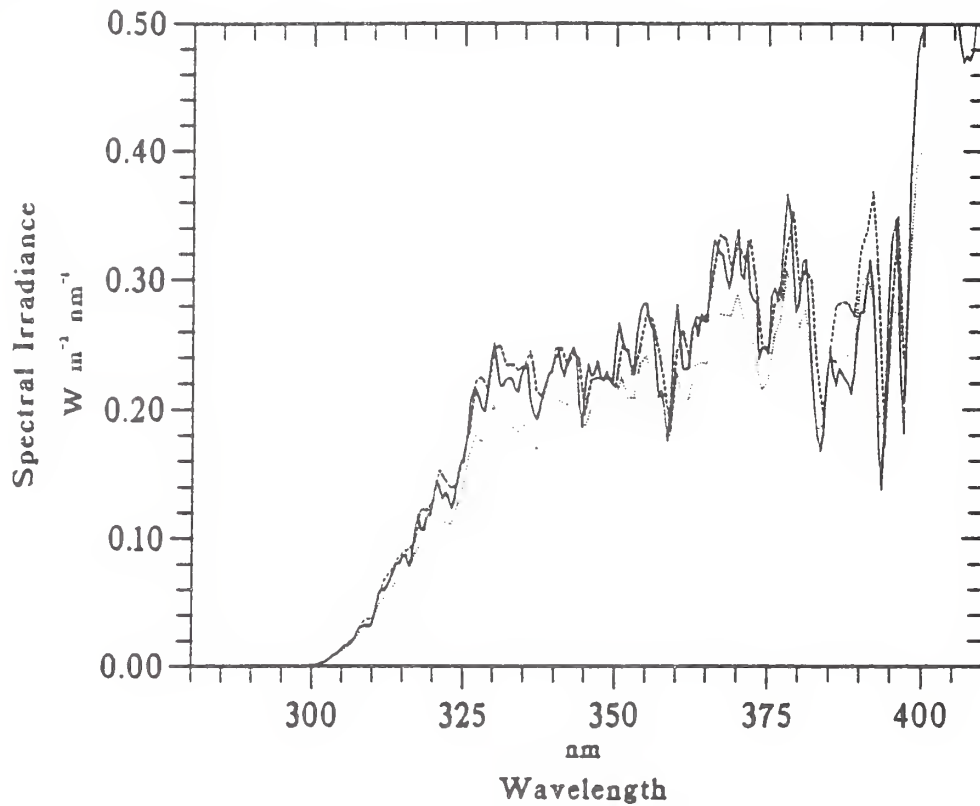


Figure 5

Ratio of Observed Global Irradiance Spectra
Greece 40°N
July 1991

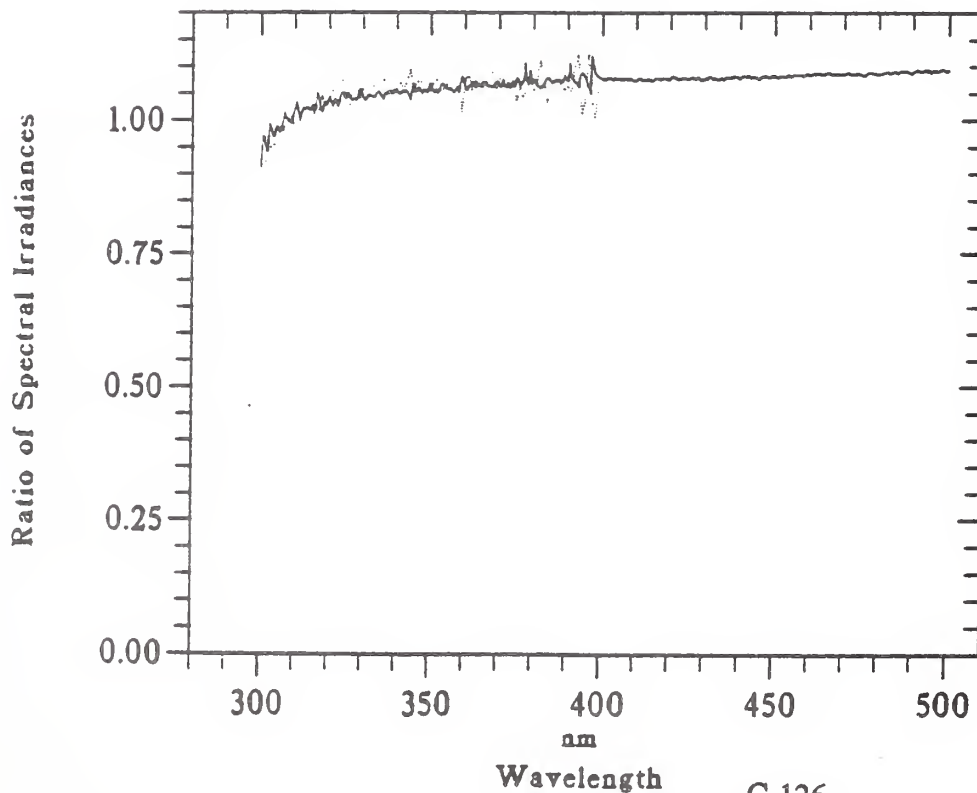


Figure 6

Sky calibrations

In the intercalibrations on the sky, all the instruments were exposed simultaneously on the roof of the building. Generally speaking, the relative spectral responses were again good, and the instruments tended to agree on the absolute irradiances slightly better than in the lamp room. Where they disagreed, there was usually an identifiable reason. Differences in slit function gave rise to very repeatable fluctuations in the ratio of the output from two instruments, as the solar irradiance in this region exhibits considerable spectral structure. At the shortest wavelengths, the instruments varied according to their dependence on dark current and stray light. Occasional small wavelength shifts were detected, and one instrument showed a tendency to become less sensitive after some hours of operation. This last problem was eventually traced to the effect of humidity on an electrical connection.

However, there were some discrepancies in the sky spectra which were not at all easy to account for. In Figure 4, which shows the ratio of three pairs of simultaneous sky spectra from the AI and GR instruments, the small oscillations are due to differences in the slit function, but the broad decline at short wavelengths is the result of stray light or some other effect which comes into play at low levels of irradiance. In the AI instrument, stray light is less than the dark current in this mode of operation, while the GR signal has been reduced to zero at 290 nm in order to remove stray light. The presence of this variation in the AI/GR ratio throughout the UVB region is therefore unexpected.

Some variations in the ratio between pairs of spectrometers were dependent on solar zenith angle, and are probably attributable to imperfect cosine response in the diffusers. This is a difficult and rather neglected aspect of spectroradiometry. If the radiation incident from different parts of the sky on a horizontal surface is not collected with uniform efficiency, there is very little prospect of correcting the results later. All instruments suffer from this problem to a greater or lesser extent.

The wavelength calibration of most instruments was satisfactorily stable. When small shifts were detected they were apparently uniform throughout the recorded spectrum and therefore easily corrected. The strong Fraunhofer features near 395 nm were particularly useful for this purpose. At 290 to 300 nm, however, where the irradiance is a steep function of wavelength, the required criteria are not yet clear and may not be easily met.

The results of the sky calibrations are illustrated in Figure 5, which shows simultaneous ultraviolet spectra from three of the instruments (AI, AW, and GB) in a broken cloud regime at a solar zenith angle of 19°. The agreement in spectral structure is encouraging, and shows what could be achieved with these instruments if the absolute calibrations were reconciled.

The agreement between two instruments in their determination of spectral ratios is even more striking. Figure 6 shows the ratio of spectra taken at the same time on two successive days. The AI and GB instruments are in complete agreement, even at the shortest wavelengths where the effect of a slightly different cloud regime on the second day is faithfully recorded.

Implications for the future

Developments in this programme will be aimed at improving the absolute calibration of the spectrometers, determining the effect of critical parameters such as slit function, dark current and stray light, and the investigation of cosine and azimuth response in individual instruments. The first step will be the construction of a mobile lamp unit which will enable more frequent intercalibration than has been possible in the past.

The most difficult aspect of ultraviolet spectroradiometry is the lack of photons at wavelengths which are strongly absorbed by ozone. It follows that future instruments must have good stray light rejection. This is easier to achieve in a double monochromator, and it therefore seems likely that photomultiplier scanning spectrometers will play a significant role. Ultraviolet instruments with a fixed grating and a detector array are likely to be most useful if confined to a limited spectral region, perhaps with large dispersion, where their ability to integrate over a long time interval will be especially valuable. As array instruments have a predetermined wavelength interval, it may be necessary to ensure adequate oversampling with respect to the slit function, in order to allow comparison of interpolated spectra in the presence of wavelength drift. In the case of photomultiplier scanning instruments, it may be necessary to operate in photon counting mode in order to obtain an adequate signal-to-noise ratio in the wavelength range below 300 nm. Eventually, directional measurements will also be required, in order to address the more subtle photobiological questions, and to provide a better tool for the comparison of experimental spectra with those derived from radiative transfer models.

References

Gardiner, B. G. and Kirsch, P. J. 1991. European intercomparison of ultraviolet spectrometers, Panorama, Greece, 3-12 July 1991. Report to the Commission of the European Communities, STEP Project 76, 62 pp.

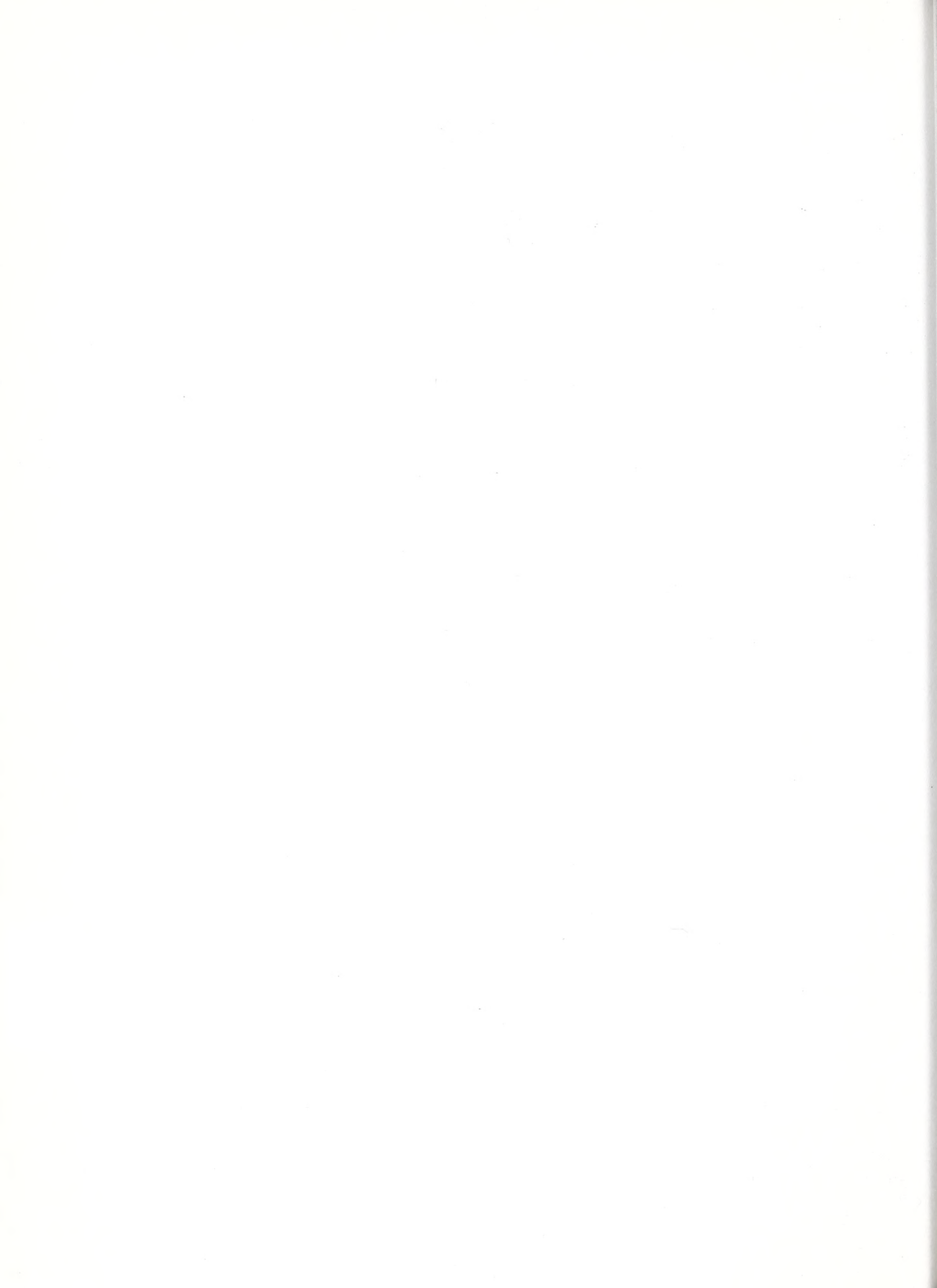
Acknowledgements

The participants acknowledge with gratitude the co-operation and assistance of their colleagues A. F. Bais and C. S. Zerefos in the University of Thessaloniki, who provided the necessary facilities throughout the campaign.

The work described in this paper was funded under Contract CT90-STEP-0076 of the STEP programme (Science and Technology for Environmental Protection) of the Commission of the European Communities.

**USDA/CSRS Instrument Development
and Preliminary Network**

Dr. Lee Harrison
State University of New York, Albany





UNIVERSITY AT ALBANY

STATE UNIVERSITY OF NEW YORK

To: Whitney Carroll
AFEAS - West Tower Suite 400
1833 H St. NW, Washington, DC 20005

From: Lee Harrison

About: Summary of Remarks at Conference

The *Solar Ultraviolet Monitoring Network for the Biosphere*, funded by the U.S. Dept. of Agriculture has the following program objectives:

Program Objectives: To develop, test, and deploy two prototype high accuracy Ultraviolet Spectroradiometers suitable for extended autonomous field operation with telemetered control and data transfer that are capable of wavelength resolution substantially better than 1 nm., and absolute accuracy approaching 1% over the wavelength range 280 nm. to 400 nm.

To then operate these instruments for one year, thereby starting the Biosphere Monitoring Program. One of the two instruments will be sited at the "Southern Great Plains" Clouds & Radiation Testbed facility of the DOE Atmospheric Radiation Measurement (ARM) program near Ponca City, OK. The site for the second instrument has not yet been selected.

These objectives push the state of the art with respect to accuracy and minimum detection limit. In order to achieve this desired performance we are developing a new UV spectroradiometer:

Technical Approach: These instruments will consist of Lambertian fore-optics developed at ASRC specially for these instruments, a dual 1/4 meter Ebert grating monochromator manufactured by RSI (Research Support Instruments), a Peltier-cooled photomultiplier detector operated in the photon counting regime, and an on-board control control & data telemetry computer derived from the Multi-filter RSR instruments (that make spectroradiometric observations through the range 350 - 1600 nm) being developed jointly by ASRC and PNL for the ARM. The instruments will also implement the automated shadowband technique to permit separate

measurements of the total horizontal irradiance and the direct beam irradiance.

The instrument will have an internal automated wavelength calibration against a Hg. vapor lamp, and a semi-automated absolute calibration against a 50 W FEL type standard lamp. This absolute calibration will use a "bootstrap" technique based on the spectral observations from the instrument itself to improve the stability of this calibration by partially compensating for the change in filament temperature caused by lamp operation. The instruments will receive laboratory testing and calibration at the National Institute for Standards Technology (NIST).

The Airy width of the spectral bandpass will be set to 0.1 nm. The precision of the grating drive mechanism is 0.02 nm., thus permitting standard spectral deconvolution techniques to "over-resolve" the Airy limit by perhaps a factor of two given that the slit-function is accurately established and sufficient measurements made.

The dual grating monochromator, and photon counting detection, are needed to achieve measurements below ≈ 300 nm, where out-of-band rejection ratios of order 10^8 are needed, and photon arrival rates may drop below 10 Hz. The time required to make an individual spectral measurement is thus set by the Poisson statistics of stochastic arrivals. At wavelengths below 290 nm. this may require several minutes to achieve 1% accuracy; in contrast at wavelengths longer than 300 nm the acquisition will typically be $\ll 0.1$ sec. (In which case the acquisition of a spectrum will be grating-drive limited.)

Since we have only just begun these engineering efforts it is premature to discuss integrated system performance, but I can show early results of the development and testing of the Lambertian Inlet optic ("cosine diffuser").

A Lambertian optic is a necessary component of any instrument that measures *total horizontal irradiance* (either spectral or broad-band). The goal of such an optic is to provide an angular acceptance function proportional to the cosine of the zenith angle for all incident radiation that arrives at the detector from angles above the horizon. This is equivalent to measuring the flux incident on a flat surface.

The performance of the inlet optic with respect to the correct integration over the sky radiance distribution is critical. In the absence of other information about the sky radiance distribution, errors introduced at this point propagate through all subsequent analysis, and generally cannot be corrected without introducing *ad hoc* assumptions, even if the deviation of the response function from the ideal cosine(Zenith Angle) is known. The instrument can be no better than its inlet optic! Unfortunately neither flat or spherical-

dome windows do this properly, a consequence of the Fresnel equations that predict reflections from surfaces.

In addition there are practical constraints stemming from the requirement that the inlet optic be suitable for field use. The optic must have a sealed entrance, and must be designed both to be readily cleaned, and to minimize the optical consequences of small (but inevitable) soiling. It also must be designed to avoid aging degradation.

Lambertian Inlet Optic and Beam Collimator: The empirical development of Lambertian diffusers optimized for various wavelengths has a venerable history (e.g., Kerr, et al. [1967]). By the time of this early work it was recognized that simple glass domes did not perform well (particularly at solar zenith angles near 70°), and that flat diffusing receivers with carefully shaped sidewall and blocking ring geometries can be much superior.

As a critical part of our design of advanced spectral radiometers for the Atmospheric Radiation Measurement Program we are developing improved Lambertian diffusers, and operate an automated test facility to measure their angular response functions. (We believe it to be the only automated facility of this kind.) The test bench consists of 500 Watt 1" aperture axial parabolic confocal Xenon arc light source manufactured by ILC corp., a 16 ft. beam-forming tube with baffles to eliminate off-axis light, and a working cavity with a 2 ft working swing radius around the central beam point. The working optical aperture is slightly greater than 2" diameter, with a measured intensity uniformity of better than 1%. The maximum beam divergence is $1/2^\circ$, with 84% of the radiance having a beam divergence less than $1/4^\circ$.

The calibration process is automated by a computer that controls the angular rotation of the apparatus under test and also samples and stores the detector output. The computer program accepts simple user inputs for the number of detector output channels (up to 16) to be measured, the angular step per measurement (minimum angle is $1/4^\circ$, with reproducibility of $\approx 0.02^\circ$), the instrument settling time per measurement, and the number of scans to average. Repeated back-and-forth scans are needed to average out the inevitable lamp fluctuations of the Xenon arc. Some of the detectors we test have slow instrument responses (as much as 20 sec for thermopile radiometers), and so a high accuracy response determination with angular increments of $1/4^\circ$ from -90° to 90° in zenith angle and ten repetitions may take as much as 10 hours and involve 7,200 measurements. This would be unbearably tedious to do by hand -- we can simply start the instrument and leave it running over night.

The automation of this calibration process is critical to the development of good Lambertian detectors (particularly if they must operate over a range of wavelengths) since repeated measurements (and some "cut-and-try" iteration) are needed to arrive at an acceptable design. In general the modern starting point for a design is usually one developed from Monte-

Carlo photon ray-tracing calculations. Unfortunately the optical properties of these materials (particularly the internal scattering phase-functions as a function of wavelength) are not sufficiently well known to permit these calculations to be sufficiently accurate to establish a design. In our case, however, the starting point design will be taken from our multi-filter instrument, because it has already been demonstrated to work well at 380 nm. Consequently we have a head start at this problem.

The complete Lambertian inlet optic for the UV spectroradiometer is shown schematically in Fig. 1 below. In addition to providing a Lambertian receiver and integrating cavity, this optic supplies a shutter (shown in the open position) and a mercury vapor lamp for automated wavelength calibration, a beam former that couples the output into the f -number optical cone that the monochromator can receive (thereby reducing stray light throughput), and an attenuator (needed at longer wavelengths to avoid photomultiplier saturation).

The inlet diffuser and integrating cavity will be made entirely from Spectralon™ (a proprietary optical plastic manufactured by Labsphere).

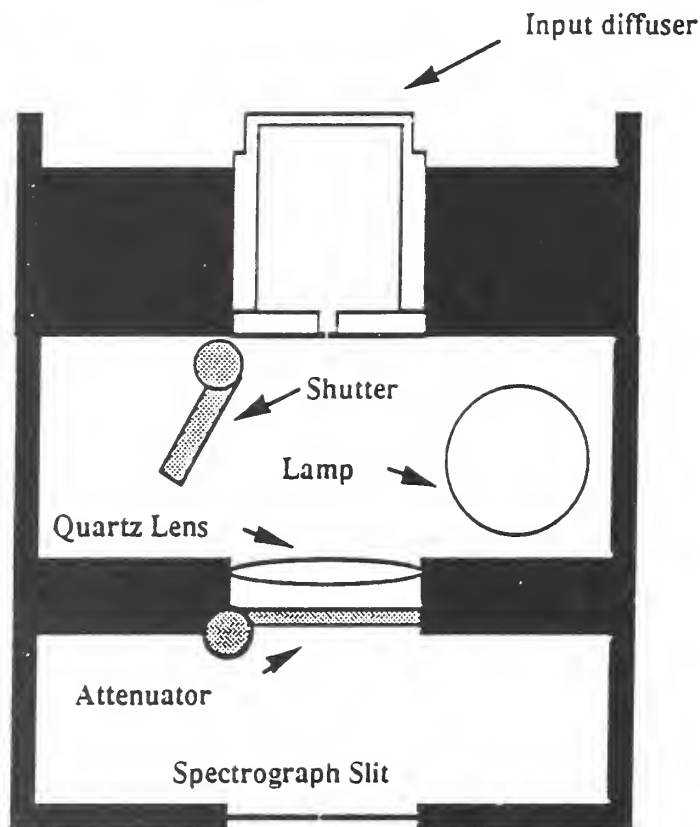


Fig 1: Schematic Diagram of Lambertian Inlet Optic -- not to scale

In general, the goal of these designs is to select the transmission of the first surface to be approximately 0.1 - 0.2. The thickness ratios of the flat face and rim sidewalls are tailored by test results to produce the best

approximation to Lambertian response. (This must, of course, be a compromise over the intended operating wavelength range.) The integrating cavity behind both improves the angular response and substantially increases the light throughput provided that the cavity albedo is good, and

$$\text{Area}_{\text{first-surface}} \times \text{Transmission}_{\text{first-surface}} \gg \text{Area}_{\text{exit}}$$

The low transmission front surface diffuser is insensitive to scattering produced by surface deposits (absorption does matter), a dramatic advantage compared to designs using high-transmission domes. Spectralon is readily cleaned, chemically inert, and has demonstrated very low aging degradation in the presence of UV.

The relay optic consisting of a quartz lens relays the image of the integrating cavity exit (that is shaped like the spectrograph slit, but slightly larger), and ensures that only rays lying within the f 4.8 throughput optic of the spectrograph impinge on the slit. This reduces stray light throughput.

An attenuator is needed at the longer wavelengths to prevent detector saturation. This attenuation *should not* be produced by a aperture that vignettes the optical path of the spectrograph, doing so reduces the number of grating lines illuminated and alters the bandpass. Consequently this attenuator (shown in the operating position) should be a stable absorption filter. (It is not necessary that this filter be "neutral density," but it is very important that its throughput at each wavelength be stable.)

We have started to develop and test this critical portion of the instrument, and our results are shown in the following figures.

Figure Captions & Discussion:

Figures 2 & 3

In most reports Lambertian inlet optic performance is shown with a figure like that of figure 2; that plots the apparent deviation of the instrument response from a fitted perfect cosine. In this figure (taken from a real detector, but anonymous since this is an illustrative example only) the response appears very good indeed.

Unfortunately plots of this form camouflage the errors we want to see. Figure 3 shows the error ratio for this same data. The error ratio is the ratio of the measured response of the detector as a function of angle, divided by a best-fit ideal cosine function. A perfect Lambertian diffuser would exhibit a horizontal line with the value 1. Figure 3 demonstrates that this detector has errors of $\approx 2\%$ through much of the angular range, and worst-case errors near 5% at 70° .

Figures 4 & 5

Very few Lambertian detectors perform as well as the previous example. Figure 3 shows the performance of three individual Eppley PSP pyranometers (a standard instrument for total horizontal irradiance). Figure 4 shows the performance of a single Kipp & Zonen CM11: a competing instrument.

Readers should note that the monotonically declining response exhibited by these detectors as the zenith angle increases is undesirable. The total measured irradiance for a *perfect* Lambertian diffuser will be

$$I = \int_0^{\pi/2} S(\vartheta) \cos(\vartheta) \sin(\vartheta) d\vartheta$$

where $S(\vartheta)$ is the sky radiance as a function of zenith angle ϑ . The weighting kernel $\cos(\vartheta)\sin(\vartheta)$ is a maximum at 45° , hence the detector performance at mid angles is very important.

Figure 6

This figure shows the Lambertian-inlet test item fabricated by RSI. This test item permits the integrating cavity protrusion and blocking ring height to be adjusted. The attenuator/shutter mechanism is missing, and the relay lens optic has been replaced by a photodiode having equal exit f -number. Current test are being done using UG-11 and BG-39 filters in series to obtain a response over the range 300 - 400 nm.

Figure 7

This figure shows the best test results to date (April 3) with this design. These results are a factor of two better than those shown at the meeting, and we are still making progress. Please note, however, that this design is already superior to those commonly used.

Useful References

Atmospheric Radiation Measurement Program Plan (1990) United States Dept. of Energy document DOE/ER-0441

Barker, R.E. Jr. (1968) "The Availability of Solar Radiation Below 290 nm and Its Importance in Photomodification of Polymers." *Photochemistry and Photobiology* 7, pp 275-295

Chai, A.T. and A.E.S. Green (1976) "Ratio Measurement of Diffuse to Direct Solar Irradiance in the Middle Ultraviolet" *Appl. Optics* 15 pp 1182-1187

Garrison, L.M., L.E. Murray, D.D. Doda, and A.E.S. Green (1976) "Diffuse-Direct Ultraviolet Ratios with a Compact Double Monochromator" *Appl. Optics* 15 pp 827-836

Garrison, L.M., L.E. Murray, and A.E.S. Green (1978) "Ultraviolet Limit of Solar Radiation at the Earth's Surface with a Photon Counting Monochromator" *Appl. Optics* 17 pp 683-684

Garrison, L.M., D.D. Doda, and A.E.S. Green (1979) "Total Ozone Determination by Spectroradiometry in the Middle Ultraviolet" Appl. Optics 18 pp 850-855

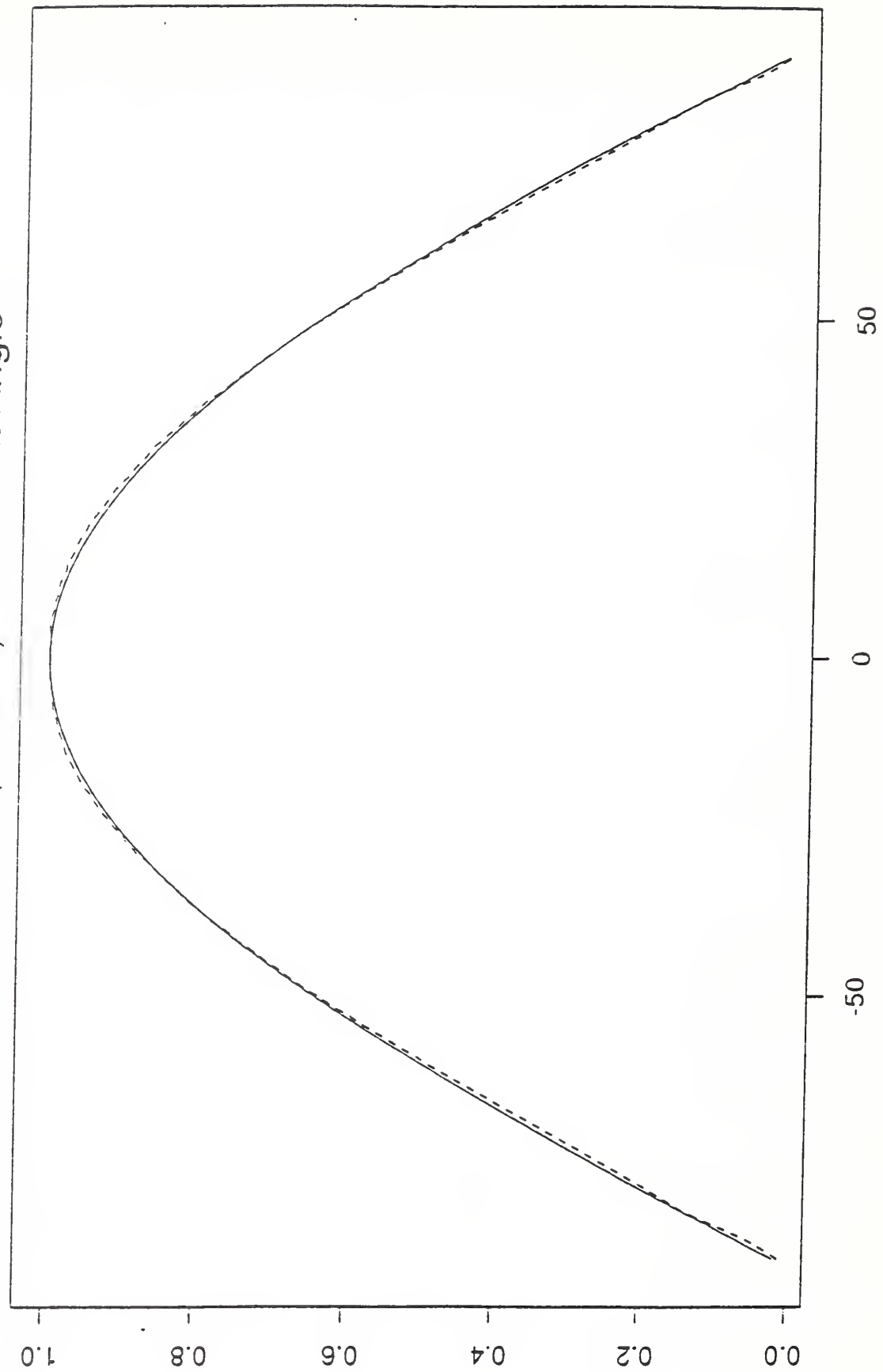
Halpern, P., J.V. Dave, and N. Breslau (1974) "Sea-Level Solar Radiation in the Biologically Active Spectrum." Science 186, pp 1204-1208

Kerr, J.P., G.W. Thurtell, and C.B. Tanner (1967) "An Integrating Pyranometer for Climatological Observer Stations and Mesoscale Networks," J. Appl. Met. 6, pp. 688-694

Kostkowski, H.J., J.L. Lean, R.D. Saunders, and L.R. Hughey (1986) "Comparison of the NBS SURF and Tungsten Ultraviolet Irradiance Standards", Appl. Optics 25, p 25

Schoeberl, M.R. and A.J. Krueger (1983) "Medium Scale Disturbances in Total Ozone During Southern Hemisphere Summer" Bull. Am. Meteor. Soc 64(12) pp 1358-1365

True Cosine Response (solid) and Measured
Response (dashed) vs Incident Angle

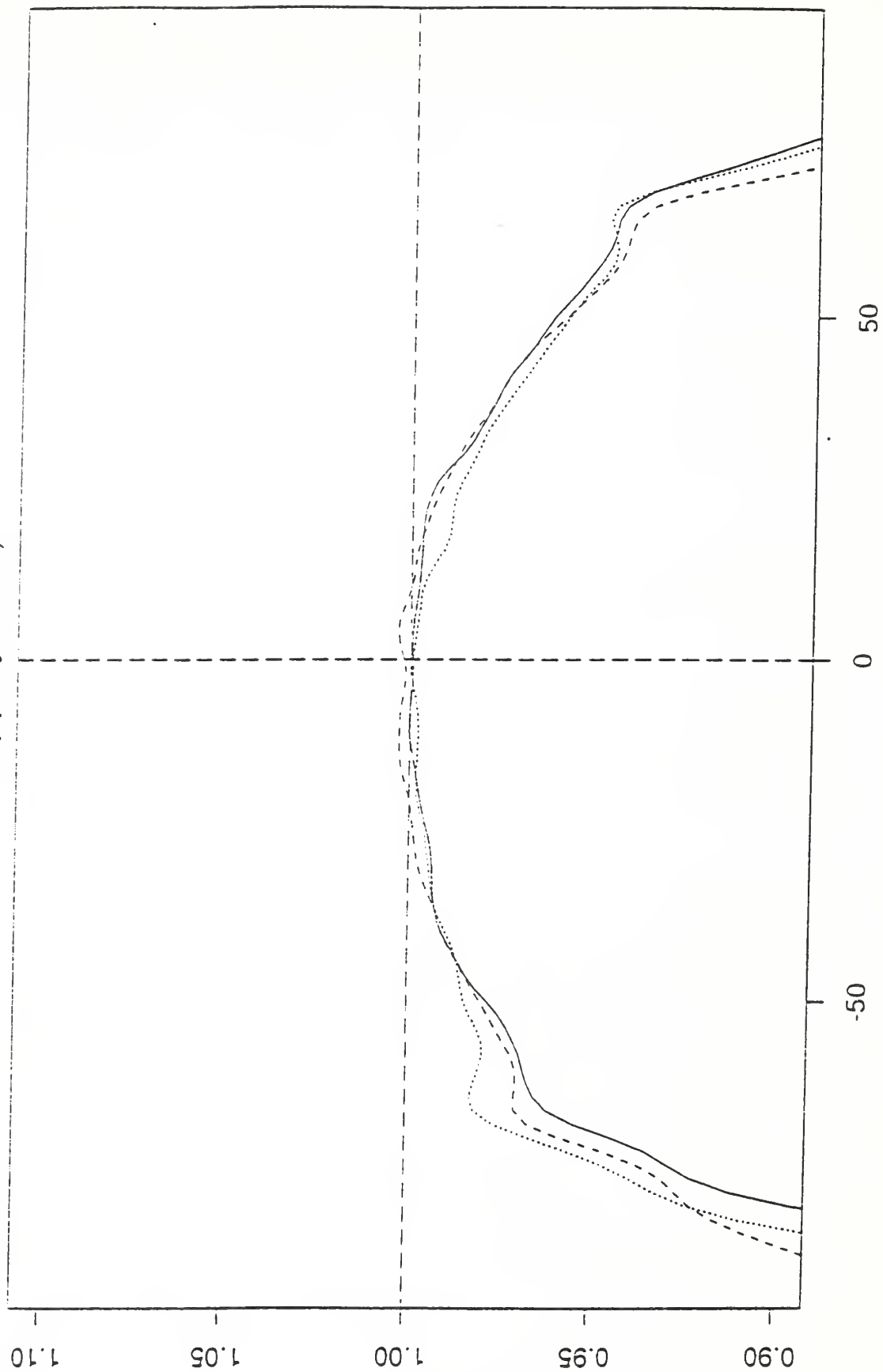


Normalized Cosine Response vs Incident Angle

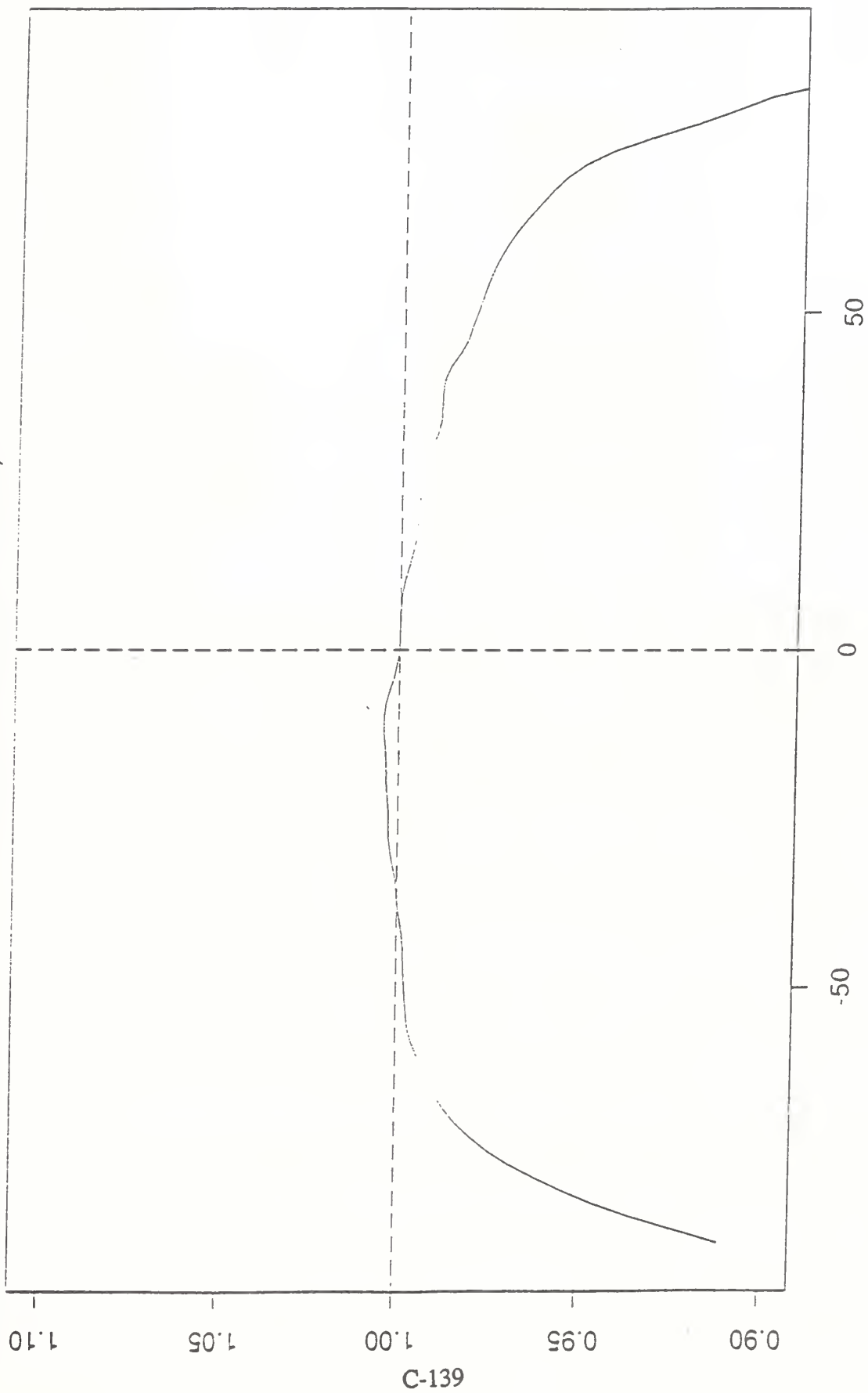


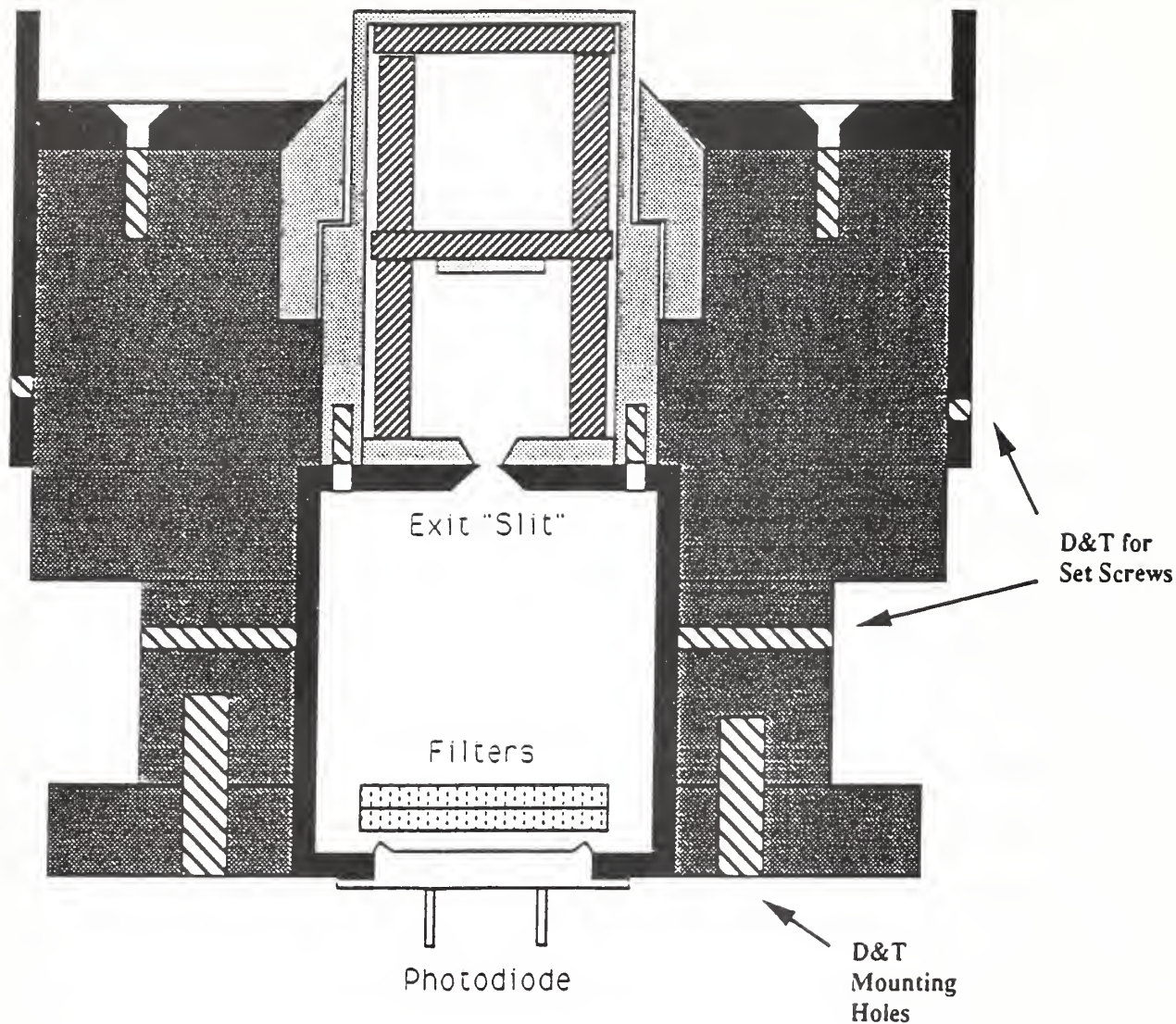
C-137





Cosine Response vs. Incident Angle
(Eppley PSP)



Cosine Response vs. Incident Angle (Kipp & Zonen CM11)



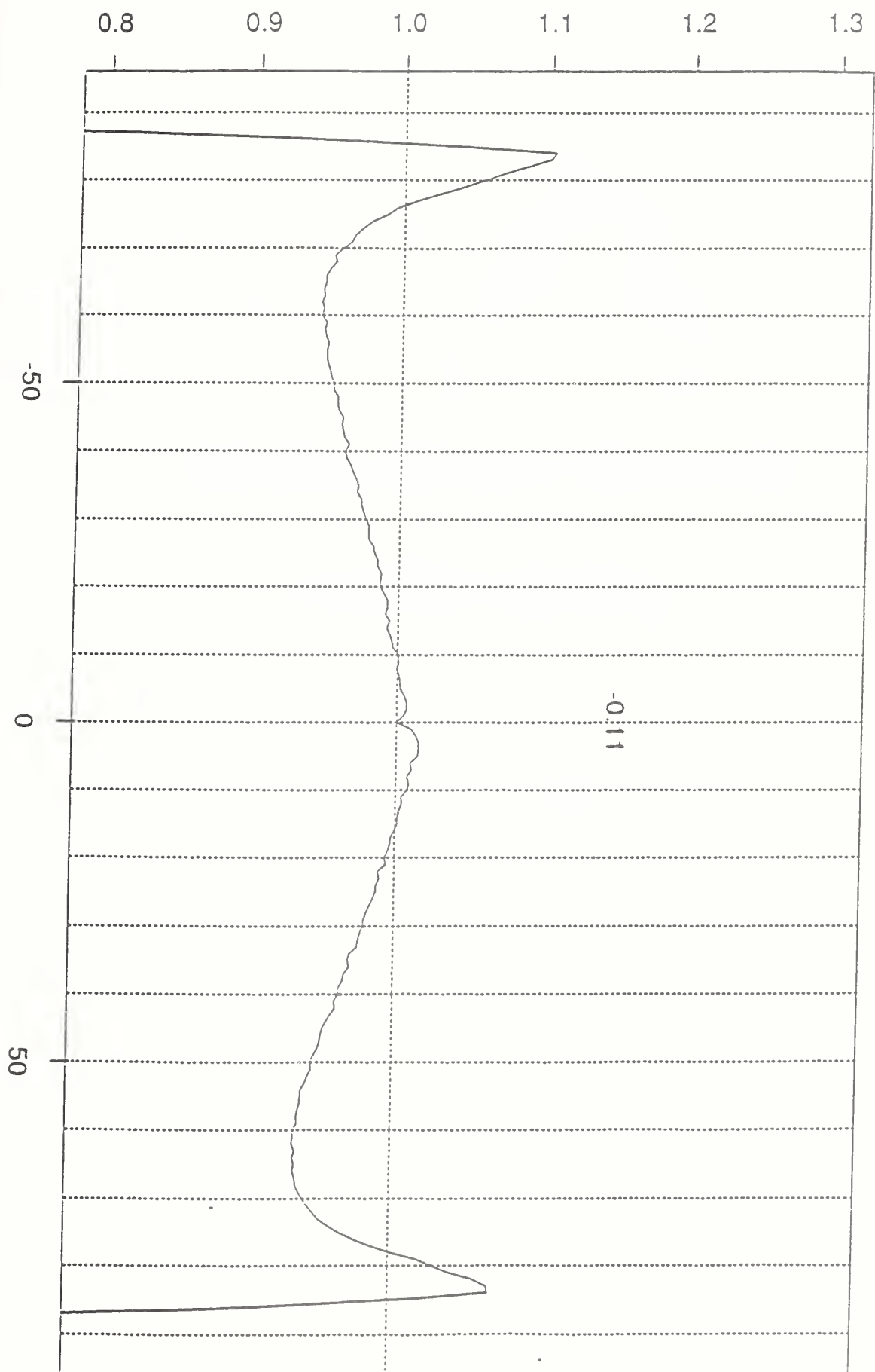


-  = Spectralon™ Optical Plastic
-  = Quartz, Fuzed Silica, or Schott WG-280
-  = Machinist's Choice of Material
-  = 6061 Aluminum, Optical Black Anodize

Mechanical Sketch: Lambertian Optical Inlet of the UV-Spectroradiometer (Test Item)

Not to Scale -- see attached notes for discussion of design and controlling dimensions -- Lee Harrison, 12/26/91

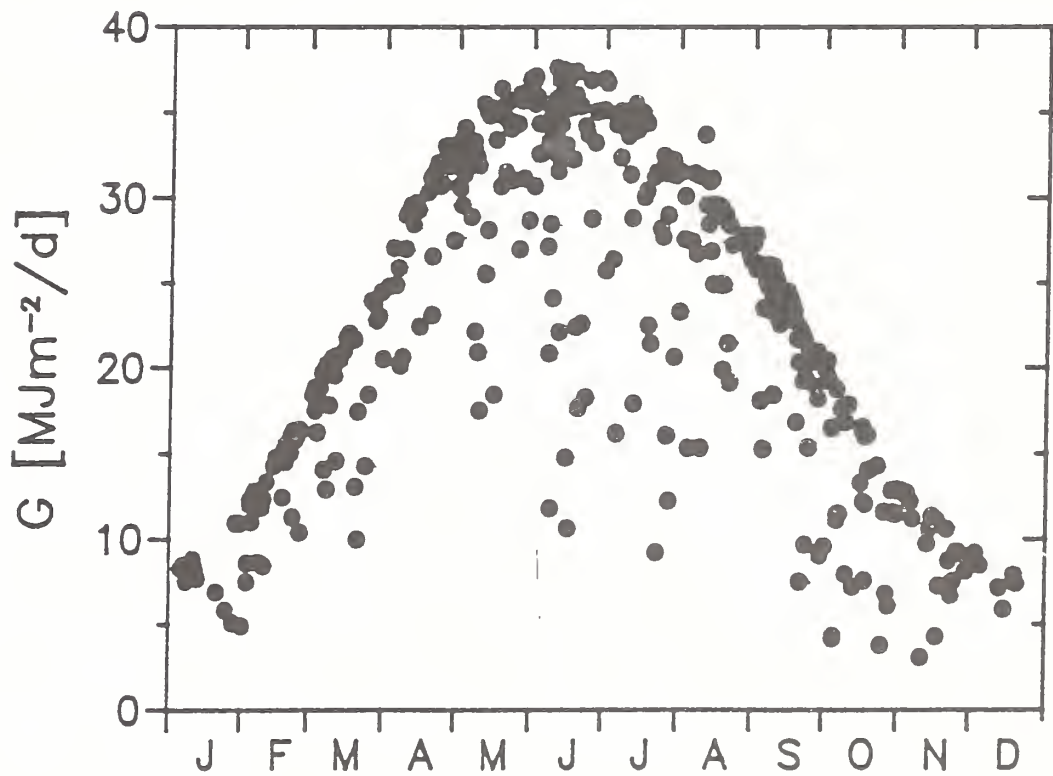
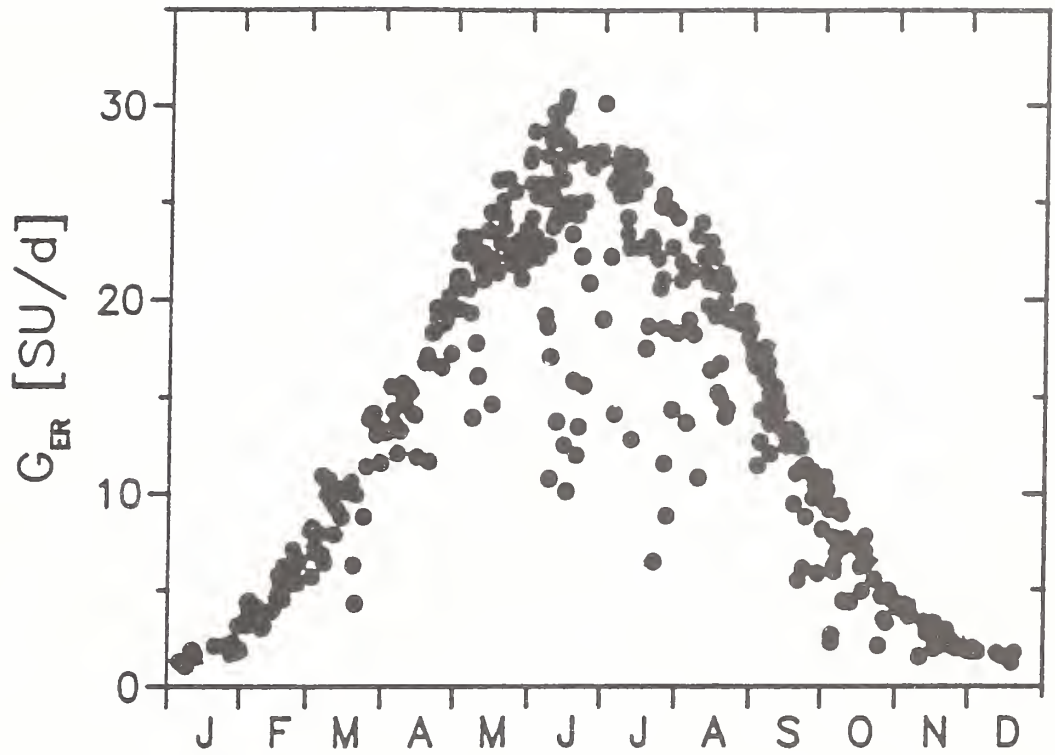
UV Depressed Diffuser 4



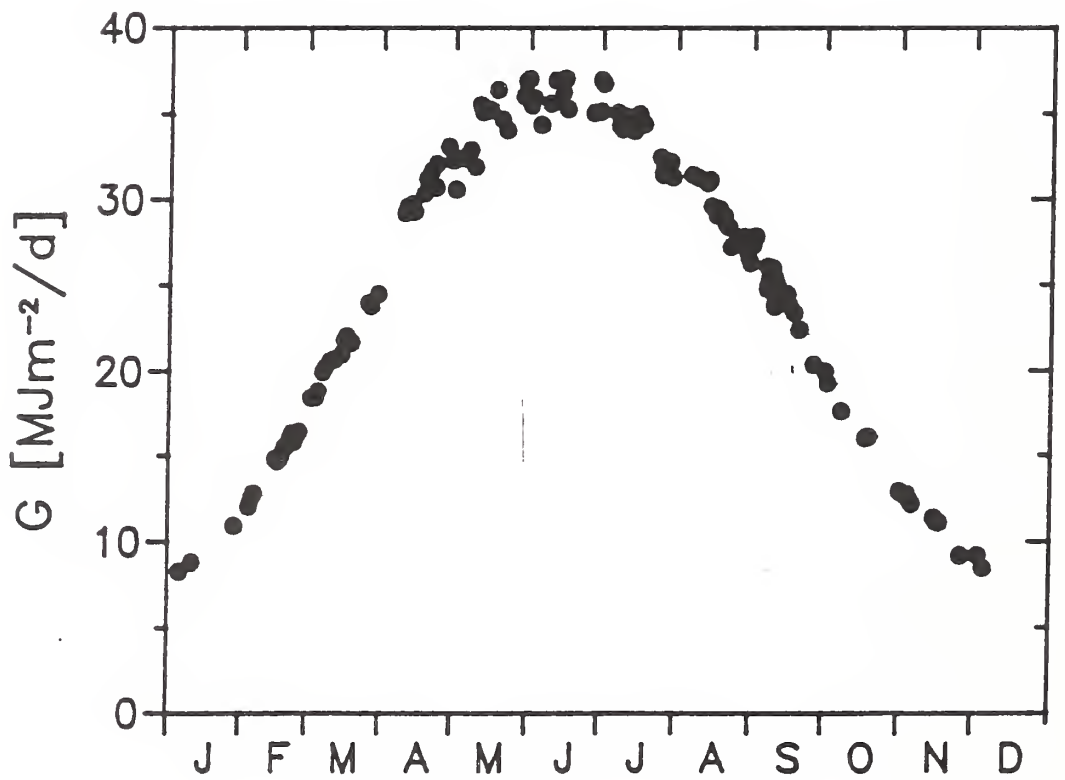
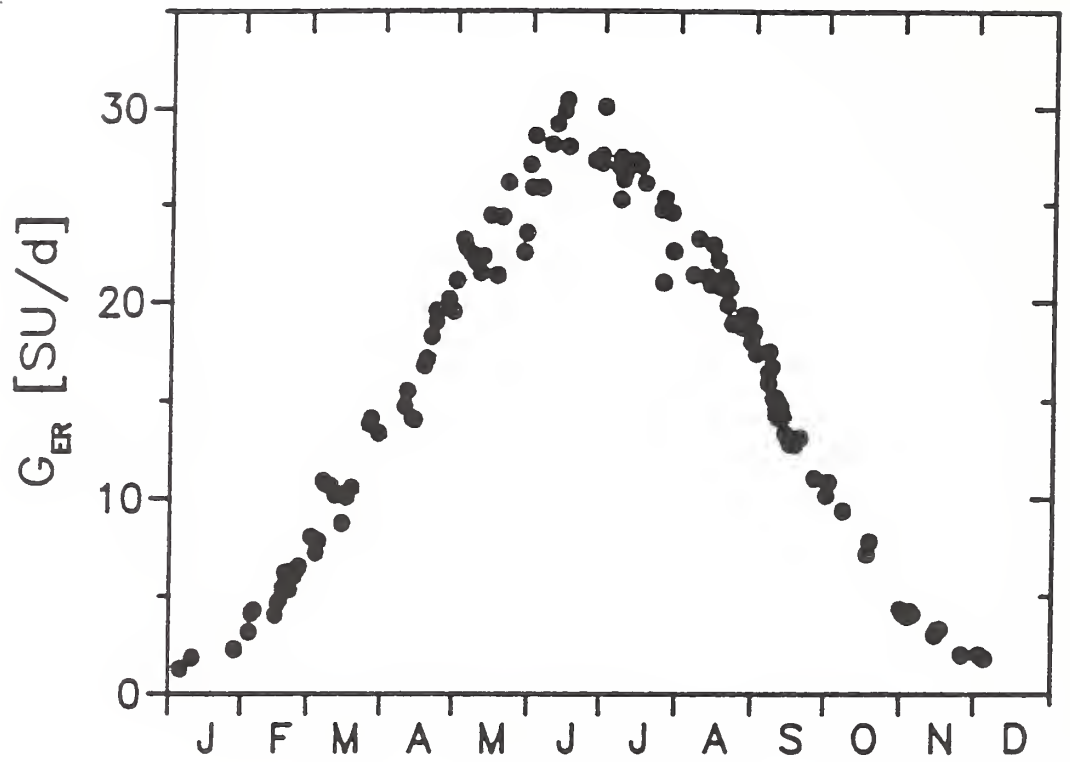
High Altitude UV-B Measurements and Trends

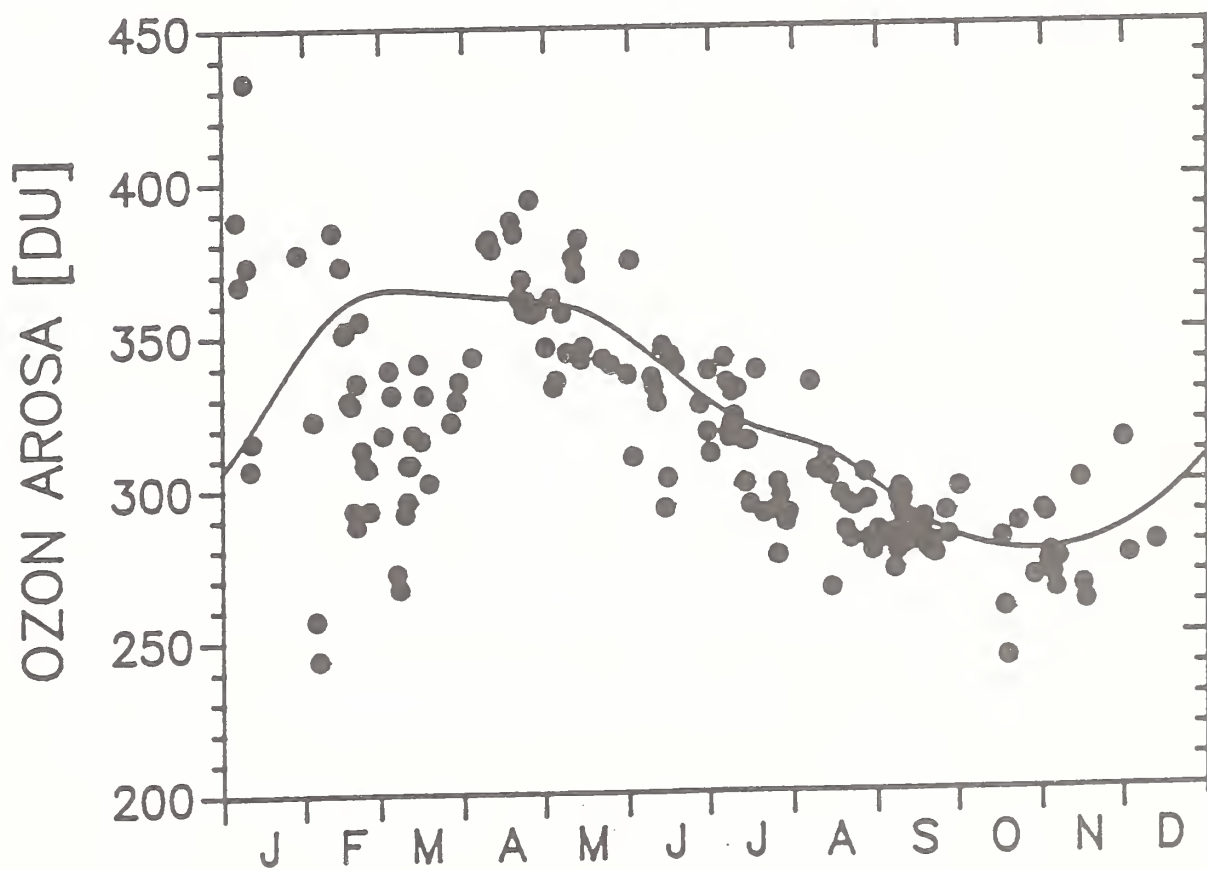
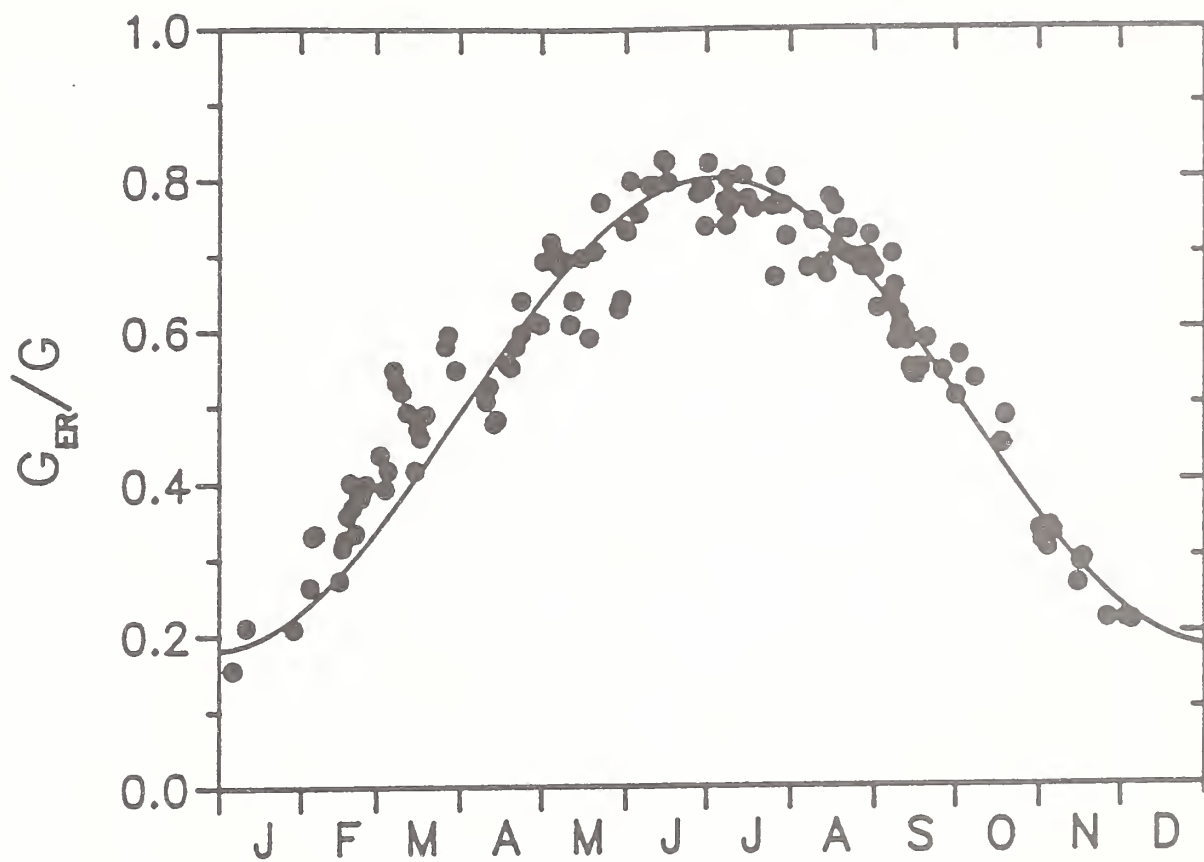
Dr. Mario Blumthaler
University of Innsbruck, Austria

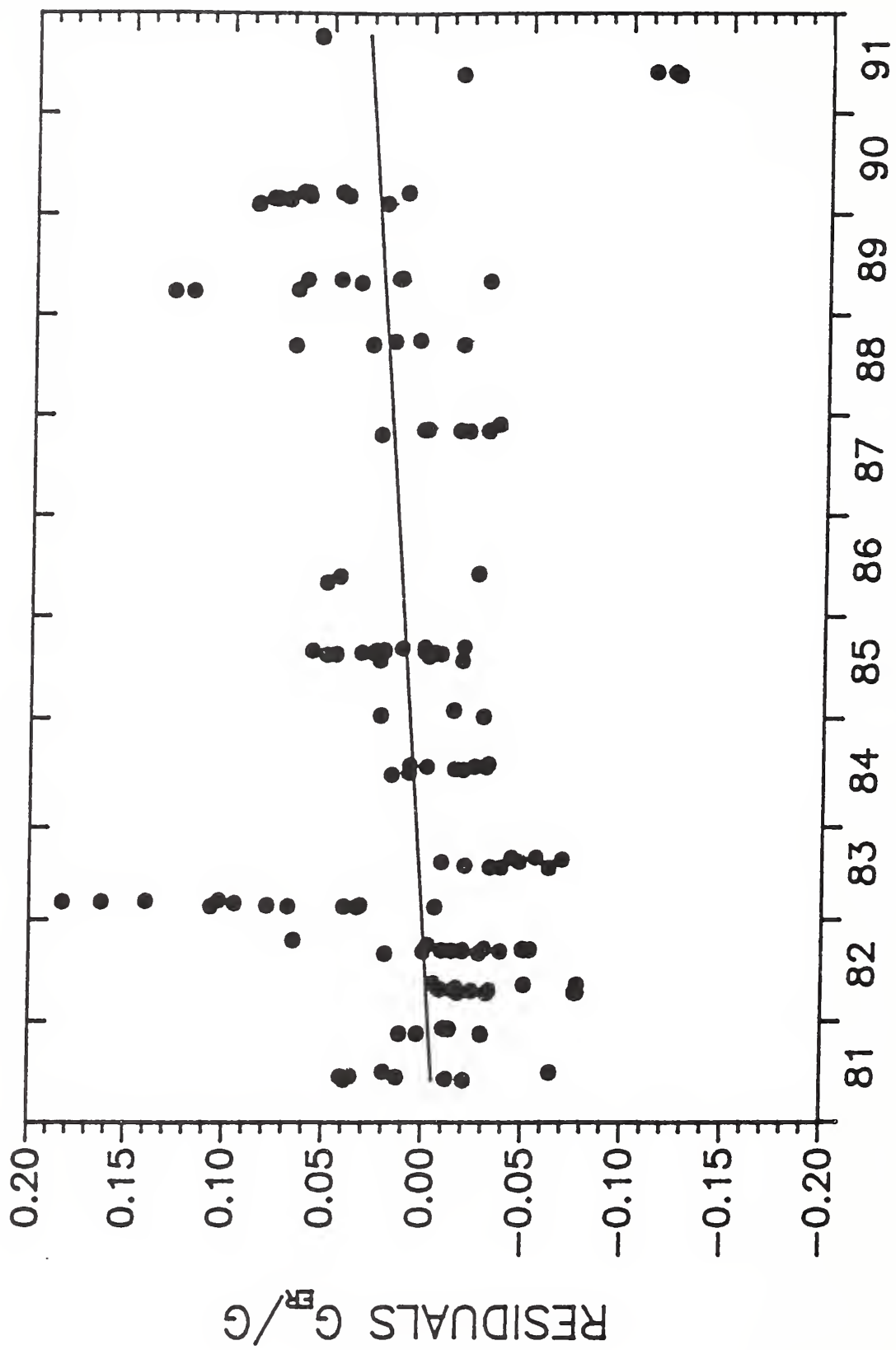
JUNGFRAUJOCH (3576 m)

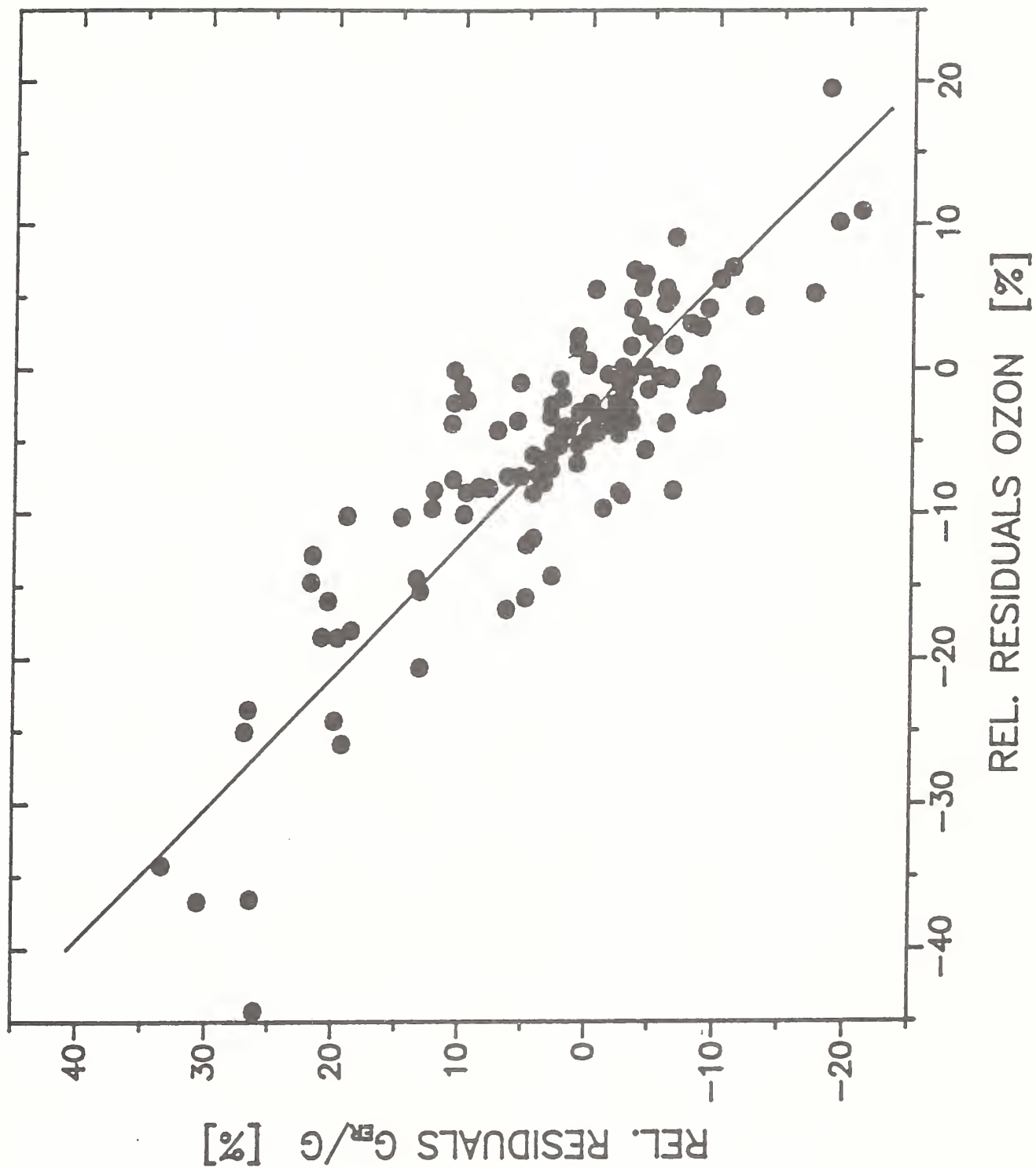


JUNGFRAUJOCH (3576 m)









UV-B Controlling Factors and Variability

**Dr. John Frederick
University of Chicago**

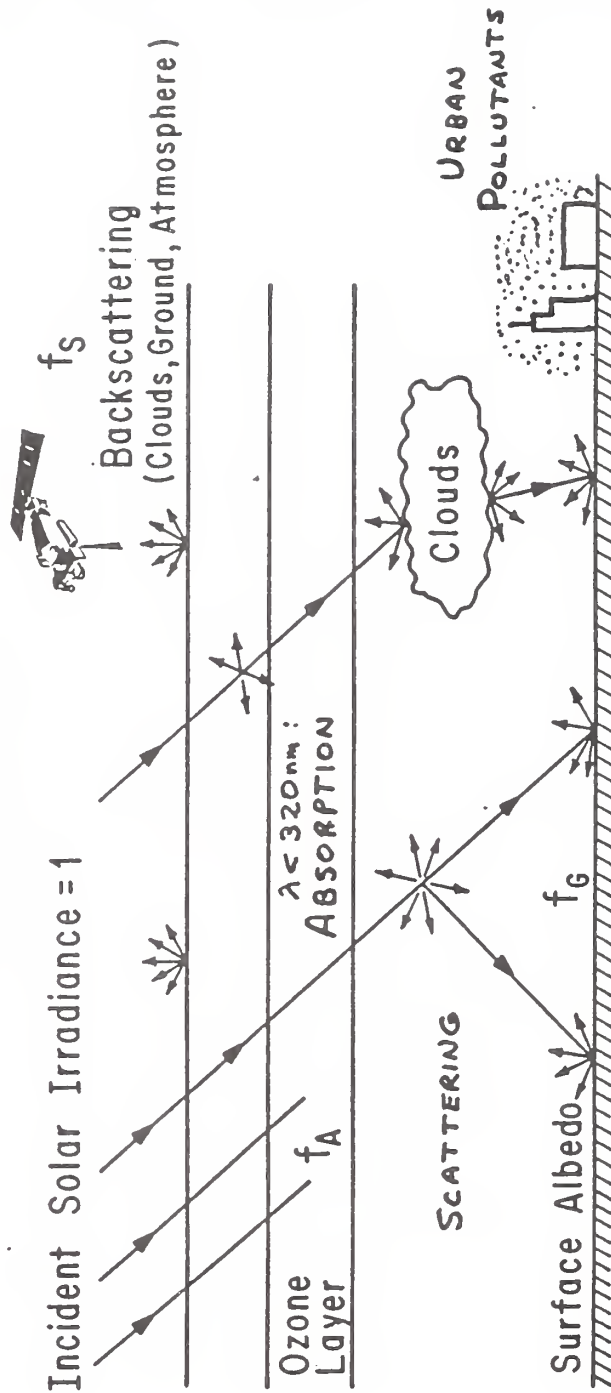
Factors That Control Surface UV-B Irradiances and Their Variation Over Time

Elizabeth C. Weatherhead & John E. Frederick

- * Identify Factors That Contribute to the Transmission of the Atmosphere**
- * Latitudinal and Temporal Variations in Erythemat Irradiances for an Ozone-Absorbing, Molecular-Scattering Atmosphere**
- * Variability Shown by UV Radiation in the Real Atmosphere**
- * Absorption by Gaseous Air Pollutants in the Boundary Layer: Magnitude and Trends**
- * A Rationale for Performing Ground-Based UV Irradiance Measurements**

The Budget of Biologically Active Ultraviolet

Solar Radiation



$$f_A + f_g + f_s = 1$$

ABSORPTION IN ATMOSPHERE

SCATTERING TO SPACE

ABSORPTION AT GROUND

Factors That Control UV-B Irradiances at the Earth's Surface

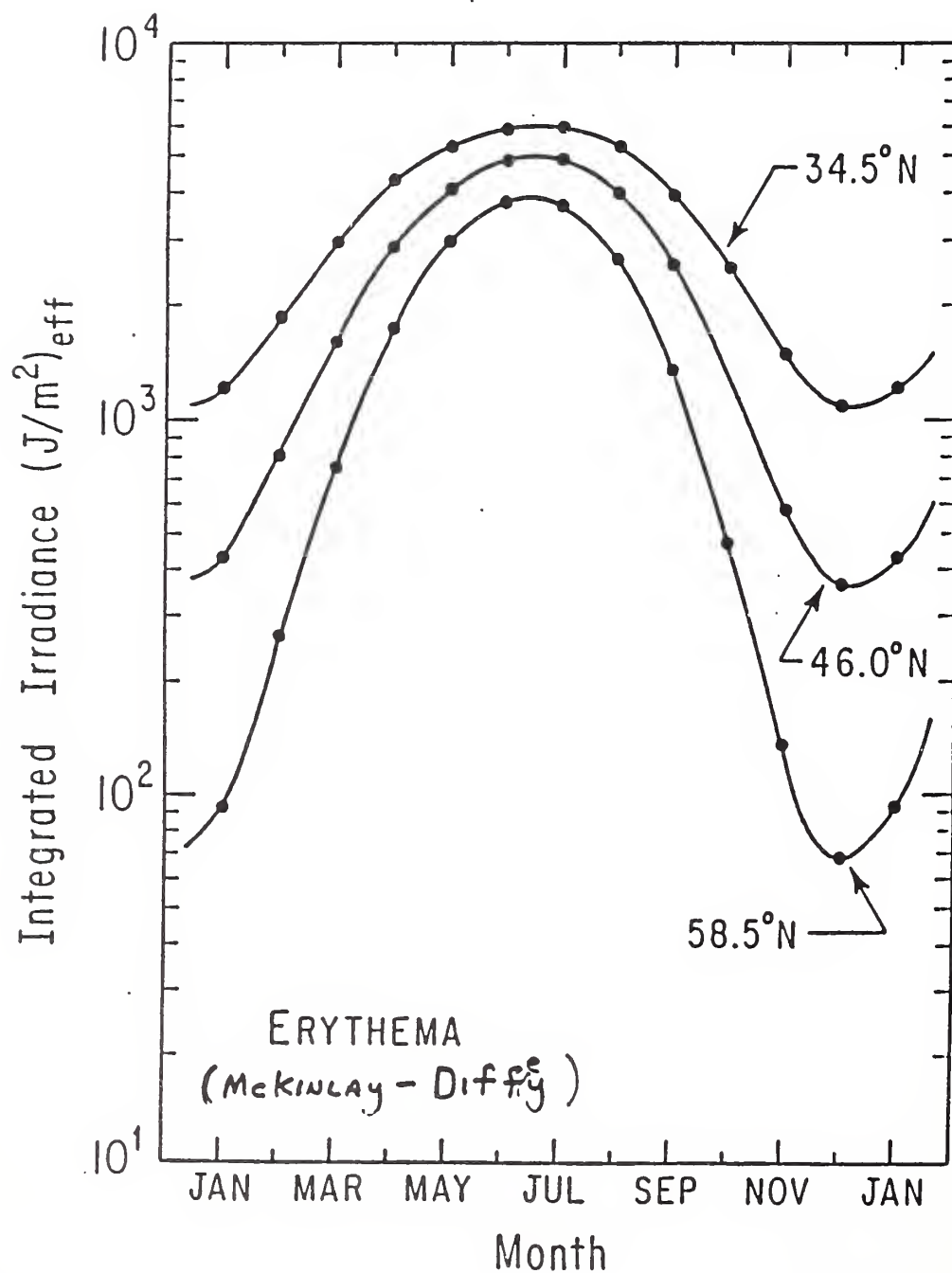
(in approximate order of increasing difficulty to model)

- * **Solar Zenith Angle**
(or elevation of sun above horizon)

- * **Stratospheric Composition**
 - Molecular Scattering
 - Absorption by Ozone
(Gases other than ozone are usually neglected)
 - Scattering by Aerosols
(very small effect, except after volcanic eruption)

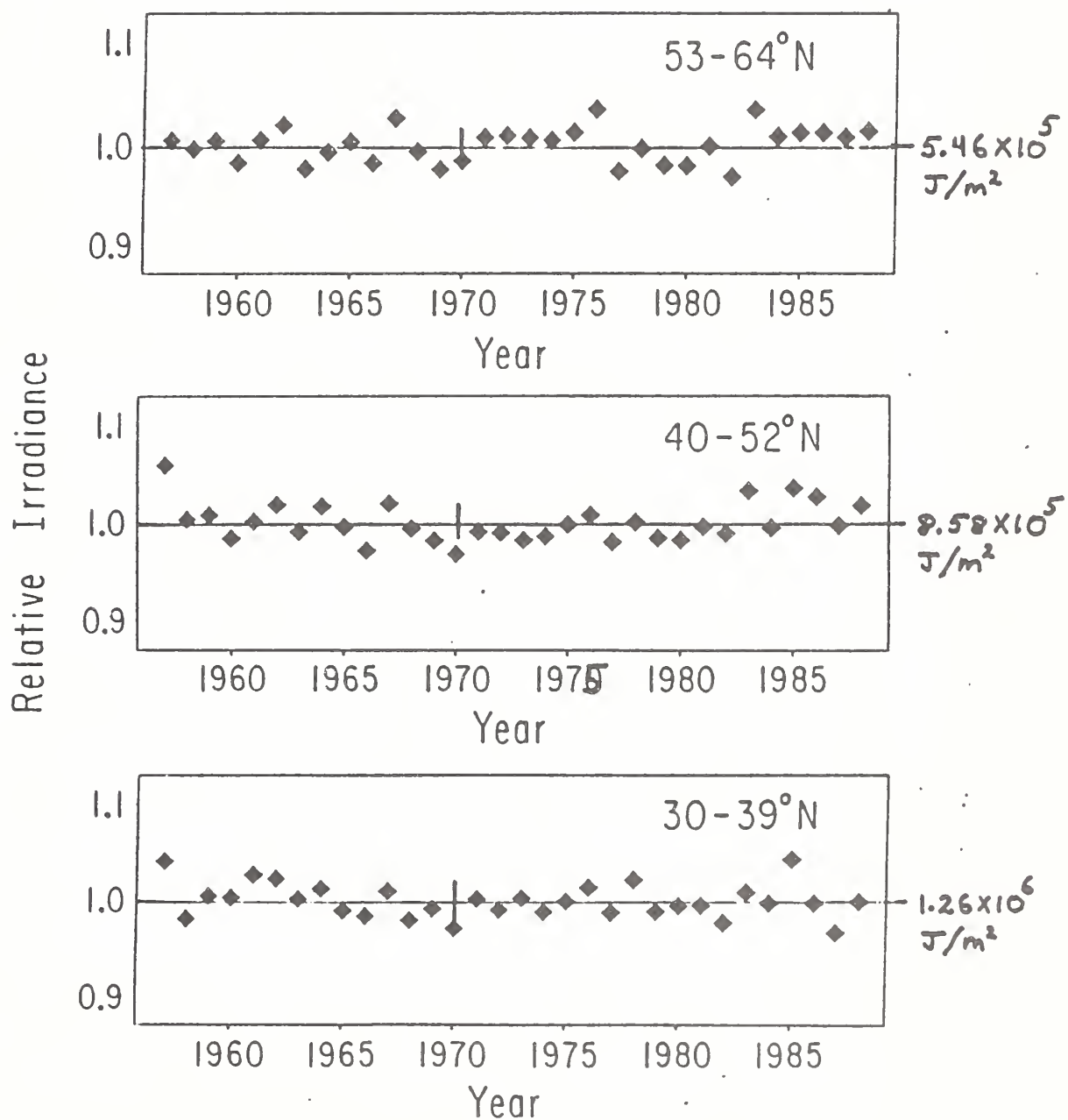
- * **Tropospheric Composition**
 - Molecular Scattering
 - Absorption by Gaseous Pollutants
(ozone, nitrogen dioxide, sulfur dioxide)
 - Scattering by Haze and Particulates
 - Scattering by Clouds

ANNUAL CYCLE IN ERYTHEMAL IRRADIANCE:
24 HOUR INTEGRALS AT NORTH AMERICAN LATITUDES

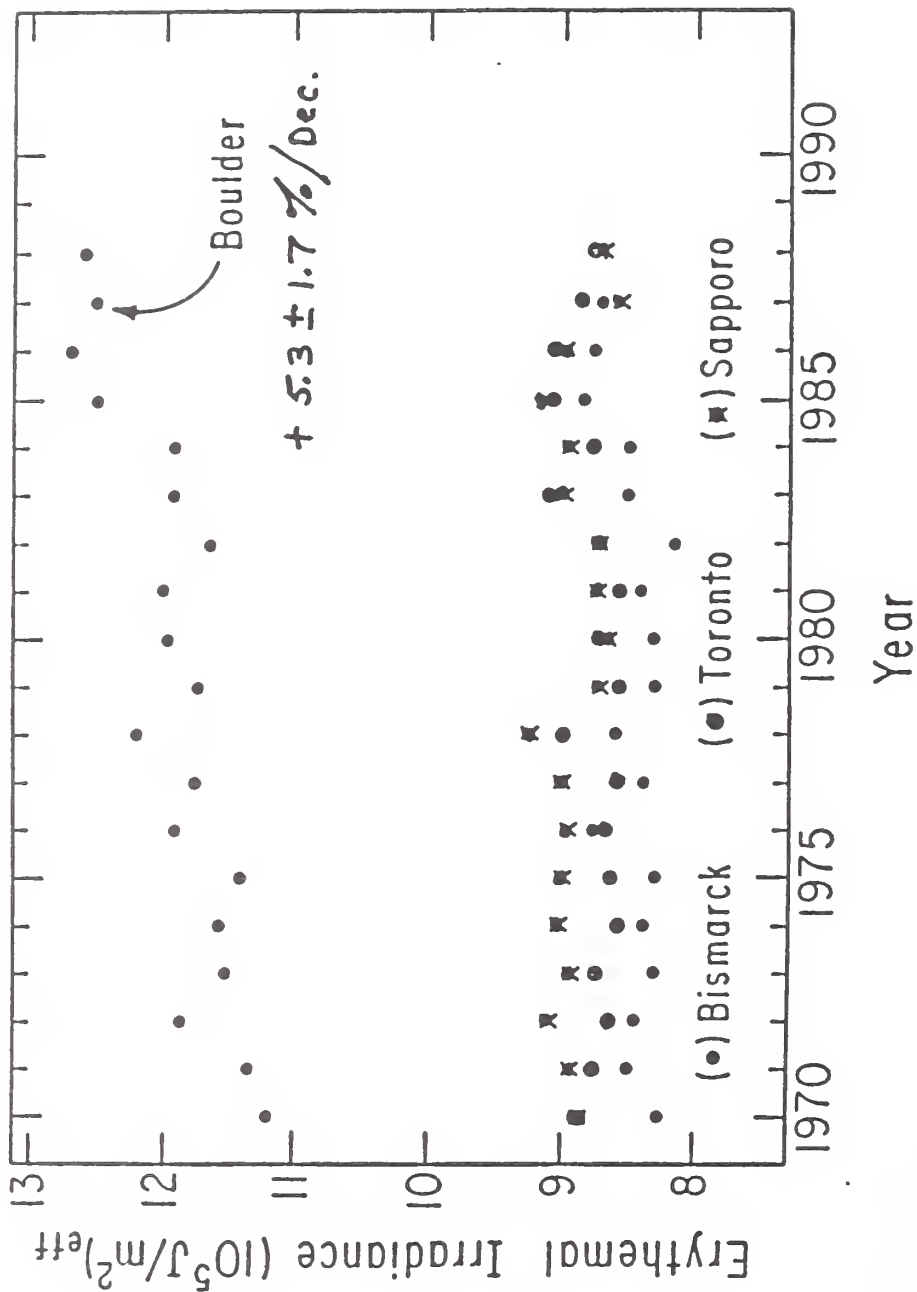


ANNUALLY INTEGRATED ERYTHEMAL IRRADIANCES BASED ON
ALL DOBSON STATIONS IN EACH LATITUDE BAND (1957-1988)

(The 32-year mean in each latitude band is
normalized to 1.0)



ANNUALLY INTEGRATED ERYTHEMAL IRRADIANCE
 BASED ON DOBSON OZONE AT FOUR SITES (1970-1988)



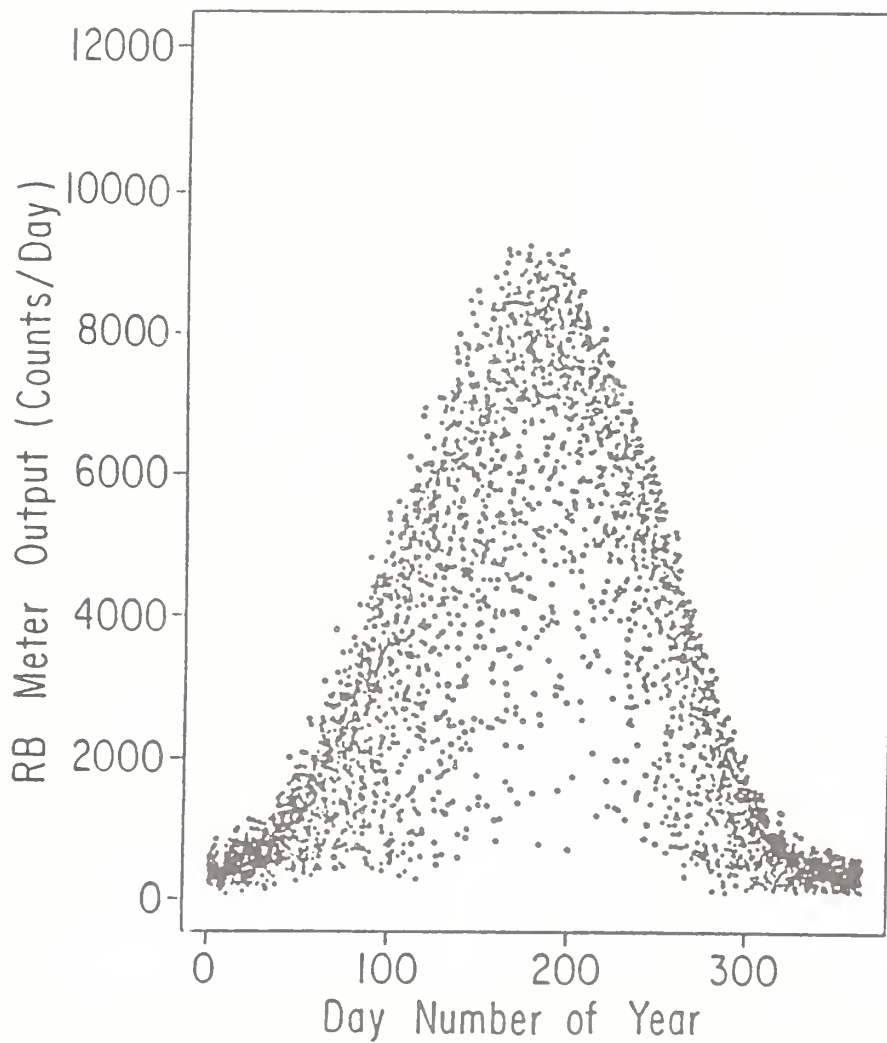
BISMARCK: $+ 2.2 \pm 2.0 \% / \text{Decade}$

TORONTO: $+ 1.7 \pm 1.5 \% / \text{Decade}$

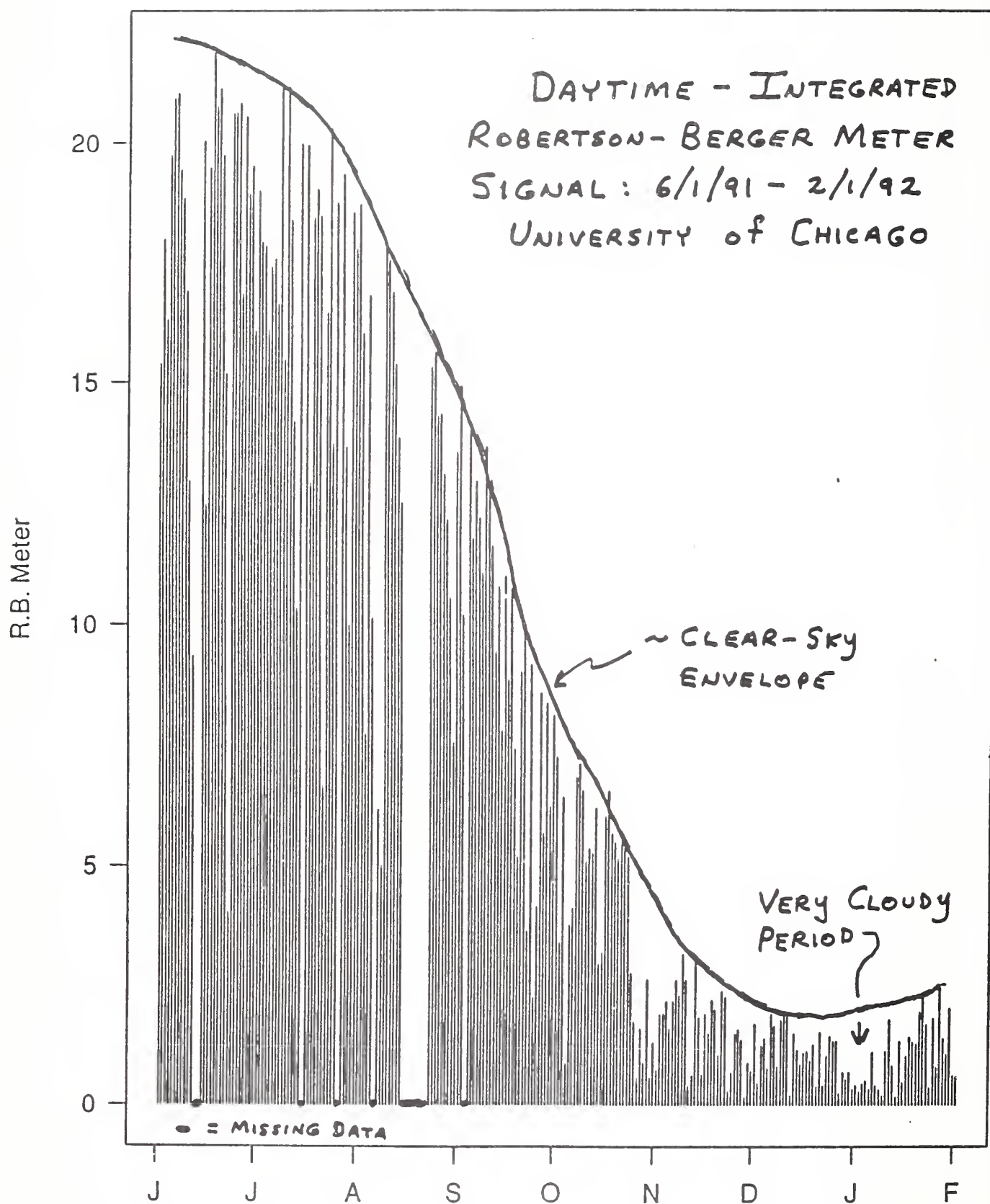
SAPPORO: $- 1.3 \pm 1.7 \% / \text{Decade}$

ELEVEN YEARS OF ULTRAVIOLET IRRADIANCE MEASUREMENTS:
24-HOUR INTEGRALS AT BISMARCK, ND

INSTRUMENT = ROBERTSON-BERGER METER



57th & Ellis



Month

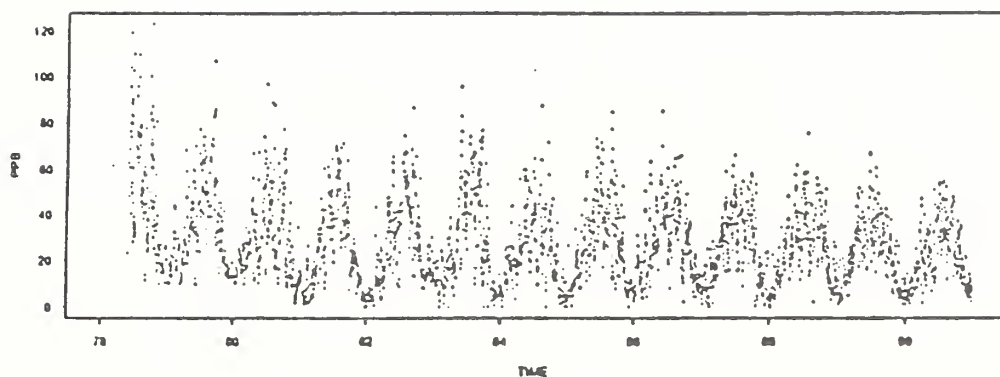
June 1 1991 to February 1 1992

C-154

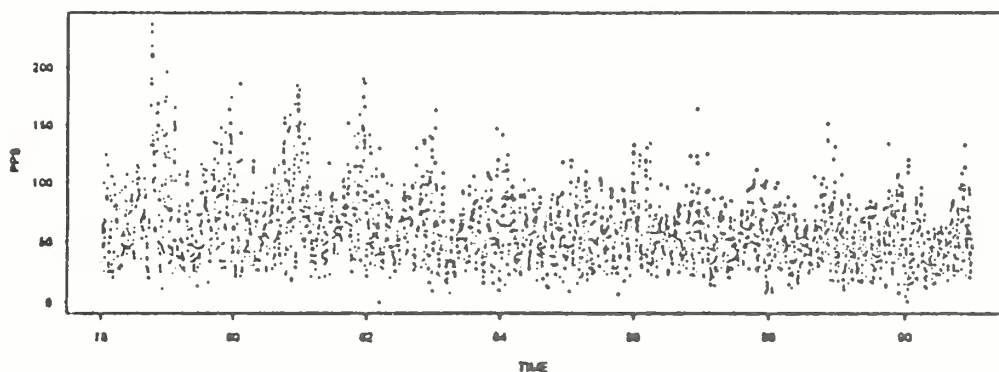
TIME SERIES OF DAYTIME-AVERAGED AIR POLLUTION DATA
FROM LOS ANGELES-BURBANK SITE (1978-1990)

(The Vertical Scale Gives Mixing Ratios In PPBV)

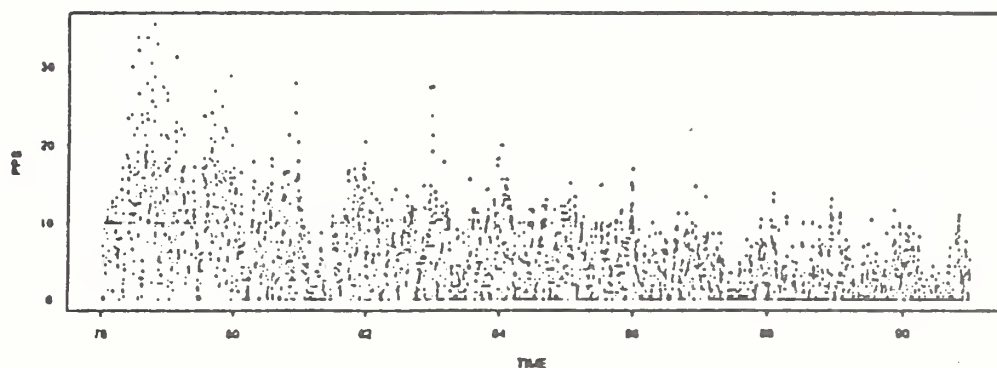
OZONE



NITROGEN DIOXIDE



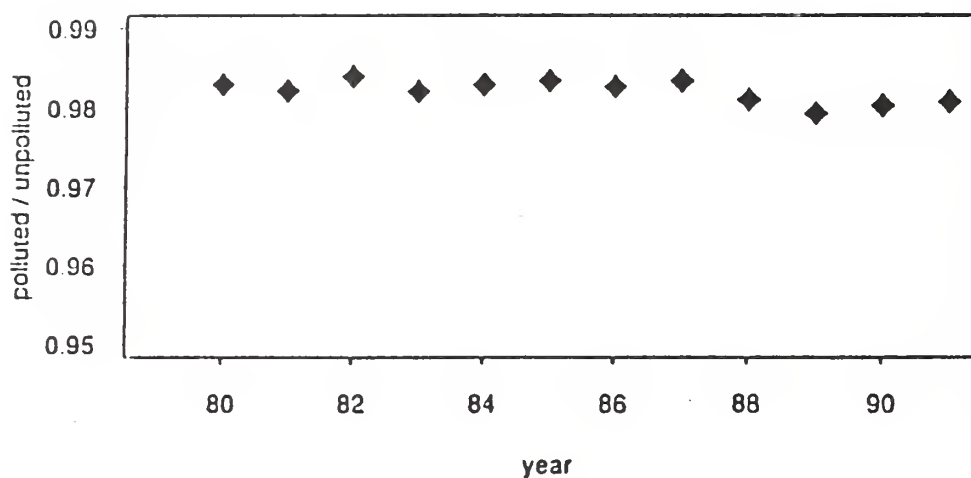
SULPHUR DIOXIDE



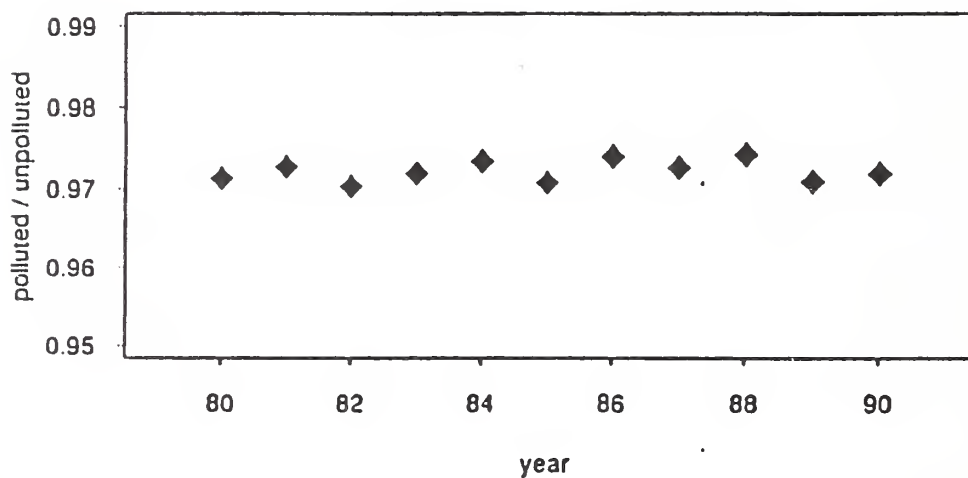
MONTHLY MEAN ATTENUATION OF ERYTHEMAL IRRADIANCE
PROVIDED BY O_3 , NO_2 , AND SO_2 IN THE BOUNDARY LAYER

(San Francisco - Pittsburg Monitoring Station)

January

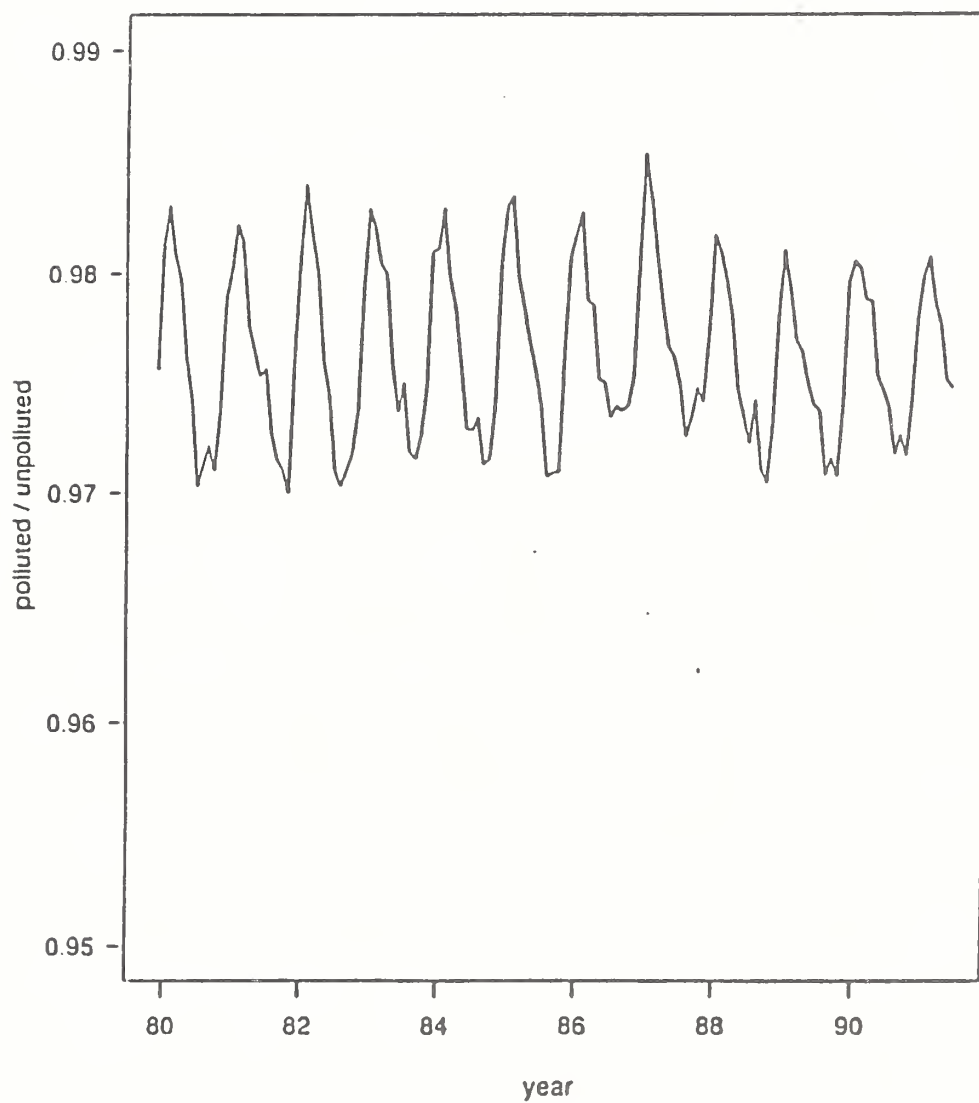


July



MONTHLY MEAN ATTENUATION OF ERYTHEMAL IRRADIANCE
PROVIDED BY O_3 , NO_2 , AND SO_2 IN THE BOUNDARY LAYER

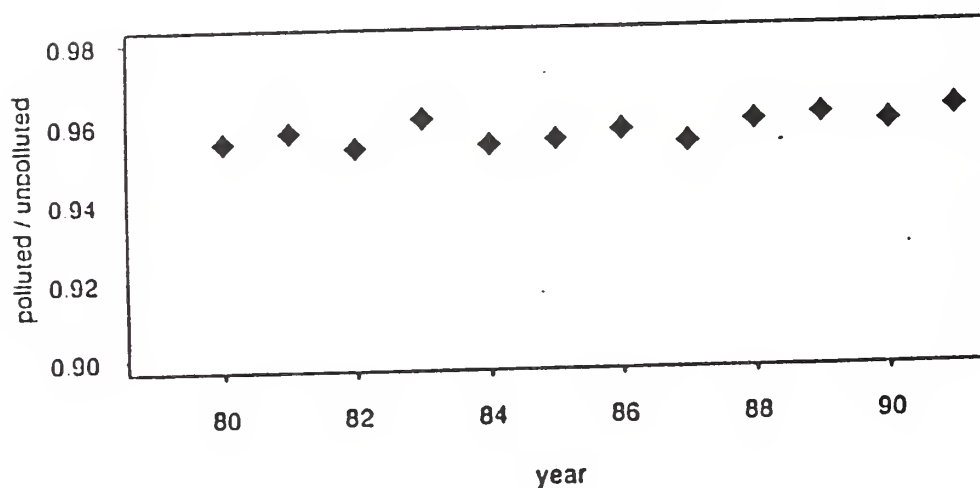
(San Francisco - Pittsburg Monitoring Station)



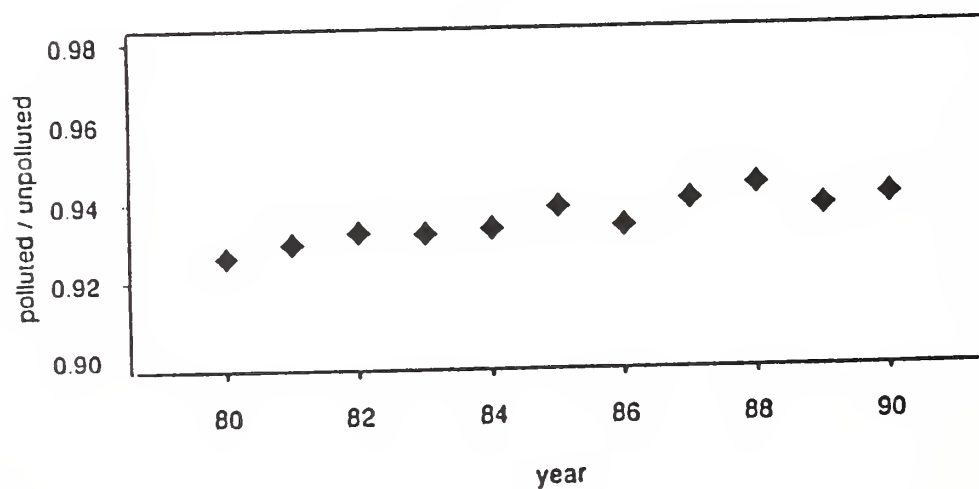
MONTHLY MEAN ATTENUATION OF ERYTHEMAL IRRADIANCE
PROVIDED BY O_3 , NO_2 , AND SO_2 IN THE BOUNDARY LAYER

(Los Angeles - Burbank Monitoring Station)

January

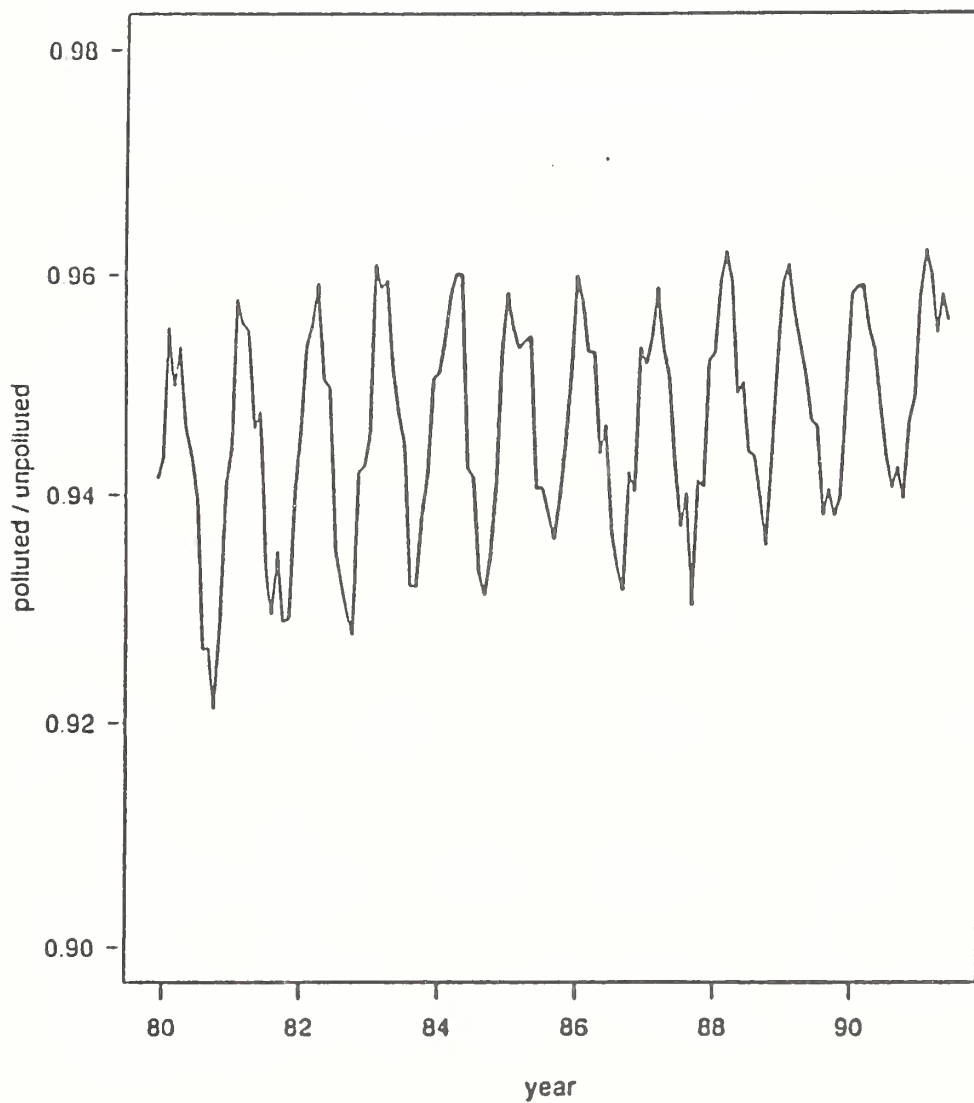


July



MONTHLY MEAN ATTENUATION OF ERYTHEMAL IRRADIANCE
PROVIDED BY O_3 , NO_2 , AND SO_2 IN THE BOUNDARY LAYER

(Los Angeles - Burbank Monitoring Station)



An Objective of Ground-Based UV Spectral Irradiance Measurements

- * To determine how clouds, haze, and gaseous pollutants alter the transmission of the troposphere

- Determine the magnitude and variability in the ratio:

$$\left(\frac{\text{True UV Spectral Irradiance}}{\text{UV Spectral Irradiance for a Clear, Unpolluted Atmosphere}} \right)$$

- This ratio will depend on meteorological conditions, season, and location
- * With the above focus, surface UV irradiance measurements are not redundant with column ozone measurements made from satellites and the Dobson network

INFLUENCE OF GASEOUS AIR
POLLUTANTS ON TRENDS IN ERYTHEMAL
IRRADIANCE : LOS ANGELES 1980-90

MONTH	"CLEAN" TREND* (%/Dec.)	"POLLUTED" TREND** (%/Dec.)	POLLUTED CLEAN
MAY	5.0	5.2	1.04
JUNE	3.2	3.9	1.22
JULY	2.2	3.3	1.50
AUGUST	2.8	3.4	1.21
SEPT.	2.5	3.4	1.36

* BASED ON TOMS OZONE ONLY

** MEAN TRENDS COMPUTED FOR FOUR
 POLLUTION MONITORING SITES.

Comparison of Measurements from R-B and Dobson Meters

**Dr. John Frederick
University of Chicago**

Comparison of Variability in UV Radiation "Data" From Two Independent Sources

Elizabeth C. Weatherhead & John E. Frederick

Data Set #1 - UV radiation measurements from Robertson-Berger (RB) meters located at Bismarck, ND and Tallahassee, FL (1974-1985)

Data Set #2 - Simulated RB signals based on a radiative transfer code using Dobson column ozone measurements from Bismarck and Tallahassee as inputs. The computed spectral irradiance is weighted by the RB meter response function.

* Both data sets are expressed as monthly mean, daytime integrated radiation levels (in relative units).

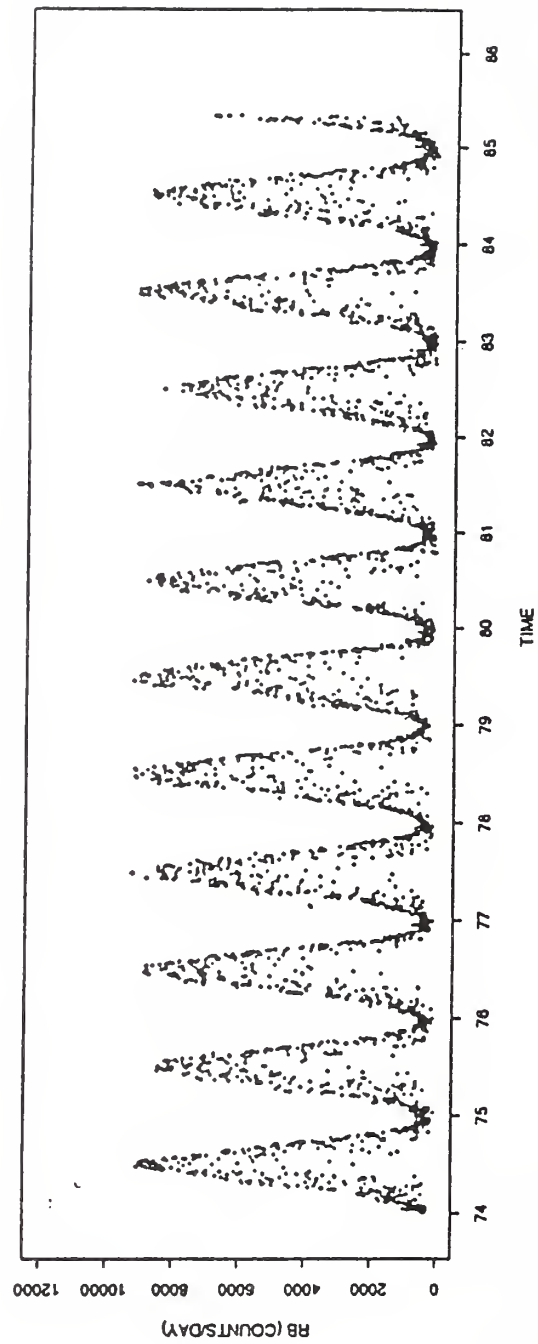
* Questions:

(1) What is the correlation between the two data sets? How much of the variability in the RB signals can be explained by variability in ozone alone ?

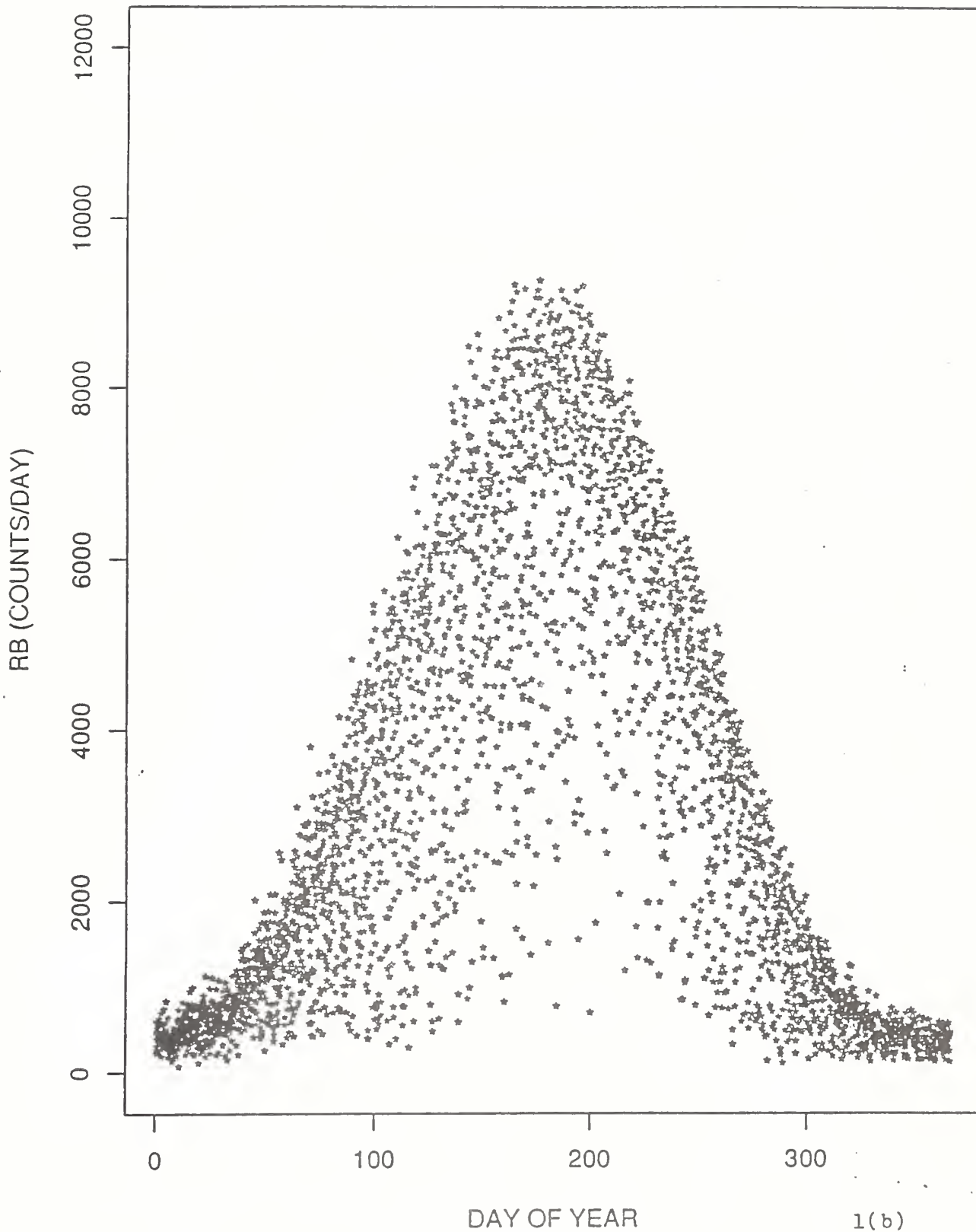
(2) How do trends in the two data sets compare to each other?

DAILY INTEGRATED ROBERTSON-BERGER METER READINGS FOR
BISMARCK, ND (LATITUDE 46.8 N), 1974-EARLY 1985

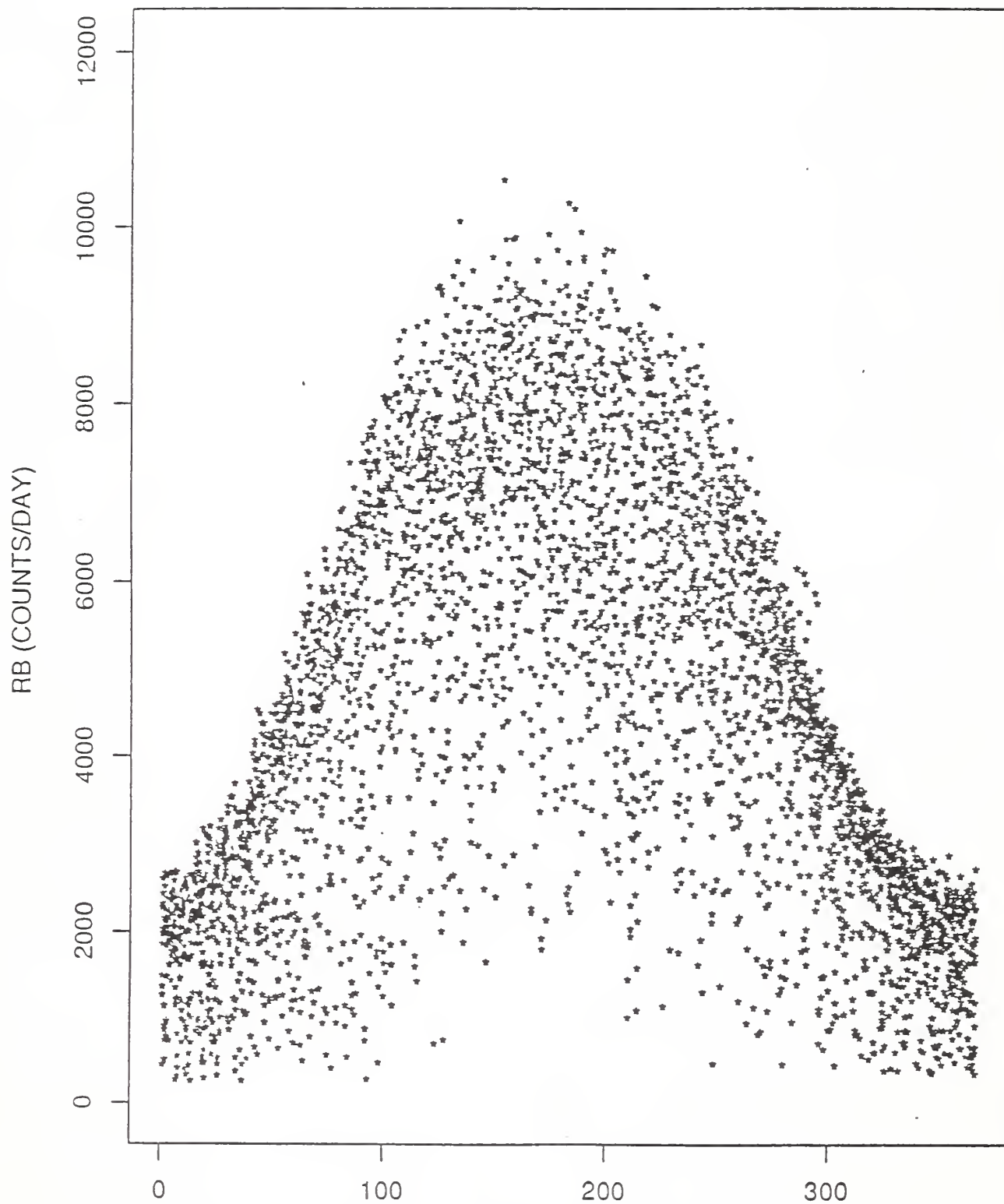
BISMARCK



DAILY INTEGRATED ROBERTSON-BERGER METER READINGS FOR
BISMARCK, ND (LATITUDE 46.8 N), 1974-EARLY 1985,
PLOTTED VERSUS DAY NUMBER OF THE YEAR



DAILY INTEGRATED ROBERTSON-BERGER METER READINGS FOR
TALLAHASSEE, FL (LATITUDE 30.4 N), 1974-EARLY 1985,
PLOTTED VERSUS DAY NUMBER OF THE YEAR

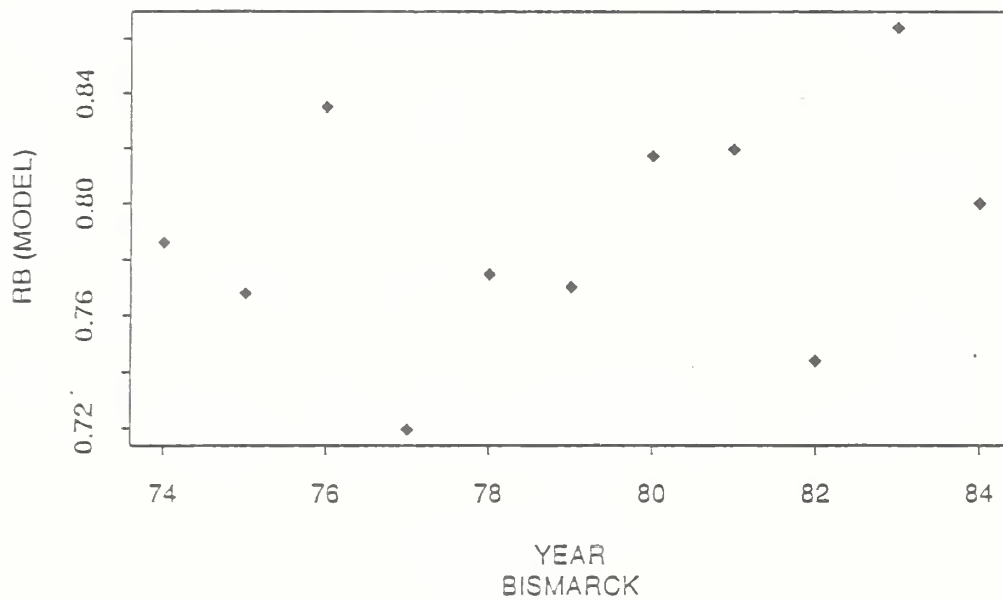


DAY OF YEAR

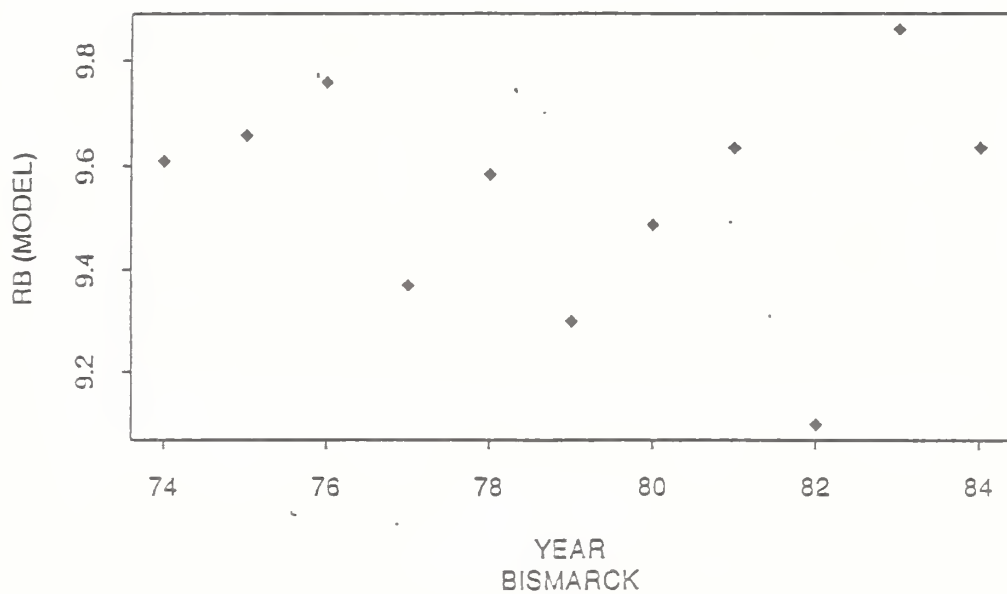
2(b)

MODELLED ROBERTSON-BERGER METER READINGS:
MONTHLY MEAN, DAYTIME INTEGRATED SIGNALS BASED ON
DOBSON COLUMN OZONE FOR BISMARCK, ND

JANUARY

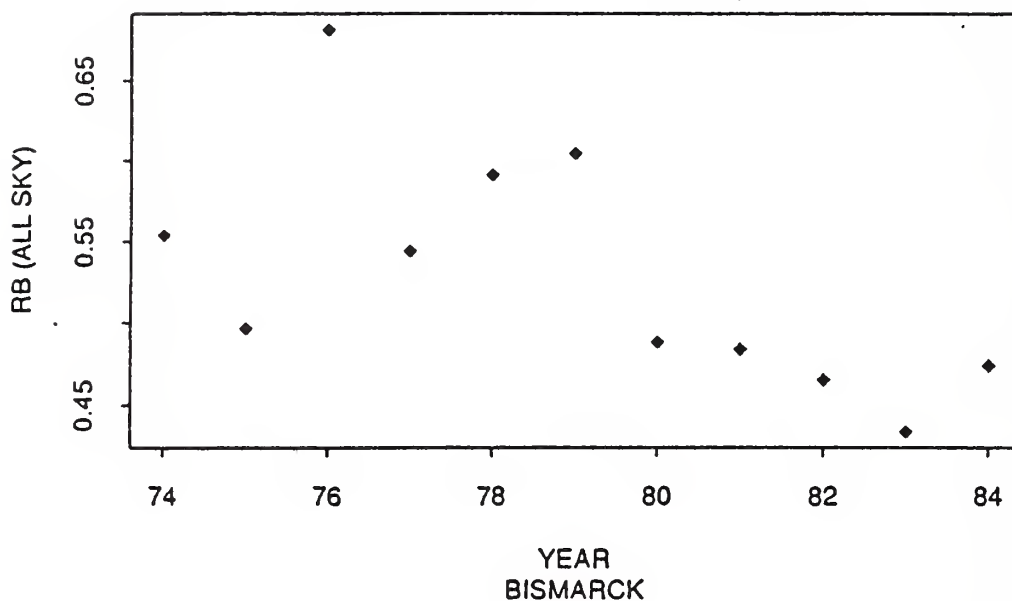


JULY

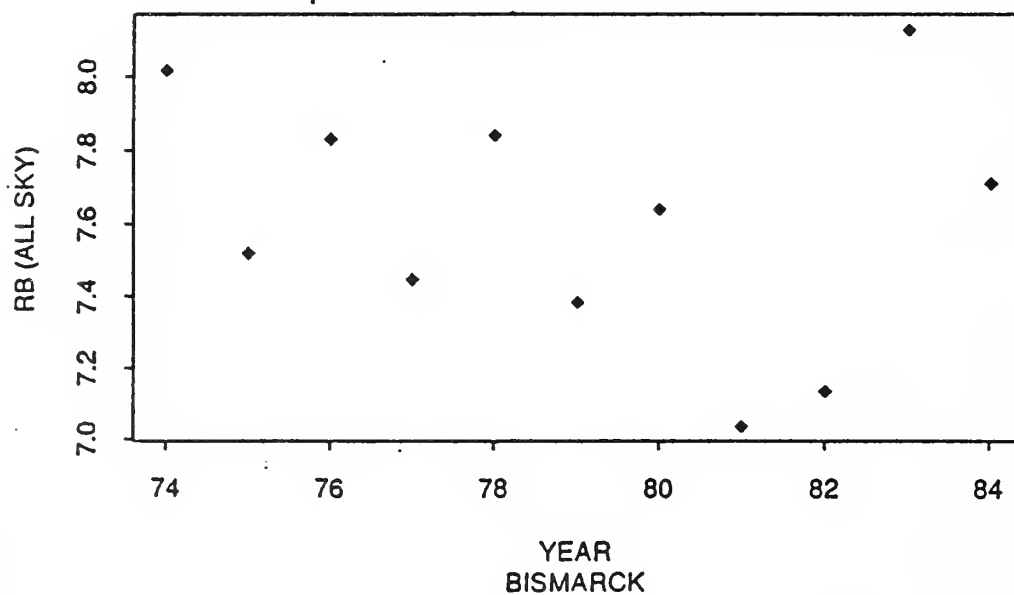


ROBERTSON-BERGER METER READINGS FOR BISMARCK, ND:
MONTHLY MEAN, DAYTIME INTEGRATED SIGNALS
INCLUDING THE INFLUENCE OF CLOUDINESS

JANUARY

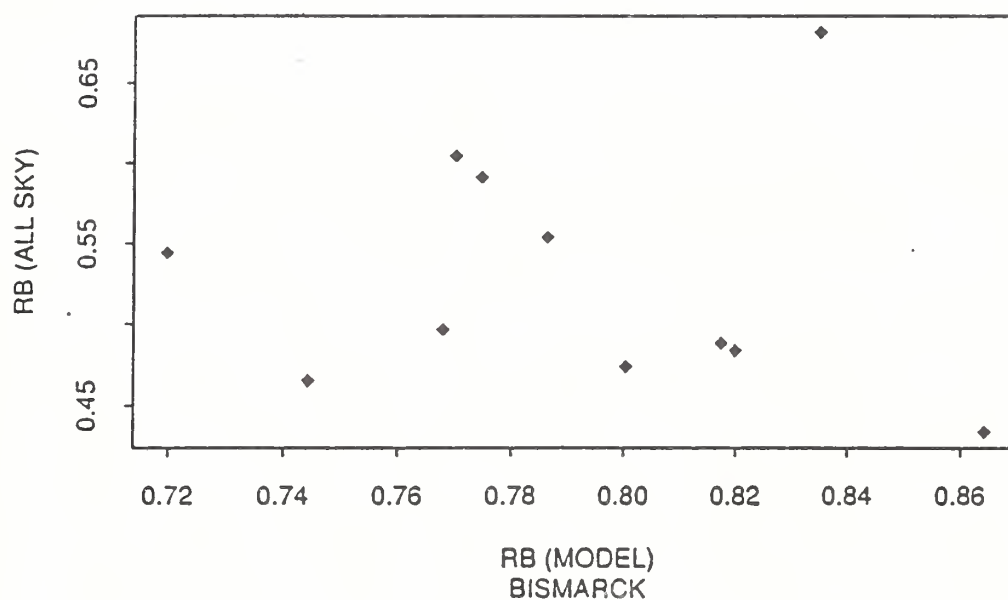


JULY

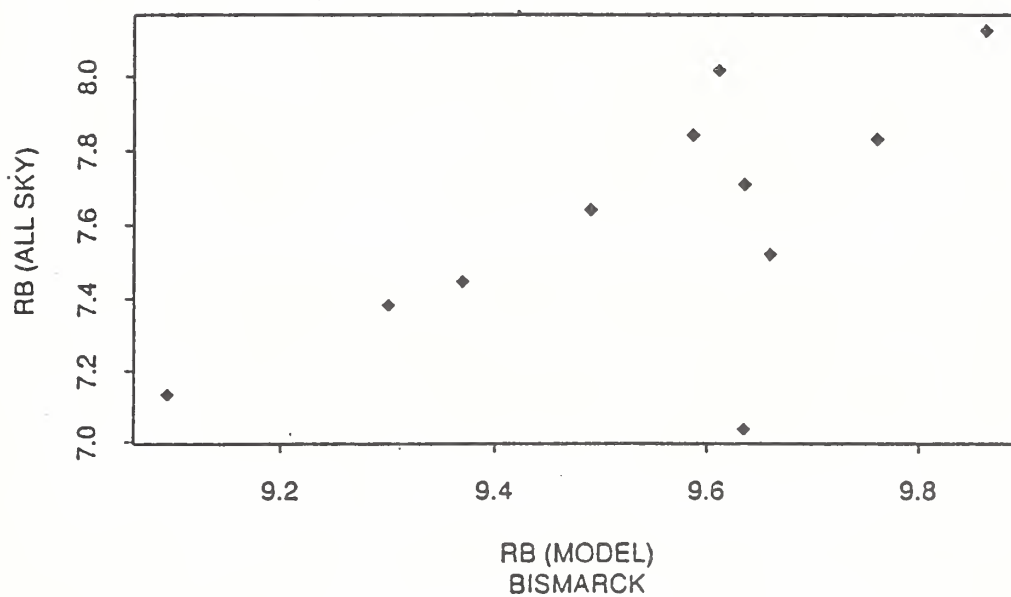


RELATIONSHIP BETWEEN MEASURED RB SIGNALS FOR
BISMARCK, ND AND CALCULATIONS BASED ON
MONTHLY MEAN DOBSON OZONE

JANUARY



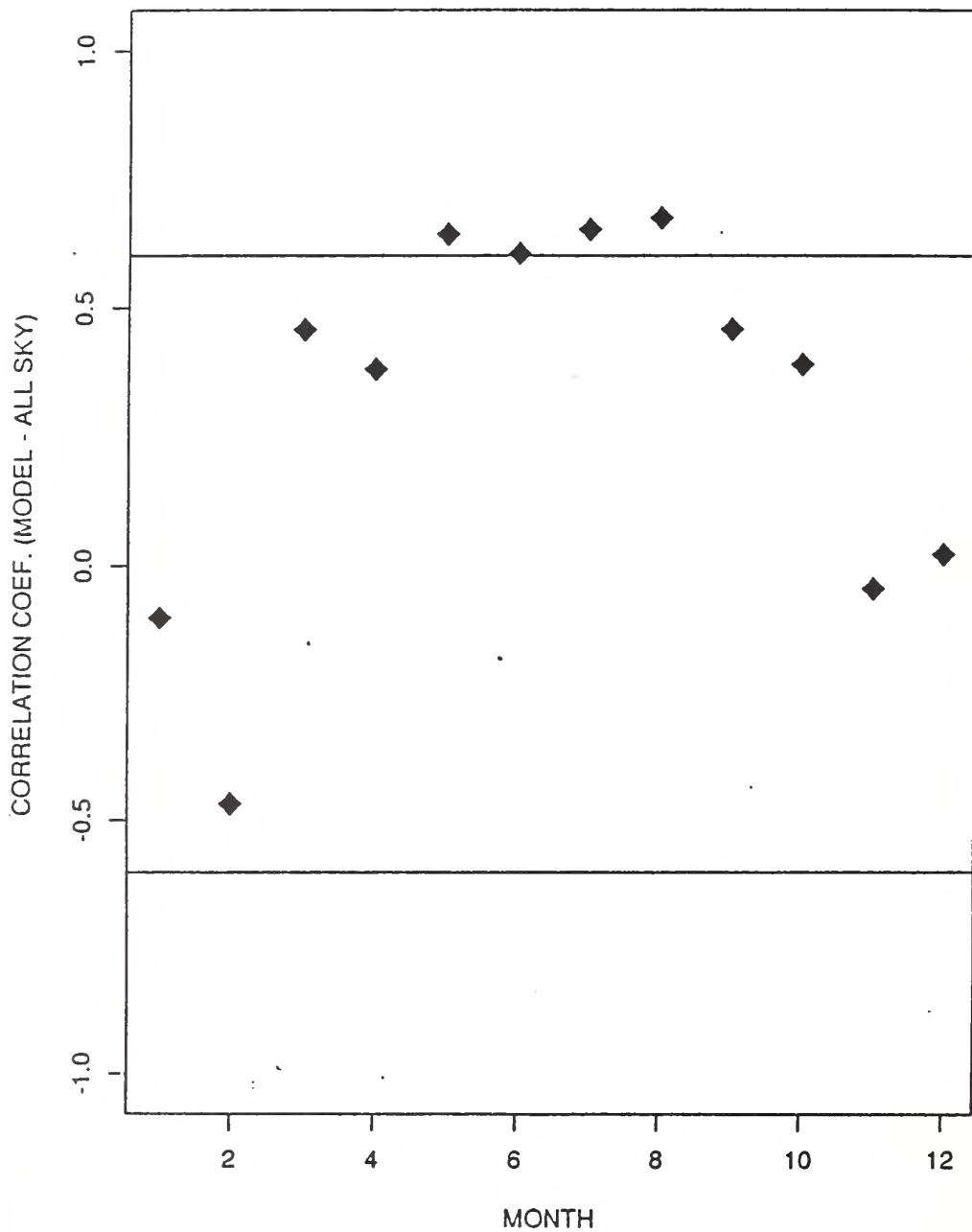
JULY



THE CORRELATION BETWEEN MEASURED AND MODELLED RB
SIGNALS FOR BISMARCK BY MONTH OF THE YEAR

(Horizontal lines indicate values required for 95%
confidence that the result does not arise by chance.)

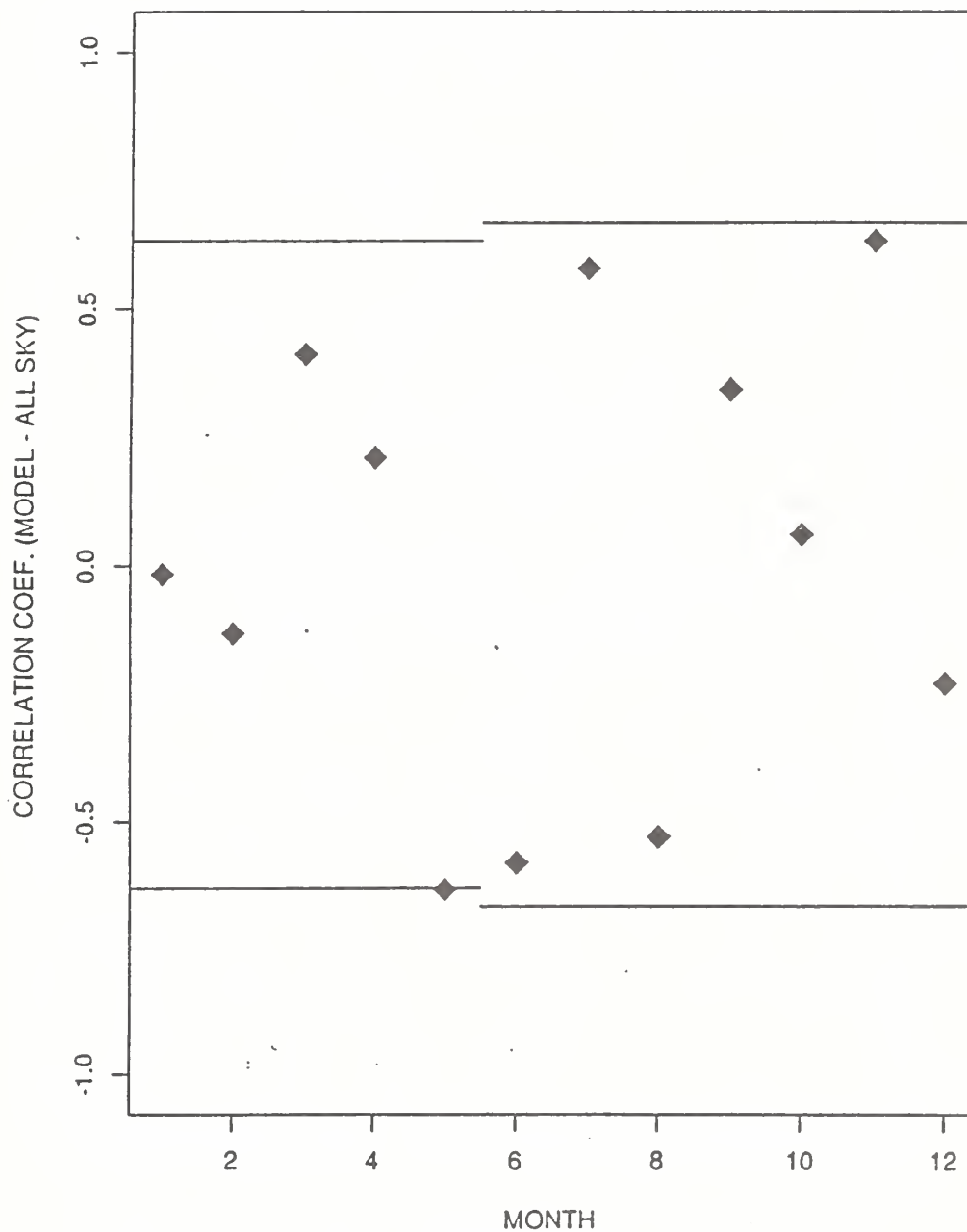
BISMARCK



THE CORRELATION BETWEEN MEASURED AND MODELLED RB
SIGNALS FOR TALLAHASSEE BY MONTH OF THE YEAR

(Horizontal lines indicate values required for 95%
confidence that the result does not arise by chance.)

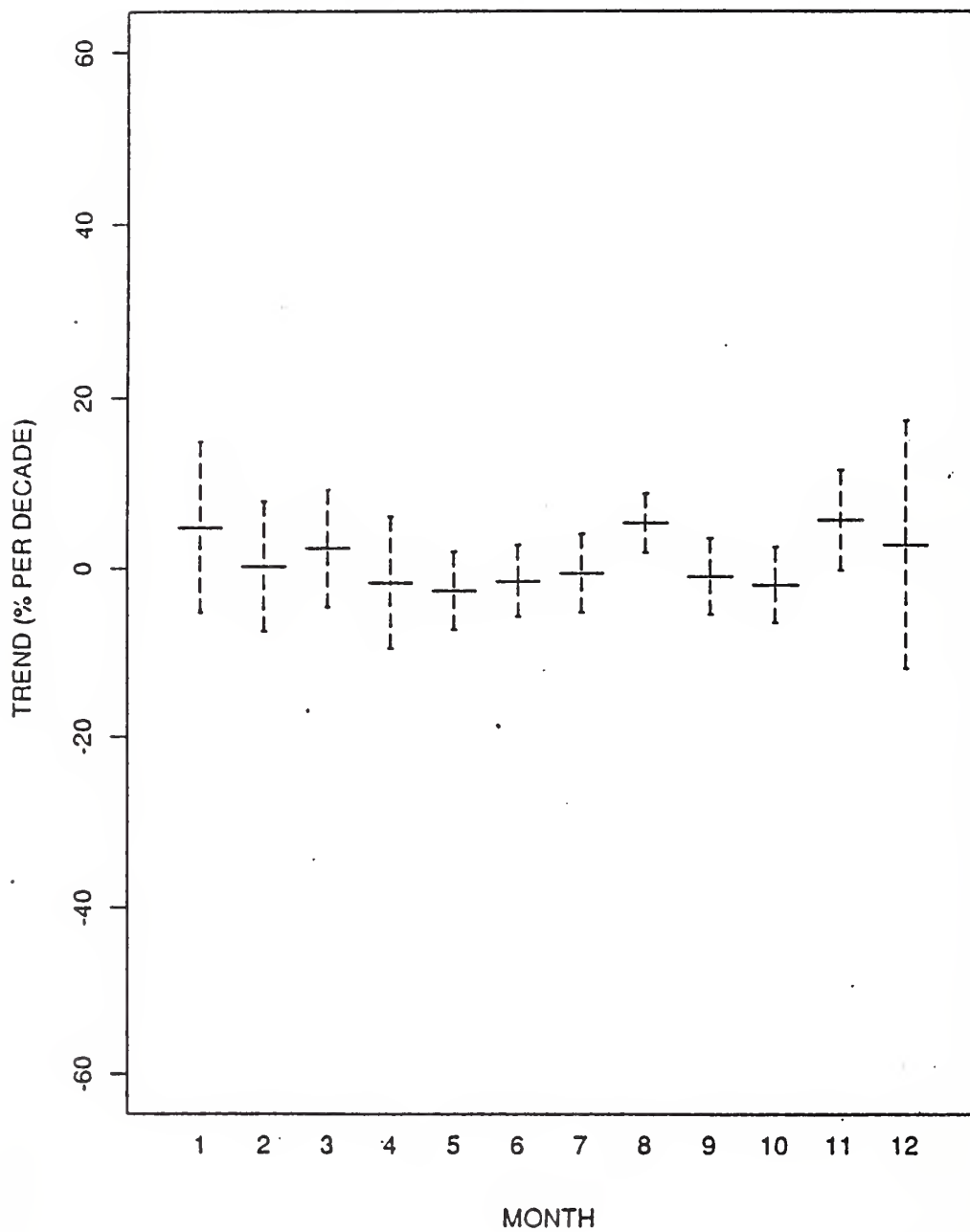
TALLAHASSEE



TRENDS BY MONTH OF THE YEAR AT BISMARCK:
MODELLED RB SIGNALS BASED ON DOBSON OZONE

(Vertical dashed lines denote 95% confidence limits)

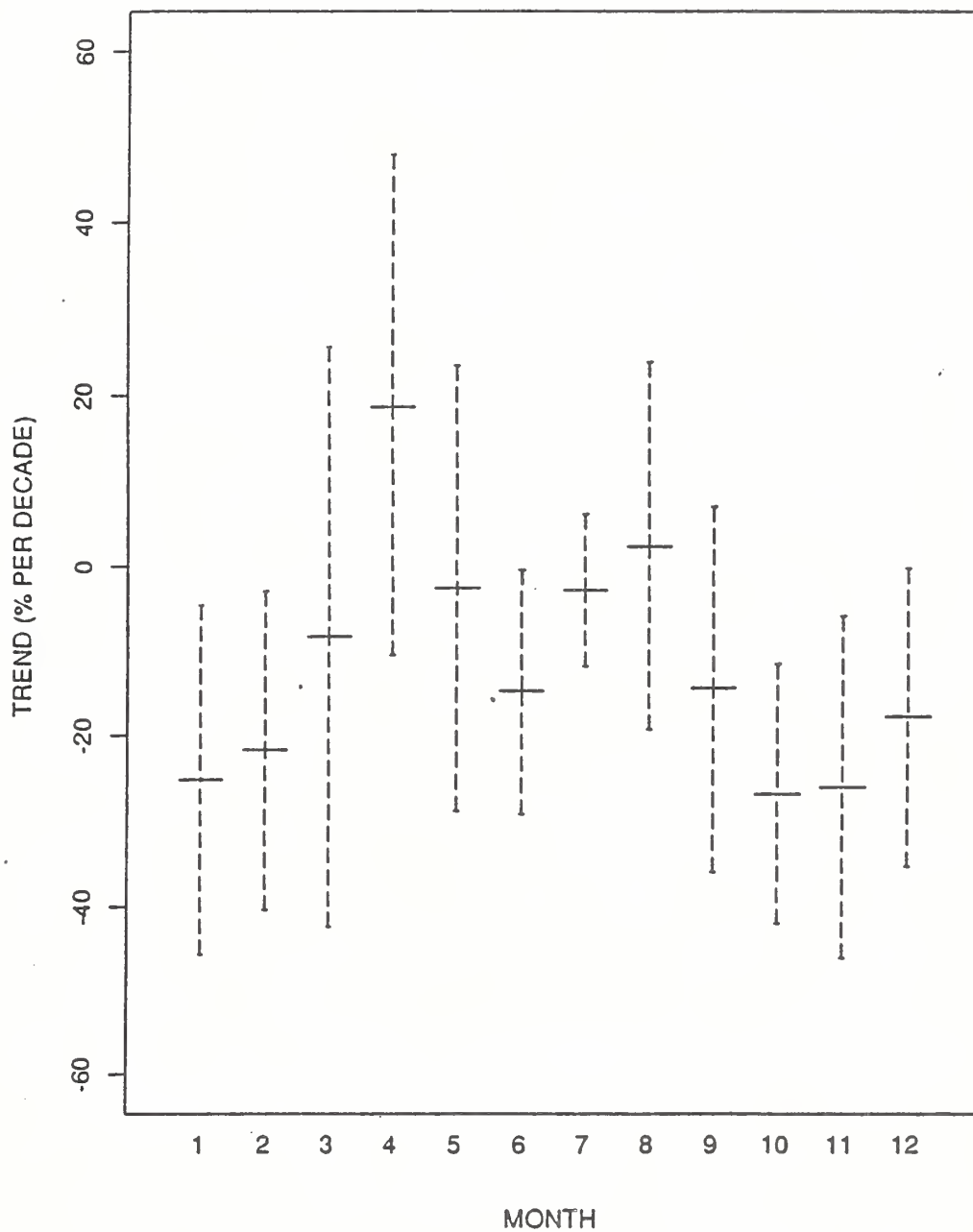
MODEL - BISMARCK



TRENDS BY MONTH OF THE YEAR AT BISMARCK:
MEASURED RB SIGNALS INCLUDING CLOUDINESS

(Vertical dashed lines denote 95% confidence limits)

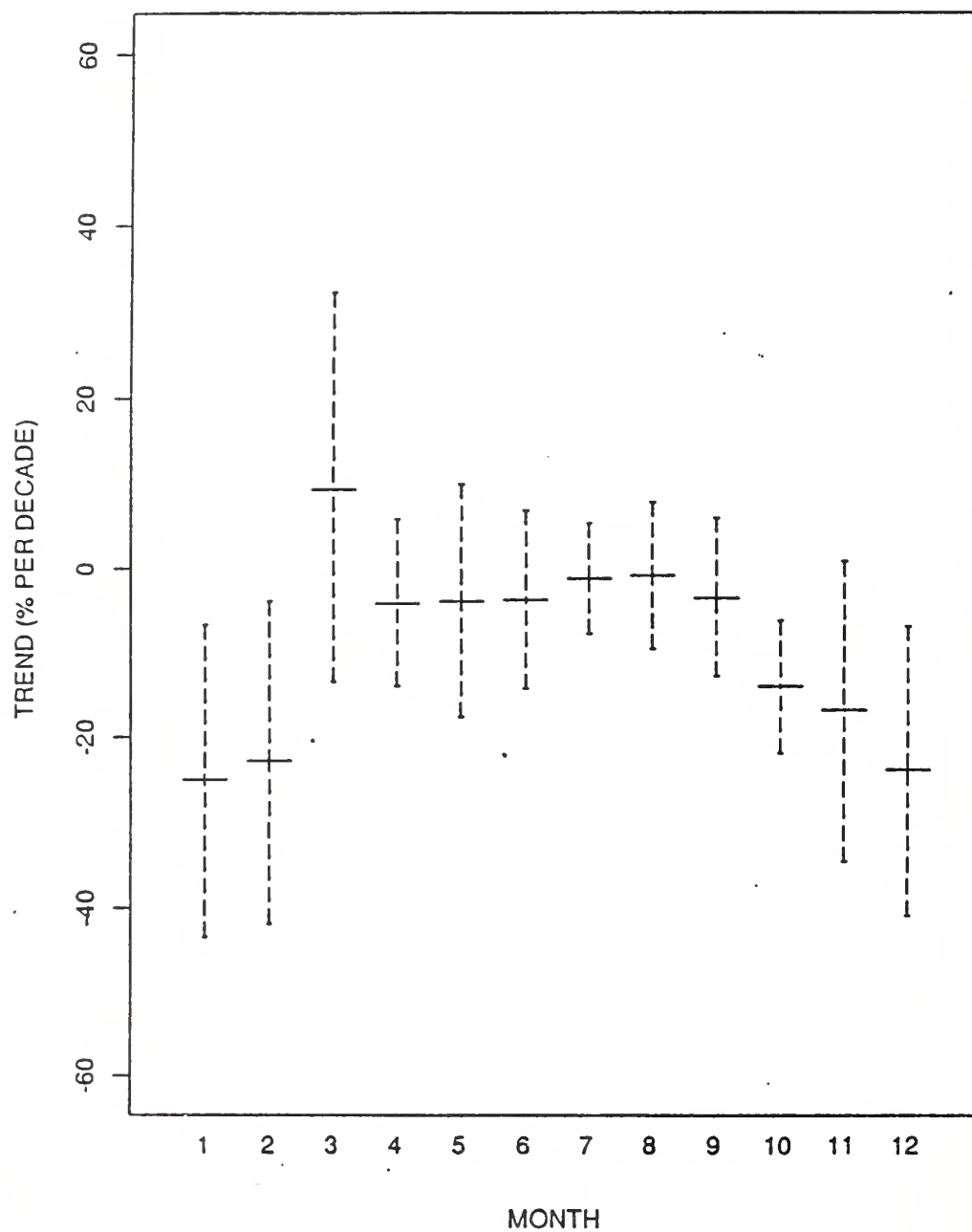
ALL SKY - BISMARCK



TRENDS BY MONTH OF THE YEAR AT BISMARCK:
MEASURED RB SIGNALS FOR APPARENT CLEAR CONDITIONS

(Vertical dashed lines denote 95% confidence limits)

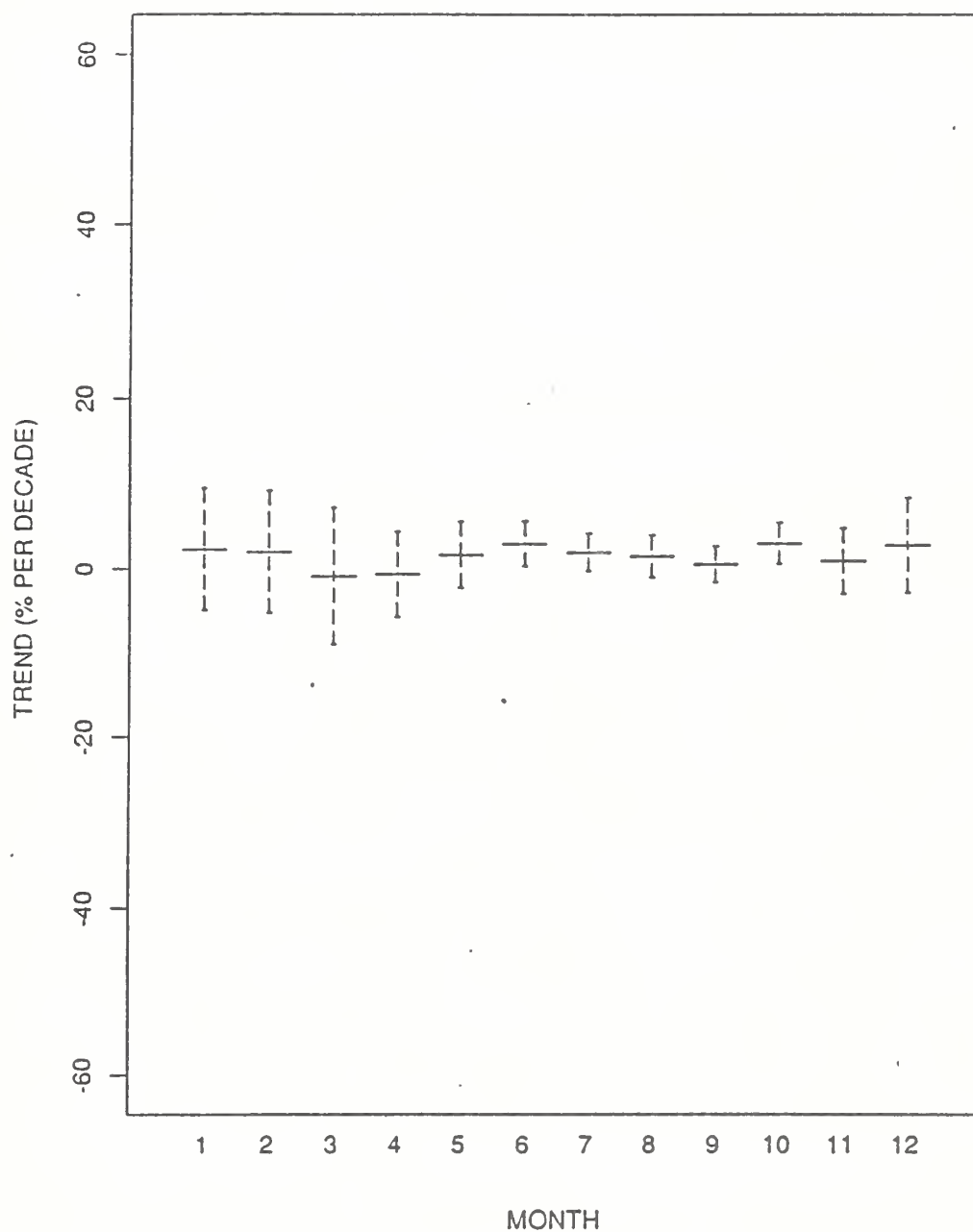
CLEAR 123 - BISMARCK



TRENDS BY MONTH OF THE YEAR AT TALLHASSEE
MODELLED RB SIGNALS BASED ON DOBSON OZONE

(Vertical dashed lines denote 95% confidence limits)

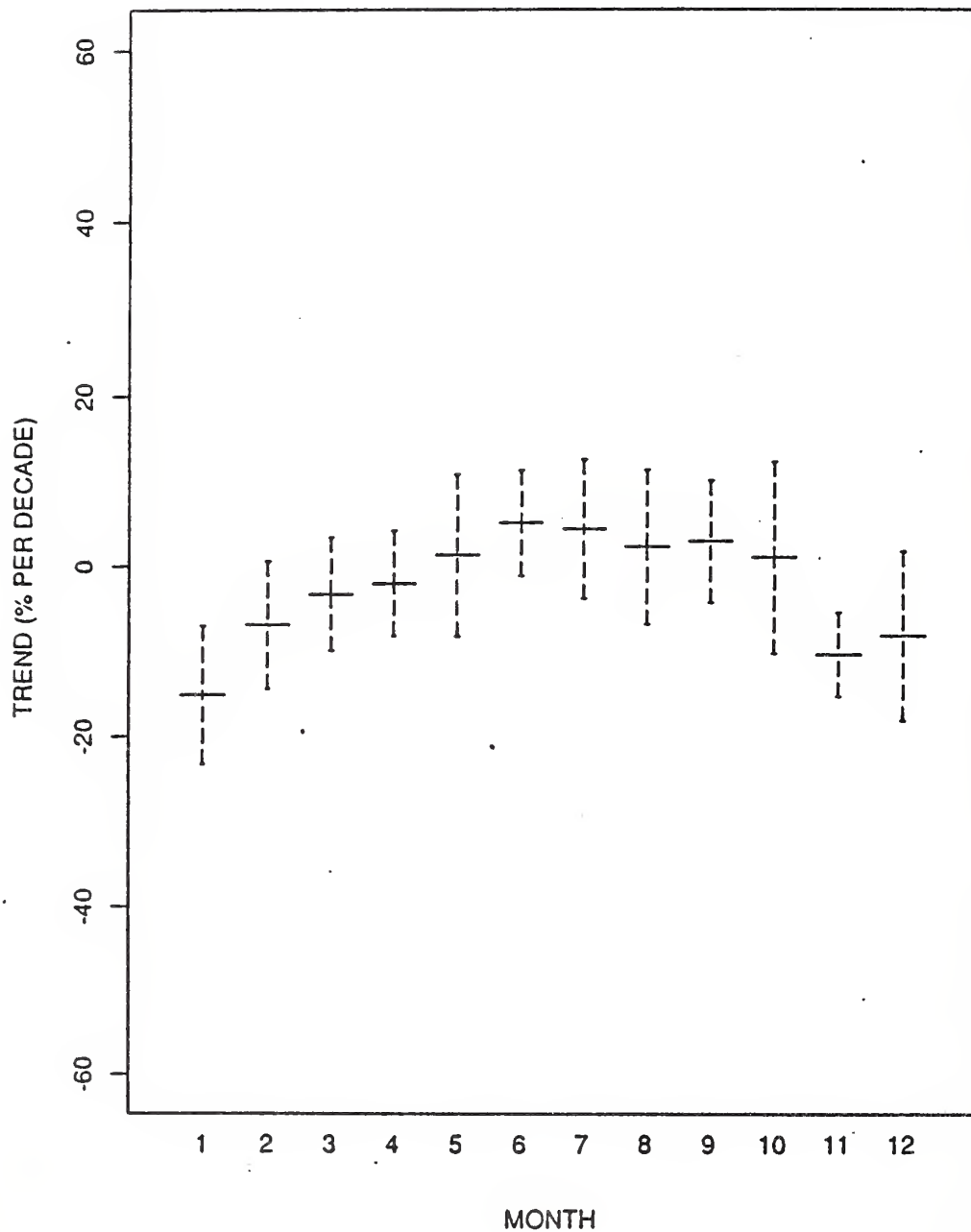
MODEL - TALLAHASSEE



TRENDS BY MONTH OF THE YEAR AT TALLHASSEE:
MEASURED RB SIGNALS FOR APPARENT CLEAR CONDITIONS

(Vertical dashed lines denote 95% confidence limits)

CLEAR 123 - TALLAHASSEE



Conclusions

- * Year-to-year variations in RB readings are not explained solely by variations in ozone. Cloudiness must make a major contribution to the year-to-year variability.
- * Trends in the RB data sets for clear skies are consistent with trends computed using Dobson ozone for months when the absolute radiation levels are greatest.
- * Negative trends (in % of the monthly mean signal per decade) exist in the RB data sets for the months of low signal levels. These trends differ in sign from predictions based on Dobson ozone data.
- * Based on this analysis alone, it is not possible to determine the origin of the discrepancy between trends computed for months of low signal levels.

U.S. R-B Meter Network and Instrument Characterization

**Dr. John DeLuisi
National Oceanic and Atmospheric Administration**

**An Examination of the Spectral Response Characteristics
of Seven Robertson-Berger Meters After Long-Term Field Use**

by

John DeLuisi, James Wendell

National Oceanic and Atmospheric Administration

Boulder, CO 80303

U.S.A.

Fred Kreiner

Cooperative Institute for Research in Environmental Sciences

University of Colorado

Boulder, CO 80303

U.S.A.

In Press. (Journal of Photochem. & Photobiol.)

Abstract

Seven Robertson-Berger ultraviolet meters located at National Weather Service stations were subjected to a laboratory analysis of their spectral response functions. The analysis revealed that all spectral response functions were similar in shape in the important erythemalogenic wavelength region of 300-330 nm; however, a few of the spectral response function wavelength positions varied slightly. The average of the spectral response functions was compared to Robertson-Berger meter spectral response functions published in the 1970s, and they agreed within experimental error. This finding suggests that the shapes of the spectral response functions did not change or changed only slightly during the meters' long-term exposure in the network. To provide insight into the problems associated with measurement of ultraviolet radiation in the UV-B region (295-320 nm), examples of errors caused by wavelength band shifts and calibration procedures are given.

1. Introduction

Concern over the possible depletion of atmospheric ozone by high-flying supersonic aircraft emissions (Climatic Impact Assessment Program, U.S. Department of Transportation), and an associated predicted increase in biologically damaging ultraviolet (UV) radiation inspired the construction,

installation, and operation of a network of instruments (Robertson-Berger meters, hereafter referred to as R-B meters) to continuously measure UV radiation. The design of these instruments, consisting of a sensor unit and a recording unit, was essentially that of Robertson (1972). They were placed at different latitudes and longitudes in the United States in the early 1970s so that seasonal and regional variations could be studied and related to human skin cancer. Table 1 lists the present network sites. A few were placed outside the mainland United States.

These instruments sense a broad wavelength band that is meant to simulate the sunburning action spectrum of Caucasian skin, similar to action spectrum of Coblentz and Stair [1934]. However, the design of the instrument did not accurately meet this requirement Berger (1976), and for this reason it had been criticized (e.g., NAS 1979). It does possess a spectral response function (SRF) that is similar in shape to the human skin erythemal action spectrum at wavelengths greater than 300 nm, but the solar UV band it senses is shifted toward longer wavelengths several nanometers beyond the human skin erythemal action spectrum. The bandwidth of solar UV radiation actually sensed by the instrument is ≈ 13 nm at half-power and at a solar zenith angle of 30° the band's maximum power wavelength is ≈ 311 nm; it should be ≈ 307 nm if the instrument were to simulate the response to the human skin action spectrum (DeLuisi and Harris, 1983).

Nevertheless, the band extends sufficiently far into the wavelength region of the Huggins ozone absorption band such that the meter is sensitive to atmospheric ozone absorption, although, not as sensitive as it would be if it accurately simulated that of the human skin action spectrum.

Scotto et al. (1988) calculated an average surface UV radiation trend of -8% from 1974 to 1985 using R-B meter data from eight stations located in mainland United States. The trends among these stations varied from -5% to -13%. The result was unexpected, because a -0.84% per decade trend in the northern hemisphere column ozone had been reported by Bojkov et al. (1990) for a similar period. However, the ozone trend is seasonally dependent: it is greatest in winter and least in summer when UV reaches its maximum.

Cloud-free sky UV radiation data analyzed by Scotto et al. (1988) essentially gave the same result analyzed for all sky conditions. Fredrick and Weatherhead (1991) examined the R-B meter data record and found good agreement with irradiance calculations based on Dobson ozone measurements for all seasons except wintertime. It seems unlikely that increases in tropospheric aerosols would account for the R-B meter results because the necessary increase to the tropospheric aerosol optical depth would be unusually large and, therefore, unlikely. Long-term aerosol depth data at the R-B meter sites are not

available and, therefore, this comment remains speculative.

Long-term monitoring of a radiation variable requires stable instrumentation and stable calibration reference standards. Sharp and Kennedy (1992) have investigated the stability of the calibration procedure used by Berger (1976) for the R-B meter network and the reader is referred to their conclusions. However, since the SRFs were not measured for each instrument in the network until this investigation, it is not possible to directly determine whether instrumentation characteristics changed. Nevertheless, examining the characteristics of a sample of several R-B meters that served in the network (about one-half the number in the network) should yield a sufficient set for determining the degree of their mutual consistency, and perhaps yield information that would bear on their stability while operating in the network. Moreover, a recheck of the R-B meter SRFs after an additional 1 to 2 years operation in the network should yield direct information on their stability.

The R-B meter sensor unit is sensitive to temperature changes. Blumthaler and Ambach (1986) reported a sensitivity change of 8% per 10°C change in sensor temperature. Sharp and Kennedy (1992) obtained a similar result, but the rate was closer to 5% per 10°C change in sensor temperature. Determining the temperature sensitivities of the network meters was not an objective of this investigation.

It was the objective of this investigation to measure the SRFs of the network R-B meters and to determine their expected performance in the field. Seven of 13 network instruments were analyzed via laboratory measurement of their SRFs, calibration of the meter sensitivity in terms of absolute radiant flux units, and assessment of performance features under varying solar zenith angles. Some results of the measured SRFs were compared with results found in the scientific literature.

2. The R-B Meter Sensor Unit

Details on the construction and design principles of the R-B meter are given by Berger (1976). Sharp and Kennedy (1992) recently examined the design features of the instrument. The diagram of Fig. 1 is a vertical cross-section schematic of the R-B meter sensor unit. The Vycor dome transparency is essentially flat in the UV band sensed by the instrument. The UG-11 filter transmits UV radiation effectively at wavelengths shorter than 320 nm. The layer of magnesium tungstate absorbs UV radiation and emits radiation in the visible region. The 4010 Corning filter transmits green light (peak transmission ~525 nm) which is detected by the photodiode. This arrangement of dome, filters and substrate called the optical head, shapes the SRF and prevents all solar radiation from reaching the detector. The output current from the photodiode charges a capacitor in the recorder unit which is set to discharge and reset when it reaches

a predetermined level. The number of discharges is tallied by the unit and printed on paper tape at one-half hour time intervals. Details of the instrument calibration are given by Berger (1976).

3. Laboratory Set-Up

The measurement of the R-B meter SRF is done for the sequential arrangement of the Vycor dome, Schott UG-11 filter, magnesium tungstate substrate, and the Corning 4010 green filter. This configuration is defined here as the optical head. The photodiode of the sensor unit, although not used in the measurement of the SRF, is assumed to respond linearly to the band of green light transmitted by the 4010 filter. The optical head, as shown in Fig. 1, is separable from the sensor unit as a single component. Figure 2 (large box) is a schematic representation of the laboratory apparatus that was used to characterize the R-B meter optical head. The basic components of the apparatus are a 75 W xenon lamp powered by an optical-feedback power regulator; a McPherson grating monochromator model number 2051; and a specially designed dark chamber mounted at the output port of the monochromator. The dark chamber holds the optical head, a beam-splitter, and a calibrated UDT silicon detector, model number QED200. An EMI model number 8558QB photomultiplier and housing are attached to the exit port of the dark chamber. The entrance and exit slits of the monochromator

are set to allow a 0.8 nm half-maximum bandwidth of exiting radiation. Wavelength accuracy is checked routinely with a mercury lamp attached to the side-entrance port of the monochromator. Experience with the optical-feedback power regulator has indicated that accurate measurements can be done without the use of a beam splitter. The stability of the regulator is sufficient to permit alternating the detector and sensor head in the path of the beam to obtain a ratio. The small box in Fig. 1 illustrates this procedure, which was adopted after the present work was completed.

Some of the radiation exiting the monochromator is reflected toward the silicon detector by the beam-splitter and some is transmitted through the beam splitter, which had been calibrated to give the ratio of reflected to transmitted radiation. Calibration results of the beam-splitter reflection-to-transmission ratio are given by DeLuisi et al. (1992). The reflected radiation is measured by the QED200 detector recently calibrated by the National Institute of Standards and Technology (NIST). The transmitted radiation is directed normally incident to the R-B meter optical head. Radiation emerging from the optical head is detected by the photomultiplier. Because the SRF of the R-B meter is normalized to a value of unity at the wavelength of maximum response, it is only necessary to determine the relative magnitudes of the UV radiation incident on the head and the radiation emitted by the head.

An R-B meter SRF, $R(\lambda)$, is obtained by the expression

$$R(\lambda) = \frac{V_{pmt}}{V_s(\lambda)} \cdot \gamma(\lambda) \quad (1)$$

where λ is wavelength, V_{pmt} is the relative power measured by the photomultiplier, V_s is the relative power measured by the silicon detector, and $\gamma(\lambda)$ is the beam-splitter ratio of transmitted-to-reflected radiation.

Outputs from the QED200 and photomultiplier detectors are recorded on a strip chart and read at 5 nm intervals. The signals from the detectors are fairly smooth and change slowly with wavelength. Therefore, the 5 nm intervals are believed sufficient for accurate numerical analyses. The strip chart is being replaced by a computerized data acquisition unit, which will improve the overall accuracy of the measurement procedure. A significant portion (i.e., ~50%) of the variations in the measured SRFs is due to chart reading error.

4. R-B Meter Spectral Response Functions

To obtain a representative measure of the SRF of an R-B meter optical head, the SRFs of five sections of one head are measured and averaged. The diagrams in Fig. 3 illustrate typical

locations and relative sizes of the measured areas of an optical head. Data for SRF plots are slightly smoothed. A few tests have shown that more than one run on a specific area is repeatable to better than 2%. Although the runs on the different areas extend over the wavelength range of 250 to 400 nm, the most important region is between 300 and 330 nm, wherein lies the meter's greatest sensitivity to the spectral distribution of the incident solar UV radiation near solar noon. In the spectral range 300-330 nm the standard deviation of the average of five sections was on the order of 5% or less. However, approximately half of this was due to chart reading error, as mentioned above.

Figure 4 contains seven plots representing the SRFs of seven R-B meters. Numerical tabulations of these plots and their standard deviations are given by DeLuisi et al. (1992). Some interesting differences are noted in the 300-330 nm wavelength region. Although all shapes in this region are quite similar, no explanation is given for the differences at this time except that variations in instrument construction (e.g., filters and substrate thickness) are likely to be a cause. The SRFs are temperature dependent, and the laboratory room temperature may have differed by a few degrees during the measurement of the response function of different days. The outlying SRFs were checked and found to be consistent. Recall that the SRF measurements were done for 5 nm intervals. A slight error in the

response function could arise if the actual maximum of the function does not fall on an interval. However, because the maximum is quite flat, normalization would have a minor effect. Aging from long-term field use may also be responsible; however, this cannot be assessed because, as mentioned earlier, no previous characterization data exist. Nevertheless, these instruments have operated in the field for several years to more than a decade and it is quite remarkable that their SRFs have retained their shape similarity. The Climate Monitoring and Diagnostics Laboratory (CMDL) plot in Fig. 5 is the average of the seven R-B meter SRFs. This plot is compared with the SRFs obtained from the literature. The present SRFs are consistent with those of Berger (1976) and Robertson (1972) (Published in CIAP Monograph 5, Part 1, 1975), which are also plotted in Fig. 5. The SRFs recently measured are close enough to earlier determinations, especially Berger's, to strongly suggest verification of the long-term stability of the R-B meter network instruments. Recall that Berger's (1976) instrument design and construction is after that of Robertson (1972). The indication that the SRF shapes may not have changed does not imply that the absolute magnitudes did not change; i.e., all SRFs have been adjusted to unity at the maximum. Nevertheless, calibration accounts for the changes in absolute magnitude. Table 2 contains the numerical values of the average and standard deviations of the CMDL plot in Fig. 5. Uncertainties in the individual SRFs are estimated to be ± 1.5 nm in wavelength and 2-3% in the

response. The impact of different SRFs on the precision of the R-B meter sensor unit is examined next.

5. R-B Meter Calibration

The R-B meter is calibrated in terms of sunburn units, defined as the UV radiation dose that causes minimal erythema (minimum erythemal dose, or MED) on untanned Caucasian skin. DeLuise and Harris (1983) investigated the absolute radiant energy of a sunburn unit by using simultaneous spectral measurements of solar UV flux obtained with a double monochromator, and measurements obtained with an R-B meter during a cloud-free sky conditions. Because the SRF of the R-B meter does not simulate the human erythemal action spectrum, a nonlinear relationship between the R-B meter count rate and an MED will exist.

This investigation considers two methods for calibration of R-B meters. The first uses the normalized SRFs and measurements of the spectral solar flux made with a Brewer spectrophotometer Kerr et al. (1984). The second compares daily total counts from an R-B meter that had been recently calibrated by the Solar Light Company. The conversion of R-B meter counts to sunburn units is 440 counts equals 1 sunburn unit; however, further work might be required to confirm this conversion.

The first method is a calibration in absolute radiant flux units made by convolving the measured solar spectral flux with the normalized R-B meter response functions shown in Fig. 4. A typical spectrum of UV spectral solar flux measured by the Brewer spectrophotometer is shown in Fig. 6. Details on the use of the Brewer are given by DeLuise et al. (1992). This calibration was done to demonstrate the effects of slightly different SRFs on absolute calibrations of broad-band instruments in the rapid fall-off region of the UV spectrum.

The portion of the solar UV spectrum $E(\Delta\lambda)$ sensed by the R-B meter is determined by the convolution integral

$$E(\Delta\lambda) = \int_0^{\infty} R(\lambda) F(\lambda) d\lambda, \quad (2)$$

where $R(\lambda)$ is the instrument's SRF (normalized to 1 at the maximum), $F(\lambda)$ is the solar flux (direct plus diffuse-sky) incident on the sensor, and $\Delta\lambda$ represents the instrument's effective band pass, which, for example, can be defined as the rectangular representation of the integrated power $E(\Delta\lambda)$ having the maximum of $R(\lambda) \cdot F(\lambda)$ as the height and the $\Delta\lambda$ as the width. Figure 7 contains six plots of the convoluted solar spectral flux with the normalized R-B meter SRFs. Convolution calculations were done from solar noon (zenith angle 18°) to the time when the solar zenith angle reached 85° . Because the spectrum of incident

solar UV flux changes in shape considerably during the increase in solar zenith angle, where the flux at the shorter wavelength is diminishing more rapidly than longer wavelengths (i.e., the band is shifting towards the longer wavelengths), the convoluted results of Fig. 7 will change as well. DeLuisi and Harris (1983) illustrated this effect, and DeLuisi et al. (1992) examined the band shift toward longer wavelengths in greater detail. For example, the present results indicate that the R-B meter's wavelength of median band power is 312.1 nm at 20° solar zenith angle and 314.0 nm at 60° solar zenith angle.

The second method, which is that followed by Berger (1976) for the network, is to adjust meter sensitivities to agree with the daily total count made by a reference instrument. When this is done, a different result is seen compared to that of the first method. Figure 8 contains plots obtained from four R-B meter one-half-hour counts that were adjusted to agree with the reference meter daily total count value. With this method the agreement is seen to be quite good. The differences are approximately a few to several percent, depending on solar zenith angle, and are caused by the wavelength differences of the SRFs and differences among the instruments' responses to the zenith angle of the sun (i.e., the cosine response, defined as the instrument's response to direct radiation at various incident angles).

The adjustment procedure involves an initial electronic adjustment to each R-B meter recording unit to obtain daily total counts within a few percent of a standard. It might require several or more days to finalize the adjustments. Slight differences of a few percent or less, are seen in instrument results from day to day; because these adjustments cannot be done precisely with the electronics, small biases may remain after several days of operation. The final adjustment is made numerically by calculating a calibration factor that is obtained by taking the daily total count ratio of the reference instrument to the test instrument. For the Fig. 8 comparison, the reference has been chosen to be represented by a standard that had been calibrated by the Solar Light Company. These calibration factors are applied to the data obtained by the respective instruments operating in the field. Berger (1976) used a reference R-B meter at Temple University as the primary calibrator, and transferred the calibration to the field instruments with a traveling secondary standard.

The reason why this method of calibration works as well as it does for a broadband UV sensor is somewhat fortuitous, and important. It turns out that the maximum of the spectral band sensed by the R-B meter is near 311 nm (see Fig. 7). If the R-B measurements are forced to agree with a prescribed value, this essentially resets the SRFs so that they are not quite normalized at their maximum values, but are readjusted to agree closer to

the 311 nm maximum of the convoluted spectra. Because the SRFs are almost parallel in this region, the instruments will sense convoluted spectra that are not exactly the same, but are close. Theoretical calculations were made to model the variations that might occur when two dissimilar SRFs are subjected to the same UV radiation spectral changes caused by various total ozone amounts and solar zenith angle. The variations do appear to be small, about 2-3%, but more work is required to fully quantify these.

If the adjustment procedure of the second approach is applied to the absolute calibration procedure of the first approach, then a similar result obtains. Figure 9 contains plots that illustrate this for seven instruments. The observations start at solar noon. The numerical values are tabulated in DeLuisi et al. (1992). The reference is the average of the daily total values of the six instruments. Again, differences of 2-3% are seen. The reader is reminded that the results of Fig. 9 are not obtained the way those of Fig. 8 are obtained because a calculated convolution is involved with the latter.

Nevertheless, an interesting cross-over in the plots is noted near 34° solar zenith angle. This result arises from a compensation caused by the different but similarly shaped SRFs. Insight into this compensation can be gained by examining Fig. 10. This plot of the convolution of solar spectral flux with SRFs of two R-B meters shows the mechanism of compensation. The meter with the SRFs biased toward the shorter wavelengths (solid

line) senses more UV on the shorter wavelength side and less on the longer wavelength side, compared to the other meter. Each spectrum has the same integrated power. The two SRFs used in this example were chosen for their exceptional difference so that maximum contrast would be acquired.

6. Discussion

Seven R-B meters were examined for their spectral response characteristics. The instruments were then exposed to solar radiation while a UV spectral radiometer recorded the solar spectral flux. The spectral flux data were then used to calculate an absolute calibration for each R-B meter. The R-B meter calibration in terms of 30-minute counts was done by a simple side-by-side comparison of the test meter with a local standard. The local standard was calibrated by comparison with a standard maintained by the Solar Light Company. The results were analyzed to determine the expected performance of each instrument as it would be while operating in the field. The 30-minute count calibration is that used for the R-B meter network.

The SRFs measured thus far were quite similar in shape in the wavelength region of importance, i.e., 300-330 nm. However, the wavelength positions among them varied by a few nanometers.

Experimental error is partially responsible for this variation. Variations in the optical components, such as filter and substrate thicknesses, are also believed to be partially responsible. The displacements have only a small impact on the agreement among the instruments when they are calibrated to agree with a standard, as is done for the network meters. On the other hand, if each instrument were separately calibrated for absolute irradiance, then considerable differences would result among them because the slight differences in their SRFs become important. The agreement among them is greatly improved if all instruments are calibrated to agree with the same daily total value.

Some determinations of the cosine responses of the optical heads suggest that the sensor units do not follow the ideal cosine response. However, because atmospheric UV radiation contains a significant diffuse sky component, the cosine response error is diminished in significance, becoming increasingly less significant as the solar zenith angle increases.

These instruments had been operating in the field for a decade or more. It is remarkable that their SRFs have retained a considerable degree of similarity. Because the functions were not measured before now, it is not possible to determine if a drift occurred. Nevertheless, the average of seven SRFs determined by our investigation is very close to the SRFs of Berger (1976) who constructed the instruments, strongly

suggesting little to no drift in the network sensor units' SRFs shapes. The indication that the SRF shape has not changed does not imply that the magnitude of the SRF has not changed, because all measured functions have been normalized to a value of unity at the maximum. However, routine calibration of the network instruments, if properly done, will account for changes in magnitude (see Berger, 1976). Improper calibration of the response level of a network of R-B type meters can result in a drift (or false trend) in the network data. Examining the SRFs after one or more years of additional field operation should shed some further light on the question of drift. The recording units were not evaluated; however, they definitely show signs of aging, and many of the components are becoming difficult to replace. An upgraded recording unit would greatly improve data quality.

Overall, the basic design principle of the R-B meter sensor unit might well be sufficient for a stable long-term UV monitoring device. Of course, the temperature dependence of the sensor unit as well as the cosine response would need further consideration, although the latter is not considered serious. In the very least, a measurement of the sensor head temperature would be very useful for making temperature corrections to the data. Another useful piece of information would be a more exact record of time, which is not now recorded along with the half-hourly printed counts.

In Summary:

- The shape of the SRF R-B meters in the present network appears not to have changed significantly with time.
- The design principle of the R-B meter might be sufficient for a stable long-term UV sensor.
- The temperature dependence of the R-B meter optical head should receive attention, although it is believed not to be responsible for instrument drift.
- Drifts in the network instruments should be avoidable by proper calibration if the SRFs remain stable.
- More work is needed to quantify the cosine response of R-B meters.

Calibration of an instrument such as the R-B meter that senses a broad band in the sharp cut-off region of atmospheric UV radiation < 320 nm must be done with care to account for changes in the transmitted solar UV spectrum due to variations in solar zenith angle and total ozone. A laboratory calibration using standard lamps is not straightforward. The calibration should be done using actually measured solar UV spectra or a solar UV simulator (that can accurately simulate various conditions) if

done in a laboratory. Procedures to account for these factors can be developed to improve the radiometric interpretation of the measurement and, therefore, its application. To our knowledge, such procedures have not been thoroughly developed for the R-B meter. Nevertheless, it would be worthwhile to develop procedures if the use of broad-band instruments is to continue and greater accuracy is deemed desirable.

Acknowledgments

This work was funded partially by the Fluorocarbon Program Panel of the Chemical Manufacturers Association. The assistance received from J. Cotton and L. Machta of NOAA's Air Resources Laboratory is greatly appreciated. A note of thanks is extended to J. Scotto and D. Berger for providing helpful information on the R-B meter network. The opportunity to interact with investigators W. Sharp, J. Kennedy, and J. Fredrick and members of the CMA Fluorocarbon Panel was very stimulating.

References

- Berger, D. (1976), The sunburning ultraviolet meter: Design and performance. *Photochem. and Photobiol.*, 24, 187-192.
- Blumthaler, M. and W. Ambach (1986), Messungen der Temperatur

Koeffizienten des Robertson-Berger Sunburn Meters und des Eppley UV-radiometer. *Arch. Met. Geophys. Biol., Ser. B*, 36, 357-373.

Bojkov, R.D., L. Bishop, W.L. Hill, G.C. Reinsel, and G.C. Tiao (1990), A statistical trend analysis of revised Dobson total ozone data over the northern hemisphere. *J. Geophys. Res.*, 95, 9785-9807.

Coblentz, M.W. and R. Stair (1934), Data on the spectral erythemic reaction of untanned human skin to ultraviolet radiation. Research Paper RB631, National Bureau of Standards, *J. Res.*, 13.

DeLuisi, J. and J. Harris (1983), A determination of the absolute energy of a Robertson-Berger meter sunburn unit. *Atmos. Environ.*, 17, No. 4, 751-758.

DeLuisi, J., J. Wendell, and F. Kreiner (1992), Performance characteristics of the Robertson-Berger ultraviolet meter. NOAA/ERL data report (in preparation, information available upon request).

Fredrick, J.E. and E.C. Weatherhead (1992), Temporal changes in surface ultraviolet radiation: A study of the Robertson-Berger meter and Dobson data records. *J. Photochem.*

Photobiol., (to be published).

Kerr, J.B., C.T. McElroy, D.I. Wardle, R.A. Olafson, and W.J.F. Evans (1984), The automated Brewer spectrometer. *Atmospheric Ozone*, International Ozone Commission, Proceedings of the Quadrennial Ozone Symposium, Halkidiki, Greece, 3-7 September, 1984, D. Reidel Publishing.

NAS (1979), Protection Against Depletion of Stratospheric Ozone by Chlorofluorocarbons. *National Academy of Sciences*, Library of Congress Card Catalog Number 79-57247, 392 pp.

Robertson, D. (1972), Solar ultraviolet radiation in relation to human skin burn and cancer. Ph.D. Thesis, No. THE4866, University of Queensland.

Scotto, J., G. Cotton, F. Urbach, D. Berger, and T. Fears (1988), Biologically effective ultraviolet radiation: Surface measurements in the United States, 1974-1985. *Science*, 293, 762-764.

Sharp, W.E. and B.C. Kennedy (1992), Validation of the Robertson-Berger meter. *J. Photochem. Photobiol.* (To be published).

Table 1. Sites in the Present R-B Meter Network
in the United States

<u>CITY</u>	<u>STATE</u>
Albuquerque	New Mexico
Barrow	Alaska
Boulder	Colorado
Chicago	Illinois
Concord	New Hampshire
Detroit	Michigan
El Paso	Texas
Fort Worth	Texas
Hilo	Hawaii
Lihue	Hawaii
Miami	Florida
Minneapolis	Minnesota
Redwood City	California
S. Burlington	Vermont
Salt Lake City	Utah
Seattle	Washington
Tucson	Arizona

Table 2. R-B Meter Normalized Response Function

<u>WAVELENGTH (nm)</u>	<u>RESPONSE</u>	<u>STD</u>
250	3.12E-03	9.53E-04
255	1.02E-02	6.16E-03
260	3.78E-02	2.59E-02
265	9.95E-02	5.55E-02
270	2.01E-01	8.40E-02
275	3.50E-01	9.78E-02
280	4.90E-01	9.32E-02
285	6.47E-01	8.05E-02
290	7.94E-01	5.99E-02
295	9.16E-01	4.10E-02
300	1.00E+00	1.33E-02
305	9.61E-01	4.07E-02
310	6.87E-01	7.31E-02
315	3.31E-01	5.97E-02
320	1.21E-01	2.44E-02
325	3.88E-02	8.19E-03
330	1.23E-02	2.37E-04
335	4.43E-03	8.99E-04
340	2.03E-03	5.08E-04
345	1.29E-03	4.55E-04
350	1.05E-03	4.79E-04
355	9.56E-04	4.97E-04
360	9.10E-04	5.04E-04
365	8.47E-04	4.84E-04
370	7.20E-04	4.01E-04
375	5.68E-04	2.86E-04
380	4.04E-04	1.84E-04
385	3.03E-04	1.70E-04
390	2.65E-04	1.81E-04
395	2.05E-04	1.75E-04
400	2.50E-04	1.77E-04

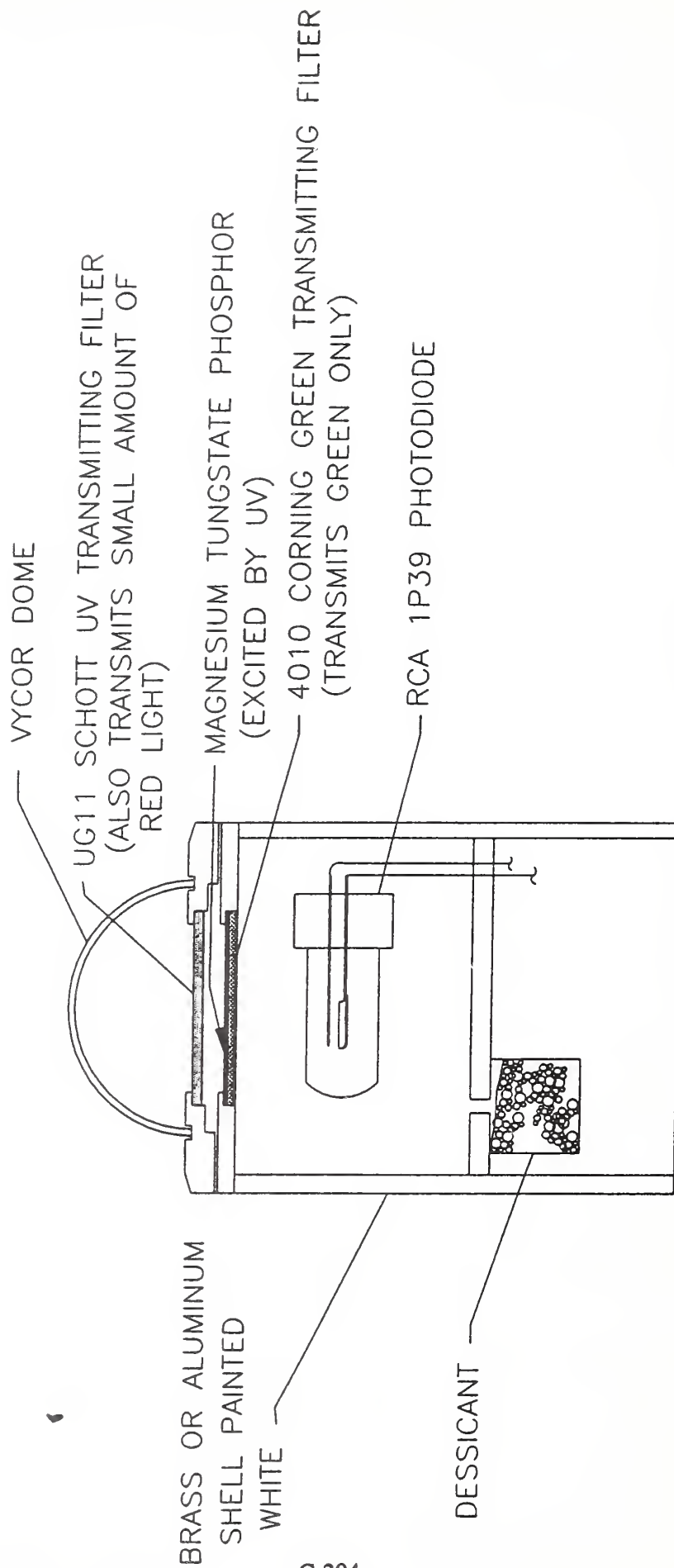
Figures

- Fig. 1. Schematic of an R-B meter sensor unit. The unit is 23 cm high.
- Fig. 2. Laboratory apparatus arrangement for measuring R-B meter response functions.
- Fig. 3. Locations and relative sizes of areas sampled on an R-B meter optical head.
- Fig. 4. Spectral response function of seven R-B meters, plotted as response versus wavelength.
- Fig. 5. Average of seven R-B meter spectral response functions (CMDL); the human erythemal action spectrum (ERYTHEMA); Berger's (1976) spectral response function (BERGER); and the NAS (1979) spectral response function (CIAP) (after Robertson, 1972).
- Fig. 6. Typical spectrum of atmospheric ultraviolet flux measured by a Brewer instrument.
- Fig. 7. UV flux convoluted with the spectral response functions of six R-B meters shown in Fig. 6.

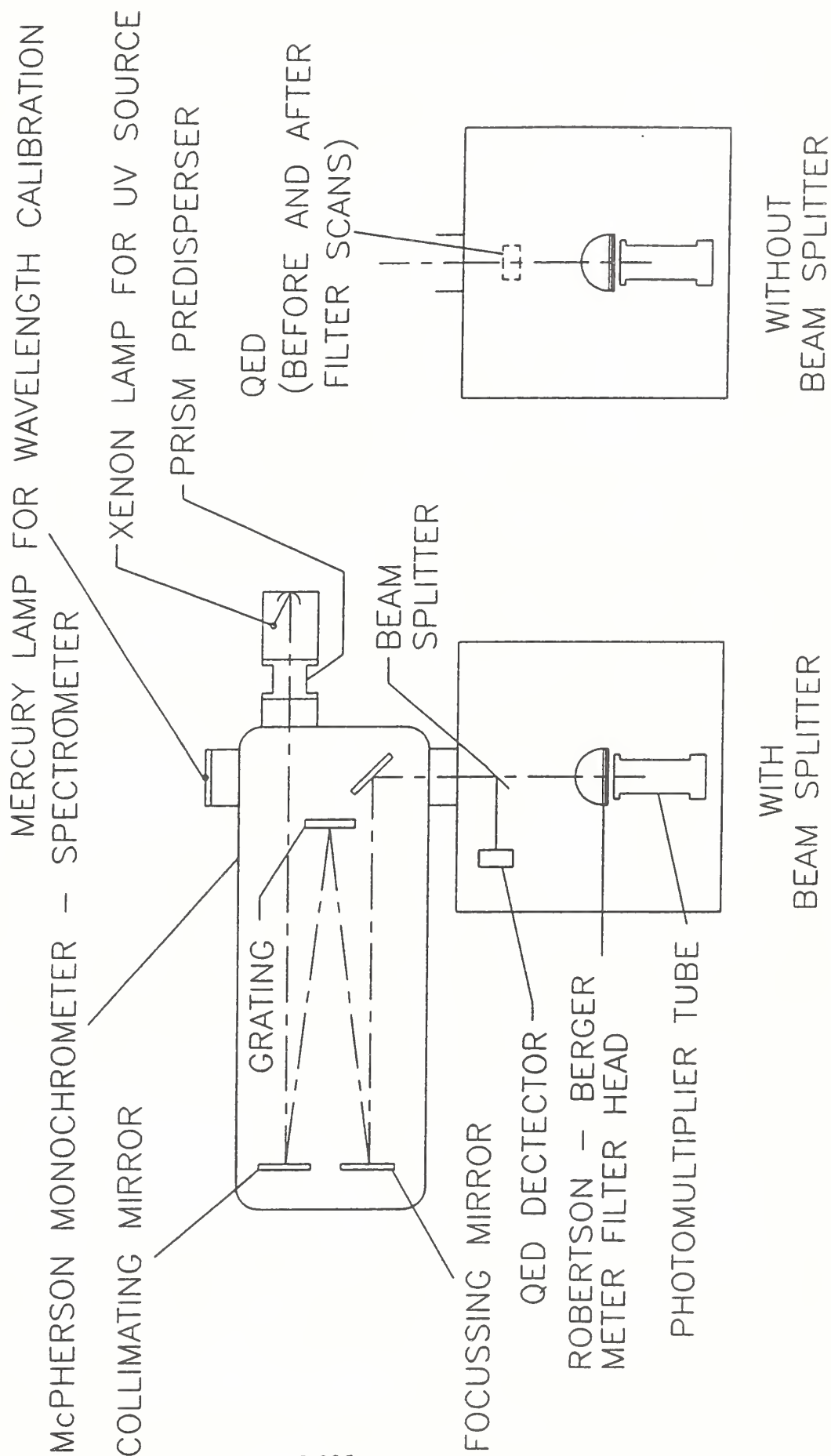
Fig. 8. Plots of four R-B meter half-hour counts versus time (over one day). The meters had been originally calibrated to give the same total daily count.

Fig. 9. Absolute radiant flux versus solar zenith angle for six R-B meters calibrated in an absolute flux mode. The instrument calibrations are adjusted to give the same daily integrated flux values.

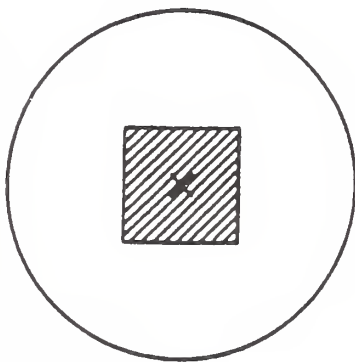
Fig. 10. UV spectrum sensed by two R-B meters with different response functions. The SRF for the solid line is shifted toward the shorter wavelengths compared to the SRF for the dashed line.



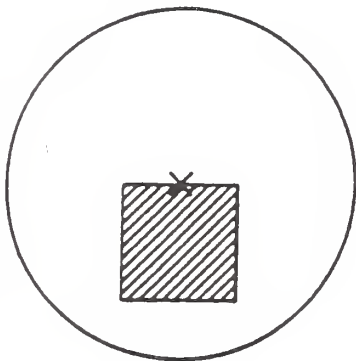
SCHEMATIC OF
ROBERTSON - BERGER UV SENSOR



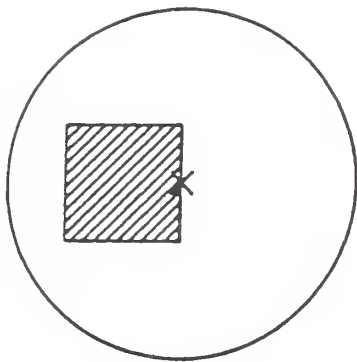
QUADRANT 0



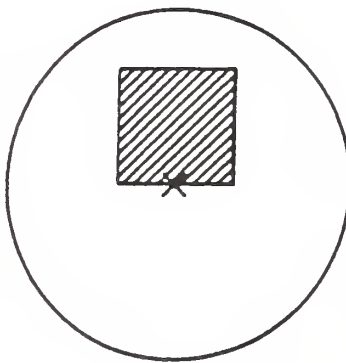
QUADRANT 1



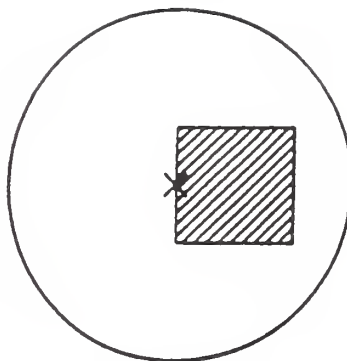
QUADRANT 2

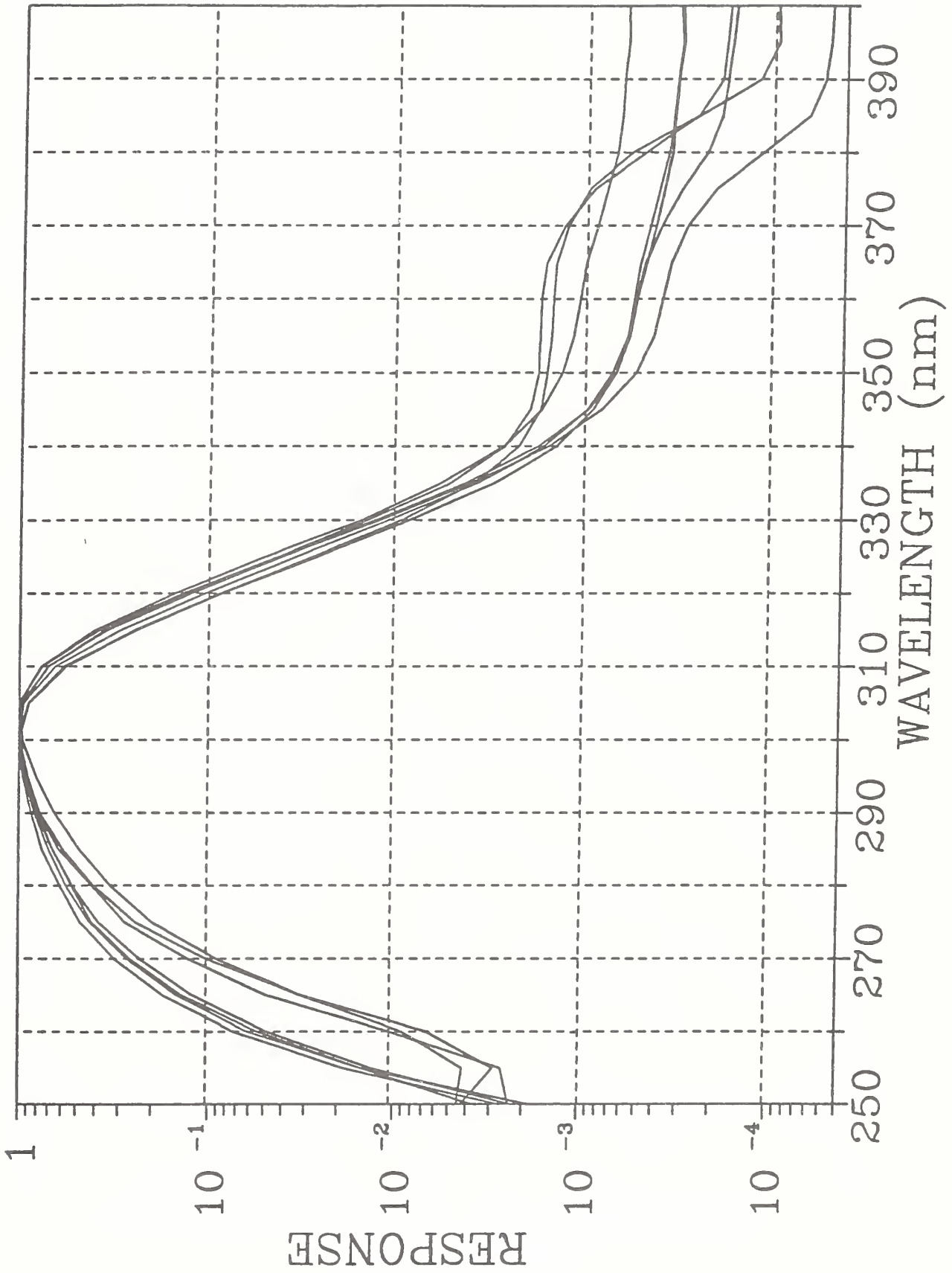


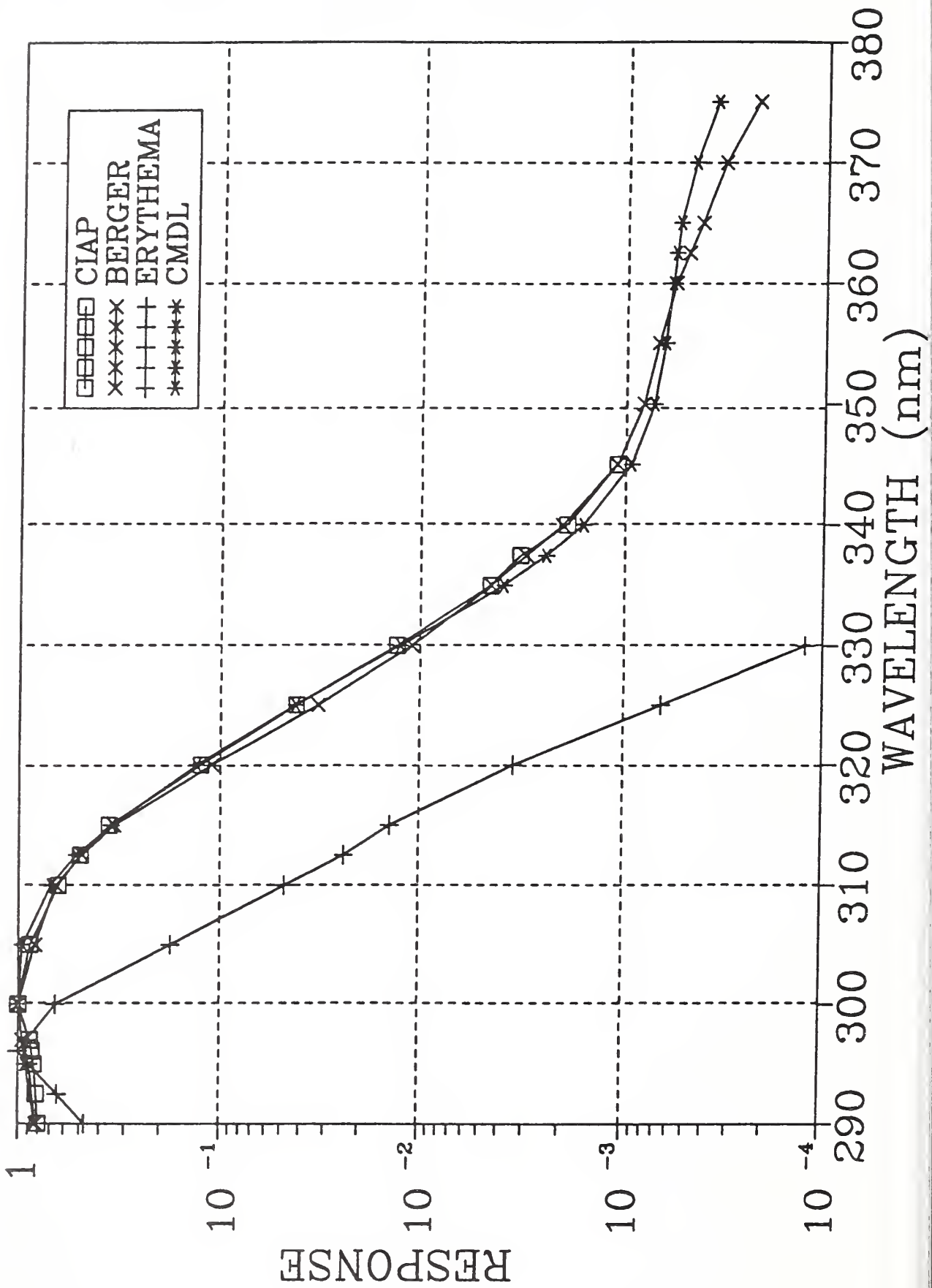
QUADRANT 3

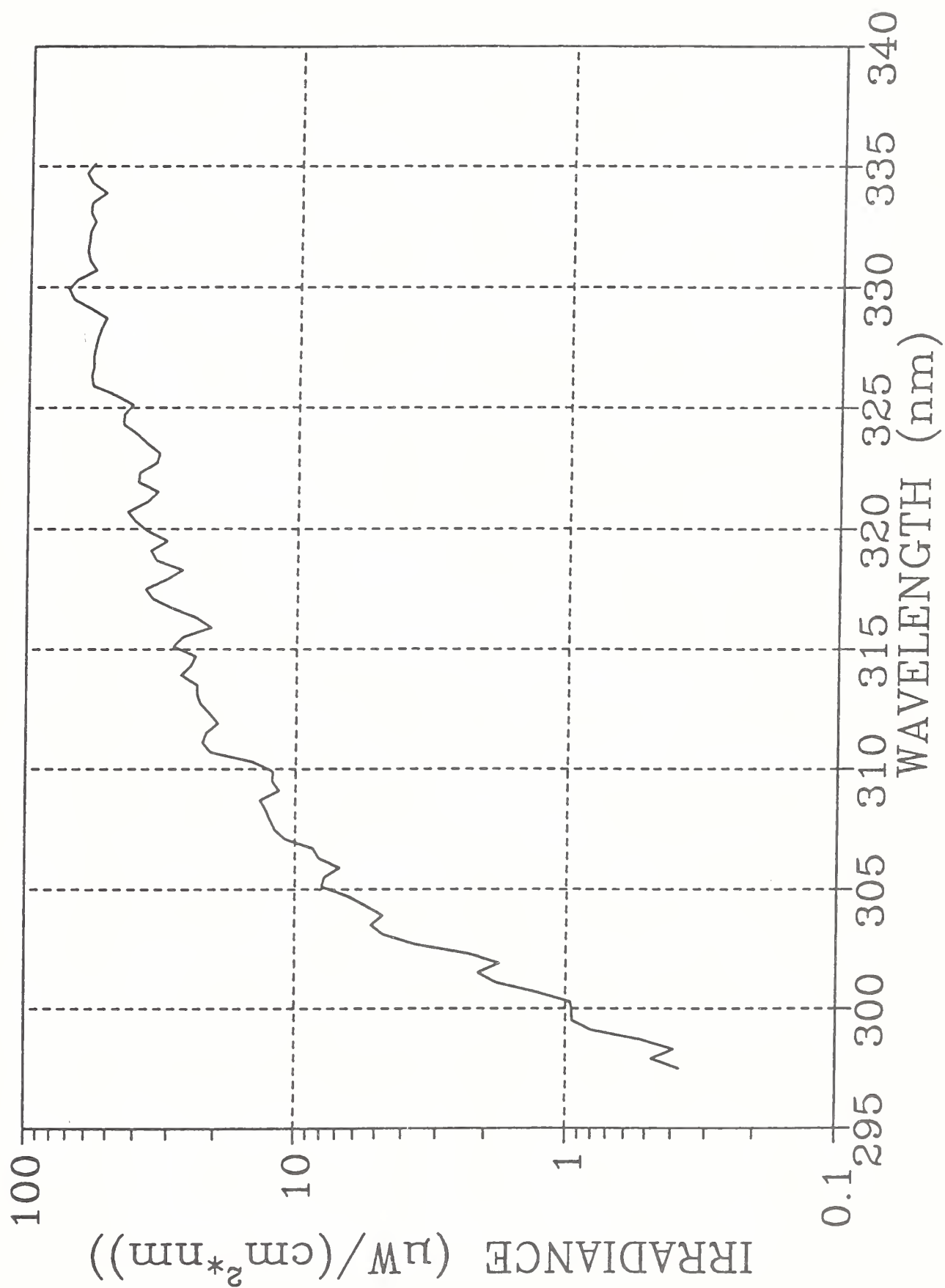


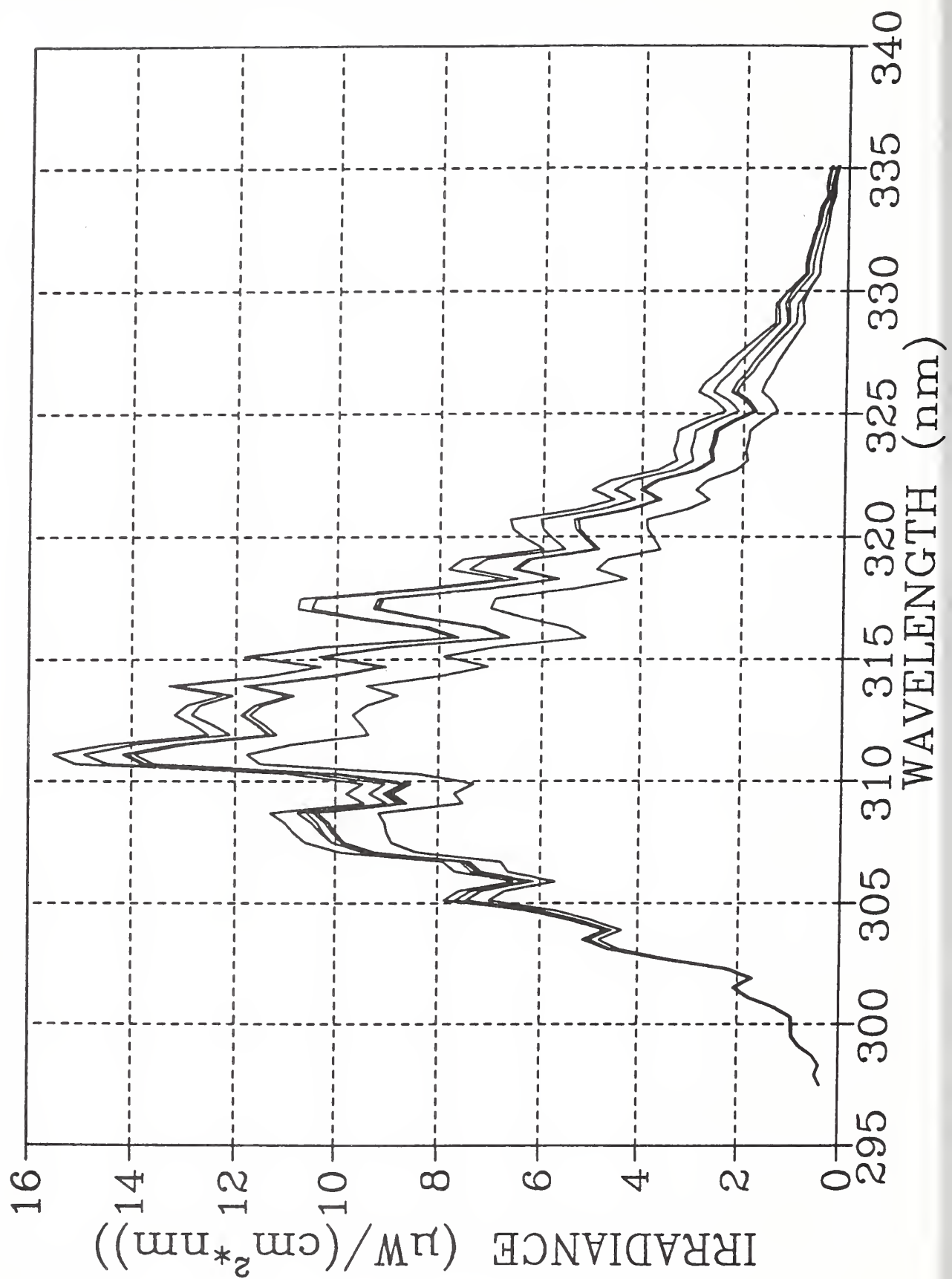
QUADRANT 4

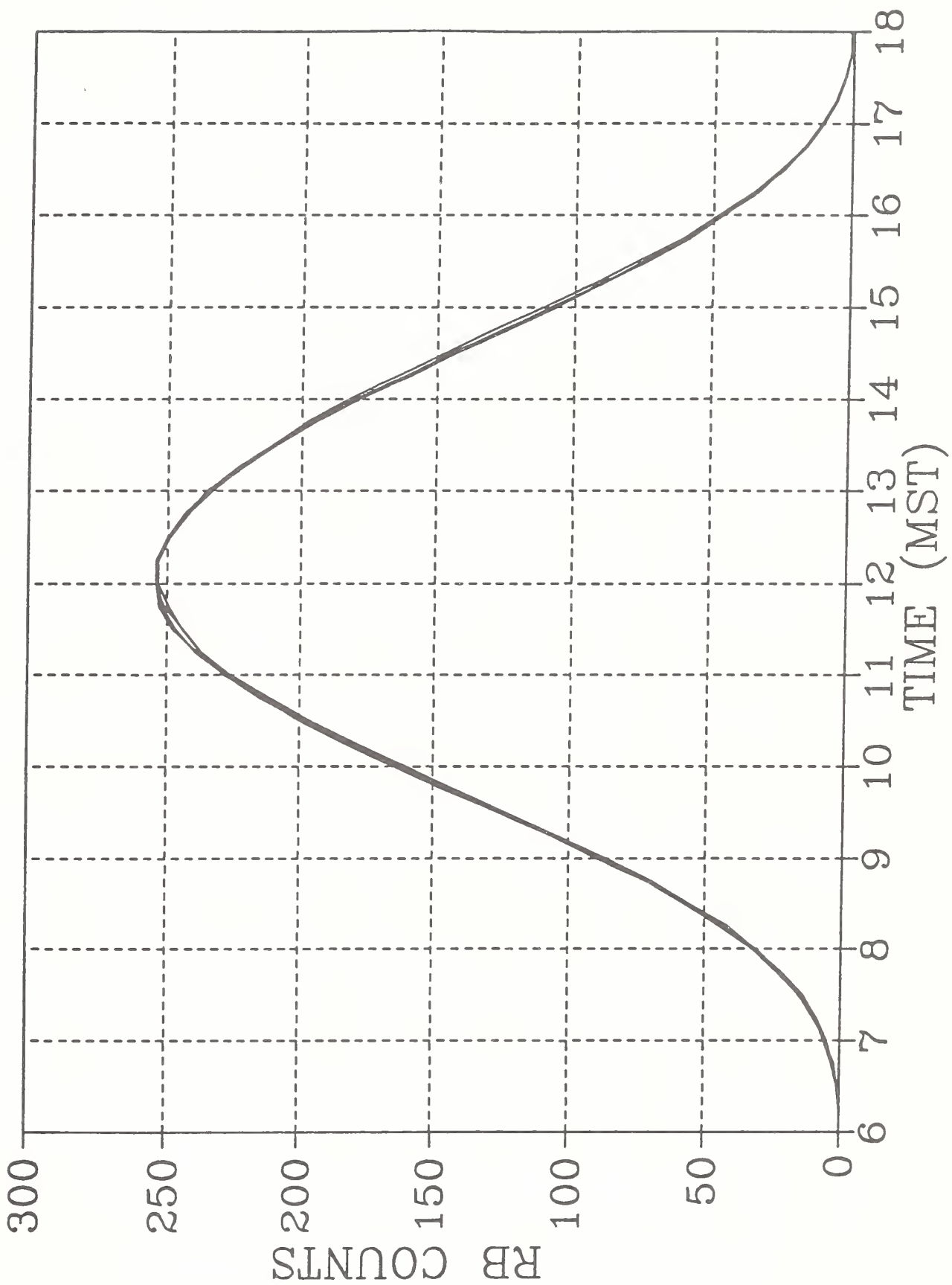


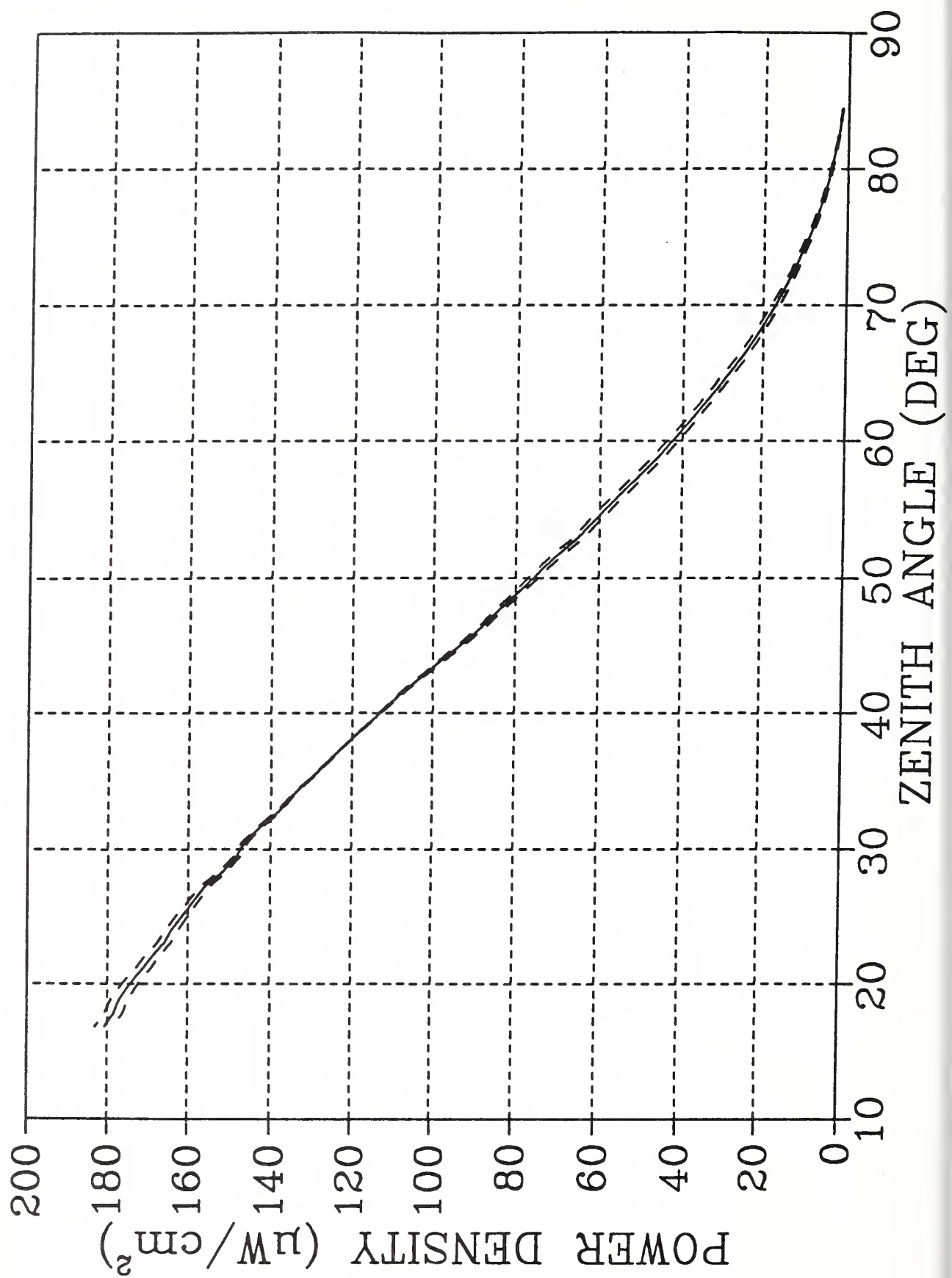


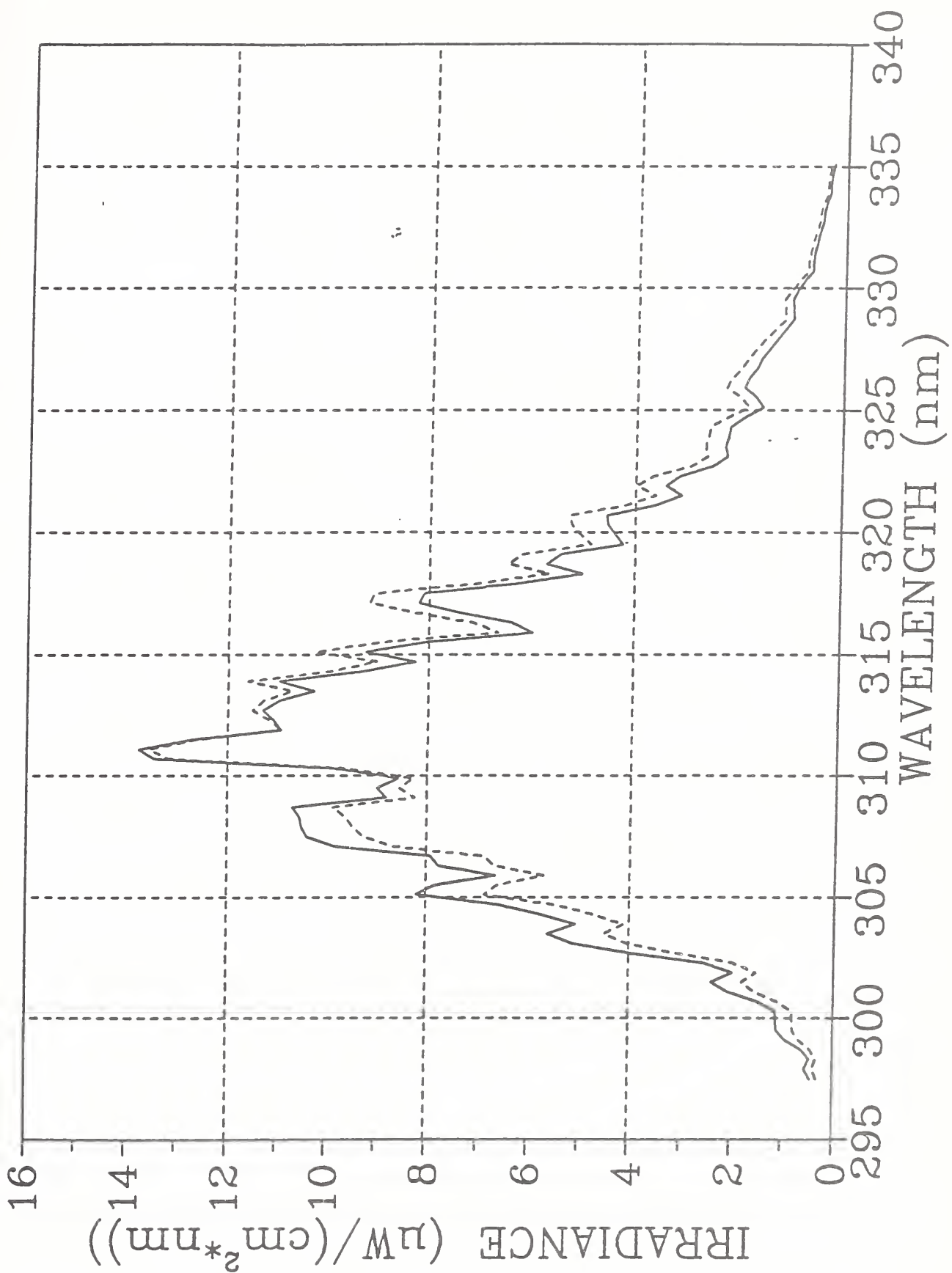


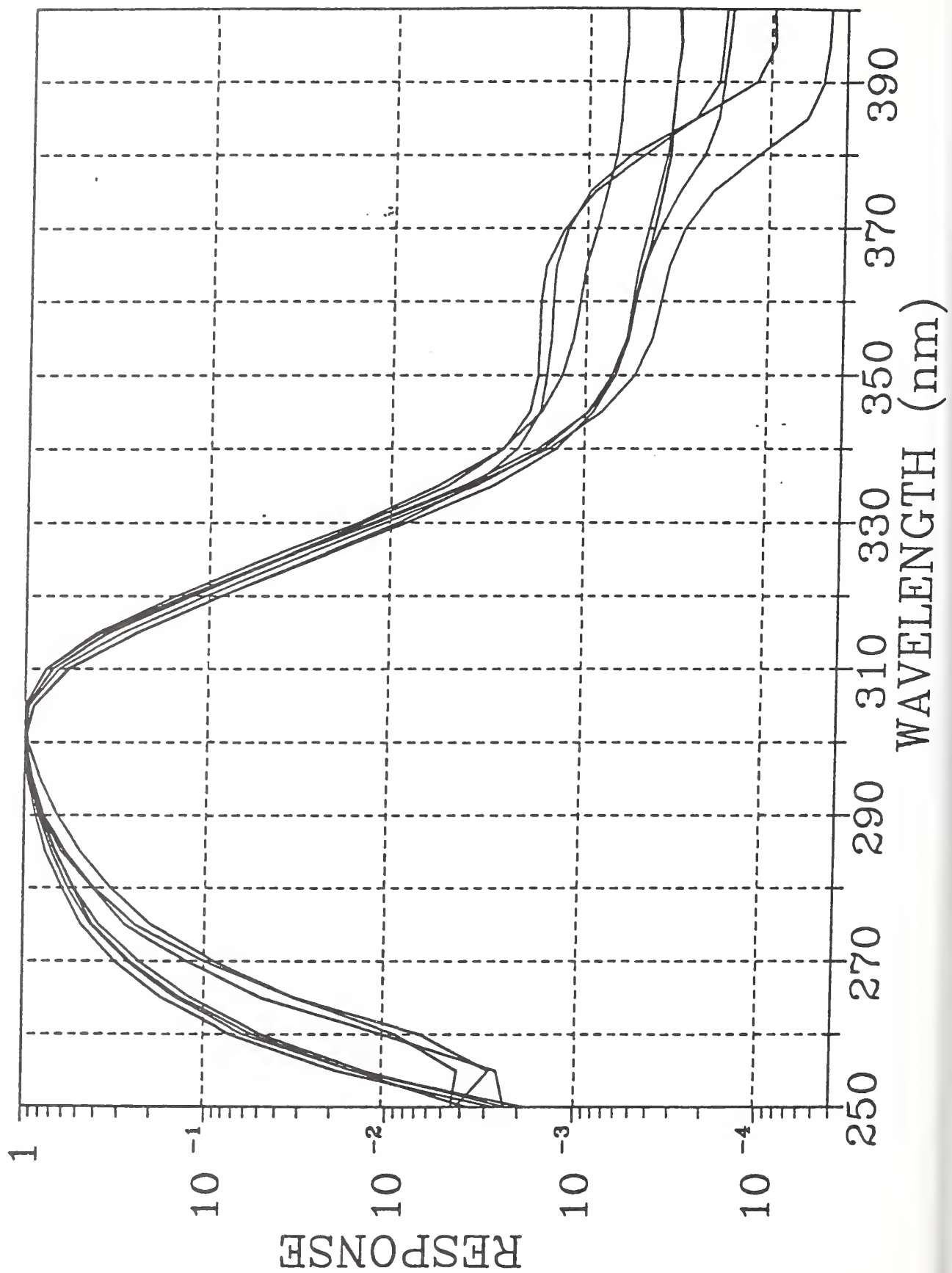


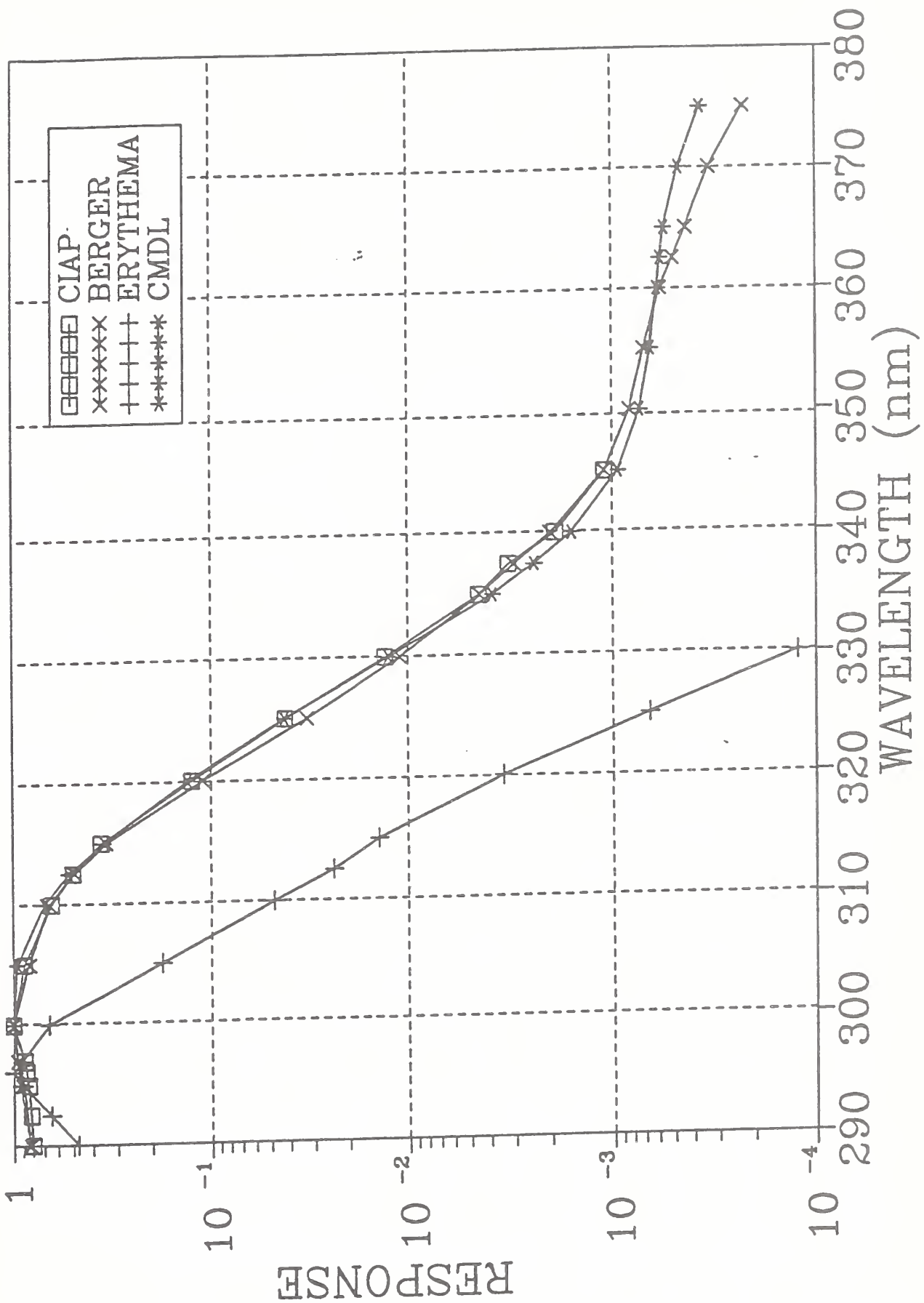


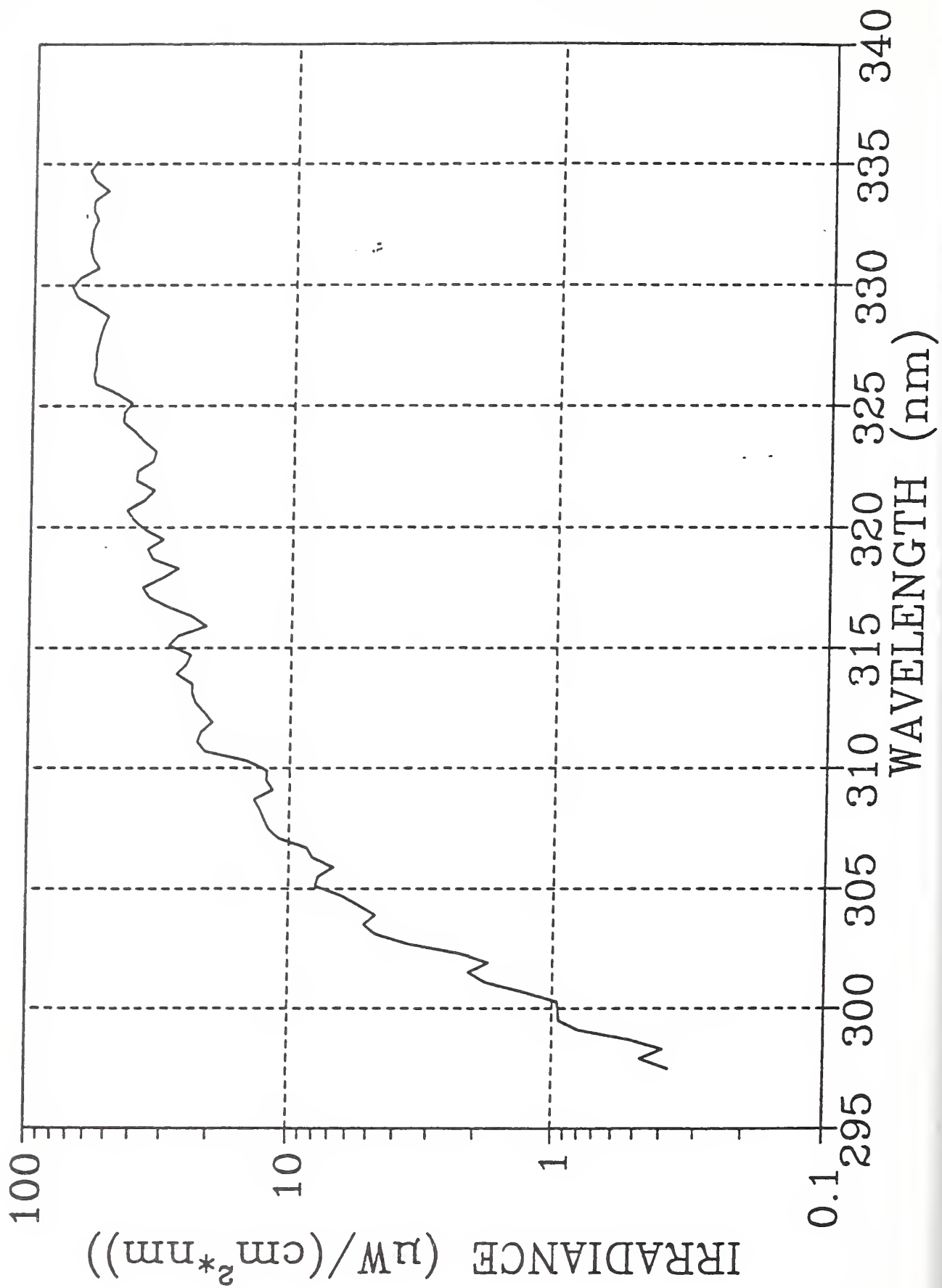


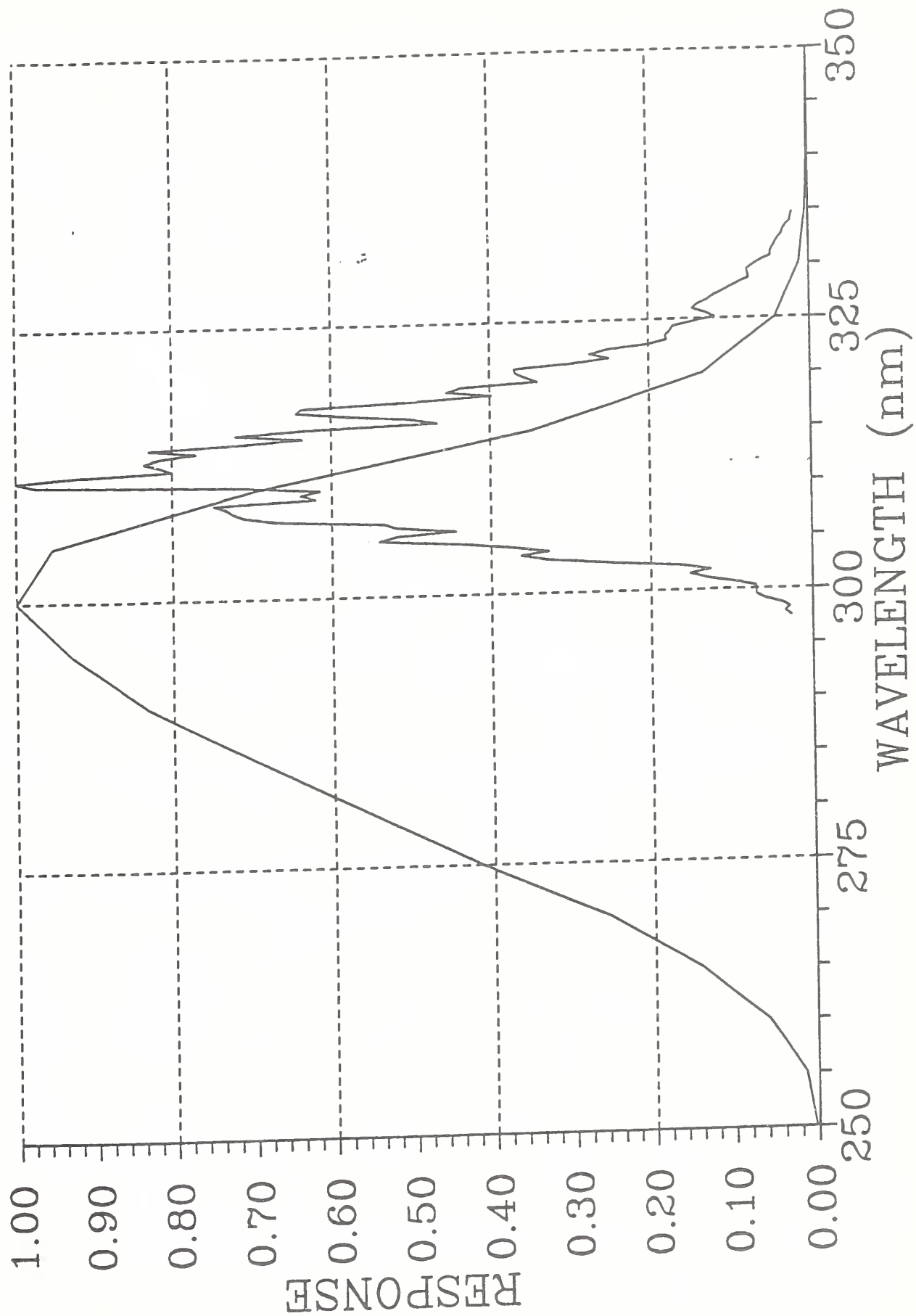


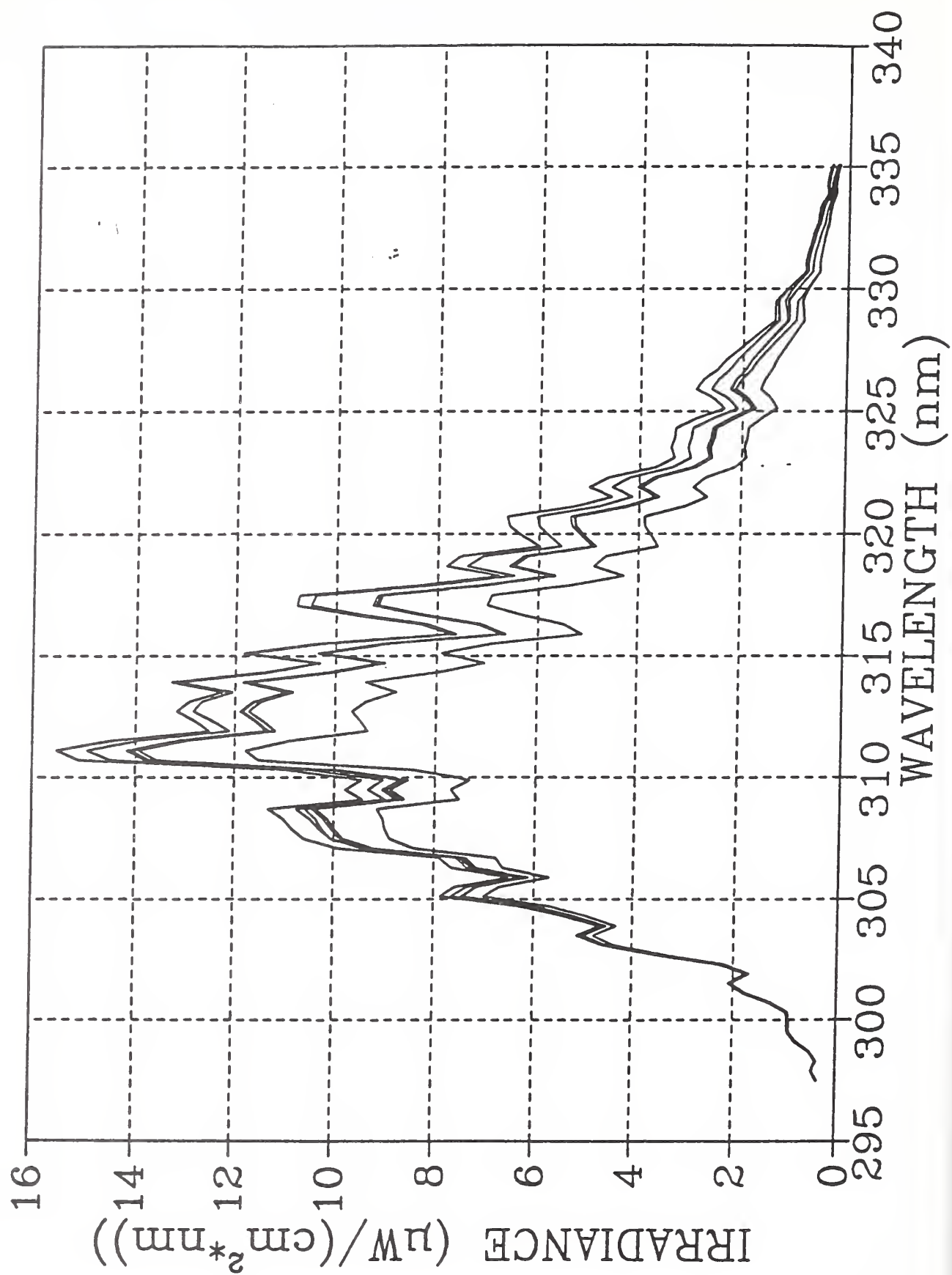


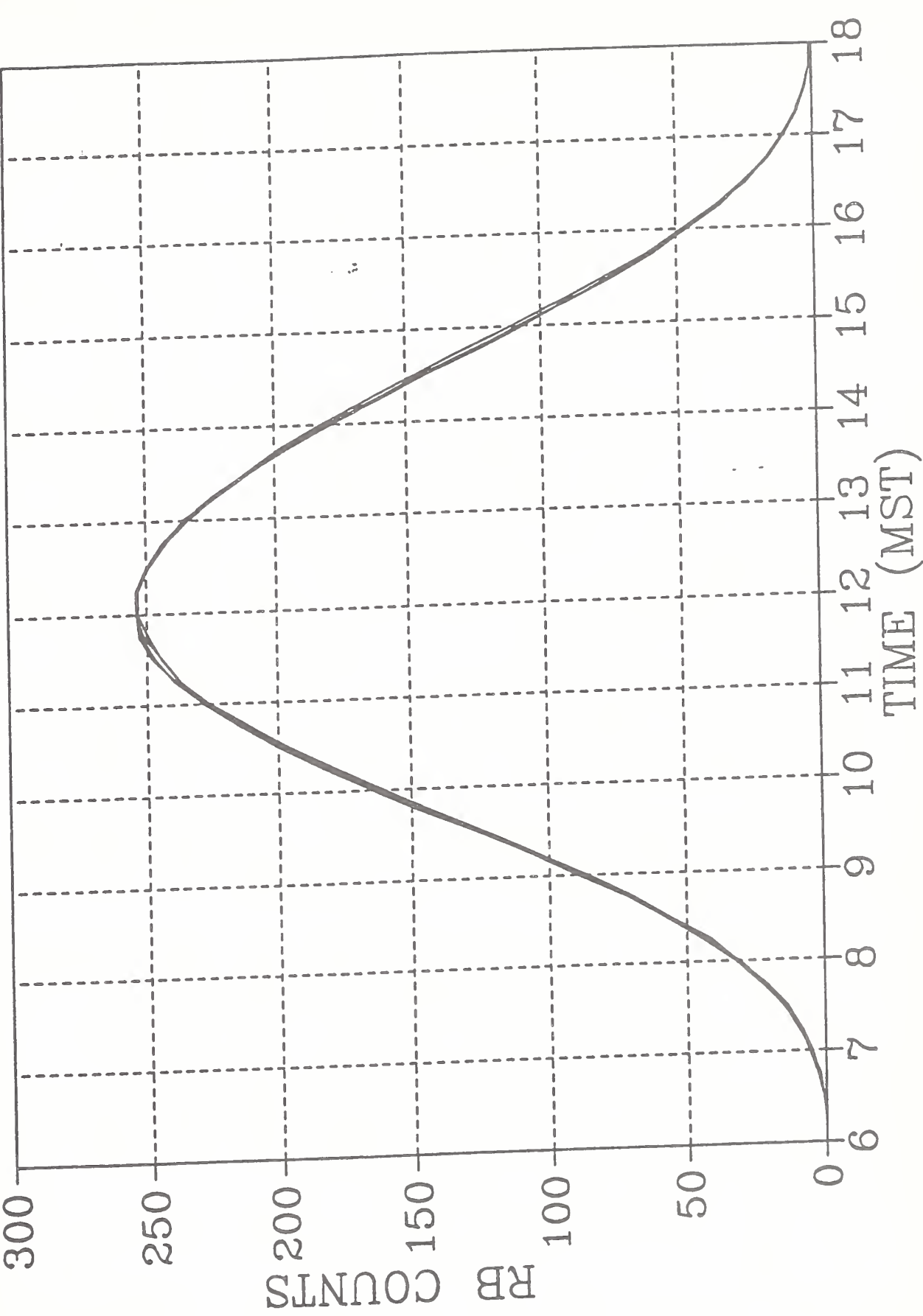


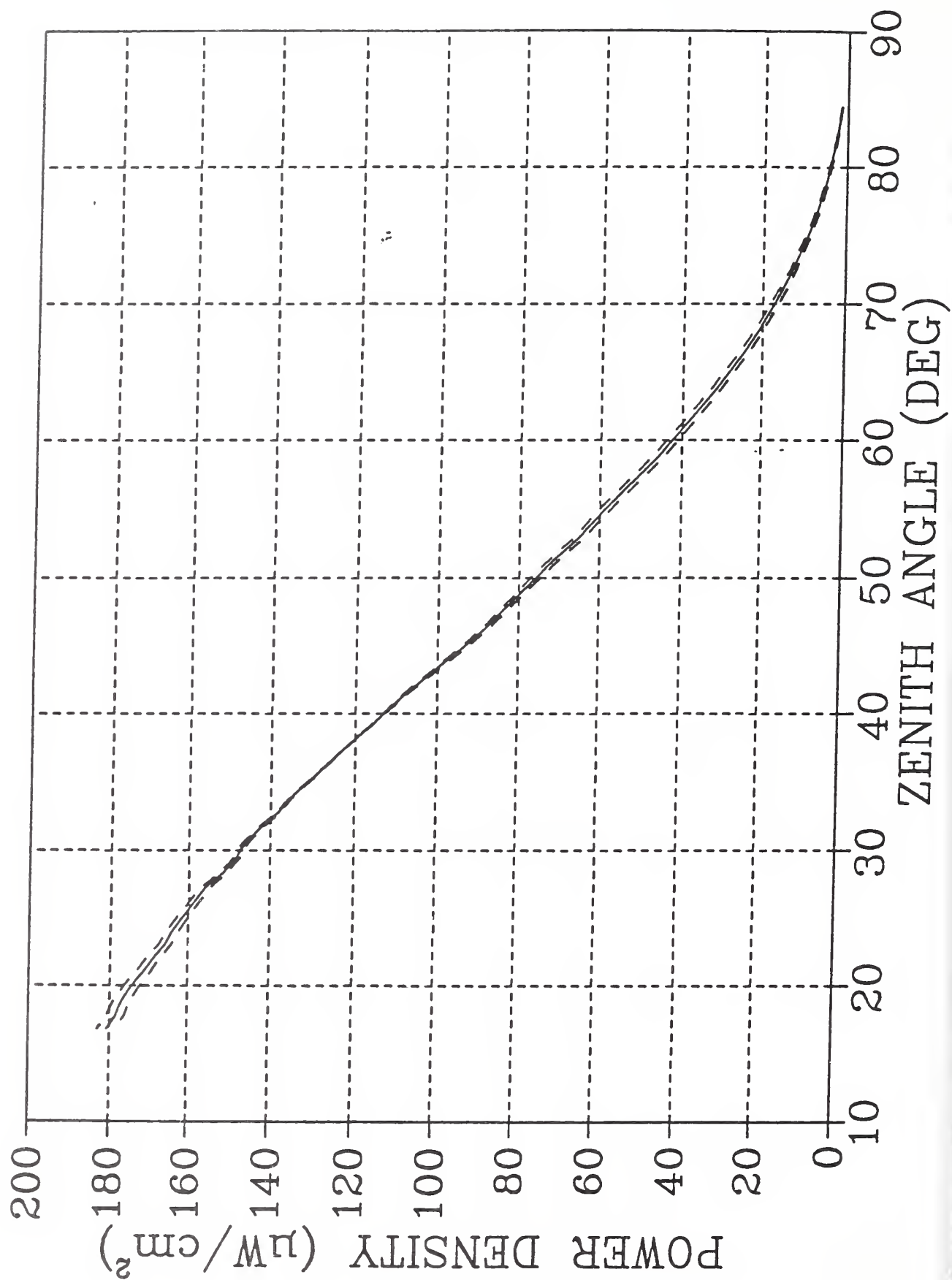


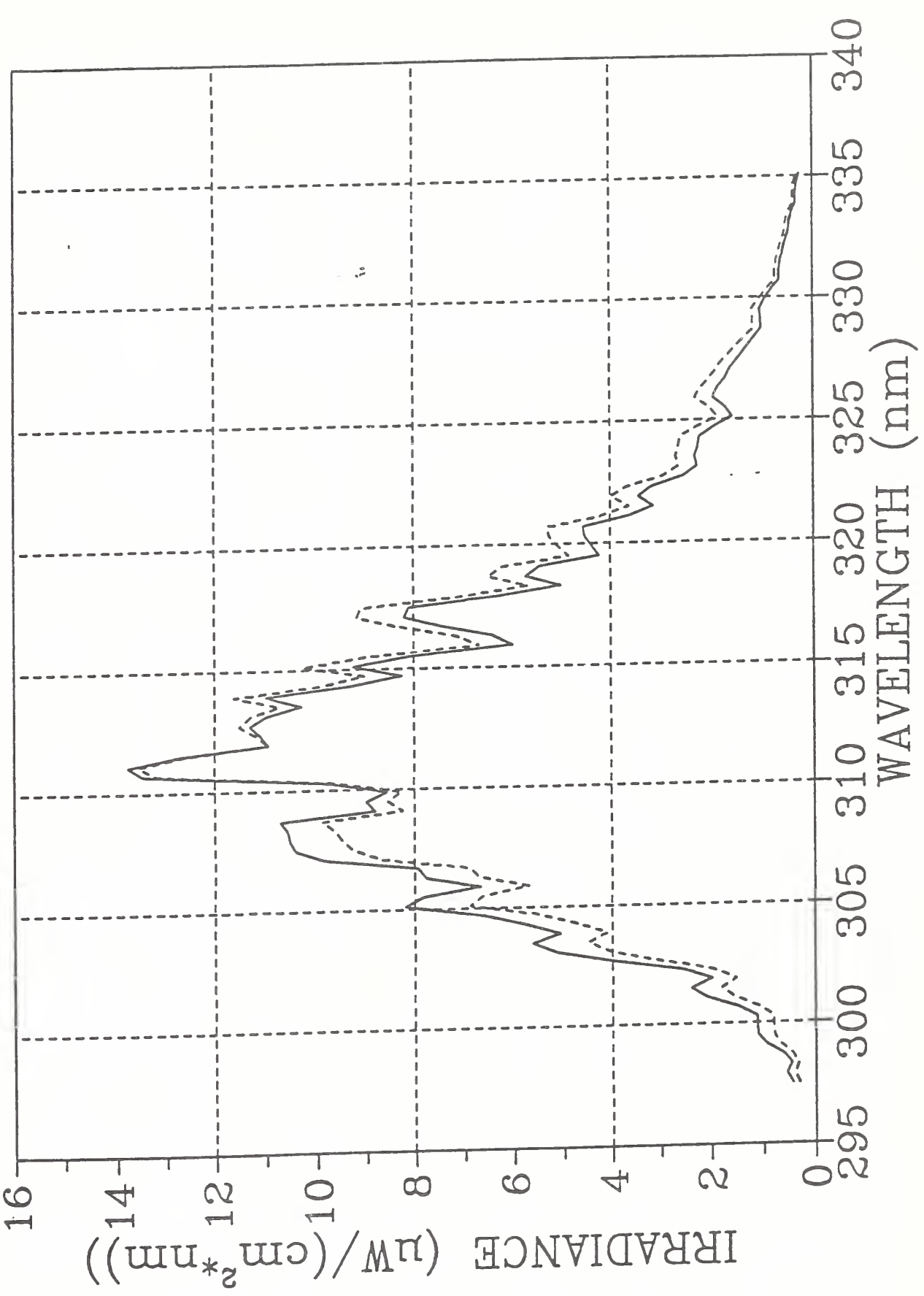




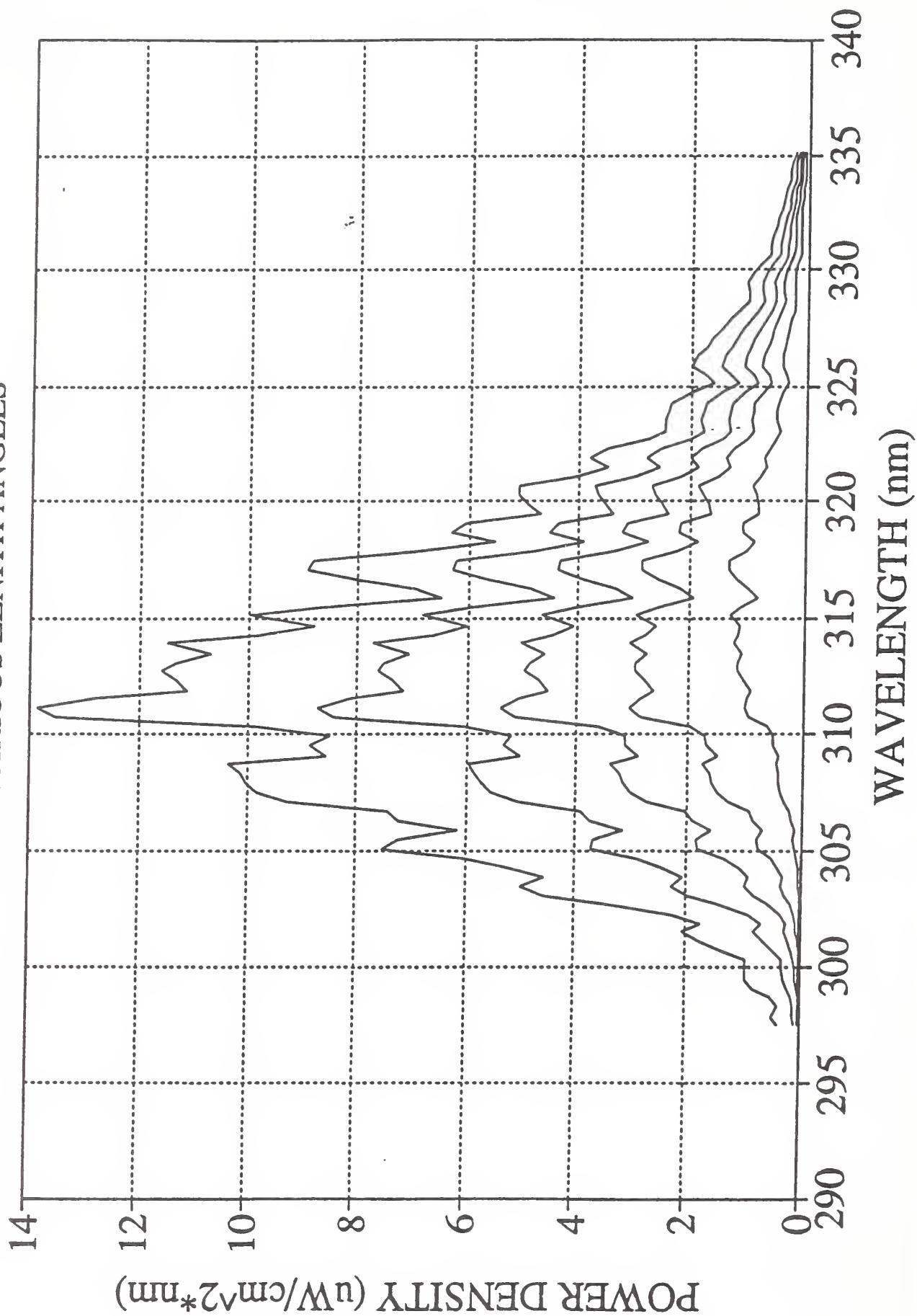




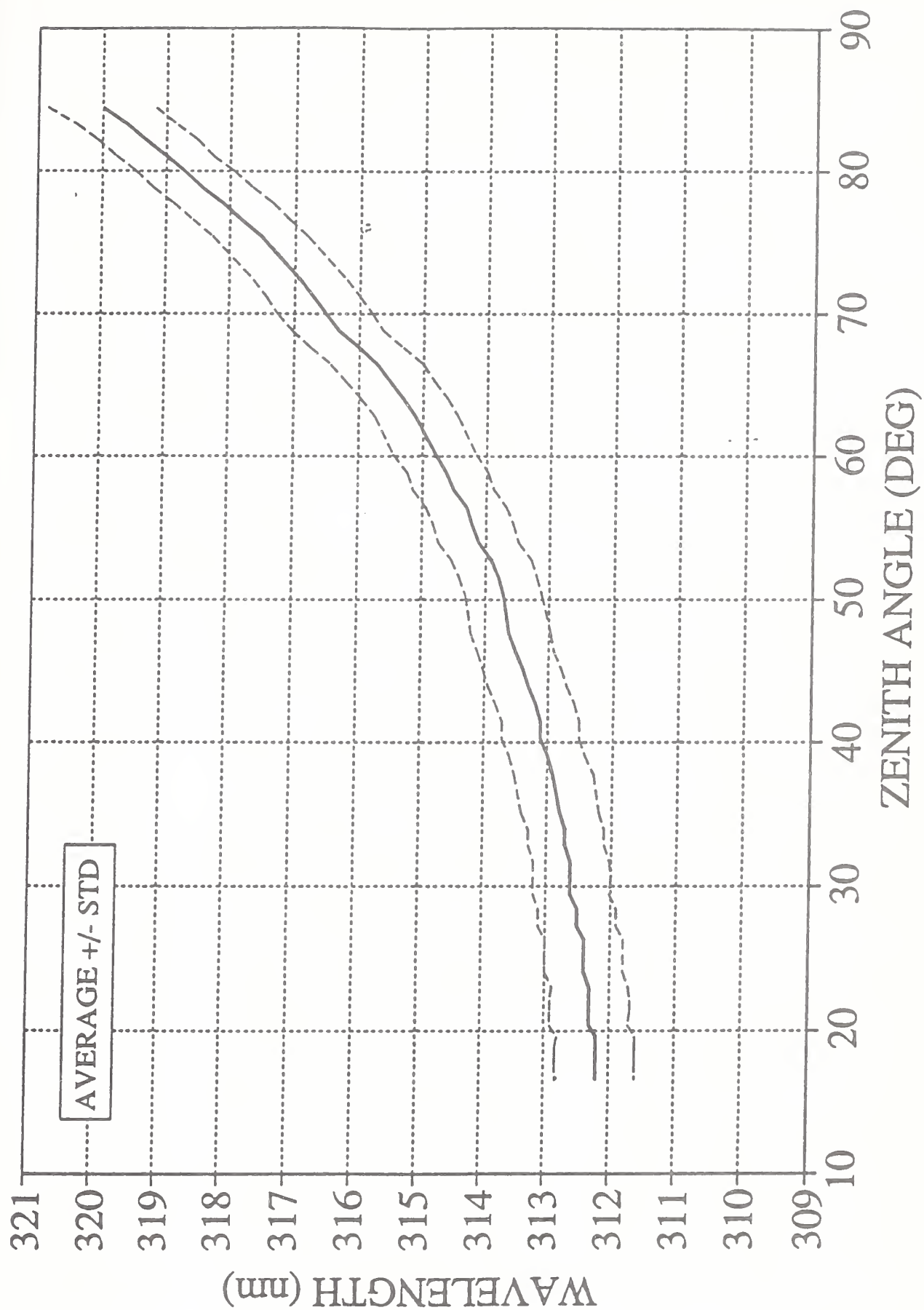




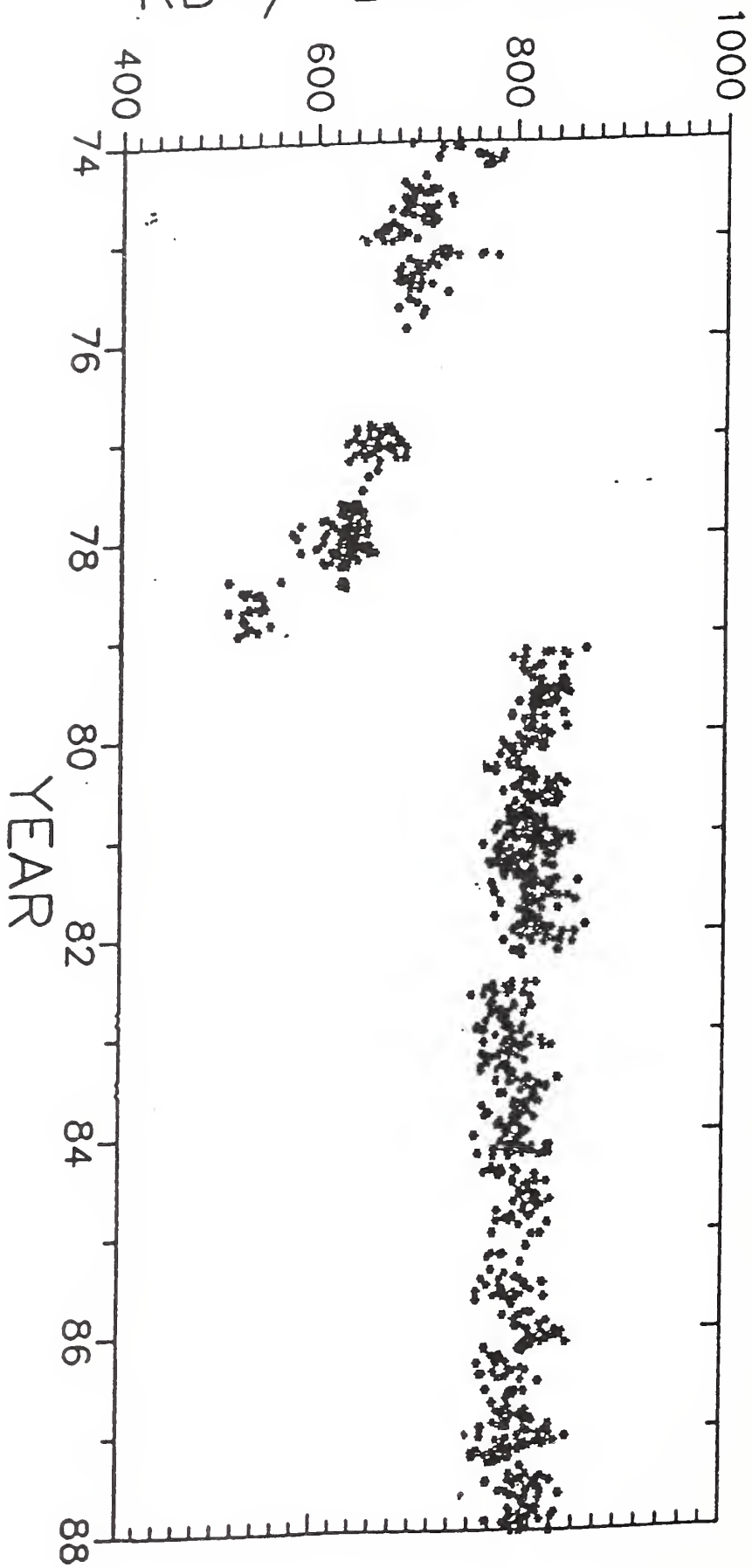
RB CONVOLUTION
AT VARIOUS ZENITH ANGLES



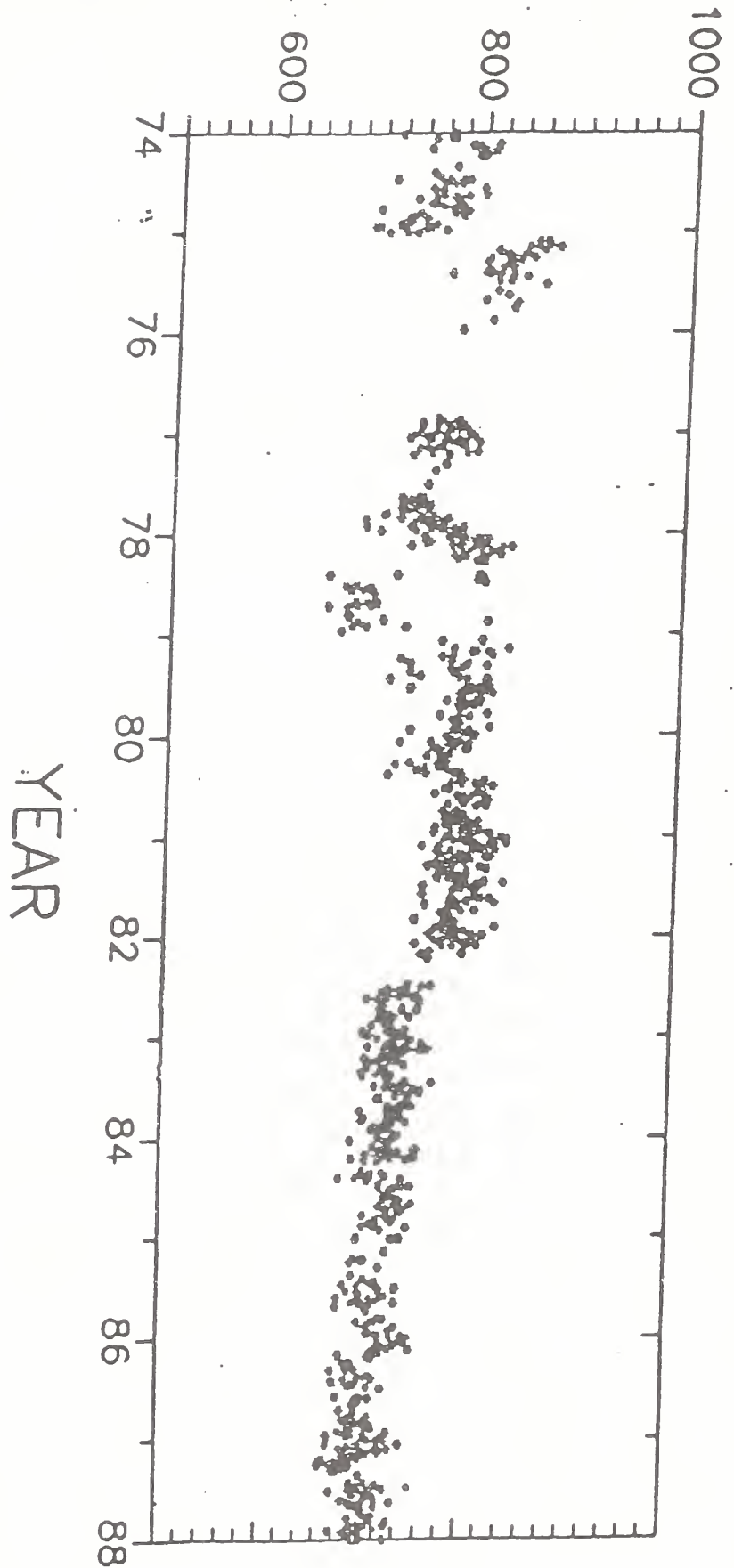
RESEARCH REPORT
JUNE 22, 1990



RB / BIRD MODEL



RB / BIRD MODEL



DOE Atmospheric Radiation Measurement Program

**Dr. Gerald Stokes
Pacific Northwest Laboratory**





UV-B Workshop Presentation

ARM measurements

- The ARM mission
- ARM Experimental Framework
- ARM Experimental Approaches
- What ARM measures
- Where ARM makes measurements



C-226



ARM measurements

Gerry Stokes
Pacific NW Laboratory



The ARM mission

- Radiative transfer
- Cloud life cycle and properties
- Emphasis on process studies

GM Stokes
March 10, 1992

ARM Experimental Framework

- The heart of ARM is the Cloud and Radiation Testbed (CART), a flexible experimental facility designed to facilitate the comparison of model predictions and observational data



ARM Experimental Approaches

- Instantaneous radiative fluxes
- Single column model
- Data Fusion and Assimilation
- Hierarchical Diagnosis



Instantaneous radiative fluxes

- Concurrent characterization of the state of the atmosphere and the consequent fluxes and their associated moments taken over both space and time under clear sky, general overcast and broken cloud conditions



What ARM measures

- Radiation measurements
- Other surface fluxes
- Basic meteorological measurements
- Cloud distribution
- Aerosols



Radiation measurements

- Broad-band radiometry: BSRN
- Spectral measurements: AERI, SORTI (NDSC)
- Flux divergence: ARM-UAV
- USDA-Harrison UV-B measurement



Other surface fluxes

- Latent and sensible heat: Bowen ratio, eddy correlation
- Precipitation: OK mesonet; NEXRAD



Radiative column; SPECTRE

- Temperature: RASS
- Water vapor: Raman lidar



Basic meteorological measurements

- Radiative column; SPECTRE
- Surface network: OK mesonet; PAM II
- Boundary measurements: profiler demo



Cloud distribution

- Visible imagery: Scripps camera
- Scanning radar: 35/94 GHz
- Satellite and UAVs



Aerosols

- Surface sampling (CMDL)
- Radiatively inferred quantities
- Lidar inferred quantities (Raman and Ceilometer)

Where ARM makes measurements

- Oklahoma-Kansas: Instrumented grid-cell
- Tropical Western Pacific: E-W Chain
- North slope: Penetrating to the marginal ice zone

Network for the Detection of Stratospheric Change

**Dr. Michael Kurylo
National Aeronautics and Space Administration**

Network for the Detection of Stratospheric Change

(NDSC)

**A set of high-quality remote-sounding research
stations for observing and understanding
the physical and chemical state of the stratosphere.**

**Complemented by secondary stations,
satellite measurements,
and existing monitoring networks.**

NDSC

Goals

Long Term:

- Provide early and continuing detection of stratospheric changes (physical & chemical).
- Provide the means to understand such changes (discern the causes).

Short Term:

- Study the temporal and spatial variability of atmospheric composition and structure.
- Provide the basis for ground truth and complementary measurements for satellite & Shuttle sensors such as UARS and ATLAS (independent calibrations).
- Provide data for testing & improving multi-dimensional stratospheric models (chemical & dynamical).

NDSC

Realities (Pluses & Minuses)

Satellites:

- Represent most promising means of obtaining extensive global data.
- Have encountered difficulties as totally independent systems for trends determinations.
- Cost and long lead time limit role in trend detection over the next decade.

Limited Network:

- Designed to detect stratospheric changes from selected specific locations.
- Not intended to provide global averages or global trends.
- Provide critical testing of multi-dimensional atmospheric models.

NDSC

Assumptions

- Existing and planned satellite systems will continue (NOAA SBUV, SAGE, UARS, etc.).
- Confidence in ozone trends determined from satellite systems is increased by comparisons with those from ground-based systems. (Note recent successes with TOMS & SAGE and anticipated results from EOS instruments.)
- ALE/GAGE and NOAA CMDL networks are *adequate* for ground level monitoring of long-lived gases (CFCl₃, CF₂Cl₂, CCl₄, CH₃CCl₃, N₂O, CH₄, and CO₂).
- Dobson network provides longest record for column ozone. (Intercomparison with NDSC & satellite instruments is critical.)
- Current temperature measurement systems are *inadequate* for accurate long-term trends.
- No systematic long term measurements exist for other stratospheric species.

NDSC

Measurement Priorities

1. Column ozone
2. Vertical profile of ozone (0 - 70 km)
3. Temperature (0 - 70 km)
4. Vertical profile of ClO
5. Vertical profile of H₂O
6. Vertical distribution of aerosols
7. Vertical profile or column of NO₂
8. Stratospheric column of HCl
9. Vertical profiles of long-lived tracers: CH₄, N₂O, etc.
10. Other species: HNO₃, OH, ClONO₂

NDSC

Priority Rationale

1. Solar UV penetration.
2. Stratospheric temperature structure (influence on circulation & climate).
3. Rates of chemical reactions; stratospheric temperature structure controlled by O₃.
4. Catalysis of O₃ destruction (predicted atmospheric concentration increasing 5% per year).
5. Radiative & chemical balance of the stratosphere; dominant source for OH.

NDSC

Priority Rationale (continued)

6. Importance in Antarctic & following major volcanic eruptions; effects on optical sensor data.
7. Catalytic control of O_3 ; coupling of NO_x and ClO_x .
8. Partitioning within ClO_x family.
9. Tracers for changes in atmospheric motion.
10. Changes in stratospheric composition.

NDSC

Instrumentation

<u>Species</u>	<u>Instrument</u>	<u>Status</u>
O ₃ column	Dobson	Operating
	Brewer	Operating
	UV/Vis.	Operating
O ₃ (0-20 km)	YAG Lidar	Operating
(15-45 km)	Excimer Lidar	Operating
(25-75 km)	Microwave	Operating
Temperature	Lidar	Operating
ClO (25-45 km)	Microwave	Under Development
H ₂ O (0-30 km)	Balloon Hygr.	Operating
(>35 km)	Microwave	Operating
(>20 km)	"	Under Development
Aerosols (0-30 km)	Lidar	Operating & Under Development

NDSC

Instrumentation (continued)

Species	Instrument	Status
NO ₂ (strat. col.)	UV/Visible	Operating
HCl (strat. col.)	IR	Operating
CH ₄ (strat. col.)	IR	Operating
N ₂ O (20-50 km)	Microwave	Demonstrated
HNO ₃ (strat. col.)	IR	Operating
ClONO ₂ (strat. col.)	IR	Demonstrated
OH (40-60 km)	UV Fluor.	Research Mode
	Excimer Lidar	Research Mode
HO ₂ (30-60 km)	Microwave	Demonstrated

NDSC

Stations

- Latitudinal distribution (minimum sampling of mid-latitude, tropical, and polar air masses => minimum of 5 sites)

Northern Hemisphere - mid & (?) high latitude

Southern Hemisphere - mid & (?) high latitude

Tropics

Polar (NH & SH)

- Co-location of instruments (~150 km?)

May be compromised by other logistical, meteorological, and chemical considerations.

- Dry, high altitude (>2000 m) sites

Minimize interferences from tropospheric water and aerosol columns (as quantified by instrument testing).

- Clear skies, view of horizon, low pollution

Instrument specific

- Maximum polar latitude

Range of solar zenith angles (IR)

NDSC

Design phase (formalized November, 1989 in Geneva)

- Requires experimentalists, theorists, statisticians, and data analysts.

Implementation & Operation (initiated Nov., 1989 in Geneva & continued June, 1990 in Washington & July, 1991 in UK)

- Scientific team infrastructure.
- Research oriented mode of atmospheric monitoring.
- Involvement of senior P.I.
 - site visits
 - quality control (calibrations & intercomp.)
 - data analysis
- Skilled local talent (daily operations).
- Continued involvement of theorists / modelers / analysts for comprehensive data interpretation.

Costs

- \$3M+ per station for instrumentation.
- \$2M+ per year operating costs (5 stations).

NDSC

NASA Activities

Instrument Development:

O ₃ Excimer Lidar	McDermid (JPL)
O ₃ Excimer Lidar (Mobile Intercomparator)	McGee (GSFC)
T & Aerosol Lidar	McGee (GSFC)
O ₃ Microwave	Parrish (Millitech), Connor (LaRC)
ClO Microwave	Parrish (Millitech) Solomon (SUNY)
H ₂ O Microwave	Schwartz, Bevilacqua (NRL)
H ₂ O Microwave (Mobile Intercomparator)	Olivero, Crosky (Penn State)
UV/Vis. Spectrometer	Mount, Solomon (NOAA)
IR Spectrometer	Murcay (U. Denver)

NDSC

NASA Activities (continued)

Other:

Table Mountain Observatory

- Test & Research Facility (calibrations, intercomparisons)
- Operational restrictions (IR & μ wave)

Stratospheric Ozone Intercomparison Campaign (STOIC), July 1989

- First major NDSC measurement activity

Satellite Ground-Truthing and Assessments

- UARS Correlative Measurements
- SBUV (TOMS) Instrument Properties

Future Intercomparisons, Testing, & Evaluation at OHP, Lauder, etc.

Microwave Retrieval Algorithm Development (Connor & Bevilacqua)

NDSC

NOAA Activities

Instrument Development:

**UV/Vis. Spectrometer - Mount, Solomon (NOAA)
(5 NDSC-quality instruments)**

Tropospheric O₃ Lidar - Proffitt (NOAA)

Other:

Upgrading of Mauna Loa Observatory

- **construction of NDSC facility**

UV/Vis. Instrument and Analysis Intercomparison

Data-Handling / Analytical Capabilities

- **examination of temperature lidar data**
- **synoptic context of NDSC data**
- **statistical analysis for site selection**

Satellite Accuracy Assessments

- **SBUV/2 error analysis (retrieval algorithms)**

Global Climate Model Analyses

- **to assist in NDSC sampling strategies**

NDSC

Current Status

Management:

- Steering Committee - primary managerial body

Internal operational oversight

Scientific oversight

Recommend implementation & funding actions

Insure existence of needed working groups
within the Science Team

- Science Team

Forum for conducting the business of operating
the NDSC

Operation via subgroups organized around

Instrument Type (lidar, microwave, etc.)

Molecule Addressed (O₃, NO₂, Cl-
containing, etc.)

Function (theory component, data
archiving, calibration / intercomparison,
site management, other network
coordination, etc.)

NDSC

Current Status (continued)

Initial Membership - Steering Committee

Chairman: M. Kurylo (NIST / NASA Hq)

Vice Chairman: A. Cox (NERC, U.K.)

P.I.'s & Alternates:

Lidar G. Megie (CNRS)
S. McDermid (JPL)

UV/Vis. A. Matthews (DSIR)
J. Pommereau (CNRS)

Microwave R. Bevilacqua (NRL)
J. De La Noe (CNRS)

IR W. Mankin (NCAR)
R. Zander (U. Liege)

Theory S. Solomon (NOAA)

Satellite J. Miller (NOAA)

NDSC

Current Status (continued)

Initial Membership - Steering Committee

Peers:

- C. Rodgers (Oxford U.)
- J. Russell (NASA LaRC)
- V. Khattatov (CAO, Moscow)
- P. Newman (NASA GSFC)
- W. Hill (Univ. Wisc.)
- R. Prinn (M.I.T.)

Ex Officio:

- R. Watson (NASA Hq)
- D. Albritton (NOAA)
- M. McFarland (AFEAS FP / CMA)
- R. Bojkov (WMO)
- P. Usher (UNEP)
- R. Cervellati (ENEA, Italy)
- D. Cadet (INSU - CNRS)
- H. Ott (CEC)

NDSC

Current Status (continued)

Initial Membership - Science Team

There are 1 or 2 P.I.'s associated with each of the instrument types at the primary NDSC sites. These P.I.'s constitute the Science Team.

Current P.I.'s are those, who (over the past couple of years) have proposed for and obtained support for the specific NDSC activity.

The addition of new P.I.'s will be a joint enterprise between the Steering Committee and the supporting organizations (via their Ex Officio members).

Co-Investigators on activities within the NDSC will play major roles in many of the Science Team's subgroups.

NDSC

Current Status (continued)

Stations / Sites:

Five primary stations have been selected -

Alpine Station - including Observatoire Haute Provence in France (44 N) and Jungfrauoch in Switzerland (46.5 N)

Mauna Loa/Mauna Kea observatory in Hawaii (20 N)

Lauder, New Zealand (45 S)

Dome C, Antarctica (74.5 S)

Arctic Station - tentatively identified to include the planned Canadian observatory at Eureka, the Ny-Alesund observatory in Spitzbergen, and Thule in Greenland. Details are being worked out regarding the qualification of instruments and the availability of site facilities and support personnel.

Several others are under consideration such as:

Reunion Island

Mt. Kenya

NDSC

Current Status (continued)

Topics being finalized by the Steering Committee:

Determination of interim measurement activities in Antarctica.

Discussions of tropical site options and evaluation of candidates.

Determination of new instrument development and existing instrument deployment priorities.

Completion and acceptance of Data Protocol.

Adoption of procedures for formal affiliation of theorists on the Science Team.

Development of a formalism for the inclusion of complementary investigators and measurement sites.

Development of complementary interfaces with other measurement programs.

Potential for Satellite Measurements

**Dr. Dan Lubin
California Space Institute
University of California, San Diego**

POTENTIAL FOR SATELLITE MEASUREMENTS OF SURFACE ULTRAVIOLET CLIMATOLOGY

Dan Lubin

California Space Institute, UCSD

AFEAS UV-B Monitoring Workshop
Washington, D.C., March 10, 1992

1. SATELLITE OZONE MEASUREMENTS -

Nimbus-7 TOMS/SBUV

2. RADIATIVE PROPERTIES OF CLOUDS -

Earth Radiation Budget Experiment (ERBE)

3. EXAMPLE -

"The Budget of Biologically Active Ultraviolet Radiation in the
Earth-Atmosphere System" (J. E. Frederick and D. Lubin)

4. RESEARCH IN PROGRESS -

"Spatial Distribution of Antarctic Surface UV Radiation Using
Satellite and In Situ Measurements" (Catherine Gautier, UCSB;
D. Lubin, CalSpace, UCSD)

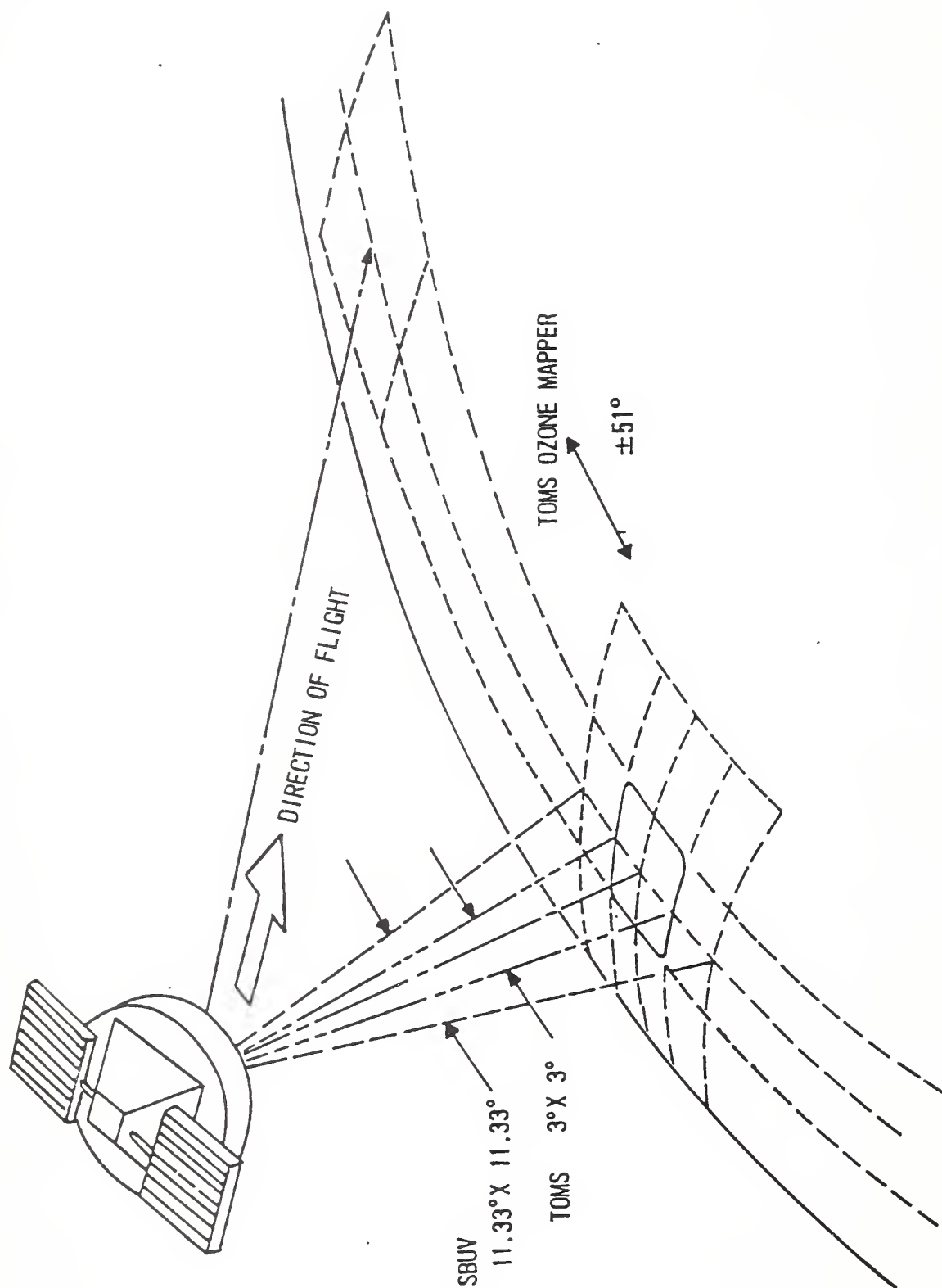


Figure 7-7 IFOV of SBUV/TOMS in the Nadir

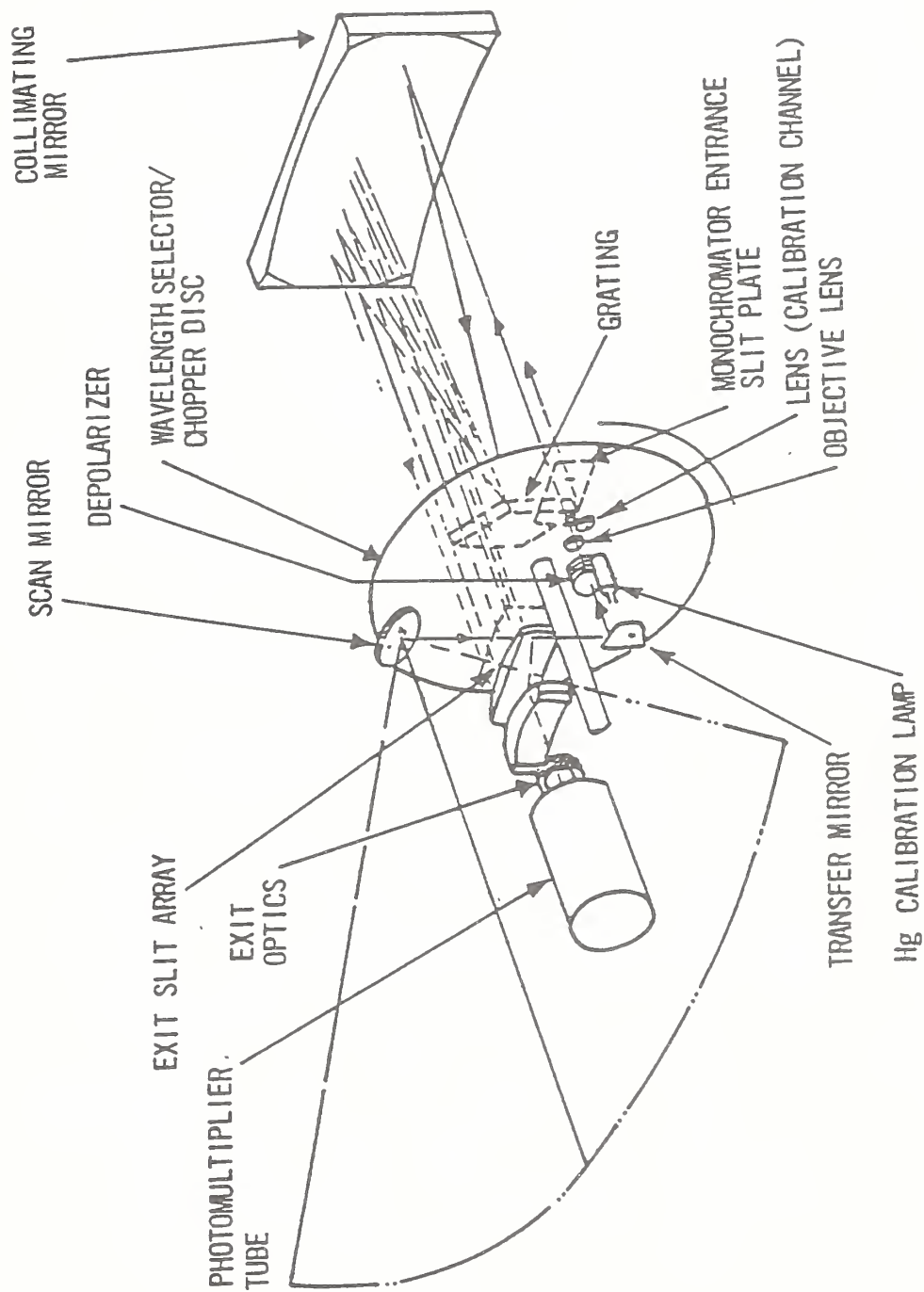


Figure 7-5 TMS Optics Diagram

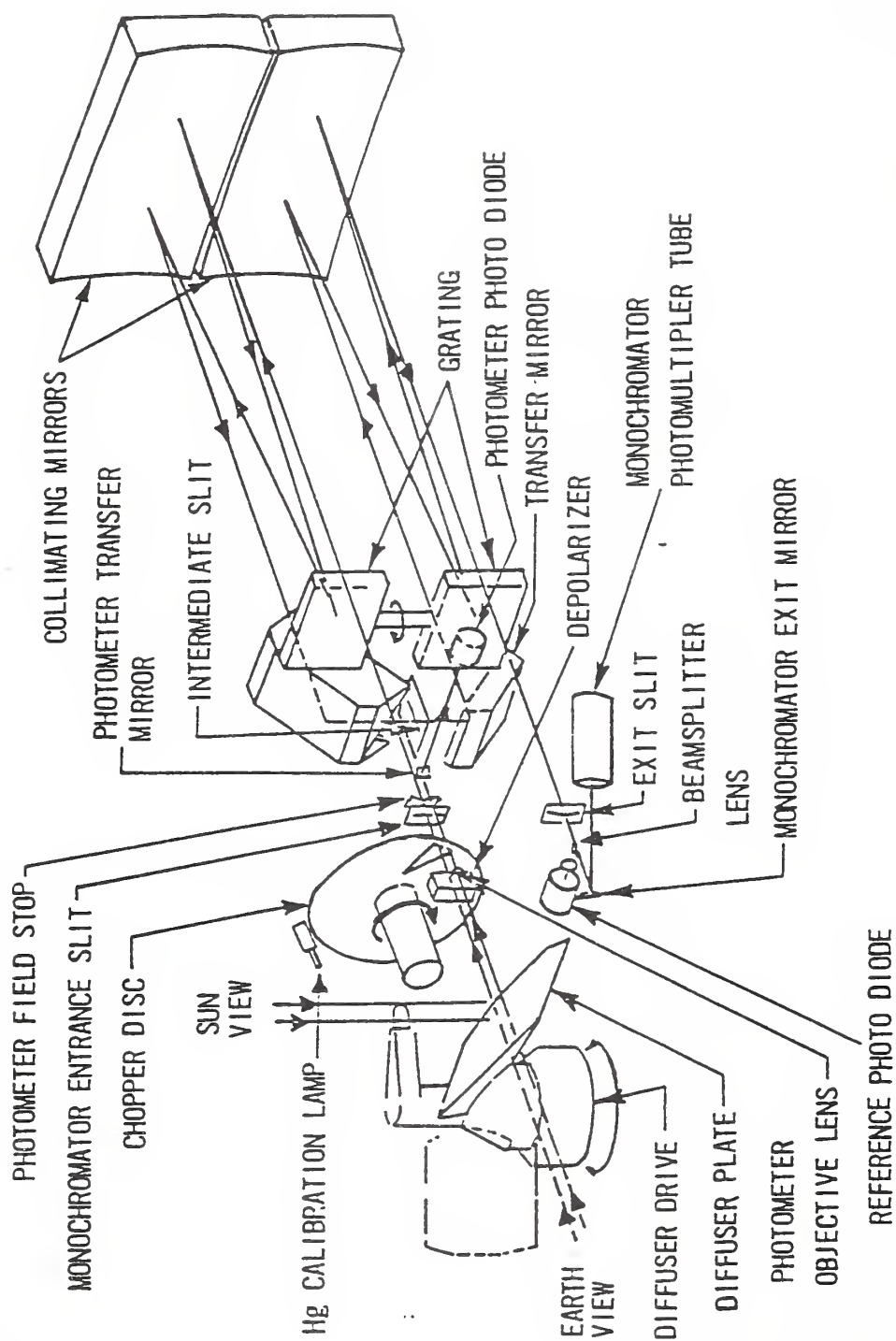


Figure 7-2 SBUV Optics Diagram

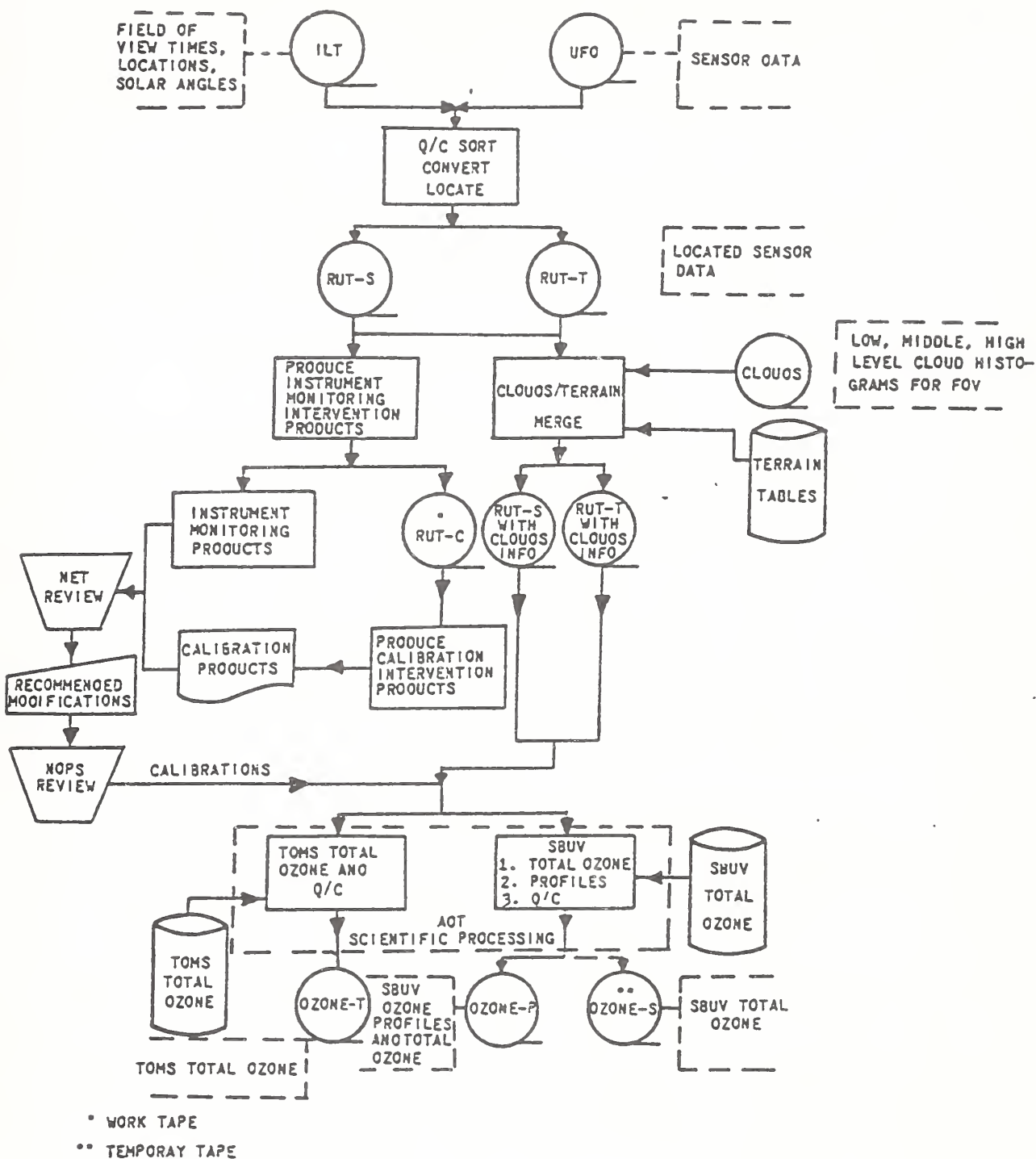


Figure 7-9a SBUV/TOMS Process Flow Chart

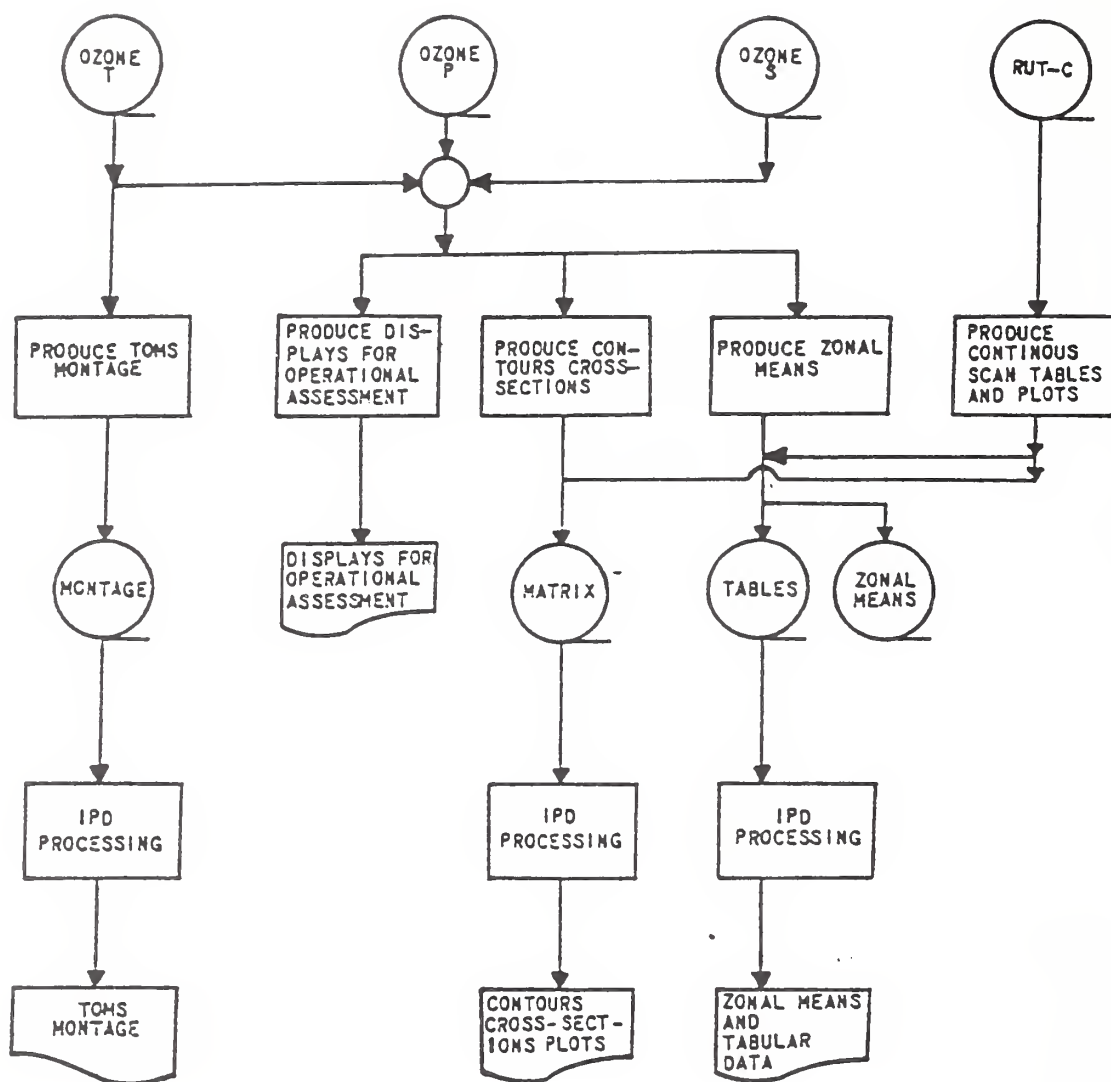


Figure 7-9b SBUV/TOMS Process Flow Chart

TOTAL OZONE MEASUREMENT BY SATELLITE

e.g., Klenk et al., *J. Appl. Meteorol.*, 21, 1672-1684, 1982.

1. Backscattered Radiance - lookup tables from radiative transfer theory
functions of ozone amount, ozone vertical profile, solar zenith angle, surface reflectivity, surface pressure
2. Effective Surface Reflectivity - computation from longest - λ UV radiances
also from reference photometer measurements made concurrently with monochromator steps, to account for small FOV changes
3. Preliminary Ozone Estimates - using differential absorption technique
wavelength pairs chosen to account for solar zenith angle dependence, e.g. {312.5 nm, 331.2 nm} for high sun, {317.5 nm, 339.8 nm} for low sun
surface pressures 1.0 ATM and 0.4 ATM
4. Determination of Surface Pressure - clear sky and/or clouds
reflectivity $R > 0.6$, assume clouds and pressure 0.4 ATM
 $R < 0.2$, assume clear skies and use surface terrain tables
 R in between, assume partly cloudy skies
5. Best Ozone Determination - interpolation using results 3 & 4.

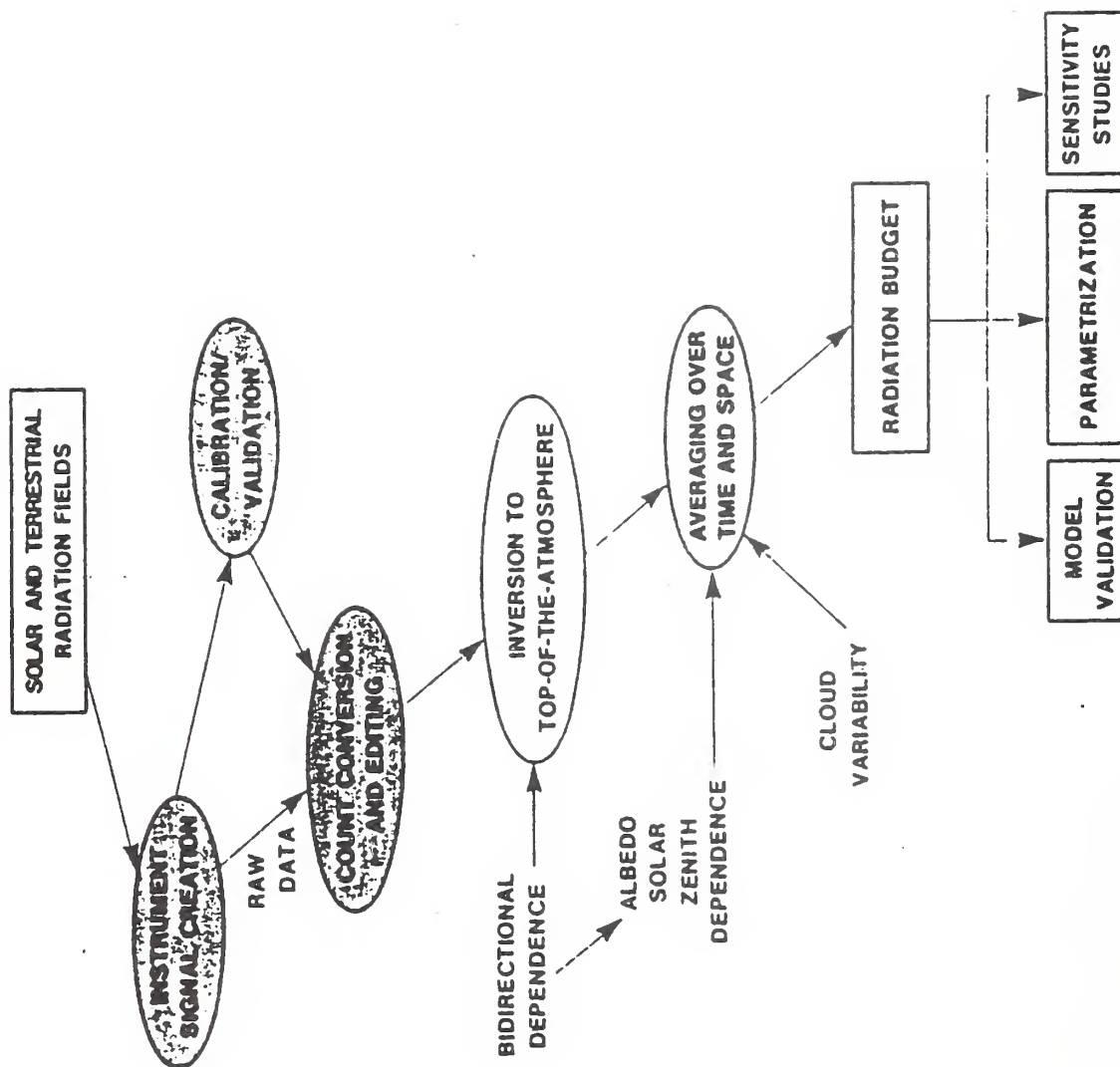
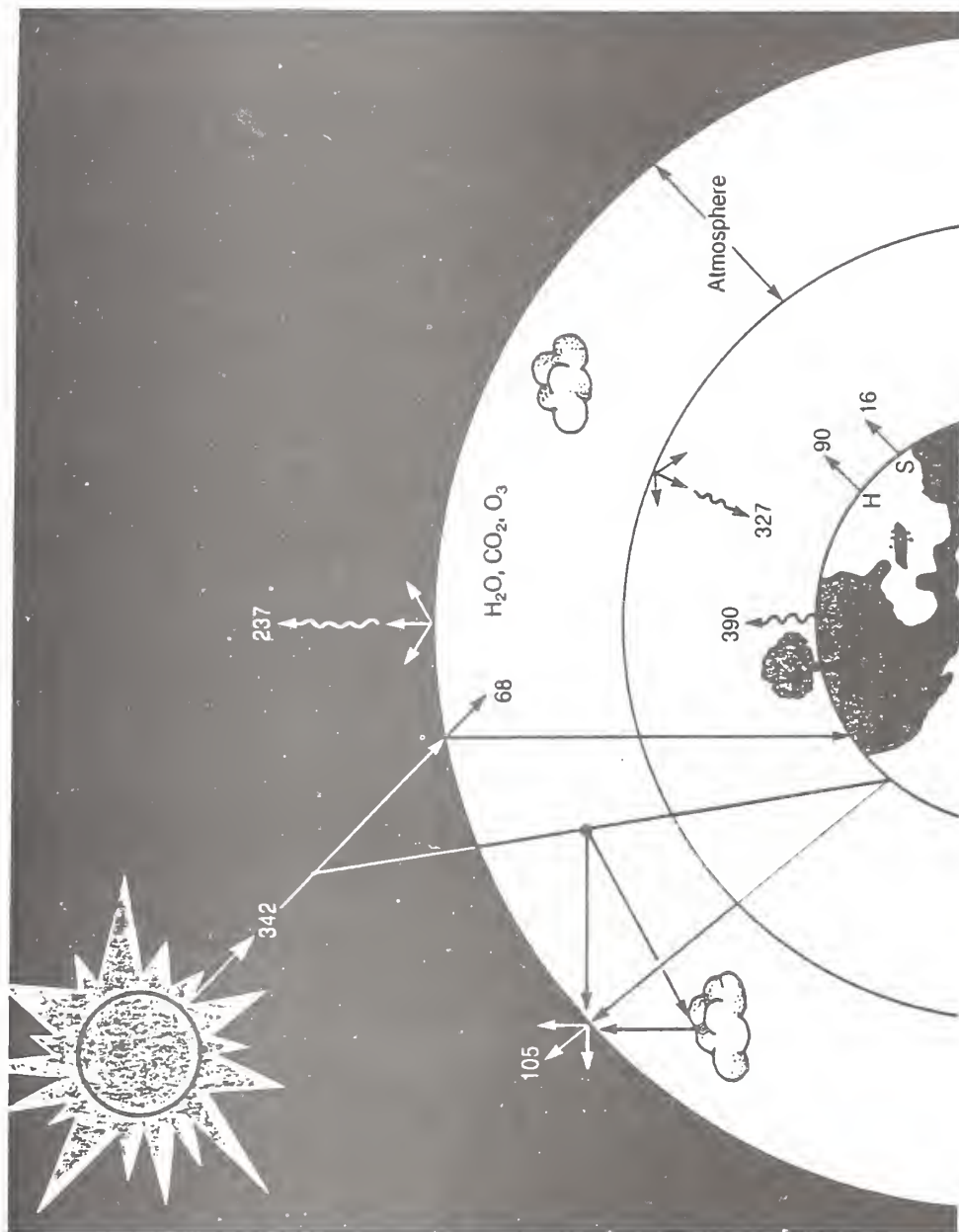


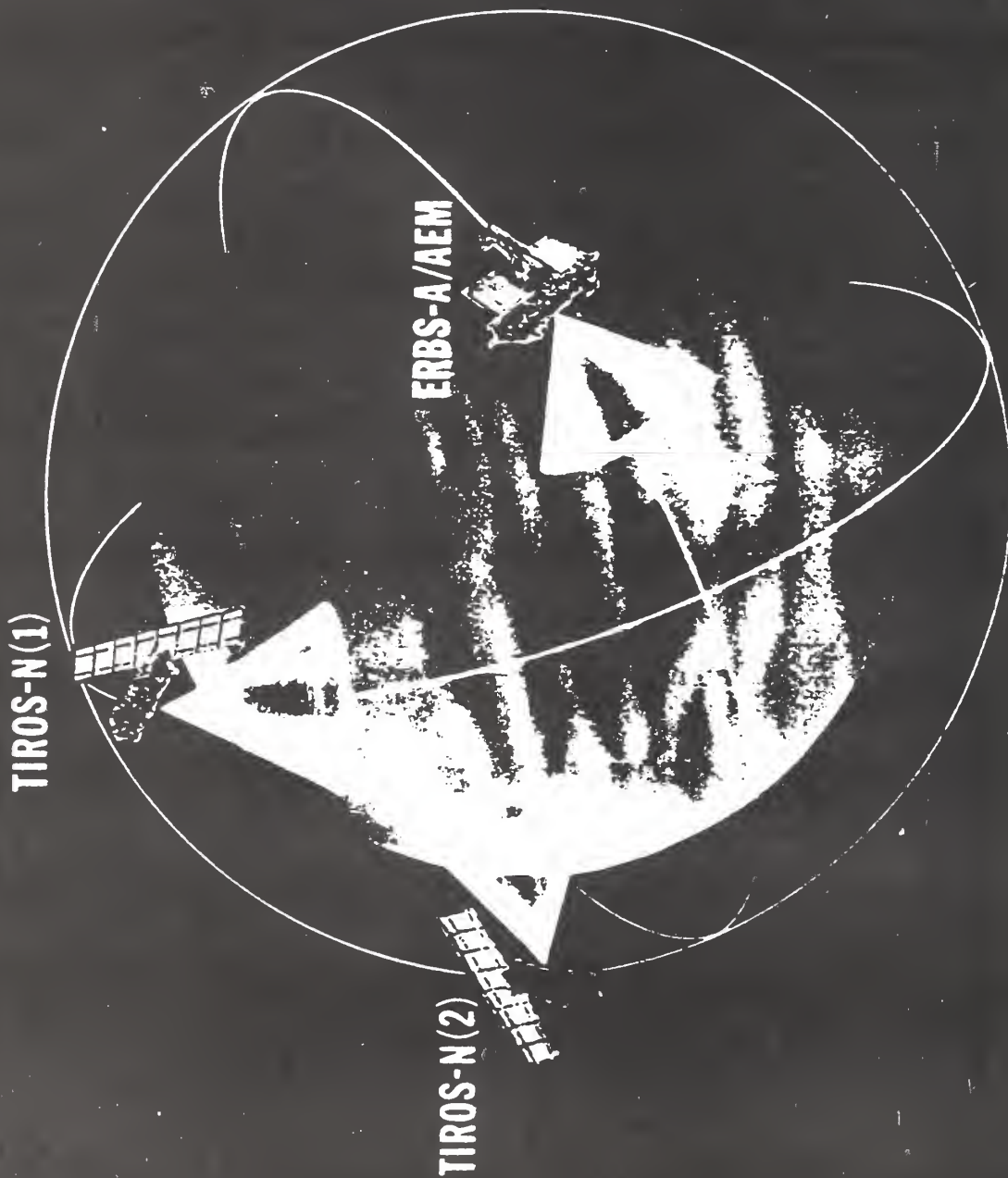
Fig. 10. Data flow chart.



Global energy balance for annual mean conditions. For the top of the atmosphere, the estimates of solar insolation (342 W/m^2), reflected solar radiation (105 W/m^2) and outgoing long-wave radiation (327 W/m^2) are obtained from satellite data. The other quantities are obtained from various published model and empirical estimates. These quantities include atmospheric absorption of solar radiation (68 W/m^2); surface absorption of solar radiation (390 W/m^2); downward long-wave emission by the atmosphere (327 W/m^2); upward long-wave emission by the surface (390 W/m^2); H , the latent heat flux from the surface (90 W/m^2); and S , the turbulent heat flux from the surface (16 W/m^2). H and S are averaged over both ocean and land. **Figure 1**

EARTH RADIATION BUDGET SATELLITE SYSTEM

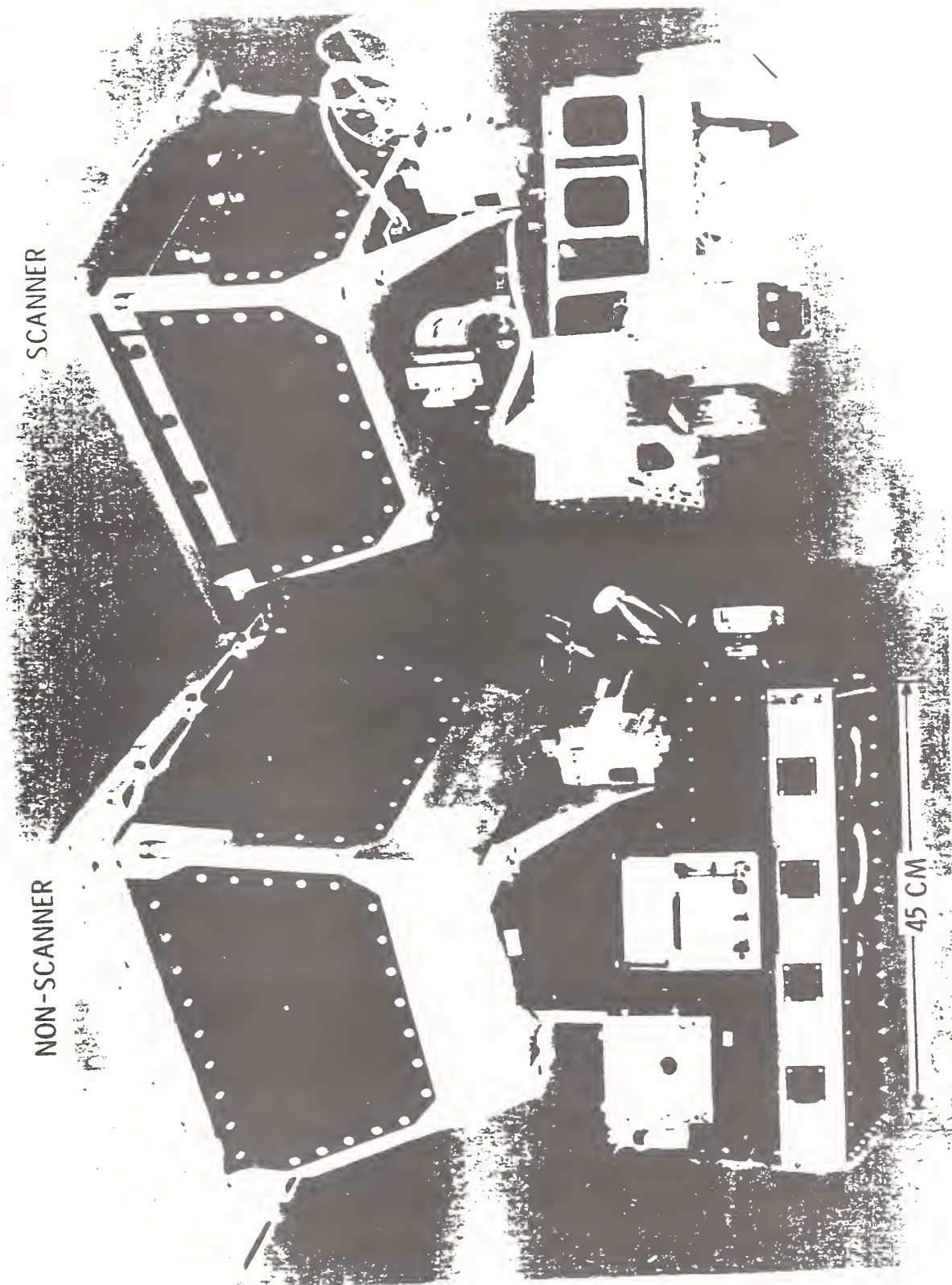
(ERBSS)



ERBE INSTRUMENTS

NON-SCANNER

SCANNER



The Budget of Biologically Active Ultraviolet Radiation in the Earth-Atmosphere System

John E. Frederick and Dan Lubin

Journal of Geophysical Research, 93(D4), 3825-32, 1988

1. Use Nimbus-7 SBUV for measuring atmospheric radiative properties
 - a) ozone via Klenk et al., J. Appl. Meteorol., 21, 1672-84, 1982.
 - b) surface and cloud albedo using measurement at 339.8 nm
 - c) "relative" radiometric calibration provided by on-board reference photodiode
2. Assume a linear relationship between fractional cloud cover q and SBUV-measured surface albedo R ,

$$q(R) = 0 \quad R \leq 0.2$$

$$q(R) = 2.5(R - 0.2) \quad 0.2 \leq R \leq 0.6$$

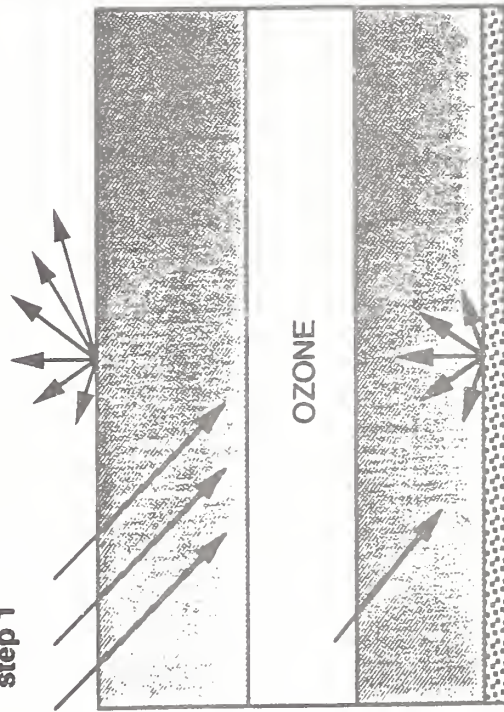
$$q(R) = 1.0 \quad R \leq 0.6.$$

3. Use a two-stream radiative transfer model to evaluate cloud optical thickness, and fractional components reflected to space, absorbed by the atmosphere, and absorbed at the ground,

$$f_s + f_a + f_g = 1.$$

ESTIMATION OF CLOUD RADIATIVE PROPERTIES USING NIMBUS-7 SBUV DATA

step 1

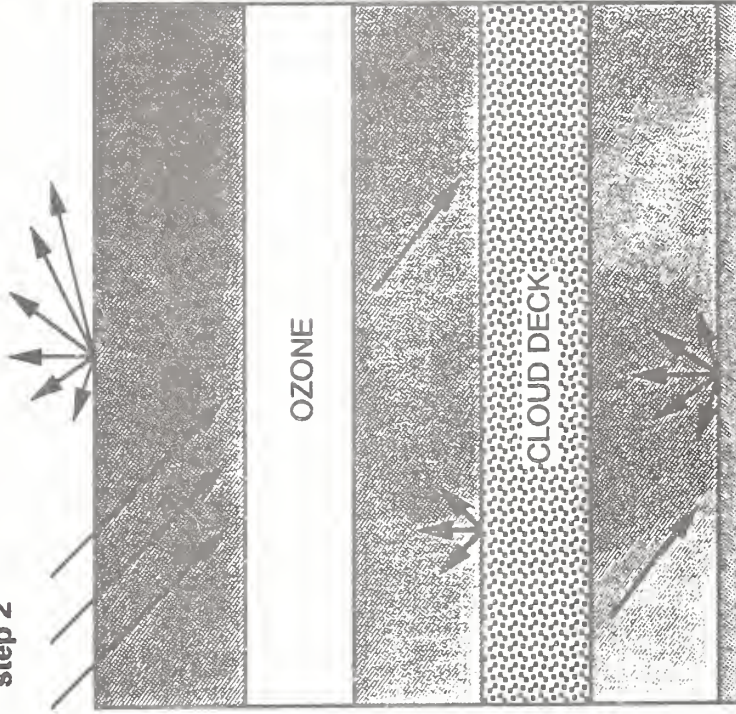


Lambertian surface at cloud top pressure

Assign cloud albedos 0.65, 0.75, 0.85

Compute planetary albedo (i.e., upward irradiance at top of atmosphere) as a function of latitude, time, and SBUV ozone amount

step 2



Lambertian surface at 1013.5 millibars

Varying cloud optical thickness, try to reproduce the planetary albedos of step 1

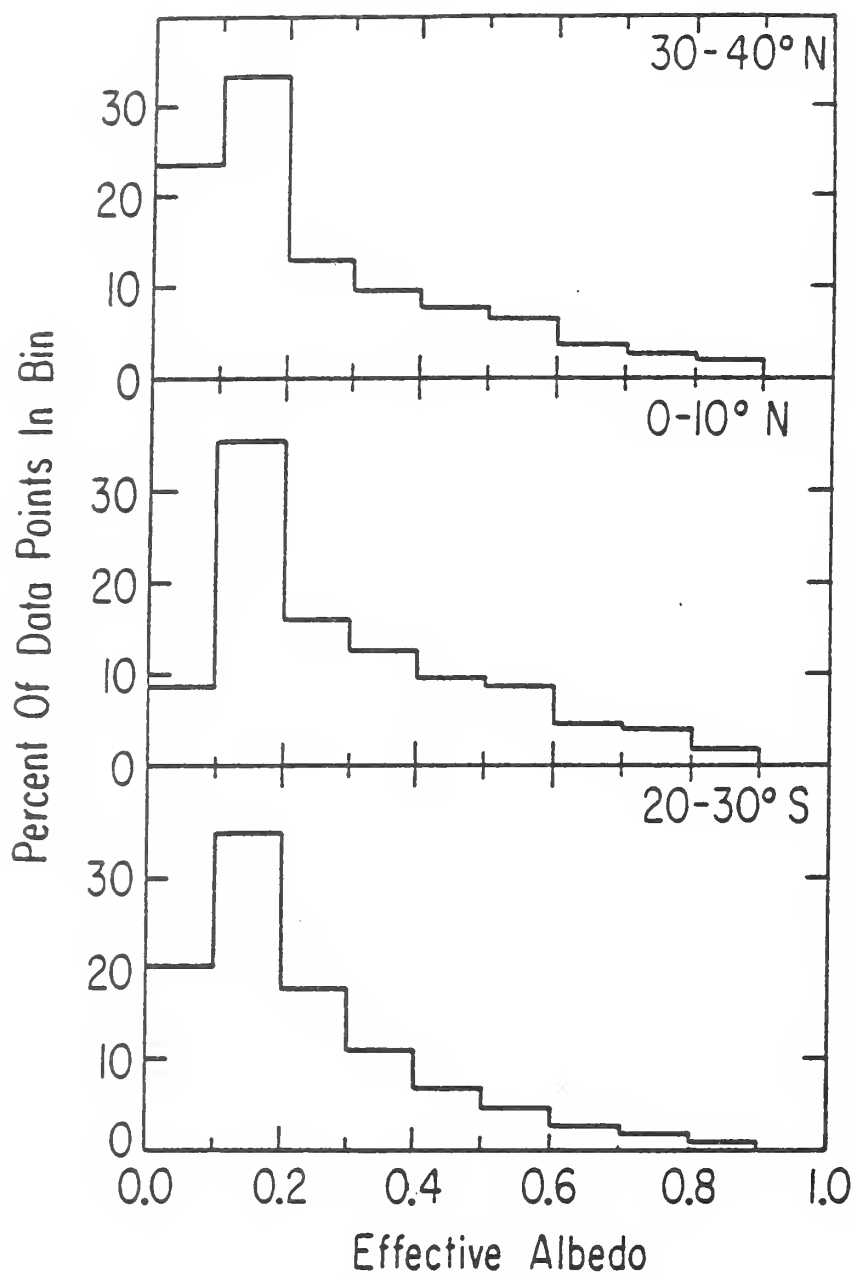


Fig. 2. Histograms of effective surface albedo derived from the Nimbus 7 SBUV instrument for July in three latitude bands. The radiation budget evaluation assumes albedos less than 0.2 to indicate clear skies. Albedos greater than 0.6 correspond to 100% cloud cover in the SBUV field of view.

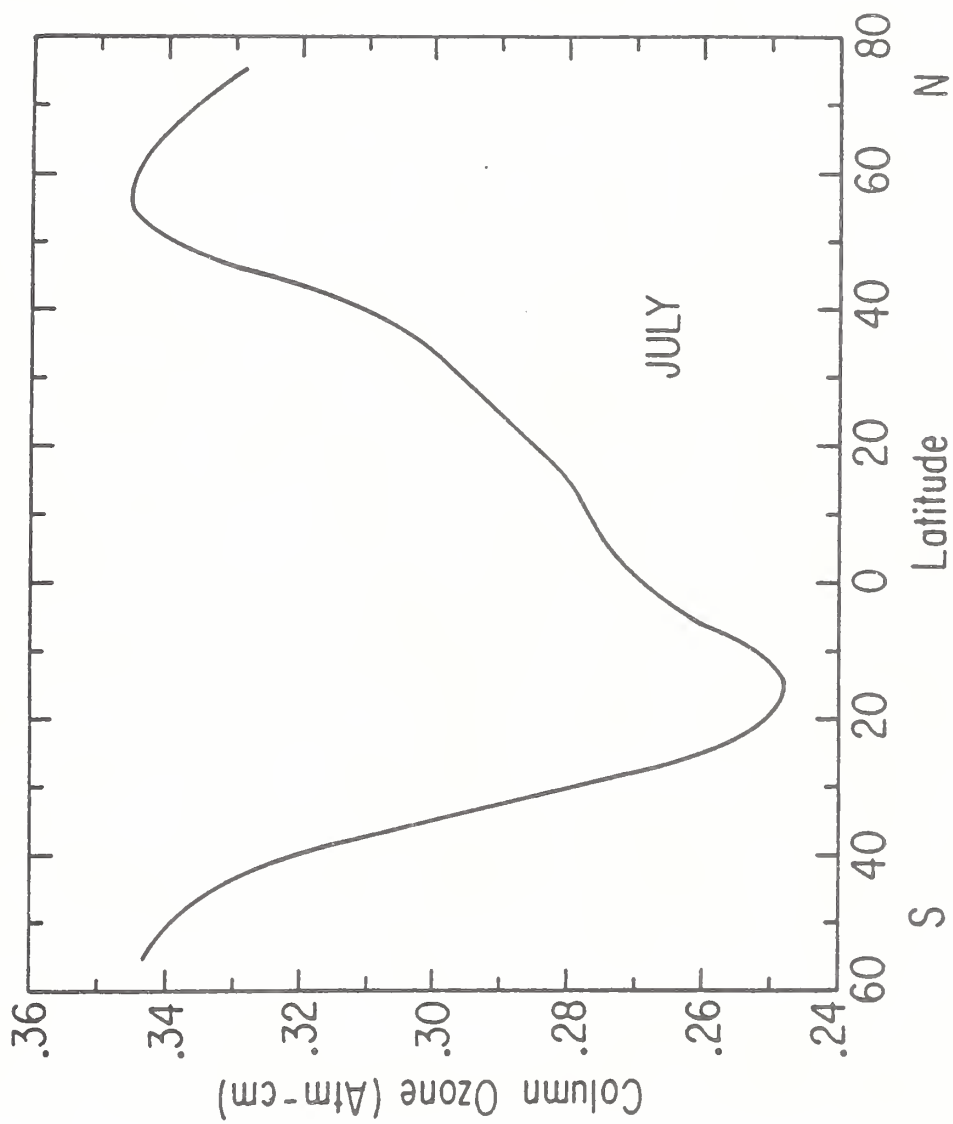


Fig. 3. Latitude distribution of total column ozone for July 1979.

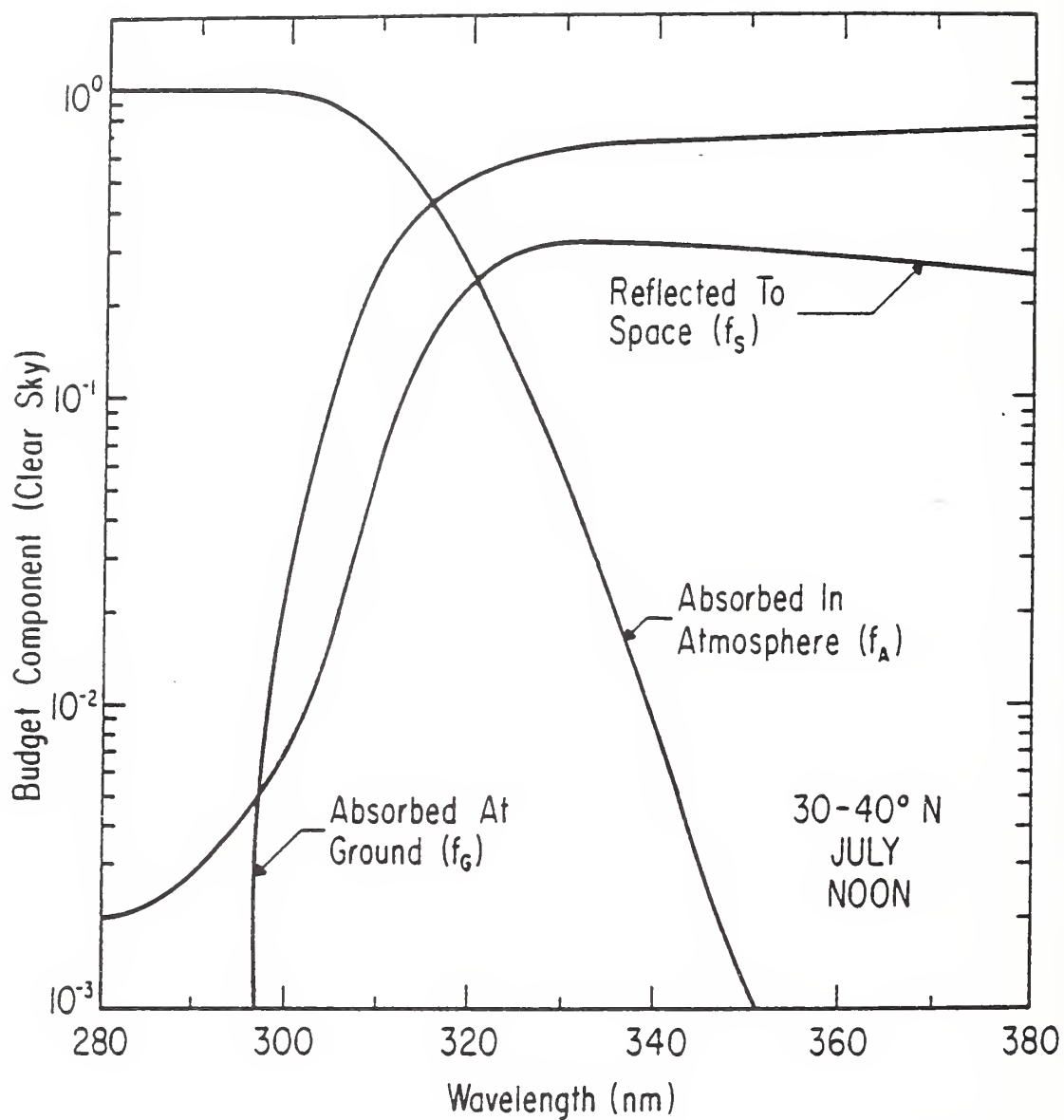


Fig. 4. Radiation budget components as functions of wavelength for the latitude band 30°-40° N, local noon, in July. Values refer to clear skies.

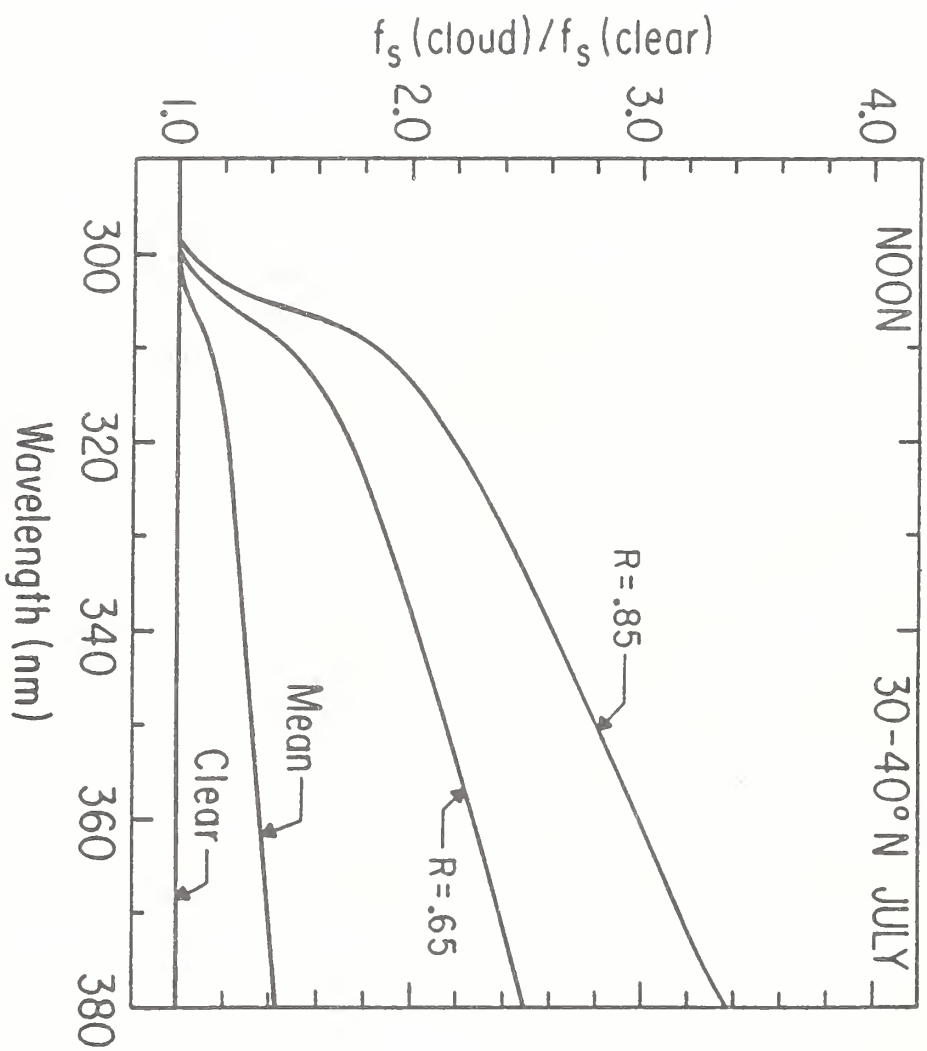


Fig. 8. Impact of cloud cover on the fraction of incident irradiance reflected to space for 30°–40°N July, local noon. The curve labeled "mean" includes all sky conditions. Effective albedos of 0.65 and 0.85 refer to 100% cloud-covered conditions.

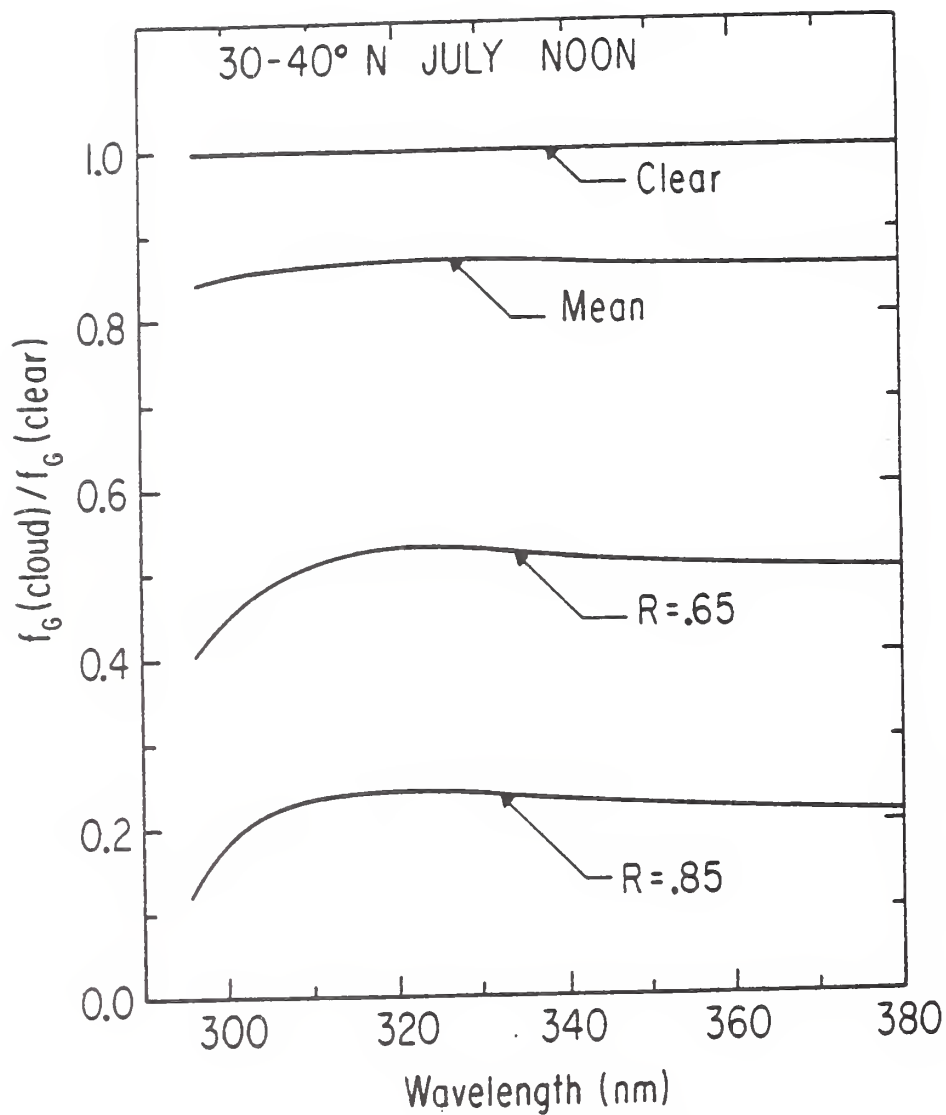


Fig. 9. Impact of cloud cover on the fraction of incident irradiance absorbed at the ground for 30°–40°N July, local noon. The curve labeled “mean” includes all sky conditions. Effective albedos of 0.65 and 0.85 refer to 100% cloud-covered conditions.

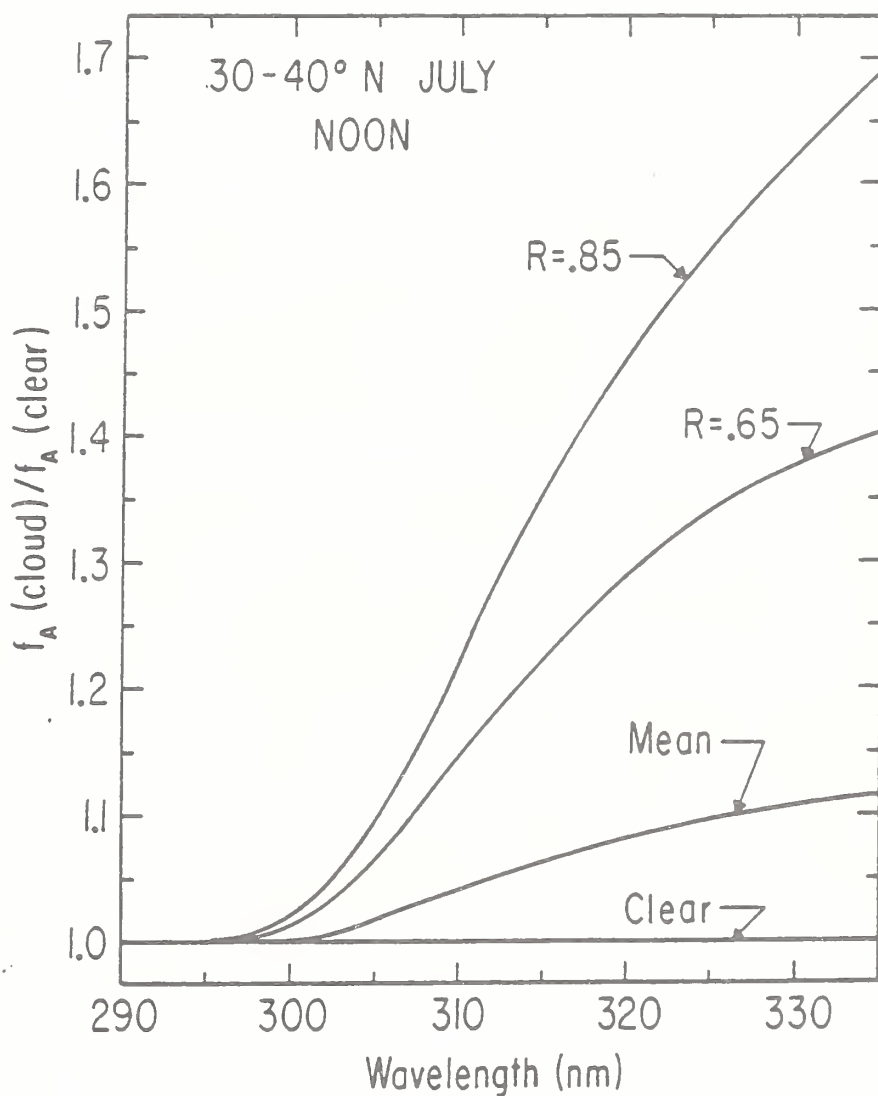


Fig. 10. Impact of cloud cover on the fraction of incident irradiance absorbed in the atmosphere for 30°–40°N July, local noon. The curve labeled "mean" includes all sky conditions. Effective albedos of 0.65 and 0.85 refer to 100% cloud-covered conditions.

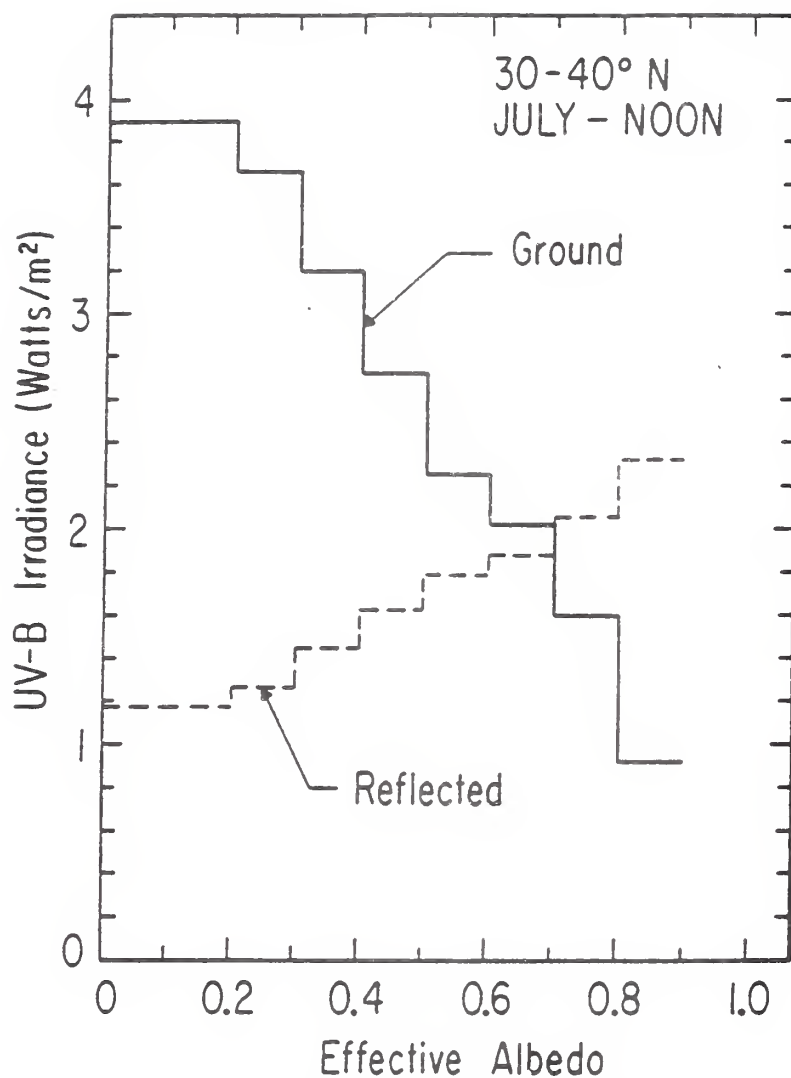
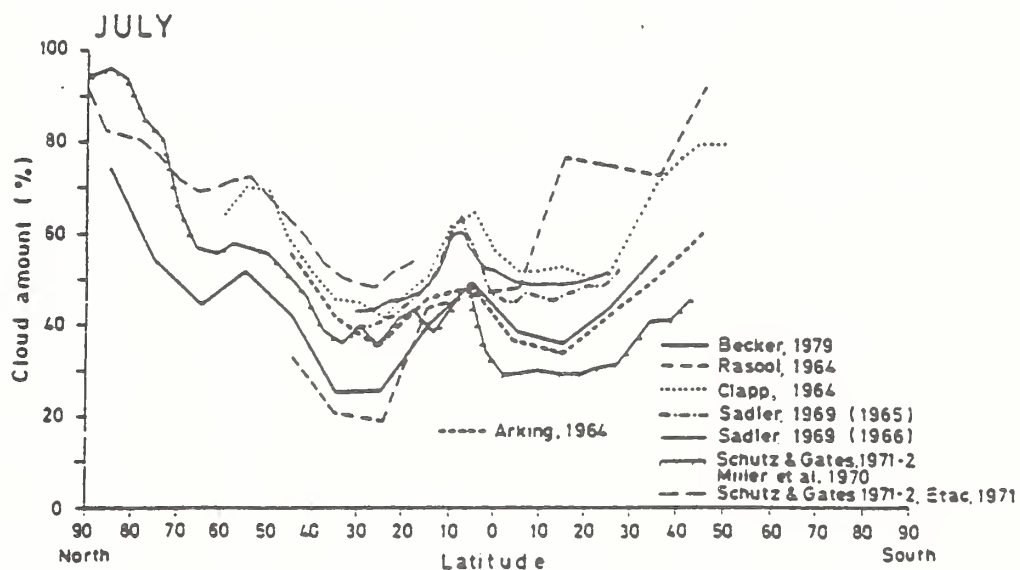
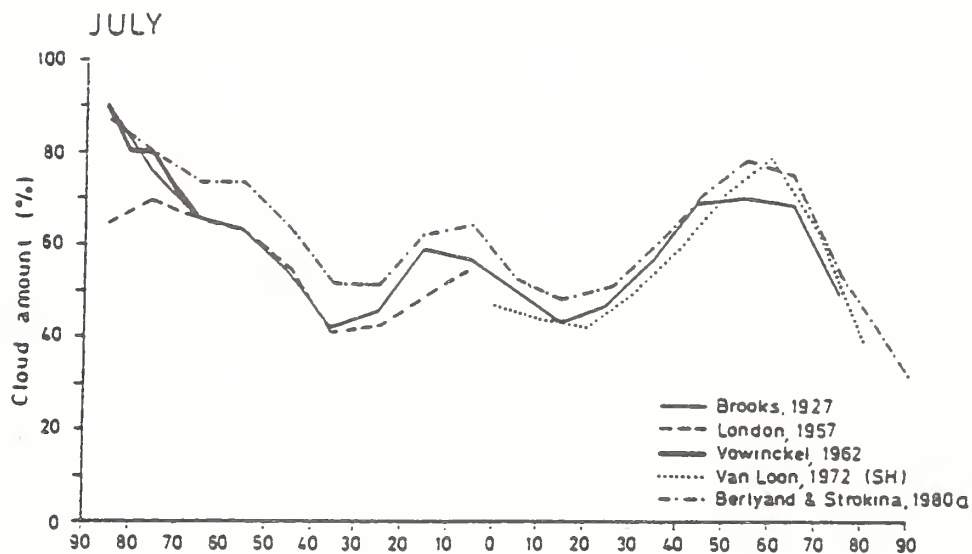


Fig. 12. Variation of total UV-B irradiances incident on the ground and reflected to space with cloud cover conditions. Results refer to 30°–40°N for July, local noon. The effective albedo combines changes in fractional cloud cover and cloud optical thickness.

Cloud climatologies for July

from Hughes, *J. Clim. Appl. Meteorol.*, 23, 724-751, 1984.



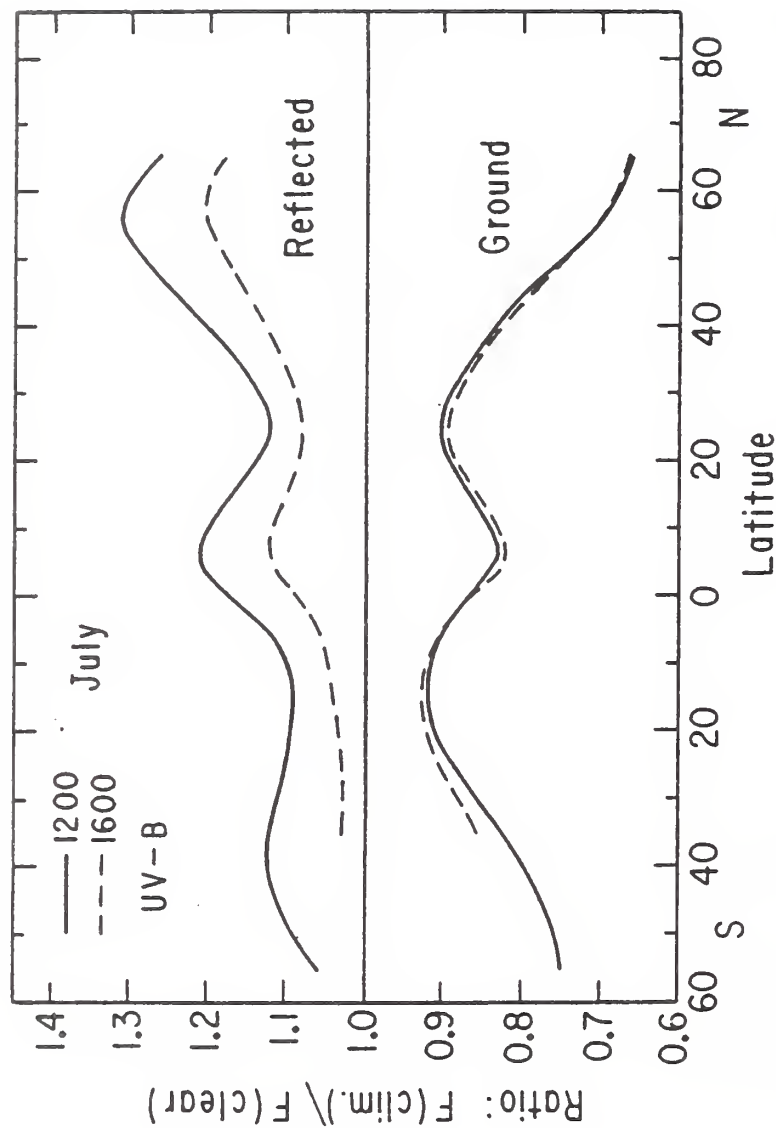


Fig. 14. Influence of climatological mean cloud cover on the total UV-B irradiances reflected to space and absorbed at the ground as functions of latitude. Results appear as ratios to the clear-sky values for July at 1200 and 1600 LT.

CONCLUSIONS

1. Measurements from the Nimbus-7 SBUV instrument enabled us to quantitatively define the budget of solar UV-A and UV-B in the earth-atmosphere system.
2. Enhanced backscattering by clouds increases the fraction of UV-B radiation absorbed by the atmosphere (up to 50% increase depending on UV-B wavelength).
3. Underneath a cloud, the UV-B radiation field is more isotropic than under clear midday skies - enhanced absorption by tropospheric ozone worth investigating.
4. The mean cloud cover (for July, in this study) reduces UV-B surface irradiance to 70-90% of the clear sky value, depending on latitude.
 - * This is comparable to DNA-effective irradiance enhancements due to projected mid-latitude ozone depletion.
 - * The "mean" cloud cover consists of mostly fractional cloud cover, the identification and treatment of which is an unresolved issue in satellite climate studies.

EXPERIMENTAL COMPONENTS

* SCRIPPS ANTARCTIC RESEARCH CENTER

1. satellite tracking facilities maintained at McMurdo & Palmer stations provide complete coverage of the Antarctic continent & Southern Ocean
2. both HRPT & DMSP capability (AVHRR, TOVS, OLS, SSM/I)

* NSF UV-MONITORING NETWORK

1. high resolution scanning spectroradiometers operating 280-625 nm
2. instruments deployed at Palmer, McMurdo, South Pole, Ushuaia (southern Argentina), and Barrow (Alaska)
3. measurements made every daylight hour

* BROADBAND SURFACE RADIOMETRY

1. Pyranometers, Pyrgeometer, PAR sensor (400-700 nm), AVHRR channels 1 & 2
2. all networked into NSF UV-monitor data stream

* ALL-SKY PHOTOGRAPHIC & VIDEO IMAGING

1. continuous daylight timelapse video using fisheye lens adapter, one image every 17 seconds
2. still photographs using Nikon 8mm fisheye lens precisely under satellite overpasses

* BOMEM FTIR SPECTRORADIOMETER

1. operating in mid-IR (500-2000 cm^{-1}) with 1 cm^{-1} resolution
2. greenhouse gas emission (under clear skies) & cloud infrared radiative properties

CLOUD PROPERTIES FROM SATELLITE DATA

* Adapt the Gautier (1981) model

In each pixel...

$$F_{\lambda}^{\downarrow} = F_{\lambda,clr}^{\downarrow} \left(\frac{1 - R_c}{1 - R_s R_c} \right)$$

$$F_{\lambda,total}^{\downarrow} = (1 - n) F_{\lambda,clr}^{\downarrow} + n F_{\lambda,c}^{\downarrow}$$

clear sky surface irradiance $F_{\lambda,clr}^{\downarrow}$ from 2-stream or δ -Eddington

Lambertian cloud reflectance R_c from AVHRR

Lambertian surface albedo R_s from clear sky composite (AVHRR or OLS)

cloud fraction n from all-sky images and satellite cloud detection algorithm

* More sophisticated radiative transfer

1. discrete ordinates (DISORT), δ -4-stream, δ -Eddington models
2. use in iterative mode to infer cloud optical & microphysical properties
3. cloud transmission & optical depth consistent with surface irradiance & TOA radiance measurements
4. cloud geometry from AVHRR channel 4,5 & FTIR measurements
5. surface and cloud bidirectional reflectance effects using DISORT
6. phase function effects (e.g., ice vs. water) using DISORT
7. spectral dependence of surface albedo

THE FAR SIDE By Gary Larson



© 1990 Universal Press Syndicate

-- The bozone layer: shielding the rest of the solar system from the Earth's harmful effects.

Non-U.S. National UV Research and Monitoring Programs

New Zealand

Dr. Richard McKenzie
Department of Scientific and Industrial Research

UVB MONITORING AND RESEARCH IN NEW ZEALAND

R. L. McKenzie

Department of Scientific and Industrial Research,
DSIR Physical Sciences, Lauder,
Central Otago, New Zealand
(Phone NZ 03-4473-411, fax NZ 03-4473-348)

*Summary of the Presentation by R. L. McKenzie
at the AFEAS UVB Workshop, Washington DC, March 11, 1992.*

The discovery of the Antarctic Ozone hole in 1985 stimulated public interest and debate in New Zealand about the incidence levels of UV irradiance at the surface, and future changes in it. By the end of the 1980s it was apparent that global ozone reductions had already occurred. In the New Zealand/Australia region there was statistical and anecdotal evidence that UV levels were already high compared with corresponding latitudes in the Northern Hemisphere, and with its close proximity to the Antarctic ozone hole, the risks of future enhanced UV levels are greater.

Before the 1980s, the only UV data available in NZ was from 2 Robertson-Berger meters. Results from these suggested that during clear sky conditions, UV levels in NZ were relatively high compared with comparable latitudes in the Northern Hemisphere (Nichol and Basher, 1987). Model calculations using a climatology of ozone measurements from the 1979-1982 period indicated that biologically active UV radiation in NZ was 10-15% higher than at comparable latitudes in the Northern hemisphere (McKenzie, 1991), and this has been suggested as a contributing factor to higher rates of incidence of skin cancer in NZ (McKenzie and Elwood, 1990).

Absolute UV spectral irradiance data are scarce in the Southern Hemisphere at mid-latitudes. In Australia measurements have been made for several years (Roy et al., 1988) but prior to 1989, the only spectroradiometric UV data available in New Zealand was from two short measurement campaigns in 1980 and 1988 (Bittar and McKenzie, 1990). In 1988 the DSIR initiated a programme to characterize the spectrum of solar ultraviolet (UV) radiation reaching the ground in New Zealand. A purpose-built instrument was developed at DSIR to enable routine measurements of cosine weighted UV irradiances incident on a horizontal surface at the ground. The aims of the UV measurement project are to determine its climatology, to identify regional differences, to understand the reasons for its variability, and to detect any long term trends.

The measurement system is based around a small, commercially-available double monochromator (focal length 100 mm, f-number f3, dispersion 10 nm/mm), which was modified, and temperature-controlled (36 ± 2 °C) to improve its stability. The instrument includes several novel features. A custom-made diffuser is used to improve on the cosine response available from commercially-manufactured diffusers. The mounting of this diffuser also incorporates a light baffle, to improve stray light rejection. A shadow band can be positioned so that the direct component of solar radiation can be masked from the instrument. This enables the diffuse and direct components of UV spectra to be studied independently. The spectral range covered is 290-450 nm, and the instrument bandpass is approximately 1 nm. However, the spectrum is sampled continuously at 0.2 nm intervals, and this oversampling enables the logged spectra to be aligned accurately (repeatability better than 0.02 nm) using a computer algorithm which compares the logged spectrum with a reference spectrum. A photomultiplier tube (pmt) detector is used, and the wide dynamic range necessary is achieved by allowing the high voltage which controls its gain to vary during the scan. Both the photomultiplier signal and the high voltage that controls the gain are logged. A supplementary diode detector samples broadband UV continuously during scans and the statistics of this data are logged so that intensity changes due to changing cloud cover during the scanning interval (200 seconds) can be identified. With the present system, useful measurements at 1 nm resolution are limited to irradiances greater than 10^{-3} mW cm⁻² nm⁻¹, which corresponds to a lower limit in wavelength in the region 290 to 295 nm (depending on the sun angle and ozone amount). This is a useful lower limit for many applications of relevance to the biosphere.

Measurements have been made routinely with this instrument at Lauder New Zealand (45°S, 170°E, elevation 370m) since December 1989. Scans are made each day at 5° intervals in solar zenith angle (SZA, for SZA > 75°), and 3 scans are also logged near local solar noon, whenever weather permits. The data is stored in binary format, and typically one month of data can be stored on a single 1.2 M Byte floppy disk. A log sheet of weather conditions (eg cloud cover, visibility), instrument changes and software changes is maintained. Absolute calibration is with reference to a 1000 W FEL lamp, traceable to NIST. After each calibration the lamp output is checked with a stable PIN diode detector, and the lamp is recalibrated annually at the DSIR irradiance standards laboratory. As further quality controls, instrument stability is assessed by means of regular stability tests (every 10 days) using a 55 W quartz halogen lamp and a mercury vapour lamp. After each day of observations, at least one of the measured spectra is graphically compared with calculated spectra.

The instrument specifications, calibration and quality control procedures, performance, and results from the first year of operation are discussed in McKenzie et al. (1992).

A range of atmospheric trace gas measurements, including total column ozone (with Dobson spectrophotometer) and ozone profiles (with ECC sondes) are available at Lauder, along with standard meteorological data, and occasional aerosol data. In addition, an all sky camera has recently been deployed to record cloud conditions during UV scans. This ancillary data greatly improves the ability to interpret the reasons for changes in UV irradiance. An application of the results, using concurrent ozone measurements to deduce the erythema (McKinlay and Diffey, 1987) Radiative Amplification Factor (RAF) resulting from changes in ozone, has been described by McKenzie et al (1991). This study showed that the RAF for erythema is 1.25 ± 0.20 , in approximate agreement with calculated RAFs of 1.1 (Madronich et al., 1991). However, changes in solar zenith angle, and changes in cloud cover are more important factors than changes in ozone in controlling erythema UV.

The spectral measurements are complemented by continuous UVB measurements using a filter instrument developed by International Light Inc. This is one of a NZ-wide network of instruments maintained by DSIR, with funding assistance from the NZ Department of Health. Data from these instruments are disseminated through the Telecom Network to local radio stations, and are used to inform the public about current UV levels in the summer. These results are expressed as "burn-times", defined as the time taken for erythemally-weighted irradiance to reach the minimum erythral dose (MED) of $21 \mu\text{J cm}^{-2}$. Typically in the summer the "burn time" is 15 to 20 minutes in NZ. In addition to this service, Television NZ includes estimates of burn times provided by the NZ Meteorological Service in televised national weather forecasts. These "forecasts" are based on calculated clear sky UV levels assuming a climatology of ozone variability. As such, they should not strictly be termed a forecasts, since ozone levels show large day-to-day and inter annual variability. However, the publicity has been useful in educating the public that it takes minutes rather than hours for UV damage to occur.

Efforts are continuing to extend and improve the quality, and geographical coverage of UV measurements in the NZ region through the deployment of new instrumentation and through participation in intercomparisons with other instruments. In addition, studies investigating the possible use of real time satellite data (eg cloud cover, ozone fields) to infer UV irradiance levels are in progress.

References

Bittar, A., and R. L. McKenzie, "Spectral UV Intensity Measurements at 45°S: 1980 and 1988.", *J. Geophys. Res.* 95 D5, p 5597-5600, (1990).

McKenzie, R. L., and J. M. Elwood, "Intensity of Solar Ultraviolet Radiation and its Implications for Skin Cancer", *NZ Medical Journal*, 103, pp 152-154, (1990).

McKenzie, R. L., "Application of a simple model to calculate latitudinal and hemispheric differences in ultraviolet radiation.", *Weather and Climate* (11), pp 3-14, (1991).

McKenzie, R. L., P. V. Johnston, M. Kotkamp, A. Bittar and J. D. Hamlin, "Solar Ultraviolet Spectro Radiometry in New Zealand: Instrumentation and sample results from 1990", *Applied Optics*, (accepted 1992).

McKenzie, R. L., W. A. Matthews and P. V. Johnston, "The relationship between erythral UV and ozone derived from spectral irradiance measurements", *Geophys. Res. Lett.*, 18(12), pp 2269-2272, (1991).

McKinlay, A. F., and B. L. Diffey, "A reference action spectrum for ultraviolet induced erythema in human skin", *CIE Journal*, 6, 1, pp 17-22 (1987).

Nichol, S. E., and R. E. Basher, "Sunburning ultraviolet radiation at Invercargill, New Zealand", *Weather and Climate*, 7, pp 21-25, 1987.

Roy, C. R., H. P. Gies, and G. Elliot, "Solar ultraviolet radiation: personal exposure and protection", *J. Occup. Health Safety - Aust NZ*, 4, 2, pp 133-139 (1988).

Madronich, S., L. O. Bjorn, M. Ilyas, and M. M. Caldwell, in Chapter 1 of UNEP report "Environmental effects of ozone depletion: 1991 update", (1991).

Non-U.S. National UV Research and Monitoring Programs

Sweden

**Dr. Ulf Wester
Swedish Radiation Protection Institute**



Dept. of Non-ionizing radiation.

March 6, 1992

5201/421/92

Summary of UVB-monitoring activities in Sweden

Natural solar UV exposure data have in Sweden often been needed as a reference in conjunction with evaluations of exposures from other sources. Such data are also needed for educating the public and some professional groups to various degrees of awareness of the sun as a possible health hazard - and limit skin cancer incidence by avoiding sunburns. The Swedish Radiation Protection Institute (an authority for protection of the public from radiation hazards) has initiated and funded projects in Sweden to measure and map biologically active natural ultraviolet radiation.

Swedish Solar UV-exposure data - present situation:

Swedish UV-data are results from studies with spectroradiometers, predictions from mathematical models, Data from a RB-meter since 1983, other UV-monitors since 1989 and network solar UV-monitoring since 1990.

Instruments:

A Dobson ozone spectrophotometer was used in Uppsala 59.9°N 1951-1966. That instrument has been modernized and is used by SMHI in Sweden at Vindeln 64.1°N (Funded by the Swedish Environmental Protection Agency).

Laboratory UV-spectroradiometers (EG&G and Optronic mod 742) have been used since 1980 for solar UV measurements during short periods since 1980 - mostly in Stockholm 59.4°N - and spectral data from it have been stored.

A Brewer Ozone spectroradiometer has been operated at the Swedish Meteorologic and Hydrologic Institute (SMHI) in Norrköping 58.6°N since 1983. Beside measurements of stratospheric ozone it is also specially designed for spectral irradiance measurements in the UVB region, and was used for such measurements 1983-85. Later it has mostly been monitoring ozone - since 1988 almost continuously.

A Berger UVB-sunburn-meter (Solar Light Co) has also been operated continuously by SMHI in Norrköping since 1983.

Two specially built filter radiometer-instruments for measuring both natural global UVB at 306 nm and UVA at 360 nm) have been monitoring solar UV since 1983 in Norrköping (continously) and in Luleå 65.5°N (with some interrupts). Data from these instruments have not yet been evaluated.

A third instrument of the same type has been monitoring solar UV in Stockholm since 1989. Data give estimates of UVA, UVB_{ACGIH}, Erythmal UV and ozone-values.

One erythmal MED-meter (Solar Light Co, mod. 500) has been tested at SMHI in Norrköping 1989.

Environmental UV-monitoring

A new project has been started with the intention to give a seasonal and geographic mapping of ultraviolet exposure data and statistics in Sweden. Six MED-monitors mod. 500 and 4 UVA-monitors (Solar Light Co) have been placed at 5 meteorologic stations (Lund 55.7°N, Norrköping 58.6°N, Borlänge 60.5°N, Umeå 63.8°N, Kiruna 67.8°N). The installations were started 1990 and completed in the summer 1991. Data is gathered in an automatic data collection network during a 5-year period, after which there will be a final evaluation of the results and available statistics.

Postadress / Mailing Address: BOX 60204, S-104 01 STOCKHOLM, SWEDEN.

Telefon / Telephone: NAT 08-729 71 00, INT +46-8-729 71 00.

Telefax / Telecopier: 08-729 71 08, 08-33 08 31 (Kärnenergiensheten, Department of Nuclear Energy).

Telex: 11771 SAFERAD S. Postgiro: 18 21 18-0.

C-279

Related reports etc.:

Josefsson Weine, 1986 "Solar Ultraviolet Radiation in Sweden", Swedish Meteorologic and Hydrologic Institute (SMHI), S-60176 Norrköping, Sweden. SMHI-report RMK 53.

Josefsson W, 1989 "Testing of the MED-Meter and a Proposal of a solar UV-network in Sweden", SMHI, S-60176 Norrköping, Sweden. Nov 1989

Josefsson W, 1990 "Measurements of total ozone 1989", SMHI, S-60176 Norrköping, Sweden. March 1990.

Josefsson W, 1988 "Measurements of the total ozone in the Nordic countries", SMHI, S-60176 Norrköping, Sweden. April 1988.

Josefsson W, 1991 "Measurements of total ozone", Swedish Environmental Programme Report 1991. Swedish Environmental Protection Agency, Information department, Marketing and Sales Section, S-171 85 Solna, Sweden. ISBN 91-620-3944-X, ISSN 0282-7298.

Josefsson W, 1991 "The intercomparison of spectroradiometers at SMHI in Norrköping 6-8 of August 1991". SMHI, S-60176 Norrköping, Sweden

Rindert S.B. 1975 "Fifteen years of ozone observations at Uppsala", Dept. of Meteorology, Uppsala University. Uppsala, Sweden. (Thesis).

Wester Ulf, 1983 "Solar ultraviolet radiation - A method for measuring and monitoring", Report RI 1983-02. Dept. of Radiation Physics, Karolinska Institute. Box 60204, S-10401 Stockholm, Sweden.

Wester U, 1984 "Solar ultraviolet radiation in Stockholm - Examples of spectral measurements and influences of measurement error parameters", Report RI 1984-03. Dept. of Radiation Physics, Karolinska Institute, Stockholm.

Wester U, 1984 "Erythmal efficiency of ultraviolet radiation from the sun and from sunlamps calculated on the basis of measured spectral data", Report RI 1984-05, Dept. of Radiation Physics, Karolinska Institute, Box 60204, S-10401 Stockholm, Sweden.

Wester U, 1987 "Solar ultraviolet radiation on the Canary Islands and in Sweden - A comparison of irradiance levels", in Human Exposure to Ultraviolet Radiation; risks and regulations, Passchier WH and Bosnjakovic PFM eds, Excerpta Medica, 339-343.

Wester U, 1990 "Monitoring of Solar UV-exposure in Stockholm 1989-90". Paper presented at Nordic Society for Radiation Protection, 9th Regular Meeting, August 29-31 1990 at Ronneby, Sweden. Swedish Radiation Protection Institute, Box 60204, S-10401 Stockholm, Sweden.

Wester U, 1991 "Monitoring of stratospheric relative ozone variations with a pair of solar UVB- and UVA-radiometers". Abstract. Proceedings of the 18th Annual meeting on the studies of the upper atmosphere by Optical methods, The Auroral Observatory, Tromsø University, Tromsø, Norway, June 17-21, 1991.

SSI-report 89-15, 1989. "Second Nordic Meeting on Non-ionizing Radiation" Page 8-9 "Solar UV-monitoring Project in Sweden", SSI-report 89-15. Swedish Radiation Protection Institute, Box 60204, S-10401 Stockholm, Sweden.

Ulf Wester

Swedish Radiation Protection Institute

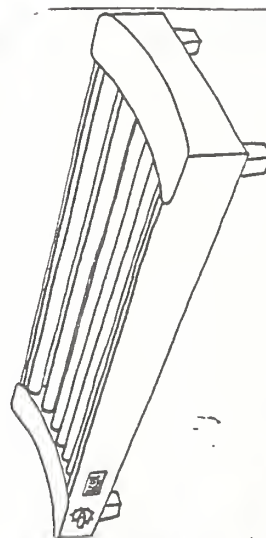
"SSI"

An authority for protection of the public
from radiation hazards

Research

Legislation

Information



"Fry now – Pay later"



Solar ultraviolet radiation research since 1980.

Objectives have varied from:

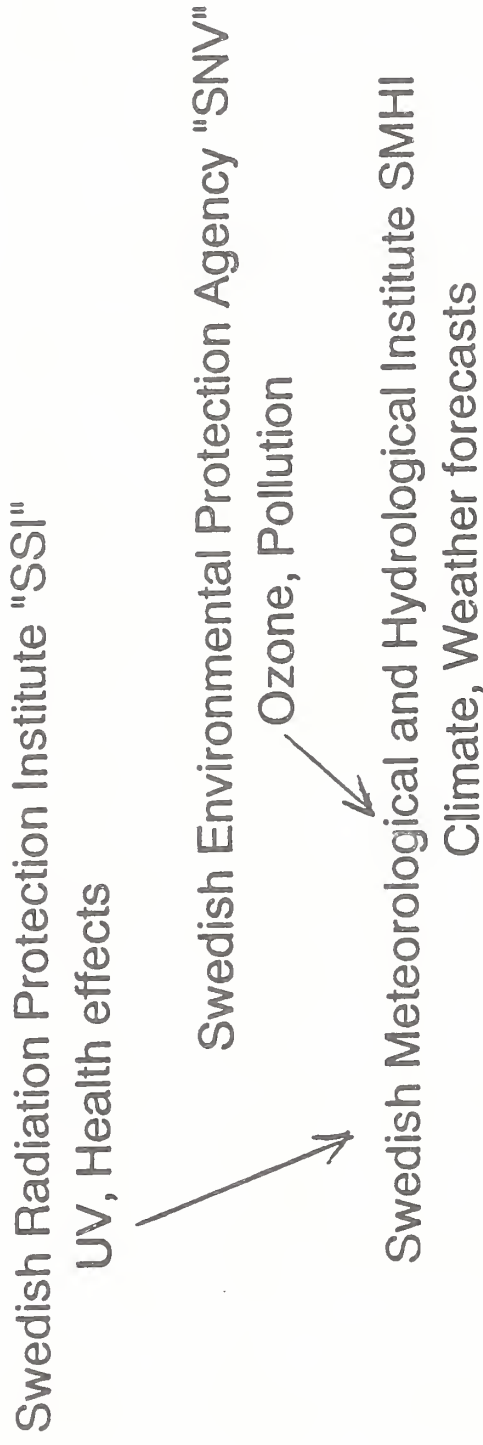
Comparisons for sunlamp legislation

Public information to reduce skincancers

Seasonal and geographic UV-mapping

(to: UVB-trends ?)

Solar UV-research – Organizations



Standard lamp calibrations:
Swedish National Testing and Research Institute "SP"

Traceability to NIST

Instruments:

- | | | | |
|---|--------------------------------------|---|----------------|
| 1 | RB-meter, 1983 | | |
| 7 | SL-500 MED, 1989-1991 | ○ | |
| 4 | SL-500 UVA 1991 | × | |
| 3 | 306nm, 360nm Filter-meters | F | 1984, 89 |
| 1 | Brewer Ozone & UVB spectroradiometer | | 1983 |
| 1 | Dobson spectrophotometer | | 1951-66, 1991- |

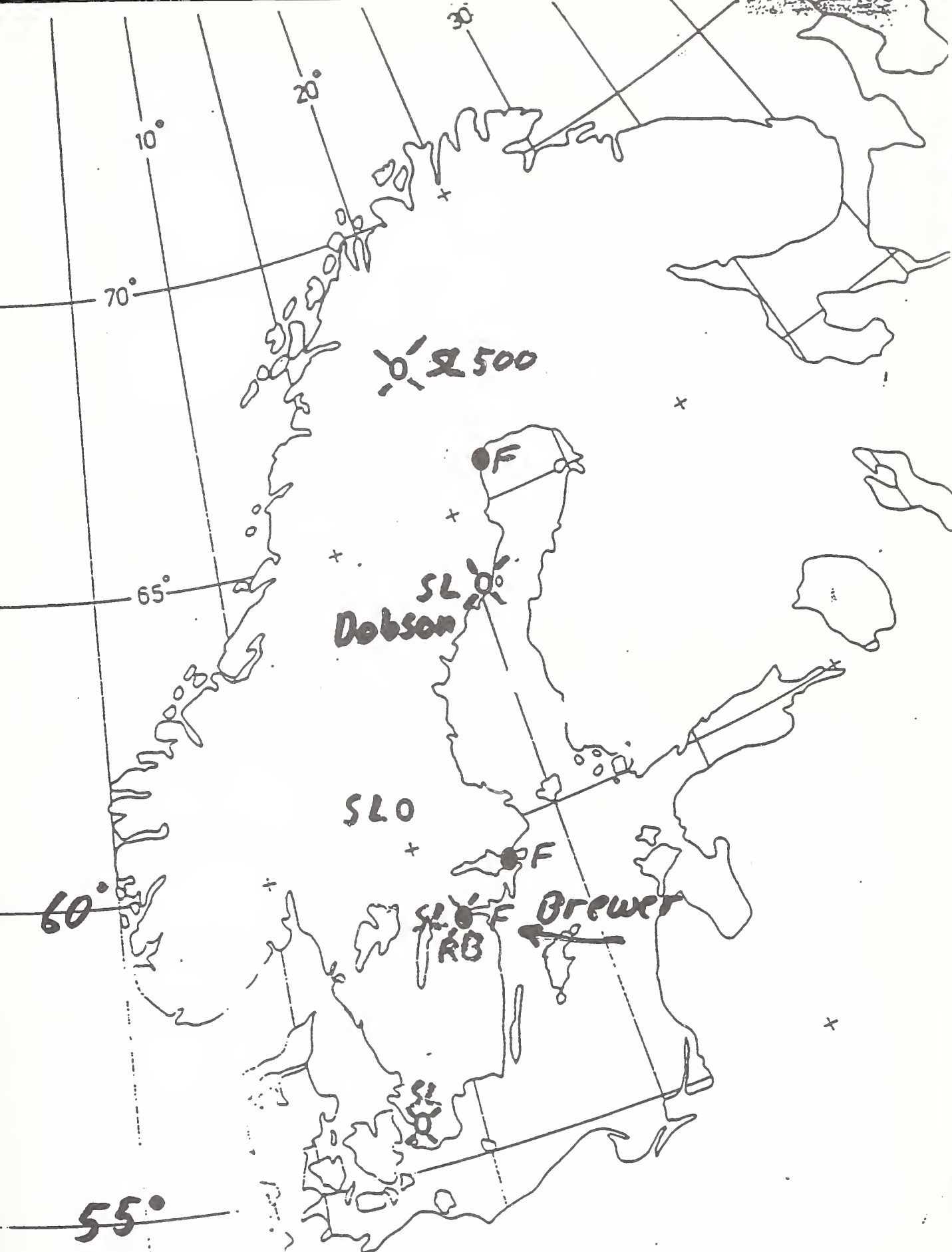


Figure 3.1 The Swedish national solar radiation network equipped by automatic data acquisition system.

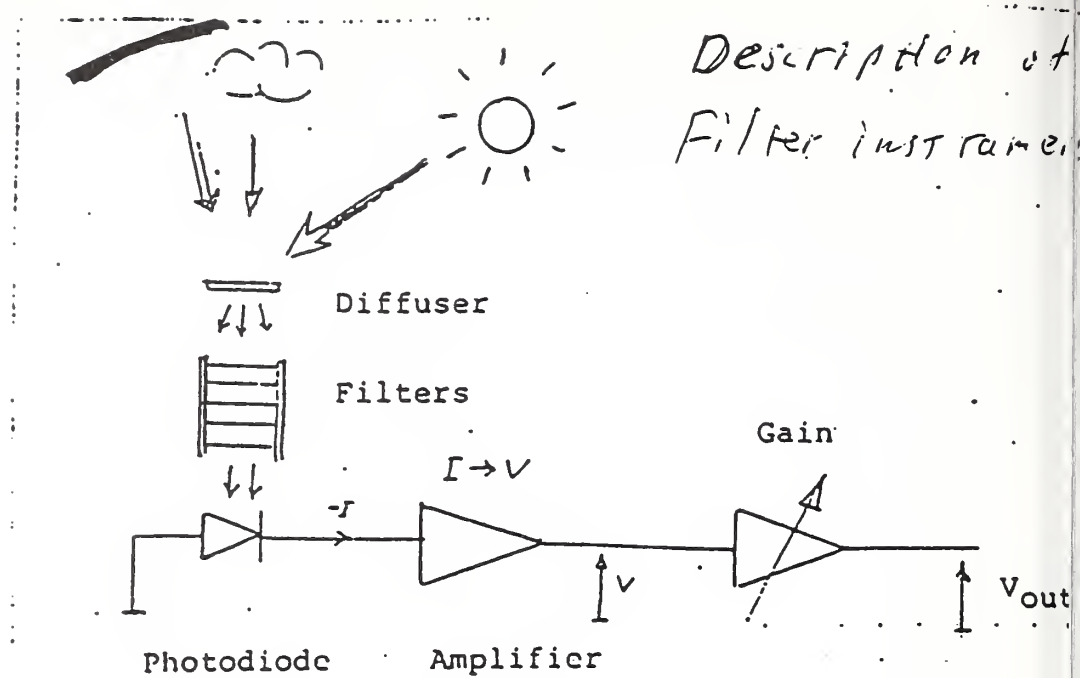
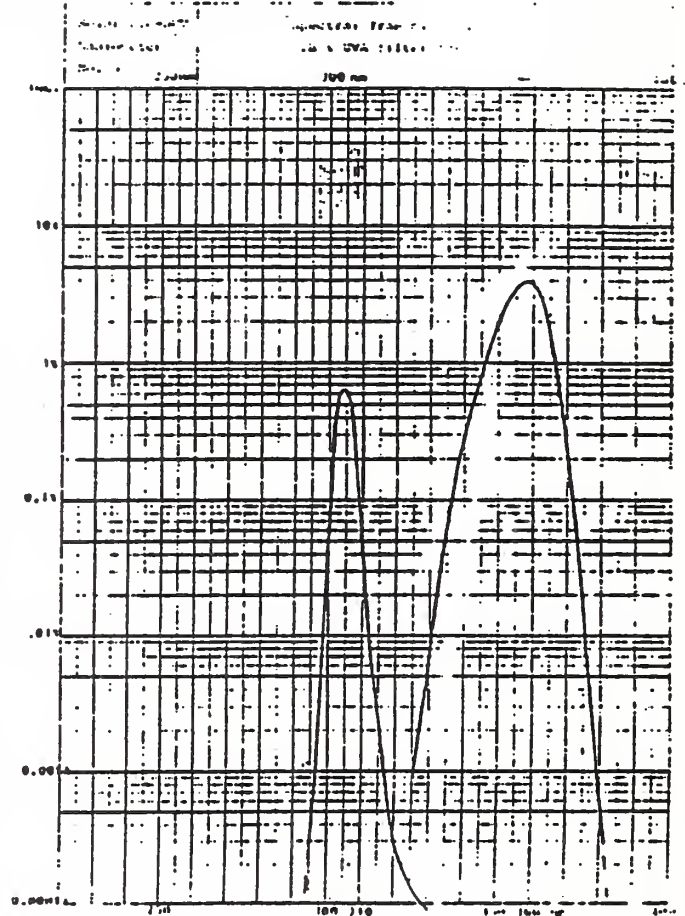
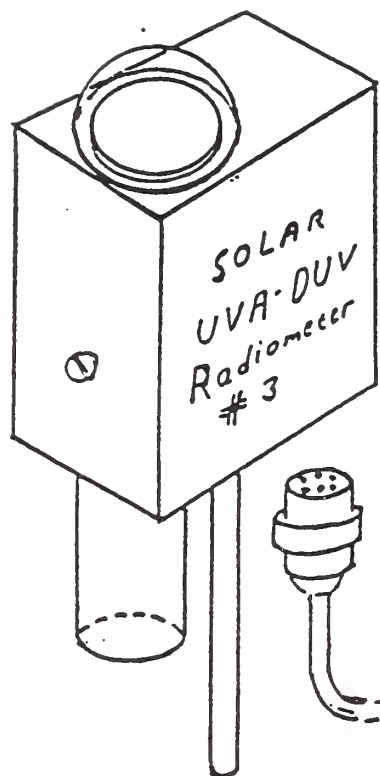


Fig A1:1 Radiometer - Instrument no. 3



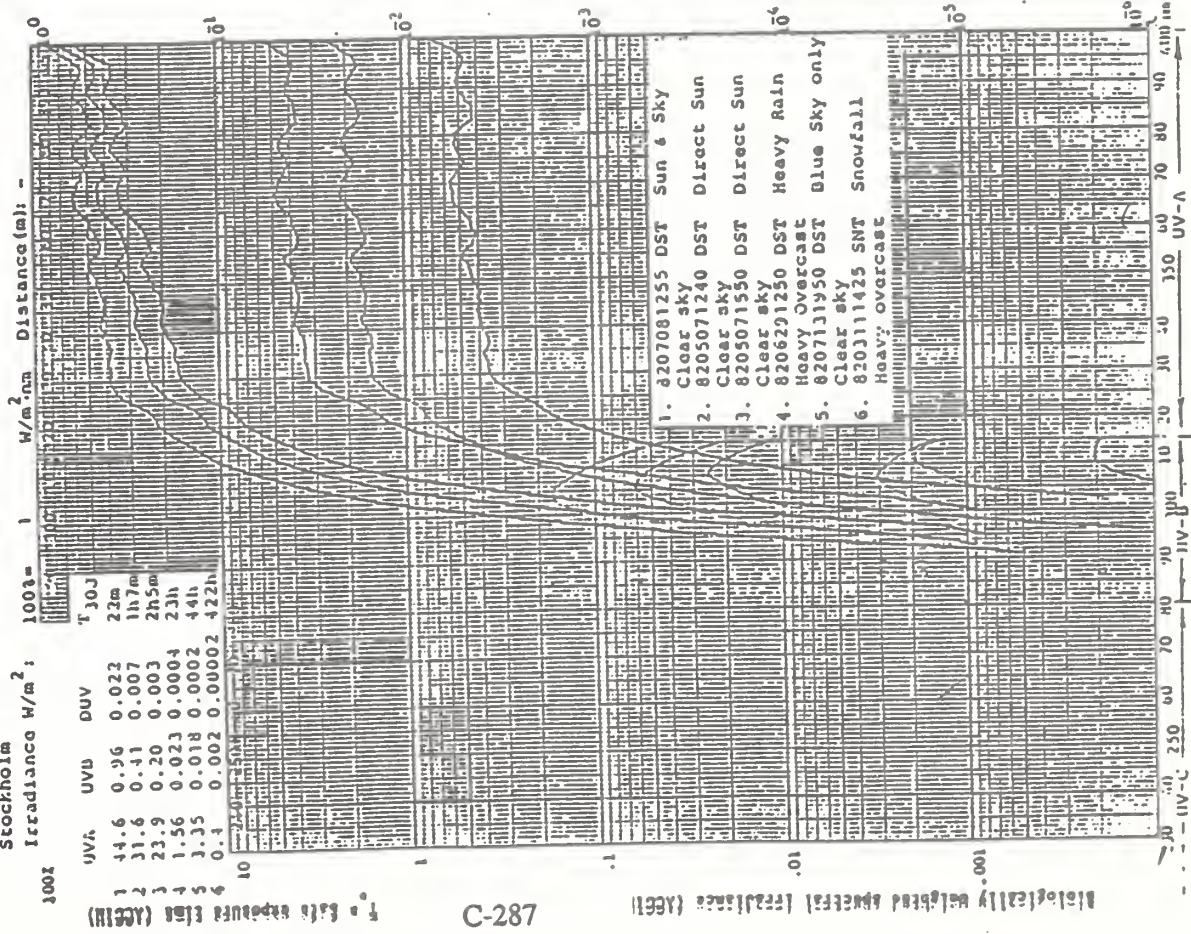


KAROLINSKA INSTITUTET
Radiolytiska institutionen
Box 4020, S-10401 Stockholm Sweden
Tel. 08-71 40 80

Diagram 3 a

Spectral Irradiance
on a surface perpendicular to
the sun or to a corresponding
noon-time sky position

W E A S U R E D O B J E C T :
Sun & Sky in various weather conditions noon-time sky position
Stockholm

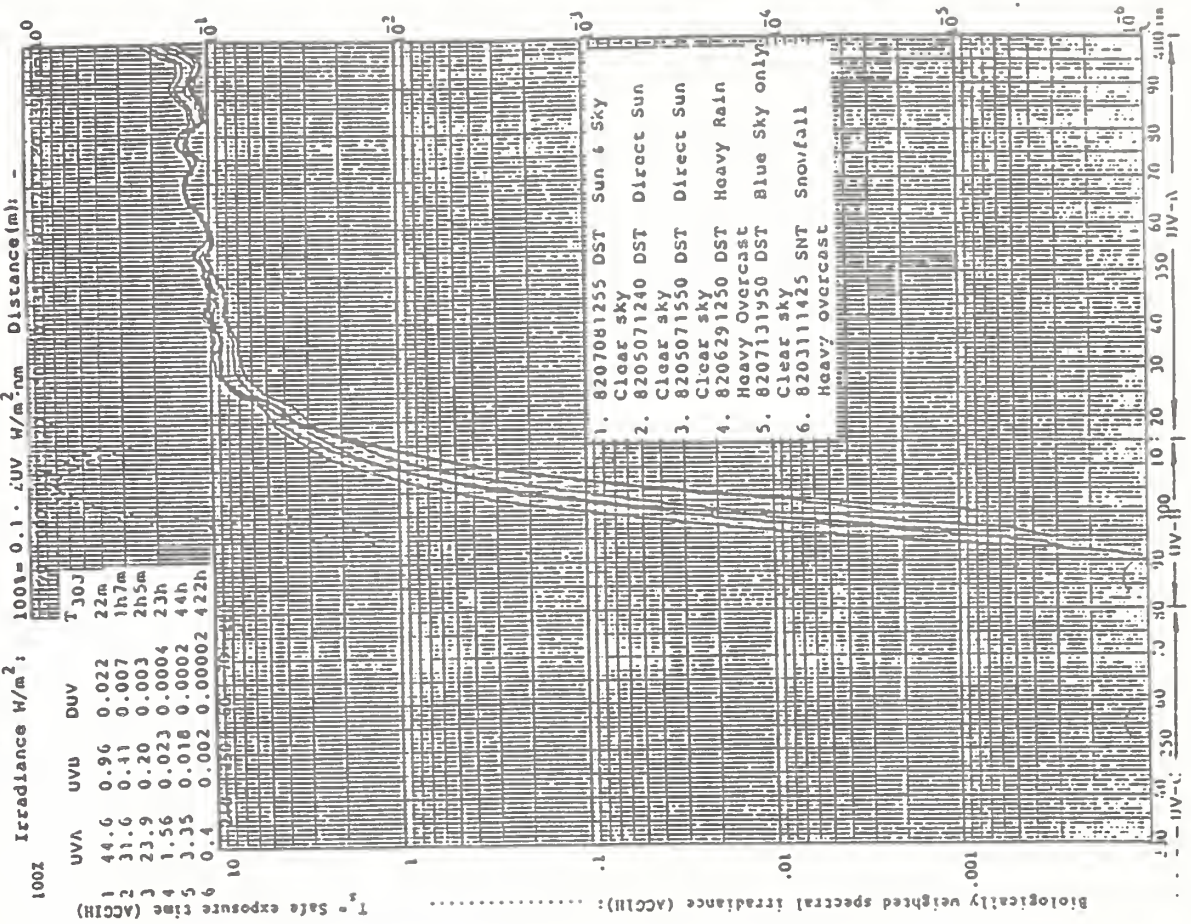


KAROLINSKA INSTITUTET
Radiolytiska institutionen
Box 4020, S-10401 Stockholm Sweden
Tel. 08-71 40 80

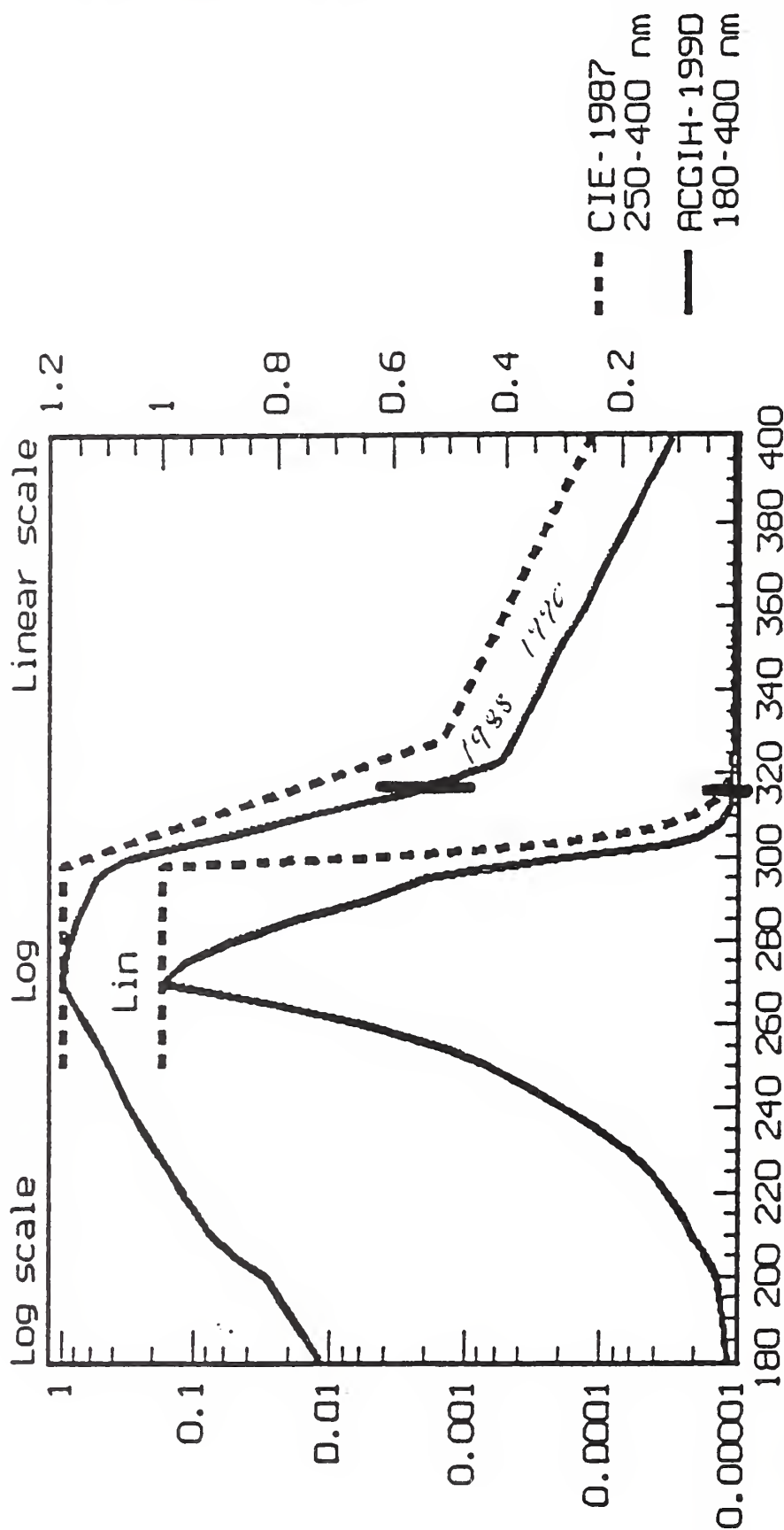
Diagram 3 b

Normalized Spectral Irradiance
on a surface perpendicular to the
sun or to a corresponding noon-time
sky position

W E A S U R E D O B J E C T :
Sun & Sky, various weather conditions
Stockholm 59°N



UV-action spectra: ACGIH-1990 & CIE-1987
 ACGIH Threshold Limit Exposure = 30 J/m^2
 CIE "Minimal Erythral Dose" = $200\text{-}300 \text{ J/m}^2$
 - Relative spectral effectiveness -

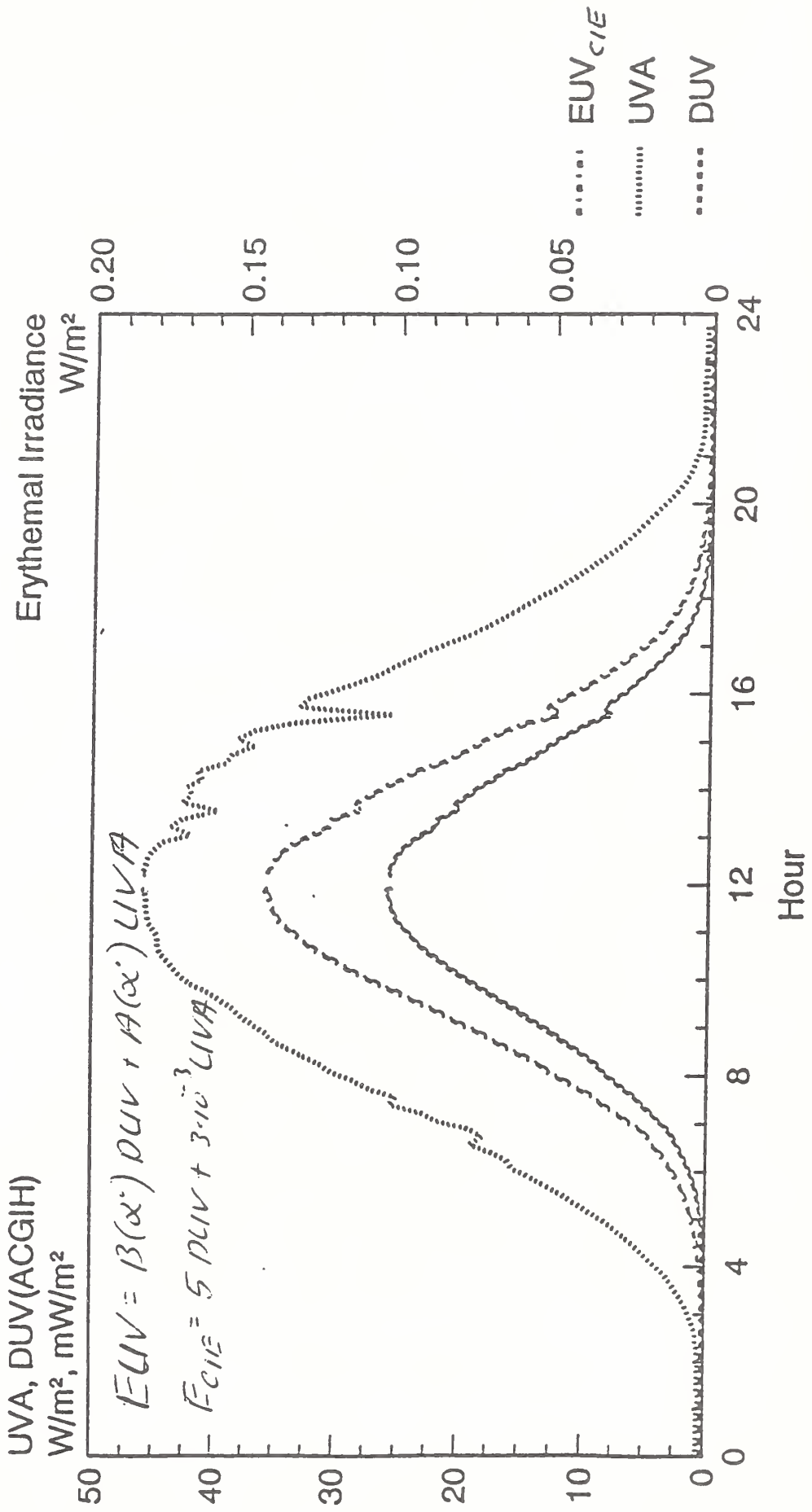


Wavelength nanometers (nm)

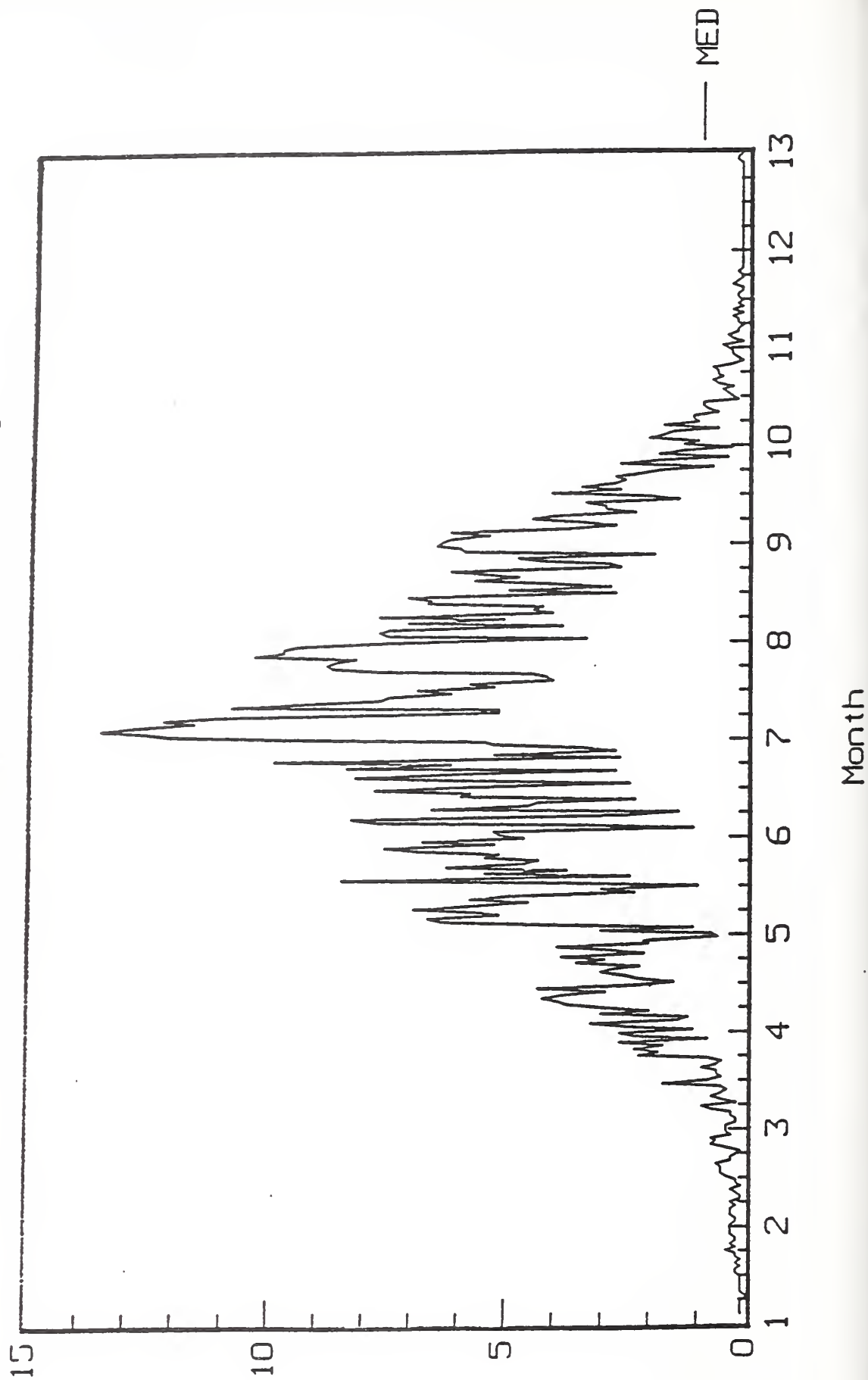
ACGIH

Figure 4: Comparison of the ACGIH hazard action spectrum & the CIE skin erythema reference action spectrum in logarithmic and linear representations.

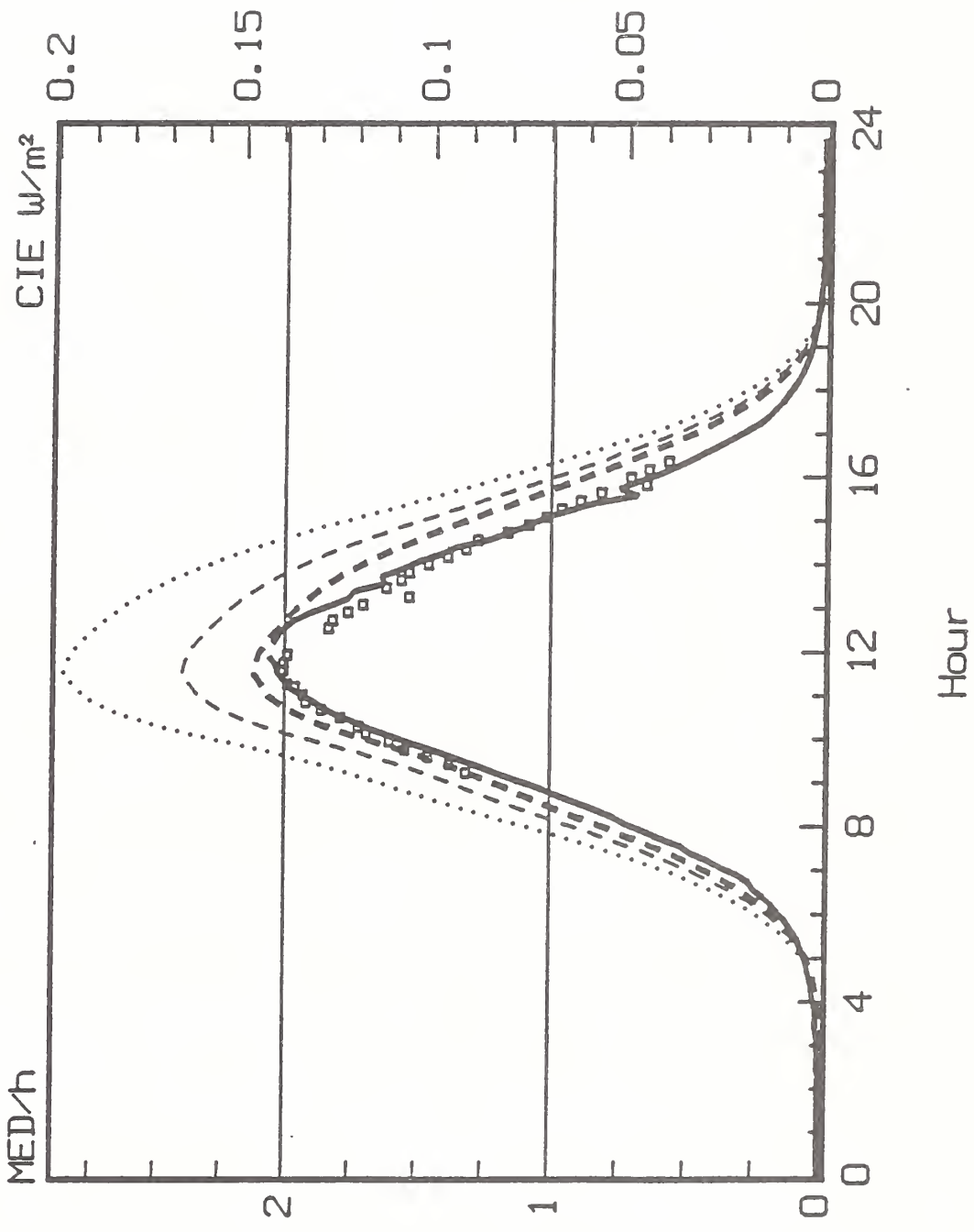
Stockholm KS, 1991-07-05
Irradiance on a horizontal surface



Number of MED/day in Stockholm 1991



Stockholm - July 5 1991 - Norrköping
 Dual passband filterinstr. - Optronic
 spectroradiometer - Solar Light mod.500
 Global erythema irradiance



Two Channel Filter-meter

DUV - UVA - METER#3 - HP711/3421A

STOCKHOLM - KS-Z6

90/06/19

Volts

10

Exposure:

DUV: 296 J/m²

UVA: 1230 kJ/m²

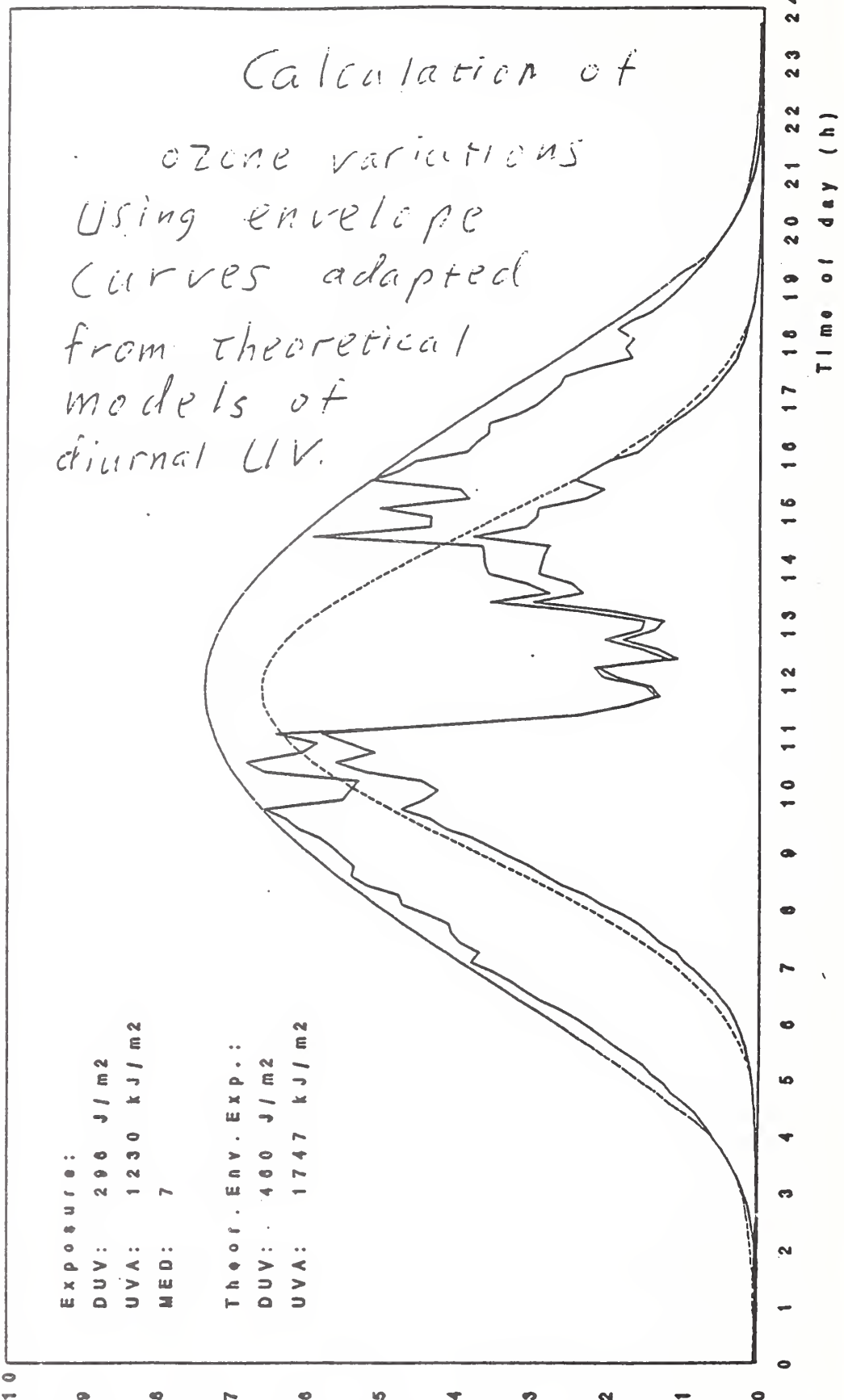
MED: 7

Theor. Env. Exp.:

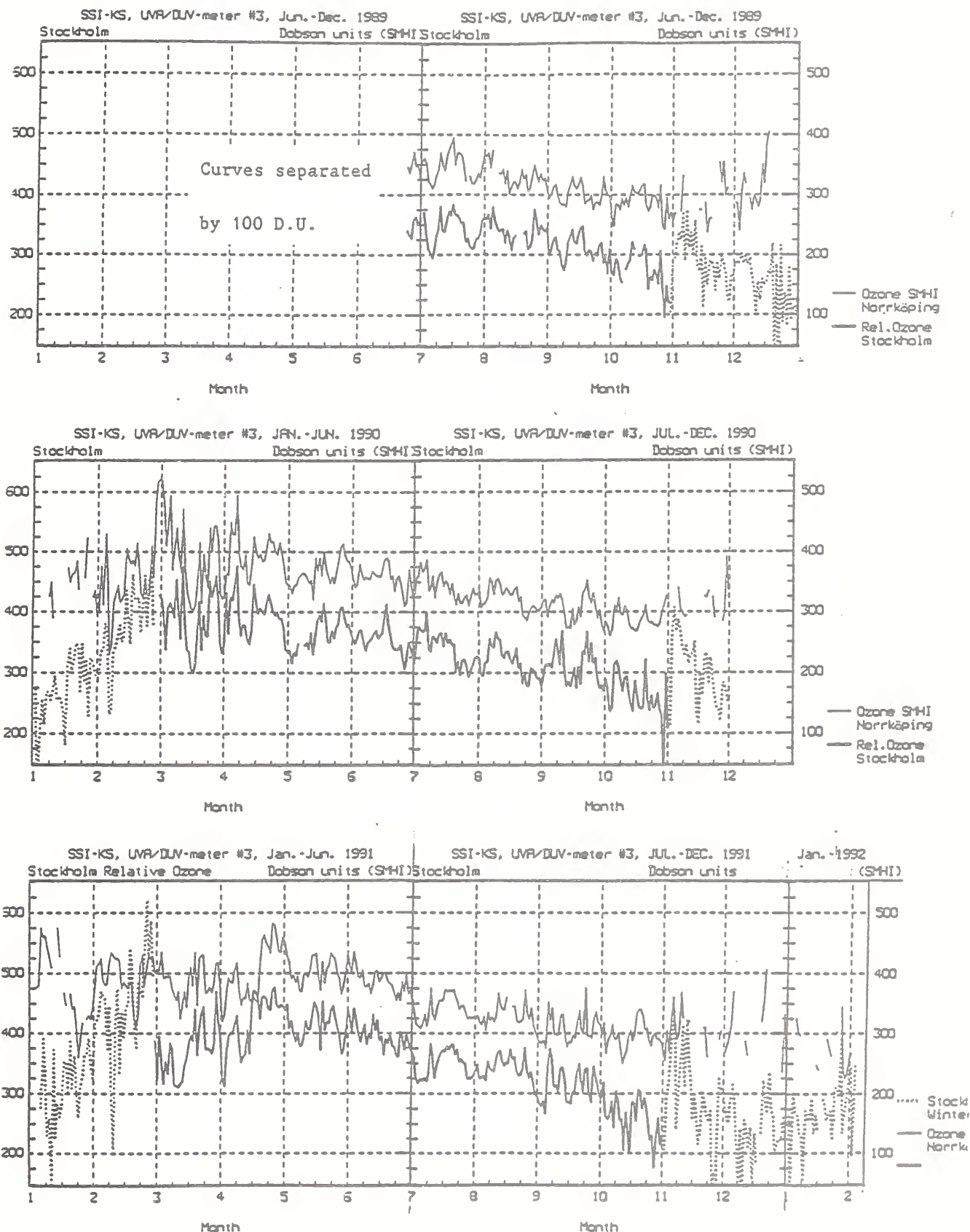
DUV: 460 J/m²

UVA: 1747 kJ/m²

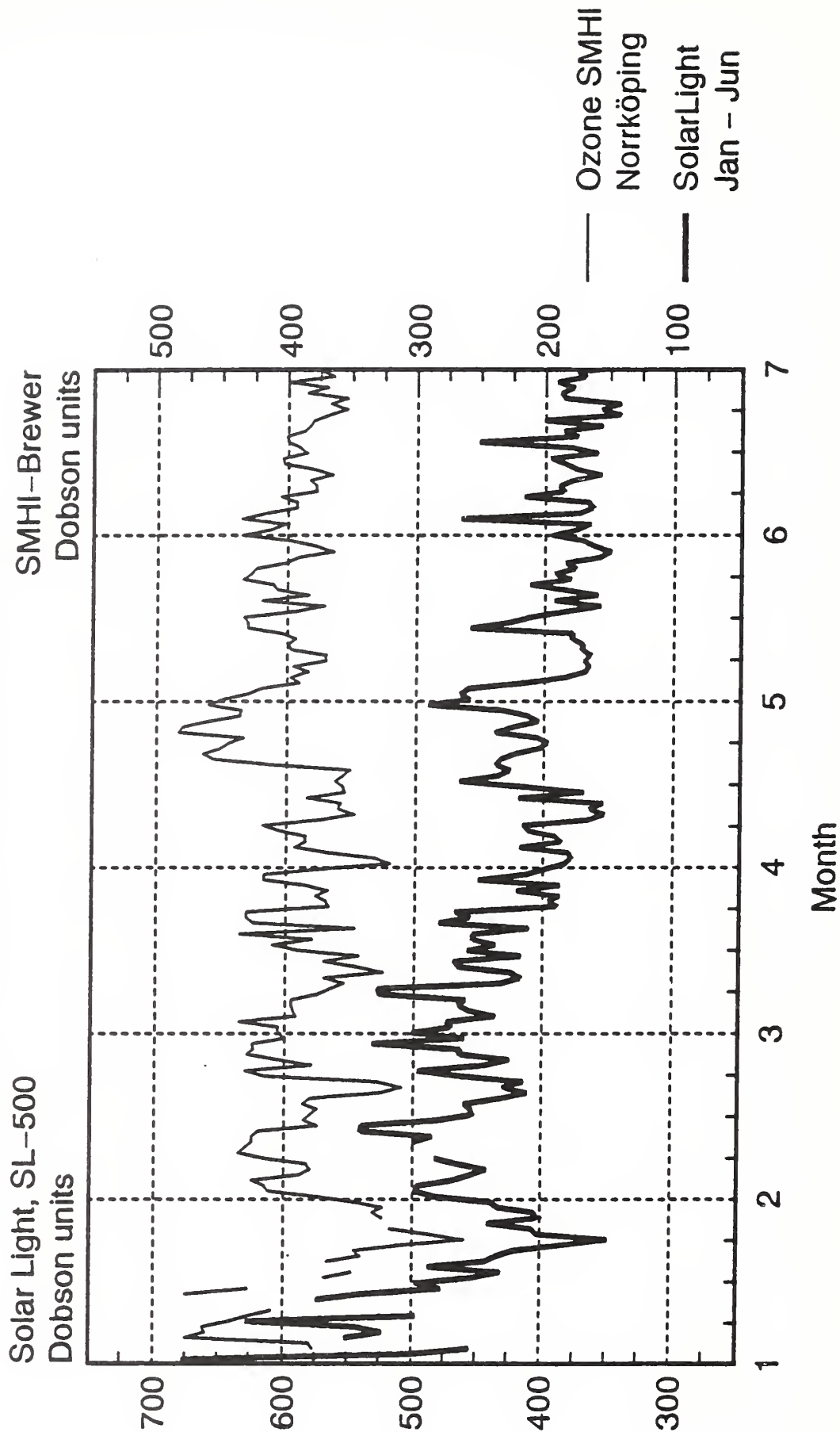
Calculation of
ozone variations
Using envelope
Curves adapted
from theoretical
models of
diurnal UV.

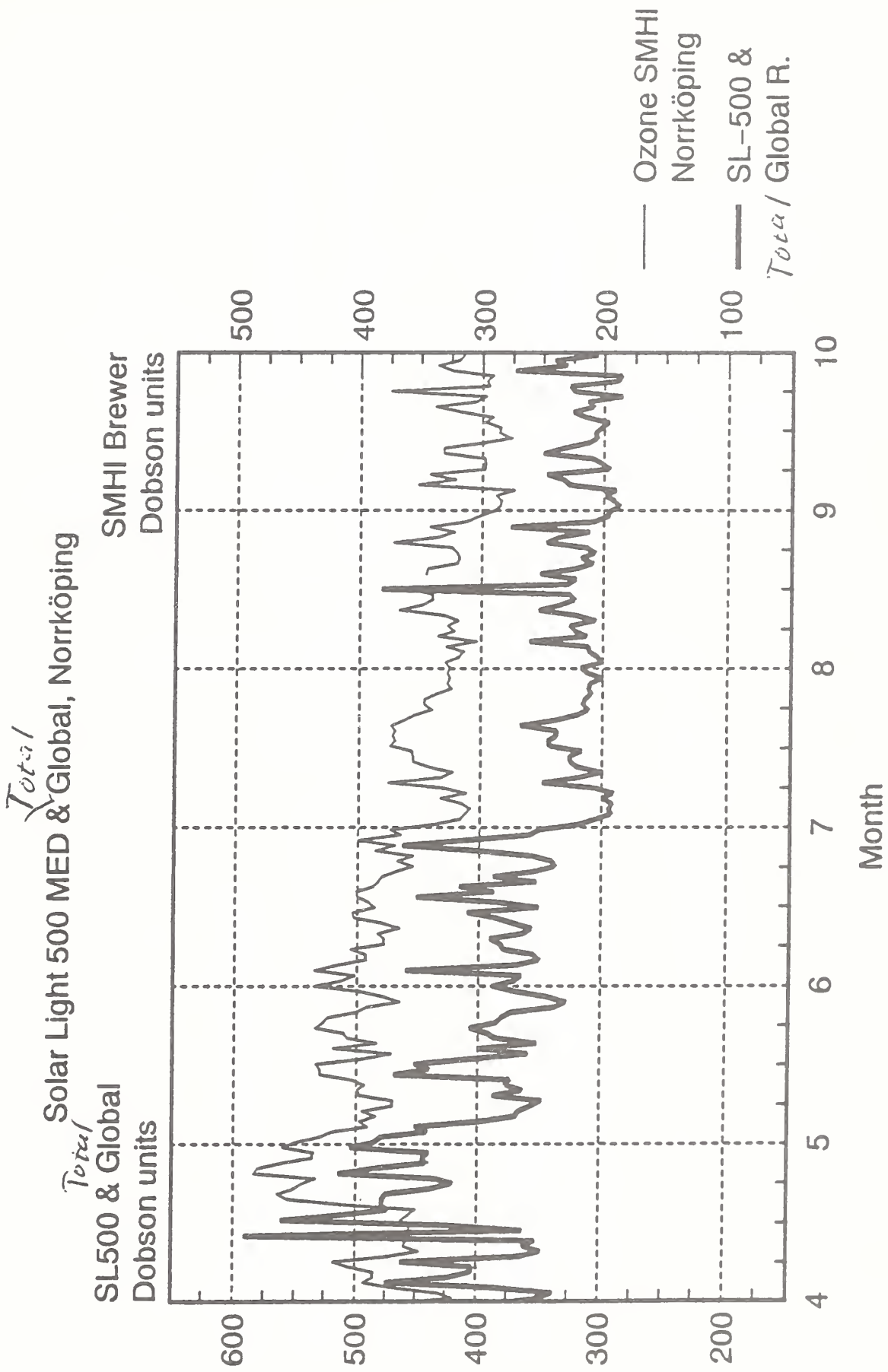


Ozone column variations measured with a dual passband filter radiometer in Stockholm 1989 - 1991 compared to reference ozone values from SMHI, Norrköping.



Ozone SMHI UVA/MED-S.Light Jan.-Jun.1991





Conclusions:

It may be possible to compare data from different types of UV-meters.

Day by day ozone-variations may be monitored to fill in temporal or geographical gaps between other ozone-spectrophotometers.

Non-U.S. National UV Research and Monitoring Programs

United Kingdom

**Dr. Colin Driscoll
U.K. National Radiological Protection Board**

BROAD-BAND SOLAR RADIATION MEASUREMENTS IN THE UK

C M H Driscoll, M J Whillock, A J Pearson, S F Dean and A F McKinlay

National Radiological Protection Board
Chilton, Didcot, Oxon OX11 0RQ

Abstract

In 1988, the National Radiological Protection Board set up three monitoring stations to make continuous measurements of terrestrial solar radiation at different latitudes within the UK. These were at the NRPB centres at Chilton (latitude $\approx 52^{\circ}\text{N}$), Leeds ($\approx 54^{\circ}\text{N}$) and Glasgow ($\approx 56^{\circ}\text{N}$). Measurements of visible (400 - 770 nm), ultraviolet UVA (320 - 400 nm) and erythemally weighted ultraviolet UVR radiation have been made simultaneously using a system based on three commercially available broad-band detectors. The measurements were designed to provide information regarding the range of variation of solar UVR at different latitudes with the time of year and to establish baseline levels for natural UVR with which measurements from artificial sources of UVR could be compared. This paper describes the measurement system, calibration and the experimental data obtained from the first three years of measurement.

Introduction

Long term repeated exposure to solar UVR, particularly in the UV-B range ($\approx 280 - 320$ nm), is clearly associated with the risk of developing non-melanoma skin cancers in susceptible white-skinned people ⁽¹⁾. High and intermittent exposure to solar UV-B appears to be a significant risk factor in malignant melanoma. Individual habits with respect to solar UVR exposure are clearly most important in assessing personal risk and baseline data on terrestrial UVR are useful data in assessing possible exposure.

Stratospheric ozone depletion and the predicted associated increase in solar ultraviolet radiation (UVR) reaching the earth's surface are important environmental issues, not only with respect to human health but also to effects on marine organisms and terrestrial plant life. Although individual organisations throughout Europe and the world have been monitoring solar UVR for many years, the measurements have not generally been co-ordinated and provide only a limited data base for epidemiological studies. In addition, most measurements have been made sporadically on a range of instruments with no cross-calibration.

In 1988, NRPB set up three monitoring stations to measure continuously terrestrial solar radiation at different latitudes within the UK. These were at the NRPB centres at Chilton (latitude $\approx 52^\circ\text{N}$), Leeds ($\approx 54^\circ\text{N}$) and Glasgow ($\approx 56^\circ\text{N}$). The measurements were designed to provide information regarding:

- (a) the range of variation of solar erythemally effective UVR and UV-A at different latitudes with the time of year;
- (b) the effects of continuing changes affecting the terrestrial measurement of solar UVR, such as from cloud cover;
- (c) establishing baseline levels for natural UVR exposure with which measurements from artificial sources of UVR could be compared.

Measurement system

The three solar radiation detectors used in the NRPB measurement system are obtainable from commercial suppliers, but have been modified according to specific requirements ⁽²⁾. They provide measurements of visible radiation (wavelength range 400 - 770 nm), UV-A (320 - 400 nm) and erythemally weighted UVR (280 - 400 nm) radiation. The UV-A and visible radiation detectors were obtained from Macam Photometrics Ltd, Scotland and the weighted UVR detector is a modified Robertson-Berger meter ⁽³⁾. The detectors were calibrated using sources traceable to national standards laboratories. In addition, the UVR detectors at Chilton were cross-calibrated against a calibrated scanning spectroradiometer using the sun at noon on a clear summer day.

In 1989, the measurement system was redesigned ⁽²⁾ to provide high stability control electronics, improved weatherproofing and better environmental control of the detector enclosure. In addition, the computer for control and data acquisition was upgraded and special control software was developed.

The redesigned system, shown in figure 1, consists of an environmentally sealed head unit in which are mounted the three detectors. The head unit is connected via a multiway cable to the data acquisition unit, which is linked to a personal computer (pc). The pc records the detector readings as data files and acts as a display and overall controller of the system.

Readings are recorded every 20 seconds and these are then used to produce a set of mean values every 5 minutes, together with associated statistical deviations. The data are written to floppy disk storage every 24 hours and are then available for compression and averaging over longer periods to enable the identification of trends.

The new monitoring system has been installed at Chilton from May 1990 and similar systems were installed at the other centres by the end of 1991.

Measurements

Comprehensive summaries of the experimental data have been published ⁽⁴⁻⁶⁾. Summaries of these data for the first 3 years of measurement (up to May 1991) at Chilton are presented as a function of the month of the year in figures 2 to 4.

The mean illuminance values at 12 GMT averaged for each month of measurement over the 3 year period are presented in figure 2 for Chilton. The highest mean value averaged over the 3 years at Chilton is observed in May at 60 klux, which is similar to that reported by the Meteorological Office ⁽⁷⁾ for Bracknell (at a similar latitude to Chilton). For comparison, the highest mean values at Leeds and Glasgow are observed at 58 klux in May and June, respectively. The illuminance values decrease to about 10 klux during the winter months, similar to the Meteorological Office data.

The mean UV-A irradiance values at 12 GMT averaged for each month of measurement over the three year period are presented in figure 3 for Chilton. The highest mean value averaged over the 3 year period at Chilton is observed in May at 25 W m^{-2} . The highest mean values at Leeds and Glasgow are similar at 24 W m^{-2} observed in May and June, respectively. These values are between 50 and 60 % of the calculated values ^(8,9) applicable to clear sky conditions at noon encountered at sea level for UK latitudes and for no reflection from the ground. On average, clear sky conditions are observed in the UK for less than 15% of the days of the year, whereas near total cloud conditions are reported for between 50 and 70% of daylight hours, depending on month and latitude. The UV-A irradiance values decrease to about 5 W m^{-2} during the winter months.

The mean UVR effective irradiance values at 12 GMT averaged for each month of measurement over the three year period are presented in figure 4 for Chilton. The highest mean value averaged over the 3 year period at Chilton is observed in May at 90 mW m^{-2} (effective). For comparison, the highest mean values at Leeds and Glasgow are observed in May at 73 mW m^{-2} (effective) and in July at 80 mW m^{-2} (effective), respectively. As with the UV-A results, these values are between 50 and 60 % of the calculated values ^(8,9) for clear sky conditions at noon. The UVR effective irradiance values decrease to about 2 mW m^{-2} (effective) during the winter months.

Site comparison

Although the highest mean illuminance and UV-A irradiance values at the three measurement sites are similar, differences in the UVR effective irradiance between the sites are observed. In figure 5, the mean monthly UVR effective irradiances at 12 GMT for the summer months (1988-90) are shown at the three UK sites.

The values at Chilton are higher during all the summer months than at the other sites. The highest mean values at Chilton are observed in May and July. These mean values are greater than 70 mW m^{-2} (effective), which is the approximate dose rate to produce a minimum erythema on sensitive skin in an hour. The highest irradiance values within the month are greater than twice the mean value, which implies that erythema would result from exposures of less than 30 minutes on some days.

The mean monthly UVR effective irradiances at 12 GMT for Glasgow peaks in July, the only month where the mean value exceeds 70 mW m^{-2} (effective). For Leeds, the highest mean value occurs in May, with a general decline as the summer progresses because of cloudier weather conditions.

Conclusions

Experience gained during the first three years of measurements has led to the solar radiation monitoring system being redesigned and modifications to the way the data are collected, analysed and presented.

It is proposed to extend the measurement network to cover the range of latitudes (from $\approx 50^\circ\text{N}$ to $\approx 60^\circ\text{N}$) appropriate to the whole of the UK. In addition, there is interest in developing a measurement network at various locations throughout Europe, especially at latitudes less than 40°N . This is important due to the increasing numbers of populations particularly at risk working, living or taking holidays in Southern Europe.

References

- 1 WHO, Nonionizing Radiation Protection, World Health Organisation Regional Publications, European Series No 25 (1989).
- 2 Dean SF, Rawlinson AI, McKinlay AF, Pearson AJ, Whillock MJ and Driscoll CMH, NRPB solar radiation measurement system, *Radiol Prot Bull*, **124**, 6 (1991).
- 3 Berger DS, The sunburning ultraviolet meter: Design and performance, *Photochem. Photobiol.*, **24**, 587 (1976).
- 4 Driscoll CMH, Whillock MJ, Gall A, Clark IE, Pearson AJ, Blackwell RP, Strong JC and McKinlay AF, Solar radiation measurements at three sites in the UK. May 1988- April 1989, Chilton, NRPB-M184 (1989).
- 5 Driscoll CMH, Whillock MJ, Pearson AJ, Gall A, Clark IE, Blackwell RP and McKinlay AF, Solar radiation measurements at three sites in the UK. May 1989- April 1990, Chilton, NRPB-M256 (1990).

6 Driscoll CMH, Whillock MJ, Dean SF, Pearson AJ, Gall A, Rawlinson AI and McKinlay AF, Solar radiation measurements at three sites in the UK. May 1990- April 1991, Chilton, NRPB-M344 (1992).

7 Littlefair PJ and Secker SM, Daylight and solar data. IN Weather data and its applications, A symposium for Building Service Engineers (organised by CIBSE, London) p 85 (1988).

8 Diffey BL, The calculation of the spectral distribution of natural ultraviolet radiation under clear day conditions, Phys Med Biol, 22, 309 (1977)

9 Diffey BL, Using a microcomputer program to avoid sunburn, Photodermatol, 1, 45 (1984)

FIGURE 1 SOLAR RADIATION MEASUREMENT SYSTEM

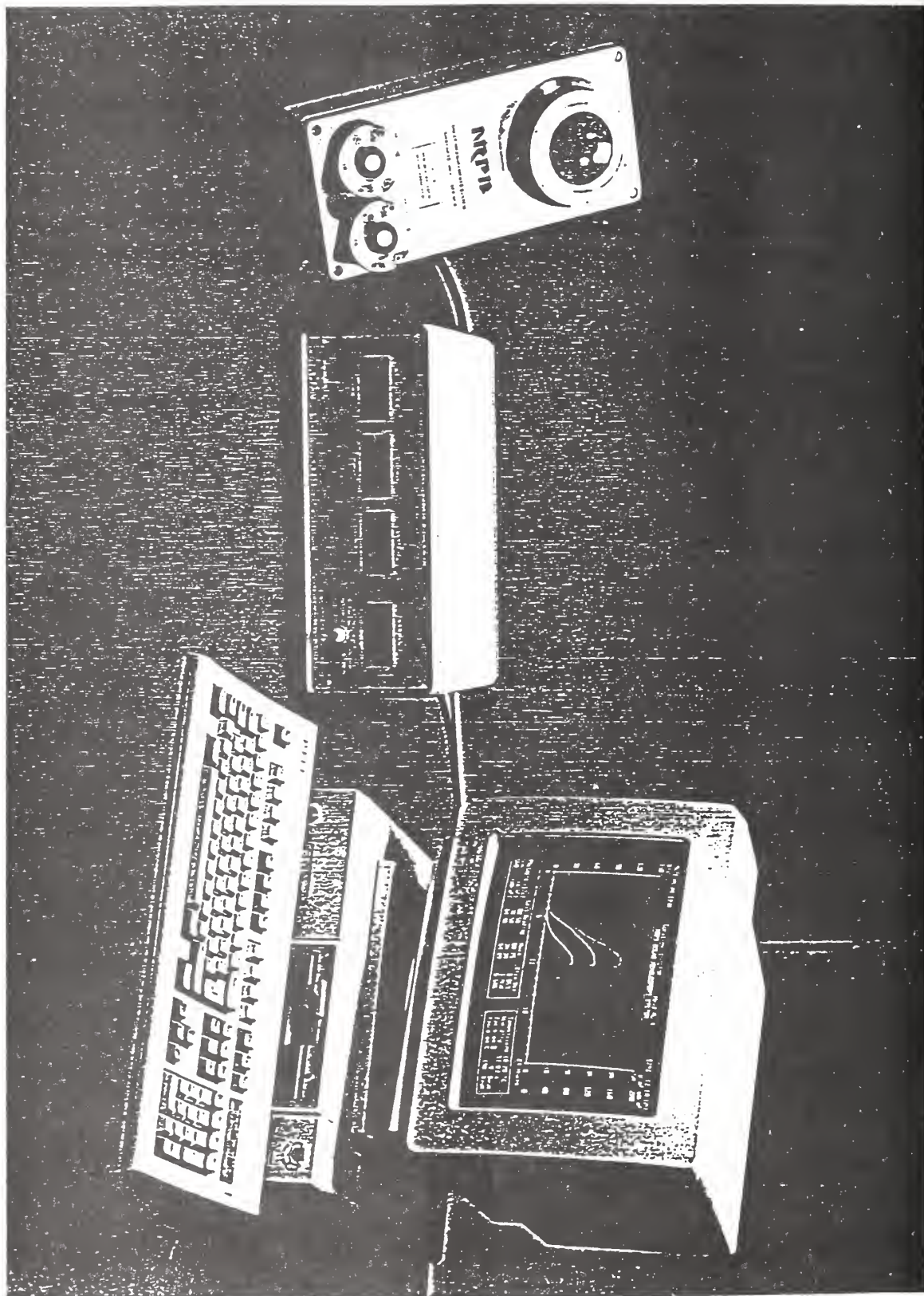


FIGURE 2 Mean monthly illuminance (12 GMT) at Chilton

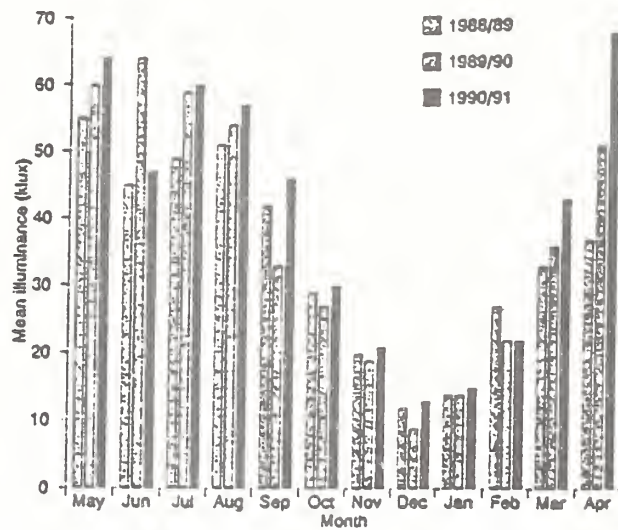


FIGURE 3 Mean monthly UV-A irradiance (12 GMT) at Chilton

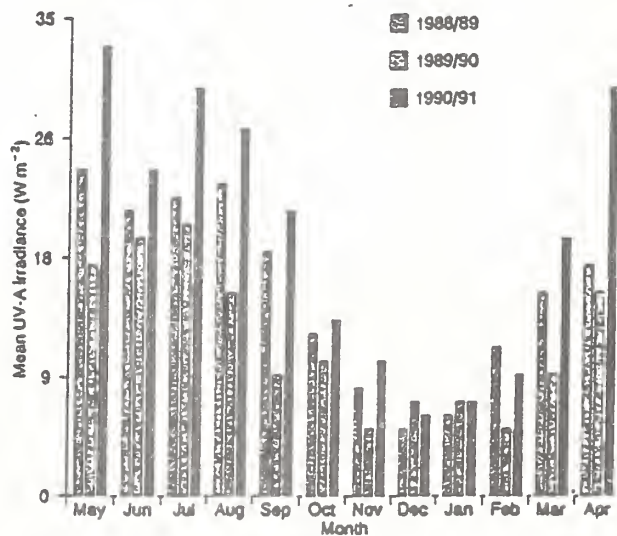
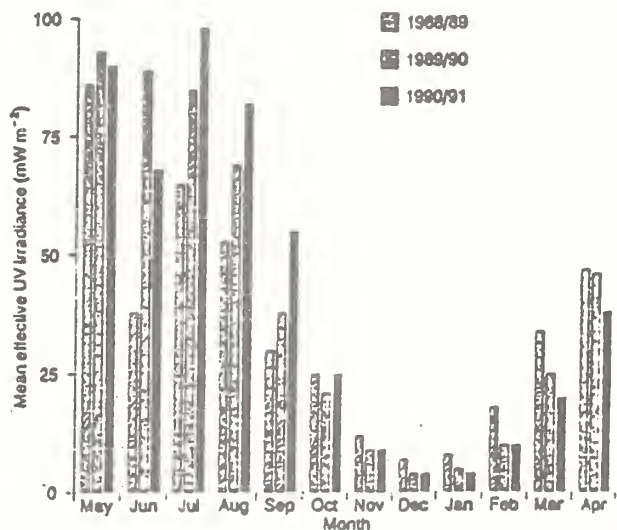


FIGURE 4 Mean monthly UV effective irradiance (12 GMT) at Chilton



Statistical Considerations in Network Design and Data Analysis

By:

Lane Bishop (Allied-Signal)

**William Hill (University of
Wisconsin, Madison)**

Network Design and Trend Analysis Issues

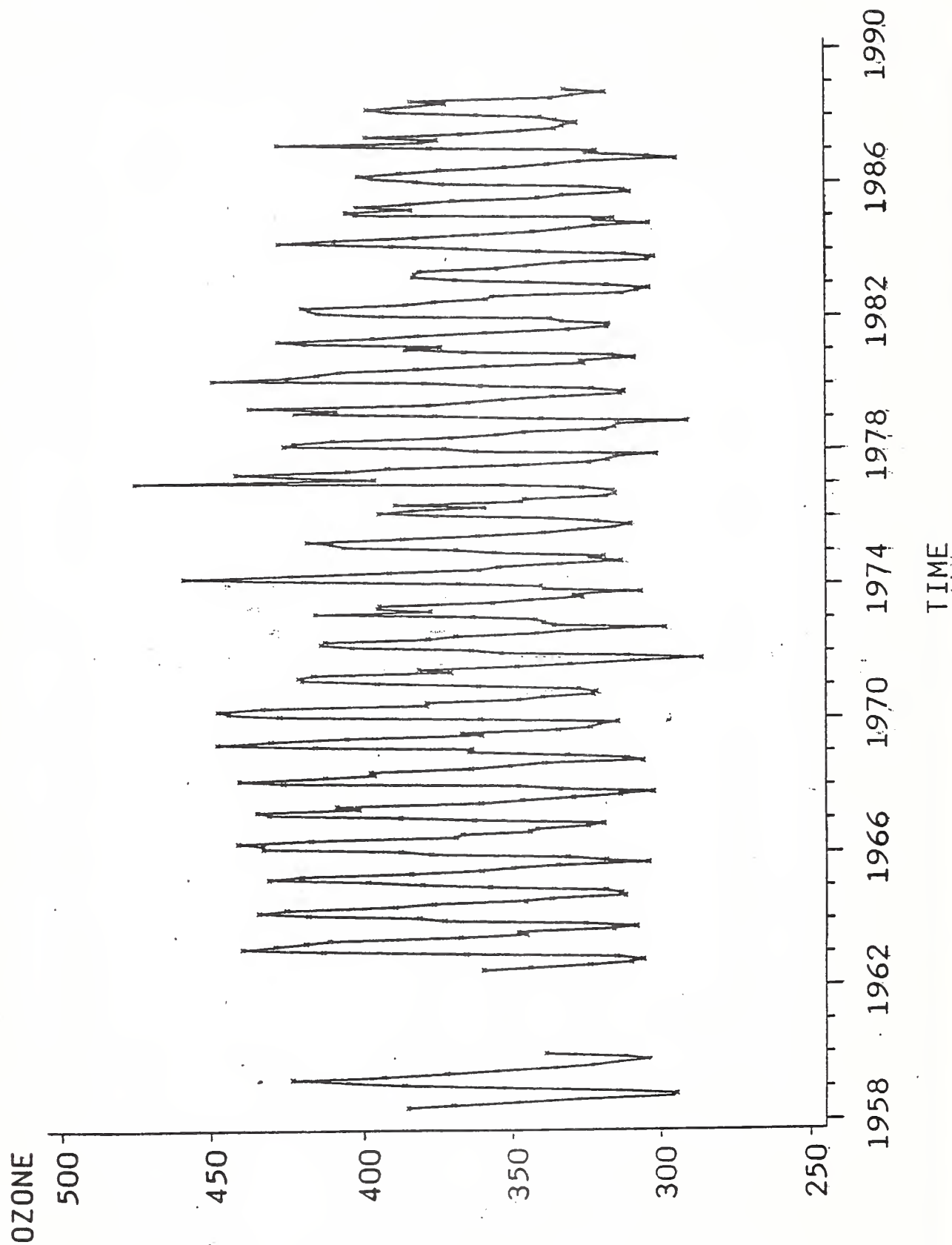
- I. Trend Detection**
- II. Coverage / Representativeness**
- III. Sampling**
- IV. Quality Assurance**

I. Trend Detection

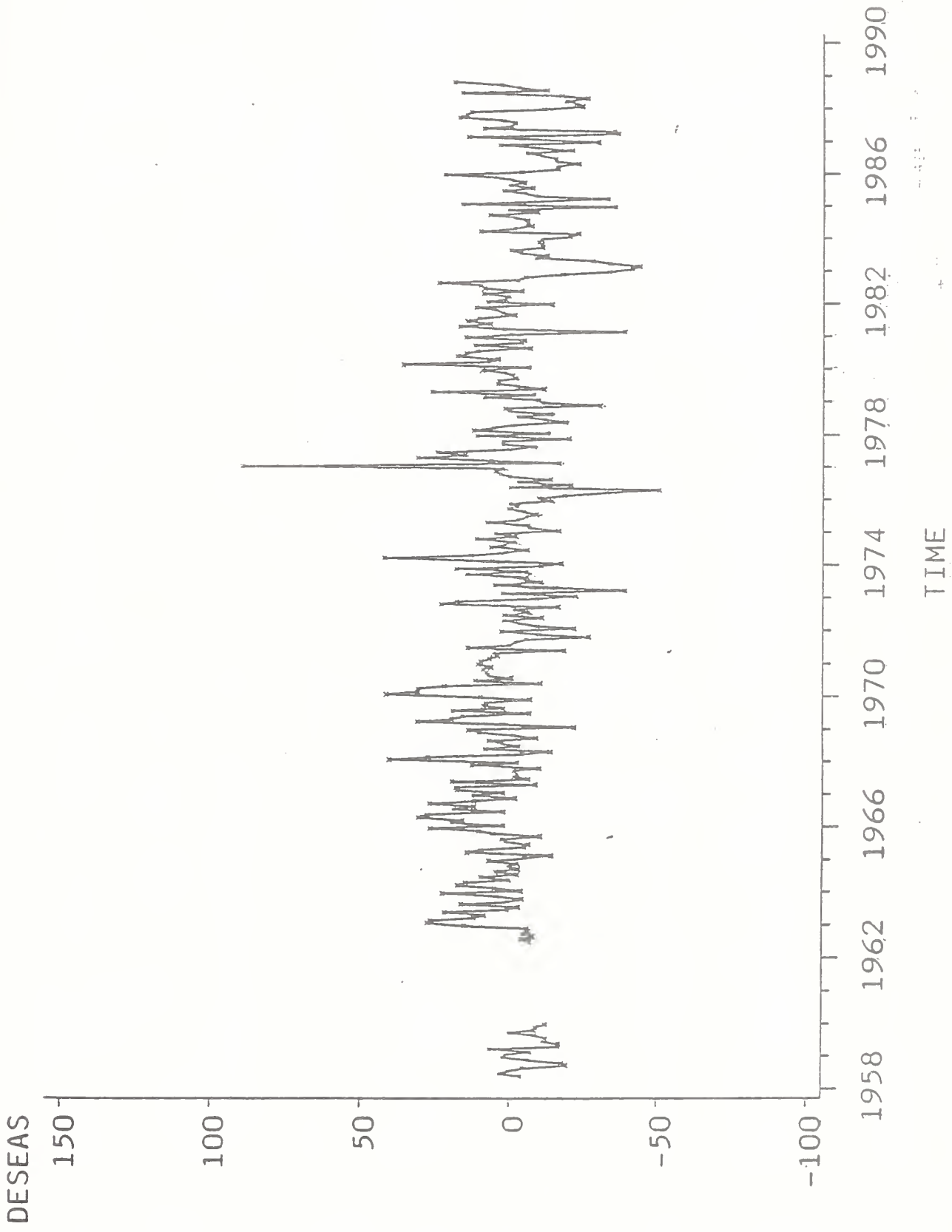
Statistical factors to be considered

1. Noise Level (ϵ)
2. Autocorrelation (ϕ)
3. Length of Record (T)
4. Sampling Rate
5. Spatial Correlation
6. Model Selection
7. Quality Assurance of Data

Total Ozone Measurements at Caribou ME



Desseasonalized Ozone at Caribou ME



Modeling (Total Ozone Example)

Multiple trends model for a monthly ozone series, y_t ,

$t = 1, 2, \dots, T$:

$$y_t = \sum_{i=1}^{12} \mu_i I_{i;t} + \sum_{i=1}^{12} \beta_i I_{i;t} R_t + \text{Trend Terms}$$

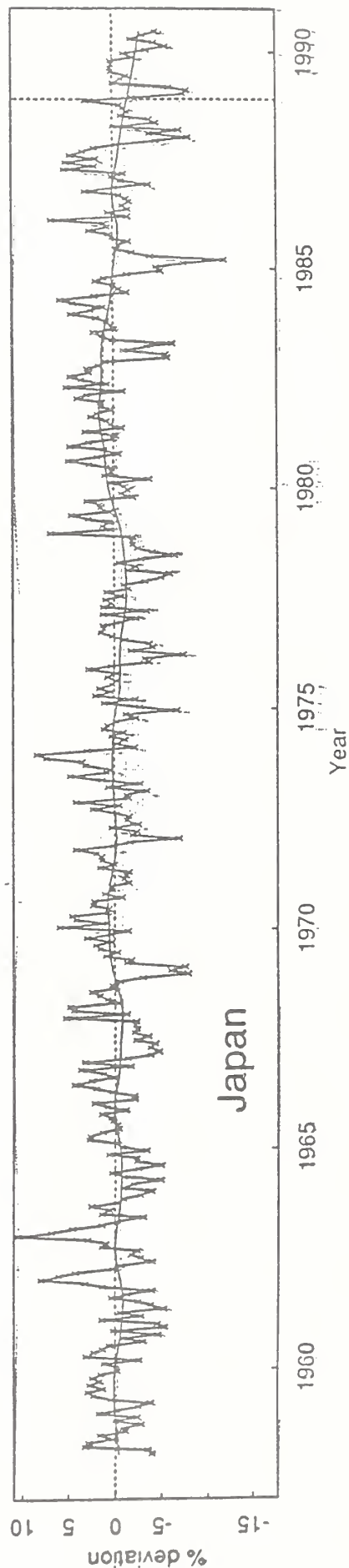
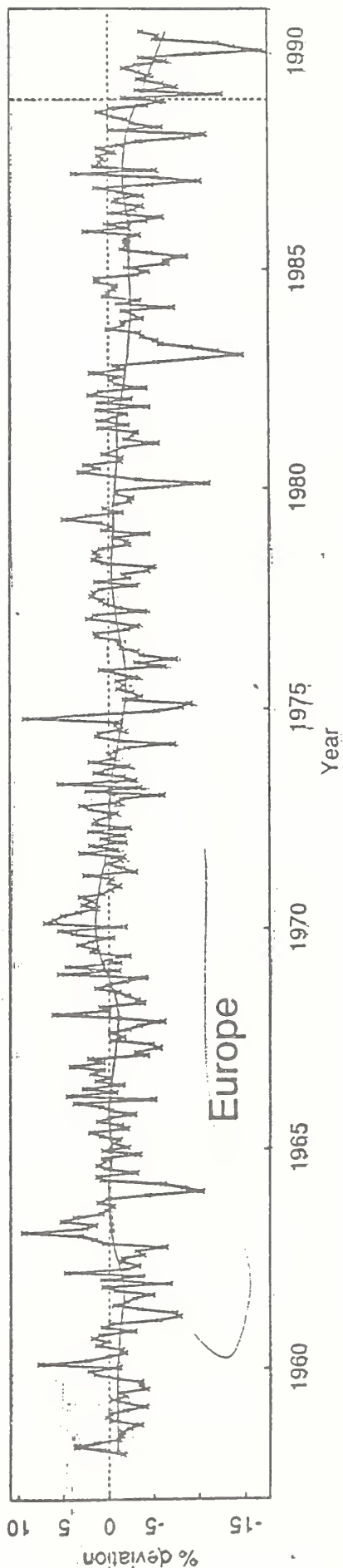
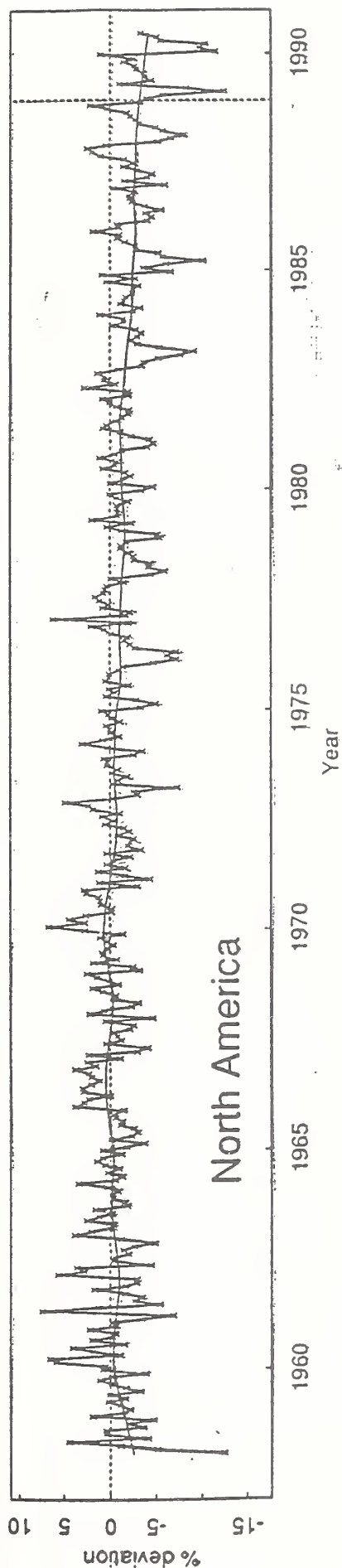
↖ Seasonal Terms

$$\gamma_1 Z_{1;t} + \gamma_2 Z_{2;t-k} + \gamma_3 Z_{3;t} + N_t$$

↖ Solar ↖ QBo ↖ Nuclear ↖ Noise

N_t series modeled

$$N_t = \phi \cdot N_{t-1} + e_t$$



Candidate Model for UV-B

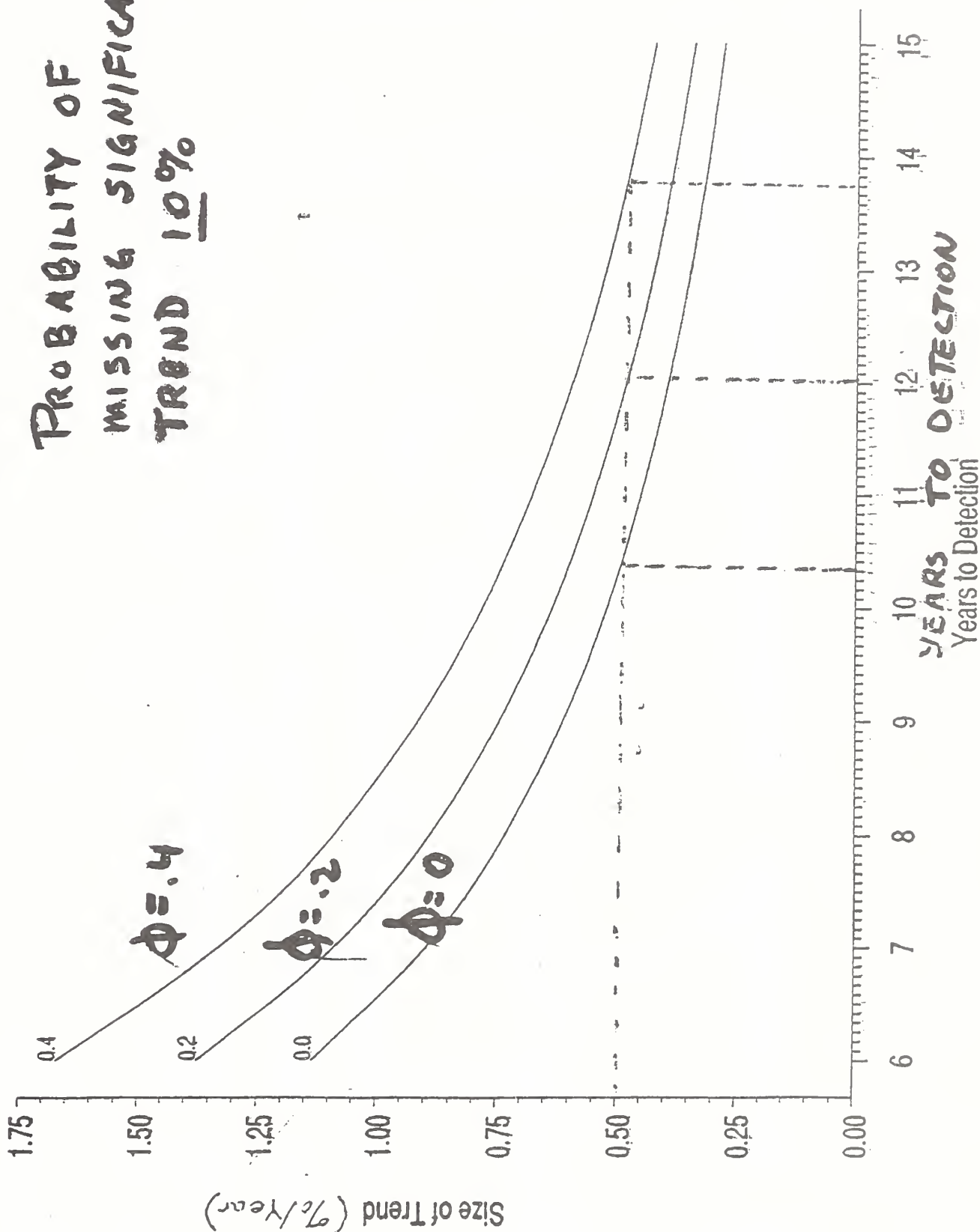
For constant solar zenith angle:

$$y_t = \mu + \text{Seasonal} + \text{Trend} \\ + \text{fn}(\text{O}_3?, \text{cloud, haze?, albedo?, etc.}) \\ + N_t$$

$$N_t = \phi N_{t-1} + e_t$$

Years to Detect Trend With Various Autocorrelations

Observation Standard Deviation of 5 Percent

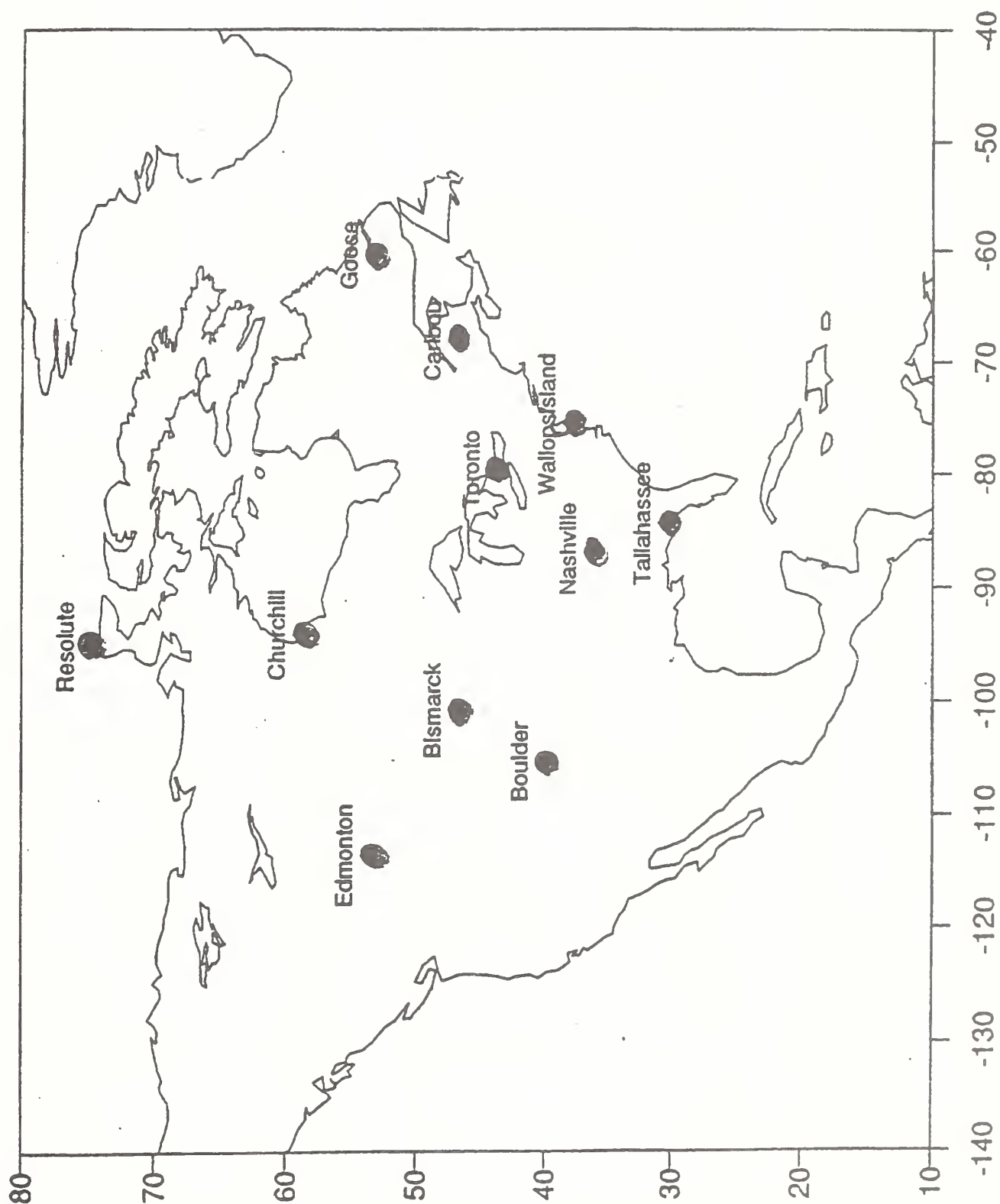


II. Coverage / Representativeness

Coverage Issues Related to:

- 1) Distance and Location**
- 2) Design Factors (e.g., cloudiness)**
- 3) Ancillary Measures**

Examples



Relationships between Stations Measuring Total Ozone Correlation Matrix of Noise Levels

C-316

Correlation Matrix of A(t) Residuals from Common Model

SERIES	CHURCH	EDMONT	GOOSE	CARIBO	BISMAR	TORONT	BOULDE	WALLOP	NASHVI	TALLAH
CHURCH	1.000	0.511	0.195	0.057	0.359	0.019	0.105	-0.124	-0.035	-0.125
EDMONT	0.511	1.000	0.078	0.014	0.466	-0.056	0.138	-0.080	-0.148	-0.075
GOOSE	0.195	0.078	1.000	0.535	-0.029	0.190	-0.112	0.098	0.014	-0.066
CARIBO	0.057	0.014	0.535	1.000	0.166	0.493	0.060	0.401	0.249	0.014
BISMAR	0.359	0.466	-0.029	0.166	1.000	0.253	0.479	0.114	0.157	-0.183
TORONT	0.019	-0.056	0.190	0.493	0.253	1.000	0.167	0.528	0.492	0.075
BOULDE	0.105	0.138	-0.112	0.060	0.479	0.167	1.000	0.051	0.177	-0.109
WALLOP	-0.124	-0.080	0.098	0.401	0.114	0.051	0.051	1.000	0.565	0.366
NASHVI	-0.035	-0.148	0.014	0.249	0.157	0.177	0.565	0.366	1.000	0.345
TALLAH	-0.125	-0.075	-0.066	0.014	-0.183	-0.109	-0.109	-0.366	0.345	1.000
LERWIC	0.061	-0.019	0.128	0.243	0.042	0.152	0.074	0.120	0.104	-0.000
LENING	-0.179	-0.166	-0.001	-0.018	-0.006	0.048	0.070	0.118	0.087	0.088
BELSK	-0.040	0.008	0.101	0.099	-0.000	0.070	0.100	0.226	0.151	0.168
BRACKN	0.070	0.084	0.057	0.170	0.130	0.241	0.044	0.191	0.182	0.067
HRADEC	0.036	0.020	0.029	0.032	0.007	0.029	0.080	0.276	0.171	0.220
HOHENP	0.041	0.041	0.048	0.009	0.090	0.128	0.122	0.251	0.228	0.178
AROSA	0.086	0.074	0.095	-0.007	0.064	0.112	0.099	0.212	0.142	0.170
VIGNA	0.069	0.131	0.071	0.013	0.034	-0.006	0.049	0.128	0.150	0.221
CAGLIA	0.053	0.073	0.143	0.048	0.052	-0.040	-0.011	0.057	0.040	0.141
SAPPOR	-0.077	0.002	0.057	0.141	0.090	-0.015	0.030	0.104	0.091	0.154
TATENO	0.055	0.011	0.155	0.121	0.089	0.029	0.107	-0.040	0.046	0.111
KAGOSH	0.043	0.013	0.013	0.021	0.106	0.057	0.136	0.011	0.080	0.083
NAHA	0.033	-0.014	0.071	0.207	0.143	0.223	0.064	0.139	0.174	0.017
QUETTA	-0.023	-0.028	0.042	0.024	0.066	-0.118	-0.067	0.018	0.041	0.070
CAIRO	-0.177	-0.144	0.007	0.142	0.104	0.099	0.058	0.184	0.173	0.082

Coverage (continued)

Depending on what we want to infer from data and trends, some important *viewing* and *societal* factors include:

	-	+
1. Cloudiness	Clear	Cloudy
2. Pollution	Clean	Dirty
3. Population	Sparse	Dense
4. Changes in ozone	Low	High
5. Altitude	Low	High
6. Latitude	Low	High
7. Crop Land	No	Yes

→ $2^7 = 128$ Combinations

→ Select some fraction: 2^{k-p} locations

**Another issue is the availability of data on
ancillary factors**

For example,

column ozone

cloudiness

aerosol and particulates

surface albedo

SO₂, NO₂, etc.

III. Sampling

- 1. If model is based on fixed solar zenith angle, need dawn to dusk data.**
- 2. Day-to-day autocorrelation influences number of days per month sampling is done.**

Effect of Sampling Rate on Trend Std. Dev.

Table 3. Summary of Ozone Trend Estimates (in % per year)

(a) Total Ozone

<u>Sampling Rate</u>	<u>Tateno</u>		<u>Hohenpeissenberg</u>	
	<u>Trend</u>	<u>S.E.</u>	<u>Trend</u>	<u>S.E.</u>
1/1	-.002	.082	-.078	.061
1/2	-.022	.082	-.099	.066
1/4	-.010	.080	-.136	.080
1/8	-.046	.073	-.103	.083
1/16	-.009	.082	-.187	.084

Effect of time lags on Station to Station Relationship

Summary of Correlation Estimates of Total Ozone

Between Arosa and Hohenpeissenberg

<u>Sampling Plan</u>	<u>Correlation</u>	<u>Sampling Plan</u>	<u>Correlation</u>
A1H1(1)	.948	A1H2(1/2)	.812
A1H1(1/2)	.943	A2H1(1/2)	.856
A1H1(1/4)	.946	A1H4(1/4)	.621
A1H1(1/8)	.950	A4H1(1/4)	.637
A1H1(1/16)	.949	A1H7(1/8)	.395
		A7H1(1/8)	.438

IV. Quality Assurance

Network Quality Assurance considerations include:

1. Calibration checks.
2. QC charts to assess "special cause" changes (e.g., drifts, outliers, etc.).
3. Robustness of measurements to viewing conditions (e.g., on target with minimum variation).
4. Intercomparison with similar or ancillary instrumental data.
5. Comparison of results with model calculations.

Conclusions / Recommendations

1. Determine trend detection target using statistical knowledge of model and variation.

Trend detection = $\text{fn}(\text{model}, \epsilon, \phi, T)$

2. Select sites that represent viewing and societal factors. Use statistical design to minimize number of sites.
3. Use sampling plan that is based away from model and data considerations (e.g., auto and spatial correlation)
4. Design quality assurance plan. (The network must be above reproach)

Commentary from Invited Experts: Effects Research

Dr. Jan van der Leun
University of Utrecht, The Netherlands

Ozone Depletion and Skin Cancer Incidence

<u>Change in Ozone</u>	<u>Predictions in NMSC</u>
- 1%	+ 6% (1971)
- 1%	+ 4% (1987)
- 1%	+ 3% (1989)
- 1%	+ 2.3% (1991)

Amplification Factors (1991)

	RAF	X	BAF	=	AF
SCC	1.4		2.5		3.5
BCC	(1.4)		1.4		2.0
					↓
SCC + BCC					2.3

Ozone Depletion



Reason for Interest

—

+

Research Effort

100

1

WHY?

FUTURE?

* NATIONAL AGRICULTURAL LIBRARY



1022438930

my

NATIONAL AGRICULTURAL LIBRARY



1022438930